

**Furo[2,3-*b*]furanones in Natural Products: Synthesis,  
Derivatization and Biological Evaluation of  
(+)-Paeonilide and Studies toward Dermatolactone**

**Dissertation**

**Zur Erlangung des Doktorgrades der Naturwissenschaften**

**Dr. rer. nat.**

**der Fakultät für Chemie und Pharmazie**

**der Universität Regensburg**



vorgelegt von

**Matthias Gnahn**

aus Leinhof

**Regensburg 2018**

Die Arbeit wurde angeleitet von: Prof. Dr. Oliver Reiser

Promotionsgesuch eingereicht am: 19.10.2018

Promotionskolloquium am: 16.11.2018

Prüfungsausschuss:

Vorsitz:	Prof. Dr. Alkwin Slenczka
1. Gutachter:	Prof. Dr. Oliver Reiser
2. Gutachter:	Prof. Dr. Julia Rehbein
3. Gutachter:	Prof. Dr. Arno Pfitzner

Der experimentelle Teil der vorliegenden Arbeit wurde im Zeitraum von November 2014 bis Oktober 2017 unter der Leitung von Prof. Dr. Oliver Reiser am Institut für Organische Chemie der Universität Regensburg angefertigt.

Herrn Prof. Dr. Oliver Reiser möchte ich herzlich für die Überlassung des äußerst interessanten Themas, die anregenden Diskussionen, sowie die stete Unterstützung während der Durchführung dieser Arbeit danken.





*Für meine Familie*



## Abbreviations

Å	angstrom	<i>et al.</i>	and others
abs	absolute	EtOH	ethanol
Ac	acetyl	g	gram(s)
APCI	atmospheric pressure chemical ionization	h	hour(s)
Bn	benzyl	HPLC	high pressure liquid chromatography
Bz	benzoyl	HRMS	high-resolution mass spectrometry
°C	degree Celsius	Hz	Hertz
calc.	calculated	IBX	2-iodoxybenzoic acid
conc.	concentrated	<i>i</i> Pr	<i>iso-propyl</i>
d	day(s)	IR	infrared
DBU	1,8-Diazabicyclo[5.4.0] undec-7-ene	LDA	Lithium diisopropylamide
DCM	dichloromethane	LiHMDS	lithium hexamethyldisilazide
DIBAL-H	diisobutylaluminum hydride	M	molar
DIPEA	<i>N,N</i> -diisopropylethylamine	MAO	monoamine oxidase
DMAP	4-dimethylaminopyridine	<i>m</i> -CPBA	<i>meta</i> -chloroperoxybenzoic acid
D-Men	D-menthyl	Me	methyl
DMF	dimethylformamide	MeCN	acetonitrile
DMP	2,2-dimethoxypropane	MeOH	methanol
DMPI	Dess–Martin periodinane	μ	micro
DMSO	dimethyl sulfoxide	min	minute(s)
<i>dr</i>	diastereomeric ratio	mL	milliliter(s)
EA	ethylacetate	mol	mole
<i>ee</i>	enantiomeric excess	m.p.	melting point
e.g.	<i>exempli gratia</i> , for example	MS	mass spectrometry
EI	electron ionization	MSA	methanesulfonic acid
equiv.	equivalent(s)		
ESI	electrospray ionization		

NBS	<i>N</i> -bromosuccinimide	TBAB	tetra- <i>N</i> -butylammonium bromide
NMO	<i>N</i> -Methylmorpholine <i>N</i> -oxide	TBAF	tetra- <i>N</i> -butylammonium fluoride
NMR	nuclear magnetic resonance	TBDMS	<i>tert</i> -butyldimethylsilyl
NOESY	nuclear Overhauser effect spectroscopy	TBDPS	<i>tert</i> -butyldiphenylsilyl
		Tf	triflyl
<i>p</i>	<i>para</i>	TFAA	trifluoroacetic anhydride
PAF	platelet-activating factor	THF	tetrahydrofuran
		TLC	thin layer chromatography
PAFR	platelet-activating factor receptor	TMS	trimethylsilyl
PCC	pyridinium chlorochromate	<i>t<sub>r</sub></i>	retention time
Pd/C	palladium on charcoal	Ts	tosyl
PE	hexanes	TSA	toluenesulfonic acid
pH	proton log units	UV	ultraviolet
Ph	phenyl	v/v	volume fraction
Piv	pivaloyl	wt%	weight percent
ppm	parts per million		
PPTS	pyridinium <i>p</i> -toluenesulfonate		
quant.	quantitative		
R	arbitrary moiety		
R <sub>f</sub>	retardation factor		
Rh/C	rhodium on charcoal		
rt	room temperature		
RT	Raumtemperatur		
sat.	saturated		
SCE	saturated calomel electrode		
SET	single electron transfer		
<i>t</i> Bu	<i>tert</i> -butyl		

## Table of contents

A. Introduction .....	1
1. Furofuranones in natural products.....	1
2. Synthesis of the furo[2,3- <i>b</i> ]furanone scaffold .....	3
3. (+)-Paeonilide.....	8
4. References .....	18
B. Main Part.....	21
1. Synthesis of (+)-paeonilide .....	21
1.1 Cyclopropanation.....	21
1.1.1 Introduction.....	21
1.1.2 Cyclopropanation of furan derivatives.....	24
1.2 Toward the furo[2,3- <i>b</i> ]furanone formation .....	29
1.2.1 Hydrogenation.....	29
1.2.2 Functionalization .....	31
1.2.3 Lactonization and Isomerization .....	35
1.3 Total synthesis of (+)-paeonilide.....	39
1.3.1 Introduction of the side chain .....	39
1.3.2 Final steps.....	41
2. Derivatization of (+)-paeonilide.....	46
3. Biological evaluation.....	54
3.1 Platelet-activating factor (PAF) .....	54
3.2 Light transmission aggregometry .....	57
3.3 Results.....	58
4. Studies toward Dermatolactone .....	62
4.1 Introduction .....	62
4.2 Visible light-mediated reactions .....	63
4.2.1 Introduction.....	63
4.2.2 Direct conjugate addition.....	65
4.2.3 Decarboxylation of <i>N</i> -acyloxyphthalimides .....	67
4.3 Ni-catalyzed coupling of <i>N</i> -acyloxyphthalimides.....	73
5. References .....	78
C. Summary .....	83
D. Zusammenfassung .....	88

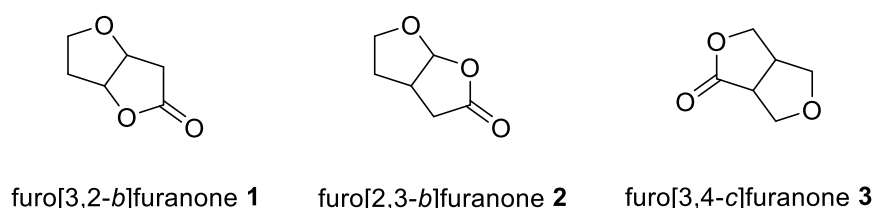
E. Experimental Part .....	93
1. General Information .....	93
2. Synthesis of compounds .....	96
2.1 Synthesis of (+)-paeonilide (49) .....	96
2.2 Derivatization of (+)-paeonilide .....	105
2.3. Studies toward dermatolactone .....	117
3. Biological evaluation.....	123
4. References .....	125
F. Appendix.....	126
1. NMR spectroscopic data.....	126
2. HPLC Chromatograms.....	163
3. X-ray crystallographic data .....	166
4. Light transmission aggregometry .....	202
5. Curriculum Vitae .....	233
G. Acknowledgement – Danksagung .....	235
H. Declaration.....	238

## A. Introduction

### 1. Furofuranones in natural products

Natural products are small organic molecules produced by living organism in nature.<sup>1</sup> Especially in medicinal chemistry, these compounds, together with their analogues and synthetic derivatives, offer a large pool of active structures, which are crucial for drug discovery and development.<sup>2,3</sup> Secondary metabolites are organic compounds which are not essential for the life cycle of cells, but provide survival functions for the organism and they are of special interest for pharmaceutical research because of their unique biological and pharmacological activities.<sup>4,5</sup> Due to their broad structural and chemical diversity, these compounds offer not only a synthetic challenge, but also an inspiration for medicinal chemistry as a rich source of novel scaffolds.<sup>6,7</sup>

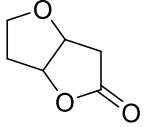
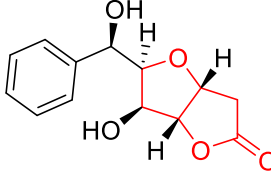
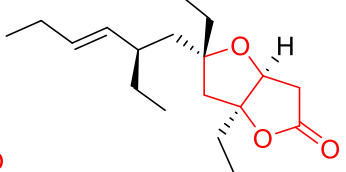
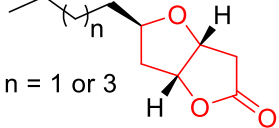
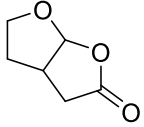
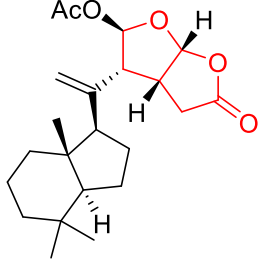
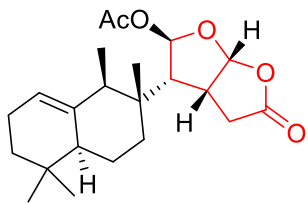
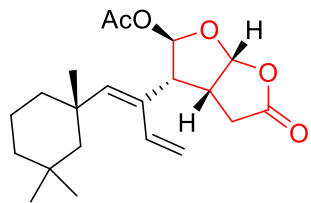
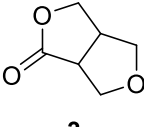
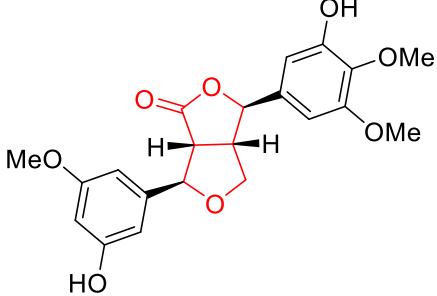
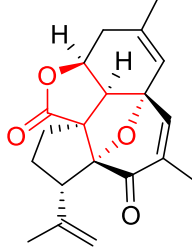
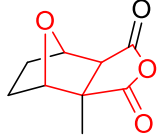
A motif frequently found in natural products is the furofuranone ring system. It was isolated from a variety of different kinds of organisms, *e.g.* marine sponges<sup>8</sup>, corals<sup>9</sup>, nudibranchs<sup>10</sup>, plants<sup>11</sup>, fungi<sup>12</sup> or insects.<sup>13</sup> There are three different types of furofuranones which are classified based on the position of the oxygen functionalities (Figure 1): the furo[3,2-*b*]furanone **1**, the furo[2,3-*b*]furanone **2** and the furo[3,4-*c*]furanone **3**.<sup>14</sup>



**Figure 1.** Classification of furofuranones.<sup>14</sup>

All three motifs can be found in a large number of naturally occurring secondary metabolites. They show great structural complexity and, as a result, display a variety of biological activities, such as antitumor<sup>9</sup>, antihelminthic<sup>15</sup> or vasodilating<sup>16</sup> effects. Furthermore, they can also act as biocontrol agents and semiochemicals.<sup>13</sup> Some representatives for natural products bearing the furofuranone scaffold as substructure are shown below (Table 1).<sup>8,9,11,13,15,16</sup>

**Table 1.** Examples for natural products bearing the furofuranone scaffold.<sup>8,9,11,13,15,16</sup>

 <p>1</p>	 <p>(+)-goniofufurone (4)</p>	 <p>(-)-plakortone E (5)</p>	 <p>(+)-Hagen's gland lactones (6)</p>
 <p>2</p>	 <p>(+)-norrisolide (7)</p>	 <p>macfarlandin C (8)</p>	 <p>spongionellin (9)</p>
 <p>3</p>	 <p>graminone B (13)</p>	 <p>(+)-intricarene (14)</p>	 <p>(-)-palasonin (15)</p>

This thesis and the herein described work is focused exclusively on the synthesis of the furo[2,3-*b*]furanone ring system and its use in natural product synthesis.

The furo[2,3-*b*]furanone scaffold is present in more than 100 natural products.<sup>17,18</sup> One example is (+)-Norrisolide (7) (see Table 1) which was first isolated in 1983 by Faulkner *et al.*

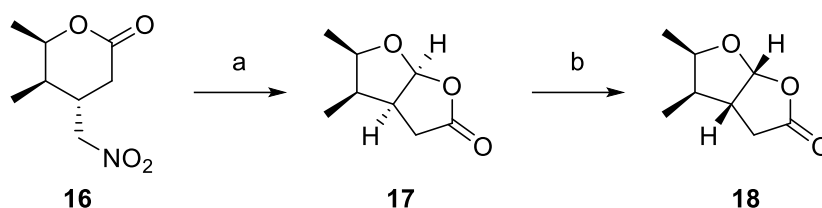


from the skin extracts of the dorid nudibranch *Chromodoris norrisi*.<sup>19</sup> Interest in **7** arose because of its ability to induce an irreversible vesiculation of the Golgi complex in intact cells, which is very useful in order to investigate the function and the dynamics of the Golgi apparatus.<sup>20</sup> Besides (+)-norrisolide (**7**), many terpenoids with a furo[2,3-*b*]furanone core structure have been isolated and synthesized. Noteworthy examples are, *e.g.* the rearranged diterpenoids macfarlandin C (**8**), spongionellin (**9**) and cheloviolene A (**11**). In all of these examples, a quaternary carbon of a hydrocarbon unit is attached to the furo[2,3-*b*]furanone fragment in the C-4 position. This hydrocarbon unit can be either on the concave or convex face of the bicyclic ring system, as shown in macfarlandin C (**8**) and cheloviolene A (**11**), respectively (see Table 1).<sup>21</sup> However, the furo[2,3-*b*]furanone scaffold can also be fused to a larger ring system, observed *e.g.* in chromodorolide B (**10**) which shows modest antitumor activity.<sup>22</sup> Recently, a new diterpene has been isolated from the Antarctic Dendroceratid sponge *Dendrilla membranosa*. The so-called “darwinolide” (**12**) shows selectivity against the biofilm phase of methicillin-resistant *Staphylococcus aureus* (MRSA).<sup>23</sup> As it is assumed that most of the human bacterial infections are correlated with biofilms and MRSA infections are especially difficult to treat, darwinolide (**12**) may provide an interesting scaffold for the development of new anti-biofilm agents.<sup>24</sup>

In summary, furo[2,3-*b*]furanones represent a class of natural products with a variety of remarkable biological activities. Therefore, synthesis of this scaffold alongside with its functionalization is of great scientific interest.

## 2. Synthesis of the furo[2,3-*b*]furanone scaffold

In the last decades, various attempts have been made to elaborate general strategies to synthesize the furo[2,3-*b*]furanone scaffold. As previously mentioned, a great variety of the biologically active compounds bearing the furo[2,3-*b*]furanone core structure is either substituted or fused to a larger ring system at the C-4 position. Therefore, focus was laid on synthetic strategies toward 4-substituted furo[2,3-*b*]furanones. The oldest route known to access such compounds was published by Nakata *et al.* in 1985 (Scheme 1).<sup>25</sup>

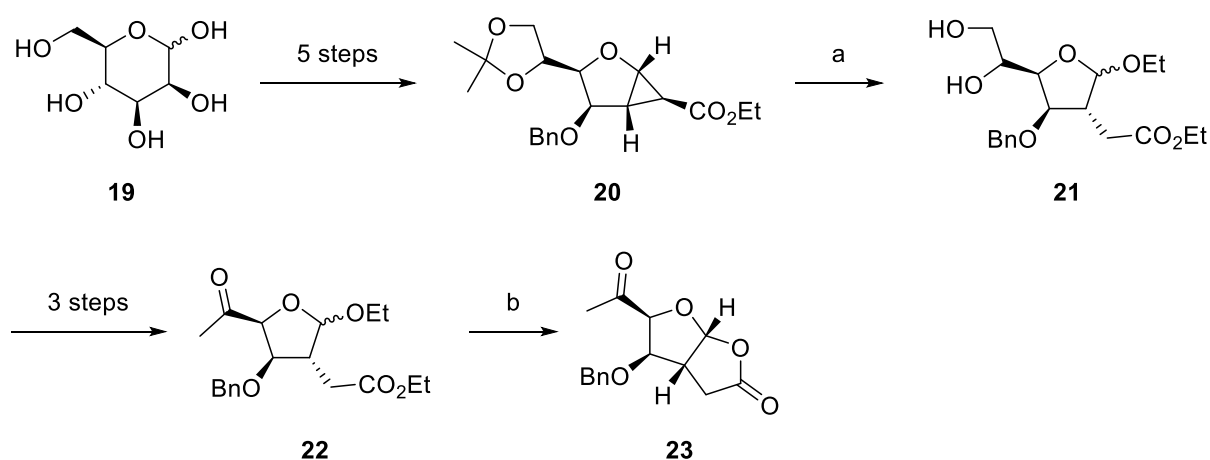


**Reagents:** a) TiCl<sub>3</sub>, Et<sub>3</sub>N; b) conc. HCl, DCM, 70% over 2 steps.

**Scheme 1.** Synthesis of furo[2,3-*b*]furanones **17** and **18** by Nakata *et al.* in 1985.<sup>25</sup>

Titanium(III)-catalyzed conversion of the nitro group of lactone **16** into an aldehyde led to the formation of the bicyclic lactone **17** which underwent isomerization to the thermodynamically favored lactone **18** upon treatment with conc. HCl.

In 1999, Theodorakis *et al.* developed a different strategy during their first approach toward (+)-norrisolide (**7**), starting from D-mannose (**19**).<sup>26</sup> The key step in this synthesis was the acid-catalyzed cyclopropane ring-opening of **20** to tetrahydrofuran **21**, followed by the acid-catalyzed lactonization to lactone **23** after previous functionalization to **22** (Scheme 2).

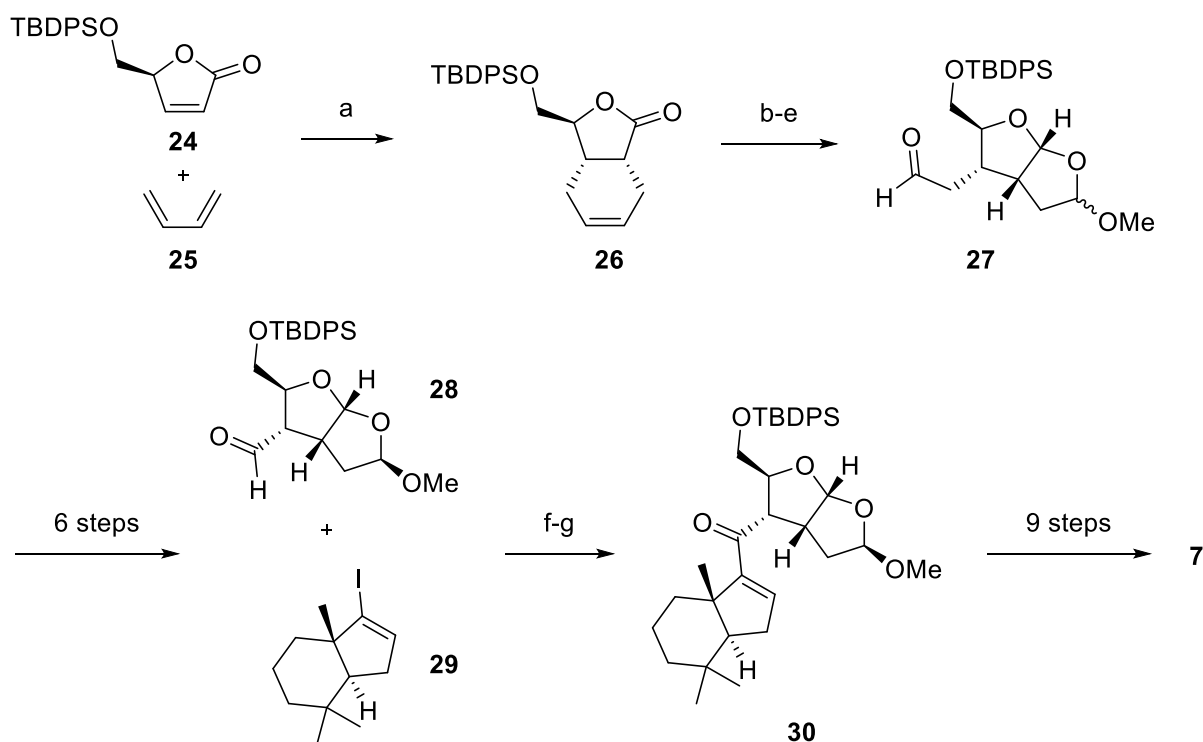


**Reagents and conditions:** a) H<sub>2</sub>SO<sub>4</sub>, EtOH, 25 °C, 48 h, 78%; b) MeSO<sub>3</sub>H, DCM, -5 to 0 °C, 12 h, 67%.

**Scheme 2.** Furo[2,3-*b*]furanone synthesis by Theodorakis *et al.* in 1999.<sup>26</sup>

Unfortunately, the introduction of the desired side chain in the C-4 position of **23** to obtain (+)-norrisolide (**7**) proved unsuccessful. Inspired by the earlier work of Corey *et al.* on the total synthesis of gracilin B and C, Theodorakis *et al.* modified their synthetic route in order to have an easily functionalizable carbonyl group in the C-4 position.<sup>27</sup> With these changes implemented, they were able to finally synthesize (+)-norrisolide (**7**) in 2004.<sup>28</sup> Therefore,

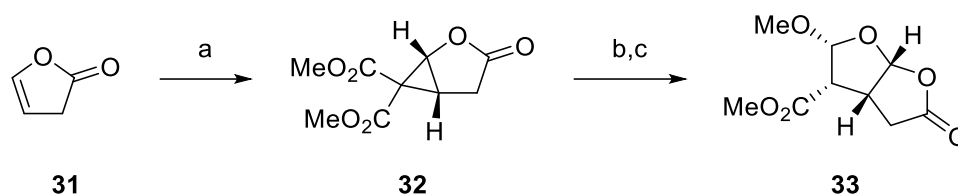
butenolide **24** and butadiene (**25**) were subjected to a Lewis acid-catalyzed Diels-Alder reaction, yielding exclusively lactone **26** with the bulky TBDPS group on the convex face of the bicyclic ring system. Subsequent reduction of the lactone moiety followed by oxidative cleavage of the alkene and methyl protection of the corresponding lactol led to aldehyde **27**. Further functionalization gave aldehyde **28** which was connected to the *trans*-fused hydrindane **29**. Subsequent oxidation of the corresponding alcohol yielded **30** which was transformed to (+)-norrisolide (**7**) in 9 steps (Scheme 3).



**Reagents and conditions:** a)  $\text{AlCl}_3$ , DCM, 60 °C, 6 d, 85%; b) DIBAL-H, DCM, -78 °C, 0.5 h, 98%; c)  $\text{OsO}_4$ , NMO, pyridine, acetone,  $\text{H}_2\text{O}$ , 25 °C, 8 h; d)  $\text{Pb}(\text{OAc})_4$ , DCM, 0 °C, 0.5 h, 64% over 2 steps; e) MeOH, Amberlyst® 15, 3 Å molecular sieves,  $\text{Et}_2\text{O}$ , 25 °C, 10 h, 77%; f) *t*BuLi, THF, -78 °C, 1.5 h, 75%; g) DMPI, DCM, 25 °C, 10 h, 95%.

**Scheme 3.** Construction of the furo[2,3-*b*]furanone structure in the total synthesis of (+)-norrisolide (**7**) by Theodorakis *et al* in 2004.<sup>28</sup>

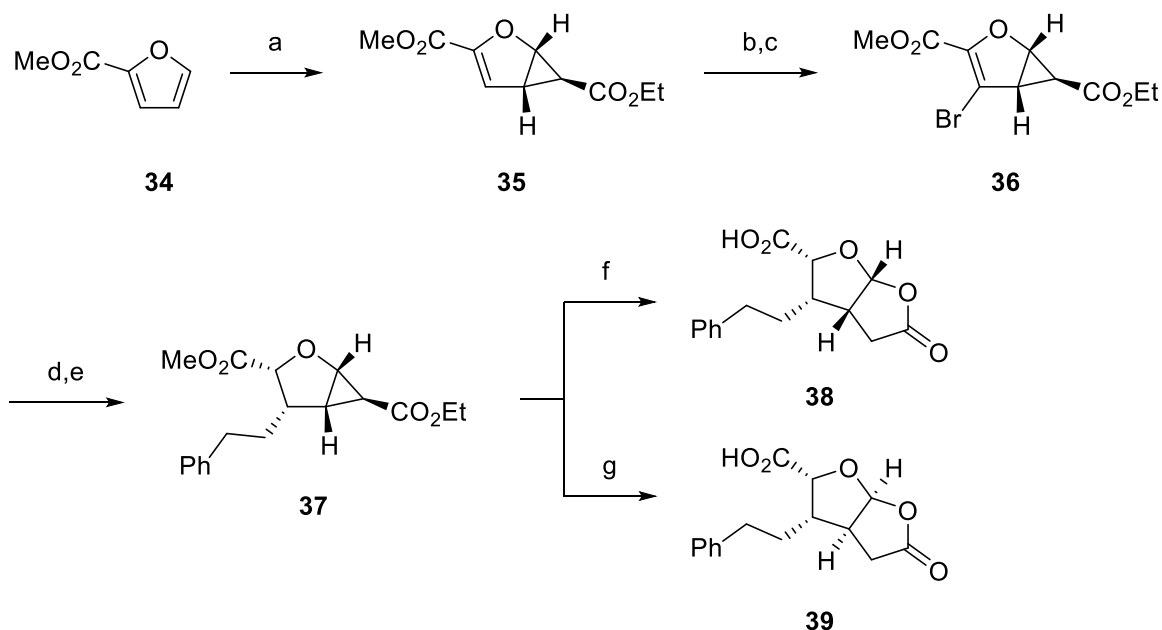
In 2012, Snapper *et al.* revisited the synthesis of (+)-norrisolide (**7**) using another strategy to synthesize the furo[2,3-*b*]furanone core structure.<sup>10</sup> Rhodium-catalyzed cyclopropanation of furanone **31** led to enantiomerically enriched cyclopropane **32**. This intermediate could then be rearranged *via* thermolysis in benzene, followed by subsequent diastereoselective hydrogenation to provide the substituted furofuranone **33** (Scheme 4).



**Reagents and conditions:** a)  $\text{Rh}_2(\text{S-NTTL})_4$ , dimethyl 2-diazomalonate, PhF, rt, 2 h, 70%, 60-70% ee; b) benzene, 185 °C, 24 h, 82%; c) Pd/C,  $\text{H}_2$ ,  $\text{Et}_3\text{N}$ , EA, rt, 3 d, 63%.

**Scheme 4.** Furo[2,3-*b*]furanone synthesis by Snapper *et al.* in 2012.<sup>10</sup>

Taking up the earlier idea of Theodorakis to synthesize the furo[2,3-*b*]furanone scaffold *via* a cyclopropane ring-opening/lactonization cascade, Reiser *et al.* published a procedure giving rise to the desired ring system bearing a substituent in the 4-position in 2005.<sup>29</sup> Interestingly, they were able to control the positioning of the substituent to be either on the concave or the convex face of the bicyclic ring system by kinetic or thermodynamic control and thus giving rise to natural products differing in the stereochemistry at the ring junction (Scheme 5).

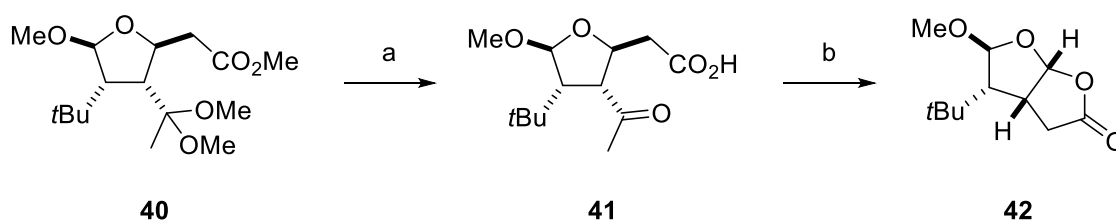


**Reagents and conditions:** a)  $\text{Cu}(\text{OTf})_2$ , (*S,S*)-*i*Pr-box,  $\text{PhNHNH}_2$ ,  $\text{N}_2\text{CHCO}_2t\text{Bu}$ , DCM, 0 °C, 38%, >99% ee; b)  $\text{Br}_2$ ,  $\text{CHCl}_3$ , 0 °C, 1 h, 70%; c) DBU,  $\text{Et}_2\text{O}$ , rt, 1 h, 94%; d)  $\text{Pd}(\text{OAc})_2$ ,  $\text{PPh}_3$ ,  $\text{Et}_3\text{N}$ , styrene, DMF, 95 °C, 24 h, 71%; e) Pd/C,  $\text{H}_2$ , MeOH, rt, 2 d, 67%; f) 6 M HCl, 1,4-dioxane, rt, 24 h, 31%; g) 6 M HCl, 1,4-dioxane, reflux, 4 h, quant., *dr* (**38**:**39** = 15:85).

**Scheme 5.** Synthesis of furo[2,3-*b*]furanones **38** and **39** by Reiser *et al.* in 2005.<sup>29</sup>

The first step in this synthesis was the asymmetric cyclopropanation of inexpensive 2-furoic acid methyl ester (**34**) to afford the cyclopropane **35**. Bromination and subsequent dehydrobromination led to vinyl bromide **36** which was then subjected to a Heck reaction with styrene. Subsequent hydrogenation gave the substituted bicycle **37**. Utilizing kinetic or thermodynamic control through carefully selected reaction conditions allowed the stereocontrol of the ring-opening/lactonization cascade resulting in lactone **38** or **39**, respectively.

In 2011, Overman *et al.* published a study on the synthesis and reactivity of bicyclic furofuranone scaffolds.<sup>30</sup> Therein, they described the synthesis of furofuranone **42**, starting from highly substituted tetrahydrofuran **40**. Saponification and ketal hydrolysis of this precursor led to the formation of acid **41**. Upon Baeyer-Villiger oxidation, **41** underwent cyclization to the desired furo[2,3-*b*]furanone **42** (Scheme 6).



**Reagents and conditions:** a) (i). 1 M NaOH, MeOH, rt, 36 h; (ii). 1 M HCl, 0 °C, 0.5 h; b) H<sub>2</sub>O<sub>2</sub>·urea, TFAA, DCM, 0 °C to rt, 1.5 h, 82% over 2 steps.

**Scheme 6.** Furo[2,3-*b*]furanone synthesis by Overman *et al.* in 2011.<sup>30</sup>

Recently, Overman *et al.* published an additional method for building up the furo[2,3-*b*]furanone scaffold in the course of their total synthesis of cheloviolenes A and B and dendrillolide C.<sup>18</sup> Herein, the starting lactone **43** could be obtained with different substituents in the 4-position through a photoredox-catalyzed coupling reaction.\* Alkylation of lactone **43** with methyl bromoacetate led to ester **44**. After reduction of the lactone moiety in **44**, the corresponding lactol was directly oxidized to the desired furo[2,3-*b*]furanone **45** (Scheme 7).

\* Methylcyclohexane was used as an exemplary substituent for the optimization studies.



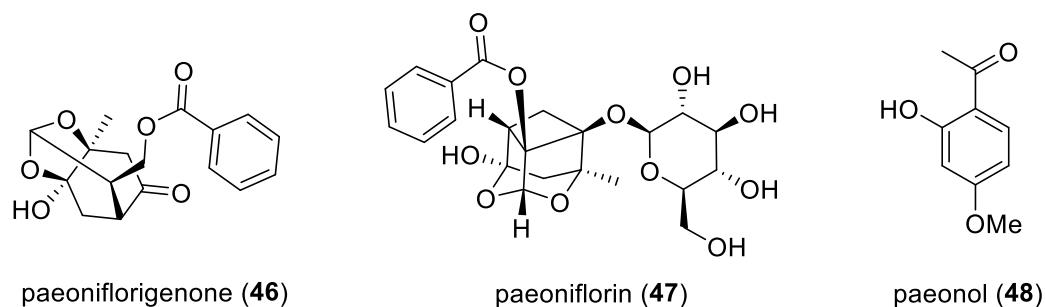


**Figure 2.** Representative biological active compounds isolated from peony root.<sup>36</sup>

In 2000, Liu *et al.* successfully isolated the highly oxygenated monoterpene (+)-paeonilide (49) for the first time from the roots of *Paeonia delavayi*, a peony which is endemic to China.<sup>44</sup> Systematically, (+)-paeonilide (49) belongs to a group of irregular acyclic monoterpenoids. Its novel molecular scaffold could be established by spectroscopic and single-crystal X-ray analyses (Figure 3).<sup>44</sup>

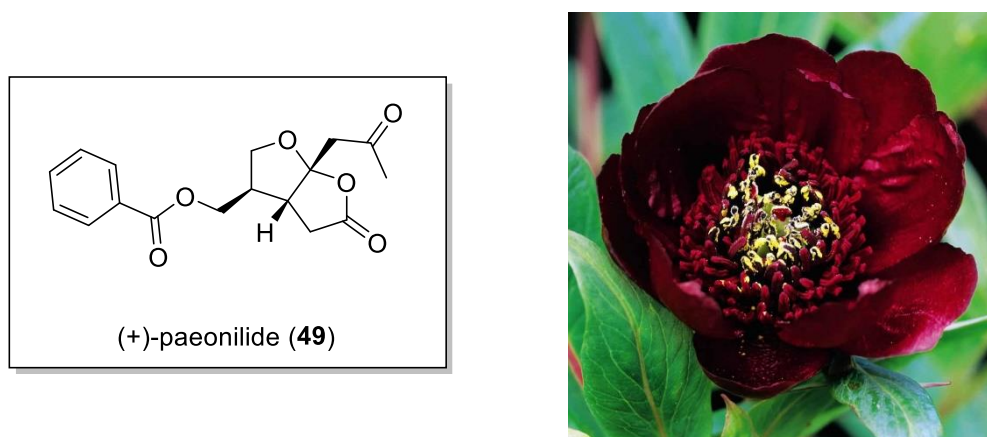


**Figure 3.** Structure of (+)-paeonilide (49) and picture of *Paeonia delavayi*.<sup>45</sup>

Noteworthy, the ring structure of (+)-paeonilide (49) is very similar to the partial ring system present in bilobalide (50) and the class of ginkgolides 51 (Figure 4). The terpene trilactones bilobalide (50) and the ginkgolides 51 are biologically active compounds exclusively isolated from the *Ginkgo biloba* tree, the last living member of the *Ginkgoaceae* which already existed over 200 million years ago in the Permian period.<sup>46,47</sup> With more than 8000 tons of dried leaves produced every year and worldwide sales over US \$1.2 billion of the finished products in 2012, the dried extracts of *Ginkgo biloba* belong to the most important herbal medicines today.<sup>48,49</sup> The leaf extracts possess a great variety of pharmacological effects and are used to treat, *e.g.* memory impairment,<sup>50</sup> Alzheimer's disease and dementia,<sup>51</sup> cerebrovascular insufficiency,<sup>52</sup>

depression<sup>53</sup> and peripheral arterial insufficiency.<sup>54</sup> Furthermore, the ginkgolides **51** were also found to specifically inhibit the platelet-activating factor (PAF, 1-*O*-alkyl-2-acetyl-*sn*-glycero-3-phosphocholine, **52**) induced platelet aggregation.<sup>55</sup>

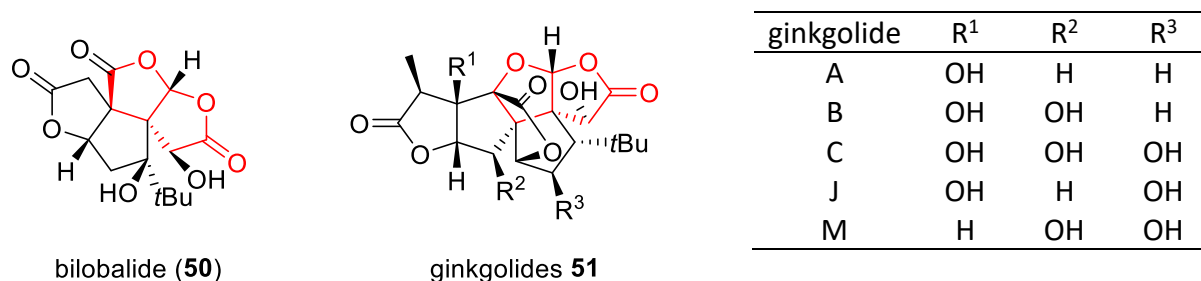


**Figure 4.** Structure of bilobalide (**50**) and ginkgolides **51** (furo[2,3-*b*]furanone substructure marked in red).<sup>46</sup>

As it bears a high structural resemblance to the ginkgolides **51**, (+)-paeonilide (**49**) was subjected to bioassays. It could be proven that **49** also acts as a selective antagonist of the PAF (**52**) induced platelet aggregation. Additionally, it did not show any effect on the arachidonic acid (AA) **53** or adenosine diphosphate (ADP) **54** induced platelet aggregation (Figure 5).<sup>44</sup>

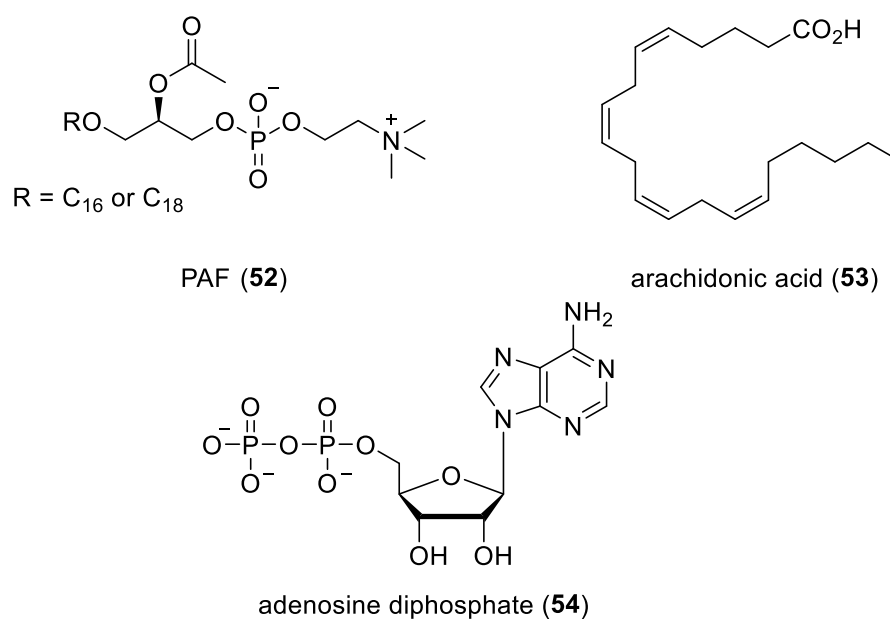


**Figure 5.** Structure of PAF (**52**), AA (**53**) and ADP (**54**).



With an IC<sub>50</sub> value of 25 μM (8 μg·mL<sup>-1</sup>), (+)-paeonilide (**49**) is within the same range as the ginkgolides **51** and, therefore, represents an interesting target for organic synthesis (Table 2).<sup>44,56</sup>

**Table 2.** IC<sub>50</sub> values of the ginkgolides **51** and (+)-paeonilide (**49**).<sup>44,56</sup>

substance <sup>[a]</sup>	IC <sub>50</sub> [μg·mL <sup>-1</sup> ]	IC <sub>50</sub> [μM]
ginkgolide A	15.6	38.2
ginkgolide B	3.5	7.5
ginkgolide C	27.4	62.2
ginkgolide J	43.5	102.5

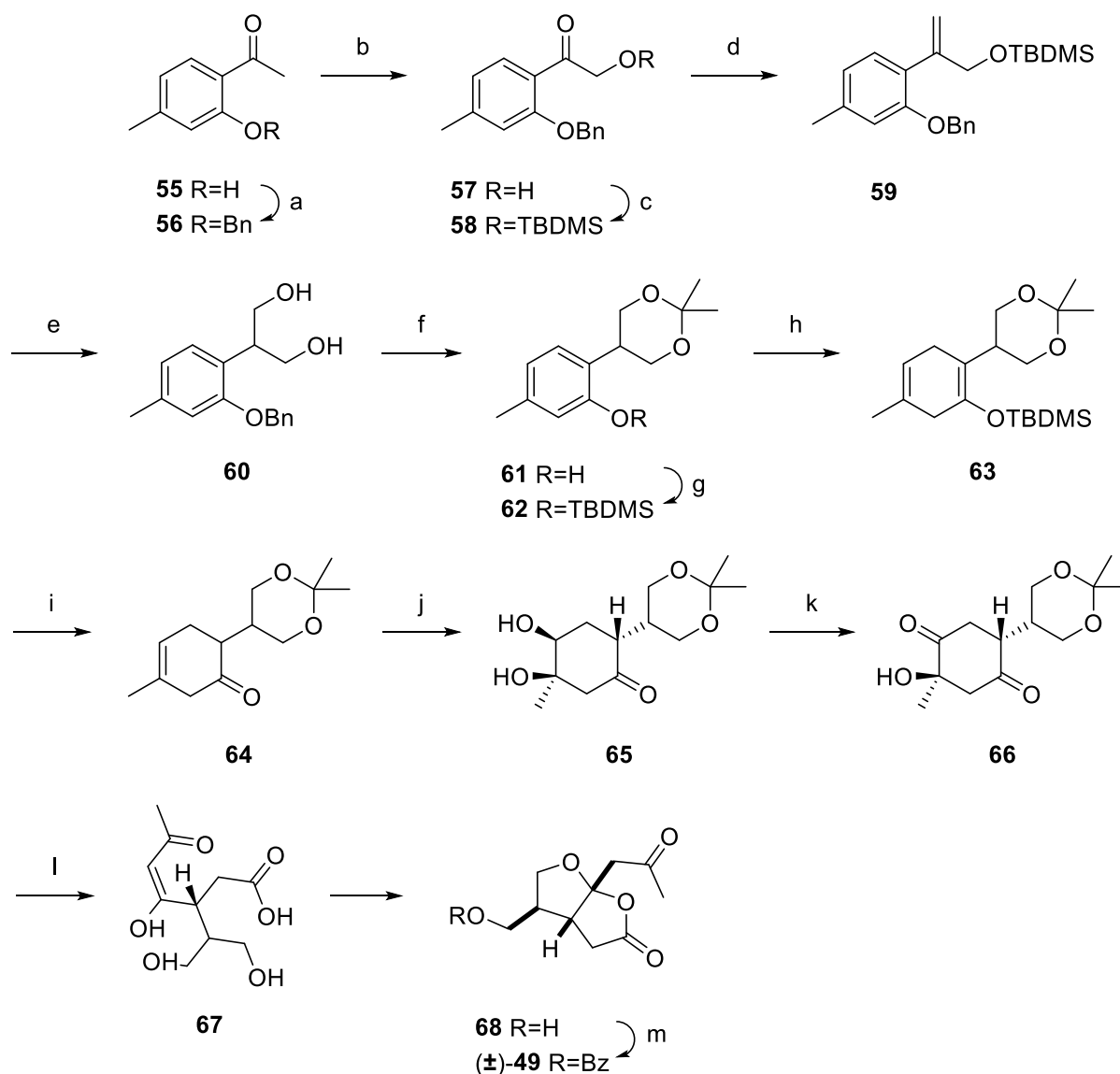
[a] Inhibition of the PAF-induced aggregation of human thrombocytes was measured for the ginkgolides **51**. In case of (+)-paeonilide (**49**) the bioassay is not specified.

Due to the structural complexity of the ginkgolides **51** and the good results of (+)-paeonilide (**49**) in the biological tests, the development of an artificial synthesis of **49** was under investigation since its discovery.

Five total syntheses are published until today, three giving racemic paeonilide (±)-**49**<sup>57,58,59</sup> and two stereoselective routes, one leading to (+)-paeonilide (**49**)<sup>60</sup> and the other to the unnatural enantiomer (-)-paeonilide (*ent*)-**49**.<sup>61</sup>

The first racemic total synthesis was published in 2006 by Zhang *et al.*, yielding (±)-**49** in 16 steps with an overall yield of 15% starting from commercially available 2-hydroxy-4-methylacetophenone (**55**).<sup>57</sup>

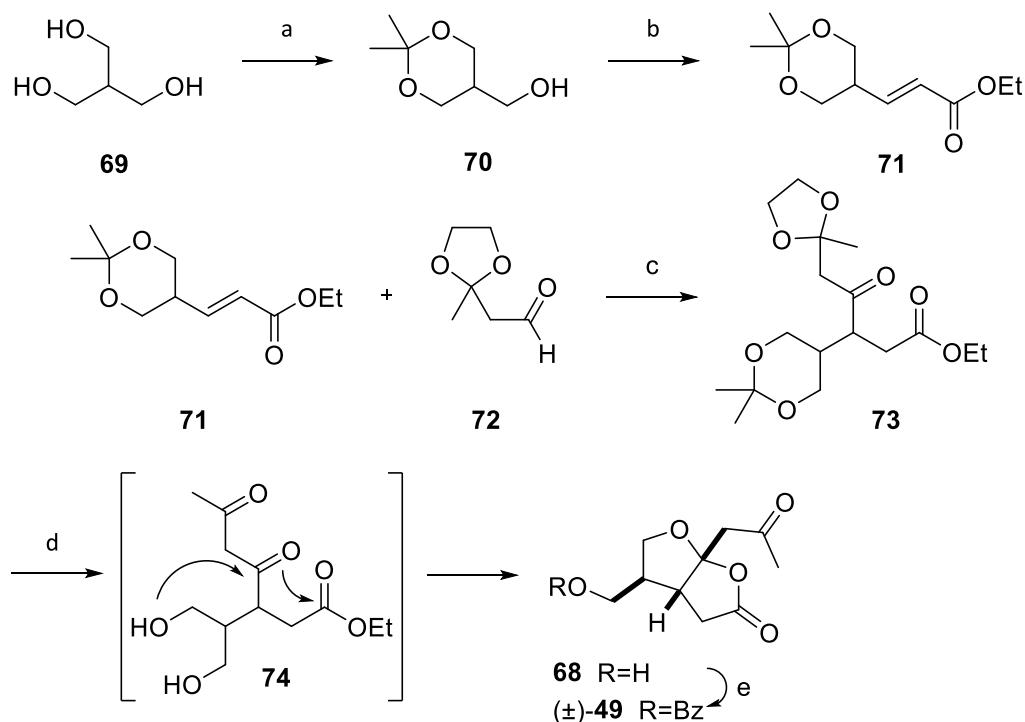
After benzyl protection of **55** to **56**, **56** was subjected to a Rubottom oxidation followed by a silyl protection to give compound **58**. In the next step, a Wittig olefination and subsequent hydroboration yielded diol **60**. This compound was deprotected by hydrogenolysis, then the 1,3-diol system was protected with DMP and finally, phenol **61** was reprotected with TBDMSCl to give **62**. Birch reduction and treatment of the resulting diene **63** with boric acid in the presence of TBAF, followed by dihydroxylation and oxidation with IBX led to diketone **66**. Deprotection and cleavage with periodic acid gave intermediate **67** which directly underwent intramolecular cyclization to obtain **68**. Finally, benzoylation of the alcohol moiety yielded the desired compound (±)-paeonilide (±)-**49** (Scheme 8).



**Reagents and Conditions:** a)  $K_2CO_3$ , KI, BnCl, MeCN, 95%; b) (i). LDA, THF, TMSCl; (ii). *m*-CPBA, DCM,  $NaHCO_3$ ; (iii). HCl, 65%; c) TBDMSCl, imidazole, DMF, quant.; d)  $Ph_3PCH_3I$ ,  $tBuOK$ , THF, 95%; e) (i).  $BH_3 \cdot THF$ , THF; (ii). 30%  $H_2O_2$ , 6 M NaOH, 90%; f) (i). Pd/C,  $H_2$ , EtOH; (ii). DMP, PPTS; 94.5% over 2 steps; g) TBDMSCl,  $Et_3N$ , DCM, quant; h) Li,  $NH_3$ , THF/EtOH (2:1), 90%; (i)  $H_3BO_3$ , TBAF, THF/ $H_2O$  (9:1), 86.7%; j)  $OsO_4$ , NMO, THF,  $tBuOH$ ,  $H_2O$ , 92%; k) IBX, EA, 94%; l)  $H_5IO_6$ , EA; m) BzCl, pyridine, DCM, 46% over four steps.

**Scheme 8.** Synthesis by Zhang *et al.* of racemic paeonilide ( $\pm$ )-**49**.<sup>57</sup>

The shortest synthesis of racemic paeonilide ( $\pm$ )-**49** was published by Du *et al.* in 2007. Starting from commercially available 2-(hydroxymethyl)propane-1,3-diol (**69**) they obtained ( $\pm$ )-**49** in five steps with an overall yield of 59% (Scheme 9).<sup>58</sup>



**Reagents and conditions:** a) DMP, TsOH, THF; b) (i). (COCl)<sub>2</sub>, DMSO, Et<sub>3</sub>N; (ii). Ph<sub>3</sub>P=CHCO<sub>2</sub>Et, DCM, 84% over 2 steps based on **83**; c) (BzO)<sub>2</sub>, benzene, 79%; d) HCl, EA, 91%; e) BzCl, pyridine, 98%.

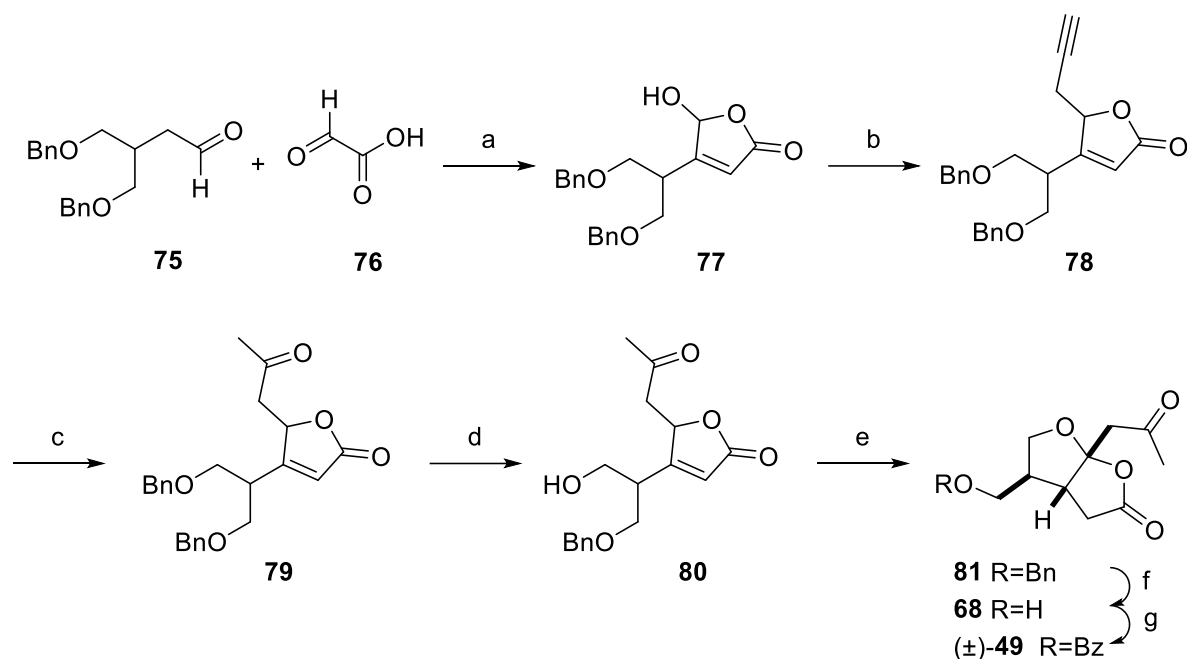
**Scheme 9.** Total synthesis of racemic paeonilide (±)-49 by Du *et al.* in 2007.<sup>58</sup>

Triol **69** was first protected with DMP, followed by a one-pot Swern oxidation and Wittig olefination to give *trans*-ester **71**. This was then subjected to a benzoyl peroxide-promoted intermolecular radical addition together with aldehyde **72** to afford keto ester **73**. Acid-catalyzed deacetylation, hemiacetal formation and lactonization led to alcohol **68** which was subsequently benzoylated to give racemic paeonilide (±)-49.

The latest synthesis of racemic paeonilide (±)-49 was published by Argade *et al.* in 2013. They utilized Umpolung chemistry for the intramolecular cyclization of 3,4-disubstituted butenolides to obtain (±)-49 in seven steps with an overall yield of 24%.<sup>59</sup>

Starting with a morpholine hydrochloride promoted aldol condensation of the protected aldehyde **75** and glyoxalic acid (**76**), they obtained butenolide **77** via a dehydrative cyclization pathway. Barbier reaction of **77** with propargyl bromide followed by oxymercuration, led to methyl ketone **79**. Deprotection of **79** in the presence of AlCl<sub>3</sub> led to monoprotected butenolide **80**. Treatment of this with *p*-TSA proceeded highly chemo- and diastereoselective to yield exclusively the desired furo[2,3-*b*]furanone **81**. Finally, hydrogenolysis of the benzyl

protection group and subsequent benzoylation of the primary alcohol gave ( $\pm$ )-**49** (Scheme 10).

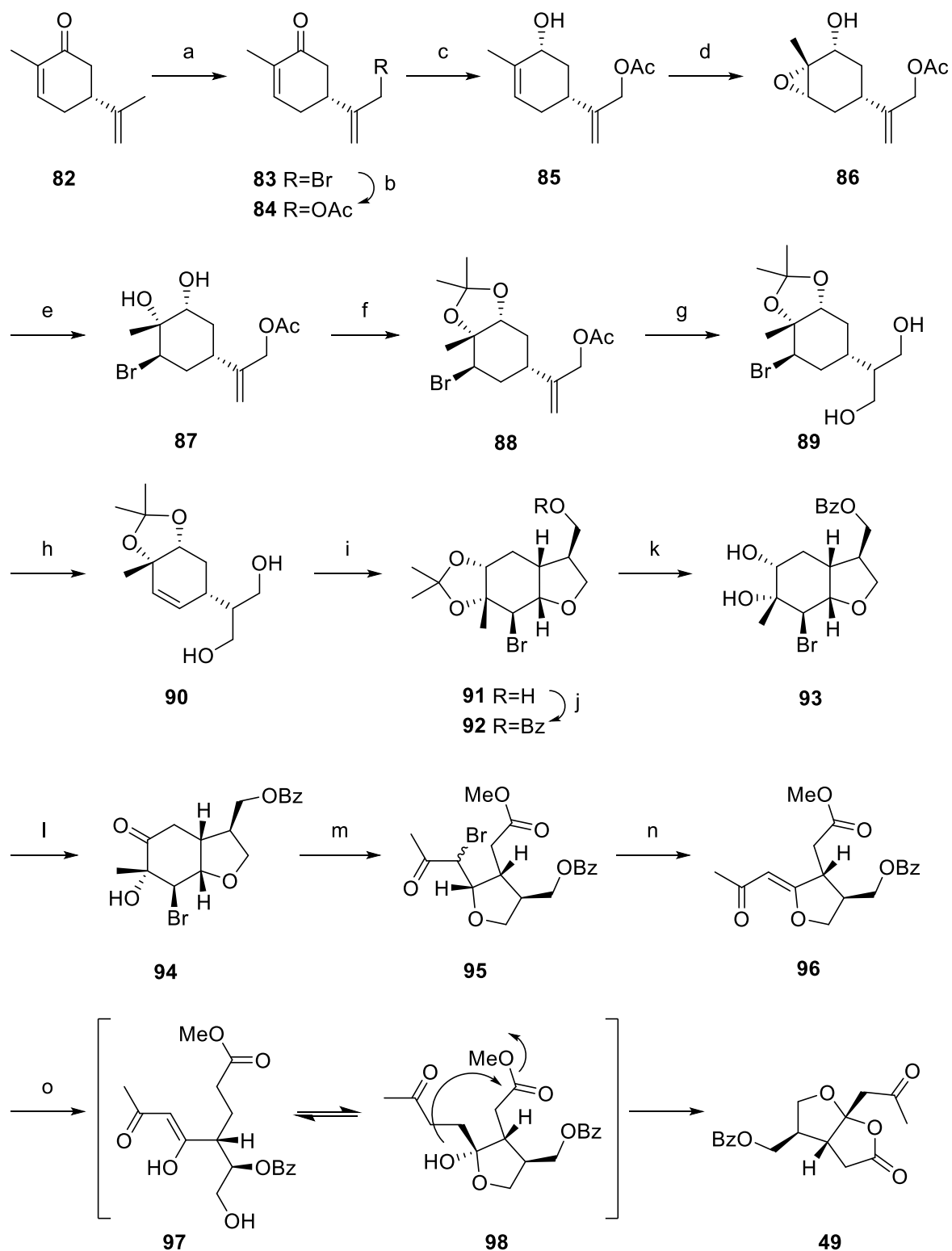


**Reagents and conditions:** a) morpholine, HCl, 1,4-dioxane, H<sub>2</sub>O, 64%; b) propargyl bromide, Zn, DMF, 82%; c) Hg(OAc)<sub>2</sub>, H<sub>2</sub>SO<sub>4</sub>, MeCN, 87%; d) AlCl<sub>3</sub>, DCM, 81%; e) *p*-TSA, toluene, 73%; f) Pd/C, H<sub>2</sub>, MeOH, 91%; g) BzCl, pyridine, DCM, 99%.

**Scheme 10.** Total synthesis of racemic paeonilide ( $\pm$ )-**49** by Argade *et al.* in 2013.<sup>59</sup>

In 2006, Zhang *et al.* also published the first stereospecific synthesis of (+)-paeonilide (**49**) and confirmed its absolute configuration. In the course of this synthesis, they obtained **49** starting from (*R*)-(-)-carvone (**82**) in 16 steps with an overall yield of 6.2% (Scheme 11).<sup>60</sup>

In the first step, (*R*)-(-)-carvone (**82**) was brominated using NBS and the resulting allyl bromide **83** was then subjected to an S<sub>N</sub>2 substitution to give acetate **84**. Luche reduction, followed by epoxidation with *m*-CPBA led to epoxide **86**. This was opened with lithium bromide and the corresponding diol was protected using DMP. Hydroboration of **88** gave the 1,3-diol **89** and subsequent dehydrobromination produced cyclohexene **90**. Treatment with NBS induced cyclization and the resulting furan derivative **91** was obtained as a single diastereomer.

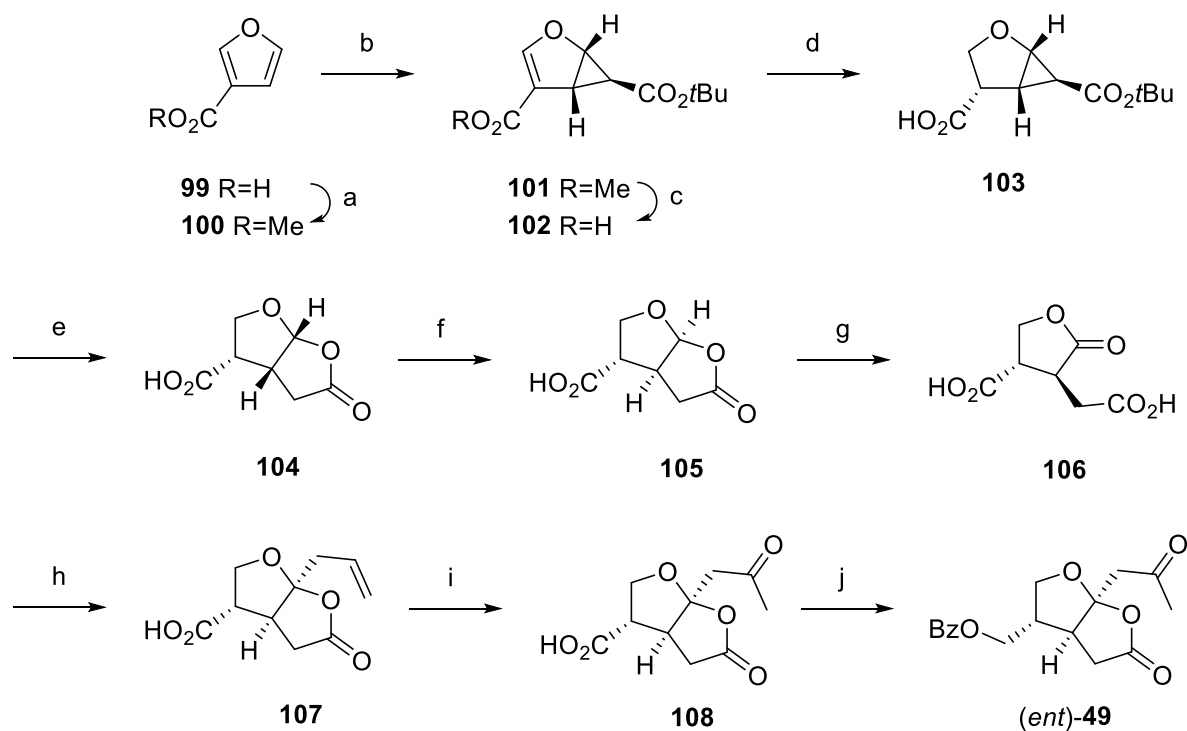


**Reagents and Conditions:** a) NBS, NaOAc, AcOH, DCM, 35%; b) AgOAc, acetone, 92%; c) NaBH<sub>4</sub>, CeCl<sub>3</sub>, MeOH, 95%; d) *m*-CPBA, DCM, NaHCO<sub>3</sub>, 93%; e) LiBr (*in situ*), THF, AcOH, 97%; f) DMP, DCM, TsOH, 95%; g) BH<sub>3</sub>·SMe<sub>2</sub>, THF, H<sub>2</sub>O<sub>2</sub>, NaOH, 89%; h) <sup>t</sup>BuOK, DMF, 95%; i) NBS, THF, 95%; j) BzCl, pyridine, DCM, 99%; k) HCl, MeOH, 92%; l) IBX, EA, 90%; m) H<sub>5</sub>IO<sub>6</sub>, EA, CH<sub>2</sub>N<sub>2</sub>, Et<sub>2</sub>O, 90%; n) DBU, benzene; o) HCl, EA, 40%.

**Scheme 11.** Total synthesis of (+)-paeonilide (**49**) by Zhang *et al.* in 2006.<sup>60</sup>

In the next step, the free alcohol moiety was benzoyl protected and the diol was first deprotected and then oxidized with IBX to give  $\alpha$ -hydroxy ketone **94**. This then underwent oxidative ring-opening upon treatment with periodic acid and the resulting carboxylic acid was directly converted to the corresponding methyl ester **95** with diazomethane. Elimination of HBr led to the unstable  $\alpha,\beta$ -unsaturated ketone **96** which was subsequently treated with HCl to cyclize and form the desired (+)-paeonilide (**49**).

In 2012, Reiser *et al.* published an enantioselective total synthesis of the unnatural enantiomer (-)-paeonilide (*ent*)-**49**, starting from commercially available 3-furoic acid (**99**) with an overall yield of 4.4% (7.7% brsm) in 12 steps (Scheme 12).<sup>61</sup>



**Reagents and Conditions:** a)  $\text{H}_2\text{SO}_4$ , MeOH, 82%; b)  $\text{Cu}(\text{OTf})_2$ , (*S,S*)-*i*-Pr-box,  $\text{PhNHNH}_2$ ,  $\text{N}_2\text{CHCO}_2^t\text{Bu}$ , DCM, 38% (53% brsm), 83% *ee.*; c) LiOH, THF,  $\text{H}_2\text{O}$ , 85% (100% brsm); d) Pd/C,  $\text{H}_2$ , EtOH, quant.; e) HCl, THF; f) pyridine,  $\text{H}_2\text{O}$ , 75% based on **55**; g) Jones reagent, acetone, 88%; h) allyl-MgBr, THF, 73%; i)  $\text{Hg}(\text{OAc})_2$ , Jones reagent, acetone, 79%; j) (i).  $\text{BH}_3\cdot\text{THF}$ , THF; (ii). BzCl,  $\text{Et}_3\text{N}$ , DCM; (iii). DMPI, DCM, 44%.

**Scheme 12.** Total synthesis of unnatural (-)-paeonilide (*ent*)-**46** by Reiser *et al.* in 2012.<sup>61</sup>

In the first step, 3-furoic acid (**99**) was esterified to **100** in order to enable a copper-catalyzed asymmetric cyclopropanation to give **101**. Saponification and subsequent hydrogenation yielded cyclopropane **103** with the carboxylic acid on the concave face of the bicyclic ring system. In order to obtain the desired furo[2,3-*b*]furanone core structure, an acid-catalyzed

cyclopropane ring-opening/lactonization cascade was applied to obtain **104** which was isomerized to the thermodynamically more stable lactone **105** bearing the carboxylic acid on the convex face upon treatment with pyridine. Oxidative ring-opening, followed by a Grignard reaction with allylmagnesium bromide, furnished the introduction of the side chain in the acetal position to obtain allyl **107**. This was subsequently subjected to an oxymercuration/oxidation yielding methyl ketone **108**. In the last step, both, the carboxylic acid and the ketone, were reduced to the corresponding alcohol with  $\text{BH}_3$ . Selective benzylation of the primary alcohol and reoxidation of the secondary alcohol finally gave the desired (-)-paeonilide (*ent*)-**49**.

The described synthesis of (-)-paeonilide (*ent*)-**49** by Reiser *et al.* is the foundation of this work. The studies presented in this thesis deal with the synthesis of (+)-paeonilide (**49**) and the improvement of the synthetic strategy concerning enantioselectivity as well as the applicability for further derivatization. Special focus was laid on the synthesis of a precursor that is not only suitable for the synthesis of enantiopure (+)-paeonilide (**49**) but also enables access to a variety of derivatives. Several derivatives could be synthesized in order to evaluate whether modification can improve the biological activity in the PAF-induced platelet aggregation compared to the natural product (+)-paeonilide (**49**). The results are presented in the following chapters.

#### 4. References

- <sup>1</sup> Chintoju, N.; Konduru, P.; Kathula, R. L.; Remella, R. *Res. Rev. J. Hosp. Clin. Pharm.* **2015**, *1* (1), 5–10.
- <sup>2</sup> Kumar, K.; Waldmann, H. *Angew. Chem. Int. Ed. Engl.* **2009**, *48* (18), 3224–3242.
- <sup>3</sup> Ji, H. F.; Li, X. J.; Zhang, H. Y. *EMBO Rep.* **2009**, *10* (3), 194–200.
- <sup>4</sup> Dickschat, J. S. *Beilstein J. Org. Chem.* **2011**, *7*, 1620–1621.
- <sup>5</sup> Ruiz, B.; Chávez, A.; Forero, A.; García-Huante, Y.; Romero, A.; Snchez, M.; Rocha, D.; Snchez, B.; Rodríguez-Sanoja, R.; Sánchez, S.; Langley, E. *Crit. Rev. Microbiol.* **2010**, *36* (2), 146–167.
- <sup>6</sup> Nicolaou, K. C. *Proc. R. Soc. A Math. Phys. Eng. Sci.* **2014**, *470* (2163).
- <sup>7</sup> Kong, D. X.; Jiang, Y. Y.; Zhang, H. Y. *Drug Discov. Today* **2010**, *15* (21–22), 884–886.
- <sup>8</sup> Akiyama, M.; Isoda, Y.; Nishimoto, M.; Narazaki, M.; Oka, H.; Kuboki, A.; Ohira, S. *Tetrahedron Lett.* **2006**, *47* (14), 2287–2290.
- <sup>9</sup> Tang, B.; Bray, C. D.; Pattenden, G. *Tetrahedron Lett.* **2006**, *47* (36), 6401–6404.
- <sup>10</sup> Granger, K.; Snapper, M. L. *European J. Org. Chem.* **2012**, No. 12, 2308–2311.
- <sup>11</sup> Ralph, M.; Ng, S.; Booker-Milburn, K. I. *Org. Lett.* **2016**, *18* (5), 968–971.
- <sup>12</sup> Mayer, A.; Köpke, B.; Anke, H.; Sterner, O. *Phytochemistry* **1996**, *43*, 375–376.
- <sup>13</sup> Gharpure, S. J.; Nanda, N.; Kumar, M. *Eur. J. Org. Chem.* **2011**, 6632–6635.
- <sup>14</sup> Lone, A. M., *Studies directed towards the synthesis of bioactive compounds*. PhD Thesis, University of Kashmir, Srinagar, 2016.
- <sup>15</sup> Fietz, O.; Dettner, K.; Görls, H.; Klemm, K.; Boland, W. *J. Chem. Ecol.* **2002**, *28* (7), 1315–1327.
- <sup>16</sup> Matsunaga, K.; Shibuya, M.; Ohizumi, Y. *J. Nat. Prod.* **1994**, *57* (12), 1734–1736.
- <sup>17</sup> Search of <http://dnp.chemnetbase.com> on 2/7/2018.
- <sup>18</sup> Slutskyy, Y.; Jamison, C. R.; Zhao, P.; Lee, J.; Rhee, Y. H.; Overman, L. E. *J. Am. Chem. Soc.* **2017**, *139* (21), 7192–7195.
- <sup>19</sup> Hochlowski, J. E.; Faulkner, D. J.; Matsumoto, G. K.; Clardy, J. *J. Org. Chem.* **1983**, *48*, 1141–1142.
- <sup>20</sup> Guizzunti, G.; Brady, T. P.; Malhotra, V.; Theodorakis, E. A. *J. Am. Chem. Soc.* **2006**, *128* (13), 4190–4191.
- <sup>21</sup> Garnsey, M. R.; Slutskyy, Y.; Jamison, C. R.; Zhao, P.; Lee, J.; Rhee, Y. H.; Overman, L. E. *J. Org. Chem.* **2017**, *83* (13), 6958–6976.
- <sup>22</sup> Rungprom, W.; Chavasiri, W.; Kokpol, U.; Kotze, A.; Garson, M. J. *Mar. Drugs* **2004**, *2*, 101–107.



- <sup>23</sup> Von Salm, J. L.; Witowski, C. G.; Fleeman, R. M.; McClintock, J. B.; Amsler, C. D.; Shaw, L. N.; Baker, B. J. *Org. Lett.* **2016**, *18* (11), 2596–2599.
- <sup>24</sup> Akers, K. S.; Mende, K.; Cheatle, K. A.; Zera, W. C.; Yu, X.; Beckius, M. L.; Aggarwal, D.; Li, P.; Sanchez, C. J.; Wenke, J. C.; Weintrob, A. C.; Tribble, D. R.; Murray, C. K. *BMC Infect Dis* **2014**, *14*, 190.
- <sup>25</sup> Nakata, T.; Nagao, S.; Oishi, T. *Tetrahedron Lett.* **1985**, *26*, 6465–6468.
- <sup>26</sup> Kim, C.; Hoang, R.; Theodorakis, E. A. *Org. Lett.* **1999**, *1* (8), 1295–1297.
- <sup>27</sup> Corey, E. J.; Letavic, M. A. *J. Am. Chem. Soc.* **1995**, *117* (48), 12017.
- <sup>28</sup> Brady, T.P.; Kim, S. H.; Wen, K.; Theodorakis, E. A. *Angew. Chem.* **2004**, *116*, 757–760; *Angew. Chem. Int. Ed.* **2004**, *43*, 739–742.
- <sup>29</sup> Weisser, R.; Yue, W.; Reiser, O. *Org. Lett.* **2005**, *7* (24), 5353–5356.
- <sup>30</sup> Schnermann, M. J.; Beaudry, C. M.; Genung, N. E.; Canham, S. M.; Untiedt, N. L.; Karanikolas, B. D. W.; Sütterlin, C.; Overman, L. E. *J. Am. Chem. Soc.* **2011**, *133* (43), 17494–17503.
- <sup>31</sup> Yuan, H.; Ma, Q.; Ye, L.; Piao, G. *Molecules* **2016**, *21* (5).
- <sup>32</sup> Fabricant, D. S.; Farnsworth, N. R. *Environ. Health Perspect.* **2001**, *109* (SUPPL. 1), 69–75.
- <sup>33</sup> Kisangau, D. P.; Herrmann, T. M. *Int. J. Biodivers. Sci. Ecosyst. Serv. Manag.* **2007**, *3*, 184–192.
- <sup>34</sup> Lin, M.-Y.; Lee, Y.-R.; Chiang, S.-Y.; Li, Y.-Z.; Chen, Y.-S.; Hsu, C.-D.; Liu, Y.-W. *Evid. Based. Complement. Alternat. Med.* **2013**, 2013.
- <sup>35</sup> Wu, M.; Gu, Z. *Evidence-based Complement. Altern. Med.* **2009**, *6* (1), 57–63.
- <sup>36</sup> Zhao, D. D.; Jiang, L. L.; Li, H. Y.; Yan, P. F.; Zhang, Y. L. *Molecules* **2016**, *21* (10), 1362–1375.
- <sup>37</sup> Kimura, M.; Kimura, I.; Nojima, H.; Takahashi, K.; Hayashi, T.; Shimizu, M.; Morita, N. *Jpn J Pharmacol* **1984**, *35* (1), 61–66.
- <sup>38</sup> Duan, W. J.; Yang, J. Y.; Chen, L. X.; Zhang, L. J.; Jiang, Z. H.; Cai, X. D.; Zhang, X.; Qiu, F. *J. Nat. Prod.* **2009**, *72* (9), 1579–1584.
- <sup>39</sup> Huang, Y.; Ohno, O.; Suenaga, K.; Miyamoto, K. *Biosci. Biotechnol. Biochem.* **2017**, *81* (6), 1106–1113.
- <sup>40</sup> Chen, T.; Fu, L.-X.; Zhang, L.-W.; Yin, B.; Zhou, P.-M.; Cao, N.; Lu, Y.-H. *Can. J. Physiol. Pharmacol.* **2016**, *94* (8), 888–894.
- <sup>41</sup> Yang, H. O.; Ko, W. K.; Kim, J. Y.; Ro, H. S. *Fitoterapia* **2004**, *75* (1), 45–49.
- <sup>42</sup> Kong, L. D.; Cheng, C. H. K.; Tan, R. X. *J. Ethnopharmacol.* **2004**, *91* (2–3), 351–355.
- <sup>43</sup> Chou, T. C. *Br. J. Pharmacol.* **2003**, *139* (6), 1146–1152.
- <sup>44</sup> Liu, J.-K. Y.; Ma, B.; Wu, D.-G.; Lu, Y.; Shen, Z.-Q.; Zheng, Q.-T.; Chen, Z.-H. *Biosci. Biotechnol. Biochem.* **2000**, *64* (7), 1511–1514.

- <sup>45</sup> [https://www.crocus.co.uk/plants/\\_/paeonia-delavayi/classid.2000003359/](https://www.crocus.co.uk/plants/_/paeonia-delavayi/classid.2000003359/) (accessed on 12.07.2018)
- <sup>46</sup> Strømgaard, K.; Nakanishi, K. *Angew. Chemie Int. Ed.* **2004**, *43* (13), 1640–1658.
- <sup>47</sup> Gnaedinger, S. *Geobios* **2012**, *45* (2), 187–198.
- <sup>48</sup> van Beek, T. A. *Bioorg. Med. Chem.* **2005**, *13* (17), 5001–5012.
- <sup>49</sup> Gafner, S. *Bot. Adulterants Bull.* **2018**, No. January, 1–8.
- <sup>50</sup> Hindmarch, I. *Presse Med* **1986**, *15* (31), 1592–1594.
- <sup>51</sup> Kanowski, S.; Herrmann, W. M.; Stephan, K.; Wierich, W.; Hörr, R. *Pharmacopsychiatry* **1996**, *29* (2), 47–56.
- <sup>52</sup> Vesper, J.; Hänsgen, K. D. *Phytomedicine* **1994**, *1* (1), 9–16.
- <sup>53</sup> Rojas, P.; Serrano-García, N.; Medina-Campos, O. N.; Pedraza-Chaverri, J.; Ögren, S. O.; Rojas, C. *Neurochem. Int.* **2011**, *59* (5), 628–636.
- <sup>54</sup> Bauer, U. *Arzneimittelforschung* **1995**, *34* (6), 716–720.
- <sup>55</sup> Braquet, P. G.; Spinnewyn, B.; Braquet, M.; Bourgain, R. H.; Taylor, J. E.; Etienne, A.; Drieu, K. *Blood Vessel* **1985**, *16*, 558–572.
- <sup>56</sup> Koch, E. *Phytomedicine* **2005**, *12* (1–2), 10–16.
- <sup>57</sup> Wang, C.; Liu, J.; Ji, Y.; Zhao, J.; Li, L.; Zhang, H. *Org. Lett.* **2006**, *8* (12), 2479–2481.
- <sup>58</sup> Du, Y.; Liu, J.; Linhardt, R. J. *J. Org. Chem.* **2007**, *72* (10), 3952–3954.
- <sup>59</sup> Deore, P. S.; Argade, N. P. *Org. Lett.* **2013**, *15* (22), 5826–5829.
- <sup>60</sup> Wang, C.; Zhang, H.; Liu, J.; Ji, Y.; Shao, Z.; Li, L. *Synlett* **2006**, No. 7, 1051–1054.
- <sup>61</sup> Harrar, K.; Reiser, O. *Chem. Comm.* **2012**, *48* (28), 3457–3459.

## B. Main Part

### 1. Synthesis of (+)-paeonilide

#### 1.1 Cyclopropanation

##### 1.1.1 Introduction

Despite its high ring strain of approximately 27 kcal·mol<sup>-1</sup>, the cyclopropane moiety is omnipresent in nature.<sup>1,2</sup> A large number of naturally occurring products, *e.g.* terpenoids, alkaloids, unusual amino acids and fatty acid metabolites, contain this three-membered carbon ring system.<sup>2,3</sup> These natural products along with their synthetic derivatives are of great scientific interest because of their broad range of biological activities.<sup>4</sup> For this reason, chemists have always been fascinated by the cyclopropane ring system.<sup>5</sup> Moreover, cyclopropanes play a crucial role as essential building block for the construction of a variety of complex structures and natural products.<sup>6</sup> Therefore, different methods to synthesize cyclopropanes have been developed over the years, *e.g.* the Simmons-Smith reaction, cycloisomerizations and the formation *via* free carbenes by  $\alpha$ -elimination. Another very powerful method for the construction of cyclopropanes is the transition-metal-catalyzed decomposition of diazo compounds.

Diazo compounds are very versatile building blocks and therefore many useful applications in organic synthesis have been found.<sup>7</sup> Transition-metal-catalyzed dediazonation of diazo compounds gives rise to highly reactive metal carbenoids which are applied, *inter alia*, in the cyclopropanation of alkenes.<sup>8</sup> Depending on their adjacent functional groups, these metal carbenoids can be divided into three groups: acceptor **109**, acceptor-acceptor **110** and donor-acceptor **111** substituted carbenoids (Figure 6).<sup>9</sup>

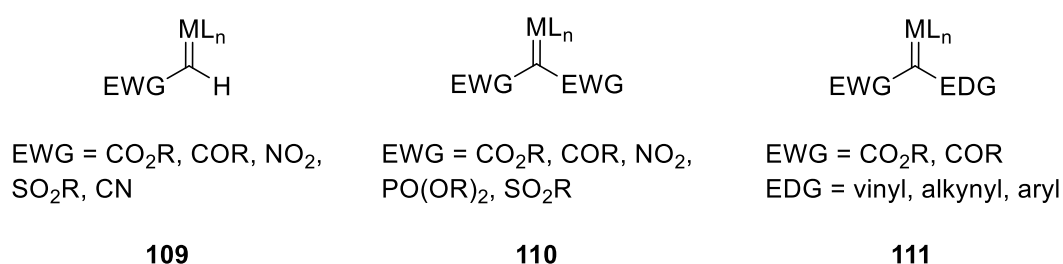
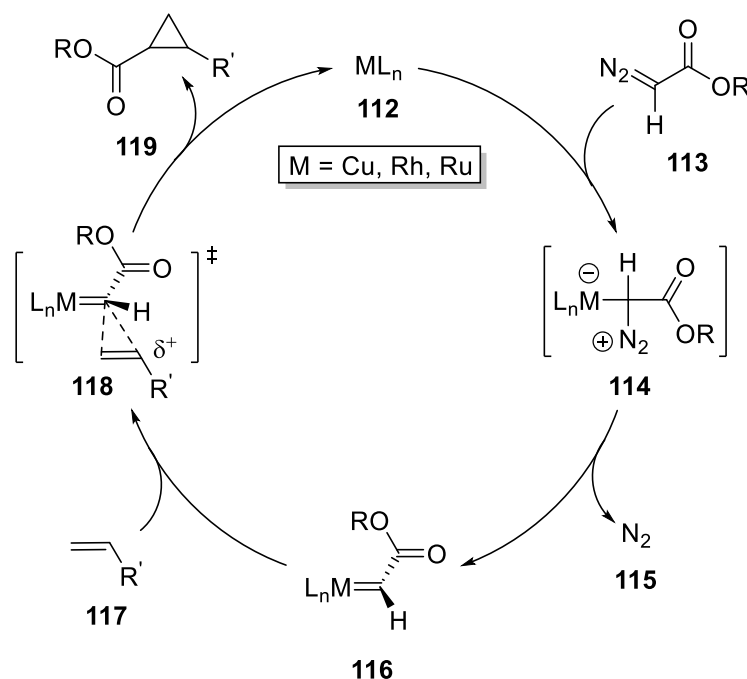


**Figure 6.** Classification of metal carbenoids (EWG = electron-withdrawing group; EDG = electron-donating group).<sup>9</sup>

On the one hand, the substitution pattern of the utilized diazo compound and on the other hand the metal-ligand system are decisive for the reactivity profile of the carbenoid, as electronic and steric factors around the metal-carbenoid center play a pivotal role.<sup>9,10</sup>

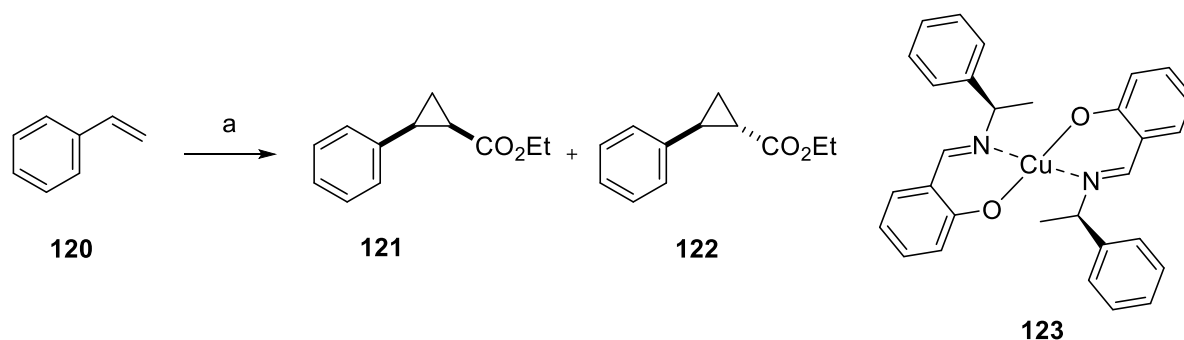
Typical metals for cyclopropanation reactions are, amongst others, Cu, Rh, Ru, Pd and Co.<sup>10</sup> The general proposed catalytic cycle for these transition-metal-catalyzed cyclopropanations of alkenes is shown below (Scheme 13).<sup>5,11</sup>



**Scheme 13.** Proposed mechanism for the transition-metal-catalyzed cyclopropanation of alkenes.<sup>5,11</sup>

In the first step, the metal-catalyst **112** is attacked by the negatively polarized carbon of the diazo compound **113** to form the zwitterionic metal alkyl complex **114**. Release of nitrogen (**115**) generates the metal-carbenoid **116** which subsequently adds to the alkene **117** in a concerted but asynchronous manner.<sup>12</sup>

Due to its abundance and relatively low cost compared to other metals, the use of copper as catalyst for cyclopropanation reactions is very attractive.<sup>13</sup> Especially copper(I) triflate, generated *in situ* by reduction of copper(II) triflate, is a highly efficient catalyst for cyclopropanations.<sup>14</sup> Moreover, the use of chiral ligands enables access to asymmetric reactions. The first enantioselective copper-catalyzed cyclopropanation was published by Nozaki *et al.* in 1966 (Scheme 14).<sup>15</sup>



**Reagents and conditions:** a)  $\text{N}_2\text{CHCO}_2\text{Et}$  (0.33 equiv.),  $\text{Cu}(\text{OTf})_2$  (1.0 mol%), (*R*)-2-((1-phenylethylimino)methyl)phenol (2.2 mol%),  $\text{PhNHNH}_2$  (1.0 mol%), 58-60 °C, 72%.

**Scheme 14.** First asymmetric copper-catalyzed cyclopropanation by Nozaki et al. in 1966.<sup>15</sup>

Styrene (**120**) was successfully cyclopropanated with ethyl diazoacetate in the presence of a catalytical amount of the chiral copper salicylidimine complex **123** to yield an optically active mixture of the *cis* and *trans* isomers **121** and **122**.

Even today, there is still a continuing interest in the development of new chiral ligands in order to generate highly efficient and stereoselective metal-catalysts. Especially popular and effective chiral ligands for the copper(I)-catalyzed asymmetric cyclopropanation are semicorrines **124**,<sup>16</sup> bis(oxazolines) **125** (box)<sup>17,18</sup> and aza-bis(oxazolines) **126** (aza-box)<sup>19</sup> (Figure 7).

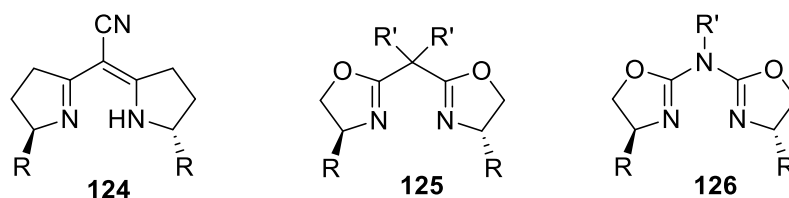


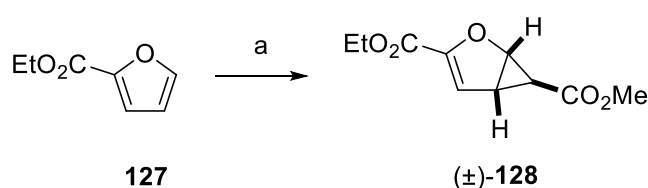
**Figure 7.** General chemical structures for semicorrines **124**, box **125** and azabox **126** ligands.

These chiral ligands are able to induce extremely high levels of enantioselectivity (up to >99% *ee*)<sup>13</sup> in cyclopropanations of a broad substrate scope, *e.g.* with substituted furan derivatives.<sup>20</sup>

### 1.1.2 Cyclopropanation of furan derivatives

Until today, several cyclopropanation reactions of furan and its derivatives are reported. As electron-rich furans tend to ring-opening, furans bearing an electron-withdrawing substituent are rather stable and allow access to the desired cyclopropanes.<sup>21</sup> Therefore, mainly furan esters are used as starting material for cyclopropanations.

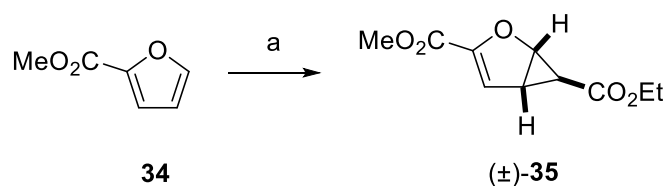
The first example of a cyclopropanated furan ester dates back to 1988 when Saltykova *et al.* used methyl diazoacetate and  $\text{Rh}_2(\text{OAc})_4$  for the cyclopropanation of 2-furoic acid ethyl ester (**127**) to synthesize racemic cyclopropane ( $\pm$ )-**128** (Scheme 15).<sup>22</sup>



**Reagents and conditions:** a)  $\text{N}_2\text{CHCO}_2\text{Me}$  (1.0 equiv.), **127** (2.9 equiv.),  $\text{Rh}_2(\text{OAc})_4$  (2.3 mol%), 20 °C, 6 h, 22%.

**Scheme 15.** Cyclopropanation of 2-furoic acid ethyl ester (**127**) by Saltykova *et al.* in 1988.<sup>22</sup>

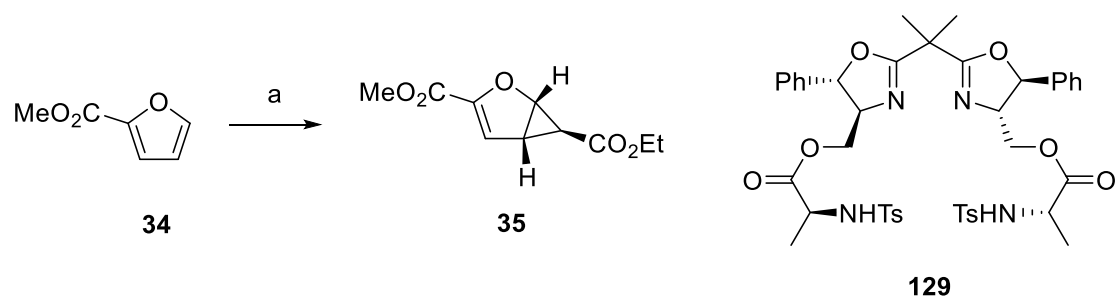
In 1990, Wenkert *et al.* reported the racemic cyclopropanation of 2-furoic acid methyl ester (**34**) to cyclopropane ( $\pm$ )-**35** under quite similar conditions, however, providing much higher yield (Scheme 16).<sup>23</sup>



**Reagents and conditions:** a)  $\text{N}_2\text{CHCO}_2\text{Et}$  (1.0 equiv.),  $\text{Rh}_2(\text{OAc})_4$  (0.3 mol%), rt, 15 h, 55%.

**Scheme 16.** Cyclopropanation of 2-furoic acid methyl ester (**34**) by Wenkert *et al.* in 1990.<sup>23</sup>

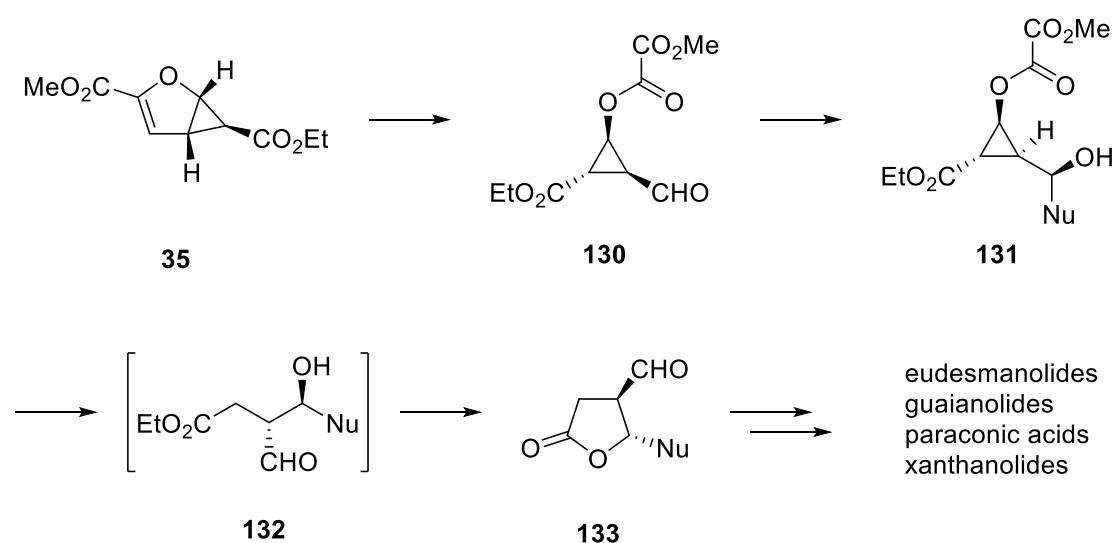
Ten years later, Reiser *et al.* published an enantioselective version of this cyclopropanation giving rise to enantiomerically pure **35** utilizing chiral box ligand **129** (Scheme 17).<sup>24</sup>



**Reagents and conditions:** a) **34** (3.4 equiv.),  $\text{N}_2\text{CHCO}_2\text{Et}$  (1.0 equiv.),  $\text{Cu}(\text{OTf})_2$  (0.7 mol%), **129** (0.7 mol%),  $\text{PhNHNH}_2$ , DCM, rt, 12 h, 36%, 91% *ee*, >99% *ee* after recrystallization from *n*-pentane.

**Scheme 17.** Asymmetric cyclopropanation of **34** by Reiser *et al.* in 2000.<sup>24</sup>

Since access to enantiomerically pure cyclopropanation product **35** is feasible, it has been extensively used as a starting point for different transformations toward the synthesis of a variety of complex structures and natural products. In 2001, Reiser *et al.* reported a powerful strategy for the construction of *anti*-4,5-disubstituted  $\gamma$ -butyrolactones **133** starting from cyclopropanated furan ester **35**.<sup>25</sup> Ozonolytic cleavage of the double bond in **35** followed by reductive work-up led to aldehyde **130**. In the next step, a diastereoselective nucleophilic attack gives rise to either the Felkin-Ahn<sup>25</sup> or the Cram-chelate product<sup>26</sup> depending on the used nucleophile. Base-induced cleavage of the oxalyl ester in **131** initiates a retro-aldol/lactonization cascade (*via* **132**) to obtain *anti*-4,5-disubstituted  $\gamma$ -butyrolactone **133** (Scheme 18).



**Scheme 18.** Synthetic sequence for the stereoselective preparation of *anti*-4,5-disubstituted  $\gamma$ -butyrolactones **133** as precursors for the synthesis of different natural product classes.<sup>25</sup>

Moreover, this methodology enables access to the core structures of a number of natural product families, including eudesmanolides, guaianolides, paraconic acids and xanthanolides.<sup>27,28</sup>

In addition to 2-furoic acid methyl ester (**34**), the enantioselective cyclopropanation of 3-furoic acid methyl ester (**100**) has also been investigated in previous work (Table 3).<sup>28,29,30,31</sup>

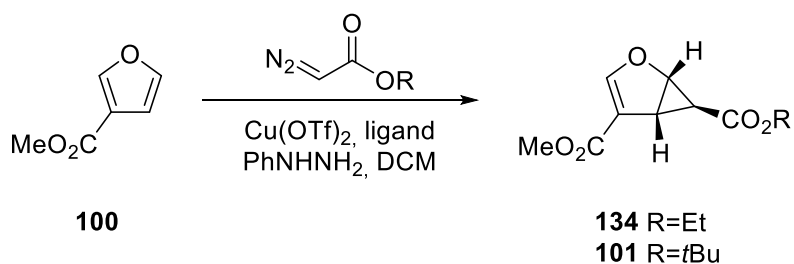
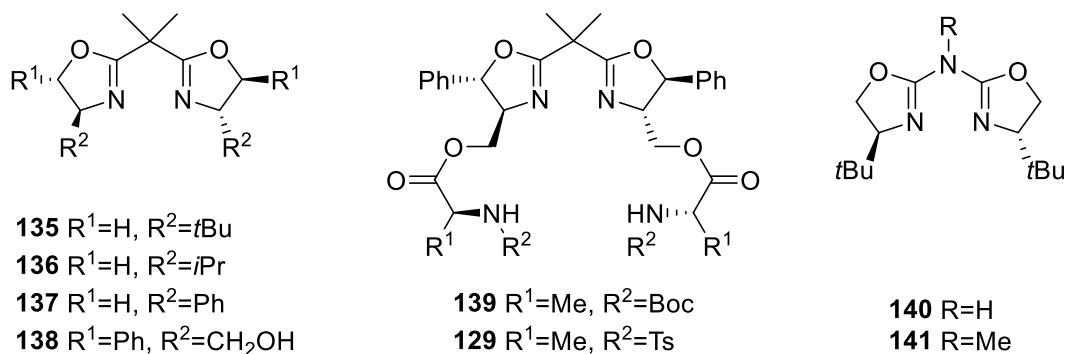


**Table 3.** Enantioselective cyclopropanation of 3-furoic acid methyl ester (**100**).<sup>28,29,30,31</sup>

entry	R	ligand	temperature	ratio Cu/ligand	yield [%]	ee <sup>[a]</sup> [%]
1	Et	<b>136</b>	0	0.8	31	83
2	Et	<b>135</b>	0	0.8	22	74
3	Et	<b>138</b>	0	0.8	27	74
4	Et	<b>139</b>	0	0.8	31	68
5	Et	<b>129</b>	0	0.8	19	40
6	tBu	<b>136</b>	0	0.8	38	83
7	tBu	<b>138</b>	0	0.8	38	65
8	tBu	<b>137</b>	0	0.8	34	19
9	tBu	<b>140</b>	0	0.5	55	92
10	tBu	<b>141</b>	0	0.5	38	94
11	tBu	<b>140</b>	-10	0.5	31	93
12	tBu	<b>141</b>	-10	0.5	21	92

[a] determined by chiral HPLC.





Comparing the reactions with ethyl diazoacetate, the best results (31%, 83% *ee*, entry 1) were obtained using *i*Pr-box ligand **136** (entries 1-5). The exchange of ethyl diazoacetate by *tert*-butyl diazoacetate showed only a small increase in yield but no effect on selectivity (entries 6 and 7), while the use of phenyl-box ligand **137** resulted in a significant drop of enantioselectivity. Later on, the reaction was screened on the dependency on temperature and Cu/ligand ratio with two azabox ligands **140** and **141** (entries 9-12). Although ligand **140** showed significantly better yields compared to ligand **141**, the difference in terms of selectivity is negligible. Moreover, it was shown that decreasing the temperature has an adverse effect on the yield. All in all, the best results were obtained with a Cu/ligand ratio of 0.5 and the use of ligand **140** at 0 °C (55%, 92% *ee*, entry 9).

However, all reactions and optimization screenings so far only yielded the (*S,R,S*)-enantiomer **101**. In this work, focus was laid on the enantioselective synthesis of the (*R,S,R*)-enantiomer **142** as starting point for the synthesis of (+)-paeonilide (**49**). Due to the fact that the required enantiomer of ligand **140** was not accessible, the copper(I)-catalyzed cyclopropanation of 3-furoic acid methyl ester (**100**) with *tert*-butyl diazoacetate was screened with different ligands (Table 4).

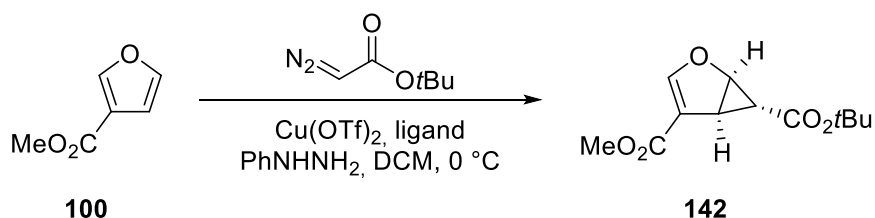
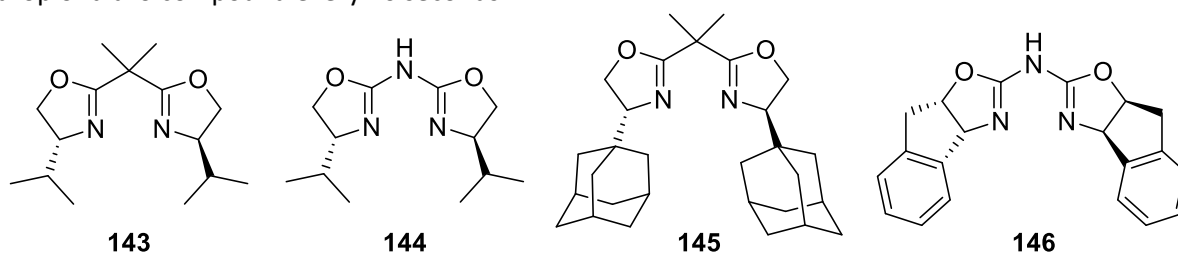


**Table 4.** Ligand screening for the synthesis of **142**.

entry <sup>[a]</sup>	ligand	yield [%]	<i>ee</i> <sup>[b]</sup> [%]
1	<b>143</b>	50 <sup>[c]</sup>	83
2	<b>144</b>	45 <sup>[c]</sup>	82
3	<b>145</b>	11 <sup>[c]</sup> , 29 <sup>[d]</sup>	93
4	<b>146</b>	20 <sup>[d]</sup>	95

[a] **100** (1.0 equiv.), N<sub>2</sub>CHCO<sub>2</sub>tBu (1.5 equiv.), Cu(OTf)<sub>2</sub> (1.0 mol%), ligand (2.2 mol%), PhNHNH<sub>2</sub> (1.0 mol%); [b] determined by chiral HPLC; [c] one drop of diazo compound every 10 seconds; [d] one drop of diazo compound every 20 seconds.



Comparing the two *iPr*-ligands **143** and **144** no change in selectivity and only a slight decrease in terms of yield could be observed (entries 1 and 2). Using box ligand **145** with bulky adamantyl-groups proved that the size of the substituent plays a crucial role regarding selectivity and yield (entry 3). As the selectivity increases, the yield significantly drops down. Reducing the addition speed of the diazo compound led to enhanced, but still unfruitful yields. The same observations could be recognized applying indanyl-azabox ligand **146** (entry 4). While an excellent *ee* value of 95% was obtained, the yield further decreased even at low addition speed.

In summary, the best results (50%, 83% *ee*) were obtained using *iPr*-box ligand **143**. Furthermore, it was possible to obtain enantiomerically pure **142** by recrystallization from *n*-pentane. However, several recrystallizations were necessary resulting in a significant loss of product. The solution to this problem is described in the following (see chapter 1.2.2). Therefore, further experiments were carried out with enantioenriched cyclopropane **142**. The analytical chiral HPLC chromatograms of racemic and enantiopure **142** are shown below (Figure 8).

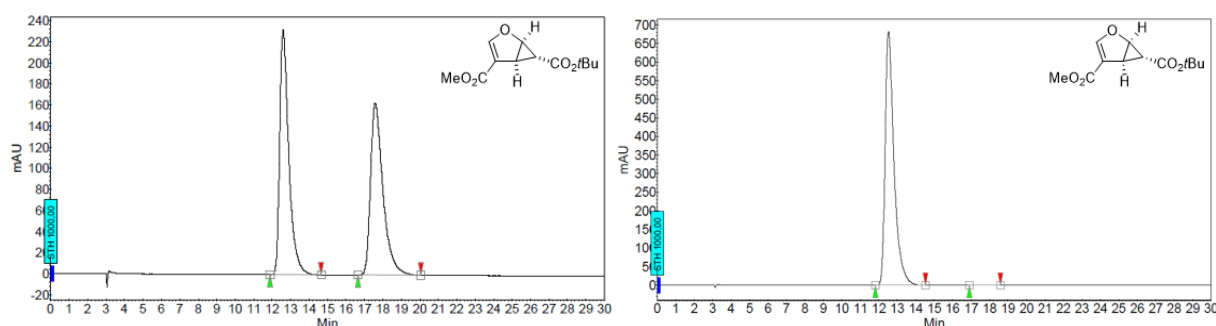


**Figure 8.** Left: analytical chiral HPLC chromatogram of racemic **142**. Right: analytical chiral HPLC chromatogram of enantiopure **142**. Conditions: Phenomenex Lux Cellulose-2, *n*-heptane/*iPr*OH 99:1, 1.0 mL/min, 254 nm): *tr* (major) = 12.59, *tr* (minor) = 17.59.

Moreover, the absolute stereochemistry of the cyclopropanated 3-furoic acid methyl ester **142** could be unambiguously confirmed by X-ray crystallography (Figure 9).

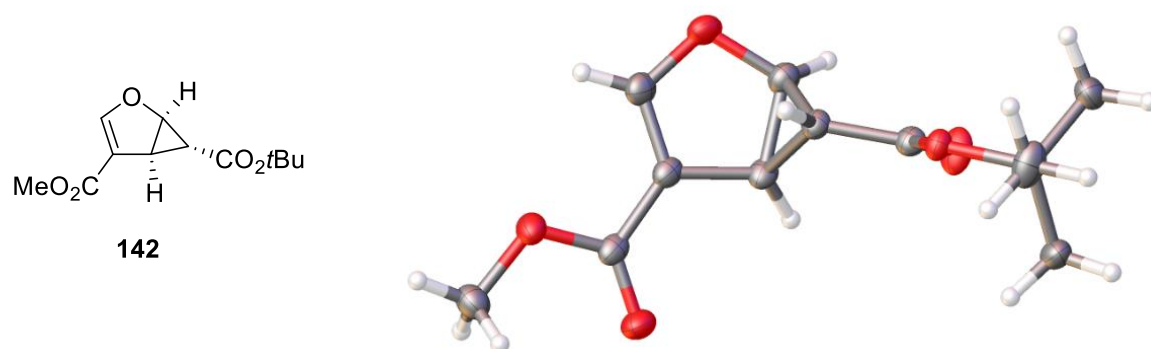


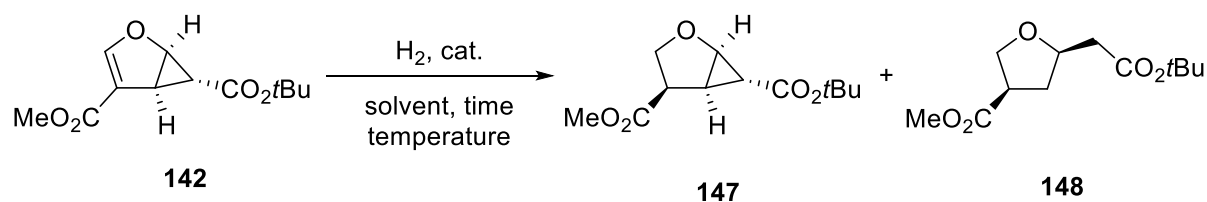
**Figure 9.** X-ray structure of **142**.

## 1.2 Toward the furo[2,3-*b*]furanone formation

### 1.2.1 Hydrogenation

Earlier studies proved that direct lactonization of the unsaturated cyclopropane **142** is not feasible.<sup>32</sup> However, a straightforward lactonization was reported with a saturated bicycle.<sup>33</sup> Therefore, a reduction of the C-C double bond of **142** was necessary. Moreover, earlier studies revealed that previous saponification of the methyl ester enabled access to the desired hydrogenation product but this synthetic route lacked in terms of diastereoselectivity and separability in the following steps.<sup>34</sup> To circumvent this problem a screening for the direct hydrogenation of enantioenriched cyclopropane **142** was conducted (Table 5).

The hydrogenation was initially performed with palladium on charcoal (Pd/C) in aqueous ethanol, as described in the synthesis of (-)-paeonilide (-)-**49**.<sup>30</sup> However, after 5 hours at an atmospheric hydrogen pressure no reaction could be observed with methyl ester **142** (entry 1). Changing the catalytic system to rhodium on charcoal (Rh/C) also resulted in no reaction (entry 2). For this reason, the applied hydrogen pressure was raised to 30 bar resulting in full conversion of the starting material, however, providing not only the desired product **147** but also the hardly separable cyclopropane ring-opening product **148** (entry 3). As these conditions at least yielded the desired product **147**, different solvents were tested in order to suppress byproduct formation (entries 4-10). The use of MeOH or toluene showed no beneficial effect on the outcome of the reaction and gave more or less the same result as aqueous ethanol (entries 4 and 5). While utilizing DMF or MeCN as solvent, even an increased formation of unwanted byproduct **148** compared to the desired product **147** was observed (entries 6 and 7).

**Table 5.** Hydrogenation of the C-C double bond.

entry <sup>[a]</sup>	cat. <sup>[b]</sup>	cat. load [mol%]	solvent <sup>[c]</sup>	p(H <sub>2</sub> ) [bar]	time [h]	yield [%] <sup>[d]</sup>	ratio <sup>[e]</sup>
1	Pd/C	3	EtOH/H <sub>2</sub> O	atm.	5	n. r.	n. d.
2	Rh/C	1	EtOH/H <sub>2</sub> O	atm.	5	n. r.	n. d.
3	Pd/C	3	EtOH/H <sub>2</sub> O	30	5	98	1.9:1
4	Pd/C	3	MeOH	30	5	90	1.7:1
5	Pd/C	3	toluene	30	5	93	2.1:1
6	Pd/C	3	DMF	30	5	67	1:2.3
7	Pd/C	3%	MeCN	30	5	71	1:1.8
8	Pd/C	3%	DCM	30	5	86	4.4:1
9	Pd/C	3%	acetone	30	5	92	6.8:1
10	Pd/C	3%	EA	30	5	97	8.3:1
11	Pd(OH) <sub>2</sub> /C	5%	EA	30	5	88	5.5:1
12	Rh/C	1%	EtOH/H <sub>2</sub> O	30	1	87	4.4:1
13	Rh/C	1%	EtOH/H <sub>2</sub> O	15	1	87	5.0:1
14	Rh/C	1%	EA	15	1	94	-
15 <sup>[f]</sup>	Rh/C	0.6%	EA	15	0.5	98	-

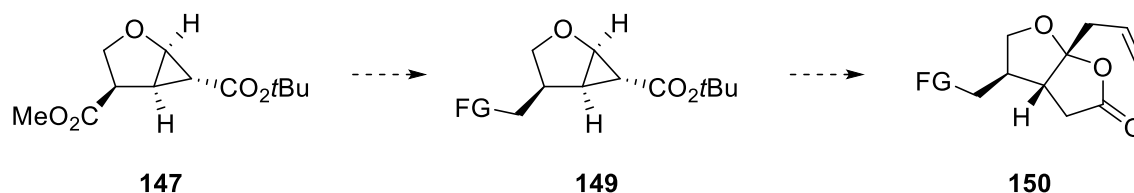
[a] 2.0 mmol **142** [b] catalysts: 10% Pd/C, 5% Rh/C, 20% Pd(OH)<sub>2</sub>/C; [c] EtOH/H<sub>2</sub>O (95:5, v/v) [d] yield of crude mixture, n. r. = no reaction; [e] determined by <sup>1</sup>H-NMR of the crude mixture, n. d. = not determined; [f] 12.6 mmol **142**.

Changing the solvent to DCM, acetone or EA resulted in an increased tendency toward the hydrogenation product **147** (entries 8-10). Additionally, two other catalysts were tested within this screening (entries 11-15). Applying the best conditions investigated so far together with palladium hydroxide on charcoal (Pd(OH)<sub>2</sub>/C) led to a decrease in yield and product ratio (entry 11). In contrast, rhodium on charcoal in aqueous ethanol showed an improved result compared to the reaction with Pd/C (entry 3 vs. 12). Reduction of the hydrogen pressure to 15 bar even increased the selectivity (entry 13). The best results were obtained using Rh/C as catalyst and EA as solvent. With these conditions, the desired product **147** was formed exclusively in excellent yield (entries 14 and 15). Gratifyingly, the reaction could be even run on large scale while decreasing the amount of catalyst and the reaction time (entry 15).

In summary, the reaction was highly dependent on the applied solvent and catalyst. In the presence of Rh/C and EA, it was feasible to isolate **147** in pure form. Moreover, the hydrogenation proceeded exclusively from the convex side of the bicyclus due to the bulky *tert*-butyl group, thus forming **147** as a single diastereomer.

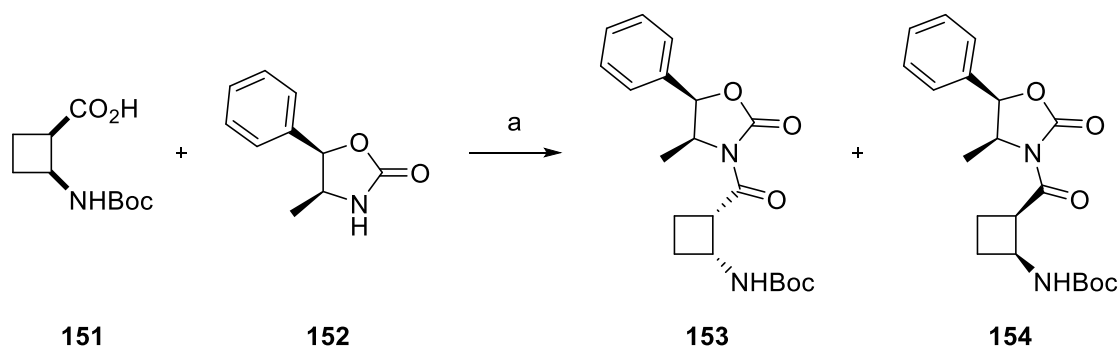
### 1.2.2 Functionalization

With the saturated bicycle **147** in hand, the direct lactonization should be possible. However, previous functionalization of the methyl ester should be advantageous for the later steps and for the synthesis of a suitable precursor **150** for derivatizations, as the methyl ester had to be transformed anyway (Scheme 19).



**Scheme 19.** From cyclopropane **147** to a suitable precursor **150** for the synthesis of (+)-paeonilide (**49**) and derivatives.

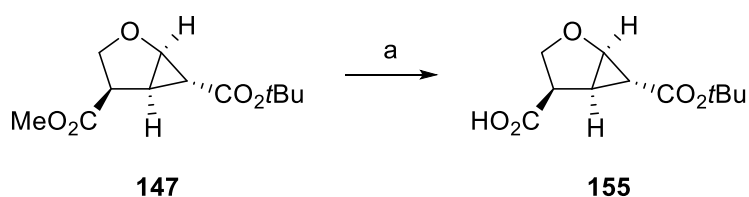
Selective reduction of the methyl ester to a hydroxyl group in the presence of the *tert*-butyl ester might be useful since a benzoate group needed to be introduced in the final steps. Starting with enantioenriched **147**, the first step should be a chiral resolution in order to obtain enantiomerically pure product. One convenient approach was reported by Aitken *et al.* in 2011.<sup>35</sup> Therein, they showed the chiral resolution of racemic amino acid **151** *via* derivatization with a chiral oxazolidin-2-one **152** which allowed easy separation of the resulting diastereomers **153** and **154** (Scheme 20).



**Reagents and conditions:** a) i) PivCl (1.05 equiv.), Et<sub>3</sub>N (1.2 equiv.), THF, 0 °C, 1 h; ii) **152** (1.0 equiv.), *n*-BuLi (1.0 equiv.), THF, -78 °C, 1 h, 46% **153** and 44% **154**.

**Scheme 20.** Chiral resolution of racemic **151** using oxazolidin-2-one **152**.<sup>35</sup>

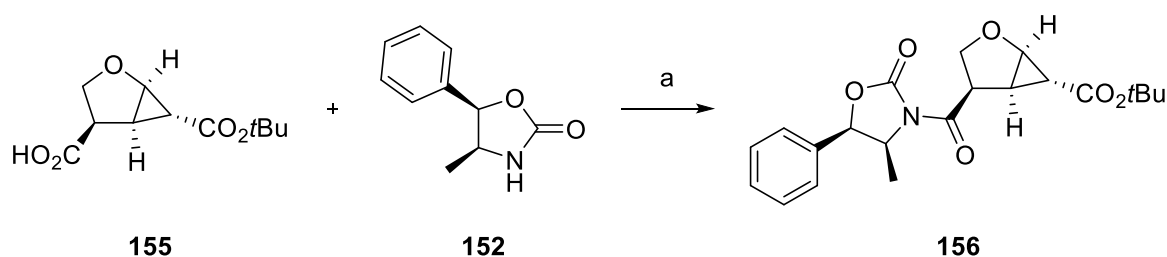
In order to perform such a chiral derivatization with cyclopropane **147**, the methyl ester had to be selectively saponified. This was accomplished under mild conditions using LiOH (Scheme 21).



**Reagents and conditions:** a) LiOH (1.1 equiv.), H<sub>2</sub>O/THF (2:1, v/v), rt, 1.5 h, 95%.

**Scheme 21.** Selective saponification of the methyl ester of **147**.

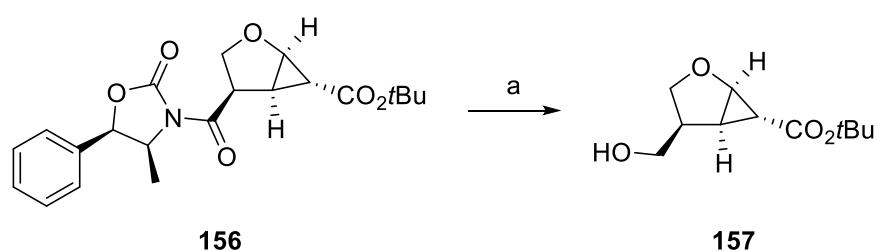
The reaction proceeded smoothly furnishing the desired acid **155** in excellent yield and thus enabling the chiral resolution. Therefore, enantioenriched acid **155** was coupled with the chiral oxazolidin-2-one **152** and the desired diastereomer **156** could be isolated in good yield (Scheme 22).<sup>35</sup>



**Reagents and conditions:** a) **155** (83% ee), PivCl (1.05 equiv.), Et<sub>3</sub>N (1.2 equiv.), THF, 0 °C, 1 h; ii) **152** (1.05 equiv.), *n*-BuLi (1.05 equiv.), THF, -78 °C, 1 h, 75%.<sup>35</sup>

**Scheme 22.** Chiral resolution of **155** using oxazolidin-2-one **152**.<sup>35</sup>

With the single diastereomer **156** in hand, a variety of reactions for the facile removal of the chiral auxiliary would be possible.<sup>36</sup> However, since a hydroxyl functionality should be introduced reductive cleavage of the oxazolidinone was the reaction of choice. Classical reductive removal of the chiral auxiliary using LAH or LiBH<sub>4</sub> was not practicable in this case, as the *tert*-butyl ester would be also reduced. But a reductive cleavage of oxazolidinones in a non-destructive way using inexpensive NaBH<sub>4</sub> in THF and water has been published, too.<sup>37</sup> Slight modifications of the reported method provided the desired alcohol **157** in excellent yield (Scheme 23).



**Reagents and conditions:** a) NaBH<sub>4</sub> (3.0 equiv.), MeOH (3 mL/mmol), THF, rt, 1 h, 98%, >99% *ee*.

**Scheme 23.** Reductive cleavage of the chiral auxiliary.<sup>37</sup>

Moreover, the removal of the chiral auxiliary proceeded with neither epimerization nor racemization and the oxazolidinone **152** could be recovered and reused. Analytical chiral HPLC unambiguously confirmed that enantiomerically pure alcohol **157** was synthesized (Figure 10).

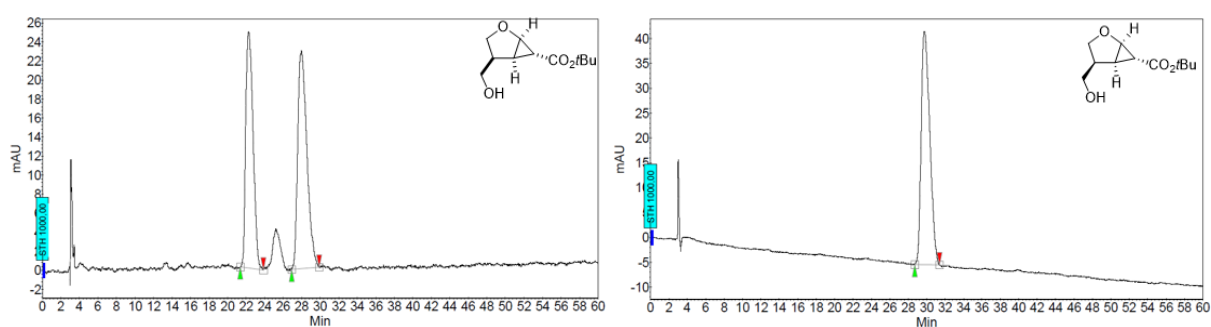
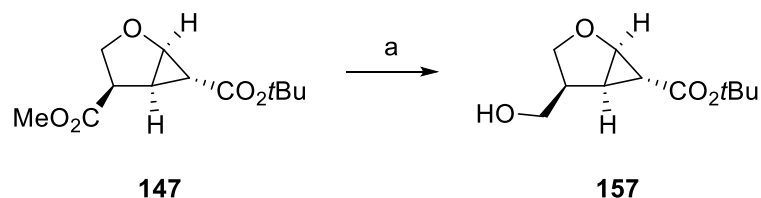


**Figure 10.** Left: analytical chiral HPLC chromatogram of racemic **142**. Right: analytical chiral HPLC chromatogram of enantiopure **142**. Conditions: Phenomenex Lux Cellulose-2, *n*-heptane/*i*PrOH 95:5, 1.0 mL/min, 215 nm): *tr* (minor) = 22.26, *tr* (major) = 27.95.

In the case of enantiomerically pure methyl ester **147** obtained by recrystallization, the synthesis of alcohol **157** was straightforward. Although NaBH<sub>4</sub> itself is not generally applicable

to the reduction of esters due to its low reactivity, the reducing power can be increased using several additives.<sup>38</sup> Thus, a direct selective reduction of the methyl ester functionality of **147** was possible with a NaBH<sub>4</sub>-MeOH system giving rise to alcohol **157** in excellent yield (Scheme 24).

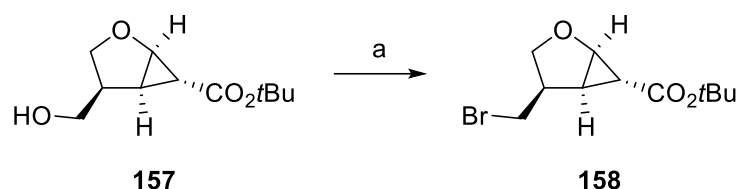


**Reagents and conditions:** a) NaBH<sub>4</sub> (4.0 equiv.), MeOH (3 mL/mmol), THF, reflux, 1.5 h, 98%.

**Scheme 24.** Direct reduction of the methyl ester of **147**.<sup>38</sup>

The next key step in the synthesis of (+)-paeonilide (**49**) should be an acid-mediated cyclopropane ring-opening/lactonization cascade in order to construct the furo[2,3-*b*]furanone core structure. However, earlier studies showed that subsequent acid-catalyzed lactonization with alcohol **157** was not feasible, as only a complex mixture of unidentified compounds was obtained.<sup>32</sup> Therefore, a suitable substituent had to be found which on the one hand enables access to the desired furo lactone and is stable against the conditions used in the later steps. On the other hand, this substituent should be able to be readily transformed in a later stage to give access to (+)-paeonilide (**49**) and derivatives. Due to its easy amenability, the conversion of the hydroxyl group to a bromide came to mind. A bromide group would be advantageous in terms of diastereoselectivity in the ensuing lactonization because of its size and furthermore it can be easily transformed by nucleophilic substitution. For the conversion of an alcohol to a bromide, several alternatives were conceivable, *e.g.* a reaction with PBr<sub>3</sub> or SO<sub>2</sub>Br.<sup>39</sup> In this work, an Appel reaction using CBr<sub>4</sub> and PPh<sub>3</sub> was applied and already the first attempt proceeded smoothly to the desired bromide **158** in excellent yield (Scheme 25).<sup>40</sup>





**Reagents and conditions:** a) CBr<sub>4</sub> (1.2 equiv.), PPh<sub>3</sub> (1.2 equiv.), DCM, rt, 1 h, 93%.

**Scheme 25.** Appel reaction of alcohol **157**.<sup>40</sup>

Moreover, the absolute stereochemistry of the bromide **158** was confirmed by X-ray crystallography (Figure 11).

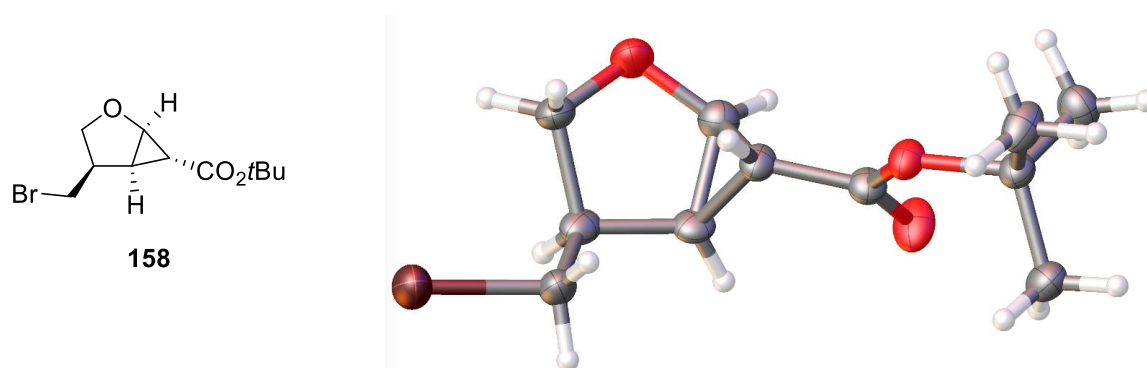
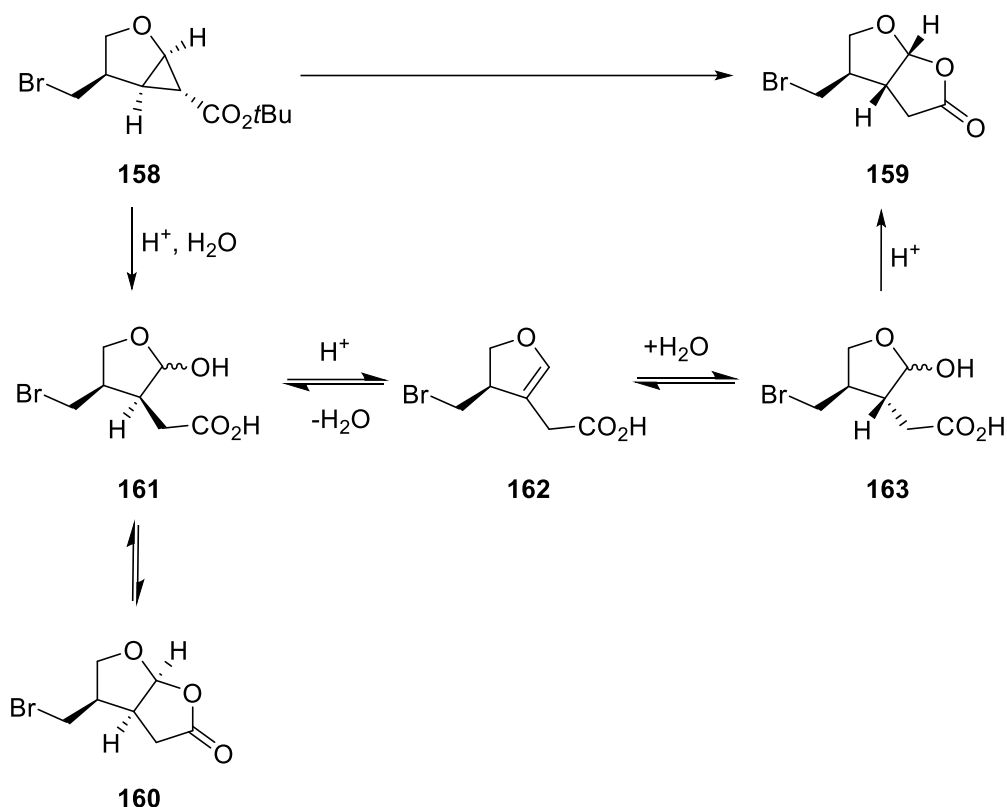


**Figure 11.** X-ray structure of **158**.

### 1.2.3 Lactonization and Isomerization

With the cyclopropanated bromide **158** in hand, the next step toward the synthesis of (+)-paeonilide (**49**) was the acid-mediated ring-opening/lactonization to furo lactone **159**. This goal could be achieved either by a two-step procedure or a one-pot reaction.<sup>41,33</sup> The latter was reported by Reiser *et al.* for the enantioselective synthesis of furo[2,3-*b*]furans.<sup>33</sup> Therein, they obtained two diastereomers regarding the position of the substituents after the ring-opening/lactonization cascade. Remarkably, they were able to control the positioning of the substituents to be either on the concave or the convex face of the bicyclic ring system by kinetic or thermodynamic control. Therefore, they postulated a mechanism to explain the formation of the two emerging diastereomers which can also be applied to the present reaction of bromide **158** (Scheme 26).



**Scheme 26.** Acid-mediated formation of furo lactone diastereomers **159** and **160**.<sup>33</sup>

Under acidic conditions, cyclopropane **158** is hydrolyzed to form lactol **161**. This can either undergo a rearrangement to the undesired kinetic product **160** or eliminate water to give the enol ether **162**. Re-addition of water under inversion of stereochemistry leads to lactol **163**, which rearranges to the desired thermodynamic product **159**.

In order to find the best reaction conditions for the direct ring-opening/lactonization of **158**, a screening was conducted (Table 6). The reaction was initially performed using 2 M HCl and cooling to 0 °C, as described in the synthesis of (-)-paeonilide (-)-**49**.<sup>30</sup> The reaction proceeded smoothly with a yield of 80%, albeit the formation of the undesired furo lactone **160** was favored (entry 1). However, this was not surprising due to the fact that the reaction outcome is controlled kinetically or thermodynamically. Thus, using low temperatures benefits the kinetic product **160** with the substituent on the concave side of the fused ring system. For this reason, harsher reaction conditions developed earlier by Reiser *et al.* were adopted that should prefer the formation of the thermodynamically favored product **159**.<sup>33</sup> Using 6 M HCl and heating to 60 °C for 4 h led to a decrease of both, yield and diastereoselectivity (entry 2). A further increase in temperature to reflux at least shifted the diastereomeric ratio to the side of the desired product **159**, but still with an unsatisfying diastereomeric ratio (entry 3). Under

microwave conditions at 110 °C, the result was strongly dependent on the reaction time (entries 4 and 5). While five minutes gave only a diastereomeric ratio of 1.5:1, increasing the reaction time to 30 minutes yielded a ratio of 5:1, however, accompanied by a drop in yield. The initial conditions together with microwave irradiation even improved the diastereoselectivity to a ratio of 6:1, but the yield further decreased to only 38% (entry 6).

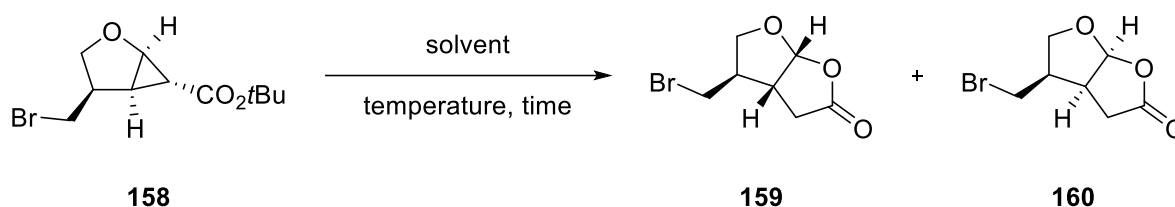


**Table 6.** Screening of the direct lactonization of **158**.

entry <sup>[a]</sup>	solvent	temperature	time	conditions	<i>dr</i> <sup>[b]</sup>	yield <sup>[c]</sup> [%]
1 <sup>[d]</sup>	THF/2 M HCl (1:3)	0 °C	15 h	-	1:1.5	80
2	dioxane/6 M HCl (1:2)	60 °C	4 h	-	1:2	75
3	dioxane/6 M HCl (1:2)	reflux	4 h	-	2:1	70
4	dioxane/6 M HCl (1:2)	110 °C	5 min	microwave	1.5:1	55
5	dioxane/6 M HCl (1:2)	110 °C	30 min	microwave	5:1	53
6	THF/2 M HCl (1:3)	110 °C	30 min	microwave	6:1	38

[a] 1.0 mmol **158**; [b] determined by <sup>1</sup>H-NMR; [c] yield of diastereomeric mixture; [d] 6.0 mmol **158**.

As the direct lactonization attempts turned out to give no adequate results in terms of diastereomeric ratio, a further screening to investigate the isomerization of a diastereomeric mixture **159/160** (*dr* = 1.5:1) toward furo lactone **159** was performed (Table 7).

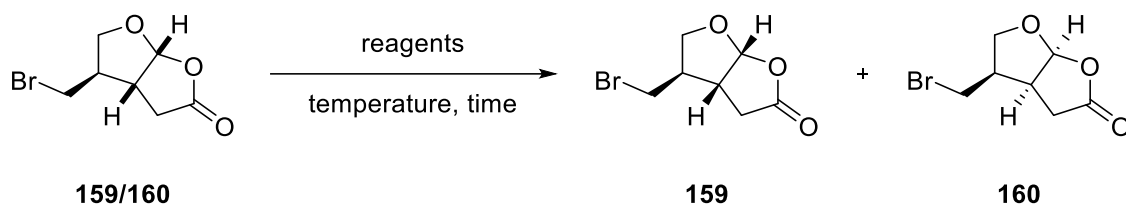


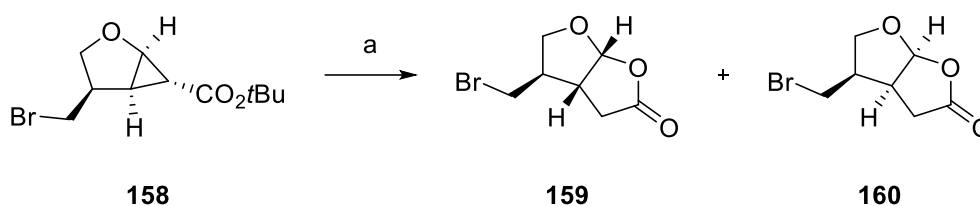
**Table 7.** Isomerization screening of the diastereomeric mixture **159/160**.

entry <sup>[a]</sup>	reagents	temperature	time [h]	<i>dr</i> <sup>[b]</sup>
1	pyridine:THF (1:2)	50 °C	1	no change
2	pyridine:THF (1:2)	50 °C	36	no change
3	H <sub>2</sub> SO <sub>4</sub> :THF (1:5)	50 °C	1	no change
4	H <sub>2</sub> SO <sub>4</sub> :THF (1:5)	50 °C	24	7:1
5	2.5 equiv. H <sub>2</sub> SO <sub>4</sub> , toluene	100 °C	18	6.5:1
6	Amberlyst® 15 (30 mg/mmol), toluene	100 °C	18	2:1:1
7	Amberlyst® 15 (30 mg/mmol), toluene	reflux	18	11.5:1
8	Al <sub>2</sub> O <sub>3</sub> (Brockmann IV) (30 mg/mmol), toluene	reflux	18	5.5:1

[a] 0.5 mmol **159/160**; [b] determined by GC.

The reaction was monitored by GC in order to follow changes in the diastereomeric ratio. In an earlier study pyridine was shown to promote the isomerization of the undesired to the desired diastereomer.<sup>32</sup> However, at elevated temperatures, no change in the diastereomeric ratio could be observed even after 36 h (entries 1 and 2). The use of H<sub>2</sub>SO<sub>4</sub> also showed no effect after 1 h, but increasing the reaction time to 24 h led to a good diastereomeric ratio of 7:1 (entries 3 and 4). Nevertheless, it has to be mentioned that under these conditions a noticeable decomposition was observed. Reducing the amount of H<sub>2</sub>SO<sub>4</sub> and running the reaction in toluene at 100 °C for 18 h again gave good results, but still accompanied by decomposition (entry 5). Using the acidic cation exchange resin Amberlyst® 15 at 100 °C only gave a ratio of 2.1:1 while refluxing the reaction for 18 h resulted in a significantly increased diastereomeric ratio of 11.5:1 (entries 6 and 7). In the last test reaction, the application of basic Al<sub>2</sub>O<sub>3</sub> (Brockmann IV) was investigated, showing also relatively good results (entry 8). In summary, both the direct lactonization and the isomerization could be indeed controlled kinetically or thermodynamically since increasing the temperature and reaction time benefits the formation of the thermodynamically favored diastereomer **159** with the substituent on the convex face of the bicycle.

As Amberlyst® 15 proved to be a suitable reagent for the isomerization of **159/160** to **159**, it should be also tested for the direct acid-catalyzed lactonization of bromide **158** (Scheme 27).



**Reagents and conditions:** a) Amberlyst® 15 (30 mg/mmol), toluene, reflux, 20 h, 81% **159** and 11% **160**.

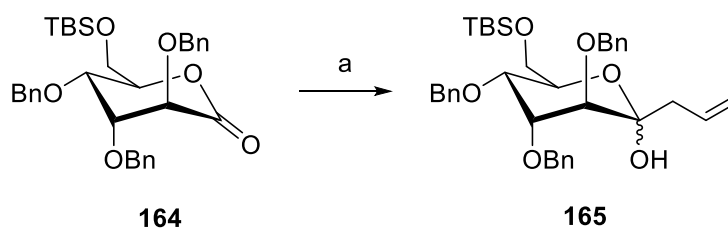
**Scheme 27.** Direct lactonization of bromide **158**.

The reaction proceeded smoothly to the two diastereomers **159** and **160**. Remarkably, after the reaction Amberlyst® 15 could be readily filtered off and no byproducts were obtained. Most importantly, it was possible to separate the two diastereomers by column chromatography to yield 81% of the desired furo lactone **159** and 11% of the undesired diastereomer **160**.

### 1.3 Total synthesis of (+)-paeonilide

#### 1.3.1 Introduction of the side chain

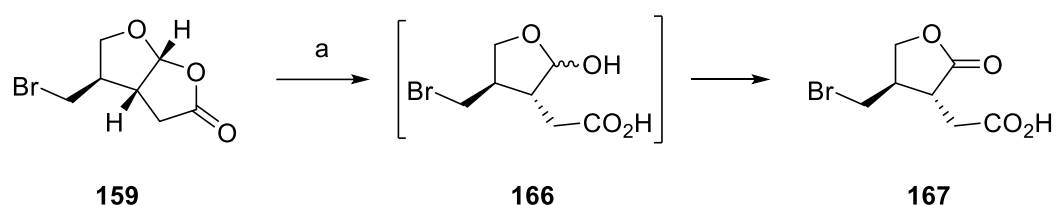
The next necessary step toward the synthesis of (+)-paeonilide (**49**) was the introduction of a suitable side chain in the acetal position. Unfortunately, all earlier attempts to achieve this goal *via* C-H insertion did not give the desired results.<sup>32</sup> However, Matsuda *et al.* reported a synthetic strategy to introduce either a vinyl or allyl group at the carbonyl center of a  $\delta$ -lactone in 2008 (Scheme 28).<sup>42</sup>



**Reagents and conditions:** a) allyl-MgBr (1.2 equiv.), THF, -78 °C, 1.5 h, 92%.

**Scheme 28.** Reaction of  $\delta$ -lactone **164** with allylmagnesium bromide.<sup>42</sup>

As already reported for the synthesis of (-)-paeonilide (-)-**49**, furo lactone **159** had to be converted to  $\alpha,\beta$ -substituted  $\gamma$ -butyrolactone **167** in order to make use of the established Grignard protocol.<sup>30</sup> Therefore, furo lactone **159** was treated with Jones reagent leading to the opening of the lactone and the formation of lactol **166** which was subsequently oxidized to the corresponding  $\alpha,\beta$ -substituted  $\gamma$ -butyrolactone **167** in excellent yield (Scheme 29).



**Reagents and conditions:** a) Jones reagent (3.0 equiv.), acetone, rt, 1.5 h, 98%.

**Scheme 29.** Oxidative ring-opening of **159**.

The absolute stereochemistry of the  $\alpha,\beta$ -substituted  $\gamma$ -butyrolactone **167** was confirmed by X-ray crystallography (Figure 12).

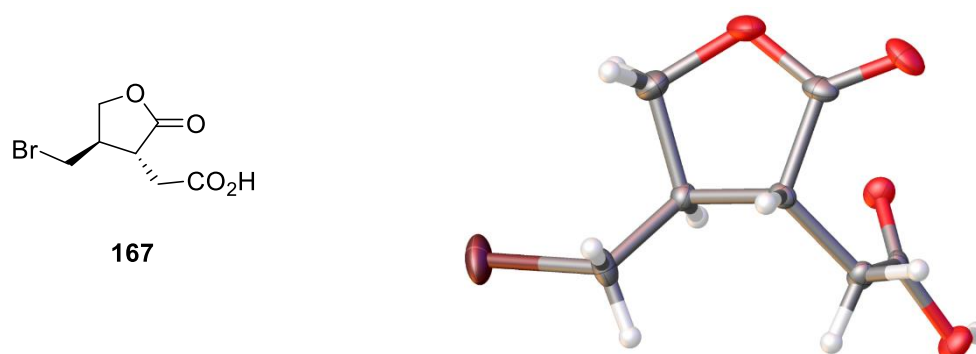
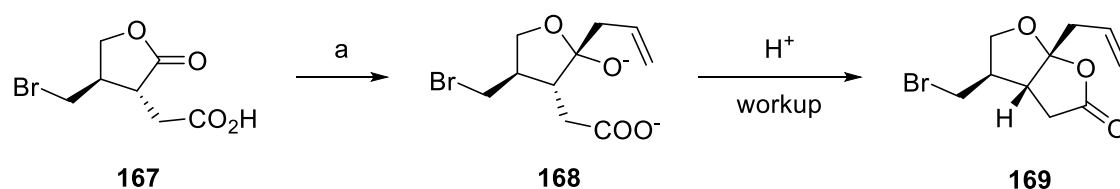


**Figure 12.** X-ray structure of **167**.

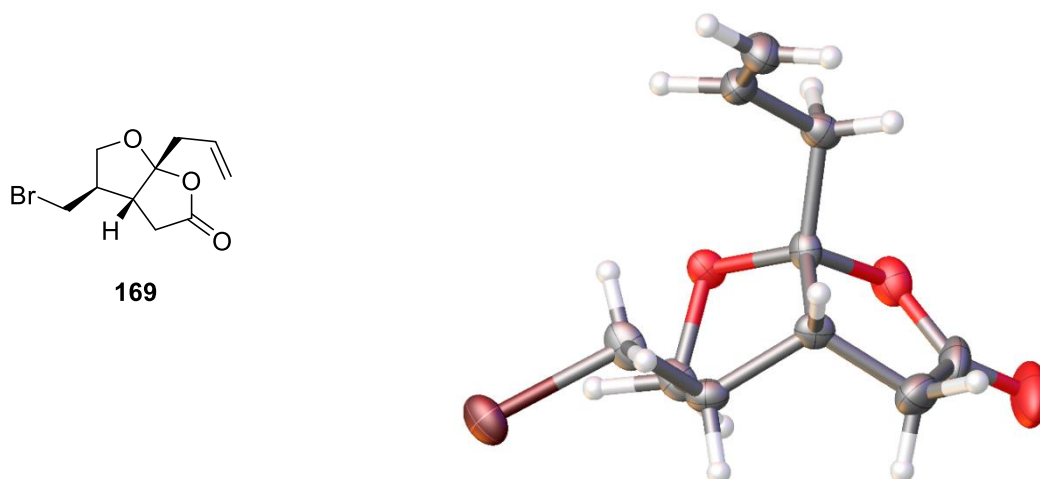
With lactone **167** in hand, the introduction of a side chain *via* a Grignard reaction should be reliable now. Due to the fact that the final product **49** bears a methyl ketone in the side chain, the use of allylmagnesium bromide seemed to be appropriate as the allyl group could be further functionalized later on. For the allylation of lactone **167**, 2.5 equiv. allyl-MgBr were used, since 1.0 equiv. was consumed by the free carboxylic acid (Scheme 30).<sup>32</sup>



**Reagents and conditions:** a) allyl-MgBr (2.5 equiv.), THF, -78 °C, 2 h, 81%.

**Scheme 30.** Grignard reaction of lactone **167**.

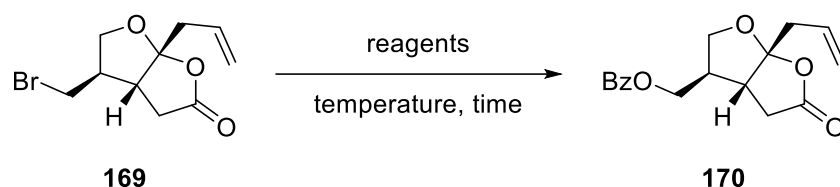
Fortunately, acidic work-up of the reaction led to subsequent lactonization yielding the desired furolactone **169** with the allyl group in the acetal position as a single diastereomer. Moreover, this compound was not only a well-suited precursor for the last steps toward (+)-paeonilide (**49**) but also a very promising starting point for several derivatizations. Especially, the terminal double bond and the primary bromide should readily enable access to a great variety of transformations. The absolute stereochemistry of bromide **169** was confirmed by X-ray crystallography (Figure 13).



**Figure 13.** X-ray structure of **169**.

### 1.3.2 Final steps

In the final steps of the synthesis of (+)-paeonilide (**49**) two further transformations had to be accomplished. On the one hand the allyl group had to be oxidized to the methyl ketone and on the other hand, the bromide should be transformed to a benzoate. Therefore, the nucleophilic substitution of bromide **169** with a suitable benzoate was investigated (Table 8).

**Table 8.** Conversion of bromide **169** to benzoate **170**.<sup>43,44</sup>

entry	reagents	temperature	time [h]	yield [%]
1	sodium benzoate, Adogen® 464, toluene/H <sub>2</sub> O (2:1)	reflux	1.5	51
2	potassium benzoate, DMF	80 °C	2	80

In the initial attempt benzoate **167** should be obtained using sodium benzoate under phase transfer conditions.<sup>43</sup> The desired product could be isolated, however, only in moderate yield. Fortunately, a second attempt utilizing potassium benzoate in DMF at 80 °C delivered **170** in 80% yield.<sup>44</sup>

Finally, the last step toward (+)-paeonilide (**49**) was the oxidation of the allyl group to the methyl ketone. For this purpose, the first reaction which came to mind was the Wacker-oxidation, as it is a well-established reaction to convert terminal alkenes to the corresponding methyl ketones.<sup>45</sup> Conventionally, Wacker-oxidation protocols apply a Pd-catalyst together with a stoichiometric redox co-catalyst (*e.g.* CuCl), under an oxygen atmosphere in aqueous solution.<sup>46,47</sup> This methodology was investigated for the oxidation of the allyl group of benzoate **170** (Table 9).

The first reaction was carried out following a procedure reported by Lowary *et al.* in 2003.<sup>48</sup> Under these conditions, only low conversion of starting material was observed at ambient temperature and therefore the reaction was heated to 60 °C (entry 1). This led to full conversion of the starting material **170** yielding 34% of the desired product **49**, however, accompanied by 37% of the corresponding aldehyde **171**. Following a procedure published by Wang *et al.*, using Pd(OAc)<sub>2</sub> as catalyst and molecular oxygen as the sole oxidant for the Wacker-oxidation, resulted in a complex mixture, but neither the methyl ketone **49** nor the aldehyde **171** were formed (entry 2).<sup>49</sup> In a third approach, Fe<sub>2</sub>(SO<sub>4</sub>)<sub>3</sub> was used as oxidant together with PdCl<sub>2</sub> as catalyst, again resulting in a complex mixture containing no product (entry 3).<sup>50</sup>



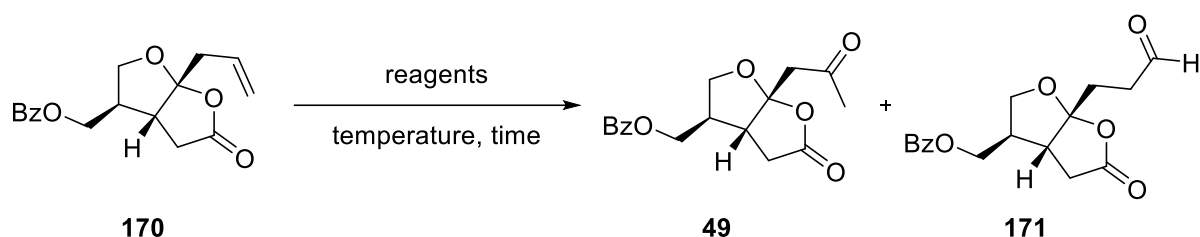
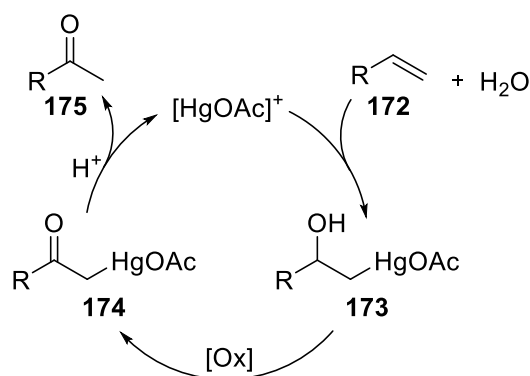


**Table 9.** Oxidation of the terminal alkene to the methyl ketone.<sup>48,49,50,51</sup>

entry	reagents	temperature	time [h]	49 [%]	168 [%]
1 <sup>[a]</sup>	PdCl <sub>2</sub> (10 mol%), CuCl (1.0 equiv.), O <sub>2</sub> , DMF/H <sub>2</sub> O (3:1)	rt to 60 °C	8	34	37
2 <sup>[a]</sup>	Pd(OAc) <sub>2</sub> (10 mol%), TFA (1.0 equiv.), O <sub>2</sub> , DMSO/H <sub>2</sub> O (10:1)	70 °C	15	-	-
3	PdCl <sub>2</sub> (5 mol%), Fe <sub>2</sub> (SO <sub>4</sub> ) <sub>3</sub> (1.5 equiv.), MeCN/H <sub>2</sub> O (7:1)	45 °C	24	-	-
4	Hg(OAc) <sub>2</sub> (0.3 equiv.), Jones reagent (3.0 equiv.), acetone/H <sub>2</sub> O (4:1)	0 °C to rt	18	63	-

[a] O<sub>2</sub> applied *via* a balloon.

As none of these Wacker-type oxidations led to satisfying results, a different method utilizing Hg(OAc)<sub>2</sub> for the oxymercuration of the olefin followed by subsequent oxidation with Jones reagent to obtain the methyl ketone was investigated (entry 4).<sup>51</sup> Advantageously, this method only requires catalytic amounts of the highly toxic mercury salt compared to common oxymercuration. In the first step, the double bond of olefin **172** attacks the mercury ion and upon regioselective attack of water the Markovnikov product **173** is formed. The reaction is driven in the direction of this thermodynamically less stable hydrated form **173**, as it is subsequently trapped by oxidation to the corresponding ketone **174**. The desired product **175** is generated by proteolysis of the C-Hg-bond under release of the catalyst (Scheme 31).



**Scheme 31.** Catalytic cycle of the oxymercuration/oxidation sequence using Hg(OAc)<sub>2</sub>.

This approach yielded (+)-paeonilide (**49**) in 63% yield without formation of the corresponding aldehyde **171**. (+)-paeonilide (**49**) was obtained as colorless needles after recrystallization from methanol and the optical rotation ( $[\alpha]_{\text{D}}^{20} = +54.2$ ,  $\text{CHCl}_3$ ,  $c = 0.22$ ) fitted perfectly with the value reported for the authentic sample ( $[\alpha]_{\text{D}}^{20} = +54.3$ ,  $\text{CHCl}_3$ ,  $c = 0.44$ ).<sup>52</sup> Furthermore, analytical chiral HPLC confirmed that enantiomerically pure (+)-paeonilide (**49**) was synthesized and no loss of enantiomeric excess occurred during the synthesis (Figure 14).

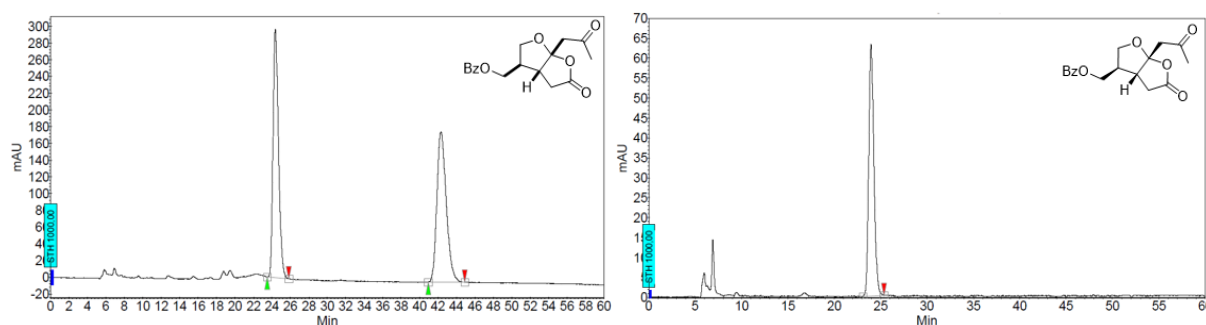


**Figure 14.** Left: analytical chiral HPLC chromatogram of (±)-**49**. Right: analytical chiral HPLC chromatogram of enantiopure **49**. Conditions: Phenomenex Lux Cellulose-1, *n*-heptane/*i*PrOH 50:50, 0.5 mL/min, 215 nm): *tr* (major) = 24.37, *tr* (minor) = 42.32.

Moreover, the absolute stereochemistry of (+)-paeonilide (**49**) was unambiguously confirmed by X-ray crystallography (Figure 15).

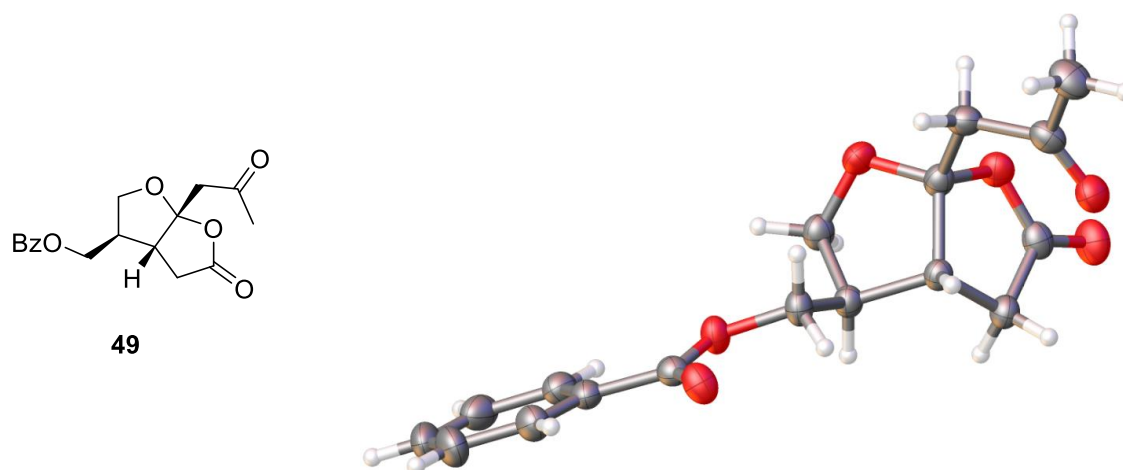


**Figure 15.** X-ray structure of (+)-paeonilide (**49**).

In summary, starting from commercially available, non-chiral 3-furoic acid methyl ester (**100**) enantiopure (+)-paeonilide (**49**) was afforded in an 11 step, straightforward synthesis with an overall yield of 10.4%. Until today, this is the only enantioselective synthesis of (+)-paeonilide (**49**). Moreover, a suitable precursor **169** for further derivatizations could be synthesized in 9 steps with an overall yield of 20.6%.

## 2. Derivatization of (+)-paeonilide

In some cases, the biological activity of naturally occurring substances can be increased by derivatization. Therefore, a library of several (+)-paeonilide derivatives should be synthesized to compare their biological activity to the synthesized (+)-paeonilide (**49**). Considering the structure of bromide **169** or benzoate **170**, three different modification sites came to mind (Figure 16). On the one hand, the methyl ketone in (+)-paeonilide (**49**) could be exchanged *via* different transformations of the double bond  $R^1$  in the side chain. On the other hand, modifications of the other side chain  $R^2$  were applicable, *inter alia*, by nucleophilic substitution of the bromide group in **169**. Furthermore, different alkyl chains  $R^3$  should be introduced in the  $\alpha$ -position of the lactone *via* alkylation of the corresponding enolate.

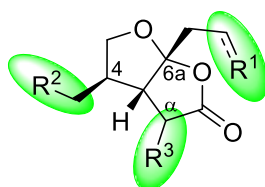
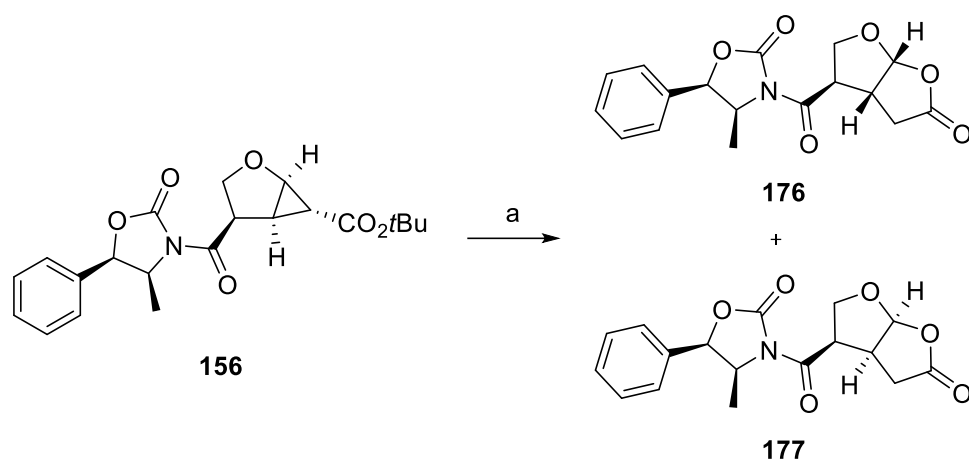


**Figure 16.** Modification sites at the paeonilide core structure.

The first derivative was supposed to bear a carboxylic acid group instead of the benzoate in the 4-position. Earlier studies revealed that the acid-mediated direct lactonization toward the furo[2,3-*b*]furanone with a carboxylic acid in the 4-position lacked in terms of diastereoselectivity and separability, therefore, oxazolidinone **156** should be used as starting point for the desired derivative.<sup>34</sup> As already mentioned before, it was possible to control the positioning of the substituents to be either on the concave or the convex face of the bicyclic ring system by kinetic or thermodynamic control. Due to the bulky oxazolidinone group in the 4-position, the formation of the thermodynamic product with the substituent on the convex side of the bicyclus should be even more favored. Using the optimized conditions, namely refluxing the reaction mixture with the acidic cation exchange resin Amberlyst® 15, resulted in the formation of 74% of the desired diastereomer **176** and 15% of the undesired one **177** (Scheme 32).



**Reagents and conditions:** a) Amberlyst® 15 (50 mg/mmol), toluene, reflux, 3 h, 74% **176** and 15% **177**.

**Scheme 32.** Acid-mediated direct lactonization of **156**.

Moreover, the two diastereomers could be readily separated by column chromatography and their absolute stereochemistry was unambiguously confirmed by X-ray crystallography (Figure 17).

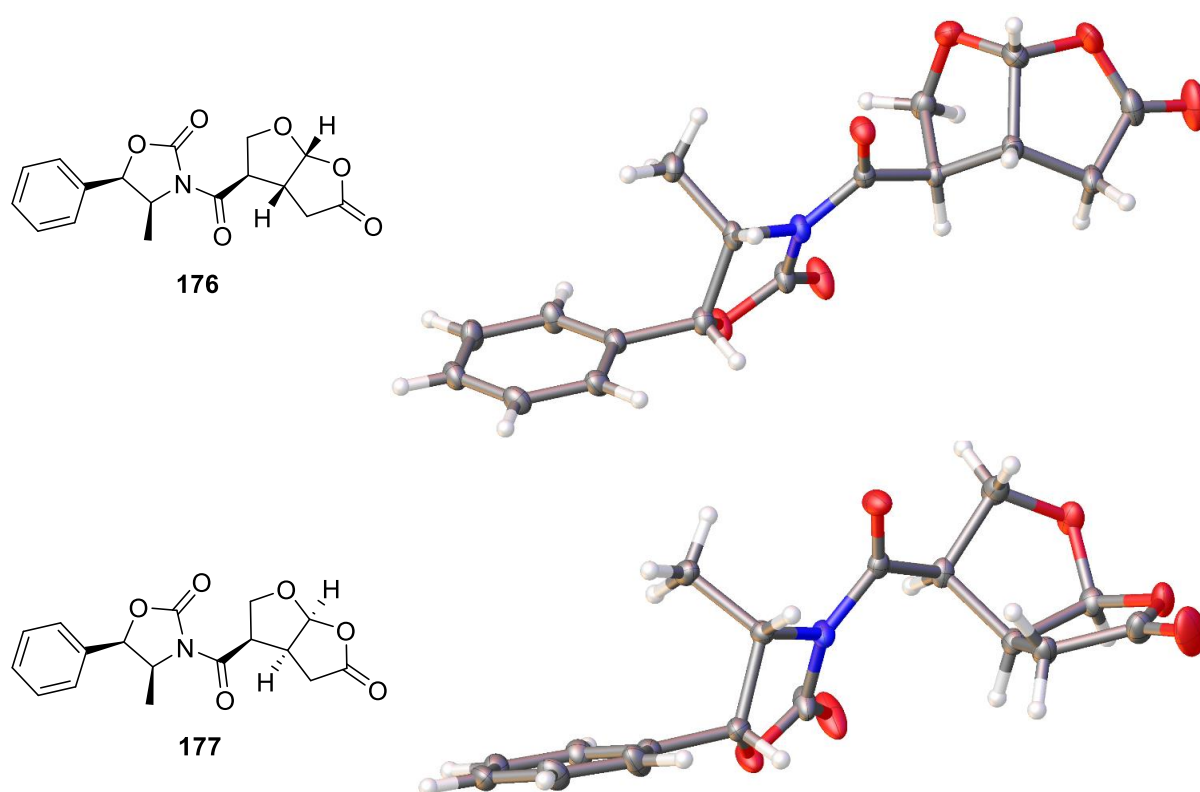
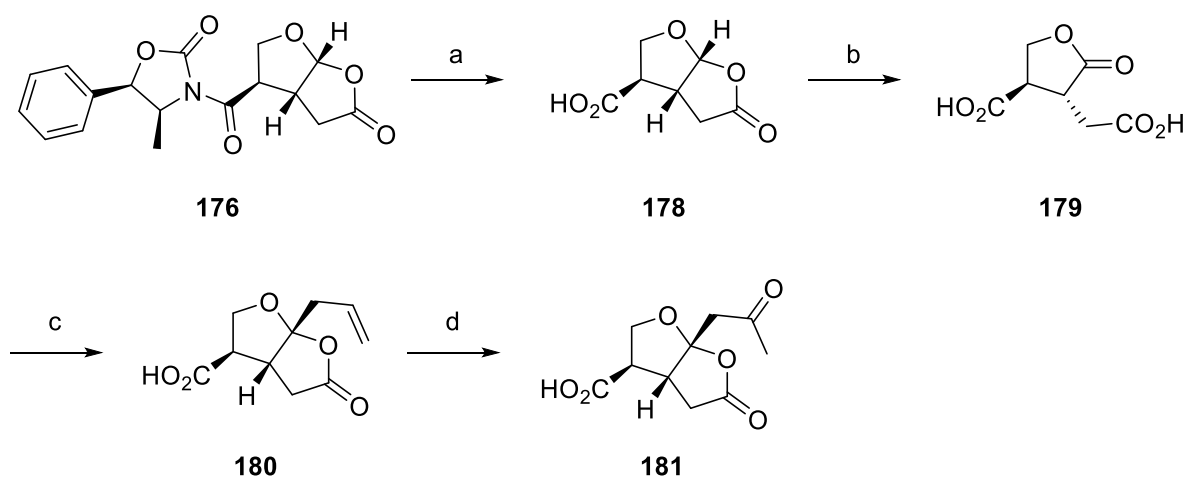


**Figure 17.** X-ray structures of **176** and **177**.

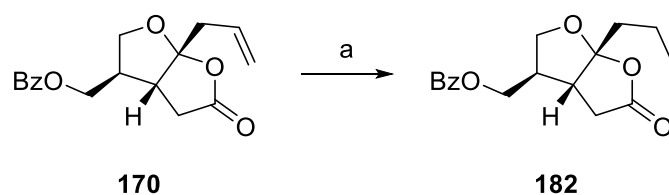
Cleavage of the chiral auxiliary was achieved in excellent yield using LiOH, thus, giving rise to diastereomerically and enantiomerically pure acid **178**.<sup>53</sup> Subsequent oxidative ring-opening to lactone **179** followed by allylation with allylmagnesium bromide (3.0 equiv. were necessary since 2.0 equiv. were consumed by the free carboxylic acids) gave **180** in good yield. In the last step, the desired acid derivative **181** was afforded in 76% yield *via* a previously established oxymercuration/oxidation protocol. Starting from cyclopropane **156** the carboxylic acid derivative **181** was obtained in 5 steps with an overall yield of 28.6% (Scheme 33).<sup>51</sup>



**Reagents and conditions:** a) LiOH (2.0 equiv.), H<sub>2</sub>O/THF (1:3, v/v), 0 °C, 0.5 h, 91%; b) Jones reagent (3.0 equiv.), acetone, rt, 5 h, 82%; c) allyl-MgBr (3.0 equiv.), THF, -78 °C, 3 h, 68%; d) Hg(OAc)<sub>2</sub> (0.4 equiv.), Jones reagent (3.0 equiv.), acetone/H<sub>2</sub>O (4:1, v/v), rt, 36 h, 76%.

**Scheme 33.** Synthesis of acid derivative **181**.<sup>51,53</sup>

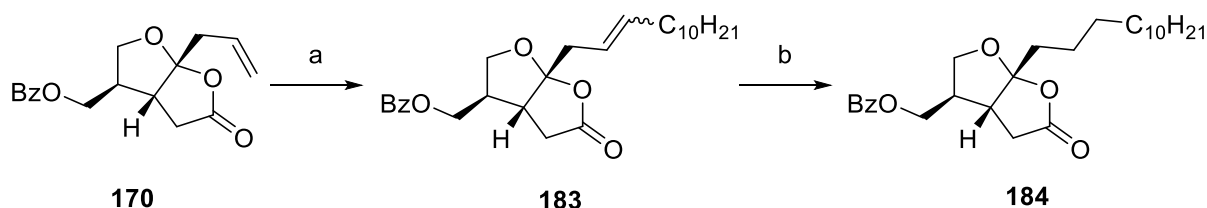
In order to analyze the influence of the methyl ketone side chain on the biological activity, several modifications were investigated. First, a derivative bearing the propyl side chain but without the ketone functionality should be synthesized. Therefore, benzoate **170** was hydrogenated using Pd/C under 1 atm. hydrogen pressure in MeOH. The reaction proceeded smoothly yielding **182** in 81% (Scheme 34).



**Reagents and conditions:** a) Pd/C (5 mol%), H<sub>2</sub> (1 atm.), MeOH, rt, 2 h, 81%.

**Scheme 34.** Synthesis of hydrogenated derivative **182**.

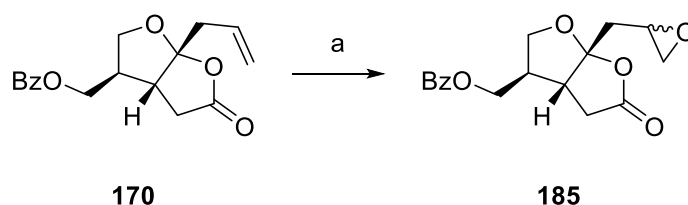
As the lipophilicity of a compound plays an important role in the ability to penetrate membranes and tissues, it also correlates strongly with the biological activity.<sup>54,55</sup> Therefore, a derivative bearing a long alkyl side chain was synthesized. Installation of the long alkyl chain was achieved *via* cross metathesis of benzoate **170** with 1-dodecene using Grubbs' II catalyst.<sup>28</sup> The saturated side chain was obtained by hydrogenation of the double bond of **183** applying Pd/C as catalyst under 1 atm. hydrogen pressure. The desired tridecyl derivative **184** was obtained in 81% over two steps (Scheme 35).



**Reagents and conditions:** a) 1-dodecene (6.0 equiv.), Grubbs' II catalyst (5 mol%), DCM, reflux, 24 h, 90%; b) Pd/C (5 mol%), H<sub>2</sub> (1 atm.), MeOH, rt, 1.5 h, 89%.

**Scheme 35.** Synthesis of derivative **184**.<sup>28</sup>

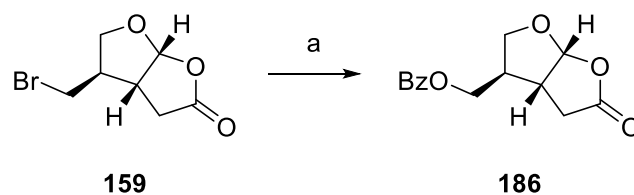
Additionally, the effect of an epoxide in the side chain should be investigated. Therefore, benzoate **170** was treated with *m*-CPBA and already the first attempt proceeded smoothly to the desired epoxide **185** (*dr* = 54:46) in very good yield (Scheme 36).



**Reagents and conditions:** a) *m*-CPBA (2.0 equiv.), DCM, rt, 72 h, 82%, *dr* = 54:46.

**Scheme 36.** Epoxidation of benzoate **170**.

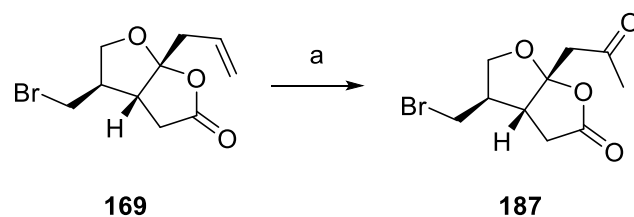
The necessity of the side chain in the acetal position for the biological activity should also be examined by synthesizing a (+)-paeonilide derivative **186** without the side chain. If the removal of the methyl ketone side chain should have no effect on the biological activity, it would be extremely beneficial, as the synthetic route toward derivative **186** was much shorter than the one for (+)-paeonilide (**49**). Nucleophilic substitution of bromide **159** using potassium benzoate afforded the desired derivative **186** in good yield (Scheme 37).



**Reagents and conditions:** a) potassium benzoate (1.6 equiv.), DMF, 80 °C, 2 h, 77%

**Scheme 37.** Synthesis of derivative **186**.

To broaden the scope of derivatives, several modifications of the functional group in the C-4 position were investigated. As the precursor **169** was already synthesized during the synthesis of (+)-paeonilide (**49**), oxidation of the allyl side chain should give rise to the bromide derivative **187**. Oxymercuration and subsequent oxidation with Jones reagent yielded the desired compound **187** in 70% (Scheme 38).



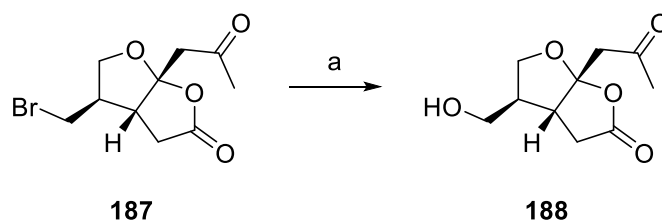
**Reagents and conditions:** a) Hg(OAc)<sub>2</sub> (0.5 equiv.), Jones reagent (3.0 equiv.), acetone/H<sub>2</sub>O (4:1, v/v), rt, 24 h, 70%.

**Scheme 38.** Oxymercuration/oxidation cascade of precursor **169**.

Proceeding from bromide derivative **187**, a hydroxyl functionality should be introduced in the C-4 position. Conversion of an alkyl halide to an alcohol is normally done under alkaline hydrolysis, but these conditions were not suitable for the reaction of **187** due to its base sensitive lactone functionality. In 2017 Shastri *et al.* reported a mild hydroxylation of alkyl



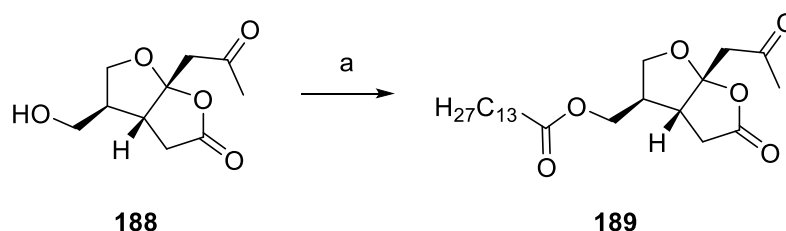
halides utilizing the nucleophilicity of water which is applicable for acid as well as base sensitive compounds.<sup>56</sup> Therefore, bromide **187** was heated to 80 °C in a DMF/H<sub>2</sub>O (1:4, v/v) mixture for 12 h resulting in the formation of the desired alcohol **188** in good yield (Scheme 39).



**Reagents and conditions:** a) DMF/H<sub>2</sub>O (1:4, v/v), 80 °C, 12 h, 72%.

**Scheme 39.** Synthesis of alcohol **188**.<sup>56</sup>

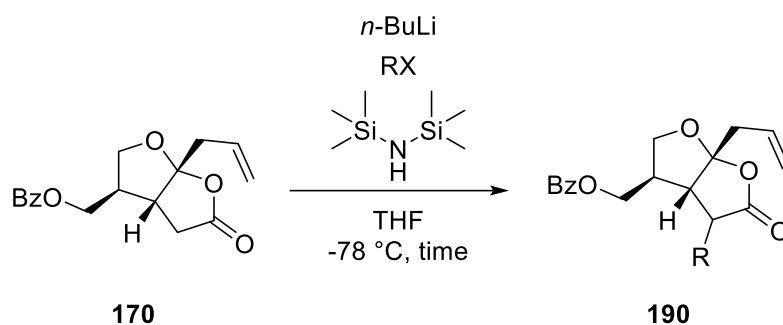
As already mentioned, the lipophilicity of a compound can have a great impact on its biological activity.<sup>54,55</sup> For this reason, alcohol **188** should be esterified in order to obtain the fatty acid ester derivative **189**. Using Et<sub>3</sub>N and catalytic amounts of DMAP, the C-13-fatty acid ester **189** was synthesized in very good yield from alcohol **188** and myristoyl chloride (Scheme 40).<sup>57</sup>



**Reagents and conditions:** a) myristoyl chloride (1.5 equiv.), DMAP (5 mol%), Et<sub>3</sub>N (1.5 equiv.), DCM, rt 3 h, 86%.

**Scheme 40.** Synthesis of the C-13-fatty acid ester **189**.<sup>57</sup>

Furthermore, different alkyl chains should be introduced in the  $\alpha$ -position of the lactone. This was accomplished *via*  $\alpha$ -alkylation using *in situ* generated LiHMDS and alkyl halides with different chain lengths (Table 10).<sup>58</sup>

**Table 10.**  $\alpha$ -alkylation of benzoate **170**.<sup>58</sup>

entry <sup>[a]</sup>	RX	time [h]	<i>dr</i> <sup>[b]</sup>	yield <sup>[c]</sup> [%]
1 <sup>[d]</sup>	CH <sub>3</sub> I	0.5	8:1	<b>190</b> <sup>[e]</sup> 64 (91% brsm)
2	C <sub>3</sub> H <sub>7</sub> I	1.5	-	-
3	C <sub>4</sub> H <sub>9</sub> Br	1.5	-	-
4	C <sub>8</sub> H <sub>17</sub> I	1.5	-	-

[a] 0.15 mmol **170**, RX (3.0 equiv.), *n*-BuLi (1.4 equiv.), HMDS (1.4 equiv.); [b] determined by <sup>1</sup>H-NMR of the crude mixture; [c] isolated yield; [d] different amounts of base were tested; [e] only the major diastereomer **191** was obtained after column chromatography.

The first reaction was carried out with MeI in order to introduce a methyl group in the  $\alpha$ -position of the lactone (entry 1). This reaction resulted in the formation of the desired product with a diastereomeric ratio of 8:1. However, no complete conversion could be achieved irrespective of the amount of base used. Moreover, after column chromatography, only the major diastereomer **191** was isolated in 64% (91% brsm). Unfortunately, the application of alkyl halides with longer chains only led to re-isolation of starting material while no product formation could be observed (entries 2-4). As even the *i*Pr and butyl halides showed no conversion, the introduction of bigger substituents than a methyl group seemed to be not feasible at this stage.

The absolute configuration of **191** was determined performing NOESY experiments. Regarding that the absolute configuration of the hydrogen at the ring junction and the hydrogens in the side chain was already unambiguously assigned, the direction of the methyl group could be determined by NOE cross peaks revealing that it is also orientated on the convex face of the bicycle (Figure 18).

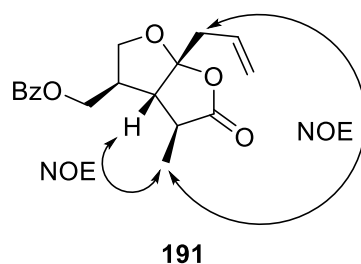
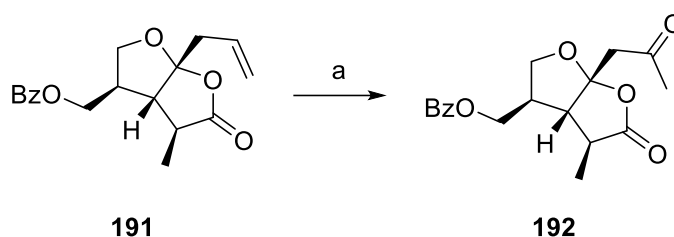


**Figure 18.** Determination of the absolute configuration of **191** by the presence of NOE cross peaks.

With **191** in hand, the allyl side chain should be oxidized to the desired methyl ketone. This was again accomplished *via* an oxymercuration/oxidation protocol and the (+)-paeonilide derivative **192** with a methyl group in the  $\alpha$ -position of the lactone was obtained in moderate yield (Scheme 41).



**Reagents and conditions:** a)  $\text{Hg}(\text{OAc})_2$  (0.5 equiv.), Jones reagent (3.0 equiv.), acetone/ $\text{H}_2\text{O}$  (4:1), rt, 30 h, 54%

**Scheme 41.** Synthesis of derivative **192**.

In summary, a small library of 9 (+)-paeonilide derivatives was successfully synthesized which could now be tested on their ability to inhibit the PAF-induced human platelet aggregation and furthermore be compared to the results obtained for the synthesized (+)-paeonilide (**49**). The results of this biological evaluation are presented in the next chapter.

### 3. Biological evaluation

#### 3.1 Platelet-activating factor (PAF)

Since its discovery in 1971 and structural elucidation in 1979, PAF (**52**) has been intensively studied, as it has been shown to be involved in a great variety of physiological and pathological functions.<sup>59,60</sup> From a chemical point of view, PAF (1-*O*-alkyl-2-acetyl-*sn*-glycero-3-phosphocholine, **52**) consists of an ether linked alkyl chain in the *sn*-1 position, an acetyl group in the *sn*-2 position and a phosphocholine group in the *sn*-3 position of the glycerol backbone.<sup>60</sup> There is a structural diversity in the ether linked alkyl chain depending on different species or cell types. However, the biologically most active species of PAF bear either a hexadecyl or an octadecyl group in the *sn*-1 position (Figure 19).<sup>61</sup>

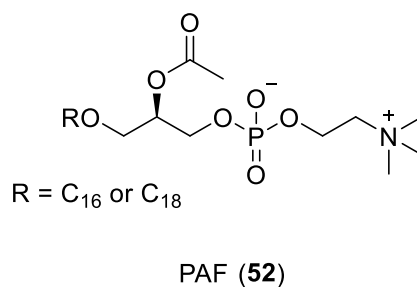
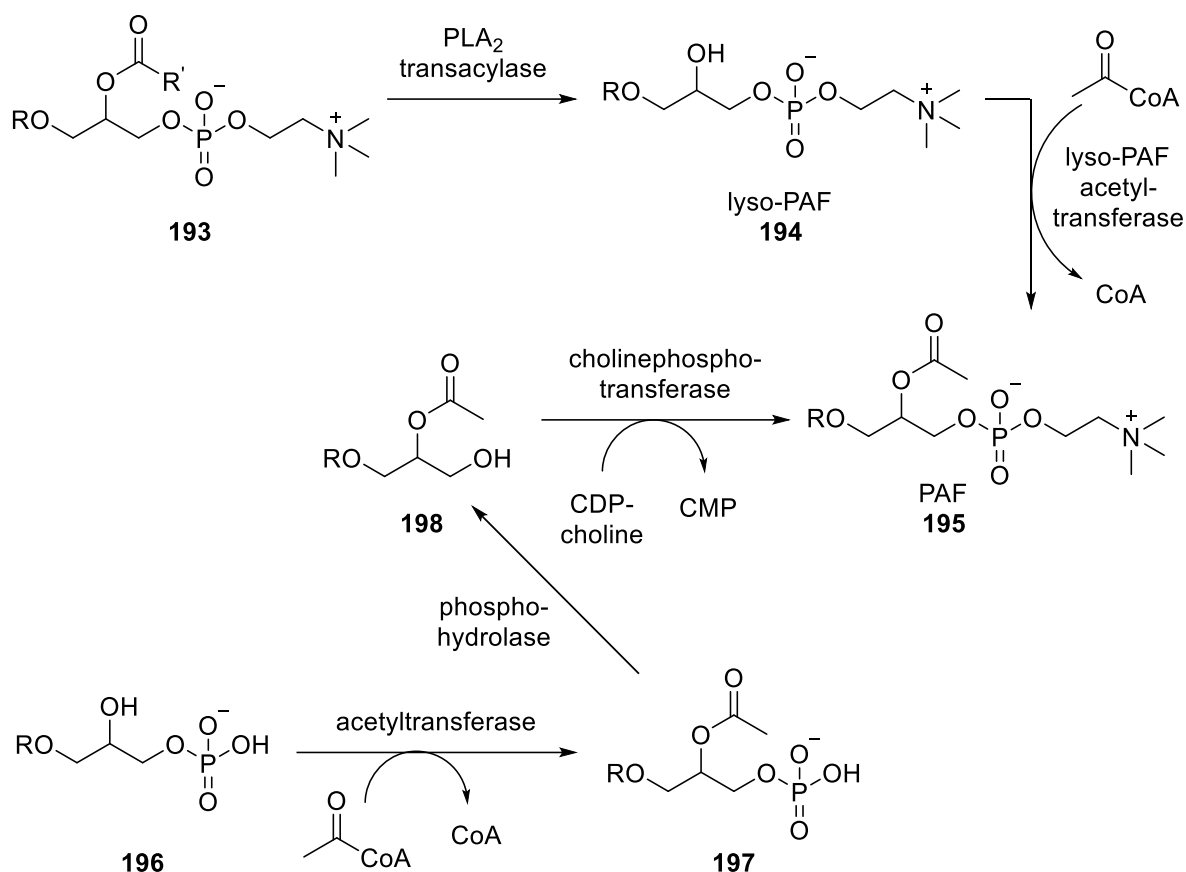


**Figure 19.** Structure of PAF (**52**).<sup>61</sup>

Despite its name, PAF (**52**) is not only involved in the activation of platelets but is also a phospholipid signaling molecule between the immune and the nervous system.<sup>60,61</sup> Moreover, it is a very potent mediator of inflammation in many different cells and tissues and therefore plays a pivotal role in acute and chronic inflammation.<sup>62</sup> In addition, PAF (**52**) may induce anaphylactic shock,<sup>63</sup> atherosclerosis<sup>64</sup> and rheumatoid arthritis.<sup>65</sup>

All kinds of PAF **195** are produced by a variety of different cells, *e.g.* endothelial cells, monocytes, neutrophils, platelets and macrophages, upon stimulation.<sup>60,66</sup> The biosynthesis can take place *via* two distinct pathways, on the one hand the remodeling pathway, and on the other hand the *de novo* pathway (Scheme 42).<sup>60,67</sup> The remodeling pathway starts with the hydrolysis of the fatty acid in the *sn*-2 position of a phospholipid **193** by phospholipase A<sub>2</sub> (PLA<sub>2</sub>) and a transacylase to produce biologically inactive lyso-PAF **194**.<sup>68</sup> PAF **195** is finally synthesized *via* acetylation of lyso-PAF **194** by an acetyl coenzyme A (acetyl-CoA) dependent acetyltransferase.<sup>60</sup>



**Scheme 42.** PAF biosynthesis *via* the remodeling (upper) pathway and the *de novo* (lower) pathway.<sup>60,67</sup>

The first step in the *de novo* biosynthesis of PAF **195** is an acetylation of **196** catalyzed by an acetyl coenzyme A (acetyl-CoA) dependent acetyltransferase. Subsequent dephosphorylation of **197** by a specific phosphohydrolase yields the alkylacetyl glycerol **198** which reacts with cytidine diphosphate choline (CDP-choline) to form PAF **195** and cytidine monophosphate (CMP) catalyzed by a cholinephosphotransferase.<sup>67</sup>

Binding of PAF (**52**) to the specific platelet-activating factor receptor (PAFR; gene name: PTAFR) starts up a signal transduction which leads to the activation of many humoral, autocrine and paracrine mechanisms.<sup>60</sup> From a chemical point of view PAFR belongs to the class of seven-transmembrane G-protein-coupled receptors and is a 342aa protein which is coded by an intronless gene. PAF (**52**) activates either the G<sub>q</sub> or the G<sub>i</sub> coupled PAFR and thus initiates several intracellular signaling pathways. However, there is a rising suspicion that PAF (**52**) can also act independently from its receptor.<sup>60</sup>

As PAF (**52**) participates in a variety of different physiological and pathological functions, the exploration of new PAFR-antagonists is of great interest. In order to determine the PAF-antagonism of a substance, mainly the inhibition of the PAF-induced aggregation of platelets

from different origins is measured.<sup>69</sup> PAF (**52**) is a very potent inducer of platelet aggregation in certain species, *inter alia* in guinea pig, rabbit and human.<sup>70</sup> On the one hand, binding of PAF (**52**) with the  $G_i$  coupled PAFR blocks the synthesis of cyclic adenosine monophosphate (cAMP) from adenosine triphosphate (ATP). On the other hand, stimulation of the  $G_q$  coupled receptor activates phospholipase C- $\beta$  (PLC $\beta$ ) leading to the formation of the second messengers inositol triphosphate (IP<sub>3</sub>) and diacylglycerol (DAG) from phosphatidylinositol 4,5-bisphosphate (PIP<sub>2</sub>). IP<sub>3</sub> binds to IP<sub>3</sub>-receptors (IP<sub>3</sub>R) - calcium channels in the dense tubular system - and leads to an increased concentration of Ca<sup>2+</sup> in the cytoplasm. DAG together with Ca<sup>2+</sup> then activates protein kinase C (PKC) causing several platelet responses (Figure 20).<sup>60,71,72</sup>

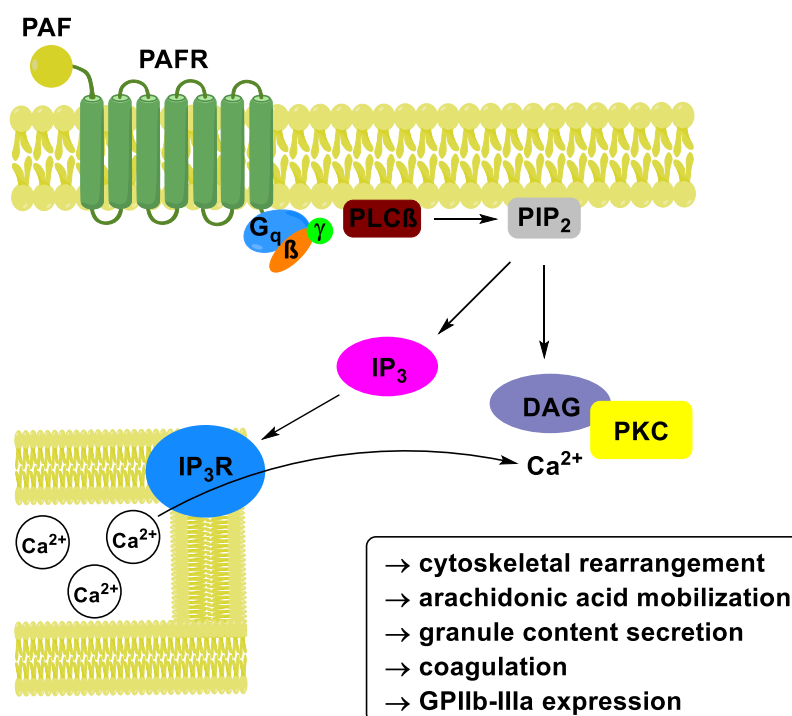


**Figure 20.** PAFR-dependent signaling pathway for platelet aggregation.<sup>60,71,72</sup>

A previous publication suggested that isolated (+)-paeonilide (**49**) might exert inhibitory effects on the PAF-induced platelet aggregation.<sup>52</sup> In this work, the PAF-antagonistic effects of the synthesized (+)-paeonilide (**49**) and derivatives on human platelets were evaluated by light transmission aggregometry.

### 3.2 Light transmission aggregometry

Since its discovery by Born *et al.* in 1967, the light transmission aggregometry is still one of the most useful methodologies for the test of *in vitro* platelet functions. An aggregometer is a spectrometer with several sample chambers kept at a temperature of 37 °C under continuous stirring. With this setup the change of absorbance of a sample after the addition of an aggregation-inducing agent can be recorded, as the agonist leads to aggregate formation and thus an increased light transmittance (Figure 21).<sup>73,74</sup>

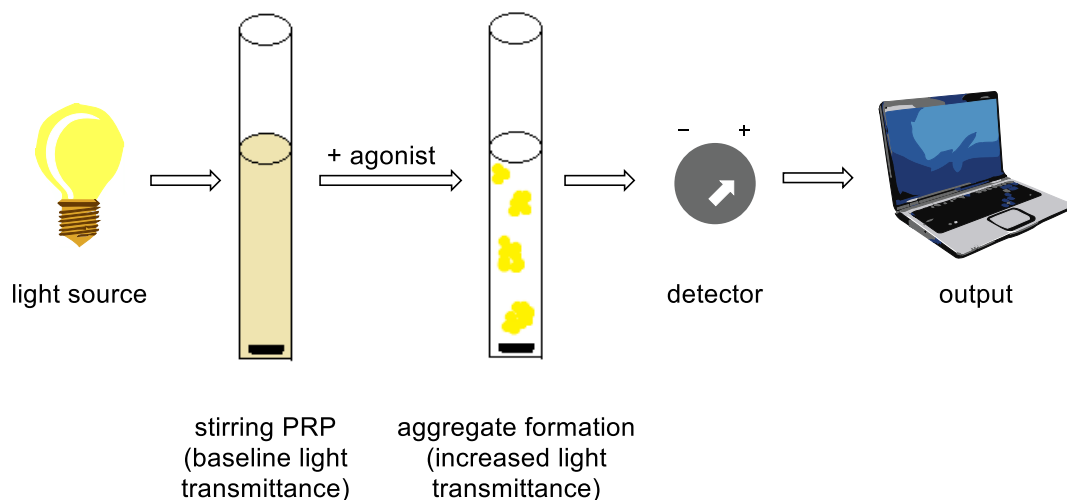


**Figure 21.** Scheme of light transmission (Born) aggregometry.

The tests were carried out in platelet rich plasma (PRP) with the use of platelet poor plasma (PPP) as reference. Both were obtained after collection and subsequent work-up of the blood. The PPP sample represented 100% transmission or 100% aggregation, respectively, and thus served as reference. One PRP sample was treated with the respective concentration of the inhibitor in DMSO. A second PRP sample was diluted to the same volume with DMSO containing no inhibitor, in order to serve as reference for the calculation of the inhibitory effect. After incubation for five minutes at 37 °C, both samples were put in a sample chamber and continuously stirred in order to simulate the shear stress of a vessel. The light transmission was set to 0% and then a specific amount of agonist was added to both PRP samples. In this way, two different graphs were obtained, one for the sample with antagonist and the other without antagonist. The potency of the antagonist could be calculated after comparison of the

two detected curves: either the difference in the maximum aggregation or the difference in the slope was used.

### 3.3 Results

In order to investigate the influence of several functional groups in different positions on the inhibition of the PAF-induced human platelet aggregation, (+)-paeonilide (**49**) and a small library of 9 derivatives were tested (Figure 22). The light transmission aggregometry was carried out independently at the University of Regensburg, Faculty of Chemistry and Pharmacy, under the supervision of Prof. Dr. Schlossmann.

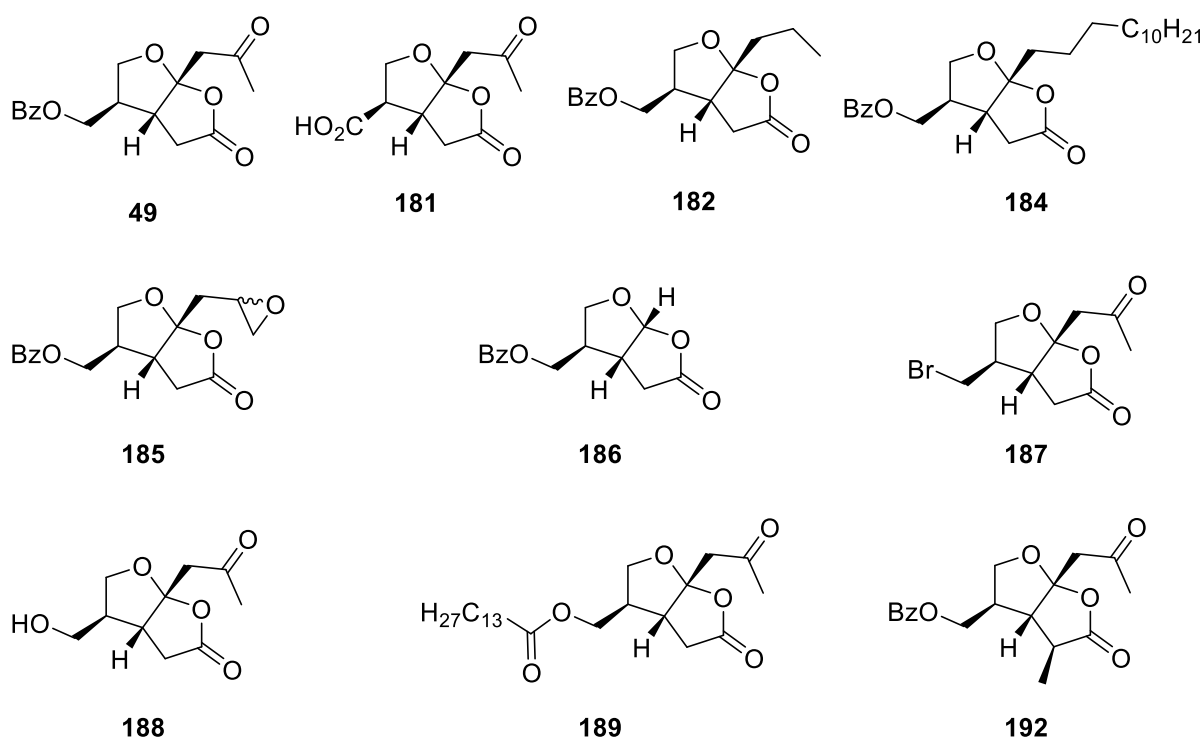


**Figure 22.** (+)-paeonilide (**49**) and derivatives for biological evaluation.

As mentioned above, the  $IC_{50}$  value was calculated using either the maximum aggregation or the slope. Using the slope for the determination of the  $IC_{50}$  value mostly resulted in slightly increased values, however, all results are highly comparable. The  $IC_{50}$  values for each compound and both calculation methods are stated in  $[\mu\text{g}\cdot\text{mL}^{-1}]$  and in order to achieve a better comparability also in  $[\mu\text{M}]$ . Furthermore, the potency of (+)-paeonilide (**49**) was



arbitrarily set to 100% in order to be able to directly compare each derivative to the synthesized (+)-paeonilide (**49**) (Table 11).

**Table 11.** Inhibition of PAF-induced platelet aggregation by (+)-paeonilide (**49**) and derivatives.

compound	maximum aggregation			slope		
	IC <sub>50</sub> [μg·mL <sup>-1</sup> ]	IC <sub>50</sub> [μM]	potency [%]	IC <sub>50</sub> [μg·mL <sup>-1</sup> ]	IC <sub>50</sub> [μM]	potency [%]
<b>49</b>	22.0	69.0	100	27.9	87.6	100
<b>181</b>	132.0	578.5	11.9	138.9	608.8	14.4
<b>182</b>	105.4	348.5	19.8	116.0	383.7	22.8
<b>184</b>	241.9	544.2	12.7	225.8	507.9	17.2
<b>185</b>	20.9	65.7	105.0	18.9	59.2	148.0
<b>186</b>	82.4	372.9	18.5	89.1	403.0	21.7
<b>187</b>	33.4	120.6	57.2	54.6	196.9	44.5
<b>188</b>	>300	>1000	-	>300	>1000	-
<b>189</b>	191.3	450.6	15.3	211.7	498.7	17.6
<b>192</b>	18.0	54.2	127.3	18.0	54.1	161.9

Although the bioassay for the natural (+)-paeonilide (**49**) was not specified, the result for the inhibition of the PAF-induced human platelet aggregation by the synthetic sample was in accordance with the literature reported IC<sub>50</sub> value (8 μg·mL<sup>-1</sup> or 25 μM).<sup>52</sup> Acid **181** as well as the two derivatives bearing an alkyl side chain **182** and **184** showed a drastic decrease in inhibitory effect. Comparison of the latter two proved that elongation of the alkyl chain had an adverse effect on the biological activity. With epoxide **185** a quite similar or even slightly increased inhibition was observed, underlining the importance of an oxygen functionality in the side chain in the acetal position. Derivative **186** bearing no side chain again showed a drop of inhibition. Bromide **187** gave at least moderate results, while alcohol **188** turned out to be completely inactive. This could maybe due to its extremely high polarity and the consequent incapability of proper binding to PAFR. Fatty acid ester **189** proved that a long alkyl chain has also an adverse effect in this position. Derivative **192** showed an increased biological activity and therefore led to the presumption that an alkyl chain in the α-position of the lactone has a beneficial effect on the inhibition of the PAF-induced platelet aggregation.

In summary, the bioassay indicated that the side chains have a great impact on the inhibitory effect. Exchange of the methyl ketone group to an alkyl chain or its complete removal resulted in a significant decrease of biological activity, while epoxidation more or less led to similar

outcome. Therefore, it could be concluded that the oxygen moiety in this side chain might play a pivotal role. Furthermore, it was shown that the benzoyl group in the other side chain was the most potent functional group so far. Moreover,  $\alpha$ -alkylation appeared to have a beneficial effect on the biological activity.

The concentration-dependent inhibition of human platelet aggregation was also graphically illustrated (Figure 23 and 24).

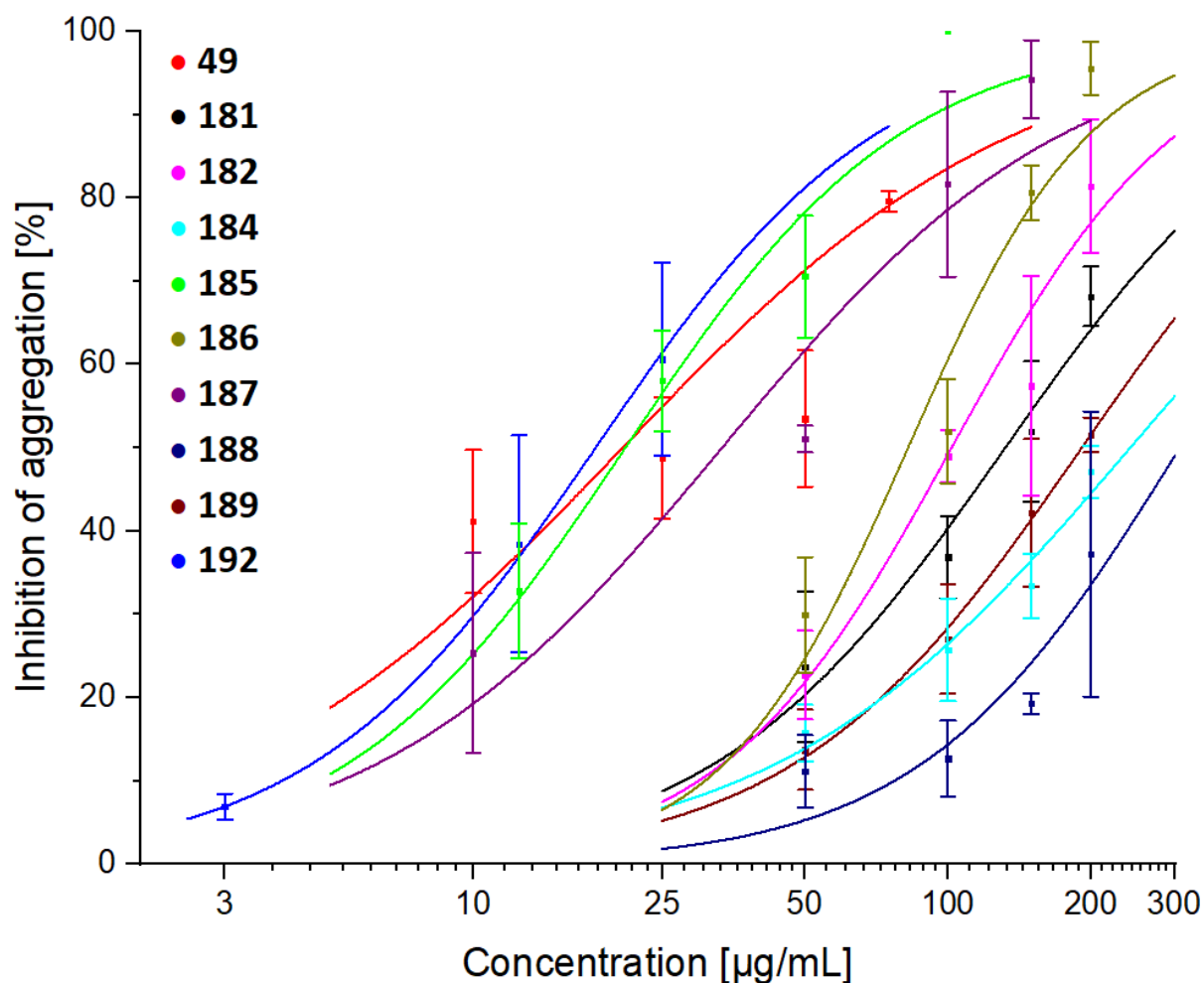


**Figure 23.** Concentration-dependent inhibition of aggregation (calculated by the maximum aggregation).

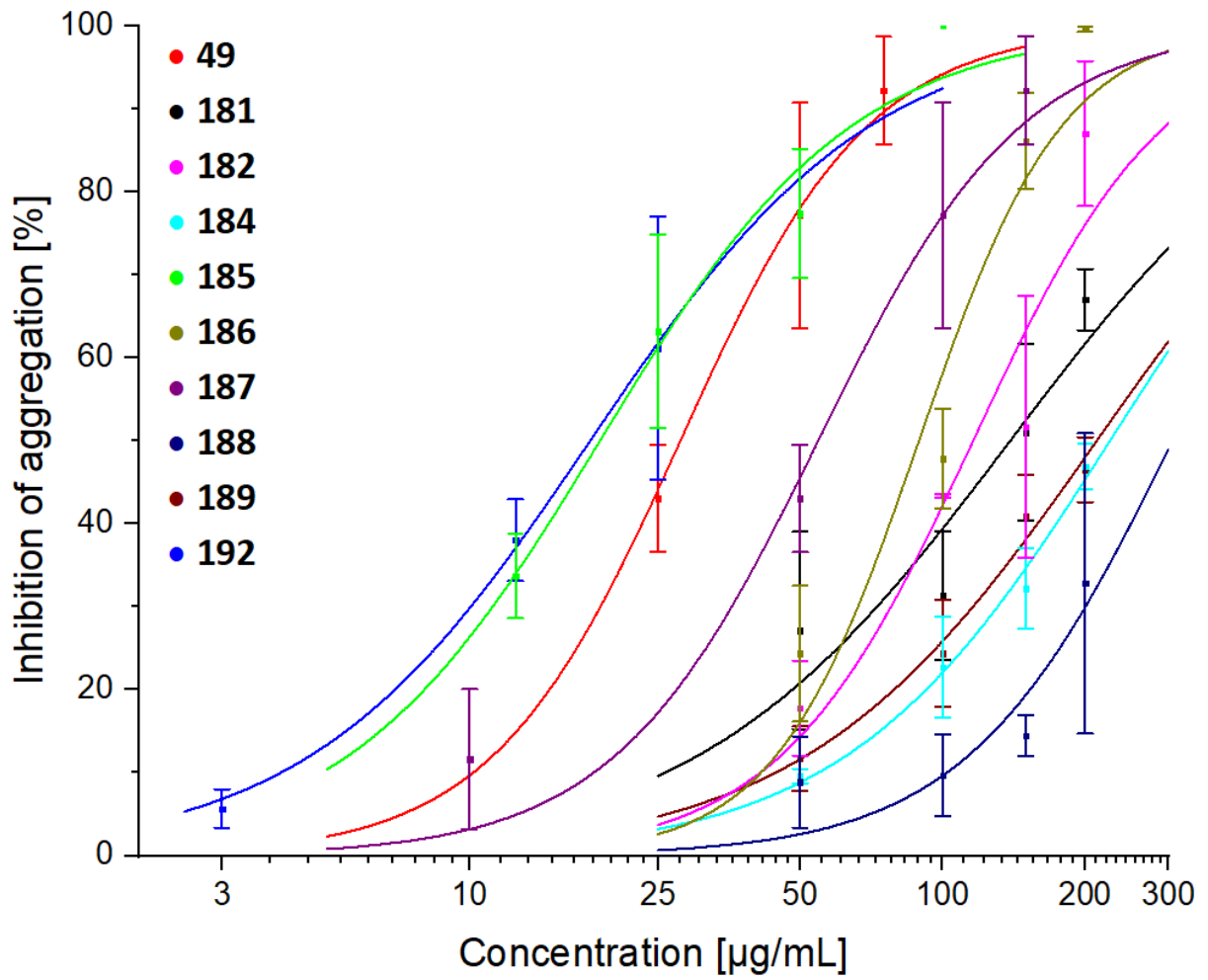


**Figure 24.** Concentration-dependent inhibition of aggregation (calculated by the slope).

## 4. Studies toward Dermatolactone

### 4.1 Introduction

Another natural product bearing the furo[2,3-*b*]furanone core structure fused to a second cyclic fragment in the C-4 position is the so-called dermatolactone (**199**). This novel sesquiterpene was first isolated from the culture broth of an ascomycete (strain A4990) in 1996. Its relative structure was established by NMR and mass spectrometry (Figure 25).<sup>75</sup>

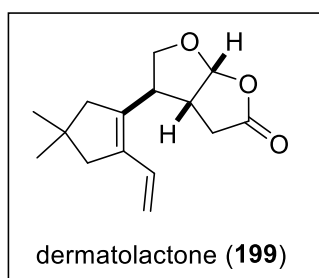
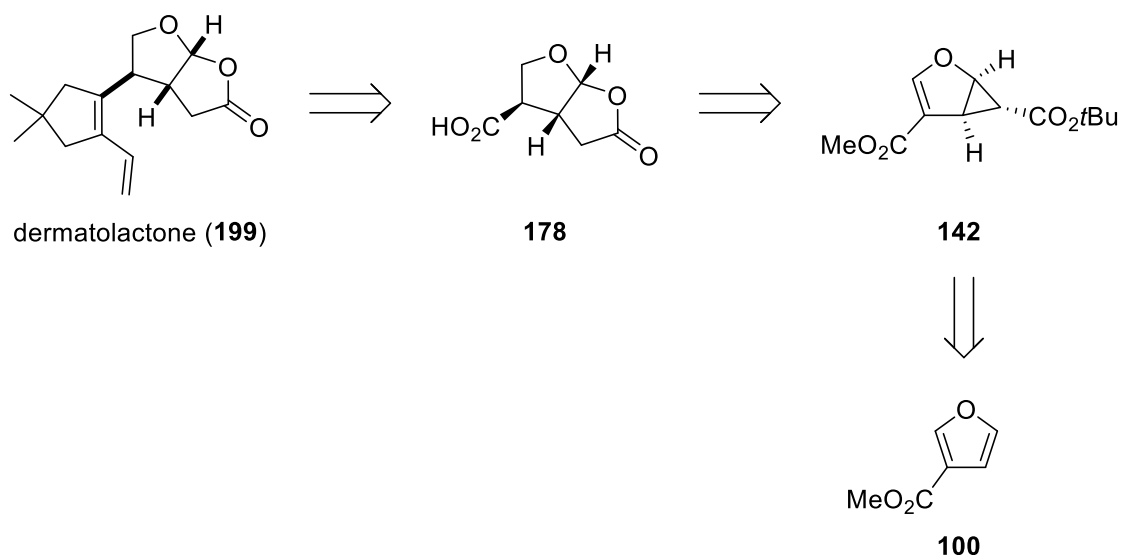


**Figure 25.** Relative structure of dermatolactone (**199**).<sup>75</sup>

Moreover, it was shown that dermatolactone (**199**) is not only cytotoxic against different mammalian cell lines but also possesses antimicrobial activity.<sup>75</sup> As the absolute stereochemistry of dermatolactone (**199**) has not yet been determined and no total synthesis has been reported until today, an artificial total synthesis would be worthwhile in order to establish the absolute structure of dermatolactone (**199**) and to investigate its still underexplored biological activity.

Since furo[2,3-*b*]furanone **178** bearing a carboxylic acid group in the C-4 position was already synthesized during the derivatization of (+)-paeonilide (**49**), it seemed to be a suitable precursor for the synthesis of dermatolactone (**199**). For this reason, the retro synthetic analysis of the target compound **199** starts similar to the synthesis of (+)-paeonilide (**49**). Cyclopropanation of 3-furoic acid methyl ester (**100**) introduces the chiral information yielding **142**. Acid-mediated cyclopropane ring-opening/lactonization gives rise to the precursor **178**. The key step in this synthesis should be a visible light-mediated conjugate addition in order to introduce the carbocyclic fragment into the side chain, which should finally be transformed to dermatolactone (**199**) (Scheme 43).



**Scheme 43.** Retrosynthesis of dermatolactone (**199**).

## 4.2 Visible light-mediated reactions

### 4.2.1 Introduction

Photochemistry is a powerful methodology to accomplish a variety of chemical reactions which actually require harsh conditions or toxic reagents.<sup>76,77</sup> Classically, molecules were directly excited in order to trigger reactivity. Since most organic molecules do not absorb light in the visible range, higher energy ultra-violet (UV) irradiation is necessary to activate them. However, the use of UV light has many drawbacks and therefore different photocatalysts, which absorb photons from visible light and transfer either energy or electrons to the reagents, have been developed in order to circumvent this problem.<sup>78</sup> The main catalysts which are employed for this purpose, are organic dyes, inorganic semiconductors or transition-metal complexes.<sup>79</sup> Common transition-metal based photocatalysts are [Ir(dF(CF<sub>3</sub>)ppy)<sub>2</sub>(dtbbpy)]<sup>+</sup> (**200**), *fac*-Ir(ppy)<sub>3</sub> (**201**), and [Ru(bpy)<sub>3</sub>]<sup>2+</sup> (**202**) (Figure 26).

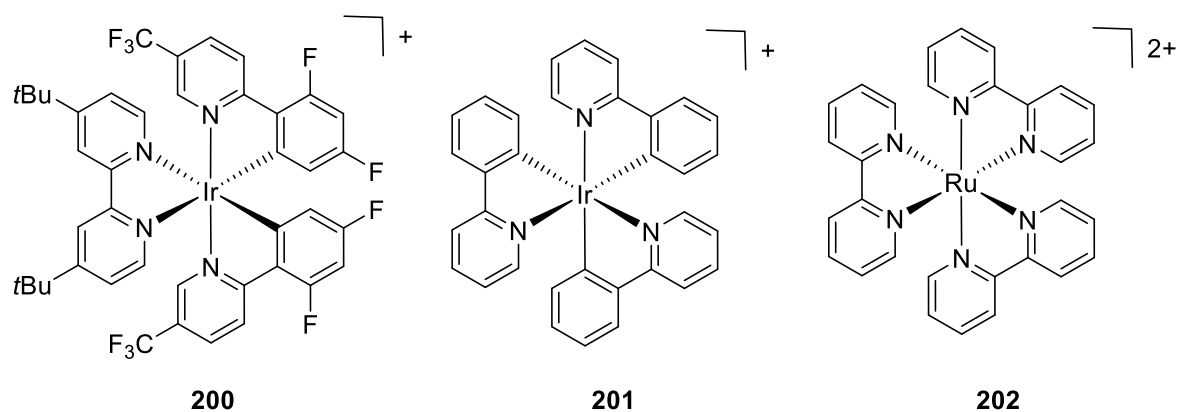
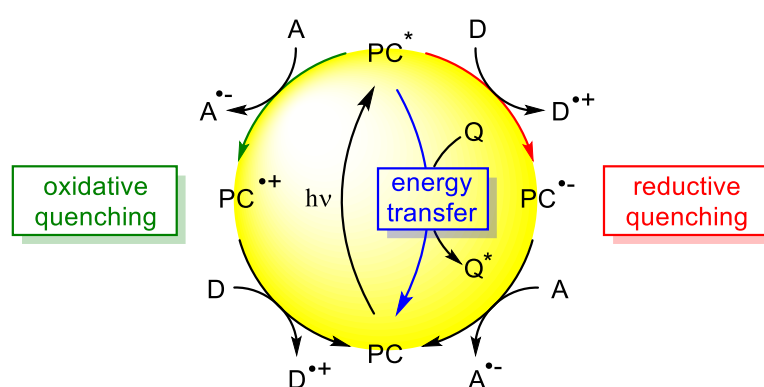


**Figure 26.** Common transition-metal photocatalysts.

A photocatalyst (PC) absorbs light in the visible range and is thereby promoted to its excited state  $\text{PC}^*$ . Subsequently, a suitable reagent can react with  $\text{PC}^*$  either in a quenching or an energy transfer process (Scheme 44).<sup>80</sup> The photoredox pathway can take place in an oxidative or a reductive quenching cycle. If an electron acceptor (A) is present in the reaction, it gets reduced *via* a single electron transfer (SET) from the excited photocatalyst ( $\text{PC}^*$ ). The cationic species  $\text{PC}^{\bullet+}$  formed in this way is then reduced by a suitable electron donor (D) in order to close the oxidative quenching cycle and regenerate the neutral photocatalyst (PC). Similarly,  $\text{PC}^*$  gets reduced in the presence of an electron donor (D) in the reductive quenching cycle. Thereby, the anionic species  $\text{PC}^{\bullet-}$  has to react with an electron acceptor (A) to form the neutral photocatalyst (PC) again.



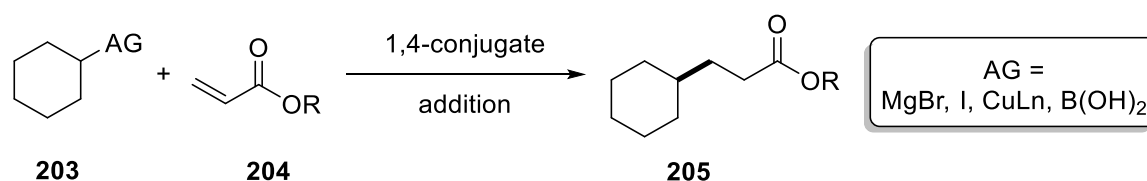
**Scheme 44.** General reaction pathway of a photoredox catalyst.<sup>31</sup>

Moreover, the photocatalyst (PC) can also act as a photosensitizer and transfer energy to a suitable substrate (Q) which has incompatible redox potentials and therefore is not able to undergo a SET.<sup>80</sup>

Especially in the last decade, a great variety of transformations was accessible by visible light-mediated photoredox catalysis. This methodology was applied, *inter alia*, for atom transfer radical additions (ATRA),<sup>81</sup> deoxygenations,<sup>82</sup> dehalogenations<sup>83</sup> or cycloadditions.<sup>84</sup> For the construction of dermatolactone (**199**), a photoinduced decarboxylative conjugate addition seemed to be an elegant reaction.

#### 4.2.2 Direct conjugate addition

1,4-conjugate additions play a pivotal role in organic chemistry for the construction of new carbon-carbon bonds. Thereby, an electrophilic olefin or Michael acceptor **204** reacts with a nucleophile or a SOMO-activated molecule **203** in a 1,4-addition to give the coupled product **205** (Scheme 45).<sup>85</sup>



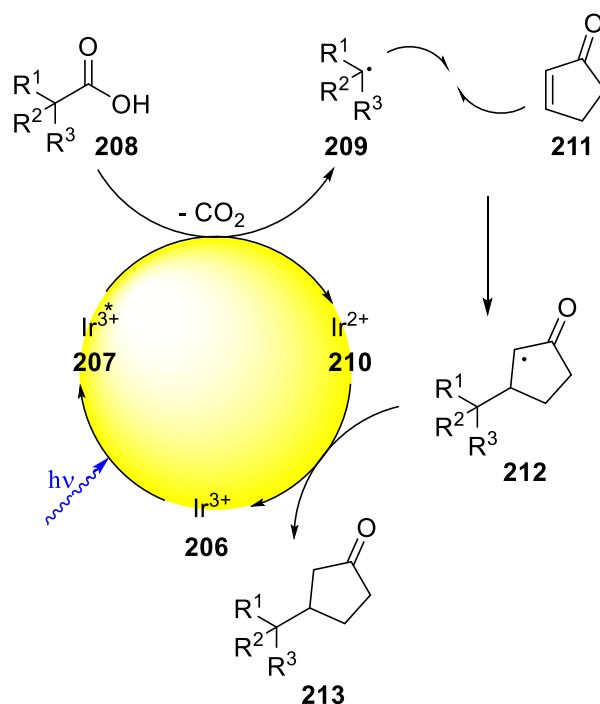
**Scheme 45.** Common 1,4-conjugate addition.<sup>85</sup>

Common activation groups (AGs) for this kind of reaction are Grignard reagents,<sup>86</sup> alkyl iodides,<sup>87</sup> organo cuprates<sup>88</sup> or boronic acids.<sup>89</sup>

In 2014, MacMillan *et al.* reported a radical 1,4-conjugate addition using carboxylic acids as a simple and traceless activation group. Decarboxylation under photoredox conditions facilitated the reaction with Michael acceptors without the need of stoichiometric amounts of organometallic compounds.<sup>85</sup>

Irradiation of an Ir(III)-photoredox catalyst **206** with visible light generates the strongly oxidizing excited state Ir(III)\* **207**. Base-mediated deprotonation of a carboxylic acid **208** followed by a single-electron transfer (SET) leads on the one hand to the formation of alkyl radical **209** under extrusion of CO<sub>2</sub>, and on the other hand to the reduced Ir(II)-species **210**. The highly nucleophilic radical **209** reacts with a Michael acceptor **211** in a conjugate addition

forming radical **212**. A second SET leads to the reduction of radical **212** by the Ir(II)-complex **210** and thus yields the desired 1,4-addition product **213** along with the regenerated photocatalyst **206** (Scheme 46).<sup>85</sup>



**Scheme 46.** Proposed mechanism for the decarboxylative conjugate addition.<sup>85</sup>

With the carboxylic acids **155** and **178** in hand, this methodology should be applied in order to introduce a suitable cyclic fragment in the side chain for the total synthesis of dermatolactone (**199**). Therefore, the reaction was carried out with 2-cyclopentenone (**211**) as model substrate and  $[\text{Ir}[\text{dF}(\text{CF}_3)\text{ppy}]_2(\text{dtbbpy})]\text{PF}_6$  as photocatalyst in DMF (Table 12). As CsF and  $\text{K}_2\text{HPO}_4$  were reported to show good results, both were applied as base for this test reactions. Using carboxylic acid **155** as Michael donor for the conjugate addition only resulted in partial decomposition and recovery of starting material (entries 1 and 2). Unfortunately, the same results were obtained with carboxylic acid **178** as starting material (entries 3 and 4). One explanation for these unfruitful results could be the oxidation potential of the used substrates. The oxidation potentials for both **155** as well as **178** were determined as more than +2.5 V versus the saturated calomel electrode (SCE) by cyclic voltammetry (CV) and were therefore unlikely for reactions with common photocatalysts.



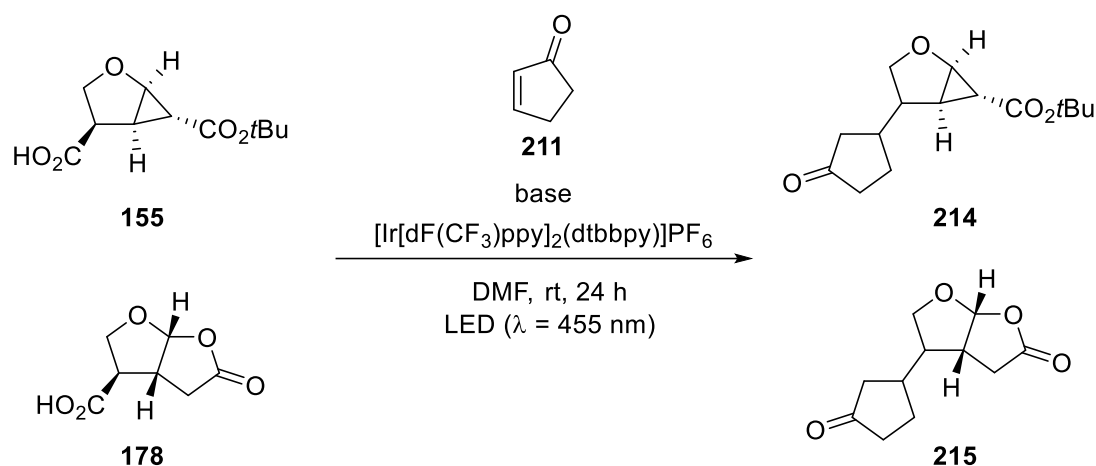


**Table 12.** Decarboxylative conjugate addition of carboxylic acid **155** and **178**.

entry <sup>[a]</sup>	substrate	base	yield [%]	recovered starting material [%]
1	<b>155</b>	$\text{K}_2\text{HPO}_4$	-	58
2	<b>155</b>	CsF	-	41
3	<b>178</b>	$\text{K}_2\text{HPO}_4$	-	73
4	<b>178</b>	CsF	-	61

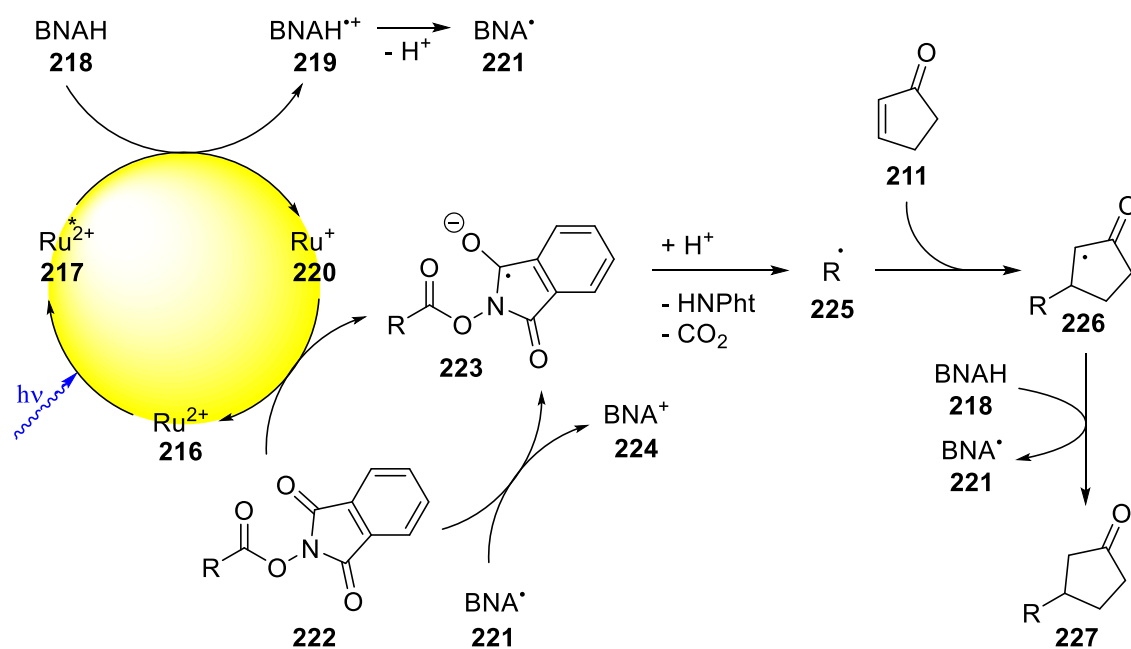
[a] 0.3 mmol **155** or **178**, 2-cyclopentenone (**211**) (3.0 equiv.),  $[\text{Ir}[\text{dF}(\text{CF}_3)\text{ppy}]_2(\text{dtbbpy})]\text{PF}_6$  (1 mol%), base (1.2 equiv.).

As none of these test reactions yielded the desired product, the reactivity of the substrates should be enhanced by transformation of the carboxylic acid group to an active ester.

#### 4.2.3 Decarboxylation of *N*-acyloxyphthalimides

Decarboxylation reactions have been intensively investigated in the last decades and are still of great interest because carboxylic acids are readily available, non-toxic and stable starting materials for synthesis.<sup>88</sup> Due to the fact that the direct transformation of the carboxylic acids **155** and **178** was not sufficient, they should be converted to more reactive derivatives. One very famous example is the decarboxylation of thiohydroxamate esters *via* homolytical cleavage of the N-O bond under thermal or photochemical conditions known as Barton decarboxylation.<sup>90</sup> An alternative active ester for decarboxylation reactions using irradiation was reported by Okada *et al.* in 1988. They used *N*-hydroxyphthalimide in order to activate the carboxylic acid moiety.<sup>91</sup> In 1991, the same group extended the scope of this methodology

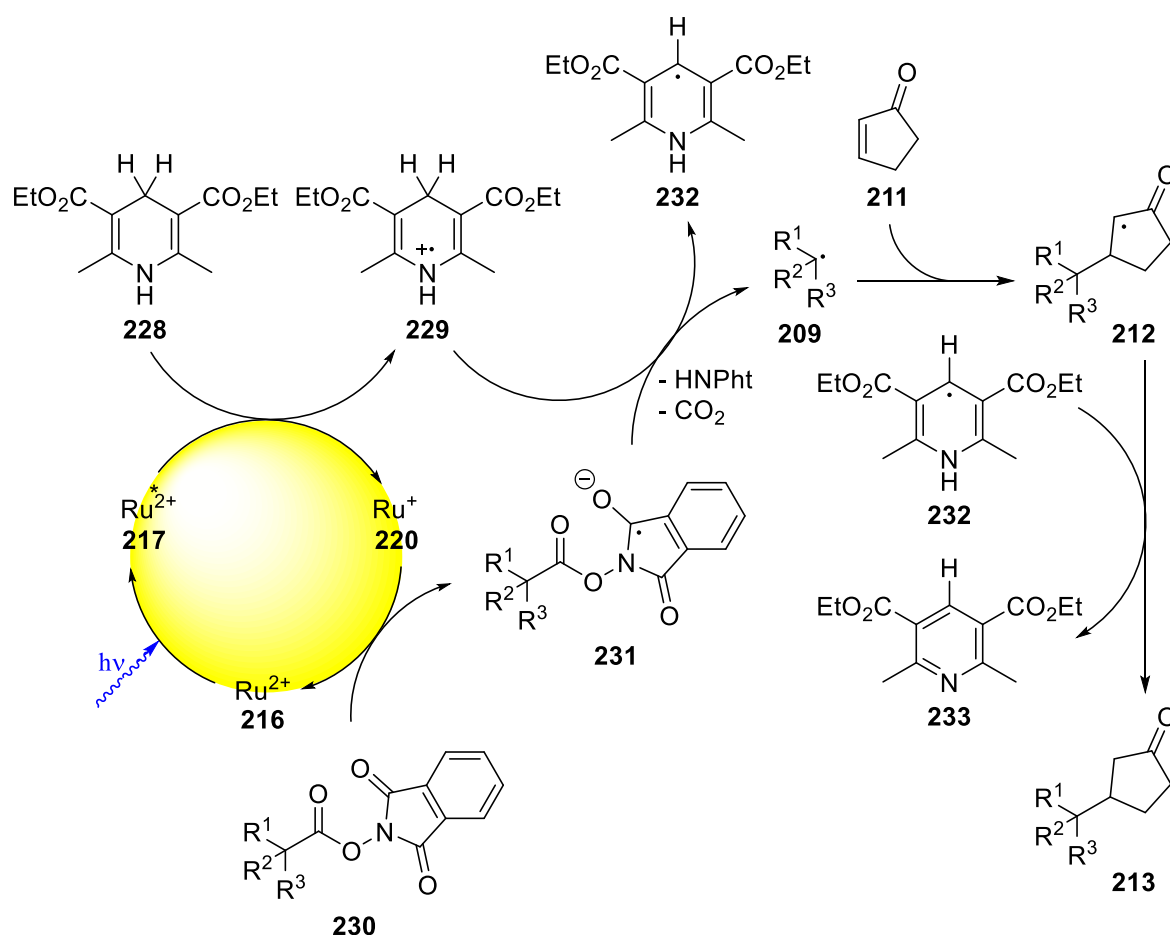
to a visible light-mediated photoredox-catalyzed Michael addition in aqueous solution (Scheme 47).<sup>92</sup>



**Scheme 47.** Proposed mechanism for the decarboxylative conjugate addition of *N*-acyloxyphthalimides **222**.<sup>92</sup>

Initially, photocatalyst **216** gets excited by visible light to **217** which undergoes a SET with 1-benzyl-1,4-dihydronicotinamide (BNAH, **218**) forming the oxidized BNAH radical cation **219** and the reduced photocatalyst **220**. **219** gets deprotonated to give BNA<sup>•</sup> **221** while the reduced photocatalyst **220** reduces the *N*-acyloxyphthalimide **222** to the radical anion **223** which can also be obtained by reduction of **222** with radical **221**. Alkyl radical **225** is then formed under cleavage of phthalimide and extrusion of CO<sub>2</sub> and adds to the electron-deficient olefin **211**. Finally, radical **226** abstracts a hydrogen-atom from BNAH **218** leading to radical **221** and the desired conjugate addition product **227**.

Taking up this earlier idea, Overman *et al.* reported a slightly modified version of the photoredox-catalyzed decarboxylative conjugate addition which could be applied even to trialkyl-substituted *N*-acyloxyphthalimides. Using a [Ru]<sup>2+</sup> photocatalyst together with Hantzsch ester **228** and DIPEA they were able to generate tertiary alkyl radicals **209** from the corresponding *N*-acyloxyphthalimide derivatives **230** (Scheme 48).<sup>93</sup>



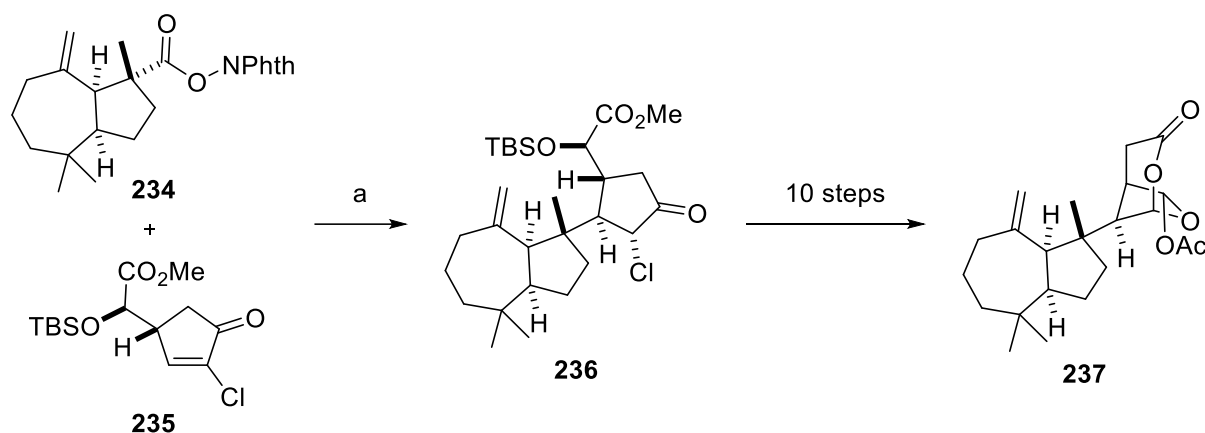
**Scheme 48.** Proposed mechanism for the decarboxylative cross-coupling of *N*-acyloxypthalimides **230** with the use of Hantzsch ester **228**.<sup>93</sup>

Initially, photocatalyst **216** is promoted to its excited state **217** upon irradiation with visible light. **217** then gets reduced by Hantzsch ester **228** to give the highly reducing Ru(I)-photocatalyst **220** which then undergoes a SET to form the radical anion **231** and regenerate the catalyst **216**. The tertiary alkyl radical **209** is generated by homolytic fragmentation and decarboxylation of **231**. Coupling of this radical **209** with a suitable Michael acceptor **211** leads to the stabilized radical **212** which abstracts a hydrogen-atom from **232** to give the desired conjugate addition product **213**.

Applying this methodology it was not only possible to couple tertiary radicals **209** with different electron-deficient olefins but also to use them for substitution reactions with allylic or vinylic halides in order to construct new C-C bonds and quaternary centers.<sup>93</sup> Moreover, this application was also used for natural product synthesis.<sup>94</sup>

Using the conditions mentioned above *N*-acyloxypthalimide **234** was successfully added to the electron-deficient olefin **235** to form the conjugate addition product **236** in 61% yield. This

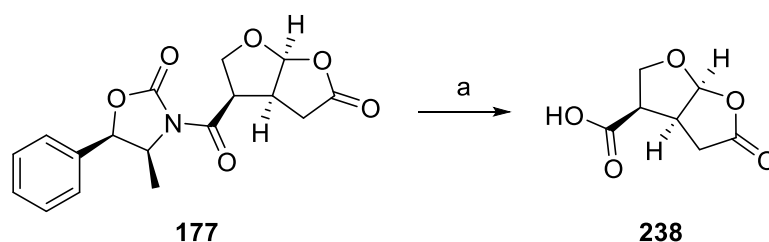
reaction represented the key step in the total synthesis of the rearranged spongian diterpene (-)-aplyviolene (**237**) (Scheme 49).<sup>94</sup>



**Reagents and conditions:** a) **235** (1.5 equiv.), Hantzsch ester (**228**) (1.5 equiv.), DIPEA (2.25 equiv.), [Ru(bpy)<sub>3</sub>](BF<sub>4</sub>)<sub>2</sub> (1 mol%), DCM, LED ( $\lambda = 455$  nm), rt, 2.5 h, 61%.

**Scheme 49.** Photoredox-catalyzed decarboxylative conjugate addition of **234** and **235** as key step in the total synthesis of (-)-aplyviolene (**237**).<sup>94</sup>

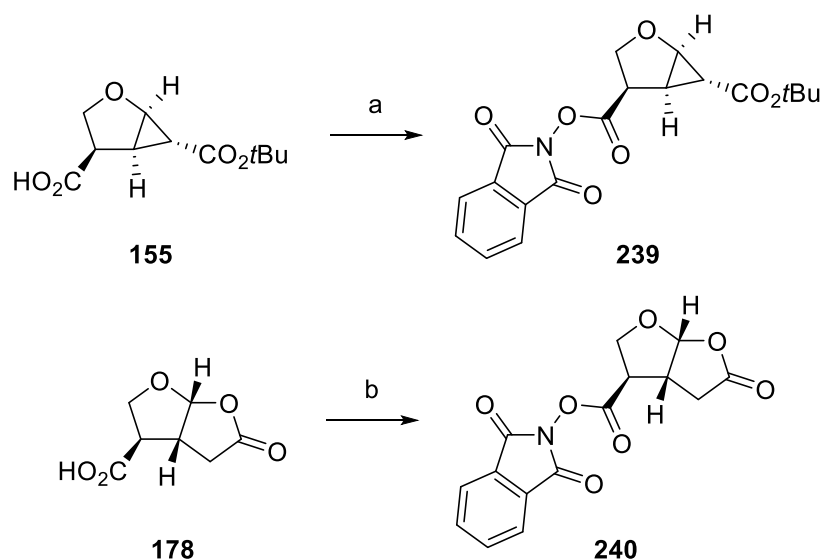
Remarkably, intermediate **236** was obtained as a single diastereomer. The diastereoselectivity of this reaction was explained by the fact that the coupling took place from the sterically less hindered convex face of the bicycle **234**. This outcome seemed to be quite promising in order to use such a decarboxylative conjugate addition for the synthesis of dermatolactone (**199**). As the absolute stereochemistry of dermatolactone (**199**) has not yet been determined, it was envisaged to develop a synthetic route which enables access to both enantiomers. With the knowledge that decarboxylative conjugate additions can be quite diastereoselective with regard to the steric hindrance of the generated alkyl radical, a furo[2,3-*b*]furanone with contrary configuration at the ring junction compared to acid **178** should be synthesized. During the synthesis of an acid derivative of (+)-paeonilide (**49**), oxazolidinone **177** was obtained which seemed to be a suitable precursor for this purpose. Cleavage of the chiral auxiliary could be achieved in very good yield under mild conditions using LiOH, thus, giving rise to diastereomerically and enantiomerically pure acid **238** (Scheme 50).<sup>53</sup>



**Reagents and conditions:** a) LiOH (2.0 equiv.), H<sub>2</sub>O/THF (1:3, v/v), 0 °C, rt, 0.5 h, 89%.

**Scheme 50.** Cleavage of the chiral auxiliary of **177**.

However, for the initial test reactions of the decarboxylative conjugate addition only the two carboxylic acids **155** and **178** were used. Therefore, these two should be transformed to their corresponding *N*-acyloxyphthalimides. In both cases, the coupling reaction with *N*-hydroxyphthalimide and DCC proceeded smoothly giving the desired active esters **239** and **240** in 91% and 84%, respectively (Scheme 51).



**Reagents and conditions:** a) *N*-hydroxyphthalimide (1.1 equiv.), DCC (1.1 equiv.), THF, rt, 20 h, 91%; b) *N*-hydroxyphthalimide (1.1 equiv.), DCC (1.1 equiv.), THF, rt, 20 h, 84%.

**Scheme 51.** Transformation of the two carboxylic acids **155** and **178** to their corresponding *N*-acyloxyphthalimides.

With these two *N*-acyloxyphthalimides in hand, the visible light-mediated decarboxylative conjugate addition should be performed. Therefore, the conditions described by Overman *et al.* using [Ru(bpy)<sub>3</sub>]<sup>2+</sup> as photocatalyst together with Hantzsch ester **228** and DIPEA were applied and 2-cyclopentenone **211** was used as model Michael acceptor (Table 13).

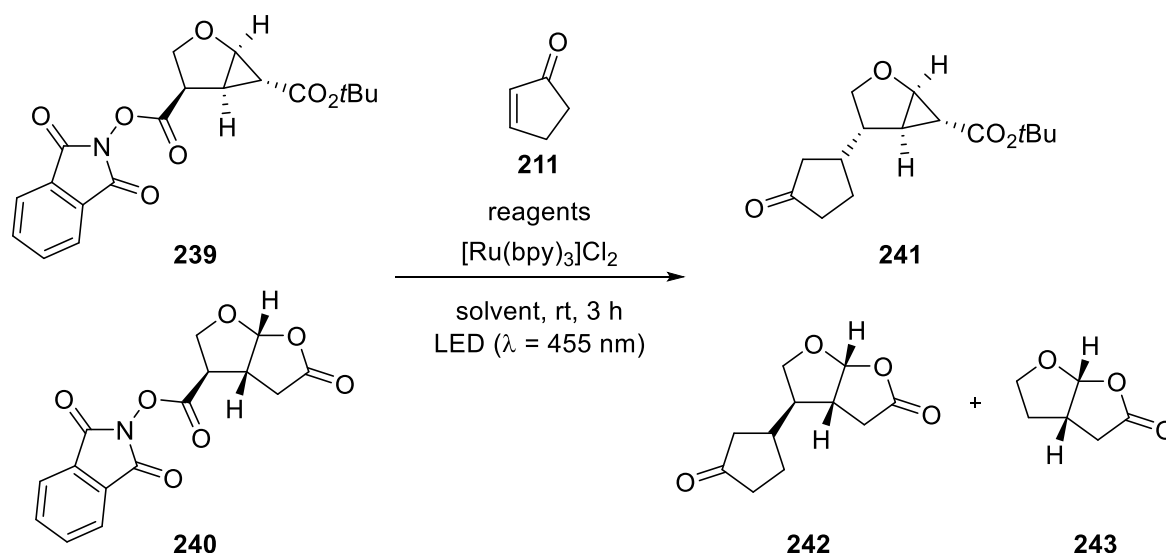


**Table 13.** Visible light-mediated decarboxylative conjugate addition of **239** and **240**.

entry	substrate	solvent	reagents	$dr^{[c]}$	yield
1 <sup>[a]</sup>	<b>239</b>	MeCN	Hantzsch ester, DIPEA	-	-
2 <sup>[a]</sup>	<b>240</b>	MeCN	Hantzsch ester, DIPEA	-	<b>243</b> 22%
3 <sup>[b]</sup>	<b>240</b>	MeCN	Hantzsch ester	1.2:1	<b>242</b> 33% <b>243</b> 26%
4 <sup>[b]</sup>	<b>240</b>	DMF	Hantzsch ester	1.1:1	<b>242</b> 21% <b>243</b> 28%
5 <sup>[b]</sup>	<b>240</b>	THF	Hantzsch ester	1.1:1	<b>242</b> 31% <b>243</b> 29%
6 <sup>[b]</sup>	<b>240</b>	Acetone/H <sub>2</sub> O	Hantzsch ester	1.2:1	<b>242</b> 30% <b>243</b> 18%

[a] 0.3 mmol **239** or **240**, 2-cyclopentenone (**211**) (5.0 equiv.), Hantzsch ester (**228**) (1.5 equiv.), DIPEA (2.25 equiv.), [Ru(bpy)<sub>3</sub>]Cl<sub>2</sub> (1 mol%); [b] 2-cyclopentenone (**211**) (8.0 equiv.), Hantzsch ester (**228**) (1.1 equiv.), [Ru(bpy)<sub>3</sub>]Cl<sub>2</sub> (1 mol%); [c] determined by <sup>1</sup>H-NMR.

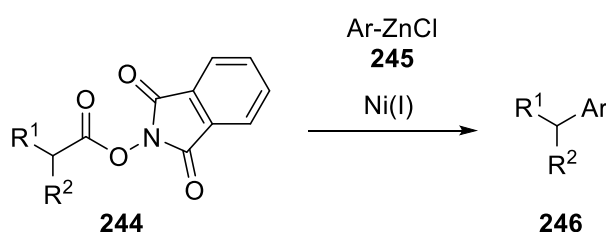
The initial test reaction using cyclopropane **239** led to full conversion of the starting material, however, no product was obtained and only decomposition was observed (entry 1). Applying the same conditions to furo[2,3-*b*]furanone **240** again resulted in full conversion, but only the decarboxylation product **243** was obtained in 22% but no formation of the conjugate addition product **242** was observed (entry 2). Omitting the use of DIPEA, finally gave the desired addition product **242** as an inseparable mixture of two diastereomers, but the decarboxylation product **243** was still formed in 26% (entry 3). The fact that only two diastereomers were obtained indicated that the decarboxylative conjugate addition took place diastereoselective because two diastereomers were expected anyhow due to the newly formed stereocenter in

the coupled cyclic fragment. This outcome would be in agreement with the literature that the alkyl radical which is formed during the reaction is selectively attacked from the convex face of the bicyclic ring system.<sup>94</sup> In order to increase the yield of the desired product **242** and suppress byproduct formation different solvents were screened (entries 4-6). However, none of these attempts was very promising, as no satisfying yield of **242** was obtained and decarboxylation without conjugate addition always took place.

Due to the fact that only poor yields of product were achieved and a suitable coupling partner in order to introduce the desired double bond in dermatolactone (**199**) was hard to find, all efforts to use the visible light-mediated conjugate addition as key step for the total synthesis of dermatolactone (**199**) were put down and an alternative reaction had to be found.

### 4.3 Ni-catalyzed coupling of *N*-acyloxyphthalimides

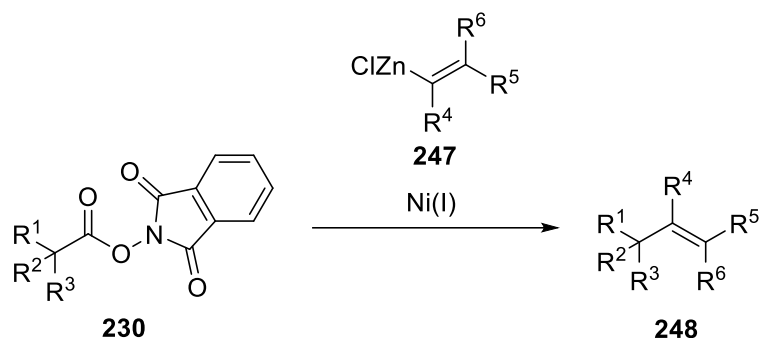
In recent years, the linkage of  $sp^2$ - $sp^3$  hybridized carbon bonds by cross-coupling reactions has been intensively studied.<sup>95</sup> Due to the lower availability of  $sp^3$ -coupling reagents, mainly alkyl halides or alkyl metal species have been utilized for this purpose.<sup>95,96</sup> Lately, it was shown that alkyl carboxylic acids can be used for Ni-catalyzed cross-coupling reactions after activation. In 2016, Baran *et al.* reported an aryl-alkyl cross-coupling of secondary *N*-acyloxyphthalimides **244** using Ni-catalysis (Scheme 52).<sup>96</sup>



**Scheme 52.** Ni-catalyzed cross-coupling of secondary *N*-acyloxyphthalimides **244**.<sup>96</sup>

Using a Ni(II)-salt and a suitable ligand, e.g. bipyridine, Baran *et al.* were able to couple several aryl zinc reagents **245** with different secondary *N*-acyloxyphthalimides **244** to achieve the cross-coupling product **246**. They further extended the scope of this reaction to the use of alkylzinc reagents in order to access  $sp^3$ - $sp^3$  hybridized carbon bond formation.<sup>97</sup> Most importantly, they reported a decarboxylative alkenylation based on this methodology which

seemed quite promising for the total synthesis of dermatolactone (**199**), due to the fact that an olefin could be directly introduced in this way (Scheme 53).<sup>98</sup>

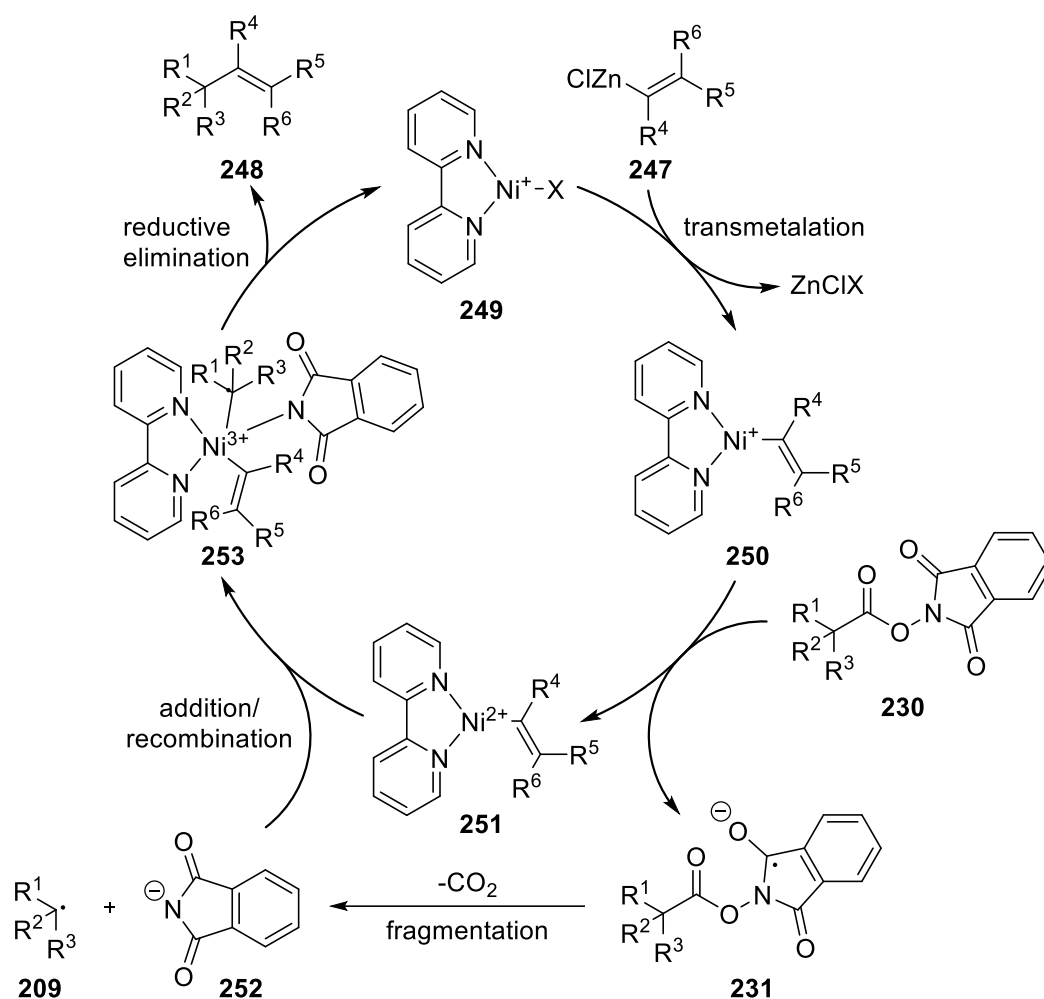


**Scheme 53.** Ni-catalyzed decarboxylative alkenylation.<sup>98</sup>

Remarkably, this reaction worked with primary, secondary and tertiary *N*-acyloxyphthalimides **230** and moreover mono-substituted to fully substituted alkylzinc reagents **247** could be applied to form the alkenylation product **248**.

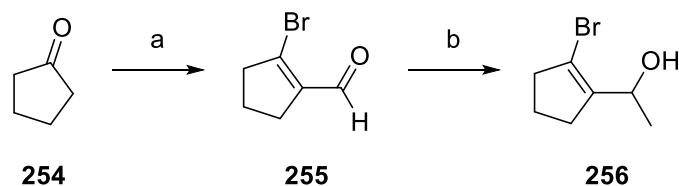
Thereby, the initially formed bipyridine-Ni(I) complex **249** undergoes transmetalation with an alkenylzinc reagent **247** to generate the alkenyl-Ni(I) complex **250**. In the next step, *N*-acyloxyphthalimide **230** receives an electron from complex **250** to form the radical anion **231** along with the Ni(II) complex **251**. Subsequent fragmentation of **231** under release of CO<sub>2</sub> leads to phthalimide anion **252** and alkyl radical **209**. Addition of the phthalimide anion **252** and the alkyl radical **209** to complex **251** generates the Ni(III) complex **253** which undergoes reductive elimination to finally produce the desired cross-coupling product **248** and regenerate the Ni(I) complex **249** (Scheme 54).





**Scheme 54.** Proposed mechanism for the decarboxylative alkenylation.<sup>98</sup>

Before such a decarboxylative alkenylation could be investigated for the synthesis of dermatolactone (**199**), a suitable olefin had to be found for the formation of the alkenylzinc reagent. Therefore, the synthesis of a cyclic  $\beta$ -hydroxy vinyl halide was envisaged which could be accomplished in a Vilsmeier-Haack reaction of cyclopentanone (**254**) followed by a Grignard reaction (Scheme 55).<sup>99,100</sup>

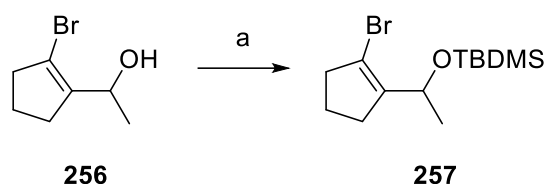


**Reagents and conditions:** a) DMF (3.0 equiv.),  $\text{PBr}_3$  (2.50 equiv.),  $\text{H}_2\text{O}/\text{THF}$  (1:3, v/v), DCM,  $0^\circ\text{C}$  to rt, 16 h; b)  $\text{MeMgBr}$  (1.1 equiv.),  $4\text{\AA}$  molecular sieve,  $\text{Et}_2\text{O}$ ,  $0^\circ\text{C}$ , 15 min, 66% over 2 steps.

**Scheme 55.** Synthesis of the cyclic  $\beta$ -hydroxy vinyl bromide **256**.<sup>99,100</sup>

The reaction of cyclopentanone (**254**) with DMF and  $\text{PBr}_3$  furnished aldehyde **255** which turned out to be not bench stable and should be directly treated with  $\text{MeMgBr}$  to form the cyclic  $\beta$ -hydroxy vinyl bromide **256**.

In order to avoid undesired side reactions, the free hydroxyl group was protected first (Scheme 56).<sup>101</sup>

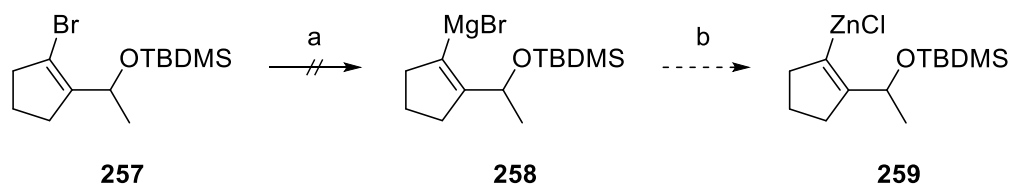


**Reagents and conditions:** a) TBDMSCl (1.5 equiv.), imidazole (2.0 equiv.), DMF, rt, 2 h, 93%.

**Scheme 56.** Protection of the free hydroxyl group of **256**.<sup>101</sup>

The protection of the hydroxyl group of **256** using TBDMSCl and imidazole proceeded smoothly yielding the desired silyl ether **257** in excellent yield.

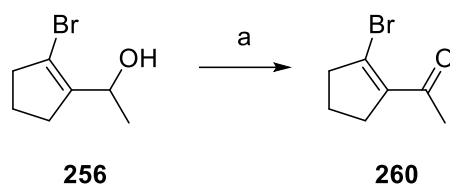
In general, alkenylzinc reagents were shown to be synthesized *via* transmetalation of an organometallic reagent or by Zn insertion. Therefore, the protected vinyl bromide **257** should be converted to its corresponding Grignard reagent **258** for the preparation of the alkenylzinc reagent **259** (Scheme 57).<sup>98</sup>



**Reagents and conditions:** a) Mg (2.5 equiv.), LiCl (1.25 equiv.), 1,2-dibromoethane (0.1 equiv.), THF, rt to reflux, 1.5 h; b)  $\text{ZnCl}_2$  (1.0 equiv.), THF, rt, 15 min.

**Scheme 57.** Synthesis of the alkenylzinc reagent **259** from the alkenyl Grignard reagent **258**.<sup>98</sup>

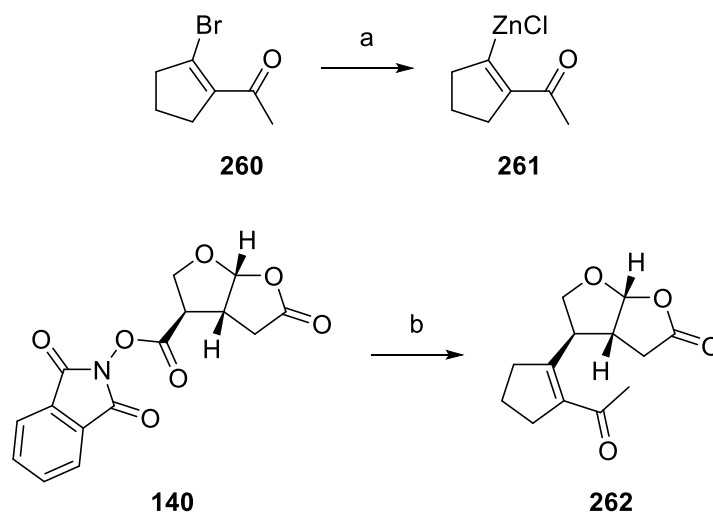
Unfortunately, already the Mg insertion did not work probably due to the fact that the protected vinyl bromide **257** is not reactive enough. In order to circumvent this problem, an  $\alpha,\beta$ -unsaturated bromide should be synthesized, as this class of compounds was shown to form alkenylzinc reagents *via* direct Zn insertion.<sup>98</sup> Therefore, alcohol **256** was oxidized to its corresponding ketone **260** with the use of *o*-iodoxybenzoic acid (IBX) (Scheme 58).<sup>102</sup>



**Reagents and conditions:** a) IBX (3.0 equiv.), EA, reflux, 3.5 h, 80%.

**Scheme 58.** Oxidation of alcohol **256** to ketone **260**.<sup>102</sup>

The reaction proceeded smoothly giving rise to the the desired ketone **260** in 80% yield. With this compound in hand, the alkenylzinc reagent **261** was generated *via* Zn insertion using Zn dust and directly used for the ensuing Ni-catalyzed decarboxylative alkenylation of *N*-acyloxyphthalimide **240** (Scheme 59).<sup>98</sup>



**Reagents and conditions:** a) Zn dust (2.0 equiv.), LiCl (2.0 equiv.), TMSCl (5 mol%), 1,2-dibromoethane (0.5 mol%), THF, rt, 1 h; b) **258** (2.0 equiv.) in THF, Ni(acac)<sub>2</sub>·xH<sub>2</sub>O (10 mol%), 2,2'-bipyridine (10 mol%), DMF, rt, 16 h, traces.

**Scheme 59.** Ni-catalyzed decarboxylative alkenylation of *N*-acyloxyphthalimide **240**.<sup>98</sup>

In this first test reaction, only traces of product **262** with impurities were obtained which were not sufficient for complete characterization. However, the decarboxylative alkenylation should be more intensively investigated and further pursued in the future to get access to dermatolactone (**199**). Alternatively, the coupling of *N*-acyloxyphthalimide **240** and  $\beta$ -hydroxy vinyl bromide **256** should be tested under photochemical conditions or a combination of photoredox and metal catalysis.<sup>103</sup>

## 5. References

- <sup>1</sup> Ebner, C.; Carreira, E. M. *Chem. Rev.* **2017**, *117* (18), 11651–11679.
- <sup>2</sup> Chen, D. Y. K.; Pouwer, R. H.; Richard, J. A. *Chem. Soc. Rev.* **2012**, *41* (13), 4631–4642.
- <sup>3</sup> Fan, Y. Y.; Gao, X. H.; Yue, J. M. *Sci. China Chem.* **2016**, *59* (9), 1126–1141.
- <sup>4</sup> Salaün, J. *Top. Curr. Chem.* **2000**, *207*, 1–67.
- <sup>5</sup> Lebel, H.; Marcoux, J. F.; Molinaro, C.; Charette, A. B. *Chem. Rev.* **2003**, *103* (4), 977–1050.
- <sup>6</sup> Reissig, H.-U.; Zimmer, R. *Chem. Rev.* **2003**, *103*, 1151–1196.
- <sup>7</sup> Maas, G. *Angew. Chemie Int. Ed.* **2009**, *48* (44), 8186–8195.
- <sup>8</sup> Zhao, X.; Zhang, Y.; Wang, J. *Chem. Commun.* **2012**, *48* (82), 10162–10173.
- <sup>9</sup> Davies, H. M. L.; Beckwith, R. E. J. *Chem. Rev.* **2003**, *103* (8), 2861–2903.
- <sup>10</sup> Gurmessa, G. T.; Singh, G. S. *Res. Chem. Intermed.* **2017**, *43* (11), 6447–6504.
- <sup>11</sup> Doyle, M. P. *Chem. Rev.* **1986**, *86* (5), 919–939.
- <sup>12</sup> Rasmussen, T.; Jensen, J. F.; Ostergaard, N.; Tanner, D.; Ziegler, T.; Norrby, P.-O. *Chemistry* **2002**, *8* (1), 177–184.
- <sup>13</sup> Fraile, J. M.; García, J. I.; Martínez-Merino, V.; Mayoral, J. a; Salvatella, L. *J. Am. Chem. Soc.* **2001**, *123* (31), 7616–7625.
- <sup>14</sup> Salomon, R. G.; Kochi, J. K. *J. Am. Chem. Soc.* **1973**, *95* (10), 3300–3310.
- <sup>15</sup> Nozaki, H.; Moriuti, S.; Takaya, H.; Noyori, R. *Tetrahedron Lett.* **1966**, *7* (43), 5239–5244.
- <sup>16</sup> Fritschi, H.; Leutenegger, U.; Pfaltz, A. *Angew. Chem. Int. Ed. Engl.* **1986**, *25*, 1005–1006; *Angew. Chem.* **1986**, *98*, 1028–1029.
- <sup>17</sup> Lowenthal, R. E.; Masamune, S. *Tetrahedron Lett.* **1991**, *32*, 7373–7376.
- <sup>18</sup> Evans, D. A.; Woerpel, K. A.; Hinman, M. M.; Faul, M. M. *J. Am. Chem. Soc.* **1991**, *113* (2), 726–728.
- <sup>19</sup> Glos, M.; Reiser, O. *Org. Lett.* **2000**, *2* (14), 2045–2048.
- <sup>20</sup> Reiser, O. *Isr. J. Chem.* **2016**, *56* (6–7), 531–539.
- <sup>21</sup> Hahn, N. D.; Nieger, M.; Dötz, K. H. *J. Organomet. Chem.* **2004**, *689* (16), 2662–2673.
- <sup>22</sup> Saltykova, L.E.; Vasil'vitskii, A.E.; Shostakovskii, V.M.; Nefedov, O. M. *Russ Chem Bull* **1988**, *37*, 2557–2560.
- <sup>23</sup> Wenkert, E.; Guo, M.; Lavilla, R.; Porter, B.; Ramachandran, K.; Sheu, J. H. *J. Org. Chem.* **1990**, *55*, 6203–6214.
- <sup>24</sup> Böhm, C.; Schinnerl, M.; Bubert, C.; Zabel, M.; Labahn, T.; Parisini, E.; Reiser, O. *Eur. J. Org. Chem.* **2000**, 2955–2965.

- <sup>25</sup> Böhm, C.; Reiser, O. *Org. Lett.* **2001**, 3 (9), 1315–1318.
- <sup>26</sup> Macabeo, A. P. G.; Kreuzer, A.; Reiser, O. *Org. Biomol. Chem.* **2011**, 9 (9), 3146–3150.
- <sup>27</sup> Nosse, B.; Chhor, R. B.; Boo Jeong, W.; Böhm, C.; Reiser, O. *Org. Lett.* **2003**, 5 (6), 941–944.
- <sup>28</sup> Chhor, R. B.; Nosse, B.; Sörgel, S.; Böhm, C.; Seitz, M.; Reiser, O. **2003**, 260–270.
- <sup>29</sup> Schinnerl, M.; Böhm, C.; Seitz, M.; Reiser, O. *Tetrahedron Asymmetry* **2003**, 14 (7), 765–771.
- <sup>30</sup> Harrar, K.; Reiser, O. *Chem. Comm.* **2012**, 48 (28), 3457–3459.
- <sup>31</sup> Pilsl, L., *Enantioselective cyclopropanation of heterocycles and the use of high-pressure techniques for the conformational analysis of peptide foldamers*. PhD Thesis, Universität Regensburg, Regensburg, 2014.
- <sup>32</sup> Harrar, K., *Enantioselective Synthesis of (-)-Paeonilide*. PhD Thesis, Universität Regensburg, Regensburg, 2011.
- <sup>33</sup> Weisser, R.; Yue, W.; Reiser, O. *Org. Lett.* **2005**, 7 (24), 5353–5356.
- <sup>34</sup> Gnahn, M., *Enantiopure Synthesis of (+)-Paeonilide*. Master Thesis, Universität Regensburg, Regensburg, 2014.
- <sup>35</sup> Declerck, V.; Aitken, D. J. *Amino Acids* **2011**, 41 (3), 587–595.
- <sup>36</sup> Heravi, M. M.; Zadsirjan, V.; Farajpour, B. *RSC Adv.* **2016**, 6 (36), 30498–30551.
- <sup>37</sup> Prashad, M.; Har, D.; Kim, H. Y.; Repic, O. *Tetrahedron Lett.* **1998**, 39 (39), 7067–7070.
- <sup>38</sup> Costa, J. C. S.; Pais, K. C.; Fernandes, E. L.; De Oliveira, P. S. M.; Mendonça, J. S.; De Souza, M. V. N.; Peralta, M. A.; Vasconcelos, T. R. A. *Arkivoc*, **2006**, 1, 128–133.
- <sup>39</sup> Bellucci, G.; Marioni, F.; Marsili, A. *Tetrahedron* **1969**, 25 (18), 4167–4172.
- <sup>40</sup> Baughman, T. W.; Sworen, J. C.; Wagener, K. B. *Tetrahedron* **2004**, 60 (48), 10943–10948.
- <sup>41</sup> Kim, C.; Hoang, R.; Theodorakis, E. A. *Org. Lett.* **1999**, 1 (8), 1295–1297.
- <sup>42</sup> Matsuda, S.; Yamanoi, T.; Watanabe, M., *Tetrahedron* **2008**, 64, 8082–8088.
- <sup>43</sup> Zahalka, H. A.; Sasson, Y. *Synthesis* **1986**, 763–765.
- <sup>44</sup> Tadic, D.; Linders, J. T. M.; Flippen-Anderson, J. L.; Jacobsen, A. E.; Rice, K. C. *Tetrahedron* **2003**, 59, 4603–4614.
- <sup>45</sup> Nishimura, T.; Kakiuchi, N.; Onoue, T.; Ohe, K.; Ucmura, S. *J. Chem. Soc. Perkin Trans. 1* **2000**, No. 12, 1915–1918.
- <sup>46</sup> Donck, S.; Gravel, E.; Shah, N.; Jawale, D. V.; Doris, E.; Namboothiri, I. N. N. *ChemCatChem* **2015**, 7 (15), 2318–2322.
- <sup>47</sup> Zhang, Z.; Kumamoto, Y.; Hashiguchi, T.; Mamba, T.; Murayama, H.; Yamamoto, E.; Ishida, T.; Honma, T.; Tokunaga, M. *ChemSusChem* **2017**, 10 (17), 3482–3489.
- <sup>48</sup> Han, J.-S.; Lowary, T. L. *J. Org. Chem.* **2003**, 68 (10), 4116–4119.

- <sup>49</sup> Wang, Y. F.; Gao, Y. R.; Mao, S.; Zhang, Y. L.; Guo, D. D.; Yan, Z. L.; Guo, S. H.; Wang, Y. Q. *Org. Lett.* **2014**, *16* (6), 1610–1613.
- <sup>50</sup> Fernandes, R. A.; Chaudhari, D. A. *J. Org. Chem.* **2014**, *79* (12), 5787–5793.
- <sup>51</sup> Rogers, H. R.; McDermott, J. X.; Whitesides, G. M. *J. Org. Chem.* **1975**, *40* (24), 3577–3580.
- <sup>52</sup> Liu, J.-K. Y.; Ma, B.; Wu, D.-G.; Lu, Y.; Shen, Z.-Q.; Zheng, Q.-T.; Chen, Z.-H. *Biosci. Biotechnol. Biochem.* **2000**, *64* (7), 1511–1514.
- <sup>53</sup> Evans, D. A.; Ellman, J. A.; Dorow, R. L. *Tetrahedron Lett.* **1987**, *28* (11), 1123–1126.
- <sup>54</sup> Hansch, C.; Dunn, W. J. *J. Pharm. Sci.* **1972**, *61* (1), 1–19.
- <sup>55</sup> Pop, E.; Oniciu, D. C.; Pape, M. E.; Cramer, C. T.; Dasseu, J.-L. H. *Croat. Chem. Acta* **2004**, *77*, 301–306.
- <sup>56</sup> Chougala, B. M.; Samundeeswari, S.; Holiyachi, M.; Shastri, L. A. *ChemistrySelect* **2017**, *2* (3), 1290–1296.
- <sup>57</sup> Wood, P.; Seo, S.; Kim, J.; Koh, S.; Ahn, Y.; Park, I. *J. Agric. Food Chem.* **2014**, *62*, 9103–9108.
- <sup>58</sup> Wu, G.; Huang, M. *Chem. Rev.* **2006**, *106* (7), 2596–2616.
- <sup>59</sup> Shukla, S. D. *Nips* **1992**, *7*, 72–75.
- <sup>60</sup> Liu, Y.; Shields, L. B. E.; Gao, Z.; Wang, Y.; Zhang, Y. P.; Chu, T.; Zhu, Q.; Shields, C. B.; Cai, J. *Mol. Neurobiol.* **2017**, *54* (7), 5563–5572.
- <sup>61</sup> Reznichenko, A.; Korstanje, R. *Am. J. Pathol.* **2015**, *185* (4), 888–896.
- <sup>62</sup> Ishii, S.; Shimizu, T. *Prog Lipid Res* **2000**, *39* (1), 41–82.
- <sup>63</sup> Im, S. Y.; Ji, S.; Ko, H. M.; Choi, J. H.; Chun, S. B.; Lee, D. G.; Lee, H. *Eur. J. Immunol.* **1997**, *27*, 2800–2804.
- <sup>64</sup> Liu, X.; Yan, Y.; Bao, L.; Chen, B.; Zhao, Y.; Qi, R. *Thromb. Res.* **2014**, *134* (5), 1066–1073.
- <sup>65</sup> Hilliquin, P.; Houbaba, H.; Aha, J.; Benveniste, J.; Menkes, C. J. *J. Rheumatol.* **1995**, *24* (3), 169–173.
- <sup>66</sup> Agrawal, V.; Jaiswal, M. K.; Ilievski, V.; Beaman, K. D.; Jilling, T.; Hirsch, E. *Biol. Reprod.* **2014**, *91* (5), 1–11.
- <sup>67</sup> Snyder, F. *Biochim. Biophys. Acta - Lipids Lipid Metab.* **1997**, *1348* (1–2), 111–116.
- <sup>68</sup> Uemura, Y.; Lee, T. C.; Snyder, F. *J. Biol. Chem.* **1991**, *266* (13), 8268–8272.
- <sup>69</sup> Koch, E. *Phytomedicine* **2005**, *12* (1–2), 10–16.
- <sup>70</sup> Levy, J. F. *Febs Lett.* **1983**, *154*(2) (2), 262–264.
- <sup>71</sup> Shah, B. H.; Rasheed, H.; Khan, F. L.; Rahman, H. B.; Hanif, S. *Exp. Mol. Med.* **2001**, *33* (4), 226–233.
- <sup>72</sup> <http://www.platelet-research.org/3/mechanisms.htm> (accessed on 26.09.2018)

- <sup>73</sup> Paniccia, R.; Priora, R.; Liotta, A. A.; Abbate, R. *Vasc. Health Risk Manag.* **2015**, *11*, 133–148.
- <sup>74</sup> Frontroth, J. P. *Haemostasis: Methods and Protocols, Methods in Molecular Biology, Chapter 17*, SSBM, New York, **2013**.
- <sup>75</sup> Mayer, A.; Köpke, B.; Anke, H.; Sterner, O. *Phytochemistry* **1996**, *43* (2), 375–376.
- <sup>76</sup> Narayanam, J. M. R.; Tucker, J. W.; Stephenson, C. R. J. *J. Am. Chem. Soc.* **2009**, *131* (25), 8756–8757.
- <sup>77</sup> Nakano, M.; Nishiyama, Y.; Tanimoto, H.; Morimoto, T.; Kakiuchi, K. *Org. Process Res. Dev.* **2016**, *20* (9), 1626–1632.
- <sup>78</sup> Schultz, D. M.; Yoon, T. P. *Science*. **2014**, *343* (6174), 985–993.
- <sup>79</sup> König, B. *European J. Org. Chem.* **2017**, *2017* (15), 1979–1981.
- <sup>80</sup> Marzo, L.; Pagire, S. K.; Reiser, O.; König, B. *Angew. Chemie Int. Ed.* **2018**, *57* (32), 10034–10072.
- <sup>81</sup> Pirtsch, M.; Paria, S.; Matsuno, T.; Isobe, H.; Reiser, O. *Chem. - A Eur. J.* **2012**, *18* (24), 7336–7340.
- <sup>82</sup> Rackl, D.; Kais, V.; Lutsker, E.; Reiser, O. *European J. Org. Chem.* **2017**, *2017* (15), 2130–2138.
- <sup>83</sup> Maji, T.; Karmakar, A.; Reiser, O. *J. Org. Chem.* **2011**, *76* (2), 736–739.
- <sup>84</sup> Lin, S.; Ischay, M. A.; Fry, C. G.; Yoon, T. P. *J. Am. Chem. Soc.* **2011**, *133* (48), 19350–19353.
- <sup>85</sup> Chu, L.; Ohta, C.; Zuo, Z.; MacMillan, D. W. C. *J. Am. Chem. Soc.* **2014**, *136* (31), 10886–10889.
- <sup>86</sup> Vila, C.; Hornillos, V.; Fañanás-Mastral, M.; Feringa, B. L. *Chem. Commun.* **2013**, *49* (53), 5933–5935.
- <sup>87</sup> Shen, Z. L.; Cheong, H. L.; Loh, T. P. *Tetrahedron Lett.* **2009**, *50* (9), 1051–1054.
- <sup>88</sup> Yamamoto, Y.; Yamamoto, S.; Yatagai, H.; Ishihara, Y.; Maruyama, K. *J. Org. Chem.* **1982**, *47* (1), 119–126.
- <sup>89</sup> Sugiura, M.; Tokudomi, M.; Nakajima, M. *Chem. Commun.* **2010**, *46* (41), 7799–7800.
- <sup>90</sup> Barton, D. H. R.; Crich, D.; Motherwell, W. B. *J. Chem. Soc., Chem. Commun.* **1983**, *18*, 939–941.
- <sup>91</sup> Okada, K.; Okamoto, K.; Oda, M. *J. Am. Chem. Soc.* **1988**, *110* (26), 8736–8738.
- <sup>92</sup> Okada, K.; Okamoto, K.; Morita, N.; Okubo, K.; Oda, M. *J. Am. Chem. Soc.* **1991**, *113* (24), 9401–9402.
- <sup>93</sup> Pratsch, G.; Lackner, G. L.; Overman, L. E. *J. Org. Chem.* **2015**, *80* (12), 6025–6036.
- <sup>94</sup> Schnermann, M. J.; Overman, L. E. *Angew. Chemie Int. Ed.* **2012**, *51* (38), 9576–9580.

- <sup>95</sup> Huihui, K. M. M.; Caputo, J. A.; Melchor, Z.; Olivares, A. M.; Spiewak, A. M.; Johnson, K. A.; Dibenedetto, T. A.; Kim, S.; Ackerman, L. K. G.; Weix, D. J. *J. Am. Chem. Soc.* **2016**, *138* (15), 5016–5019.
- <sup>96</sup> Cornella, J.; Edwards, J. T.; Qin, T.; Kawamura, S.; Wang, J.; Pan, C. M.; Gianatassio, R.; Schmidt, M.; Eastgate, M. D.; Baran, P. S. *J. Am. Chem. Soc.* **2016**, *138* (7), 2174–2177.
- <sup>97</sup> Qin, T.; Cornella, J.; Li, C.; Malins, L. R.; Edwards, J. T.; Kawamura, S.; Maxwell, B. D.; Eastgate, M. D.; Baran, P. S. *Science*. **2016**, *352* (6287), 801.
- <sup>98</sup> Edwards, J. T.; Merchant, R. R.; McClymont, K. S.; Knouse, K. W.; Qin, T.; Malins, L. R.; Vokits, B.; Shaw, S. A.; Bao, D. H.; Wei, F. L.; Zhou, T.; Eastgate, M. D.; Baran, P. S. *Nature* **2017**, *545* (7653), 213–218.
- <sup>99</sup> Lin, M. Y.; Das, A.; Liu, R. S. *J. Am. Chem. Soc.* **2006**, *128* (29), 9340–9341.
- <sup>100</sup> Xia, Y.; Qu, P.; Liu, Z.; Ge, R.; Xiao, Q.; Zhang, Y.; Wang, J. *Angew. Chemie Int. Ed.* **2013**, *52* (9), 2543–2546.
- <sup>101</sup> Corey, E. J.; Venkateswarlu, A. *J. Am. Chem. Soc.* **1972**, *94* (17), 6190–6191.
- <sup>102</sup> More, J. D.; Finney, N. S. *Org. Lett.* **2002**, *4* (17), 3001–3003.
- <sup>103</sup> Noble, A.; McCarver, S. J.; MacMillan, D. W. C. *J. Am. Chem. Soc.* **2015**, *137* (2), 624–627.

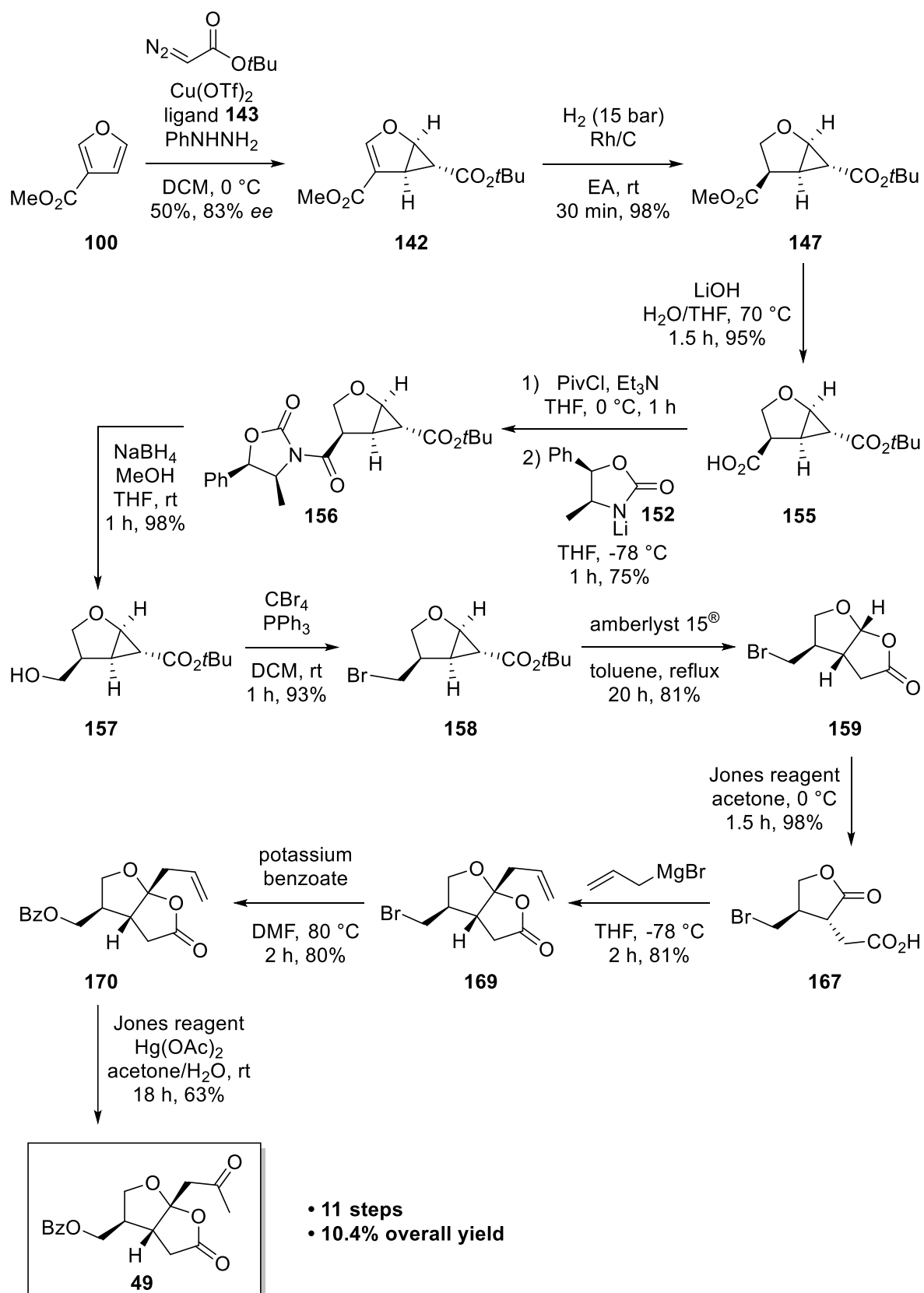


## C. Summary

The furo[2,3-*b*]furanone moiety is present in more than 100 natural products. Two representatives of this class which are substituted in the C-4 position are the highly oxygenated monoterpenoid (+)-paeonilide (**49**) and the sesquiterpene dermatolactone (**199**). In the present thesis, an enantioselective synthesis of (+)-paeonilide (**49**) and derivatives was developed and their biological activity against the PAF-induced human platelet aggregation was evaluated. Furthermore, studies toward the total synthesis of dermatolactone (**199**) were conducted.

The first chapter describes the enantioselective synthesis of (+)-paeonilide (**49**) starting from achiral 3-furoic acid methyl ester (**100**). The key step in order to introduce chirality was the asymmetric Cu(I)-catalyzed cyclopropanation to obtain bicyclus **142**. As this reaction only gave an enantiomeric excess of 83% and recrystallization led to great loss of product, a chiral resolution was carried out to achieve enantiomerically pure product. Therefore, **142** was first hydrogenated and then the methyl ester was selectively saponified. After the coupling of oxazolidin-2-one **152**, it was possible to separate the two diastereomers and reductive cleavage of the chiral auxiliary led to enantiomerically pure alcohol **157**. Transformation of the hydroxyl group to a bromide and subsequent acid-mediated ring-opening/lactonization resulted in the formation of furo[2,3-*b*]furanone **159** which could be obtained as single diastereomer after purification. Oxidative ring-opening then enabled access to the introduction of an allyl group in the acetal position. Finally, substitution of the bromide using potassium benzoate and oxidation of the allyl side chain applying an oxymercuration/oxidation protocol gave the desired (+)-paeonilide (**49**) (Scheme 60).

In this way, (+)-paeonilide (**49**) was afforded in an 11 step, straightforward synthesis with an overall yield of 10.4%. Remarkably, this is the only enantioselective synthesis of (+) paeonilide (**49**) until today. Moreover, this synthetic route allowed several modifications and one suitable precursor **169** for further derivatizations could be synthesized in 9 steps with an overall yield of 20.6%.

Scheme 60. Enantioselective synthesis of (+)-paeonilide (**49**).

The second chapter describes the synthesis of a small library of (+)-paeonilide derivatives. In total, 9 derivatives with modifications either in the two side chains or in the  $\alpha$ -position of the lactone were synthesized (Figure 27).

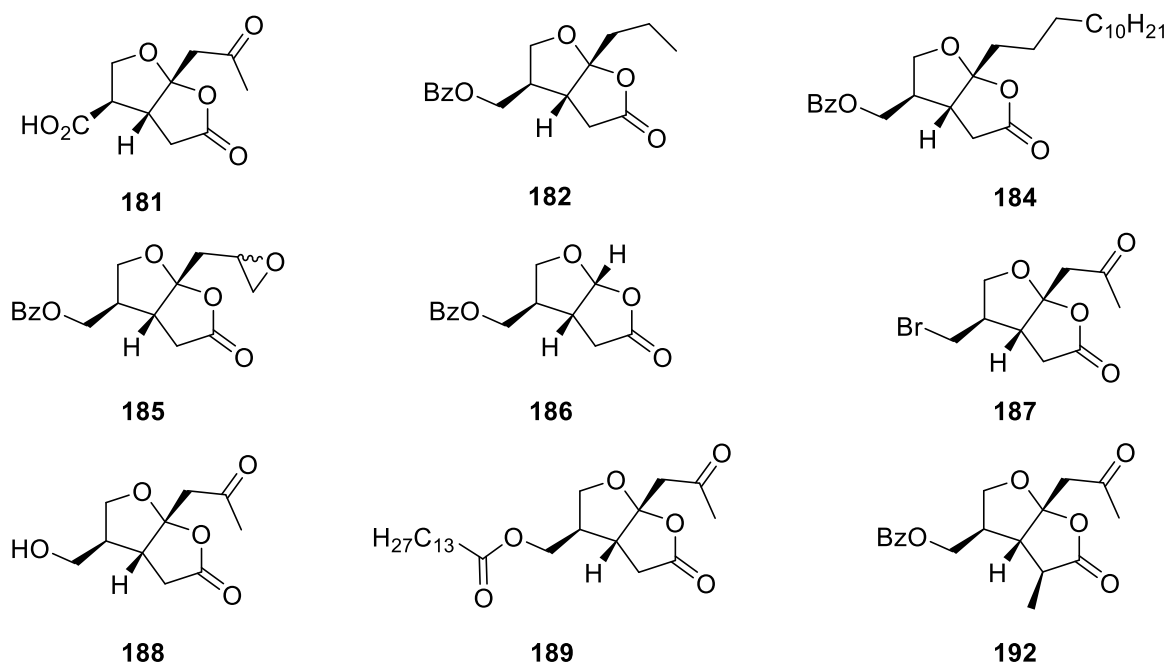


**Figure 27.** Synthesized (+)-paeonilide derivatives.

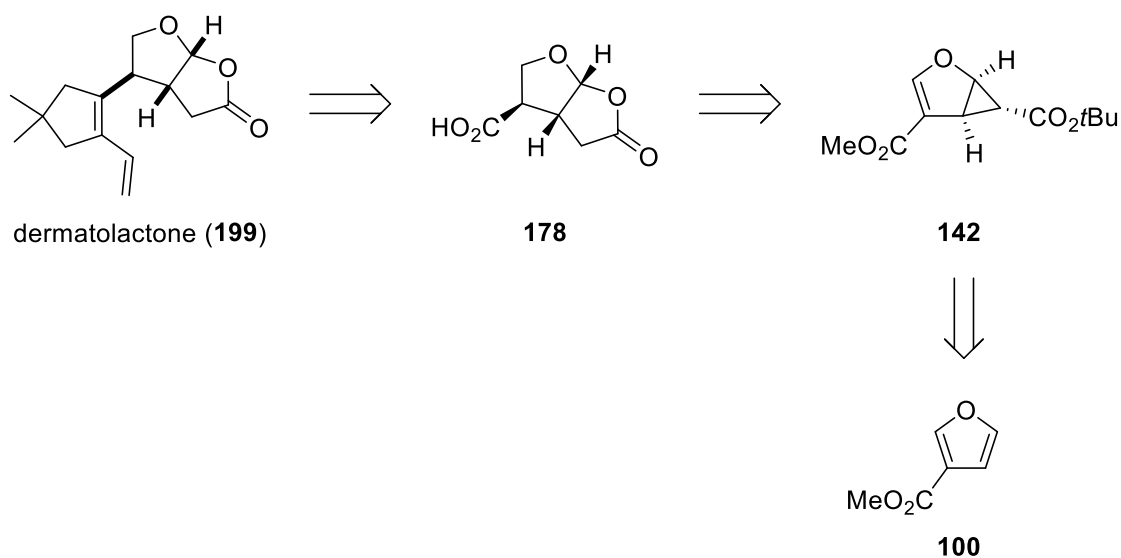
These derivatives and the synthesized (+)-paeonilide (**49**) were tested for the inhibition of the PAF-induced platelet aggregation and the results are described in the third chapter (Table 14).

**Table 14.** Inhibition of PAF-induced human platelet aggregation by (+)-paeonilide (**49**) and derivatives.

compound	maximum aggregation			slope		
	IC <sub>50</sub> [ $\mu\text{g}\cdot\text{mL}^{-1}$ ]	IC <sub>50</sub> [ $\mu\text{M}$ ]	potency [%]	IC <sub>50</sub> [ $\mu\text{g}\cdot\text{mL}^{-1}$ ]	IC <sub>50</sub> [ $\mu\text{M}$ ]	potency [%]
<b>49</b>	22.0	69.0	100	27.9	87.6	100
<b>181</b>	132.0	578.5	11.9	138.9	608.8	14.4
<b>182</b>	105.4	348.5	19.8	116.0	383.7	22.8
<b>184</b>	241.9	544.2	12.7	225.8	507.9	17.2
<b>185</b>	20.9	65.7	105.0	18.9	59.2	148.0
<b>186</b>	82.4	372.9	18.5	89.1	403.0	21.7
<b>187</b>	33.4	120.6	57.2	54.6	196.9	44.5
<b>188</b>	>300	>1000	-	>300	>1000	-
<b>189</b>	191.3	450.6	15.3	211.7	498.7	17.6
<b>192</b>	18.0	54.2	127.3	18.0	54.1	161.9

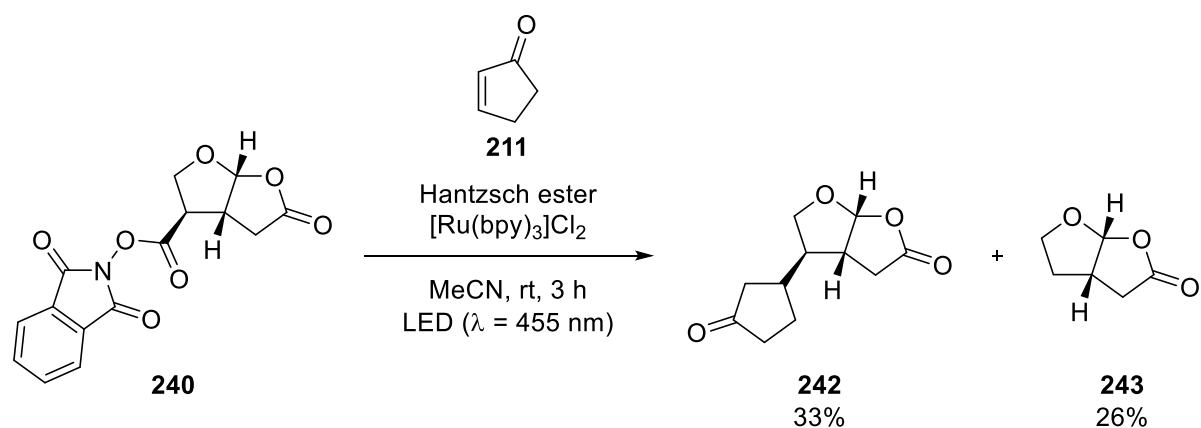
The bioassay indicated that the functional groups in both side chains have a great impact on the biological activity of the compound. Especially the oxygen functionality seemed to play a crucial role, as all deoxygenated derivatives (**182**, **184** and **186**) showed a big drop in inhibitory effect. Furthermore, the introduction of long alkyl groups in the side chains (**184** and **189**) had an adverse effect on the biological activity. Comparing the different functional groups in the C-4 position, the benzoate (**49**) proved to be the best followed by the bromide (**187**) while the alcohol (**188**) was revealed to be completely inactive. The introduction of an alkyl group in the  $\alpha$ -position of the lactone (**192**) showed a beneficial effect on the biological activity.

The last chapter deals with studies toward the total synthesis of dermatolactone (**199**). The key step in this synthesis should be a decarboxylative cross-coupling of carboxylic acid **178** which was already obtained during the synthesis of (+)-paeonilide (**49**) (Scheme 61).



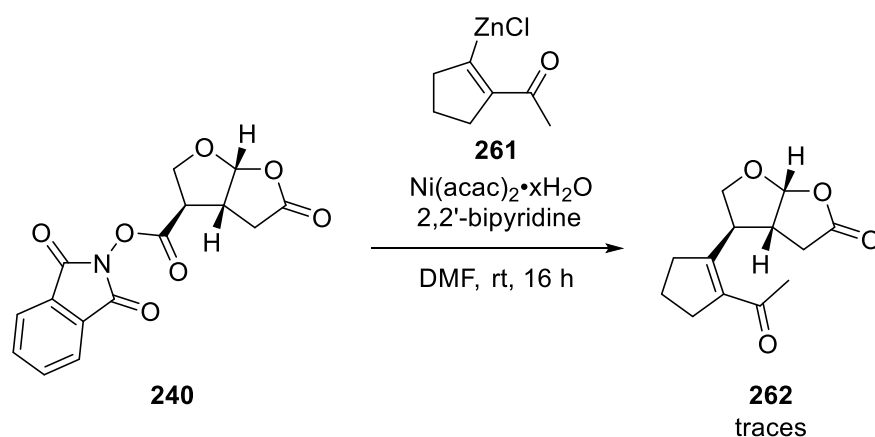
**Scheme 61.** Retrosynthesis of dermatolactone (**199**).

As acid **178** was shown to be insufficient for a photocatalyzed decarboxylative conjugate addition, it was converted to its corresponding active ester **240**. This compound underwent visible light-mediated cross-coupling with Michael acceptor **211** to form the addition product **242**, however, accompanied by undesired decarboxylation product **243** (Scheme 62).



**Scheme 62.** Visible light-mediated decarboxylative cross-coupling of **240**.

As this reaction did not give the desired result, it was looked for an alternative synthetic route. In order to directly introduce an olefin, a Ni-catalyzed decarboxylative alkenylation was envisaged. Therefore, a suitable model substrate was synthesized first. After preparation of the corresponding alkenylzinc reagent **261** *in situ*, it should be coupled with *N*-acyloxyphthalimide **240** (Scheme 63).



**Scheme 63.** Ni-catalyzed decarboxylative alkenylation of **240**.

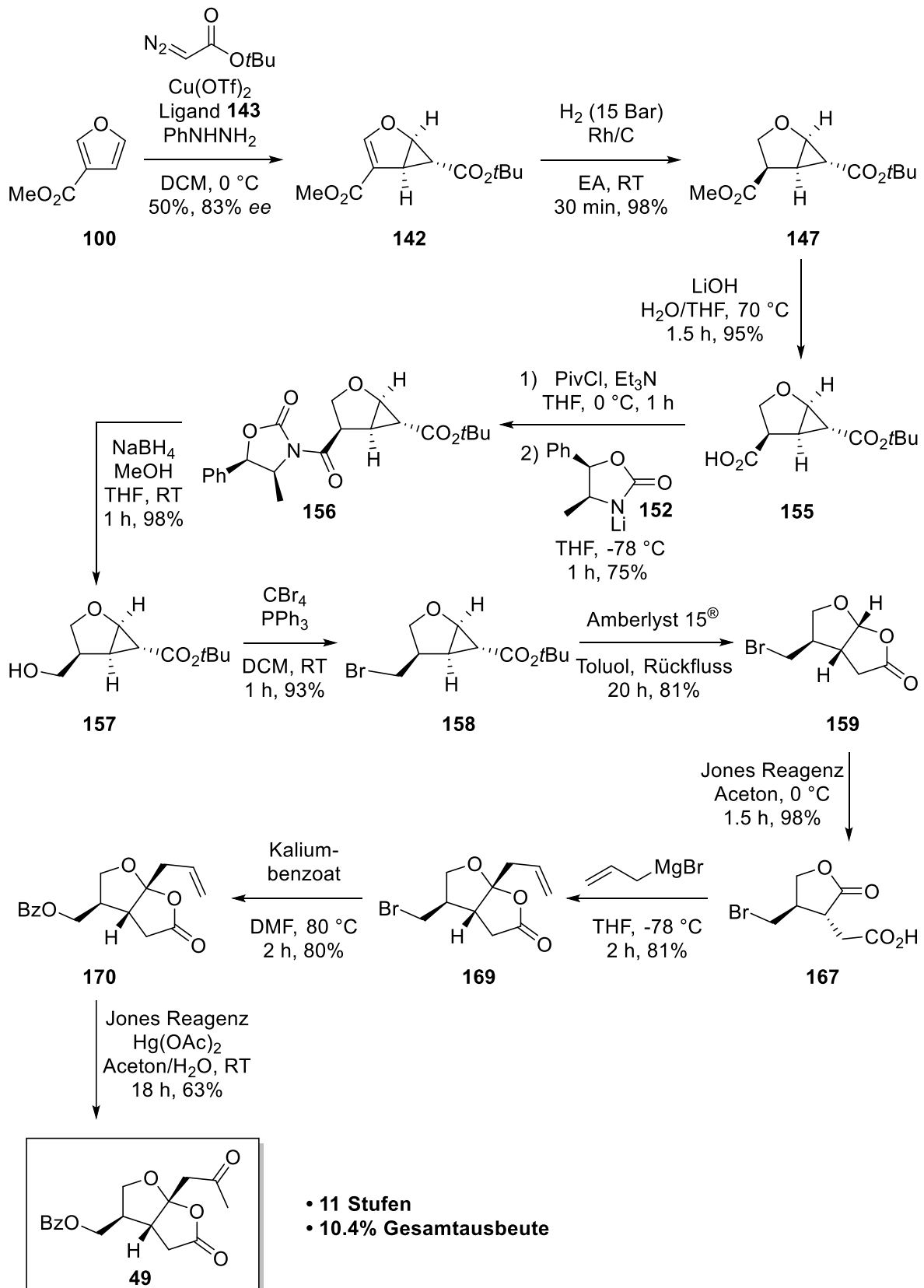
Unfortunately, only traces of the desired product **262** were obtained in a first test reaction. However, this strategy or a combination of photoredox and metal catalysis should be more intensively investigated in the future to enable access to the synthesis of dermatolactone (**199**).

## D. Zusammenfassung

Die Furo[2,3-*b*]furanonstruktur kommt in mehr als 100 Naturstoffen vor. Zwei Vertreter dieser Klasse, welche in der C-4-Position substituiert sind, sind das sauerstoffreiche Monoterpen (+)-Paeonilid (**49**) und das Sesquiterpen Dermatolacton (**199**). In der vorliegenden Arbeit wurde eine enantioselektive Synthese von (+)-Paeonilid (**49**) und verschiedenen Derivaten entwickelt und deren biologische Aktivität gegen die PAF-induzierte humane Plättchenaggregation bestimmt. Des Weiteren wurden Studien zur Totalsynthese von Dermatolacton (**199**) durchgeführt.

Das erste Kapitel beschreibt die enantioselektive Synthese von (+)-Paeonilid (**49**) ausgehend von achiralem 3-Furansäuremethylester (**100**). Der Schlüsselschritt um Chiralität zu induzieren war eine asymmetrische, Cu(I)-katalysierte Cyclopropanierung, welche den Bicyklus **142** lieferte. Da diese Reaktion nur einen Enantiomerenüberschuss von 83% ergab und Umkristallisation zu erhöhten Produktverlust führte, wurde eine Racematspaltung durchgeführt, um enantiomerenreines Produkt zu erhalten. Dazu wurde **142** zuerst hydriert und anschließend wurde der Methylester selektiv verseift. Nach der Kopplung mit dem 2-Oxazolidinon **152** war es möglich die beiden entstandenen Diastereomere zu trennen und eine reduktive Abspaltung des chiralen Auxiliars lieferte den enantiomerenreinen Alkohol **157**. Die Umwandlung der Hydroxygruppe in ein Bromid und anschließende säurekatalysierte Ringöffnung/Lactonisierung resultierten in der Bildung des Furo[2,3-*b*]furanons **159** welches nach Aufreinigung als einzelnes Diastereomer erhalten wurde. Eine oxidative Ringöffnung erlaubte nun die Einführung einer Allylgruppe in der Acetalposition. Das gewünschte (+)-Paeonilid (**49**) konnte schließlich durch eine Substitution des Bromids mit Kaliumbenzoat und eine Oxidation der Allyl-Seitenkette unter Verwendung einer Oxymyrcurierung mit sofortiger Oxidation erhalten werden (Schema 1).

Auf diese Weise wurde (+)-Paeonilid (**49**) in einer elfstufigen, unkomplizierten Synthese mit einer Gesamtausbeute von 10.4% erhalten. Bemerkenswerterweise ist dies die bis heute einzige enantioselektive Synthese von (+)-Paeonilid (**49**). Des Weiteren erlaubte diese Syntheseroute mehrere Modifikationen und ein geeigneter Vorläufer **169** für weitere Derivatisierungen konnte in 9 Stufen mit einer Gesamtausbeute von 20.6% hergestellt werden.



Schema 1. Enantioselektive Synthese von (+)-Paeonilid (**49**).

Das zweite Kapitel beschreibt die Herstellung einer kleinen Bibliothek an (+)-Paeonilid Derivaten. Insgesamt wurden neun Derivate mit Veränderungen in entweder einer der beiden Seitenketten oder in der  $\alpha$ -Position des Lactons synthetisiert (Abbildung 1).

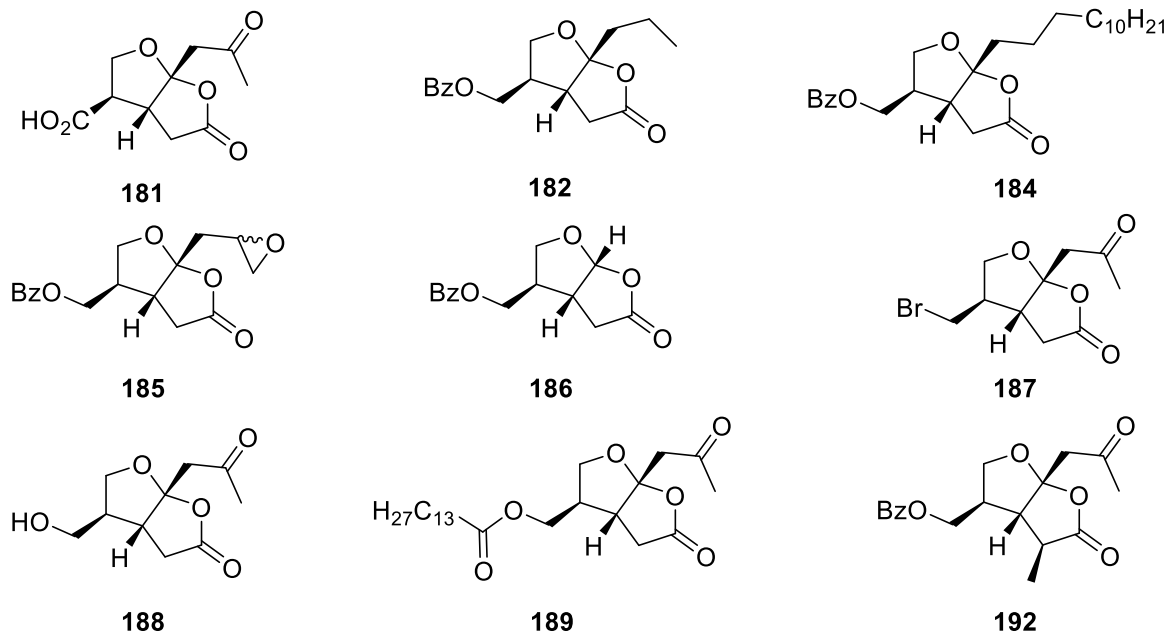


**Abbildung 1.** Hergestellte (+)-Paeonilid Derivative.

Diese Derivate und das künstlich hergestellte (+)-Paeonilid (**49**) wurden auf ihre Fähigkeit die PAF-induzierte Plättchenaggregation zu inhibieren getestet und die Ergebnisse sind in Kapitel 3 beschrieben (Tabelle 1).

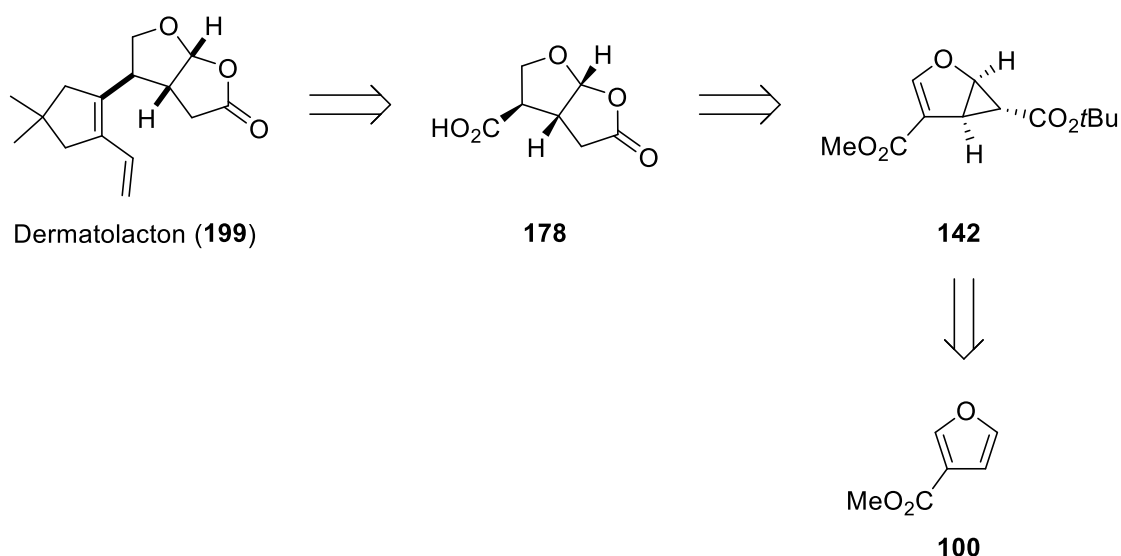
**Tabelle 1.** Inhibierung der PAF-induzierten humanen Plättchenaggregation.

Verbindung	Maximale Aggregation			Steigung		
	IC <sub>50</sub> [ $\mu\text{g}\cdot\text{mL}^{-1}$ ]	IC <sub>50</sub> [ $\mu\text{M}$ ]	Potenz [%]	IC <sub>50</sub> [ $\mu\text{g}\cdot\text{mL}^{-1}$ ]	IC <sub>50</sub> [ $\mu\text{M}$ ]	Potenz [%]
<b>49</b>	22.0	69.0	100	27.9	87.6	100
<b>181</b>	132.0	578.5	11.9	138.9	608.8	14.4
<b>182</b>	105.4	348.5	19.8	116.0	383.7	22.8
<b>184</b>	241.9	544.2	12.7	225.8	507.9	17.2
<b>185</b>	20.9	65.7	105.0	18.9	59.2	148.0
<b>186</b>	82.4	372.9	18.5	89.1	403.0	21.7
<b>187</b>	33.4	120.6	57.2	54.6	196.9	44.5
<b>188</b>	>300	>1000	-	>300	>1000	-
<b>189</b>	191.3	450.6	15.3	211.7	498.7	17.6
<b>192</b>	18.0	54.2	127.3	18.0	54.1	161.9



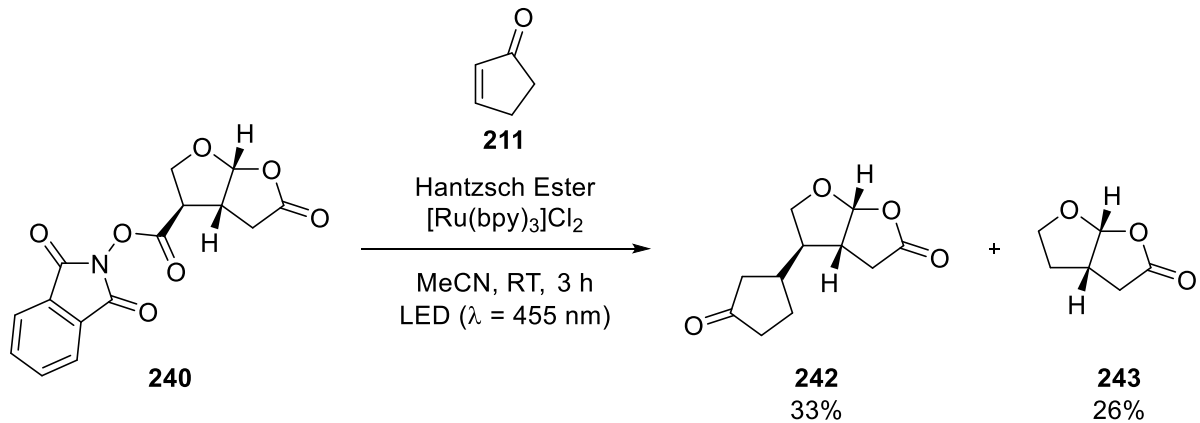
Die biologischen Versuche zeigten, dass die funktionellen Gruppen in beiden Seitenkette einen großen Einfluss auf die biologische Aktivität der Verbindung haben. Vor allem die Sauerstoffgruppe scheint eine entscheidende Rolle zu spielen, da alle deoxygenierten Derivate (**182,184** und **186**) eine drastisch verschlechterte Inhibierung zeigten. Des Weiteren hatte die Einführung von langen Alkylgruppen in den Seitenketten (**184** und **189**) einen schlechten Effekt auf die biologische Aktivität. Beim Vergleichen der funktionellen Gruppen in der C-4-Position stellte sich heraus, dass das Benzoat (**49**) die beste war, gefolgt von dem Bromid (**187**), während sich der Alkohol (**188**) als komplett inaktiv herausstellte. Die Einführung einer Alkylgruppe in der  $\alpha$ -Position des Lactons (**192**) zeigte einen positiven Einfluss auf die biologische Aktivität.

Das letzte Kapitel behandelt Studien zur Totalsynthese von Dermatolacton (**199**). Der Schlüsselschritt in dieser Synthese sollte eine decarboxylierende Kreuzkopplung der Carbonsäure **178** sein, welche bereits in der Synthese von (+)-Paeonilid (**49**) erhalten wurde (Schema 2).



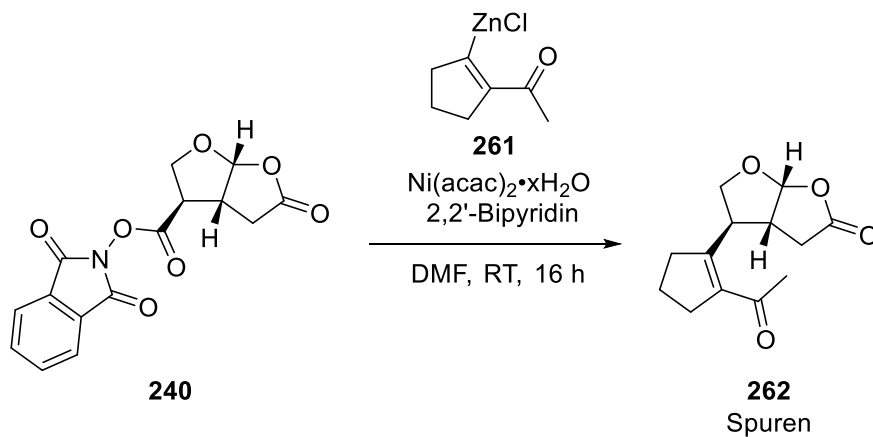
**Schema 2.** Retrosynthese von Dermatolacton (**199**).

Da die Säure **178** als unzureichend für photokatalysierte, decarboxylierende konjugierte Addition gezeigt wurde, wurde sie in den entsprechenden Aktivester **240** umgewandelt. Diese Verbindung durchläuft die durch sichtbares Licht vermittelte Kreuzkopplung, um mit dem Michael-Akzeptor **211** das Additionsprodukt **242** zu formen, welches jedoch von dem ungewollten Decarboxylierungsprodukt **243** begleitet wurde (Schema 3).



**Schema 3.** Durch sichtbares Licht vermittelte Kreuzkopplung von **240**.

Da diese Reaktion nicht den gewünschten Erfolg brachte, wurde nach einer alternativen Syntheseroute gesucht. Um direkt ein Olefin einzuführen, wurde eine Ni-katalysierte, decarboxylierende Alkenylierung vorgesehen. Dafür musste als erstes ein geeignetes Modellsubstrat synthetisiert werden. Nach der Herstellung der entsprechenden Alkenylzinkverbindung **261**, sollte diese mit dem *N*-acyloxyphthalimid **240** gekoppelt werden (Schema 4).



**Scheme 13.** Ni-katalysierte decarboxylierende Alkenylierung von **240**.

Leider ergab eine erste Testreaktion nur Spuren des gewünschten Produktes **262**. Diese Strategie oder eine Kombination aus Photoredox- und Metallkatalyse sollten in Zukunft jedoch genauer untersucht werden, um eine Synthese von Dermatolacton zu ermöglichen.

## E. Experimental Part

### 1. General Information

#### <sup>1</sup>H-NMR spectroscopy

<sup>1</sup>H-NMR spectra were recorded on a Bruker Avance 300 (300 MHz) and a Bruker Avance 400 spectrometer (400 MHz) at ambient temperature. The spectra were recorded in CDCl<sub>3</sub>, CD<sub>3</sub>CN and (CD<sub>3</sub>)<sub>2</sub>CO. Chemical shifts are reported as  $\delta$ , parts per million (ppm), relative to the center of the residual solvent signal: CDCl<sub>3</sub> = 7.26 ppm, CD<sub>3</sub>CN = 1.94 ppm and (CD<sub>3</sub>)<sub>2</sub>CO = 2.05 ppm. The spectra were analyzed by first order and the coupling constants (*J*) are reported in Hertz (Hz). The multiplicity of the signals is given as follows: s = singlet, bs = broad singlet, d = doublet, t = triplet, q = quartet, quint = quintet, m = multiplet, dd = doublet of doublets, ddd = doublet of doublets of doublets, dt = doublet of triplets, ddt = doublet of doublets of triplets, dtd = doublet of triplets of doublets. The integrals display the relative number of hydrogen atoms associated with the signals.

#### <sup>13</sup>C-NMR spectroscopy

<sup>13</sup>C-NMR spectra were recorded on a Bruker Avance 300 (75 MHz) and a Bruker Avance 400 spectrometer (101 MHz) at ambient temperature. The spectra were recorded in CDCl<sub>3</sub>, CD<sub>3</sub>CN and (CD<sub>3</sub>)<sub>2</sub>CO. Chemical shifts are reported as  $\delta$ , parts per million (ppm), relative to the center of the residual solvent signal: CDCl<sub>3</sub> = 77.2 ppm, CD<sub>3</sub>CN = 1.3 ppm and 118.3 ppm and (CD<sub>3</sub>)<sub>2</sub>CO = 29.8 ppm and 206.3 ppm. <sup>13</sup>C-NMR resonance assignment was aided by the use of DEPT 135 and DEPT 90 techniques (DEPT = distortionless enhancement by polarization transfer) to determine the number of hydrogens attached to each carbon atom and is declared as: + = primary or tertiary (CH<sub>3</sub>, CH, positive DEPT signal), - = secondary (CH<sub>2</sub>, negative DEPT signal) and C<sub>q</sub> = quarternary (no DEPT signal) carbon atoms.

#### Chiral high-performance liquid chromatography (chiral HPLC)

Chiral HPLC was performed on a Varian 920-LC with DAD using a Phenomenex Lux Cellulose-1 or Cellulose-2 column (4.6 x 250 mm, 5  $\mu$ m).

### **Column chromatography**

(Flash-) Column chromatography was performed using Merck Gerduran 60 (0.063-0.200 mm) or Merck flash silica gel 60 (0.040-0.063 mm).

### **Cyclic voltammetry**

Cyclic voltammetry measurements were carried out on an Autolab PGSTAT 302N set-up at 20 °C in acetonitrile, containing tetrabutyl ammonium tetrafluoroborate as supporting electrolyte. A conventional undivided electrochemical cell equipped with a glassy carbon working electrode, platinum wire as the counter electrode and silver wire as the reference electrode was used. The solvent was degassed by vigorous nitrogen bubbling prior to the measurements. Redox potentials were referenced against ferrocene as an internal standard. All values are reported in reference to the SCE electrode.

### **Gas chromatography**

Gas chromatography was carried out on a Fisons GC 8000 Series with a flame ionization detector (FID). As stationary phase DB1 (100% dimethylpolysiloxane, 30 m, ID 0.25 mm, 0.25 µm Film) was used. GC instrument conditions: Inlet temperature = 250 °C; detector temperature = 300 °C. GC method: starting temperature 140 °C, then temperature ramp (5 °C/min) for 12 min to 200 °C followed by an isothermal period at 200 °C for 5 min.

### **Infrared spectroscopy (IR)**

ATR-IR spectroscopy was carried out on a Bio-Rad Excalibur FTS 3000 MX equipped with a Specac Golden Gate Diamond Single Reflection ATR-System and an Agilent Cary 630 FT-IR spectrometer. Solid as well as liquid compounds were measured neat. The wavenumbers are reported as  $\text{cm}^{-1}$ .

### **Light Transmission Aggregometry**

Light transmission aggregometry was carried out on a ChronoLog 490 Optical Aggregometer and was recorded on a computer with the AGGRO/LINK software.

### **Mass spectrometry (MS)**

Mass spectrometry was performed in the Analytical Department of the University of Regensburg on a Jeol AccuTOF GCX, a Finnigan MAT SSQ 710 A, a Finnigan Thermoquest TSQ 7000 or an Agilent Technologies Q-TOF 6540 UHD.

### **Melting points:**

The melting points were measured on a SRS MPA 100 OptiMelt apparatus with a silicon oil bath. Thus obtained values were not corrected.

### **Optical rotation:**

The optical rotation was determined using a Perkin Elmer 241 polarimeter or an Anton Paar MCP 500 at 589 nm wavelength (sodium-*d*-line) in a 1.0 dm measuring cell with an inner volume of approximately 2 mL and the specified solvent.

### **Solvents and chemicals**

DCM, ethyl acetate and hexanes (petroleum ether, PE (60/40)) were distilled prior to use for column chromatography. Anhydrous solvents were prepared according to standard procedures. Commercially available chemicals were used as received, without further purification.

### **Thin layer chromatography (TLC)**

Thin layer chromatography was performed on aluminum plates coated with silica gel (Merck silica gel 60 F<sub>254</sub> and Machery-Nagel ALUGRAM® Xtra SIL G/UV<sub>254</sub>). Visualization was accomplished by UV light ( $\lambda = 254$  nm) and through the use of TLC stains, *e.g.* vanillin/sulfuric acid solution, potassium permanganate solution, *Seebach's Magic Stain* or bromocresol green, followed by heating.

### **X-ray crystallography**

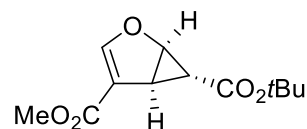
X-ray crystallography was performed in the Analytical Department of the University of Regensburg on an Agilent Technologies SuperNova, an Agilent Technologies Gemini R Ultra, an Agilent GV 50 or a Rigaku GV 50.

## 2. Synthesis of compounds

Following compounds were already available on stock in our laboratories or were synthesized according to literature procedures and spectroscopic data matched well with those reported:

4-methylbenzenesulfonyl azide,<sup>1</sup> *tert*-butyl 2-diazoacetate,<sup>2</sup> 3-furoic acid methyl ester (**100**), ligands **143**, **144**, **145** and **146**, (4*S*,5*R*)-4-methyl-5-phenyloxazolidin-2-one (**152**), Jones reagent,<sup>3</sup> Grubbs' II catalyst.

### 2.1 Synthesis of (+)-paeonilide (**49**)

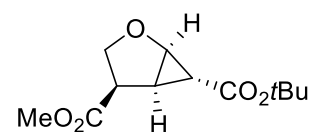


#### 6-(*tert*-Butyl) 4-methyl (1*R*,5*S*,6*R*)-2-oxabicyclo[3.1.0]hex-3-ene-4,6-dicarboxylate (**142**)

In a flame dried 25 mL Schlenk flask under N<sub>2</sub>-atmosphere Cu(OTf)<sub>2</sub> (172 mg, 476 μmol, 1.00 mol%) was dissolved in dry DCM (10 mL) and (*R,R*)-*i*Pr-bis(oxazoline)-ligand **143** (298 mg, 1.12 mmol, 2.20 mol%) was added resulting in a deep blue solution. After stirring for 20 min at rt, the copper complex solution was transferred into a flame dried 250 mL Schlenk flask under N<sub>2</sub>-atmosphere containing a solution of 3-furoic acid methyl ester **100** (6.00 g, 47.6 mmol, 1.00 equiv.) in dry DCM (20 mL) at 0 °C. Subsequently, phenylhydrazine (53.8 μL, 59.2 mg, 547 μmol, 1.00 mol%) was added, causing the solution to turn into a dark red-brown color, followed by dropwise addition of *tert*-butyl 2-diazoacetate (10.2 g, 71.4 mmol, 1.50 equiv., 74.6 g of a 13.6 wt% solution in dry DCM) with the aid of a syringe pump (one drop every 10 seconds). After complete addition, the reaction mixture was allowed to warm to ambient temperature and filtered through basic Al<sub>2</sub>O<sub>3</sub>, which was then washed with DCM (200 mL). Concentration under reduced pressure afforded a yellow oil which was purified by column chromatography (silica, PE/EA = 15:1) to give **142** (5.74 g, 23.9 mmol, 50%, 83% *ee*) as a white solid.

*R*<sub>f</sub> = 0.56 (PE/EA = 5:1, Vanillin); <sup>1</sup>H-NMR (400 MHz, CDCl<sub>3</sub>) δ = 7.17 (s, 1H), 4.93 (d, *J* = 5.6 Hz, 1H), 3.74 (s, 3H), 3.01 (dd, *J* = 5.6, 2.9 Hz, 1H), 1.43 (s, 9H), 1.03 (d, *J* = 2.5 Hz, 1H); <sup>13</sup>C-NMR (101 MHz, CDCl<sub>3</sub>) δ = 170.72 (C<sub>q</sub>), 164.16 (C<sub>q</sub>), 156.36 (+), 115.79 (C<sub>q</sub>), 81.42 (C<sub>q</sub>),

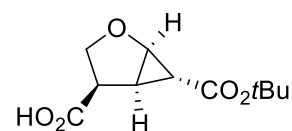
68.91 (+), 51.49(+), 29.07(+), 28.12(+), 22.52 (+); **IR** (neat):  $\tilde{\nu}$  (cm<sup>-1</sup>) = 3112, 3052, 2973, 1703, 1599, 1444, 1367, 1323, 1272, 1161, 1099, 1045, 976, 831, 792, 761, 721; **LRMS** (+ESI):  $m/z$  = 263 [M+Na]<sup>+</sup>, 258 [M+NH<sub>4</sub>]<sup>+</sup>, 241 [M+H]<sup>+</sup>, 185 [M+H-C<sub>4</sub>H<sub>8</sub>]<sup>+</sup>; **HRMS** (+ESI):  $m/z$  = 241.1069 [M+H]<sup>+</sup>; calc. for [C<sub>12</sub>H<sub>17</sub>O<sub>5</sub>]<sup>+</sup> = 241.1071; **HPLC analysis** (Phenomenex Lux Cellulose-2, *n*-heptane/*i*PrOH 99:1, 1.0 mL/min, 254 nm):  $t_r$  (major) = 12.59,  $t_r$  (minor) = 17.59, 83% *ee*;  $[\alpha]_D^{20}$  = +26.2 (DCM, *c* = 1.0); **m.p.** = 78 - 79 °C.



### 6-(*tert*-Butyl) 4-methyl (1*R*,4*R*,5*R*,6*R*)-2-oxabicyclo[3.1.0]hexane-4,6-dicarboxylate (**147**)

A solution of **142** (3.02 g, 12.6 mmol, 1.00 equiv.) in EA (5 mL) was transferred into an autoclave, charged with Rh/C (151 mg, 73.4 μmol, 0.58 mol%, 5% Rh on charcoal) and was stirred under 20 bar hydrogen pressure for 30 min at ambient temperature. Afterward, the reaction mixture was filtered through two folded filters and washed with EA. The solvent was removed under reduced pressure to obtain the pure product **147** (2.99 g, 12.3 mmol, 98%) as a colorless oil.

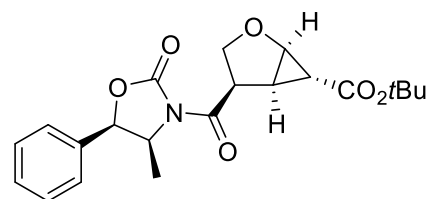
$R_f$  = 0.46 (PE/EA = 5:1, Vanillin); **<sup>1</sup>H-NMR** (400 MHz, CDCl<sub>3</sub>)  $\delta$  = 4.17 – 4.09 (m, 2H), 3.74 (s, 3H), 3.68 (t, *J* = 9.8 Hz, 1H), 3.36 (td, *J* = 9.5, 5.4 Hz, 1H), 2.35 (td, *J* = 5.4, 3.8 Hz, 1H), 2.18 (dd, *J* = 3.7, 0.7 Hz, 1H), 1.41 (s, 9H); **<sup>13</sup>C-NMR** (101 MHz, CDCl<sub>3</sub>)  $\delta$  = 172.01 (C<sub>q</sub>), 169.84 (C<sub>q</sub>), 80.91 (C<sub>q</sub>), 67.98 (-), 65.71 (+), 52.25 (+), 44.23 (+), 28.11 (+), 27.50 (+), 22.67 (+); **IR** (neat):  $\tilde{\nu}$  (cm<sup>-1</sup>) = 2978, 1737, 1711, 1439, 1394, 1368, 1319, 1256, 1200, 1155, 1118, 1070, 980, 928, 864, 838, 786, 719; **LRMS** (+APCI):  $m/z$  = 248 [M+NH<sub>4</sub>]<sup>+</sup>, 231 [M+H]<sup>+</sup>, 187 [M+H-C<sub>4</sub>H<sub>8</sub>]<sup>+</sup>; **HRMS** (+APCI):  $m/z$  = 243.1228 [M+H]<sup>+</sup>; calc. for [C<sub>12</sub>H<sub>19</sub>O<sub>5</sub>]<sup>+</sup> = 243.1227;  $[\alpha]_D^{20}$  = -70.6 (DCM, *c* = 1.0).



**(1R,4R,5R,6R)-6-(tert-Butoxycarbonyl)-2-oxabicyclo[3.1.0]hexane-4-carboxylic acid (155)**

Ester **147** (3.00 g, 12.4 mmol, 1.00 equiv.) was dissolved in an H<sub>2</sub>O/THF (2:1, v/v) mixture (90 mL) resulting in a turbid solution. Subsequently, LiOH (326 mg, 13.6 mmol, 1.10 equiv.) was added and the mixture was stirred for 1.5 h at ambient temperature. The reaction mixture was extracted with Et<sub>2</sub>O (2 x 20 mL) to remove undesired side products. Afterward, the aqueous phase was acidified to pH 2 with 2 M HCl and extracted with Et<sub>2</sub>O (3 x 30 mL). The combined organic layers were dried over Na<sub>2</sub>SO<sub>4</sub>, filtered and concentrated under reduced pressure to afford the desired acid **155** (2.68 g, 11.7 mmol, 95%) as a white solid.

$R_f$  = 0.37 (PE/EA = 3:1 + 1% formic acid, KMnO<sub>4</sub>); <sup>1</sup>H-NMR (400 MHz, CDCl<sub>3</sub>)  $\delta$  = 11.25 (bs, 1H), 4.20 (dd,  $J$  = 5.4, 1.2 Hz, 1H), 4.16 (t,  $J$  = 9.4 Hz, 1H), 3.68 (t,  $J$  = 9.8 Hz, 1H), 3.42 (td,  $J$  = 9.5, 5.4 Hz, 1H), 2.41 (td,  $J$  = 5.4, 3.9 Hz, 1H), 2.21 (dd,  $J$  = 3.7, 0.7 Hz, 1H), 1.42 (s, 9H); <sup>13</sup>C-NMR (101 MHz, CDCl<sub>3</sub>)  $\delta$  = 177.65 (C<sub>q</sub>), 170.16 (C<sub>q</sub>), 81.56 (C<sub>q</sub>), 68.04 (-), 66.04 (+), 44.60 (+), 28.40 (+), 27.71 (+), 23.06 (+); IR (neat):  $\tilde{\nu}$  (cm<sup>-1</sup>) = 3194, 2937, 2900, 1703, 1402, 1368, 1320, 1257, 1200, 1155, 1118, 1076, 980, 928, 887, 842, 779, 716, 678; LRMS (+ESI):  $m/z$  = 251 [M+Na]<sup>+</sup>, 246 [M+NH<sub>4</sub>]<sup>+</sup>, 173 [M+H-C<sub>4</sub>H<sub>8</sub>]<sup>+</sup>; HRMS (+ESI):  $m/z$  = 229.1072 [M+H]<sup>+</sup>; calc. for [C<sub>11</sub>H<sub>17</sub>O<sub>5</sub>]<sup>+</sup> = 229.1071; [ $\alpha$ ]<sub>D</sub><sup>20</sup> = -68.5 (MeOH, c = 1.0); m.p. = 76 - 77 °C.



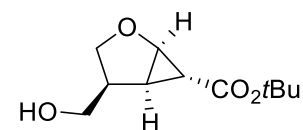
**tert-Butyl (1R,4R,5R,6R)-4-((4S,5R)-4-methyl-2-oxo-5-phenyloxazolidine-3-carbonyl)-2-oxabicyclo[3.1.0]hexane-6-carboxylate (156)**

In a flame dried 100 mL Schlenk flask under N<sub>2</sub>-atmosphere acid **155** (3.44 g, 15.1 mmol, 1.00 equiv.) was dissolved in dry THF (15 mL) and Et<sub>3</sub>N (2.50 mL, 1.83 g, 18.1 mmol, 1.20 equiv.) was added. The reaction mixture was cooled to -78 °C, pivaloyl chloride (1.94 mL, 1.91 g, 15.8 mmol, 1.05 equiv.) was added dropwise and subsequently the mixture was stirred



for 1 h at 0 °C. In a separate flame dried 25 mL Schlenk flask under N<sub>2</sub>-atmosphere oxazolidin-2-one **152** (2.80 g, 15.8 mmol, 1.05 equiv.) was dissolved in dry THF (8 mL), cooled to -40 °C and *n*-BuLi (5.85 mL, 15.8 mmol, 1.05 equiv., 2.70 M solution in toluene) was added dropwise. After stirring for 5 min, this solution was transferred to the reaction mixture which was then stirred for 1 h at -78 °C. Afterward, the reaction mixture was allowed to warm to 0 °C and was quenched with a sat. NaHCO<sub>3</sub>-solution (100 mL). THF was removed under reduced pressure followed by extraction with DCM (4 x 30 mL). The combined organic layers were washed with brine (30 mL), dried over NaSO<sub>4</sub>, filtered and concentrated under reduced pressure. The crude product was purified by column chromatography (silica, PE/EA = 5:1) to give pure **156** (4.40 g, 11.4 mmol, 75%) as a white solid.

$R_f$  = 0.51 (PE/EA = 3:1, KMnO<sub>4</sub>); <sup>1</sup>H-NMR (400 MHz, CDCl<sub>3</sub>)  $\delta$  = 7.45 – 7.34 (m, 3H), 7.33 – 7.27 (m, 2H), 5.74 (d, *J* = 7.3 Hz, 1H), 4.82 (p, *J* = 6.7 Hz, 1H), 4.57 (td, *J* = 9.2, 5.3 Hz, 1H), 4.21 – 4.12 (m, 2H), 3.90 (t, *J* = 9.5 Hz, 1H), 2.53 (td, *J* = 5.4, 4.0 Hz, 1H), 2.21 (dd, *J* = 3.8, 0.8 Hz, 1H), 1.42 (s, 9H), 0.89 (d, *J* = 6.6 Hz, 3H); <sup>13</sup>C-NMR (101 MHz, CDCl<sub>3</sub>)  $\delta$  = 170.98 (C<sub>q</sub>), 170.10 (C<sub>q</sub>), 153.04 (C<sub>q</sub>), 133.32 (C<sub>q</sub>), 129.19 (+), 129.07 (+), 125.93 (+), 81.20 (C<sub>q</sub>), 79.34 (+), 68.18 (-), 66.10 (+), 55.37 (+), 43.92 (+), 28.40 (+), 28.23 (+), 23.09 (+), 14.83 (+); IR (neat):  $\tilde{\nu}$  (cm<sup>-1</sup>) = 2978, 2933, 2363, 1778, 1700, 1457, 1349, 1320, 1241, 1197, 1156, 1118, 1066, 977, 920, 839, 768, 723, 701; LRMS (+ESI): *m/z* = 797 [2M+Na]<sup>+</sup>, 410 [M+Na]<sup>+</sup>, 405 [M+NH<sub>4</sub>]<sup>+</sup>, 332 [M+H-C<sub>4</sub>H<sub>8</sub>]<sup>+</sup>; HRMS (+ESI): *m/z* = 388.1755 [M+H]<sup>+</sup>; calc. for [C<sub>21</sub>H<sub>26</sub>NO<sub>6</sub>]<sup>+</sup> = 388.1755; [ $\alpha$ ]<sub>D</sub><sup>20</sup> = -94.4 (CHCl<sub>3</sub>, *c* = 1.0); m.p. = 62 - 63 °C.

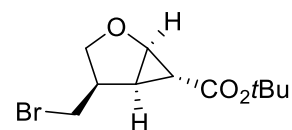


**tert-Butyl (1R,4S,5R,6R)-4-(hydroxymethyl)-2-oxabicyclo[3.1.0]hexane-6-carboxylate (157)**

Oxazolidinone **156** (1.94 g, 5.01 mmol, 1.00 equiv.) was dissolved in THF (40 mL) and NaBH<sub>4</sub> (569 mg, 15.0 mmol, 3.00 equiv.) followed by MeOH (15 mL, 3 mL/mmol) were added. After stirring for 1 h at ambient temperature the reaction was quenched with a sat. NH<sub>4</sub>Cl-solution (6 mL). The reaction mixture was extracted with EA (3 x 60 mL) and the combined organic layers were dried over NaSO<sub>4</sub>, filtered and concentrated under reduced pressure. The crude

product was purified by column chromatography (silica, PE/EA = 2:1) to yield **157** (1.05 g, 4.92 mmol, 98%) as a white solid.

$R_f$  = 0.34 (PE/EA = 1:1, KMnO<sub>4</sub>); **<sup>1</sup>H-NMR** (400 MHz, CDCl<sub>3</sub>)  $\delta$  = 4.14 (d,  $J$  = 5.5 Hz, 1H), 4.05 (t,  $J$  = 9.1 Hz, 1H), 3.74 (dd,  $J$  = 10.6, 6.9 Hz, 1H), 3.61 (dd,  $J$  = 10.6, 6.9 Hz, 1H), 3.12 (t,  $J$  = 9.8 Hz, 1H), 2.79 (qd,  $J$  = 12.0, 6.9 Hz, 1H), 2.35 (bs, 1H), 2.11 (dd,  $J$  = 9.3, 5.1 Hz, 1H), 1.91 (d,  $J$  = 3.9 Hz, 1H), 1.39 (s, 9H); **<sup>13</sup>C-NMR** (101 MHz, CDCl<sub>3</sub>)  $\delta$  = 170.68 (C<sub>q</sub>), 81.10 (C<sub>q</sub>), 69.48 (-), 65.99 (+), 63.30 (-), 42.74 (+), 28.46 (+), 27.19 (+), 22.21 (+); **IR** (neat):  $\tilde{\nu}$  (cm<sup>-1</sup>) = 3507, 3396, 3313, 2982, 2937, 2878, 1707, 1700, 1457, 1394, 1368, 1312, 1256, 1200, 1156, 1107, 1066, 980, 947, 924, 835, 772; **LRMS** (+ESI):  $m/z$  = 237 [M+Na]<sup>+</sup>, 215 [M+H]<sup>+</sup>, 159 [M+H-C<sub>4</sub>H<sub>8</sub>]<sup>+</sup>, 143 [M+H-C<sub>4</sub>H<sub>8</sub>-H<sub>2</sub>O]<sup>+</sup>; **HRMS** (+ESI):  $m/z$  = 215.1282 [M+H]<sup>+</sup>; calc. for [C<sub>11</sub>H<sub>19</sub>O<sub>4</sub>]<sup>+</sup> = 215.1278; **HPLC analysis** (Phenomenex Lux Cellulose-2, *n*-heptane/*i*PrOH 95:5, 1.0 mL/min, 215 nm):  $t_r$  (minor) = 22.28,  $t_r$  (major) = 27.95, >99% *ee*;  $[\alpha]_D^{20}$  = -82.6 (CHCl<sub>3</sub>, *c* = 1.0); **m.p.** = 81 - 83 °C.

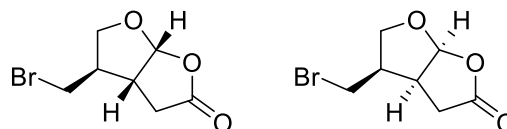


***tert*-Butyl (1*R*,4*R*,5*S*,6*R*)-4-(bromomethyl)-2-oxabicyclo[3.1.0]hexane-6-carboxylate (158)**

Alcohol **157** (1.83 g, 8.54 mmol, 1.00 equiv.) was dissolved in DCM (30 mL) and cooled to 0 °C. At this temperature PPh<sub>3</sub> (2.69 g, 10.3 mmol, 1.20 equiv.) and CBr<sub>4</sub> (3.40 g, 10.3 mmol, 1.20 equiv.) were added and the reaction was allowed to stir for 1 h at ambient temperature. The reaction mixture was concentrated under reduced pressure and the crude product was purified by column chromatography (silica, PE/EA = 8:1) to yield **158** (2.19 g, 7.90 mmol, 93%) as a white solid.

$R_f$  = 0.60 (PE/EA = 5:1, KMnO<sub>4</sub>); **<sup>1</sup>H-NMR** (400 MHz, CDCl<sub>3</sub>)  $\delta$  = 4.24 (dd,  $J$  = 5.4, 0.9 Hz, 1H), 4.14 (dd,  $J$  = 8.9, 7.9 Hz, 1H), 3.54 (dd,  $J$  = 10.0, 6.1 Hz, 1H), 3.29 (dd,  $J$  = 9.8, 8.8 Hz, 1H), 3.17 – 3.01 (m, 2H), 2.17 (dd,  $J$  = 9.5, 4.4 Hz, 1H), 1.96 (d,  $J$  = 3.8 Hz, 1H), 1.42 (s, 9H); **<sup>13</sup>C-NMR** (101 MHz, CDCl<sub>3</sub>)  $\delta$  = 170.23 (C<sub>q</sub>), 81.31 (C<sub>q</sub>), 71.34 (-), 66.44 (+), 43.06 (+), 32.07 (-), 28.85 (+), 28.44 (+), 21.91 (+); **IR** (neat):  $\tilde{\nu}$  (cm<sup>-1</sup>) = 3068, 2986, 2933, 2896, 1707, 1457, 1401, 1367, 1334, 1282, 1245, 1159, 1122, 1059, 995, 943, 872, 842, 775, 727; **LRMS** (+APCI):  $m/z$  = 294

$[M+NH_4]^+$ , 277  $[M+H]^+$ , 221  $[M+H-C_4H_8]^+$ ; **HRMS** (+APCI):  $m/z = 277.0430 [M+H]^+$ ; calc. for  $[C_{11}H_{18}BrO_3]^+ = 277.0434$ ;  $[\alpha]_D^{20} = -32.6$  (CHCl<sub>3</sub>, c = 1.0); **m.p.** = 97 - 98 °C.



**(3aR,4R,6aR)-4-(Bromomethyl)tetrahydrofuro[2,3-b]furan-2(3H)-one (159)**

**(3aS,4R,6aS)-4-(Bromomethyl)tetrahydrofuro[2,3-b]furan-2(3H)-one (160)**

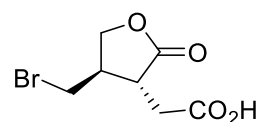
Bromide **158** (937 mg, 3.38 mmol, 1.00 equiv.) was dissolved in toluene (25 mL) and Amberlyst® 15 (101 mg, 30 mg/mmol) was added. The reaction mixture was refluxed for 20 h and the diastereomeric ratio was monitored by GC. Afterward, the mixture was filtrated and concentrated under reduced pressure. The crude product was purified by column chromatography (silica, PE/EA = 2:1) to yield minor diastereomer **160** (79.3 mg, 359 μmol, 11%) and major diastereomer **159** (604 mg, 2.73 mmol, 81%) both as a slightly yellow oil.

**Major Diastereomer 159:**

$R_f = 0.56$  (PE/EA = 1:1, KMnO<sub>4</sub>); **<sup>1</sup>H-NMR** (400 MHz, CDCl<sub>3</sub>)  $\delta = 6.09$  (d,  $J = 5.2$  Hz, 1H), 4.10 (dd,  $J = 10.0, 5.9$  Hz, 1H), 3.97 (dd,  $J = 10.0, 2.3$  Hz, 1H), 3.40 (dd,  $J = 10.3, 7.4$  Hz, 1H), 3.33 (dd,  $J = 10.3, 7.7$  Hz, 1H), 3.04 – 2.97 (m, 1H), 2.92 (dd,  $J = 18.1, 10.4$  Hz, 1H), 2.55 – 2.45 (m, 2H); **<sup>13</sup>C-NMR** (101 MHz, CDCl<sub>3</sub>)  $\delta = 174.63$  (C<sub>q</sub>), 108.15 (+), 70.98 (-), 48.85 (+), 44.25 (+), 34.73 (-), 34.23 (-); **IR** (neat):  $\tilde{\nu}$  (cm<sup>-1</sup>) = 2963, 2885, 1774, 1483, 1416, 1356, 1297, 1237, 1170, 1103, 1044, 969, 891, 831, 678; **LRMS** (+APCI):  $m/z = 238 [M+NH_4]^+$ , 221  $[M+H]^+$ ; **HRMS** (+APCI):  $m/z = 220.9810 [M+H]^+$ ; calc. for  $[C_7H_{10}BrO_3]^+ = 220.9808$ ;  $[\alpha]_D^{20} = +22.7$  (CHCl<sub>3</sub>, c = 1.0).

**Minor Diastereomer 160:**

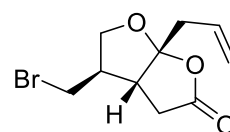
$R_f = 0.61$  (PE/EA = 1:1, KMnO<sub>4</sub>); **<sup>1</sup>H-NMR** (400 MHz, CDCl<sub>3</sub>)  $\delta = 6.13$  (d,  $J = 5.5$  Hz, 1H), 4.16 (dd,  $J = 9.2, 7.1$  Hz, 1H), 3.57 (dd,  $J = 11.2, 9.2$  Hz, 1H), 3.42 (dd,  $J = 10.5, 7.1$  Hz, 1H), 3.33 – 3.22 (m, 2H), 2.96 – 2.84 (m, 1H), 2.70 (dd,  $J = 19.0, 10.7$  Hz, 1H), 2.55 (dd,  $J = 19.0, 5.3$  Hz, 1H); **<sup>13</sup>C-NMR** (101 MHz, CDCl<sub>3</sub>)  $\delta = 174.94$  (C<sub>q</sub>), 108.35 (+), 70.38 (-), 44.31 (+), 41.74 (+), 27.89 (-), 27.81 (-); **IR** (neat):  $\tilde{\nu}$  (cm<sup>-1</sup>) = 2970, 2870, 1780, 1484, 1442, 1375, 1342, 1293, 1230, 1178, 1126, 1051, 984, 895; **LRMS** (+APCI):  $m/z = 238 [M+NH_4]^+$ , 221  $[M+H]^+$ ;  $[\alpha]_D^{20} = -64.4$  (CHCl<sub>3</sub>, c = 0.5).



### 2-((3R,4R)-4-(Bromomethyl)-2-oxotetrahydrofuran-3-yl)acetic acid (**167**)

Lactone **159** (515 mg, 2.33 mmol, 1.00 equiv.) was dissolved in acetone (15 mL) and cooled to 0 °C. At this temperature Jones reagent (2.33 mL of a 3.00 M solution, 6.99 mmol, 3.00 equiv.) was added and the reaction mixture was stirred for 1.5 h at ambient temperature. After quenching the reaction with 2-propanol (3 mL), the chromium salts were dissolved with H<sub>2</sub>O (20 mL) and the reaction mixture was extracted with EA (4 x 25 mL). The combined organic layers were dried over Na<sub>2</sub>SO<sub>4</sub>, filtered and concentrated under reduced pressure to afford the desired acid **167** (542 mg, 2.29 mmol, 98%) as a white solid.

$R_f$  = 0.30 (PE/EA = 1:1 + 1% formic acid, KMnO<sub>4</sub>); <sup>1</sup>H-NMR (400 MHz, CDCl<sub>3</sub>)  $\delta$  = 4.53 (dd,  $J$  = 9.2, 7.8 Hz, 1H), 4.06 (dd,  $J$  = 9.2, 8.6 Hz, 1H), 3.59 (dd,  $J$  = 10.7, 4.6 Hz, 1H), 3.48 (dd,  $J$  = 10.7, 6.9 Hz, 1H), 2.99 – 2.77 (m, 4H); <sup>13</sup>C-NMR (101 MHz, CDCl<sub>3</sub>)  $\delta$  = 177.06 (C<sub>q</sub>), 176.37 (C<sub>q</sub>), 70.64 (-), 42.54 (+), 41.03 (+), 33.44 (-), 32.84 (-); IR (neat):  $\tilde{\nu}$  (cm<sup>-1</sup>) = 2971, 2922, 1715, 1483, 1409, 1334, 1271, 1238, 1170, 1096, 1014, 835, 682; LRMS (+ESI):  $m/z$  = 495 [2M+Na]<sup>+</sup>, 259 [M+Na]<sup>+</sup>, 237 [M+H]<sup>+</sup>, 219 [M+H-H<sub>2</sub>O]<sup>+</sup>; HRMS (+ESI):  $m/z$  = 236.9760 [M+H]<sup>+</sup>; calc. for [C<sub>7</sub>H<sub>10</sub>BrO<sub>4</sub>]<sup>+</sup> = 236.9757; [ $\alpha$ ]<sub>D</sub><sup>20</sup> = +57.1 (MeOH,  $c$  = 1.0); m.p. = 96 - 98 °C.



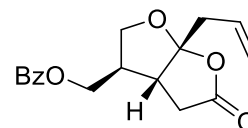
### (3aR,4R,6aR)-6a-Allyl-4-(bromomethyl)tetrahydrofuro[2,3-*b*]furan-2(3H)-one (**169**)

In a flame dried 25 mL Schlenk flask under N<sub>2</sub>-atmosphere acid **167** (317 mg, 1.34 mmol, 1.00 equiv.) was dissolved in dry THF (13 mL) and cooled to -78 °C. At this temperature allylmagnesium bromide (3.34 mL, 3.34 mmol, 2.50 equiv., 1.00 M solution in Et<sub>2</sub>O) was added dropwise and the reaction mixture was stirred for 2 h at -78 °C. After quenching with H<sub>2</sub>O (10 mL), the reaction mixture was acidified to pH 2 with 2 M HCl and extracted with Et<sub>2</sub>O (4 x 30 mL). The combined organic layers were dried over NaSO<sub>4</sub>, filtered and concentrated

under reduced pressure The crude product was purified by column chromatography (silica, PE/EA = 3:1 + 1% formic acid) to yield **169** (282 mg, 1.08 mmol, 81%) as a white solid.

**Note:** In some cases when an older allylmagnesium bromide solution was used the double bond isomerization product was obtained as an inseparable byproduct. The product is not very stable and therefore should not be stored too long.

$R_f$  = 0.38 (PE/EA = 2:1, Vanillin);  $^1\text{H-NMR}$  (400 MHz,  $\text{CDCl}_3$ )  $\delta$  = 5.85 – 5.71 (m, 1H), 5.30 – 5.23 (m, 2H), 4.12 (dd,  $J$  = 10.0, 6.0 Hz, 1H), 3.95 (dd,  $J$  = 10.0, 2.1 Hz, 1H), 3.41 (dd,  $J$  = 10.2, 7.4 Hz, 1H), 3.33 (dd,  $J$  = 10.2, 8.0 Hz, 1H), 2.94 (dd,  $J$  = 18.6, 10.1 Hz, 1H), 2.73 (dt,  $J$  = 10.2, 2.5 Hz, 1H), 2.70 – 2.61 (m, 2H), 2.56 (dd,  $J$  = 18.6, 2.4 Hz, 1H), 2.49 – 2.41 (m, 1H);  $^{13}\text{C-NMR}$  (101 MHz,  $\text{CDCl}_3$ )  $\delta$  = 173.82 ( $\text{C}_q$ ), 130.43 (+), 121.00 (-), 118.13 ( $\text{C}_q$ ), 70.79 (-), 49.78 (+), 46.10 (+), 41.51 (-), 36.29 (-), 34.15 (-); **IR** (neat):  $\tilde{\nu}$  ( $\text{cm}^{-1}$ ) = 3083, 2948, 2889, 2363, 1774, 1640, 1480, 1416, 1320, 1267, 1211, 1126, 1059, 965, 928, 831, 742, 712, 667; **LRMS** (+APCI):  $m/z$  = 278  $[\text{M}+\text{NH}_4]^+$ , 261  $[\text{M}+\text{H}]^+$ ; **HRMS** (+APCI):  $m/z$  = 261.0124  $[\text{M}+\text{H}]^+$ ; calc. for  $[\text{C}_{10}\text{H}_{14}\text{BrO}_3]^+$  = 261.0121;  $[\alpha]_{\text{D}}^{20}$  = +9.6 ( $\text{CHCl}_3$ ,  $c$  = 1.0); **m.p.** = 49 - 51 °C.

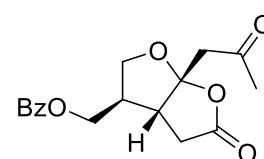


**((3R,3aR,6aR)-6a-Allyl-5-oxohexahydrofuro[2,3-b]furan-3-yl)methyl benzoate (170)**

Allyl **169** (261 mg, 1.00 mmol, 1.00 equiv.) was dissolved in DMF (10 mL) and potassium benzoate (421 mg, 2.63 mmol, 2.63 equiv.) was added at ambient temperature. Subsequently, the reaction mixture was stirred for 2 h at 80 °C. After cooling to ambient temperature the reaction mixture was diluted with  $\text{H}_2\text{O}$  (50 mL) and extracted with  $\text{Et}_2\text{O}$  (5 x 50 mL). The combined organic layers were washed with  $\text{H}_2\text{O}$  (2 x 30 mL), dried over  $\text{NaSO}_4$ , filtered and concentrated under reduced pressure. The crude product was purified by column chromatography (silica, PE/EA = 4:1 → 3:1) to yield **170** (241 mg, 798  $\mu\text{mol}$ , 80%) as a white solid.

$R_f$  = 0.32 (PE/EA = 2:1, Vanillin);  $^1\text{H-NMR}$  (400 MHz,  $\text{CDCl}_3$ )  $\delta$  = 8.05 – 7.98 (m, 2H), 7.63 – 7.55 (m, 1H), 7.50 – 7.42 (m, 2H), 5.87 – 5.71 (m, 1H), 5.29 – 5.17 (m, 2H), 4.31 (dd,  $J$  = 11.0, 7.1 Hz, 1H), 4.23 (dd,  $J$  = 11.0, 7.8 Hz, 1H), 4.13 (dd,  $J$  = 9.8, 6.0 Hz, 1H), 4.03 (dd,  $J$  = 9.8, 2.4 Hz, 1H),

2.94 (dd,  $J = 18.4, 9.9$  Hz, 1H), 2.78 – 2.47 (m, 5H);  $^{13}\text{C-NMR}$  (101 MHz,  $\text{CDCl}_3$ )  $\delta = 174.32$  ( $\text{C}_q$ ), 166.59 ( $\text{C}_q$ ), 133.74 (+), 130.85 (+), 129.90 (+), 129.80 ( $\text{C}_q$ ), 128.86 (+), 121.18 (-), 118.51 ( $\text{C}_q$ ), 69.49 (-), 65.13 (-), 46.60 (+), 44.10 (+), 41.80 (-), 36.60 (-); **IR** (neat):  $\tilde{\nu}$  ( $\text{cm}^{-1}$ ) = 3075, 2956, 1774, 1714, 1643, 1602, 1454, 1420, 1390, 1316, 1267, 1207, 1178, 1111, 1070, 1025, 973, 917, 805, 708; **LRMS** (+ESI):  $m/z = 627$  [ $2\text{M}+\text{Na}$ ] $^+$ , 325 [ $\text{M}+\text{Na}$ ] $^+$ , 303 [ $\text{M}+\text{H}$ ] $^+$ ; **HRMS** (+ESI):  $m/z = 303.1231$  [ $\text{M}+\text{H}$ ] $^+$ ; calc. for [ $\text{C}_{17}\text{H}_{19}\text{O}_5$ ] $^+$  = 303.1227;  $[\alpha]_{\text{D}}^{20} = +25.4$  ( $\text{CHCl}_3$ ,  $c = 1.0$ ); **m.p.** = 71 – 73 °C.



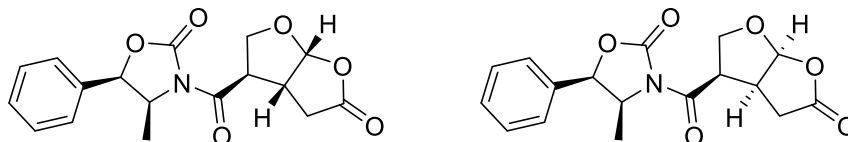
**((3R,3aR,6aR)-5-Oxo-6a-(2-oxopropyl)hexahydrofuro[2,3-b]furan-3-yl)methyl benzoate (49)**

Benzoate **170** (31.6 mg, 105  $\mu\text{mol}$ , 1.00 equiv.) was dissolved in an acetone/ $\text{H}_2\text{O}$  (4:1, v/v) mixture (2 mL) and  $\text{Hg}(\text{OAc})_2$  (10.0 mg, 31.4  $\mu\text{mol}$ , 0.30 equiv.) was added at 0 °C. After stirring for 10 min at 0 °C, Jones reagent (105  $\mu\text{L}$  of a 3.00 M solution, 314  $\mu\text{mol}$ , 3.00 equiv.) was added and the reaction mixture was stirred for 18 h at ambient temperature. After quenching the reaction with a few drops of 2-propanol the chromium salts were dissolved with  $\text{H}_2\text{O}$  (5 mL) and the reaction mixture was extracted with EA (4 x 10 mL). The combined organic layers were dried over  $\text{Na}_2\text{SO}_4$ , filtered and concentrated under reduced pressure. The crude product was purified by column chromatography (silica, PE/EA = 2:1) to yield **49** (21.1 mg, 66.3  $\mu\text{mol}$ , 63%) as a white solid.

$R_f = 0.42$  (PE/EA = 1:1, Vanillin);  $^1\text{H-NMR}$  (400 MHz,  $\text{CDCl}_3$ )  $\delta = 8.05 - 7.97$  (m, 2H), 7.64 – 7.56 (m, 1H), 7.51 – 7.43 (m, 2H), 4.29 (dd,  $J = 11.0, 7.3$  Hz, 1H), 4.18 (dd,  $J = 11.0, 8.1$  Hz, 1H), 4.07 – 3.99 (m, 2H), 3.41 (d,  $J = 17.8$  Hz, 1H), 3.35 (dd,  $J = 18.6, 10.6$  Hz, 1H), 3.00 – 2.91 (m, 2H), 2.59 – 2.50 (m, 2H), 2.20 (s, 3H);  $^{13}\text{C-NMR}$  (101 MHz,  $\text{CDCl}_3$ )  $\delta = 204.69$  ( $\text{C}_q$ ), 174.77 ( $\text{C}_q$ ), 166.68 ( $\text{C}_q$ ), 133.76 (+), 129.95 (+), 129.85 ( $\text{C}_q$ ), 128.89 (+), 115.30 ( $\text{C}_q$ ), 68.29 (-), 65.24 (-), 49.87 (-), 47.08 (+), 44.74 (+), 36.96 (-), 31.28 (+); **IR** (neat):  $\tilde{\nu}$  ( $\text{cm}^{-1}$ ) = 2924, 1763, 1707, 1453, 1409, 1372, 1316, 1282, 1178, 1118, 1074, 1044, 977, 951, 924, 715; **LRMS** (+ESI):  $m/z = 659$  [ $2\text{M}+\text{Na}$ ] $^+$ , 357 [ $\text{M}+\text{K}$ ] $^+$ , 341 [ $\text{M}+\text{Na}$ ] $^+$ , 319 [ $\text{M}+\text{H}$ ] $^+$ ; **HRMS** (+ESI):  $m/z = 319.1184$  [ $\text{M}+\text{H}$ ] $^+$ ; calc. for [ $\text{C}_{17}\text{H}_{19}\text{O}_6$ ] $^+$  = 319.1176; **HPLC analysis** (Phenomenex Lux Cellulose-1,

*n*-heptane/*i*PrOH 50:50, 0.5 mL/min, 215 nm):  $t_r$  (major) = 24.37,  $t_r$  (minor) = 42.32;  $[\alpha]_D^{20} = +54.2$  (CHCl<sub>3</sub>, *c* = 0.22), >99% *ee*; lit:  $[\alpha]_D^{20} = +54.3$  (CHCl<sub>3</sub>, *c* = 0.44); **m.p.** = 143 - 145 °C.

## 2.2 Derivatization of (+)-paeonilide



**(4*S*,5*R*)-4-Methyl-3-((3*R*,3*aR*,6*aR*)-5-oxohexahydrofuro[2,3-*b*]furan-3-carbonyl)-5-phenyl-oxazolidin-2-one (176)**

**(4*S*,5*R*)-4-Methyl-3-((3*R*,3*aS*,6*aS*)-5-oxohexahydrofuro[2,3-*b*]furan-3-carbonyl)-5-phenyl-oxazolidin-2-one (177)**

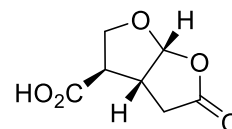
Oxazolidone **156** (931 mg, 2.40 mmol, 1.00 equiv.) was dissolved in toluene (24 mL) and Amberlyst® 15 (120 mg, 50 mg/mmol) was added. Subsequently, the reaction mixture was refluxed for 3 h. Afterward, the mixture was filtrated and concentrated under reduced pressure. The crude product was purified by column chromatography (silica, PE/EA = 3:1) to yield minor diastereomer **177** (123 mg, 371 μmol, 15%) and major diastereomer **176** (590 mg, 1.78 mmol, 74%) both as a white solid.

Major Diastereomer **176**:

$R_f = 0.23$  (PE/EA = 1:1, KMnO<sub>4</sub>); **<sup>1</sup>H-NMR** (400 MHz, CDCl<sub>3</sub>)  $\delta = 7.47 - 7.36$  (m, 3H), 7.35 - 7.27 (m, 2H), 6.18 (d, *J* = 5.6 Hz, 1H), 5.72 (d, *J* = 7.4 Hz, 1H), 4.78 (p, *J* = 6.7 Hz, 1H), 4.33 (dd, *J* = 10.3, 6.4 Hz, 1H), 4.26 (dd, *J* = 10.3, 1.0 Hz, 1H), 3.96 (d, *J* = 6.4 Hz, 1H), 3.70 - 3.62 (m, 1H), 2.95 (dd, *J* = 19.0, 10.9 Hz, 1H), 2.61 (dd, *J* = 19.0, 4.2 Hz, 1H), 0.91 (d, *J* = 6.6 Hz, 3H); **<sup>13</sup>C-NMR** (101 MHz, CDCl<sub>3</sub>)  $\delta = 174.45$  (C<sub>q</sub>), 170.80 (C<sub>q</sub>), 153.08 (C<sub>q</sub>), 132.72 (C<sub>q</sub>), 129.08 (+), 128.87 (+), 125.60 (+), 108.46 (+), 79.54 (+), 69.82 (-), 55.01 (+), 51.22 (+), 40.64 (+), 33.82 (-), 14.50 (+); **IR** (neat):  $\tilde{\nu}$  (cm<sup>-1</sup>) = 2993, 1774, 1700, 1372, 1249, 1197, 1126, 977, 764, 701; **LRMS** (+ESI): *m/z* = 685 [2M+Na]<sup>+</sup>, 354 [M+Na]<sup>+</sup>, 349 [M+NH<sub>4</sub>]<sup>+</sup>, 332 [M+H]<sup>+</sup>; **HRMS** (+ESI): *m/z* = 332.1132 [M+H]<sup>+</sup>; calc. for [C<sub>17</sub>H<sub>18</sub>NO<sub>6</sub>]<sup>+</sup> = 332.1129;  $[\alpha]_D^{20} = +41.1$  (CHCl<sub>3</sub>, *c* = 1.0); **m.p.** = 174 - 175.5 °C.

Minor Diastereomer **177**:

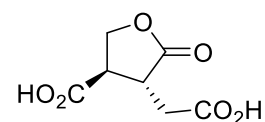
$R_f = 0.46$  (PE/EA = 1:1,  $\text{KMnO}_4$ );  $^1\text{H-NMR}$  (400 MHz,  $\text{CDCl}_3$ )  $\delta = 7.48 - 7.37$  (m, 3H), 7.33 – 7.27 (m, 2H), 6.16 (d,  $J = 5.6$  Hz, 1H), 5.72 (d,  $J = 7.3$  Hz, 1H), 4.79 (p,  $J = 6.7$  Hz, 1H), 4.40 – 4.20 (m, 3H), 3.69 (ddt,  $J = 10.6, 8.7, 5.1$  Hz, 1H), 2.69 (dd,  $J = 18.8, 10.8$  Hz, 1H), 2.49 (dd,  $J = 18.8, 4.8$  Hz, 1H), 0.92 (d,  $J = 6.6$  Hz, 3H);  $^{13}\text{C-NMR}$  (101 MHz,  $\text{CDCl}_3$ )  $\delta = 174.28$  ( $\text{C}_q$ ), 169.07 ( $\text{C}_q$ ), 152.58 ( $\text{C}_q$ ), 132.62 ( $\text{C}_q$ ), 129.11 (+), 128.88 (+), 125.63 (+), 107.93 (+), 79.43 (+), 67.75 (-), 55.11 (+), 46.88 (+), 40.12 (+), 29.57 (-), 14.53 (+); **IR** (neat):  $\tilde{\nu}$  ( $\text{cm}^{-1}$ ) = 2989, 2363, 1778, 1692, 1457, 1357, 1308, 1249, 1200, 1152, 1070, 984, 768; **LRMS** (+ESI):  $m/z = 685$  [ $2\text{M}+\text{Na}$ ] $^+$ , 354 [ $\text{M}+\text{Na}$ ] $^+$ , 349 [ $\text{M}+\text{NH}_4$ ] $^+$ , 332 [ $\text{M}+\text{H}$ ] $^+$ ; **HRMS** (+ESI):  $m/z = 332.1131$  [ $\text{M}+\text{H}$ ] $^+$ ; calc. for [ $\text{C}_{17}\text{H}_{18}\text{NO}_6$ ] $^+$  = 332.1129;  $[\alpha]_{\text{D}}^{20} = -49.6$  ( $\text{CHCl}_3$ ,  $c = 1.0$ ); **m.p.** = 159 - 160 °C.

**(3R,3aR,6aR)-5-Oxohexahydrofuro[2,3-*b*]furan-3-carboxylic acid (178)**

Oxazolidinone **176** (354 mg, 1.07 mmol, 1.00 equiv.) was dissolved in an  $\text{H}_2\text{O}/\text{THF}$  (1:3, v/v) mixture (10 mL) and cooled to 0 °C. At this temperature, LiOH (51.2 mg, 2.14 mmol, 2.00 equiv.) was added and the mixture was stirred for 0.5 h. Afterward, the reaction mixture was extracted with EA (2 x 20 mL) to remove undesired side products. Subsequently, the aqueous phase was acidified to pH 2 with 2 M HCl and extracted with EA (3 x 30 mL). The combined organic layers were dried over  $\text{Na}_2\text{SO}_4$ , filtered and concentrated under reduced pressure to afford the desired acid **178** (167 mg, 972  $\mu\text{mol}$ , 91%) as a white solid.

$R_f = 0.45$  (PE/EA = 1:1 + 1% formic acid,  $\text{KMnO}_4$ );  $^1\text{H-NMR}$  (400 MHz, Acetone)  $\delta = 6.09$  (d,  $J = 5.5$  Hz, 1H), 4.30 (dd,  $J = 9.5, 2.3$  Hz, 1H), 4.17 (dd,  $J = 9.5, 6.5$  Hz, 1H), 3.61 (dtd,  $J = 8.7, 5.9, 3.2$  Hz, 1H), 3.15 (dt,  $J = 6.4, 2.5$  Hz, 1H), 2.98 (dd,  $J = 18.6, 10.6$  Hz, 1H), 2.62 (dd,  $J = 18.6, 3.7$  Hz, 1H);  $^{13}\text{C-NMR}$  (101 MHz, Acetone)  $\delta = 174.53$  ( $\text{C}_q$ ), 172.79 ( $\text{C}_q$ ), 108.12 (+), 69.19 (-), 49.73 (+), 41.66 (+), 33.37 (-); **IR** (neat):  $\tilde{\nu}$  ( $\text{cm}^{-1}$ ) = 3183, 1771, 1737, 1700, 1420, 1360, 1256, 1179, 1103, 977, 857, 816, 787, 671; **LRMS** (+ESI):  $m/z = 195$  [ $\text{M}+\text{Na}$ ] $^+$ , 190 [ $\text{M}+\text{NH}_4$ ] $^+$ , 173 [ $\text{M}+\text{H}$ ] $^+$ ; **HRMS** (+ESI):  $m/z = 173.0445$  [ $\text{M}+\text{H}$ ] $^+$ ; calc. for [ $\text{C}_7\text{H}_9\text{O}_5$ ] $^+$  = 173.0444;  $[\alpha]_{\text{D}}^{20} = +58.5$  (Acetone,  $c = 1.0$ ); **m.p.** = 183 - 184 °C.

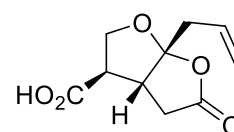




**(3R,4R)-4-(Carboxymethyl)-5-oxotetrahydrofuran-3-carboxylic acid (179)**

Lactone **178** (1.37 g, 7.96 mmol, 1.00 equiv.) was dissolved in acetone (30 mL) and cooled to 0 °C. At this temperature Jones reagent (7.97 mL of a 3.00 M solution, 23.9 mmol, 3.00 equiv.) was added and the reaction mixture was stirred for 5 h at ambient temperature. After quenching the reaction with 2-propanol (10 mL) the chromium salts were dissolved with H<sub>2</sub>O (30 mL) and the reaction mixture was extracted with EA (5 x 40 mL). The combined organic layers were dried over Na<sub>2</sub>SO<sub>4</sub>, filtered and concentrated under reduced pressure. The crude product was purified by column chromatography (silica, PE/EA = 1:1 + 1% formic acid) to afford the desired diacid **179** (1.23 g, 6.54 mmol, 82%) as a white solid.

$R_f$  = 0.20 (PE/EA = 1:1 + 1% formic acid, bromocresol green);  $^1\text{H-NMR}$  (400 MHz, CD<sub>3</sub>CN)  $\delta$  = 8.28 (s,  $J$  = 2H), 4.51 (t,  $J$  = 9.0 Hz, 1H), 4.26 (t,  $J$  = 9.1 Hz, 1H), 3.44 (dt,  $J$  = 10.4, 9.1 Hz, 1H), 3.13 (dt,  $J$  = 10.5, 5.3 Hz, 1H), 2.84 – 2.72 (m, 2H);  $^{13}\text{C-NMR}$  (101 MHz, CD<sub>3</sub>CN)  $\delta$  = 177.63 (C<sub>q</sub>), 172.96 (C<sub>q</sub>), 172.64 (C<sub>q</sub>), 67.99 (-), 45.03 (+), 39.76 (+), 33.21 (-); **IR** (neat):  $\tilde{\nu}$  (cm<sup>-1</sup>) = 3027, 2978, 1722, 1700, 1424, 1379, 1331, 1260, 1189, 1159, 1029, 932, 887, 842, 693; **LRMS** (+ESI):  $m/z$  = 399 [2M+Na]<sup>+</sup>, 211 [M+Na]<sup>+</sup>, 206 [M+NH<sub>4</sub>]<sup>+</sup>, 189 [M+H]<sup>+</sup>, 171 [M+H-H<sub>2</sub>O]<sup>+</sup>, 153 [M+H-2H<sub>2</sub>O]<sup>+</sup>; **HRMS** (+ESI):  $m/z$  = 189.0397 [M+H]<sup>+</sup>; calc. for [C<sub>7</sub>H<sub>9</sub>O<sub>6</sub>]<sup>+</sup> = 189.0394;  $[\alpha]_D^{20}$  = +43.0 (Acetone,  $c$  = 1.0); **m.p.** = 134 - 136 °C.



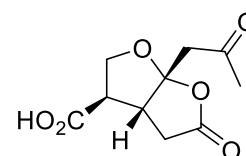
**(3R,3aR,6aR)-6a-Allyl-5-oxohexahydrofuro[2,3-*b*]furan-3-carboxylic acid (180)**

In a flame dried 100 mL Schlenk flask under N<sub>2</sub>-atmosphere acid **179** (779 mg, 4.14 mmol, 1.00 equiv.) was dissolved in dry THF (50 mL) and cooled to -78 °C. At this temperature allylmagnesium bromide (12.4 mL, 12.4 mmol, 3.00 equiv., 1.00 M solution in Et<sub>2</sub>O) was added dropwise and the reaction mixture was stirred for 3 h at -78 °C. After quenching with H<sub>2</sub>O (10 mL), the reaction mixture was acidified to pH 2 with 2 M HCl and extracted with EA

(4x 70 mL). The combined organic layers were dried over NaSO<sub>4</sub>, filtered and concentrated under reduced pressure. The crude product was purified by column chromatography (silica, PE/EA = 2:1 + 1% formic acid) to yield **180** (600 mg, 2.83 mmol, 68%) as a colorless oil.

**Note:** In some cases when an older allylmagnesium bromide solution was used the double bond isomerization product was obtained as an inseparable byproduct. The product is not very stable and therefore should not be stored too long.

$R_f$  = 0.51 (PE/EA = 1:1 + 1% formic acid, Vanillin); **<sup>1</sup>H-NMR** (400 MHz, Acetone)  $\delta$  = 5.79 (ddt,  $J$  = 17.3, 10.1, 7.1 Hz, 1H), 5.17 (dd,  $J$  = 27.1, 13.5 Hz, 2H), 4.30 (d,  $J$  = 8.1 Hz, 1H), 4.13 (dd,  $J$  = 9.0, 6.9 Hz, 1H), 3.36 (d,  $J$  = 10.3 Hz, 1H), 3.15 – 3.05 (m, 1H), 2.99 (dd,  $J$  = 18.7, 10.3 Hz, 1H), 2.75 – 2.57 (m, 3H); **<sup>13</sup>C-NMR** (101 MHz, Acetone)  $\delta$  = 173.83 (C<sub>q</sub>), 173.43 (C<sub>q</sub>), 131.48 (+), 119.19 (-), 117.80 (C<sub>q</sub>), 69.43 (-), 51.05 (+), 43.81 (+), 41.05 (-), 35.10 (-); **IR** (neat):  $\tilde{\nu}$  (cm<sup>-1</sup>) = 3410, 1731, 1709, 1418, 1296, 1268, 1203, 1093, 972, 923, 637, 625; **LRMS** (+ESI):  $m/z$  = 213 [M+H]<sup>+</sup>, 167 [M+H-HCOOH]<sup>+</sup>; **HRMS** (+ESI):  $m/z$  = 213.0759 [M+H]<sup>+</sup>; calc. for [C<sub>10</sub>H<sub>13</sub>O<sub>5</sub>]<sup>+</sup> = 213.0757; [ $\alpha$ ]<sub>D</sub><sup>20</sup> = +23.2 (MeOH, c = 1.0).

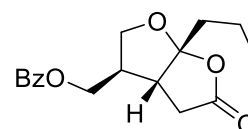


**(3R,3aR,6aR)-5-Oxo-6a-(2-oxopropyl)hexahydrofuro[2,3-*b*]furan-3-carboxylic acid (181)**

Acid **180** (276 mg, 1.30 mmol, 1.00 equiv.) was dissolved in an acetone/H<sub>2</sub>O (4:1, v/v) mixture (5 mL) and Hg(OAc)<sub>2</sub> (166 mg, 520  $\mu$ mol, 0.40 equiv.) was added at 0 °C. After stirring for 10 min Jones reagent (1.30 mL of a 3.00 M solution, 3.90 mmol, 3.00 equiv.) was added and the reaction mixture was stirred for 36 h at ambient temperature. After quenching the reaction with 2-propanol (2 mL) the chromium salts were dissolved with H<sub>2</sub>O (10 mL) and the reaction mixture was extracted with EA (4 x 20 mL). The combined organic layers were dried over Na<sub>2</sub>SO<sub>4</sub>, filtered and concentrated under reduced pressure. The crude product was purified by column chromatography (silica, PE/EA = 1:1 + 1% formic acid) to yield **181** (224 mg, 982  $\mu$ mol, 76%) as a slightly yellow oil.

$R_f$  = 0.25 (PE/EA = 1:1 + 1% formic acid, Vanillin); **<sup>1</sup>H-NMR** (400 MHz, CD<sub>3</sub>CN)  $\delta$  = 4.24 – 4.20 (m, 1H), 4.02 (dd,  $J$  = 9.8, 6.0 Hz, 1H), 3.38 – 3.30 (m, 2H), 3.14 (dt,  $J$  = 9.9, 7.1 Hz, 1H), 3.03 (d,

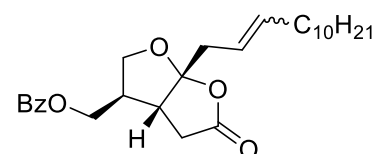
$J = 18.1$  Hz, 1H), 2.98 (dt,  $J = 5.9, 1.5$  Hz, 1H), 2.54 (dd,  $J = 18.7, 3.6$  Hz, 1H), 2.12 (s, 3H);  $^{13}\text{C-NMR}$  (101 MHz,  $\text{CD}_3\text{CN}$ )  $\delta = 206.23$  ( $\text{C}_q$ ), 175.90 ( $\text{C}_q$ ), 174.07 ( $\text{C}_q$ ), 116.15 ( $\text{C}_q$ ), 69.36 (-), 51.79 (+), 49.90 (-), 45.22 (+), 36.29 (-), 30.85 (+); **IR** (neat):  $\tilde{\nu}$  ( $\text{cm}^{-1}$ ) = 3528, 2965, 2927, 2360, 1767, 1714, 1648, 1404, 1373, 1275, 1215, 1175, 1035, 954, 787, 687, 634; **LRMS** (+ESI):  $m/z = 479$  [ $2\text{M}+\text{Na}$ ] $^+$ , 246 [ $\text{M}+\text{NH}_4$ ] $^+$ , 229 [ $\text{M}+\text{H}$ ] $^+$ ; **HRMS** (+ESI):  $m/z = 229.0705$  [ $\text{M}+\text{H}$ ] $^+$ ; calc. for [ $\text{C}_{10}\text{H}_{13}\text{O}_6$ ] $^+$  = 229.0707;  $[\alpha]_{\text{D}}^{20} = +40.8$  ( $\text{CH}_3\text{CN}$ ,  $c = 1.0$ ).



**((3R,3aR,6aR)-5-Oxo-6a-propylhexahydrofuro[2,3-b]furan-3-yl)methyl benzoate (182)**

In a 25 mL Schlenk flask benzoate **170** (51.1 mg, 169  $\mu\text{mol}$ , 1.00 equiv.) was dissolved in MeOH (5 mL) and Pd/C (8.99 mg, 8.45  $\mu\text{mol}$ , 5.00 mol%, 10% Pd on charcoal) was added. Hydrogen was applied *via* a balloon and the flask was flushed with  $\text{H}_2$  several times and then stirred for 2 h at ambient temperature. The reaction mixture was filtered through two folded filters and subsequently the solvent was removed under reduced pressure. The crude product was purified by column chromatography (silica, PE/EA = 2:1) to afford **182** (41.7 mg, 137  $\mu\text{mol}$ , 81%) as a white solid.

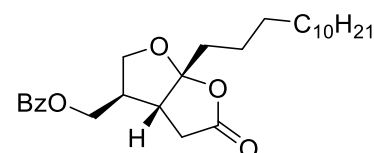
$R_f = 0.36$  (PE/EA = 2:1, Vanillin);  $^1\text{H-NMR}$  (400 MHz,  $\text{CDCl}_3$ )  $\delta = 8.05 - 7.98$  (m, 2H), 7.63 - 7.56 (m, 1H), 7.49 - 7.43 (m, 2H), 4.31 (dd,  $J = 11.0, 7.2$  Hz, 1H), 4.23 (dd,  $J = 11.0, 7.9$  Hz, 1H), 4.11 (dd,  $J = 9.8, 6.0$  Hz, 1H), 4.02 (dd,  $J = 9.8, 2.2$  Hz, 1H), 2.97 (dd,  $J = 18.5, 9.9$  Hz, 1H), 2.71 - 2.65 (m, 1H), 2.61 (dd,  $J = 18.5, 2.2$  Hz, 1H), 2.55 - 2.47 (m, 1H), 1.96 - 1.81 (m, 2H), 1.54 - 1.44 (m, 2H), 0.96 (t,  $J = 7.4$  Hz, 3H);  $^{13}\text{C-NMR}$  (101 MHz,  $\text{CDCl}_3$ )  $\delta = 174.19$  ( $\text{C}_q$ ), 166.41 ( $\text{C}_q$ ), 133.53 (+), 129.71 (+), 129.65 ( $\text{C}_q$ ), 128.66 (+), 119.36 ( $\text{C}_q$ ), 69.01 (-), 65.14 (-), 46.48 (+), 44.70 (+), 39.59 (-), 36.41 (-), 17.12 (-), 14.12 (+); **IR** (neat):  $\tilde{\nu}$  ( $\text{cm}^{-1}$ ) = 2963, 2878, 1774, 1722, 1454, 1316, 1275, 1215, 1178, 1115, 1074, 1029, 951, 917, 717; **LRMS** (+ESI):  $m/z = 631$  [ $2\text{M}+\text{Na}$ ] $^+$ , 327 [ $\text{M}+\text{Na}$ ] $^+$ , 305 [ $\text{M}+\text{H}$ ] $^+$ ; **HRMS** (+ESI):  $m/z = 305.1385$  [ $\text{M}+\text{H}$ ] $^+$ ; calc. for [ $\text{C}_{17}\text{H}_{21}\text{O}_5$ ] $^+$  = 305.1384;  $[\alpha]_{\text{D}}^{20} = +24.6$  ( $\text{CHCl}_3$ ,  $c = 1.0$ ); **m.p.** = 75.5 - 77  $^{\circ}\text{C}$ .



**((3*R*,3*aR*,6*aR*)-5-Oxo-6*a*-(tridec-2-en-1-yl)hexahydrofuro[2,3-*b*]furan-3-yl)methyl benzoate (183)**

In a flame dried 10 mL Schlenk flask under N<sub>2</sub>-atmosphere allyl **170** (30.0 mg, 99.2 μmol, 1.00 equiv.) was dissolved in dry DCM (3 mL). Subsequently, Grubbs' II catalyst (4.21 mg, 4.96 μmol, 5.00 mol%) and 1-dodecene (132 μL, 100 mg, 595 μmol, 6.00 equiv.) were added and the reaction mixture was refluxed for 24 h. After cooling to ambient temperature the solvent was evaporated and the crude product was purified by column chromatography (silica, PE/EA = 5:1) to yield **183** with traces of isomer (39.7 mg, 89.7 μmol, 90%) as a white solid.

$R_f$  = 0.34 (PE/EA = 5:1, Vanillin); <sup>1</sup>H-NMR (400 MHz, CDCl<sub>3</sub>) δ = 8.05 – 7.99 (m, 2H), 7.63 – 7.56 (m, 1H), 7.49 – 7.43 (m, 2H), 5.69 – 5.58 (m, 1H), 5.42 – 5.31 (m, 1H), 4.29 (dd,  $J$  = 11.0, 7.1 Hz, 1H), 4.23 (dd,  $J$  = 11.0, 7.9 Hz, 1H), 4.13 (dd,  $J$  = 9.8, 6.0 Hz, 1H), 4.03 (dd,  $J$  = 9.8, 2.3 Hz, 1H), 2.91 (dd,  $J$  = 18.5, 10.0 Hz, 1H), 2.77 – 2.46 (m, 5H), 2.06 – 1.95 (m, 2H), 1.33 – 1.18 (m, 16H), 0.87 (t,  $J$  = 6.8 Hz, 3H); <sup>13</sup>C-NMR (101 MHz, CDCl<sub>3</sub>) δ = 174.26 (C<sub>q</sub>), 166.41 (C<sub>q</sub>), 137.64 (+), 133.55 (+), 129.73 (+), 129.67 (C<sub>q</sub>), 128.69 (+), 121.65 (+), 118.85 (C<sub>q</sub>), 69.26 (-), 65.00 (-), 46.47 (+), 43.78 (+), 40.44 (-), 36.54 (-), 32.74 (-), 32.05 (-), 29.76 (-), 29.75 (-), 29.60 (-), 29.47 (-), 29.37 (-), 29.36 (-), 22.82 (-), 14.27 (+); IR (neat):  $\tilde{\nu}$  (cm<sup>-1</sup>) = 2922, 2855, 1778, 1722, 1454, 1349, 1316, 1271, 1219, 1111, 1074, 1029, 973, 917, 712; LRMS (+ESI):  $m/z$  = 908 [2M+Na]<sup>+</sup>, 443 [M+H]<sup>+</sup>; HRMS (+ESI):  $m/z$  = 443.2799 [M+H]<sup>+</sup>; calc. for [C<sub>27</sub>H<sub>39</sub>O<sub>5</sub>]<sup>+</sup> = 443.2792.

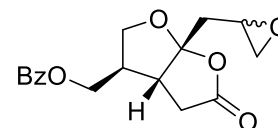


**((3*R*,3*aR*,6*aR*)-5-Oxo-6*a*-tridecylhexahydrofuro[2,3-*b*]furan-3-yl)methyl benzoate (184)**

In a 10 mL Schlenk flask benzoate **183** (33.4 mg, 75.5 μmol, 1.00 equiv.) was dissolved in MeOH (4 mL) and Pd/C (4.02 mg, 3.77 μmol, 5.00 mol%, 10% Pd on charcoal) was added. Hydrogen was applied *via* a balloon and the flask was flushed with H<sub>2</sub> several times and then stirred for 1.5 h at ambient temperature. The reaction mixture was filtered through two folded filters

and the solvent was removed under reduced pressure. The crude product was purified by column chromatography (silica, PE/EA = 5:1) to afford **184** (30.0 mg, 67.5  $\mu\text{mol}$ , 89%) as a white solid.

$R_f$  = 0.30 (PE/EA = 5:1, Vanillin);  $^1\text{H-NMR}$  (400 MHz,  $\text{CDCl}_3$ )  $\delta$  = 8.05 – 7.99 (m, 2H), 7.63 – 7.56 (m, 1H), 7.49 – 7.43 (m, 2H), 4.32 (dd,  $J$  = 11.0, 7.1 Hz, 1H), 4.24 (dd,  $J$  = 11.0, 7.8 Hz, 1H), 4.12 (dd,  $J$  = 9.8, 6.0 Hz, 1H), 4.02 (dd,  $J$  = 9.8, 2.3 Hz, 1H), 2.97 (dd,  $J$  = 18.4, 9.8 Hz, 1H), 2.70 – 2.65 (m, 1H), 2.61 (dd,  $J$  = 18.5, 2.2 Hz, 1H), 2.55 – 2.49 (m, 1H), 1.97 – 1.83 (m, 2H), 1.49 – 1.40 (m, 2H), 1.32 – 1.21 (m, 20H), 0.87 (t,  $J$  = 6.8 Hz, 3H);  $^{13}\text{C-NMR}$  (101 MHz,  $\text{CDCl}_3$ )  $\delta$  = 174.10 ( $\text{C}_q$ ), 166.32 ( $\text{C}_q$ ), 133.43 (+), 129.63 (+), 129.56 ( $\text{C}_q$ ), 128.57 (+), 119.39 ( $\text{C}_q$ ), 68.96 (-), 65.05 (-), 46.40 (+), 44.62 (+), 37.45 (-), 36.37 (-), 31.94 (-), 29.70 (-), 29.66 (-), 29.65 (-), 29.62 (-), 29.52 (-), 29.42 (-), 29.37 (-), 23.60 (-), 22.71 (-), 14.14 (+); **IR** (neat):  $\tilde{\nu}$  ( $\text{cm}^{-1}$ ) = 2926, 2855, 1774, 1722, 1454, 1349, 1316, 1275, 1178, 1115, 1073, 1029, 939, 712, 686; **LRMS** (+ESI):  $m/z$  = 912 [ $2\text{M}+\text{Na}$ ] $^+$ , 445 [ $\text{M}+\text{H}$ ] $^+$ ; **HRMS** (+ESI):  $m/z$  = 445.2953 [ $\text{M}+\text{H}$ ] $^+$ ; calc. for [ $\text{C}_{27}\text{H}_{41}\text{O}_5$ ] $^+$  = 445.2949;  $[\alpha]_{\text{D}}^{20}$  = +15.9 ( $\text{CHCl}_3$ ,  $c$  = 0.5); **m.p.** = 52 - 53  $^{\circ}\text{C}$ .



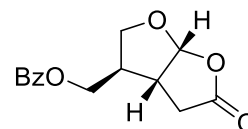
**((3R,3aR,6aR)-6a-(Oxiran-2-ylmethyl)-5-oxohexahydrofuro[2,3-*b*]furan-3-yl)methyl benzoate (185)**

In a flame dried 10 mL Schlenk flask under  $\text{N}_2$ -atmosphere allyl **170** (160 mg, 529  $\mu\text{mol}$ , 1.00 equiv.) was dissolved in dry DCM (5 mL). Subsequently, *m*-CPBA (261 mg, 1.06 mmol, 2.00 equiv., 70% purity) was added and the reaction mixture was stirred for 72 h at ambient temperature. Afterward, the solvent was evaporated and the crude product was purified by column chromatography (silica, PE/EA = 2:1) to yield **185** as a mixture of diastereomers (139 mg, 435  $\mu\text{mol}$ , 82%) as a white solid.

**Note:** In the proton NMR the signals of the diastereomers are overlapping and the characteristic peaks of the major and minor diastereomer are marked.

$R_f$  = 0.44 (PE/EA = 1:1, Vanillin);  $^1\text{H-NMR}$  (300 MHz,  $\text{CDCl}_3$ )  $\delta$  = 8.06 – 7.96 (m, 4H), 7.63 – 7.55 (m, 2H), 7.50 – 7.41 (m, 4H), 4.38<sup>minor</sup> (dd,  $J$  = 11.1, 7.1 Hz, 1H), 4.34 – 4.21 (m, 3H), 4.21 – 4.07

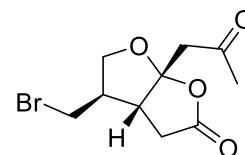
(m, 3H), 4.03<sup>major</sup> (dd,  $J = 9.8, 2.2$  Hz, 1H), 3.24 – 3.10 (m, 2H), 3.08 – 2.93 (m, 4H), 2.84 – 2.78 (m, 2H), 2.68 – 2.64 (m, 1H), 2.63 – 2.52 (m, 6H), 2.49<sup>minor</sup> (dd,  $J = 10.1, 2.9$  Hz, 1H), 1.76<sup>minor</sup> (dd,  $J = 14.7, 8.2$  Hz, 1H), 1.71<sup>major</sup> (dd,  $J = 14.7, 8.4$  Hz, 1H); <sup>13</sup>C-NMR (75 MHz, CDCl<sub>3</sub>) major:  $\delta = 174.28$  (C<sub>q</sub>), 166.31 (C<sub>q</sub>), 133.44 (+), 129.62 (+), 129.51 (C<sub>q</sub>), 128.57 (+), 117.50 (C<sub>q</sub>), 68.62 (-), 65.00 (-), 47.50 (+), 46.63 (-), 46.47 (+), 44.60 (+), 40.34 (-), 36.12 (-); minor:  $\delta = 173.69$  (C<sub>q</sub>), 166.29 (C<sub>q</sub>), 133.39 (+), 129.63 (+), 129.57 (C<sub>q</sub>), 128.55 (+), 117.81 (C<sub>q</sub>), 69.50 (-), 64.80 (-), 47.71 (+), 46.30 (+), 46.00 (-), 44.32 (+), 39.54 (-), 35.96 (-); IR (neat):  $\tilde{\nu}$  (cm<sup>-1</sup>) = 2960, 2926, 2900, 1782, 1722, 1275, 1208, 1115, 1025, 977, 917, 716; LRMS (+ESI):  $m/z = 659$  [2M+Na]<sup>+</sup>, 336 [M+NH<sub>4</sub>]<sup>+</sup>, 319 [M+H]<sup>+</sup>; HRMS (major) (+ESI):  $m/z = 319.1180$  [M+H]<sup>+</sup>; calc. for [C<sub>17</sub>H<sub>19</sub>O<sub>6</sub>]<sup>+</sup> = 319.1176; HRMS (minor) (+ESI):  $m/z = 319.1177$  [M+H]<sup>+</sup>; calc. for [C<sub>17</sub>H<sub>19</sub>O<sub>6</sub>]<sup>+</sup> = 319.1176.



**((3R,3aR,6aR)-5-Oxohexahydrofuro[2,3-*b*]furan-3-yl)methyl benzoate (186)**

Bromide **159** (150 mg, 679  $\mu$ mol, 1.00 equiv.) was dissolved in DMF (7 mL) and potassium benzoate (177 mg, 1.11 mmol, 1.63 equiv.) was added at ambient temperature. Subsequently, the reaction mixture was stirred for 2 h at 80 °C. After cooling to ambient temperature the reaction mixture was diluted with H<sub>2</sub>O (20 mL) and extracted with EA (5 x 40 mL). The combined organic layers were dried over NaSO<sub>4</sub>, filtered and concentrated under reduced pressure. The crude product was purified by column chromatography (silica, PE/EA = 2:1) to yield **186** (137 mg, 523  $\mu$ mol, 77%) as a white solid.

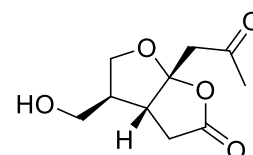
$R_f = 0.52$  (PE/EA = 1:1, KMnO<sub>4</sub>); <sup>1</sup>H-NMR (400 MHz, CDCl<sub>3</sub>)  $\delta = 8.05 - 7.98$  (m, 2H), 7.63 – 7.56 (m, 1H), 7.50 – 7.42 (m, 2H), 6.14 (d,  $J = 5.2$  Hz, 1H), 4.32 (dd,  $J = 11.1, 7.0$  Hz, 1H), 4.25 (dd,  $J = 11.1, 7.5$  Hz, 1H), 4.15 (dd,  $J = 9.8, 5.9$  Hz, 1H), 4.05 (dd,  $J = 9.8, 2.4$  Hz, 1H), 3.05 – 2.99 (m, 1H), 2.94 (dd,  $J = 18.0, 10.4$  Hz, 1H), 2.61 – 2.51 (m, 2H); <sup>13</sup>C-NMR (101 MHz, CDCl<sub>3</sub>)  $\delta = 174.52$  (C<sub>q</sub>), 166.38 (C<sub>q</sub>), 133.55 (+), 129.70 (+), 129.60 (C<sub>q</sub>), 128.68 (+), 108.13 (+), 69.33 (-), 64.93 (-), 45.46 (+), 41.92 (+), 34.63 (-); IR (neat):  $\tilde{\nu}$  (cm<sup>-1</sup>) = 2960, 2892, 1774, 1715, 1454, 1357, 1316, 1271, 1178, 1103, 1074, 1025, 977, 895, 712; LRMS (+ESI):  $m/z = 547$  [2M+Na]<sup>+</sup>, 280 [M+NH<sub>4</sub>]<sup>+</sup>, 263 [M+H]<sup>+</sup>; HRMS (+ESI):  $m/z = 263.0918$  [M+H]<sup>+</sup>; calc. for [C<sub>14</sub>H<sub>15</sub>O<sub>5</sub>]<sup>+</sup> = 263.0914;  $[\alpha]_D^{20} = +32.1$  (CHCl<sub>3</sub>,  $c = 1.0$ ); m.p. = 96 - 97 °C.



**(3aR,4R,6aR)-4-(Bromomethyl)-6a-(2-oxopropyl)tetrahydrofuro[2,3-b]furan-2(3H)-one  
(187)**

Bromide **169** (50.0 mg, 191  $\mu\text{mol}$ , 1.00 equiv.) was dissolved in an acetone/ $\text{H}_2\text{O}$  (4:1, v/v) mixture (2 mL) and  $\text{Hg}(\text{OAc})_2$  (30.5 mg, 95.7  $\mu\text{mol}$ , 0.50 equiv.) was added at 0 °C. After stirring for 10 min at 0 °C, Jones reagent (191  $\mu\text{L}$  of a 3.00 M solution, 574  $\mu\text{mol}$ , 3.00 equiv.) was added and the reaction mixture was stirred for 24 h at ambient temperature. After quenching the reaction with a few drops of 2-propanol, the chromium salts were dissolved with  $\text{H}_2\text{O}$  (5 mL) and the reaction mixture was extracted with EA (4 x 20 mL). The combined organic layers were dried over  $\text{Na}_2\text{SO}_4$ , filtered and concentrated under reduced pressure. The crude product was purified by column chromatography (silica, PE/EA = 2:1) to yield **187** (37.0 mg, 134  $\mu\text{mol}$ , 70%) as a slightly yellow oil.

$R_f$  = 0.18 (PE/EA = 2:1, Vanillin);  $^1\text{H-NMR}$  (400 MHz,  $\text{CDCl}_3$ )  $\delta$  = 4.00 (dd,  $J$  = 10.1, 5.4 Hz, 1H), 3.94 (dd,  $J$  = 10.0, 1.1 Hz, 1H), 3.38 – 3.23 (m, 4H), 2.98 – 2.89 (m, 2H), 2.53 – 2.43 (m, 2H), 2.18 (s, 3H);  $^{13}\text{C-NMR}$  (101 MHz,  $\text{CDCl}_3$ )  $\delta$  = 204.46 ( $\text{C}_q$ ), 174.43 ( $\text{C}_q$ ), 115.07 ( $\text{C}_q$ ), 69.66 (-), 50.16 (+), 49.44 (-), 46.85 (+), 36.64 (-), 34.36 (-), 31.04 (+); IR (neat):  $\tilde{\nu}$  ( $\text{cm}^{-1}$ ) = 2960, 1782, 1718, 1409, 1372, 1305, 1275, 1204, 1174, 1111, 1036, 1003, 954; LRMS (+APCI):  $m/z$  = 294  $[\text{M}+\text{NH}_4]^+$ , 277  $[\text{M}+\text{H}]^+$ ; HRMS (+APCI):  $m/z$  = 277.0071  $[\text{M}+\text{H}]^+$ ; calc. for  $[\text{C}_{10}\text{H}_{14}\text{BrO}_4]^+$  = 277.0070;  $[\alpha]_D^{20}$  = +37.3 ( $\text{CHCl}_3$ ,  $c$  = 1.0).

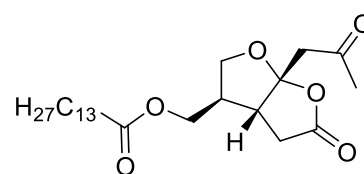


**(3aR,4S,6aR)-4-(Hydroxymethyl)-6a-(2-oxopropyl)tetrahydrofuro[2,3-b]furan-2(3H)-one  
(188)**

Bromide **187** (63.0 mg, 227  $\mu\text{mol}$ , 1.00 equiv.) was dissolved in a DMF/ $\text{H}_2\text{O}$  (1:4, v/v) mixture (1 mL) and heated to 80 °C. After stirring for 12 h the reaction mixture was extracted with EA (4 x 10 mL). The combined organic layers were dried over  $\text{Na}_2\text{SO}_4$ , filtered and concentrated

under reduced pressure. The crude product was purified by column chromatography (silica, EA) to yield **188** (35.1 mg, 164  $\mu\text{mol}$ , 72%) as a slightly yellow oil.

$R_f$  = 0.20 (EA, *Seebach's Magic Stain*);  $^1\text{H-NMR}$  (400 MHz,  $\text{CDCl}_3$ )  $\delta$  = 3.99 (dd,  $J$  = 9.7, 5.5 Hz, 1H), 3.94 (dd,  $J$  = 9.7, 1.4 Hz, 1H), 3.57 (d,  $J$  = 6.9 Hz, 2H), 3.35 – 3.23 (m, 2H), 2.99 – 2.91 (m, 2H), 2.51 (dd,  $J$  = 18.5, 2.7 Hz, 1H), 2.19 (s, 3H), 1.78 (bs, 1H);  $^{13}\text{C-NMR}$  (101 MHz,  $\text{CDCl}_3$ )  $\delta$  = 204.72 ( $\text{C}_q$ ), 175.07 ( $\text{C}_q$ ), 115.49 ( $\text{C}_q$ ), 68.43 (-), 63.73 (-), 49.56 (+), 49.39 (-), 44.06 (+), 36.84 (-), 31.01 (+); **IR** (neat):  $\tilde{\nu}$  ( $\text{cm}^{-1}$ ) = 3414, 2930, 2885, 1359, 1763, 1715, 1409, 1372, 1305, 1282, 1208, 1174, 1107, 1036, 951, 921, 850, 798; **LRMS** (+ESI):  $m/z$  = 451 [ $2\text{M}+\text{Na}$ ] $^+$ , 215 [ $\text{M}+\text{H}$ ] $^+$ ; **HRMS** (+ESI):  $m/z$  = 215.0916 [ $\text{M}+\text{H}$ ] $^+$ ; calc. for [ $\text{C}_{10}\text{H}_{15}\text{O}_5$ ] $^+$  = 215.0914;  $[\alpha]_D^{20}$  = +25.9 ( $\text{CHCl}_3$ ,  $c$  = 1.0).



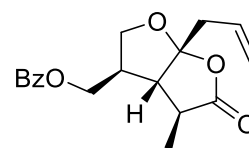
**((3R,3aR,6aR)-5-Oxo-6a-(2-oxopropyl)hexahydrofuro[2,3-b]furan-3-yl)methyl tetradecanoate (189)**

In a flame dried 10 mL Schlenk flask under  $\text{N}_2$ -atmosphere alcohol **188** (19.0 mg, 88.7  $\mu\text{mol}$ , 1.00 equiv.) was dissolved in dry DCM (2 mL) and cooled to 0  $^\circ\text{C}$ . Subsequently, DMAP (542  $\mu\text{g}$ , 4.43  $\mu\text{mol}$ , 5.00 mol%),  $\text{Et}_3\text{N}$  (18.5  $\mu\text{L}$ , 13.5 mg, 133  $\mu\text{mol}$ , 1.50 equiv.) and myristoyl chloride (36.2  $\mu\text{L}$ , 32.8 mg, 133  $\mu\text{mol}$ , 1.50 equiv.) were added and the reaction mixture was allowed to warm to ambient temperature. After stirring for 3 h at ambient temperature, sat.  $\text{NH}_4\text{Cl}$ -solution (2 mL) was added and the reaction mixture was extracted with  $\text{Et}_2\text{O}$  (4 x 10 mL). The combined organic layers were dried over  $\text{Na}_2\text{SO}_4$ , filtered and concentrated under reduced pressure. The crude product was purified by column chromatography (silica, PE/EA = 3:1) to yield **189** (32.2 mg, 75.8  $\mu\text{mol}$ , 86%) as a white solid.

$R_f$  = 0.23 (PE/EA = 3:1, Vanillin);  $^1\text{H-NMR}$  (400 MHz,  $\text{CDCl}_3$ )  $\delta$  = 4.04 (dd,  $J$  = 11.0, 7.4 Hz, 1H), 3.97 (dd,  $J$  = 9.9, 5.4 Hz, 1H), 3.94 – 3.85 (m, 2H), 3.38 (d,  $J$  = 17.7 Hz, 1H), 3.30 (dd,  $J$  = 18.5, 10.6 Hz, 1H), 2.92 (d,  $J$  = 17.7 Hz, 1H), 2.85 (d,  $J$  = 10.5 Hz, 1H), 2.49 (dd,  $J$  = 18.5, 2.9 Hz, 1H), 2.38 – 2.28 (m, 3H), 2.20 (s, 3H), 1.65 – 1.56 (m, 2H), 1.25 (s, 20H), 0.88 (t,  $J$  = 6.8 Hz, 3H);



$^{13}\text{C-NMR}$  (101 MHz,  $\text{CDCl}_3$ )  $\delta$  = 204.48 ( $\text{C}_q$ ), 174.61 ( $\text{C}_q$ ), 173.82 ( $\text{C}_q$ ), 115.06 ( $\text{C}_q$ ), 68.03 (-), 64.38 (-), 49.66 (-), 46.74 (+), 44.41 (+), 36.72 (-), 34.28 (-), 32.06 (-), 31.09 (+), 29.81 (-), 29.78 (-), 29.74 (-), 29.59 (-), 29.49 (-), 29.38 (-), 29.27 (-), 25.04 (-), 22.83 (-), 14.26 (+); **IR** (neat):  $\tilde{\nu}$  ( $\text{cm}^{-1}$ ) = 2926, 2855, 2363, 2334, 1782, 1737, 1457, 1372, 1204, 1174, 1111, 1040, 954, 667; **LRMS** (+APCI):  $m/z$  = 442 [ $\text{M}+\text{NH}_4$ ] $^+$ , 425 [ $\text{M}+\text{H}$ ] $^+$ ; **HRMS** (+APCI):  $m/z$  = 425.2904 [ $\text{M}+\text{H}$ ] $^+$ ; calc. for  $[\text{C}_{24}\text{H}_{41}\text{O}_6]^+$  = 425.2898;  $[\alpha]_{\text{D}}^{20}$  = +27.4 ( $\text{CHCl}_3$ ,  $c$  = 1.0); **m.p.** = 52.5 - 53 °C.

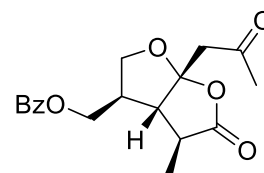


**((3R,3aS,4S,6aR)-6a-Allyl-4-methyl-5-oxohexahydrofuro[2,3-b]furan-3-yl)methyl benzoate (191)**

In a flame dried 10 mL Schlenk flask under  $\text{N}_2$ -atmosphere HMDS (93.6  $\mu\text{L}$ , 72.1 mg, 447  $\mu\text{mol}$ , 1.50 equiv.) was dissolved in dry THF (1 mL) and cooled to -78 °C. Subsequently, *n*-BuLi (165  $\mu\text{L}$ , 447  $\mu\text{mol}$ , 1.50 equiv., 2.70 M solution in toluene) was added and the reaction mixture was allowed to warm for 5 min. After cooling to -78 °C benzoate **170** (90.0 mg, 298  $\mu\text{mol}$ , 1.00 equiv.) in dry THF (1 mL) was added and the reaction mixture was stirred for 2 h. Subsequently, MeI (92.7  $\mu\text{L}$ , 211 mg, 1.49 mmol, 5.00 equiv.) was added and the reaction mixture was stirred for further 30 min. Afterward, the reaction was quenched with sat.  $\text{NH}_4\text{Cl}$ -solution (3 drops), diluted with DCM (15 mL) and dried over  $\text{Na}_2\text{SO}_4$ , filtered and concentrated under reduced pressure. The crude product was purified by column chromatography (silica, PE/EA = 3:1) to yield **191** (60.3 mg, 191  $\mu\text{mol}$ , 64%, 91% brsm) as a colorless oil.

$R_f$  = 0.51 (PE/EA = 2:1, Vanillin);  $^1\text{H-NMR}$  (400 MHz,  $\text{CDCl}_3$ )  $\delta$  = 7.84 – 7.79 (m, 2H), 7.43 – 7.36 (m, 1H), 7.29 – 7.23 (m, 2H), 5.59 (ddt,  $J$  = 17.5, 10.4, 7.3 Hz, 1H), 5.06 – 4.97 (m, 2H), 4.09 (dd,  $J$  = 11.0, 7.5 Hz, 1H), 4.01 (dd,  $J$  = 11.0, 8.2 Hz, 1H), 3.88 (dd,  $J$  = 9.9, 5.2 Hz, 1H), 3.83 (dd,  $J$  = 9.8, 1.2 Hz, 1H), 2.54 – 2.44 (m, 3H), 2.35 (dd,  $J$  = 13.1, 7.6 Hz, 1H), 2.19 (d,  $J$  = 2.4 Hz, 1H), 1.16 (d,  $J$  = 7.6 Hz, 3H);  $^{13}\text{C-NMR}$  (101 MHz,  $\text{CDCl}_3$ )  $\delta$  = 177.45 ( $\text{C}_q$ ), 166.25 ( $\text{C}_q$ ), 133.42 (+), 131.09 (+), 129.57 ( $\text{C}_q$ ), 129.55 (+), 128.58 (+), 120.72 (-), 116.55 ( $\text{C}_q$ ), 68.96 (-), 64.66 (-), 51.19 (+), 46.66 (+), 42.98 (+), 42.72 (-), 17.46 (+); **IR** (neat):  $\tilde{\nu}$  ( $\text{cm}^{-1}$ ) = 2974, 2881, 1363, 1774,

1722, 1453, 1316, 1275, 1208, 1115, 1029, 999, 947, 716; **LRMS** (+ESI):  $m/z = 655 [2M+Na]^+$ , 317  $[M+H]^+$ ; **HRMS** (+ESI):  $m/z = 317.1382 [M+H]^+$ ; calc. for  $[C_{18}H_{21}O_5]^+ = 317.1384$ ;  $[\alpha]_D^{20} = +2.7$  (CHCl<sub>3</sub>,  $c = 1.0$ ).

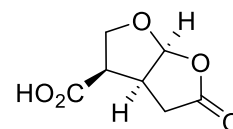


**((3R,3aS,4S,6aR)-4-Methyl-5-oxo-6a-(2-oxopropyl)hexahydrofuro[2,3-b]furan-3-yl)methyl benzoate (192)**

Benzoate **191** (40.8 mg, 129  $\mu\text{mol}$ , 1.00 equiv.) was dissolved in an acetone/H<sub>2</sub>O (4:1, v/v) mixture (2.5 mL) and Hg(OAc)<sub>2</sub> (20.6 mg, 64.5  $\mu\text{mol}$ , 0.50 equiv.) was added at 0 °C. After stirring for 10 min at 0 °C, Jones reagent (129  $\mu\text{L}$  of a 3.00 M solution, 387  $\mu\text{mol}$ , 3.00 equiv.) was added and the reaction mixture was stirred for 30 h at ambient temperature. After quenching the reaction with a few drops of 2-propanol the chromium salts were dissolved with H<sub>2</sub>O (5 mL) and the reaction mixture was extracted with EA (4 x 20 mL). The combined organic layers were dried over Na<sub>2</sub>SO<sub>4</sub>, filtered and concentrated under reduced pressure. The crude product was purified by column chromatography (silica, PE/EA = 2:1) to yield **192** (23.1 mg, 69.5  $\mu\text{mol}$ , 54%) as a white solid.

$R_f = 0.27$  (PE/EA = 2:1, Vanillin); **<sup>1</sup>H-NMR** (400 MHz, CDCl<sub>3</sub>)  $\delta = 8.05 - 7.98$  (m, 2H), 7.63 – 7.56 (m, 1H), 7.50 – 7.43 (m, 2H), 4.29 (dd,  $J = 11.1, 7.6$  Hz, 1H), 4.18 (dd,  $J = 11.1, 8.1$  Hz, 1H), 4.07 – 4.00 (m, 2H), 3.36 (d,  $J = 17.6$  Hz, 1H), 2.95 (d,  $J = 17.6$  Hz, 1H), 2.71 (d,  $J = 5.1$  Hz, 1H), 2.69 – 2.61 (m, 1H), 2.61 – 2.54 (m, 1H), 2.19 (s, 3H), 1.51 (d,  $J = 7.3$  Hz, 3H); **<sup>13</sup>C-NMR** (101 MHz, CDCl<sub>3</sub>)  $\delta = 204.37$  (C<sub>q</sub>), 177.44 (C<sub>q</sub>), 166.47 (C<sub>q</sub>), 133.58 (+), 129.70 (+), 129.66 (C<sub>q</sub>), 128.72 (+), 113.08 (C<sub>q</sub>), 68.48 (-), 64.76 (-), 51.70 (+), 50.30 (-), 46.68 (+), 43.08 (+), 31.12 (+), 16.30 (+); **IR** (neat):  $\tilde{\nu}$  (cm<sup>-1</sup>) = 2952, 2922, 2359, 1759, 1714, 1454, 1372, 1282, 1208, 1178, 1122, 1036, 992, 939, 716; **LRMS** (+ESI):  $m/z = 687 [2M+Na]^+$ , 355  $[M+Na]^+$ , 350  $[M+NH_4]^+$ , 333  $[M+H]^+$ ; **HRMS** (+ESI):  $m/z = 333.1340 [M+H]^+$ ; calc. for  $[C_{18}H_{21}O_6]^+ = 333.1333$ ;  $[\alpha]_D^{20} = +34.5$  (CHCl<sub>3</sub>,  $c = 0.5$ ); **m.p.** = 152 – 153 °C.

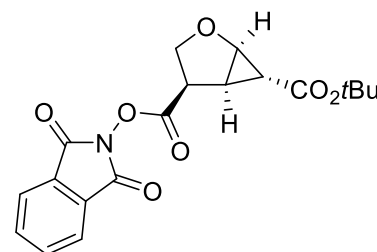
### 2.3. Studies toward dermatolactone



#### (3*R*,3*aS*,6*aS*)-5-Oxohexahydrofuro[2,3-*b*]furan-3-carboxylic acid (**238**)

Oxazolidinone **177** (106 mg, 318  $\mu\text{mol}$ , 1.00 equiv.) was dissolved in an  $\text{H}_2\text{O}/\text{THF}$  (1:3, v/v) mixture (4 mL) and cooled to 0 °C. At this temperature, LiOH (15.3 mg, 637  $\mu\text{mol}$ , 2.00 equiv.) was added and the mixture was stirred for 0.5 h. Next, the reaction mixture was extracted with EA (2 x 20 mL) to remove undesired side products. Afterward, the aqueous phase was acidified to pH 2 with 2 M HCl and extracted with EA (3 x 30 mL). The combined organic layers were dried over  $\text{Na}_2\text{SO}_4$ , filtered and concentrated under reduced pressure to afford the desired acid **238** (48.9 mg, 284  $\mu\text{mol}$ , 89%) as a white solid.

$R_f = 0.41$  (PE/EA = 1:1 + 1% formic acid,  $\text{KMnO}_4$ );  $^1\text{H-NMR}$  (400 MHz, Acetone)  $\delta = 6.11$  (d,  $J = 5.5$  Hz, 1H), 4.19 (dd,  $J = 8.9, 7.7$  Hz, 1H), 4.00 (dd,  $J = 10.9, 9.3$  Hz, 1H), 3.59 (ddd,  $J = 15.6, 10.4, 5.2$  Hz, 1H), 3.48 – 3.40 (m, 1H), 2.81 (dd,  $J = 18.8, 10.6$  Hz, 1H), 2.52 (dd,  $J = 18.8, 4.9$  Hz, 1H);  $^{13}\text{C-NMR}$  (101 MHz, Acetone)  $\delta = 175.38$  ( $\text{C}_q$ ), 171.60 ( $\text{C}_q$ ), 108.75 (+), 68.32 (-), 47.34 (+), 41.20 (+), 30.58 (-); IR (neat):  $\tilde{\nu}$  ( $\text{cm}^{-1}$ ) = 3027, 1722, 1416, 1372, 1297, 1193, 1133, 965, 865, 734, 664; LRMS (+ESI):  $m/z = 345$  [ $2\text{M}+\text{H}$ ] $^+$ , 190 [ $\text{M}+\text{NH}_4$ ] $^+$ , 173 [ $\text{M}+\text{H}$ ] $^+$ ; HRMS (+ESI):  $m/z = 173.0445$  [ $\text{M}+\text{H}$ ] $^+$ ; calc. for [ $\text{C}_7\text{H}_9\text{O}_5$ ] $^+$  = 173.0444;  $[\alpha]_{\text{D}}^{20} = -14.8$  (MeOH,  $c = 1.0$ ); m.p. = 135 - 136 °C.

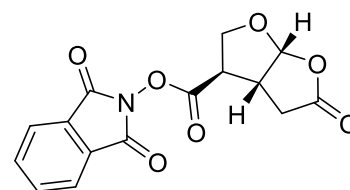


#### 6-(*tert*-Butyl) 4-(1,3-dioxoisindolin-2-yl) (1*R*,4*R*,5*R*,6*R*)-2-oxabicyclo[3.1.0]hexane-4,6-dicarboxylate (**239**)

In a flame dried 25 mL Schlenk flask under  $\text{N}_2$ -atmosphere acid **155** (130 mg, 571  $\mu\text{mol}$ , 1.00 equiv.) was dissolved in dry THF (7 mL) and *N*-hydroxyphthalimide (102 mg, 628  $\mu\text{mol}$ ,

1.10 equiv.) and DCC (130 mg, 628  $\mu\text{mol}$ , 1.10 equiv.) were added at ambient temperature. After stirring for 20 h, 1 M HCl (10 mL) was added and the reaction mixture was extracted with EA (3 x 20 mL). The combined organic layers were dried over  $\text{NaSO}_4$ , filtered and concentrated under reduced pressure. For purification, the residue was dissolved in EA (5 ml) and cooled overnight in the fridge. The precipitated DCC urea was removed by filtration and the solvent was evaporated to yield **239** (193 mg, 517  $\mu\text{mol}$ , 91%) as a white solid.

$R_f = 0.26$  (PE/EA = 3:1,  $\text{KMnO}_4$ );  $^1\text{H-NMR}$  (400 MHz,  $\text{CDCl}_3$ )  $\delta = 7.90 - 7.85$  (m, 2H), 7.81 - 7.77 (m, 2H), 4.37 - 4.30 (m, 1H), 4.27 (dd,  $J = 5.4, 1.0$  Hz, 1H), 3.81 - 3.70 (m, 2H), 2.54 (dd,  $J = 8.9, 5.2$  Hz, 1H), 2.25 (dd,  $J = 2.7, 0.9$  Hz, 1H), 1.43 (s, 9H);  $^{13}\text{C-NMR}$  (101 MHz,  $\text{CDCl}_3$ )  $\delta = 169.43$  ( $\text{C}_q$ ), 168.45 ( $\text{C}_q$ ), 161.65 ( $\text{C}_q$ ), 134.98 (+), 128.91 ( $\text{C}_q$ ), 124.15 (+), 81.26 ( $\text{C}_q$ ), 68.13 (-), 66.03 (+), 42.21 (+), 28.16 (+), 27.16 (+), 23.32 (+); **IR** (neat):  $\tilde{\nu}$  ( $\text{cm}^{-1}$ ) = 2982, 2933, 2363, 1789, 1744, 1721, 1394, 1371, 1323, 1185, 1159, 1118, 977, 880, 697; **LRMS** (+ESI):  $m/z = 769$  [ $2\text{M}+\text{Na}$ ] $^+$ , 391 [ $\text{M}+\text{NH}_4$ ] $^+$ , 374 [ $\text{M}+\text{H}$ ] $^+$ ; **HRMS** (+ESI):  $m/z = 374.1236$  [ $\text{M}+\text{H}$ ] $^+$ ; calc. for [ $\text{C}_{19}\text{H}_{20}\text{NO}_7$ ] $^+$  = 374.1234;  $[\alpha]_{\text{D}}^{20} = -22.8$  ( $\text{CHCl}_3$ ,  $c = 1.0$ ); **m.p.** = 99 - 100  $^{\circ}\text{C}$ .

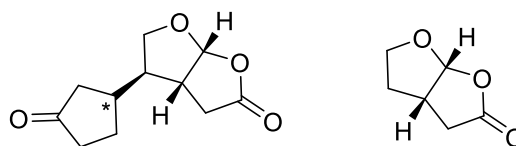


### 1,3-Dioxoisindolin-2-yl (3R,3aR,6aR)-5-oxohexahydrofuro[2,3-b]furan-3-carboxylate (**240**)

In a flame dried 25 mL Schlenk flask under  $\text{N}_2$ -atmosphere acid **178** (168 mg, 974  $\mu\text{mol}$ , 1.00 equiv.) was dissolved in dry THF (10 mL) and *N*-hydroxyphthalimide (175 mg, 1.07 mmol, 1.10 equiv.) and DCC (221 mg, 1.07 mmol, 1.10 equiv.) were added at ambient temperature. After stirring for 20 h, 1 M HCl (15 mL) was added and the reaction mixture was extracted with EA (3 x 25 mL). The combined organic layers were dried over  $\text{NaSO}_4$ , filtered and concentrated under reduced pressure. For purification, the residue was dissolved in EA (7 ml) and cooled overnight in the fridge. The precipitated DCC urea was removed by filtration and the solvent was evaporated to yield **240** (260 mg, 819  $\mu\text{mol}$ , 84%) as a white solid.

$R_f = 0.39$  (PE/EA = 1:1,  $\text{KMnO}_4$ );  $^1\text{H-NMR}$  (400 MHz,  $\text{CDCl}_3$ )  $\delta = 7.93 - 7.88$  (m, 2H), 7.85 - 7.79 (m, 2H), 6.22 (d,  $J = 5.4$  Hz, 1H), 4.59 (dd,  $J = 10.0, 2.2$  Hz, 1H), 4.33 (dd,  $J = 10.0, 6.8$  Hz, 1H),

3.68 (ddd,  $J = 13.1, 5.6, 2.9$  Hz, 1H), 3.36 – 3.30 (m, 1H), 3.05 (dd,  $J = 18.8, 10.4$  Hz, 1H), 2.67 (dd,  $J = 18.8, 3.2$  Hz, 1H);  $^{13}\text{C-NMR}$  (101 MHz,  $\text{CDCl}_3$ )  $\delta = 173.53$  ( $\text{C}_q$ ), 168.71 ( $\text{C}_q$ ), 161.72 ( $\text{C}_q$ ), 135.22 (+), 128.84 ( $\text{C}_q$ ), 124.36 (+), 107.90 (+), 69.24 (-), 48.00 (+), 42.66 (+), 34.39 (-); **IR** (neat):  $\tilde{\nu}$  ( $\text{cm}^{-1}$ ) = 2997, 2933, 1786, 1741, 1368, 1185, 1118, 1081, 1029, 988, 880, 701; **LRMS** (+ESI):  $m/z = 657$  [ $2\text{M}+\text{Na}$ ] $^+$ , 335 [ $\text{M}+\text{NH}_4$ ] $^+$ , 318 [ $\text{M}+\text{H}$ ] $^+$ ; **HRMS** (+ESI):  $m/z = 318.0616$  [ $\text{M}+\text{H}$ ] $^+$ ; calc. for [ $\text{C}_{15}\text{H}_{12}\text{NO}_7$ ] $^+$  = 318.0608;  $[\alpha]_{\text{D}}^{20} = +43.8$  (Acetone,  $c = 0.5$ ); **m.p.** = 161.5 - 162 °C.



**(3aR,4R,6aR)-4-((R)-3-Oxocyclopentyl)tetrahydrofuro[2,3-b]furan-2(3H)-one (242)**

**(3aS,6aR)-Tetrahydrofuro[2,3-b]furan-2(3H)-one (243)**

A flame dried 10 mL Schlenk tube under  $\text{N}_2$ -atmosphere was charged with *N*-acyloxyphthalimide **240** (99.2 mg, 313  $\mu\text{mol}$ , 1.00 equiv.), Hantzsch ester (87.1 mg, 344  $\mu\text{mol}$ , 1.10 equiv.), 2-cyclopentenone **211** (210  $\mu\text{L}$ , 205 mg, 2.50 mmol, 8.00 equiv.) and the photocatalyst  $[\text{Ru}(\text{bpy})_3]\text{Cl}_2$  (2.3 mg, 3.13  $\mu\text{mol}$ , 1.00 mol%) in dry  $\text{CH}_3\text{CN}$  (3 mL). The solution was degassed using three freeze-pump-thaw cycles and closed with a Teflon-sealed inlet for a glass rod, through which irradiation with a 455 nm high power LED took place. After stirring for 3 h at ambient temperature, the photoreaction was stopped and the reaction mixture was directly purified by column chromatography (silica, PE/EA = 2:1) to yield decarboxylation product **243** (10.4 mg, 81.2  $\mu\text{mol}$ , 26%) and coupling product **242** (21.6 mg, 103  $\mu\text{mol}$ , 33%,  $dr = 1.2:1$ ) both as a colorless oil.

In the proton NMR of the coupling product the signals of the diastereomers are overlapping and the characteristic peaks of the major and minor diastereomer are marked. In the carbon NMR the peaks of both diastereomers are listed.

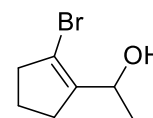
Coupling product **242**:

$R_f = 0.14$  (PE/EA = 1:1, Vanillin);  $^1\text{H-NMR}$  (400 MHz,  $\text{CDCl}_3$ )  $\delta = 6.02$  (d,  $J = 5.0$  Hz, 2H), 4.07<sup>minor</sup> (dd,  $J = 6.4, 2.9$  Hz, 1H), 4.05<sup>major</sup> (dd,  $J = 6.3, 2.9$  Hz, 1H), 3.91<sup>major</sup> (dd,  $J = 9.7, 3.1$  Hz, 1H), 3.80<sup>minor</sup> (dd,  $J = 9.6, 3.3$  Hz, 1H), 2.94 – 2.77 (m, 4H), 2.49 – 2.25 (m, 6H), 2.22 – 2.07 (m, 6H), 1.99 (ddd,  $J = 12.1, 6.3, 3.1$  Hz, 2H), 1.87 – 1.76 (m, 2H), 1.58 – 1.43 (m, 2H);

**<sup>13</sup>C-NMR** (101 MHz, CDCl<sub>3</sub>) δ = 217.14 (C<sub>q</sub>), 217.06 (C<sub>q</sub>), 174.61 (C<sub>q</sub>), 174.60 (C<sub>q</sub>), 108.36 (-), 108.28 (-), 71.13 (+), 70.33 (+), 50.98 (-), 50.86 (-), 43.59 (-), 43.37 (+), 43.33 (+), 42.91 (-), 39.82 (-), 39.78 (-), 38.55 (+), 38.47 (+), 35.03 (+), 34.93 (+), 27.98 (+), 27.90 (+); **IR** (neat):  $\tilde{\nu}$  (cm<sup>-1</sup>) = 2960, 2930, 1778, 1737, 1405, 1357, 1320, 1170, 1107, 977, 898; **LRMS** (+EI):  $m/z$  = 210 [M]<sup>+</sup>, 192 [M-H<sub>2</sub>O]<sup>+</sup>, 166 [M-CO<sub>2</sub>]<sup>+</sup>; **HRMS** (+EI):  $m/z$  = 210.0887 [M]<sup>+</sup>; calc. for [C<sub>11</sub>H<sub>14</sub>O<sub>4</sub>]<sup>+</sup> = 210.0887.

Decarboxylation product **243**:

**R<sub>f</sub>** = 0.45 (PE/EA = 1:1, KMnO<sub>4</sub>); **<sup>1</sup>H-NMR** (400 MHz, CDCl<sub>3</sub>) δ = 6.01 (d, *J* = 5.3 Hz, 1H), 4.07 – 3.99 (m, 1H), 3.93 – 3.85 (m, 1H), 3.17 – 3.05 (m, 1H), 2.82 (dd, *J* = 18.6, 10.3 Hz, 1H), 2.38 (dd, *J* = 18.7, 3.2 Hz, 1H), 2.22 – 2.07 (m, 1H), 1.79 – 1.67 (m, 1H); **<sup>13</sup>C-NMR** (101 MHz, CDCl<sub>3</sub>) δ = 175.39 (C<sub>q</sub>), 108.48 (+), 67.33 (-), 38.40 (+), 34.93 (-), 32.26 (-); **IR** (neat):  $\tilde{\nu}$  (cm<sup>-1</sup>) = 2982, 2885, 1771, 1454, 1420, 1357, 1297, 1252, 1170, 1107, 1003, 962, 932, 869, 831, 787; **LRMS** (+ESI):  $m/z$  = 146 [M+NH<sub>4</sub>]<sup>+</sup>, 129 [M+H]<sup>+</sup>; **HRMS** (+ESI):  $m/z$  = 129.0549 [M+H]<sup>+</sup>; calc. for [C<sub>6</sub>H<sub>9</sub>O<sub>3</sub>]<sup>+</sup> = 129.0546.

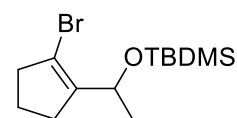


### 1-(2-Bromocyclopent-1-en-1-yl)ethan-1-ol (**256**)<sup>4,5</sup>

DMF (4.42 mL, 4.17 g, 57.0 mmol, 3.00 equiv.) was dissolved in DCM (35 mL) and cooled to 0 °C. At this temperature PBr<sub>3</sub> (4.52 mL, 12.87 g, 47.6 mmol, 2.50 equiv.) was added dropwise and the reaction mixture was stirred for 30 min at 0 °C resulting in a cloudy white solution. Subsequently, cyclopentanone **254** (1.68 mL, 1.60 g, 19.0 mmol, 1.00 equiv.) was added and the yellow solution was stirred for 16 h at ambient temperature. Afterward, the reaction mixture was poured into a sat. NaHCO<sub>3</sub>-solution (100 mL) and extracted with DCM (3 x 50 mL). The combined organic layers were dried over NaSO<sub>4</sub>, filtered and concentrated under reduced pressure. The residue was dissolved in dry Et<sub>2</sub>O (30 mL) and activated 4Å molecular sieve (3.00 g) was added. The reaction mixture was cooled to 0 °C and methylmagnesium bromide (6.98 mL, 20.9 mmol, 1.10 equiv., 3.00 M solution in Et<sub>2</sub>O) was added over a period of 15 min. After complete addition, the reaction was quenched by addition of sat. NH<sub>4</sub>Cl-solution (40 mL) and the reaction mixture was extracted with Et<sub>2</sub>O (4 x 30 mL). The combined organic layers

were dried over Na<sub>2</sub>SO<sub>4</sub>, filtered and concentrated under reduced pressure. The crude product was purified by column chromatography (silica, PE/EA = 5:1) to yield **256** (2.40 g, 12.6 mmol, 66%) as a yellow oil.

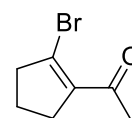
$R_f$  = 0.36 (PE/EA = 5:1, Vanillin); **<sup>1</sup>H-NMR** (400 MHz, CDCl<sub>3</sub>)  $\delta$  = 4.72 (q,  $J$  = 6.5 Hz, 1H), 2.64 – 2.56 (m, 2H), 2.50 – 2.40 (m, 1H), 2.33 (tddd,  $J$  = 10.0, 7.5, 4.9, 2.4 Hz, 1H), 2.19 (s, 1H), 1.97 – 1.86 (m, 2H), 1.24 (d,  $J$  = 6.5 Hz, 3H); **<sup>13</sup>C-NMR** (101 MHz, CDCl<sub>3</sub>)  $\delta$  = 143.30 (C<sub>q</sub>), 116.17 (C<sub>q</sub>), 65.66 (+), 40.24 (-), 29.28 (-), 21.59 (-), 20.79 (+); **IR** (neat):  $\tilde{\nu}$  (cm<sup>-1</sup>) = 3321, 2967, 2855, 1651, 1446, 1368, 1316, 1290, 1111, 1070, 1025, 921, 861; **LRMS** (+EI):  $m/z$  = 190 [M]<sup>+</sup>, 175 [M-CH<sub>3</sub>]<sup>+</sup>, 111 [M-Br]<sup>+</sup>; **HRMS** (+EI):  $m/z$  = 189.9984 [M]<sup>+</sup>; calc. for [C<sub>7</sub>H<sub>11</sub>BrO]<sup>+</sup> = 189.9988.



#### **(1-(2-Bromocyclopent-1-en-1-yl)ethoxy)(tert-butyl)dimethylsilane (257)**

Alcohol **256** (1.00 g, 5.23 mmol, 1.00 equiv.) was dissolved in DMF (35 mL) and imidazole (713 mg, 10.5 mmol, 2.00 equiv.) and TBDMSCl (1.18 g, 7.85 mmol, 1.50 equiv.) were added. After stirring for 2 h at ambient temperature, the reaction mixture was diluted with H<sub>2</sub>O (50 mL) and extracted with EA (5 x 50 mL). The combined organic layers were washed with H<sub>2</sub>O (2 x 30 mL), dried over NaSO<sub>4</sub>, filtered and concentrated under reduced pressure. The crude product was purified by column chromatography (silica, PE/EA = 5:1) to yield **257** (1.49 g, 4.89 mmol, 93%) as a colorless oil.

$R_f$  = 0.5 (PE/EA = 5:1, Vanillin); **<sup>1</sup>H-NMR** (400 MHz, CDCl<sub>3</sub>)  $\delta$  = 4.71 (q,  $J$  = 6.4 Hz, 1H), 2.60 (ddd,  $J$  = 8.6, 4.7, 2.3 Hz, 2H), 2.48 – 2.30 (m, 2H), 1.96 – 1.86 (m, 2H), 1.19 (d,  $J$  = 6.4 Hz, 3H), 0.88 (s, 9H), 0.04 (d,  $J$  = 17.2 Hz, 6H); **<sup>13</sup>C-NMR** (101 MHz, CDCl<sub>3</sub>)  $\delta$  = 144.36 (C<sub>q</sub>), 113.77 (C<sub>q</sub>), 66.44 (+), 40.10 (-), 29.26 (-), 25.84 (+), 22.03 (+), 21.61 (-), 18.15 (C<sub>q</sub>), -4.88 (+), -4.99 (+); **IR** (neat):  $\tilde{\nu}$  (cm<sup>-1</sup>) = 2956, 2896, 2855, 1472, 1364, 1316, 1252, 1122, 1085, 1036, 995, 951, 898, 831, 775, 667; **LRMS** (+APCI):  $m/z$  = 305 [M]<sup>+</sup>, 322 [M+NH<sub>4</sub>]<sup>+</sup>; **HRMS** (+APCI):  $m/z$  = 305.0928 [M]<sup>+</sup>; calc. for [C<sub>13</sub>H<sub>26</sub>BrOSi]<sup>+</sup> = 305.0931.

**1-(2-Bromocyclopent-1-en-1-yl)ethan-1-one (260)**

Alcohol **256** (1.30 g, 6.80 mmol, 1.00 equiv.) was dissolved in EA (50 mL) and IBX (5.72 g, 20.4 mmol, 3.00 equiv.) was added. After refluxing for 3.5 h, the reaction mixture was filtered and concentrated under reduced pressure. The crude product was purified by column chromatography (silica, PE) to yield **260** (1.03 g, 5.45 mmol, 80%) as a colorless oil.

$R_f$  = 0.62 (PE/EA = 5:1, Vanillin);  $^1\text{H-NMR}$  (400 MHz,  $\text{CDCl}_3$ )  $\delta$  = 2.81 (ddd,  $J$  = 8.1, 4.4, 2.1 Hz, 2H), 2.58 (ddd,  $J$  = 9.8, 4.5, 2.2 Hz, 2H), 2.41 (s, 3H), 1.92 – 1.80 (m, 2H);  $^{13}\text{C-NMR}$  (101 MHz,  $\text{CDCl}_3$ )  $\delta$  = 196.20 ( $\text{C}_q$ ), 140.53 ( $\text{C}_q$ ), 130.35 ( $\text{C}_q$ ), 44.00 (-), 33.33 (-), 30.18 (+), 21.23 (-); **IR** (neat):  $\tilde{\nu}$  ( $\text{cm}^{-1}$ ) = 2967, 2851, 1730, 1662, 1599, 1431, 1364, 1320, 1293, 1264, 1208, 1129, 1043, 895, 746; **LRMS** (+EI):  $m/z$  = 188 [ $\text{M}$ ] $^+$ , 173 [ $\text{M}-\text{CH}_3$ ] $^+$ , 109 [ $\text{M}-\text{Br}$ ] $^+$ ; **HRMS** (+EI):  $m/z$  = 187.9835 [ $\text{M}$ ] $^+$ ; calc. for [ $\text{C}_7\text{H}_9\text{BrO}$ ] $^+$  = 187.9831.



### 3. Biological evaluation

#### Materials and methods:<sup>6</sup>

Platelet-activating-factor (PAF, 1-O-Octadecyl-2-Oacetyl-sn-glycero-3-phosphorylcholine, Bachem, Heidelberg, Germany) was diluted in DMSO (2 mg/ml) and the stock solutions were stored at -20 °C.

#### The final composition of the used buffers was as follows:<sup>6,7</sup>

Buffer for dilution of PRP: NaCl (137 mM), MgCl<sub>2</sub> (2.1 mM), CaCl<sub>2</sub> (1.36 mM), KCl (2.7mM), NaH<sub>2</sub>PO<sub>4</sub> (0.42mM), NaHCO<sub>3</sub> (15.6 mM), D-glucose (1 g/l) and heparin (2 I.U./ml) (Braun AG, Melsungen, Germany, 5000 I.U./mL).

Buffer for dilution of the PAF stock solution: NaCl (137 mM), MgCl<sub>2</sub> (2.1 mM), CaCl<sub>2</sub> (1.36 mM), KCl (2.7mM), NaH<sub>2</sub>PO<sub>4</sub> (0.42mM), NaHCO<sub>3</sub> (15.6 mM), D-glucose (1 g/l) and 2.5 g/l BSA.

Citrate buffer: Na<sub>3</sub>C<sub>6</sub>H<sub>5</sub>O<sub>7</sub> (85 mM), C<sub>6</sub>H<sub>8</sub>O<sub>7</sub> (70 mM) and D-glucose (110 mmol).

#### Collection of blood and preparation of PRP and PPP:<sup>7</sup>

Blood (4 x 9 mL) was collected from the antecubital vein of a 28 year old, healthy male donor using a butterfly needle, which drained into a 10 mL syringe containing citrate buffer (1 mL). For the preparation of PRP, the citrated blood (4 x 10 ml) was each transferred to a 15 mL Falcon tube and centrifuged at 190 g for 20 min at room temperature. The supernatant was transferred to a new Falcon tube and centrifuged at 190 g for further 10 min at room temperature. The supernatant was collected as PRP and 1 mL was centrifuged again at 1500 g for 15 min at room temperature to obtain PPP. The concentration of thrombocytes in PRP was measured using a *Neubauer* counting chamber and adjusted with buffer to a final concentration of 1.0 – 1.2·10<sup>8</sup> cells/mL.

#### Assay of platelet aggregation:<sup>7</sup>

Platelet aggregation in PRP was measured on a Chrono-Log 490 Optical Aggregometer (Chrono-Log Corp., Havertown Pa., USA) by following the change of light transmission of a PRP-sample (0.5 mL) in a glass cuvette and the aggregation process was recorded on a computer with the AGGRO/LINK<sup>®</sup> software. Before each measurement, 0% and 100% aggregation was standardized in relation to a cuvette containing PPP (0.5 ml).

The PRP samples were preincubated for 5 min at 37 °C with the respective compound dissolved in DMSO and afterward continuously stirred (1200 rpm) and maintained at a temperature of 37 °C. Aggregation was induced by the addition of 1 µL diluted PAF (final PAF concentration was 200 ng/mL). The progress of aggregation was followed for a period of 2 min. Inhibition of platelet aggregation versus a solvent control was calculated in percent using the maximal aggregation and slope, respectively. Half-maximal inhibition concentrations (IC<sub>50</sub>-values) were determined by non-linear regression analysis using the software package Origin 2018 (OriginLab Corporation, Northampton, MA, USA).

#### 4. References

<sup>1</sup> Jaschinski, T.; Hiersemann, M. *Org. Lett.* **2012**, *14* (16), 4114–4117.

<sup>2</sup> Regitz, M. *Angew. Chem. Int. Ed.* **1967**, *6* (9), 733–749.

<sup>3</sup> Eisenbraun E. J. *Org. Synth.* **1965**, *45*, 28–32.

<sup>4</sup> Lin, M. Y.; Das, A.; Liu, R. S. *J. Am. Chem. Soc.* **2006**, *128* (29), 9340–9341.

<sup>5</sup> Xia, Y.; Qu, P.; Liu, Z.; Ge, R.; Xiao, Q.; Zhang, Y.; Wang, J. *Angew. Chem. Int. Ed.* **2013**, *52* (9), 2543–2546.

<sup>6</sup> Koch, E. *Phytomedicine* **2005**, *12* (1–2), 10–16.

<sup>7</sup> Antl, M.; Von Brühl, M. L.; Eiglsperger, C.; Werner, M.; Konrad, I.; Kocher, T.; Wilm, M.; Hofmann, F.; Massberg, S.; Schlossmann, J. *Blood* **2007**, *109* (2), 552–559.

## **F. Appendix**

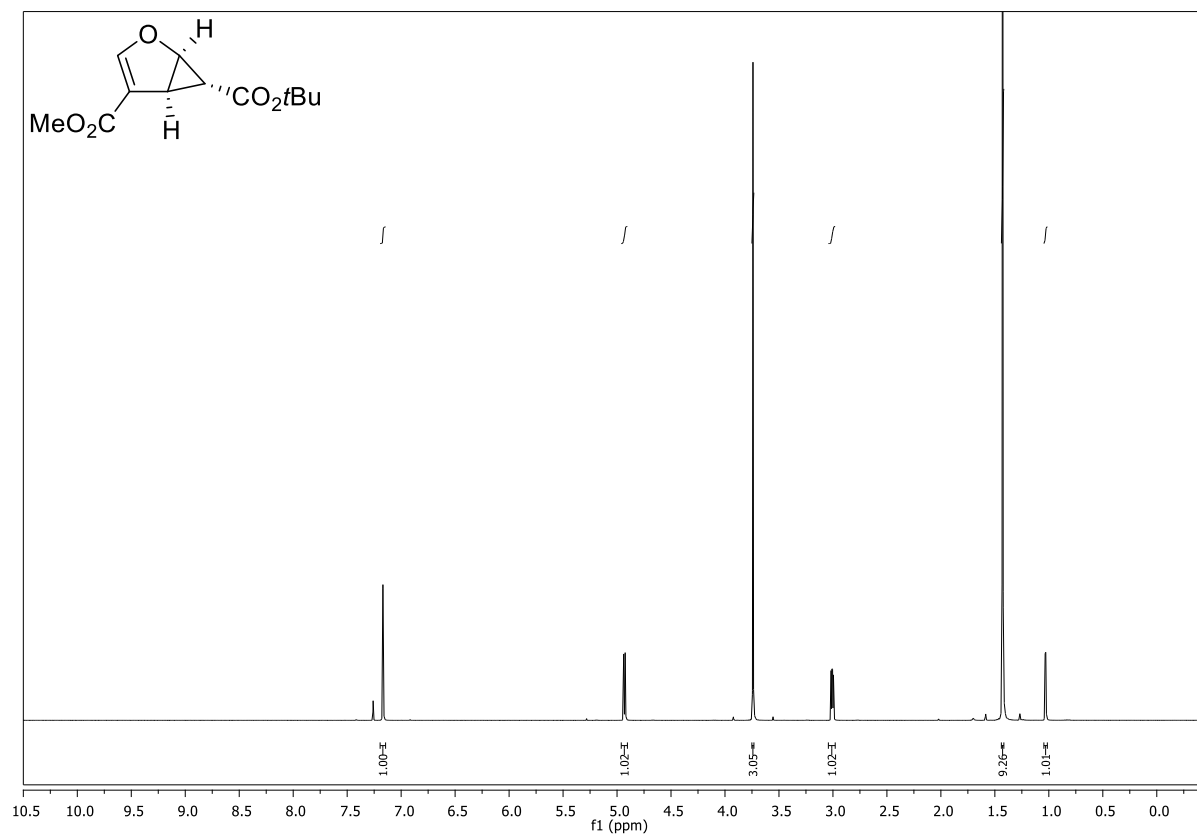
### **1. NMR spectroscopic data**

$^1\text{H}$ -NMR spectra:                      upper image

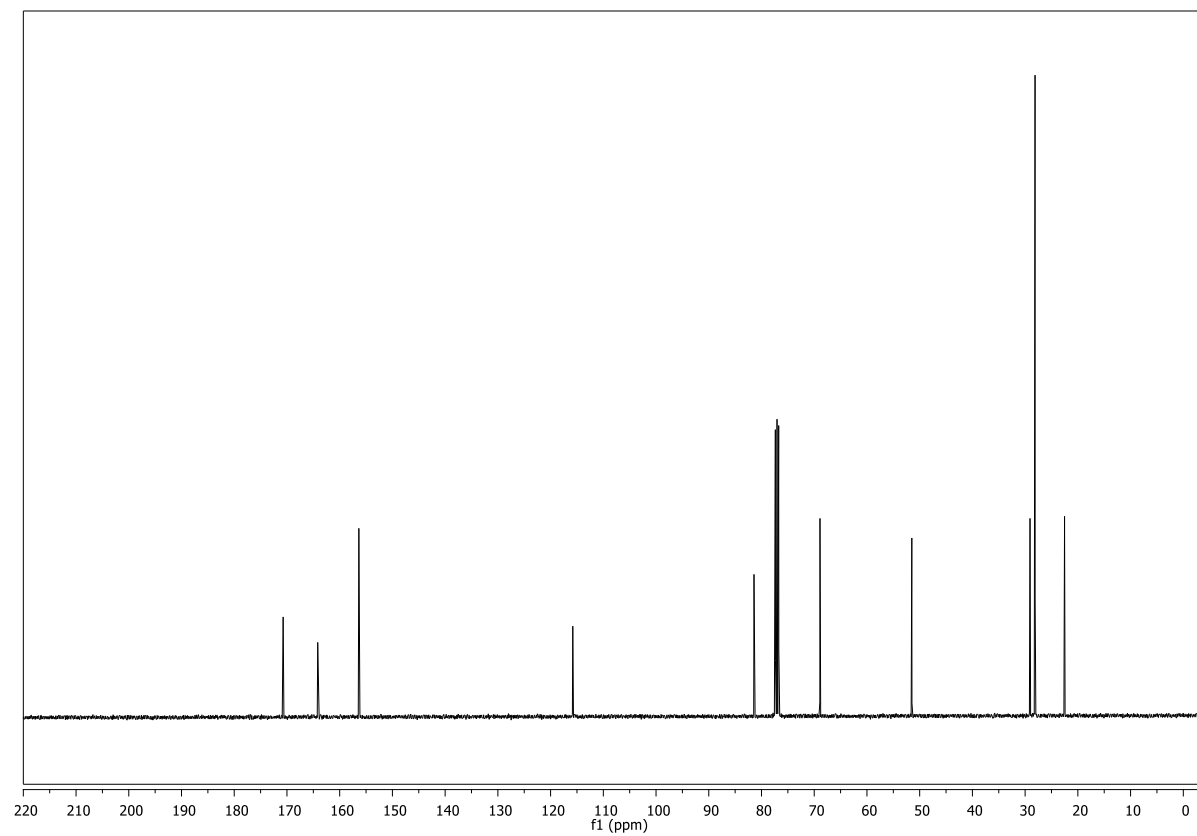
$^{13}\text{C}$ -NMR spectra:                      lower image

Solvent and frequency are stated at each spectrum.

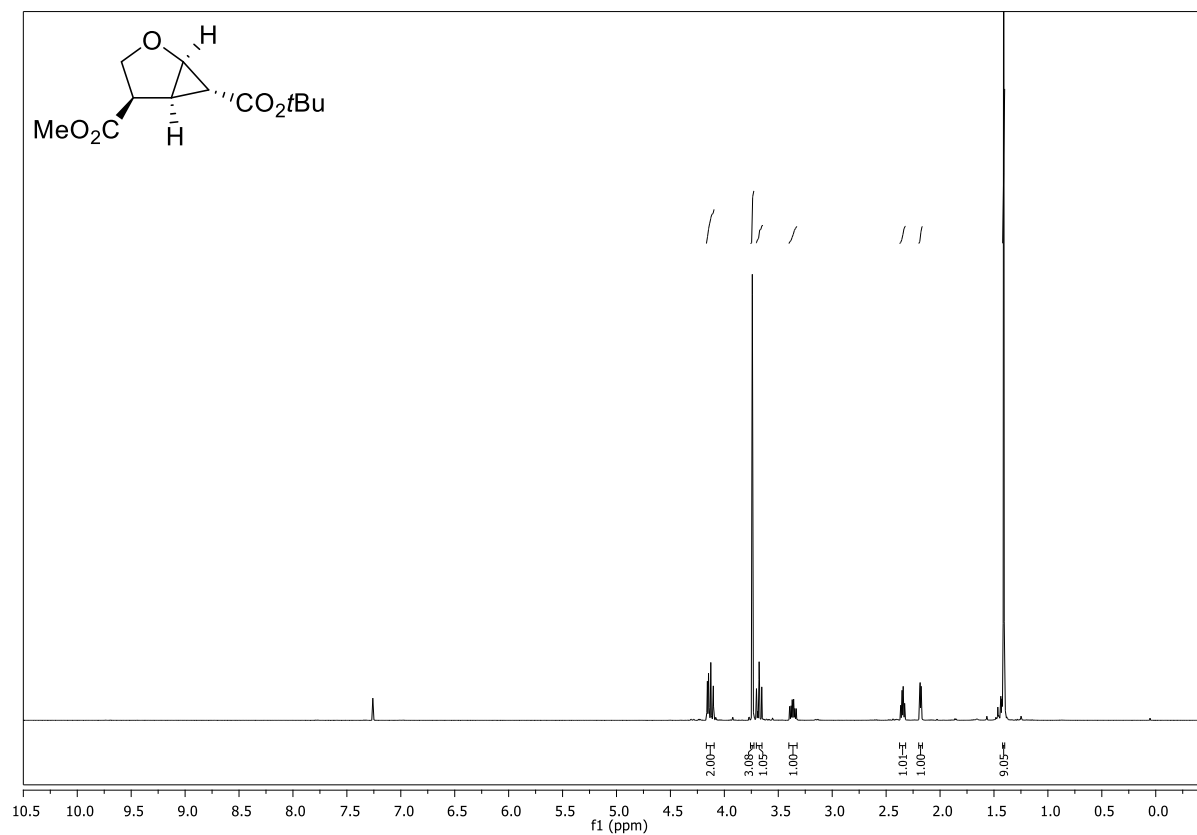
**6-(*tert*-Butyl) 4-methyl (1*R*,5*S*,6*R*)-2-oxabicyclo[3.1.0]hex-3-ene-4,6-dicarboxylate (142)**  
**(CDCl<sub>3</sub>, 400 MHz)**



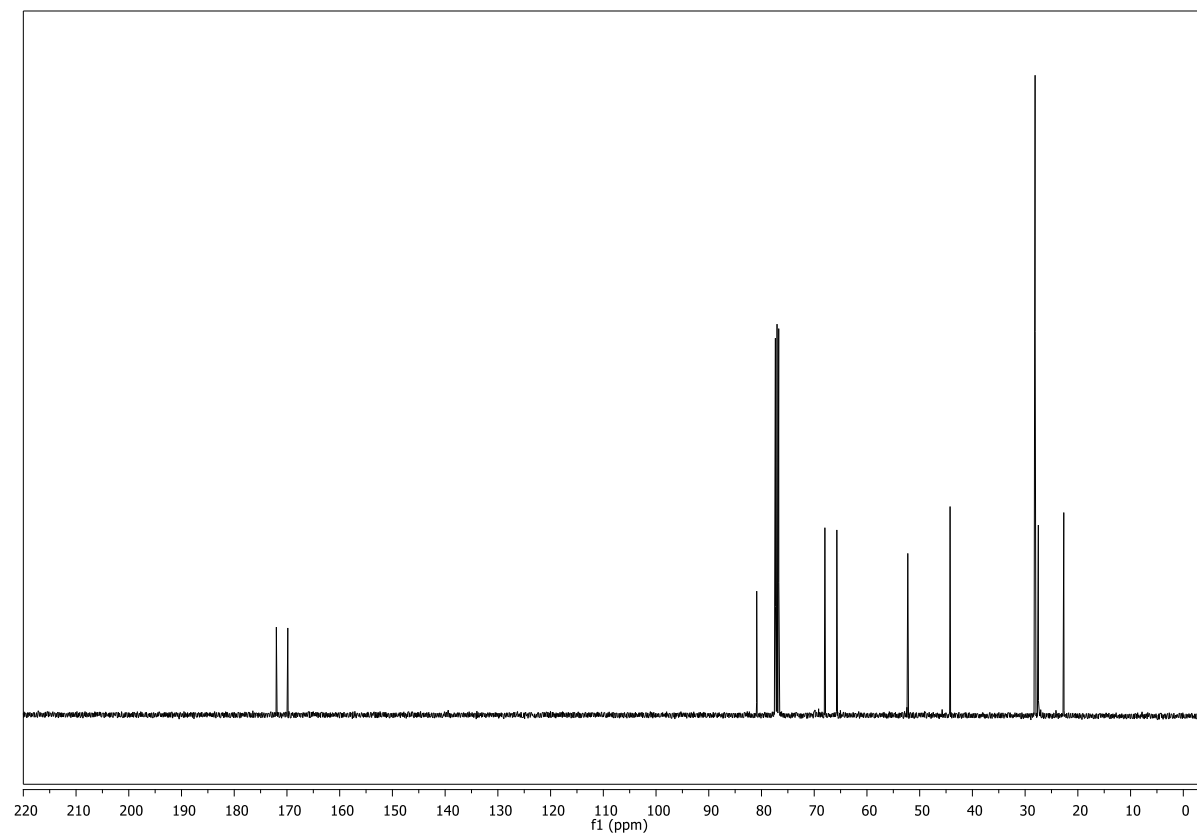
**(CDCl<sub>3</sub>, 101 MHz)**

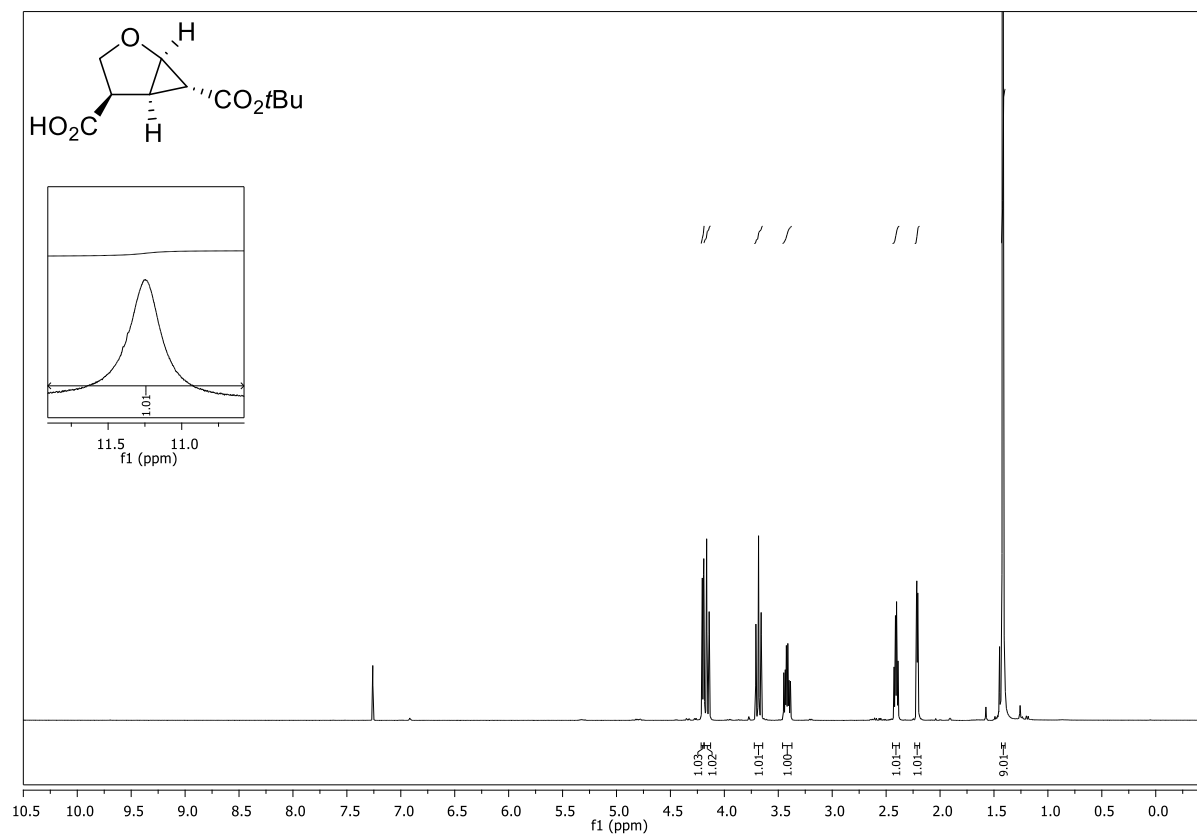
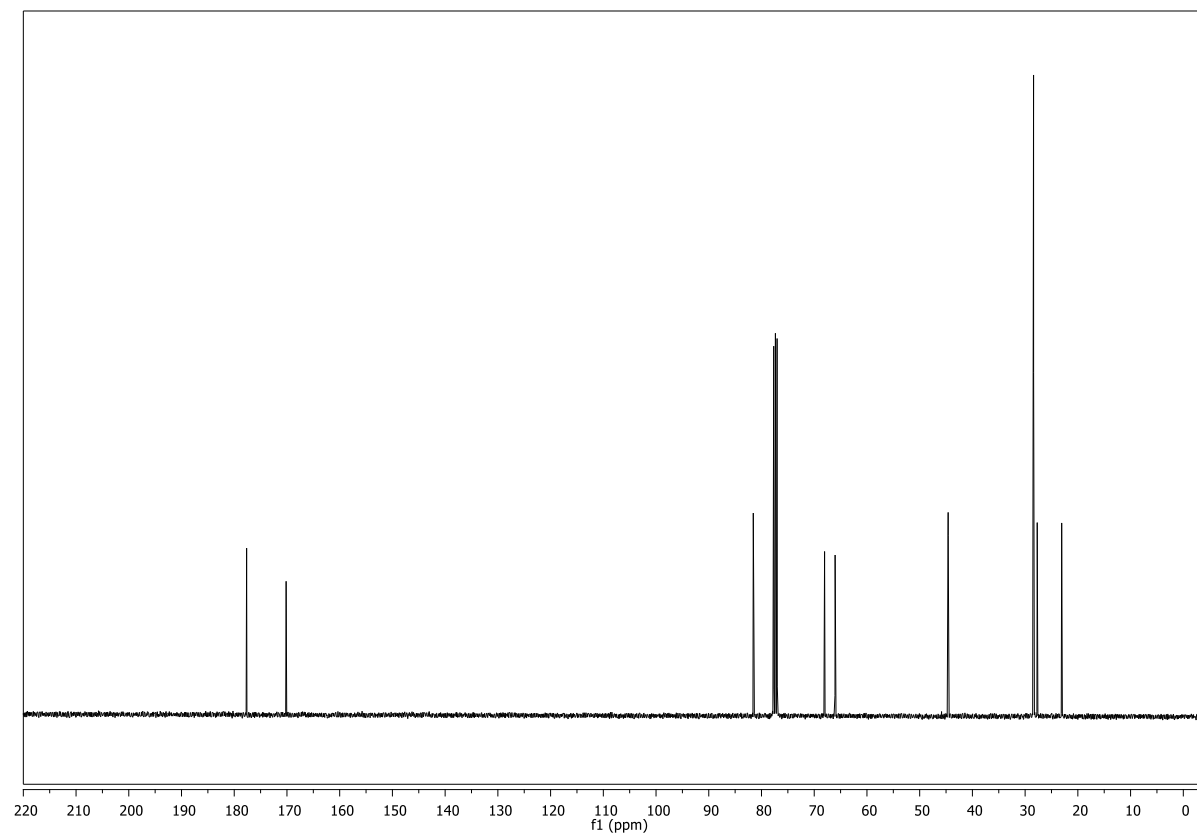


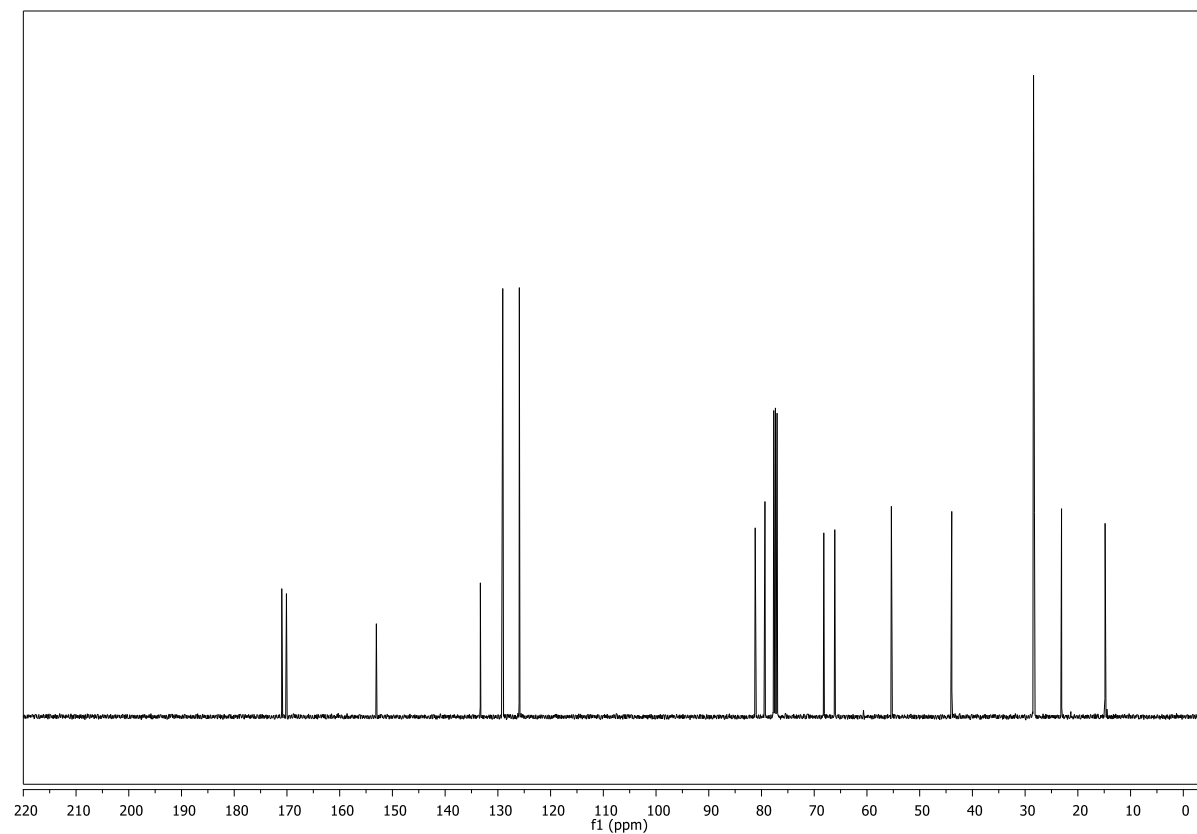
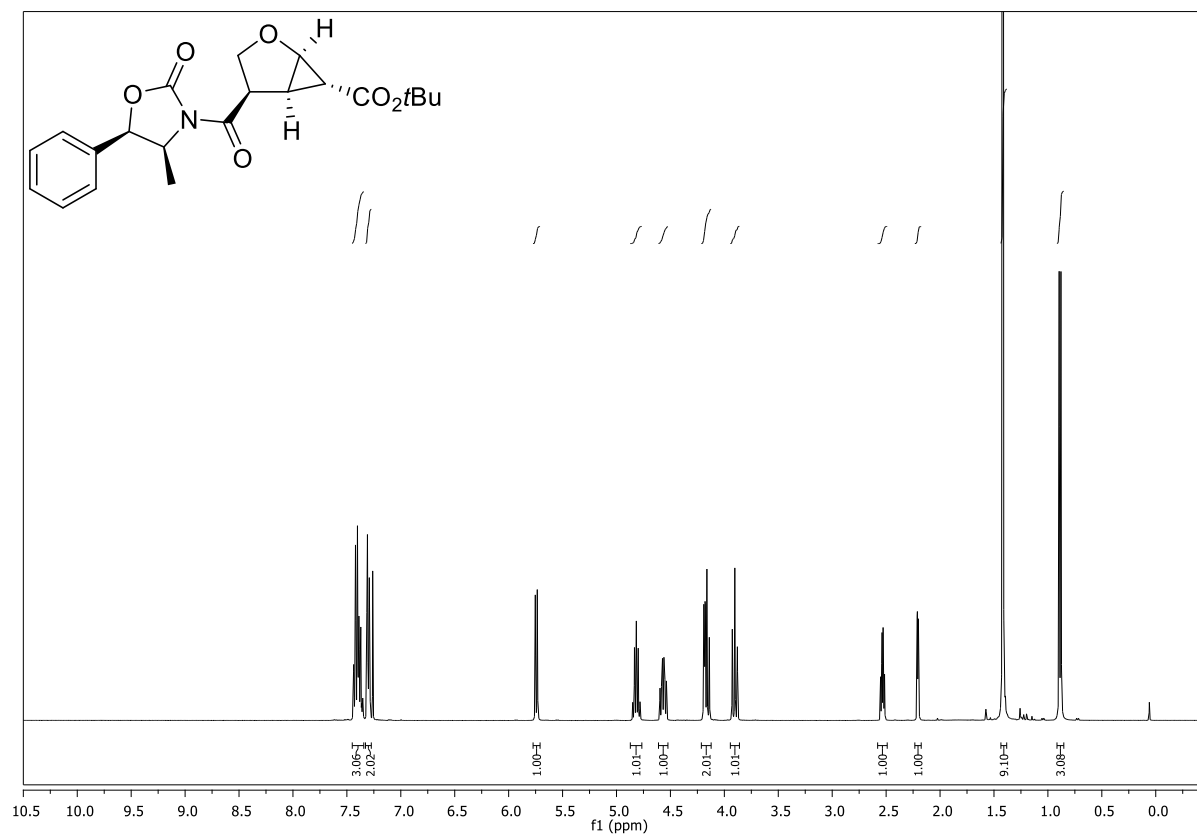
**6-(tert-Butyl) 4-methyl (1*R*,4*R*,5*R*,6*R*)-2-oxabicyclo[3.1.0]hexane-4,6-dicarboxylate (147)**  
**(CDCl<sub>3</sub>, 400 MHz)**



**(CDCl<sub>3</sub>, 101 MHz)**

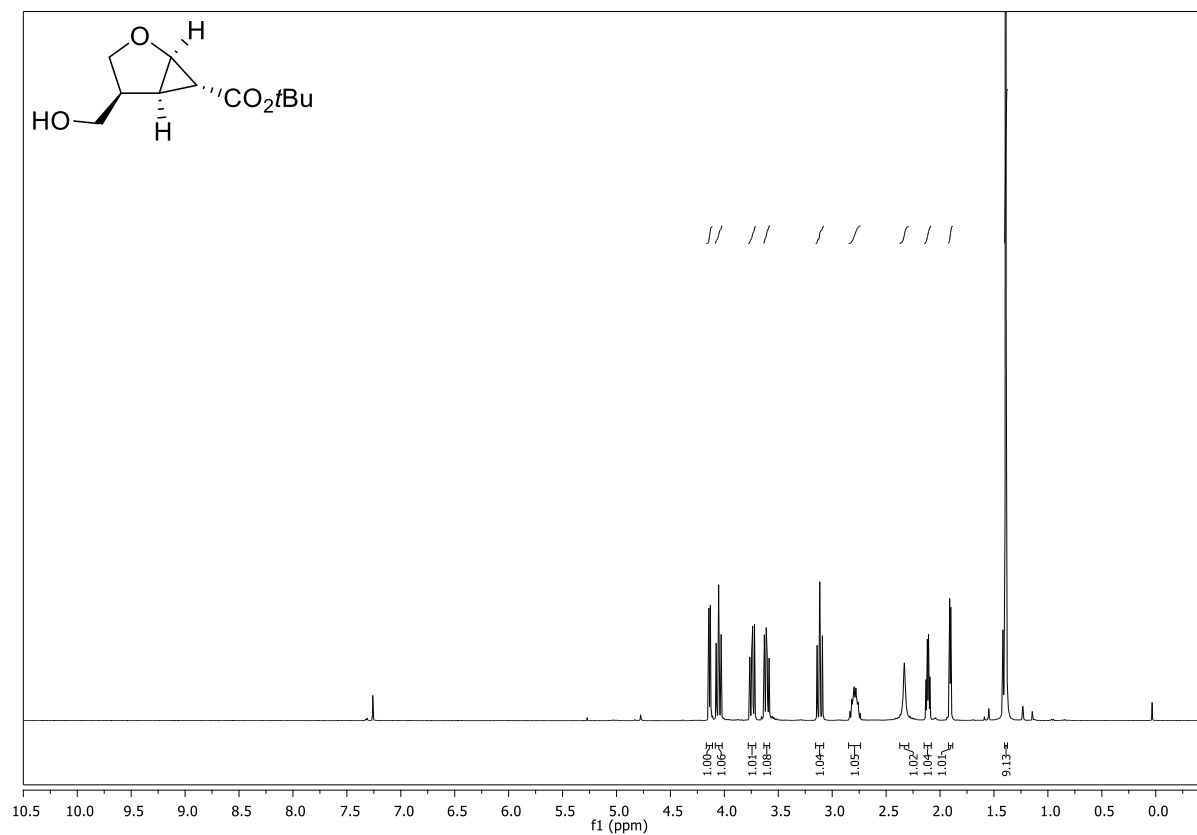


**(1*R*,4*R*,5*R*,6*R*)-6-(*tert*-Butoxycarbonyl)-2-oxabicyclo[3.1.0]hexane-4-carboxylic acid (155)****(CDCl<sub>3</sub>, 400 MHz)****(CDCl<sub>3</sub>, 101 MHz)**

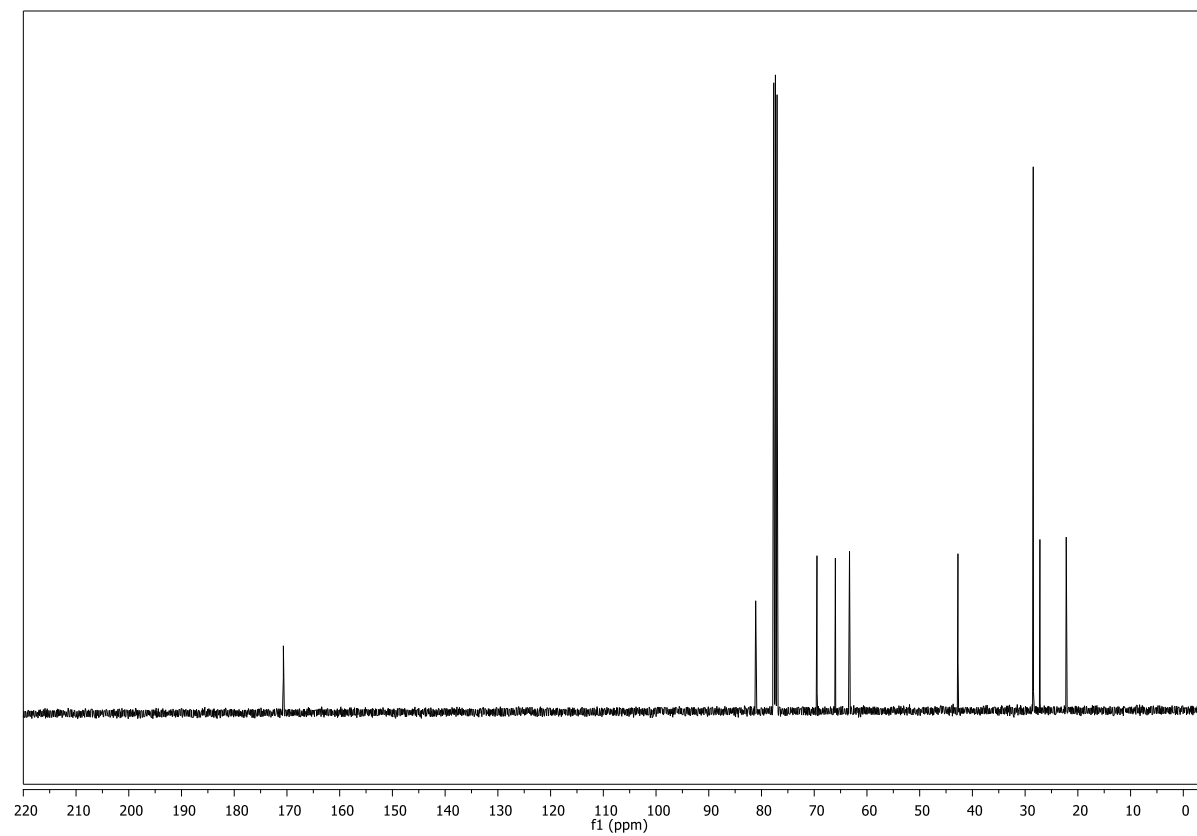
**tert-Butyl (1*R*,4*R*,5*R*,6*R*)-4-((4*S*,5*R*)-4-methyl-2-oxo-5-phenyloxazolidine-3-carbonyl)-2-oxa-bicyclo[3.1.0]hexane-6-carboxylate (156) (CDCl<sub>3</sub>, 400 MHz)**



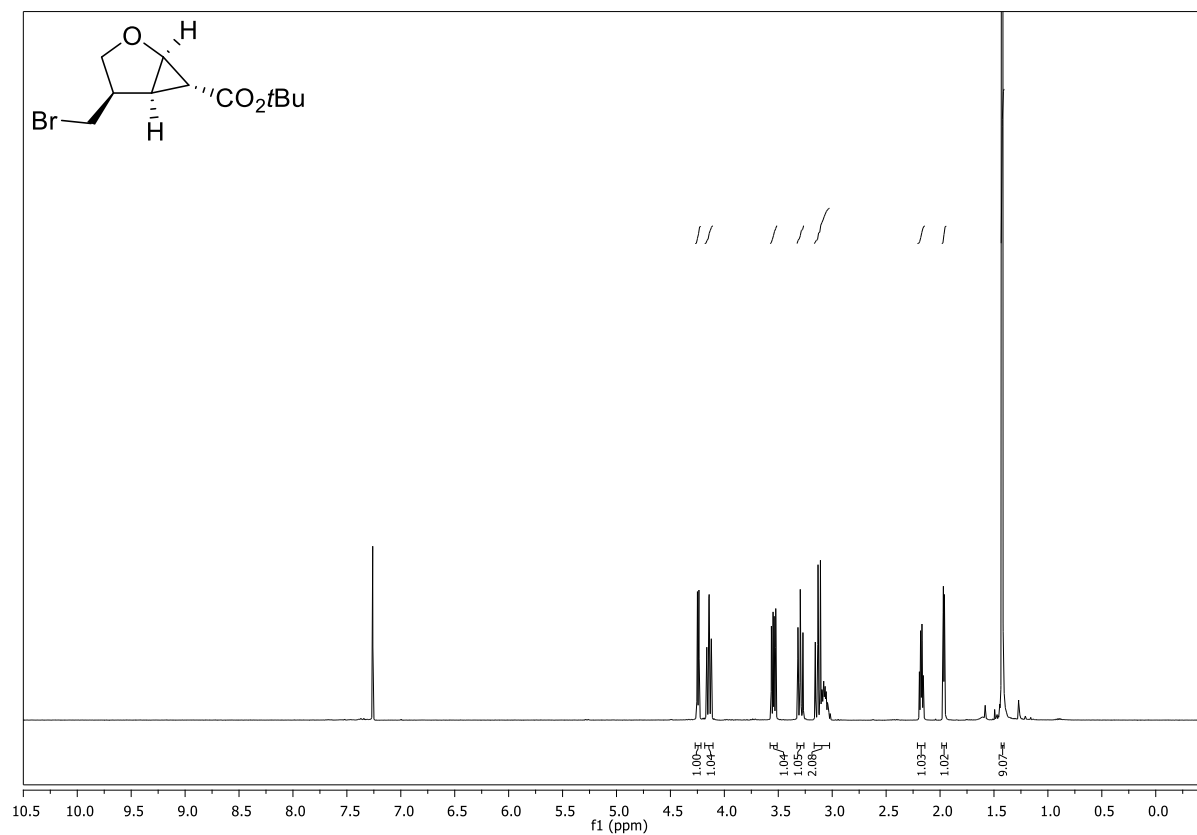
**tert-Butyl (1*R*,4*S*,5*R*,6*R*)-4-(hydroxymethyl)-2-oxabicyclo[3.1.0]hexane-6-carboxylate (157)**  
**(CDCl<sub>3</sub>, 400 MHz)**



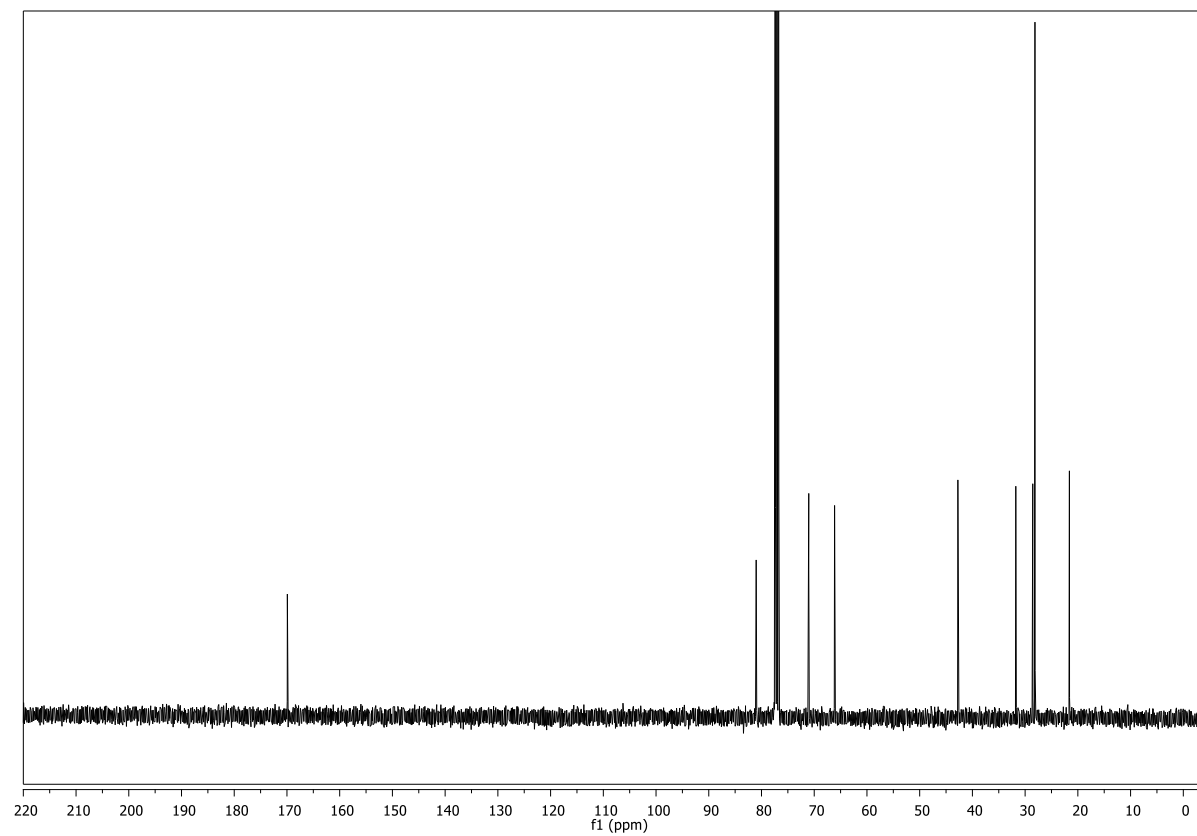
**(CDCl<sub>3</sub>, 101 MHz)**

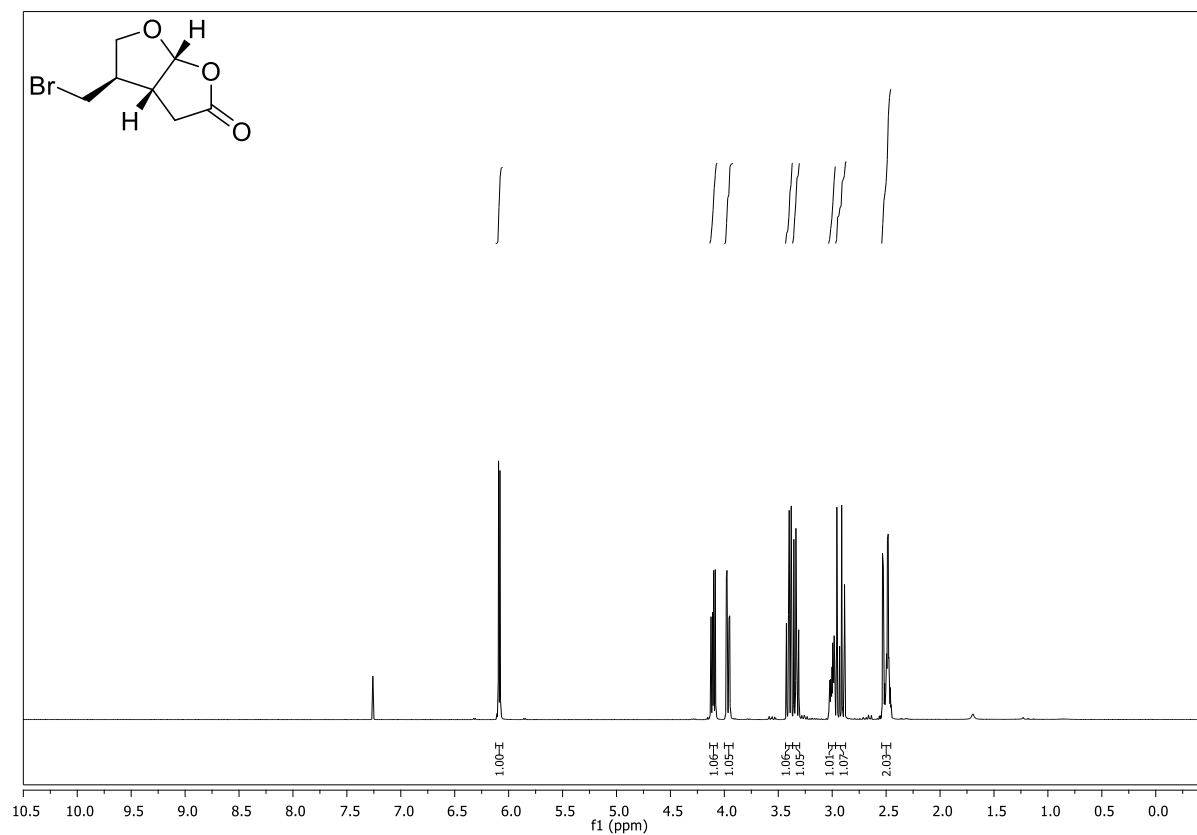
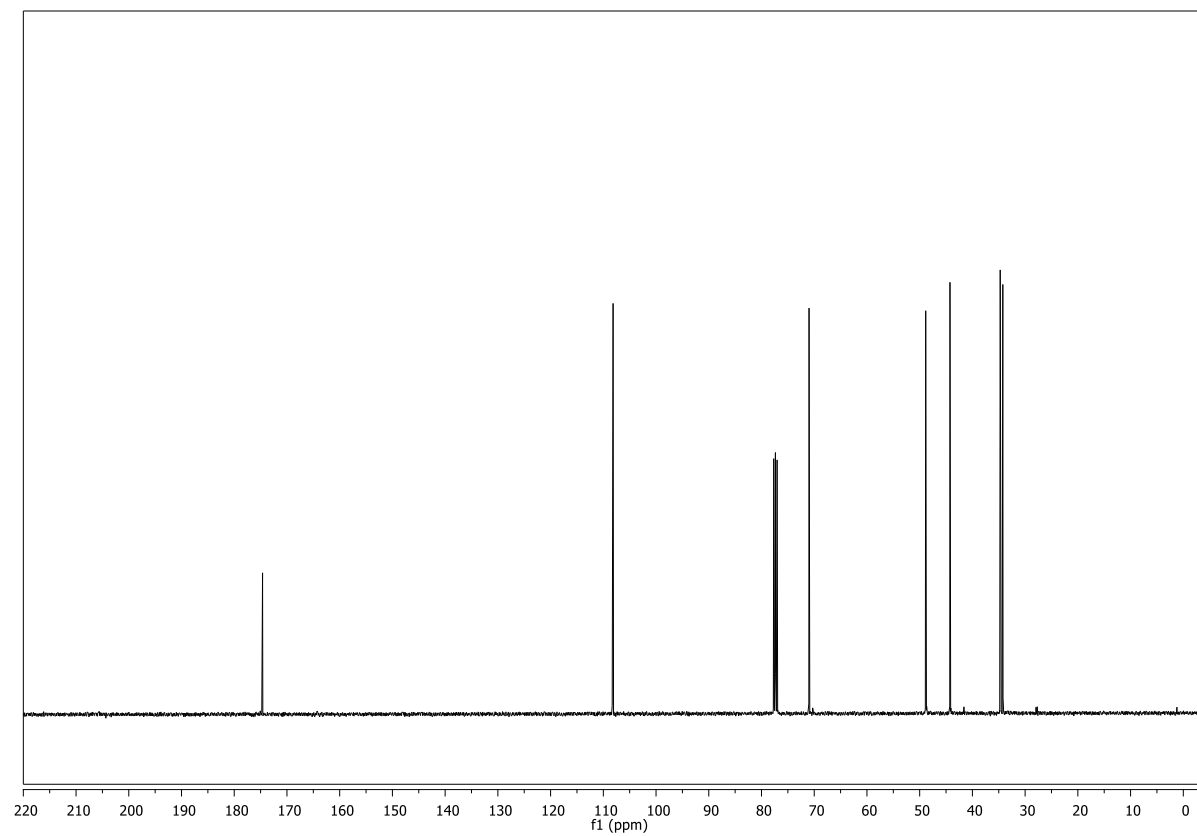


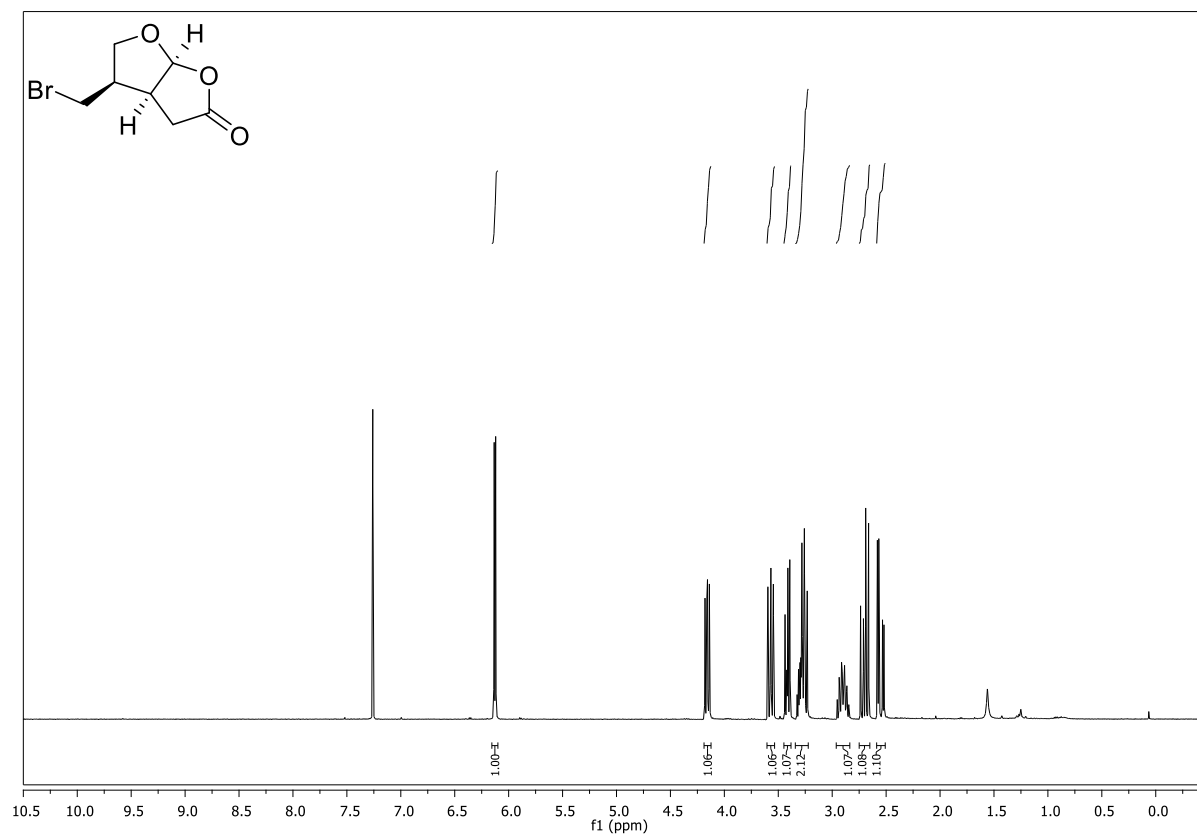
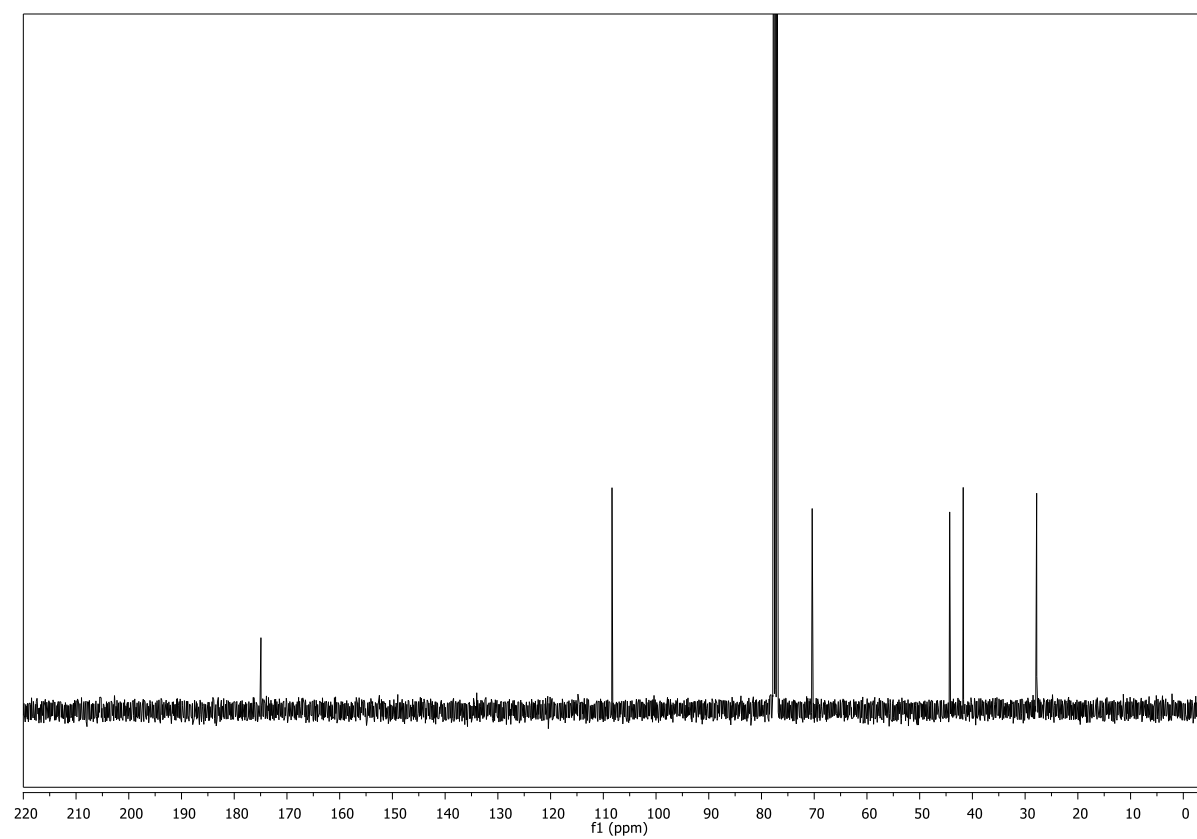
**tert-Butyl (1*R*,4*R*,5*S*,6*R*)-4-(bromomethyl)-2-oxabicyclo[3.1.0]hexane-6-carboxylate (158)**  
**(CDCl<sub>3</sub>, 400 MHz)**

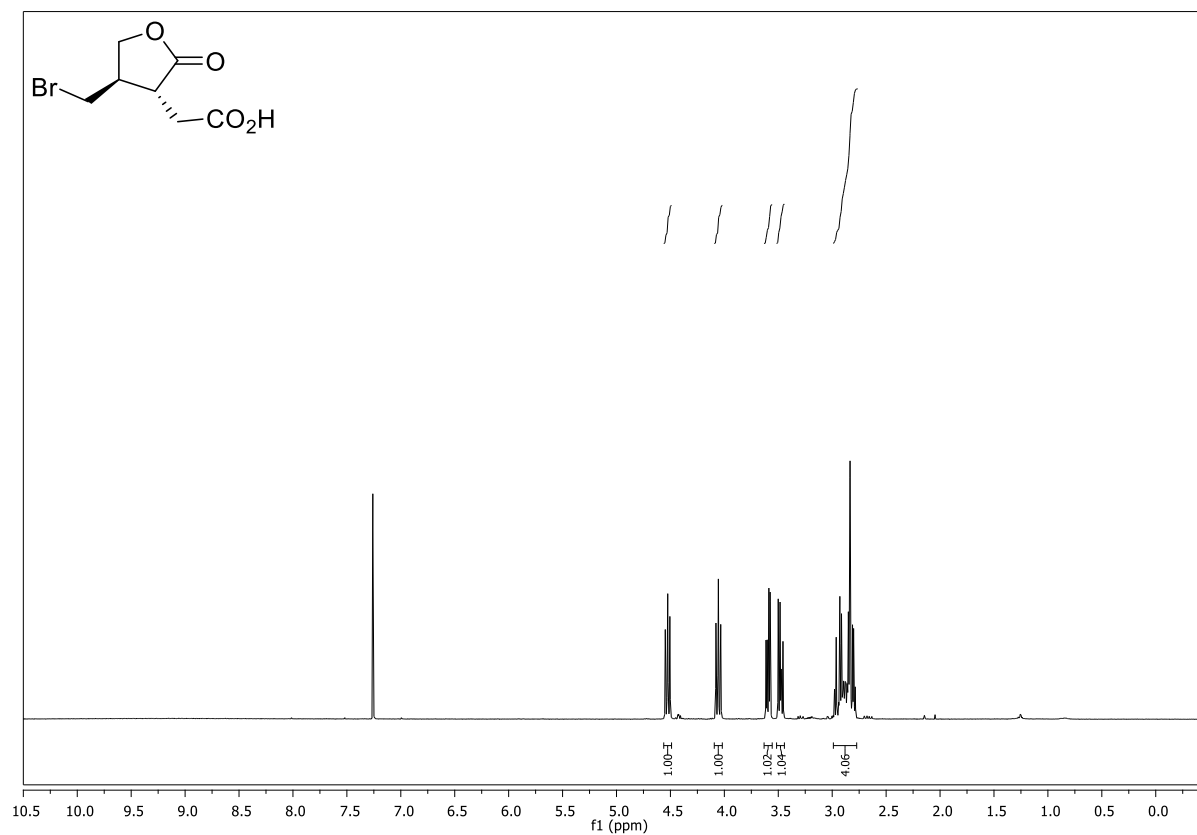
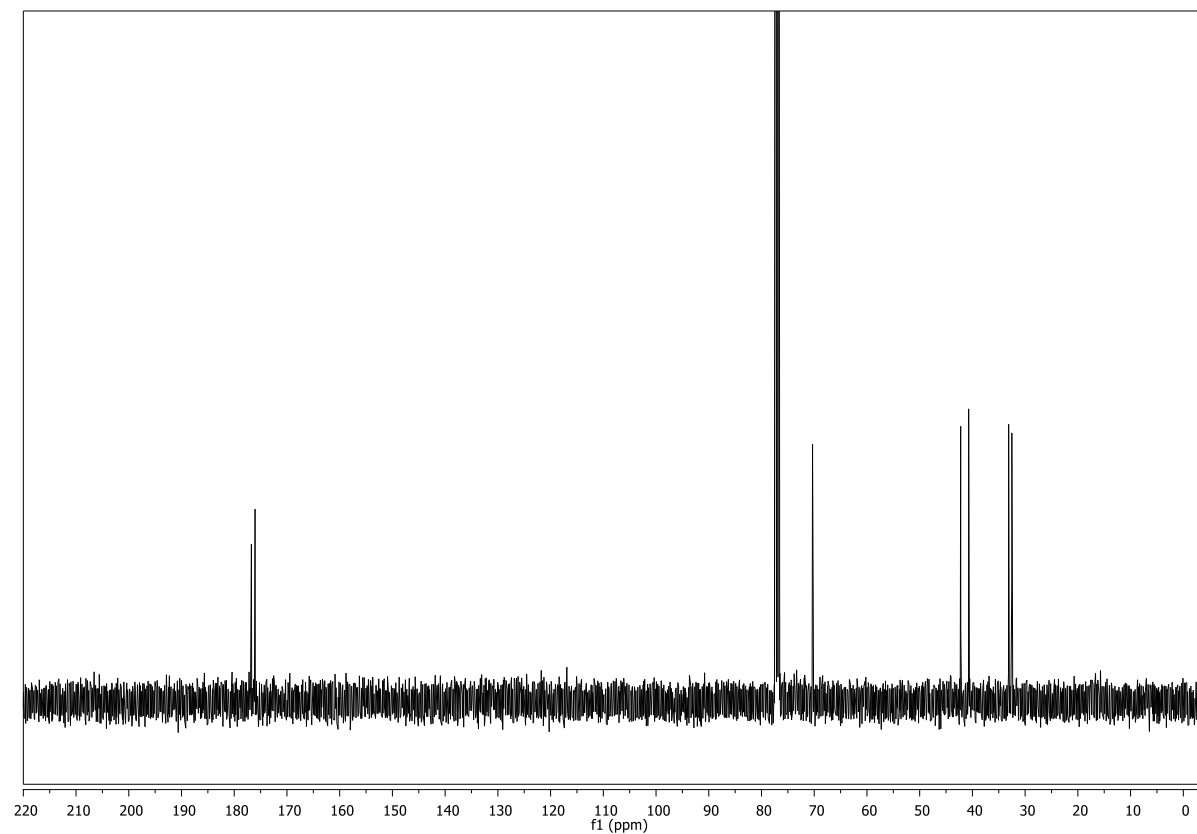


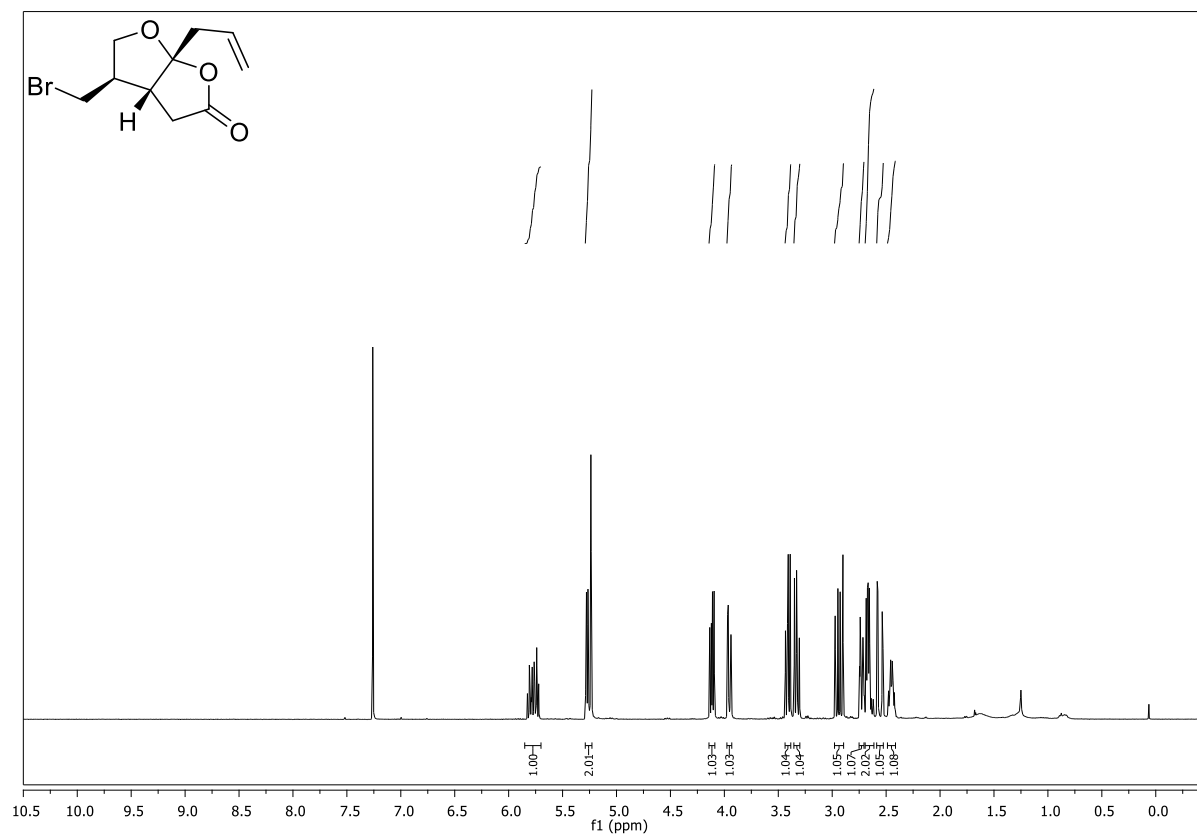
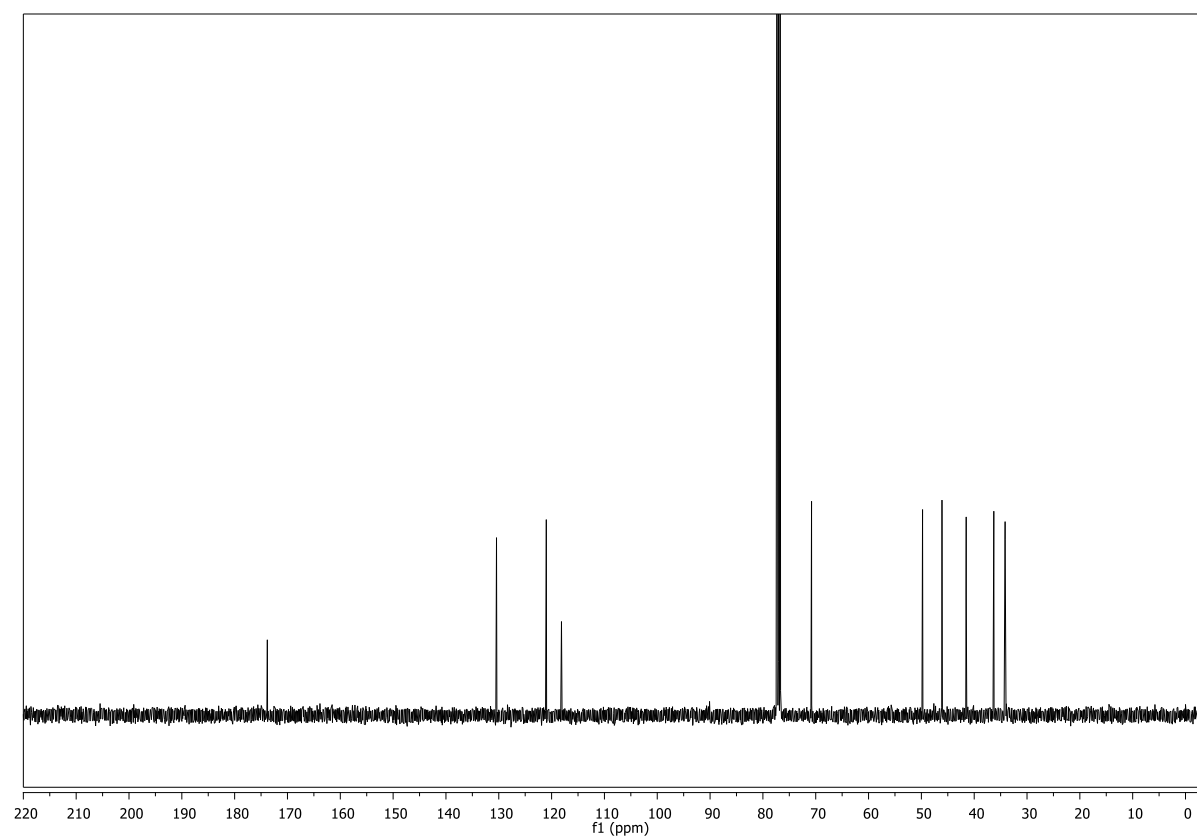
**(CDCl<sub>3</sub>, 101 MHz)**

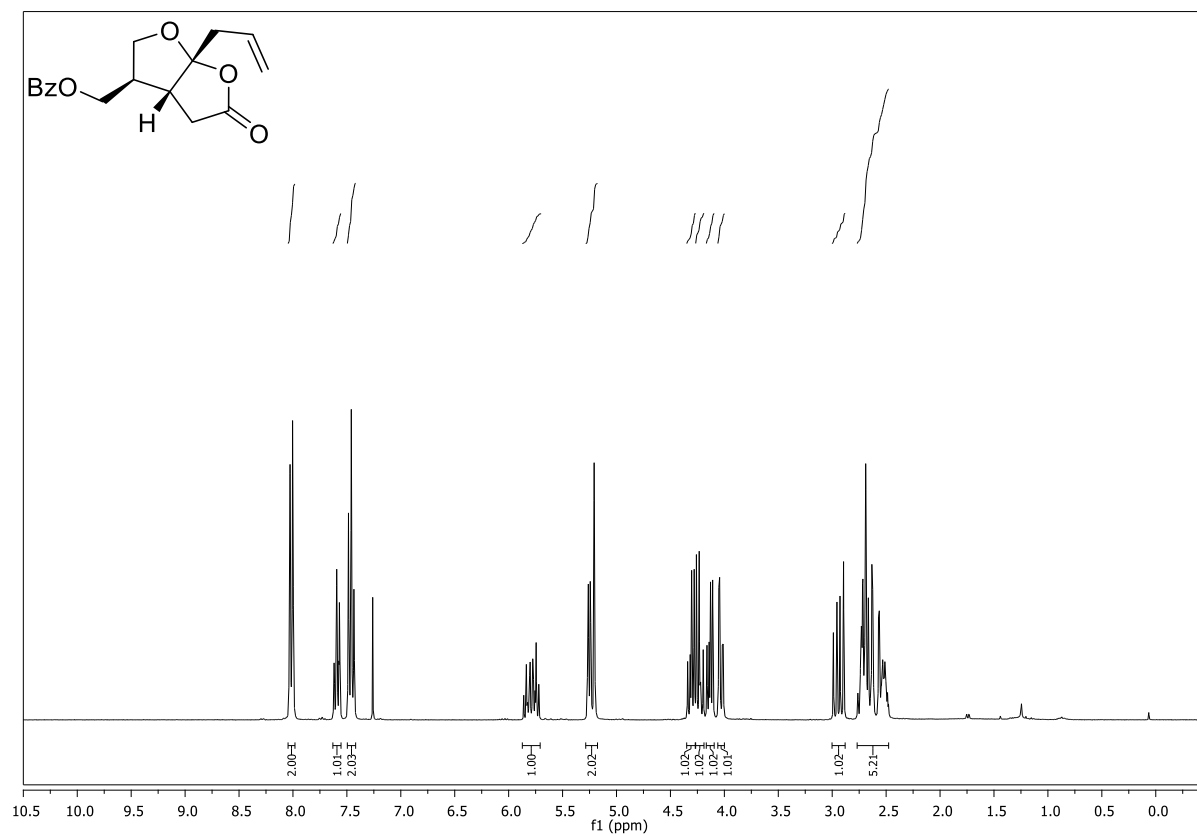
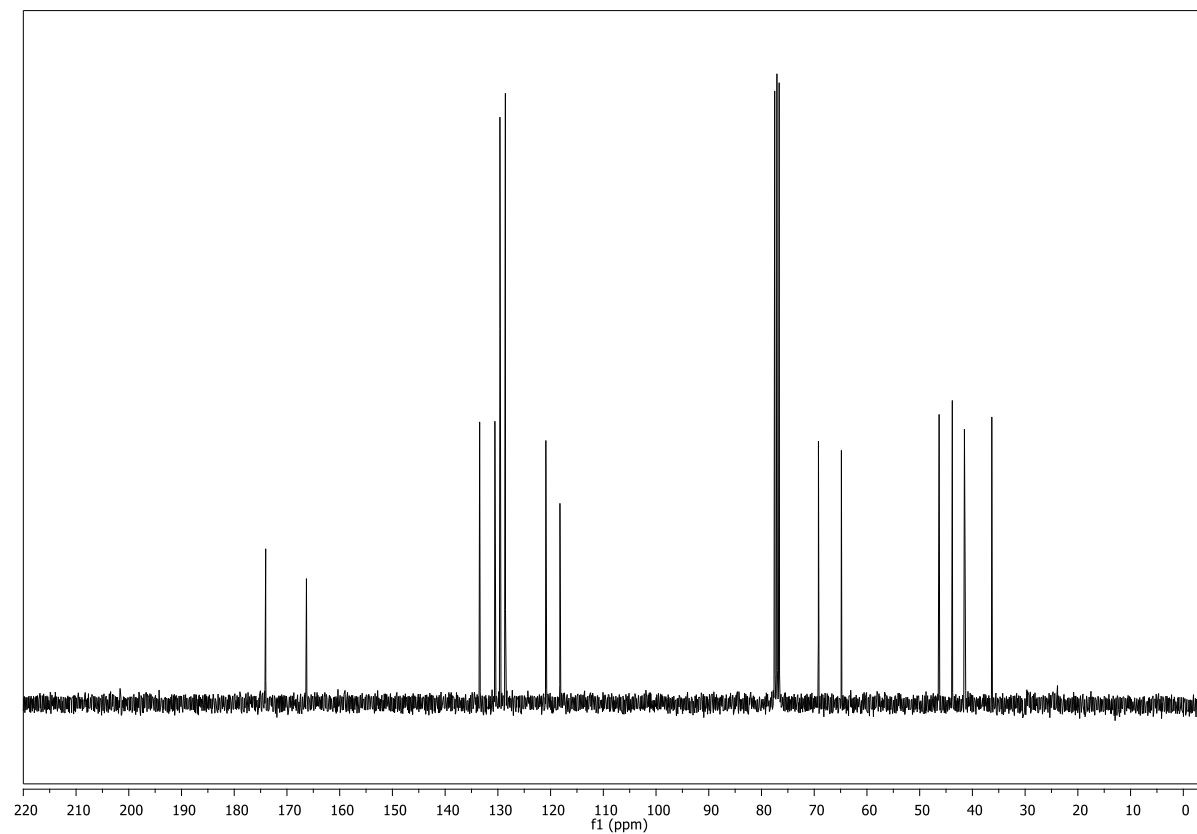


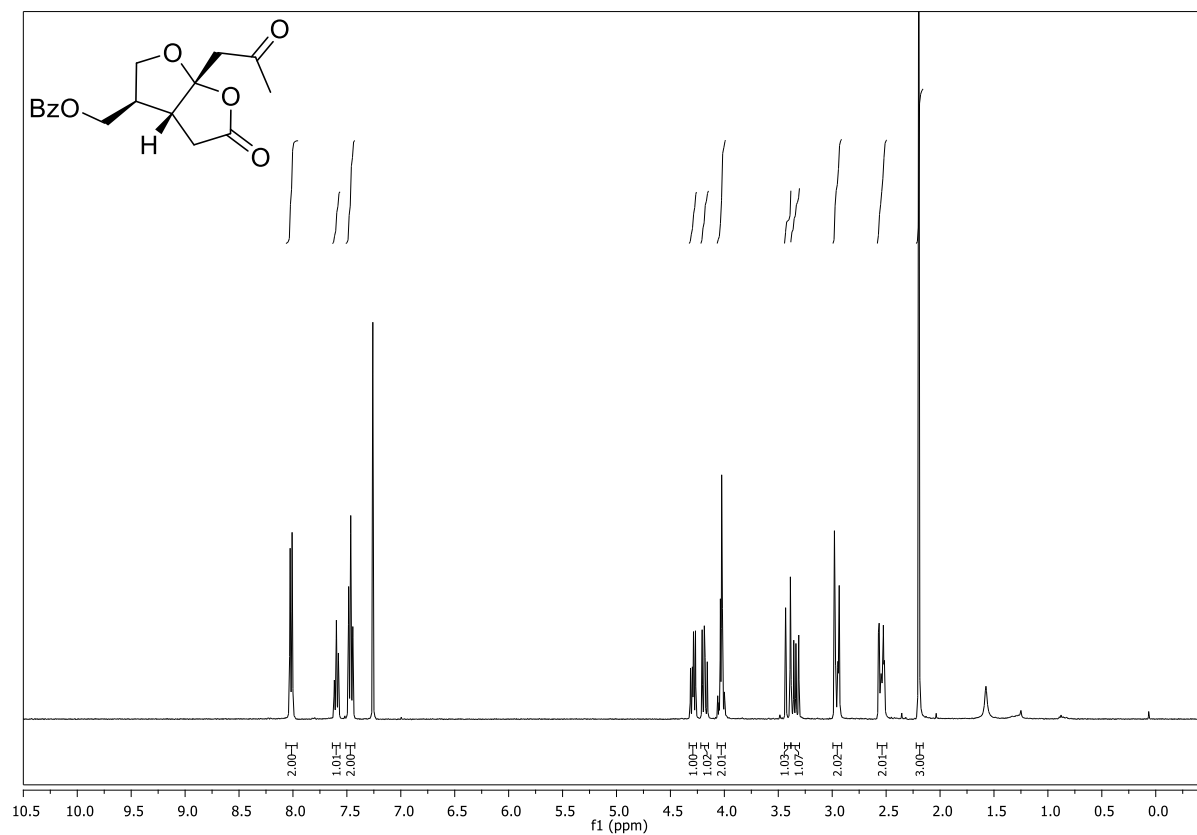
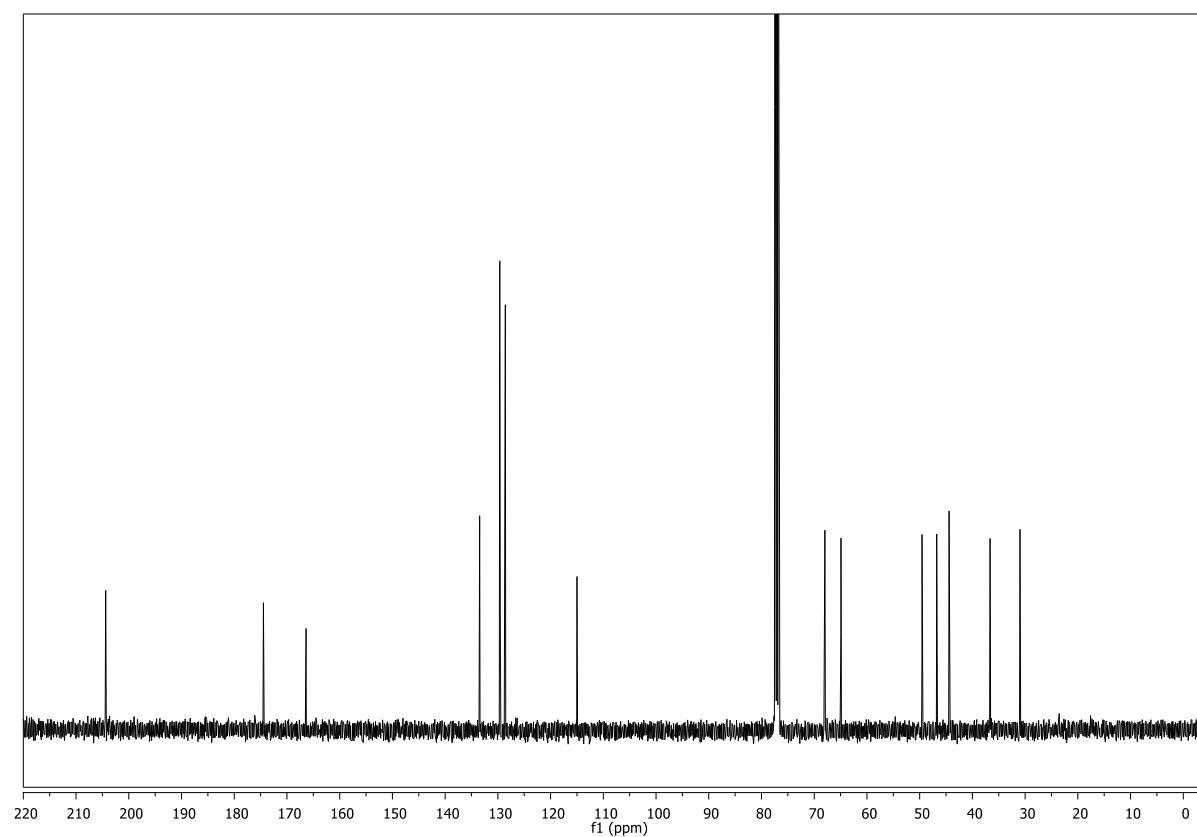
**(3aR,4R,6aR)-4-(Bromomethyl)tetrahydrofuro[2,3-b]furan-2(3H)-one (159)****(CDCl<sub>3</sub>, 400 MHz)****(CDCl<sub>3</sub>, 101 MHz)**

**(3a*S*,4*R*,6a*S*)-4-(Bromomethyl)tetrahydrofuro[2,3-*b*]furan-2(3*H*)-one (160)****(CDCl<sub>3</sub>, 400 MHz)****(CDCl<sub>3</sub>, 101 MHz)**

**2-((3*R*,4*R*)-4-(Bromomethyl)-2-oxotetrahydrofuran-3-yl)acetic acid (167)****(CDCl<sub>3</sub>, 400 MHz)****(CDCl<sub>3</sub>, 101 MHz)**

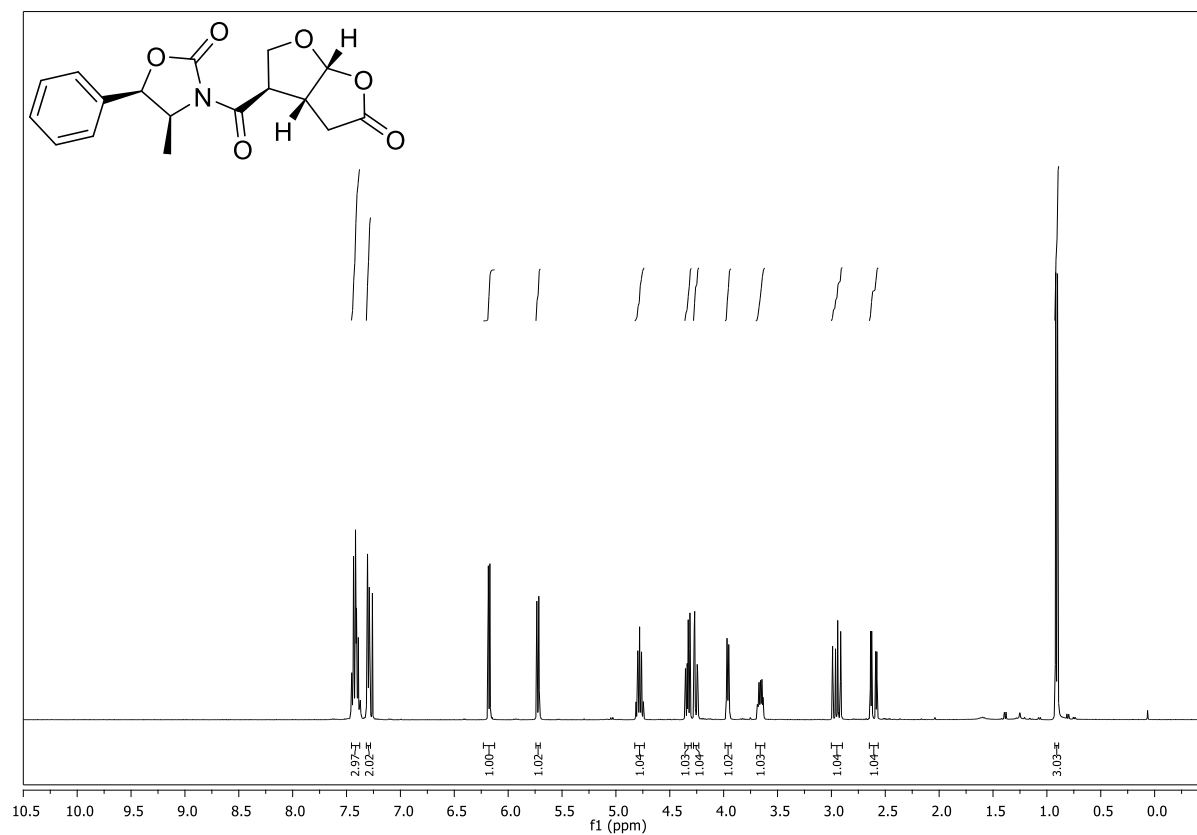
**(3aR,4R,6aR)-6a-Allyl-4-(bromomethyl)tetrahydrofuro[2,3-b]furan-2(3H)-one (169)****(CDCl<sub>3</sub>, 400 MHz)****(CDCl<sub>3</sub>, 101 MHz)**

**((3*R*,3*aR*,6*aR*)-6*a*-Allyl-5-oxohexahydrofuro[2,3-*b*]furan-3-yl)methyl benzoate (170)****(CDCl<sub>3</sub>, 400 MHz)****(CDCl<sub>3</sub>, 101 MHz)**

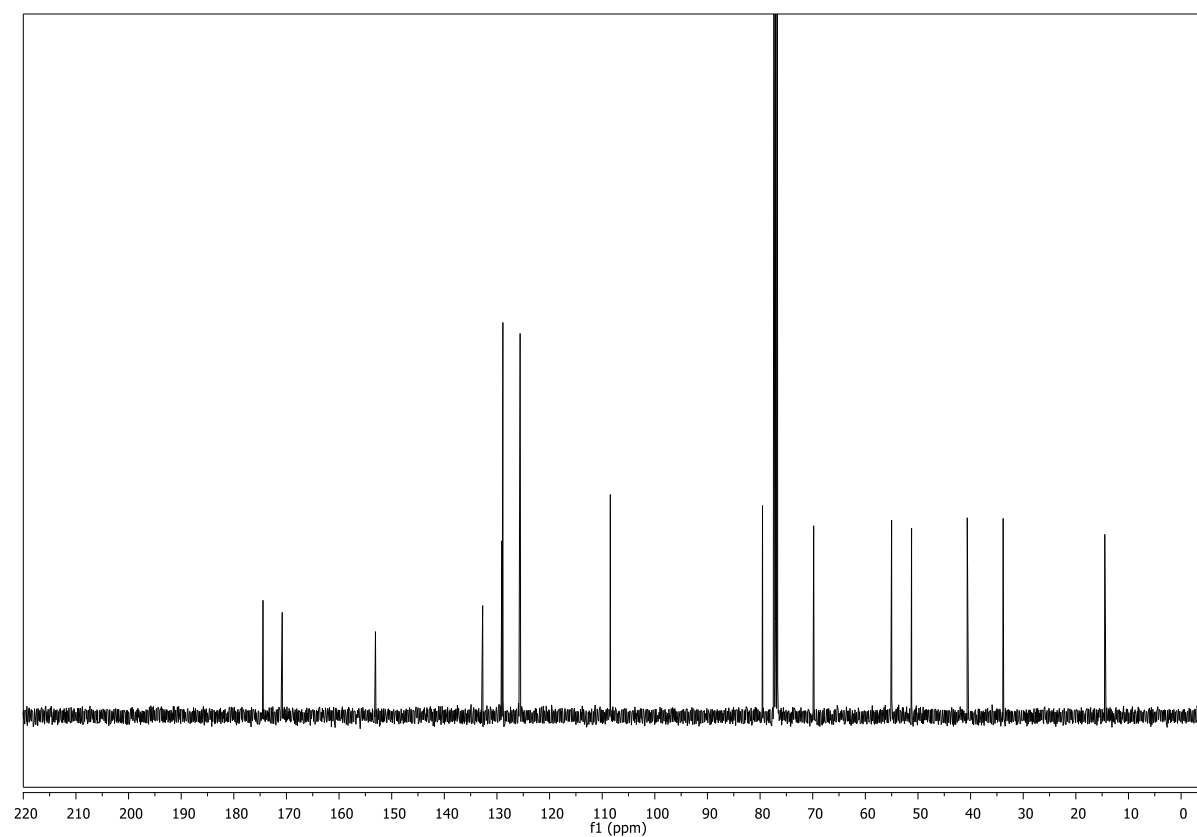
**((3*R*,3*aR*,6*aR*)-5-Oxo-6a-(2-oxopropyl)hexahydrofuro[2,3-*b*]furan-3-yl)methyl benzoate (49)****(CDCl<sub>3</sub>, 400 MHz)****(CDCl<sub>3</sub>, 101 MHz)**



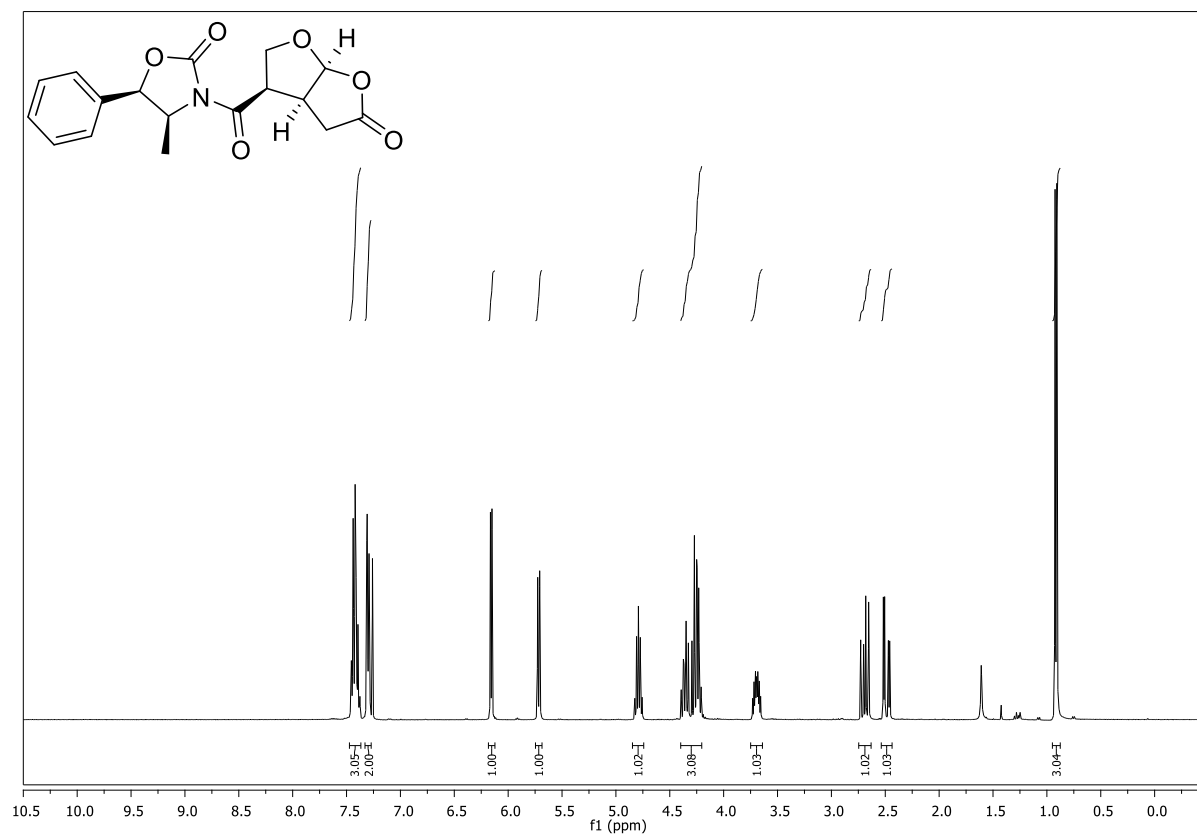
**(4*S*,5*R*)-4-Methyl-3-((3*R*,3*aR*,6*aR*)-5-oxohexahydrofuro[2,3-*b*]furan-3-carbonyl)-5-phenyloxazolidin-2-one (176) (CDCl<sub>3</sub>, 400 MHz)**



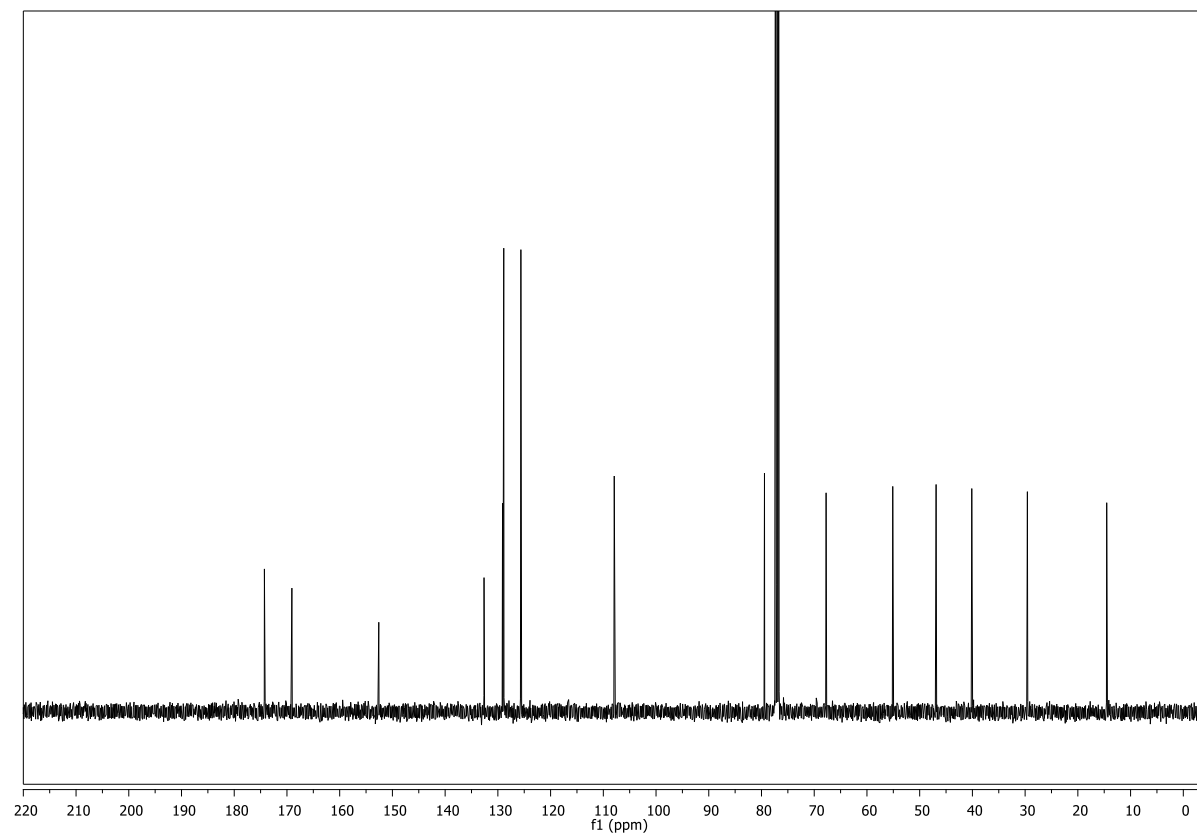
**(CDCl<sub>3</sub>, 101 MHz)**

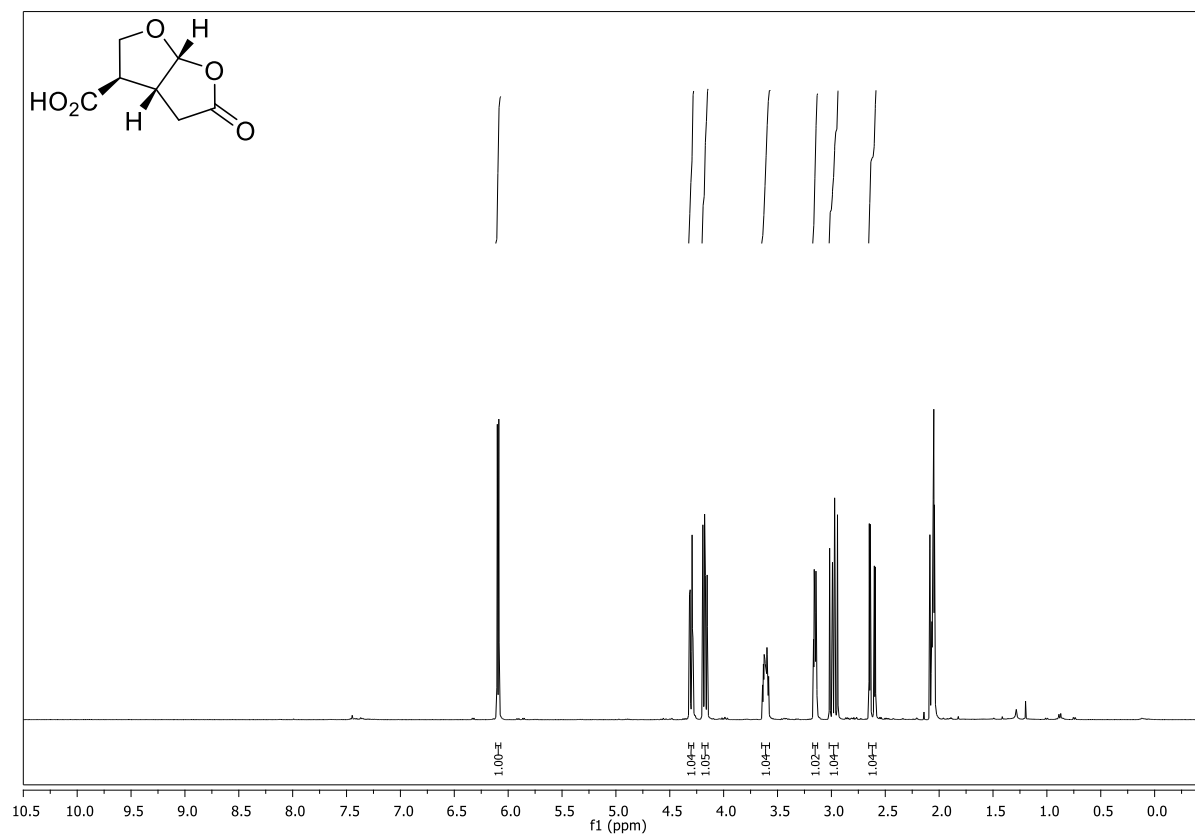
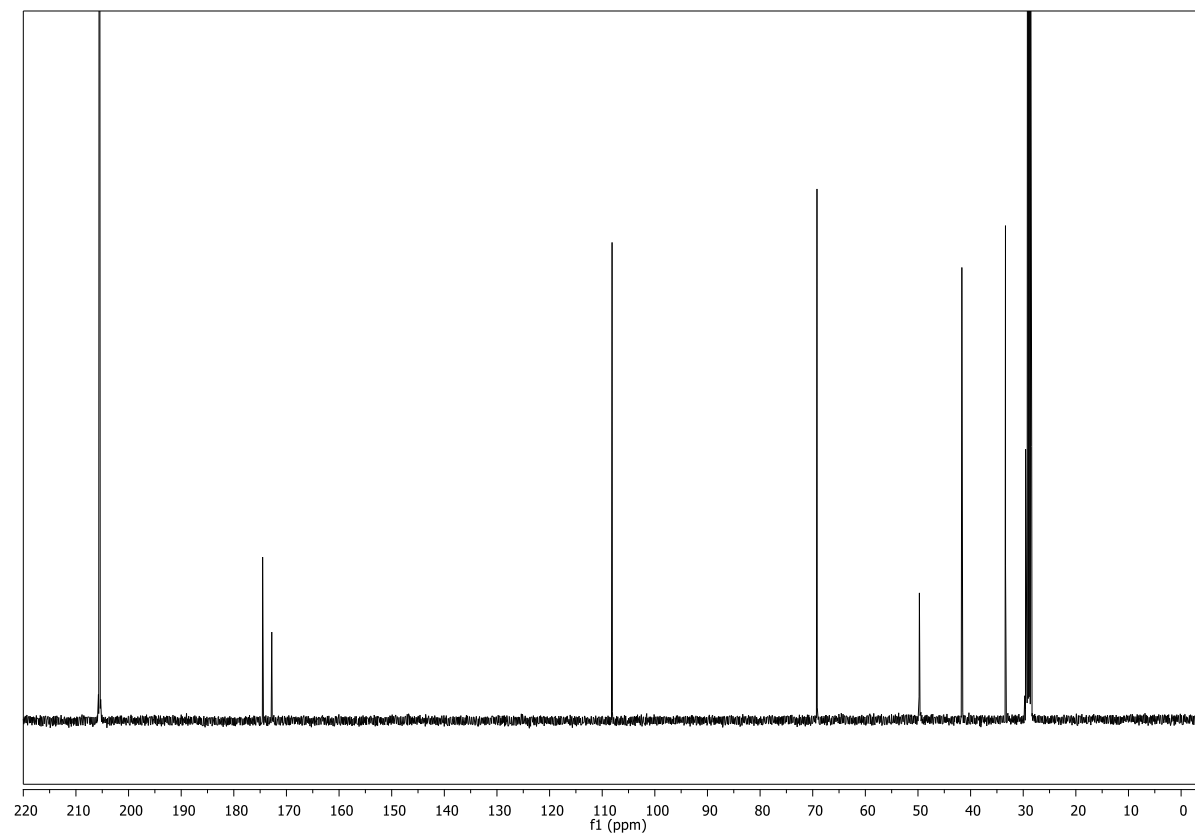


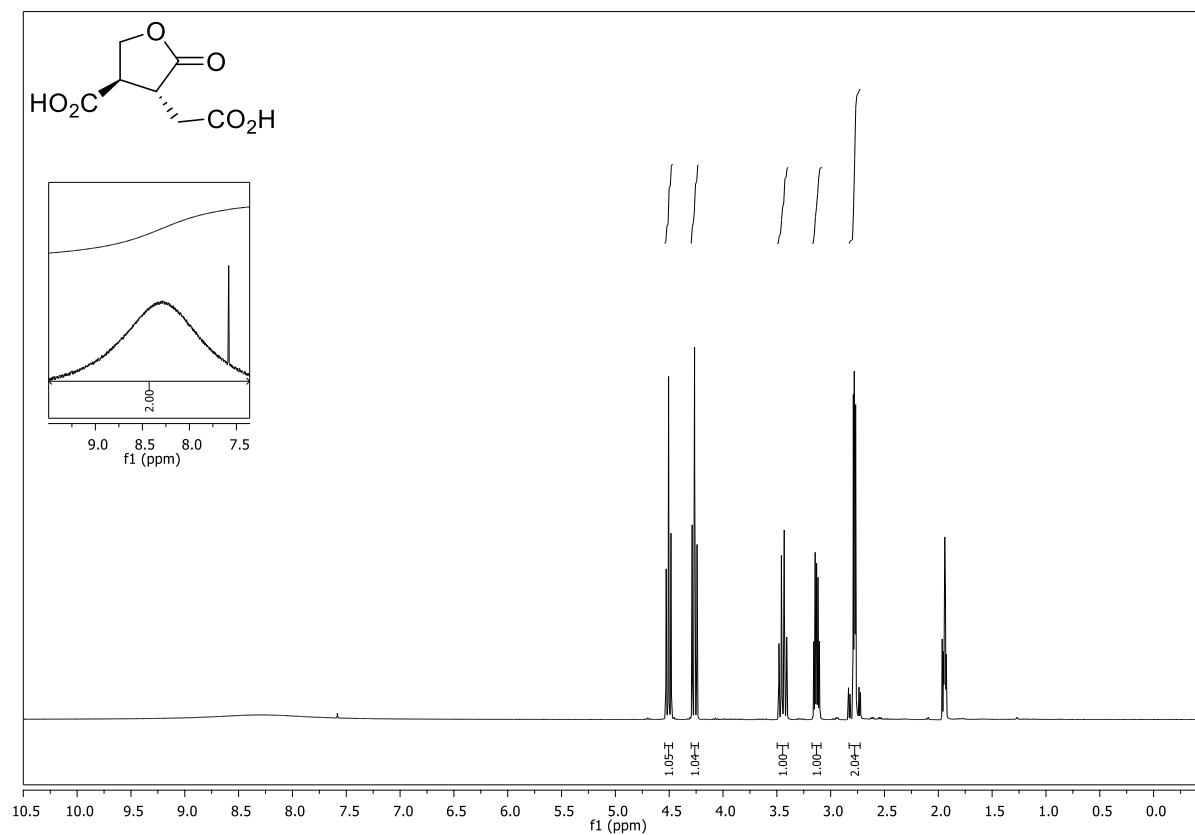
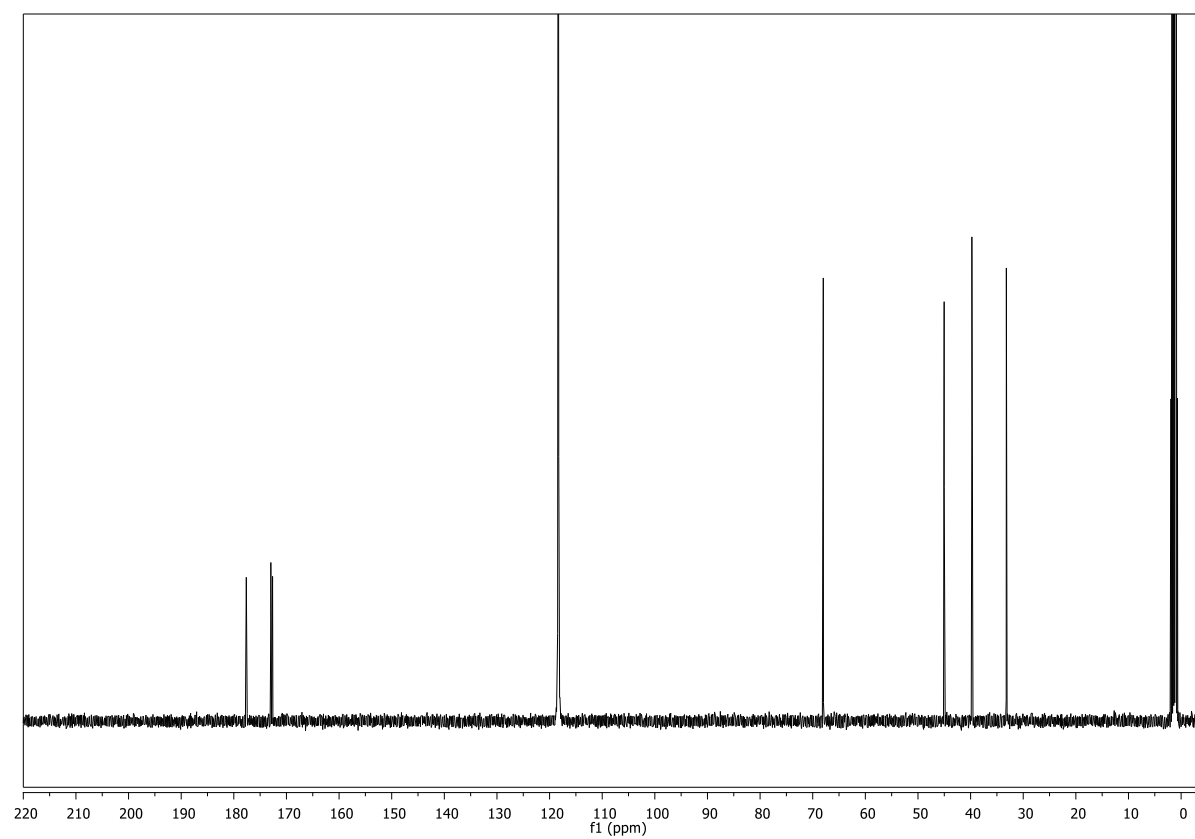
**(4*S*,5*R*)-4-Methyl-3-((3*R*,3*aS*,6*aS*)-5-oxohexahydrofuro[2,3-*b*]furan-3-carbonyl)-5-phenyloxazolidin-2-one (177) (CDCl<sub>3</sub>, 400 MHz)**

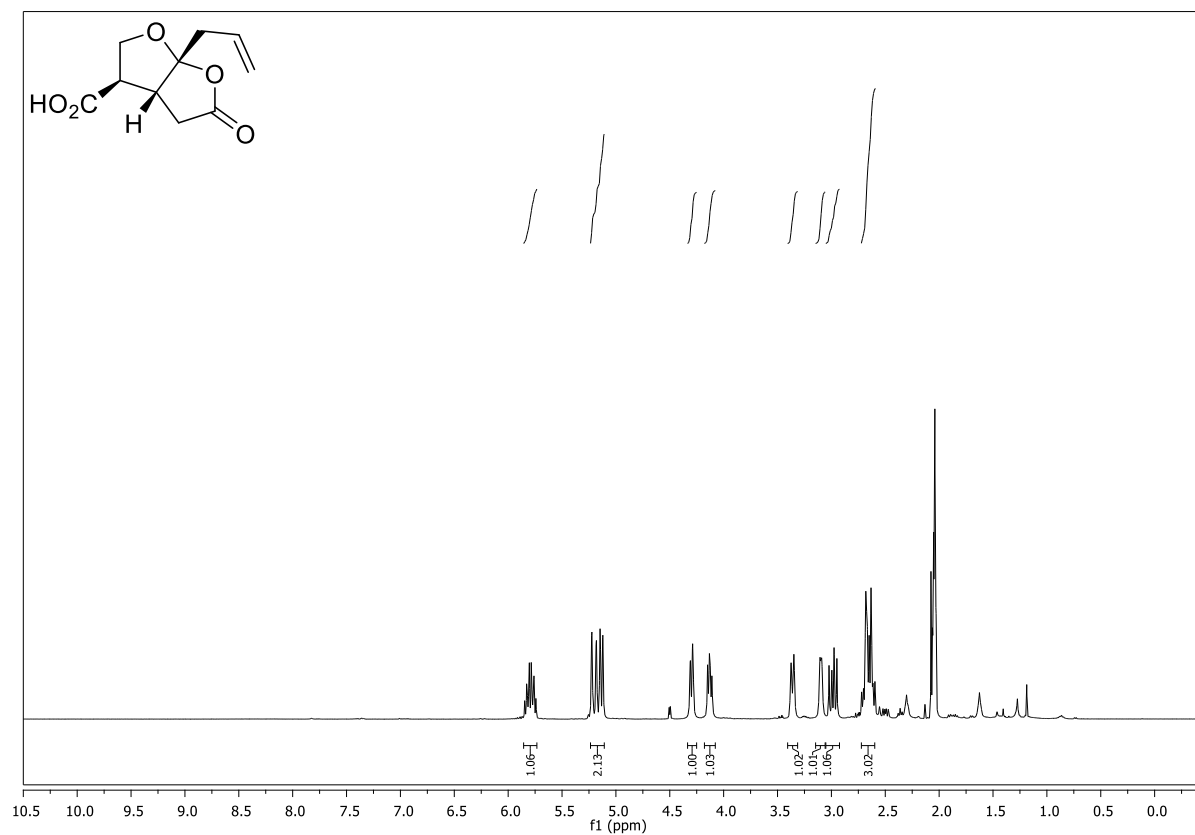
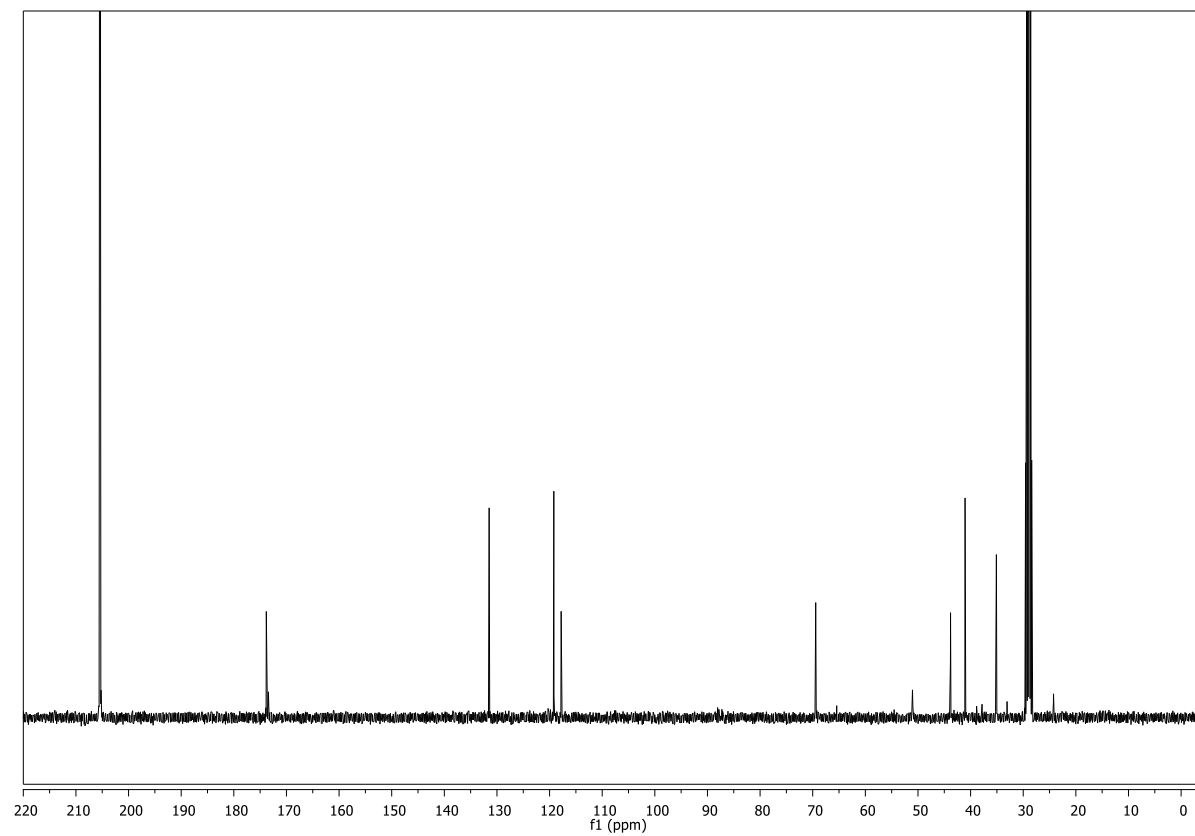


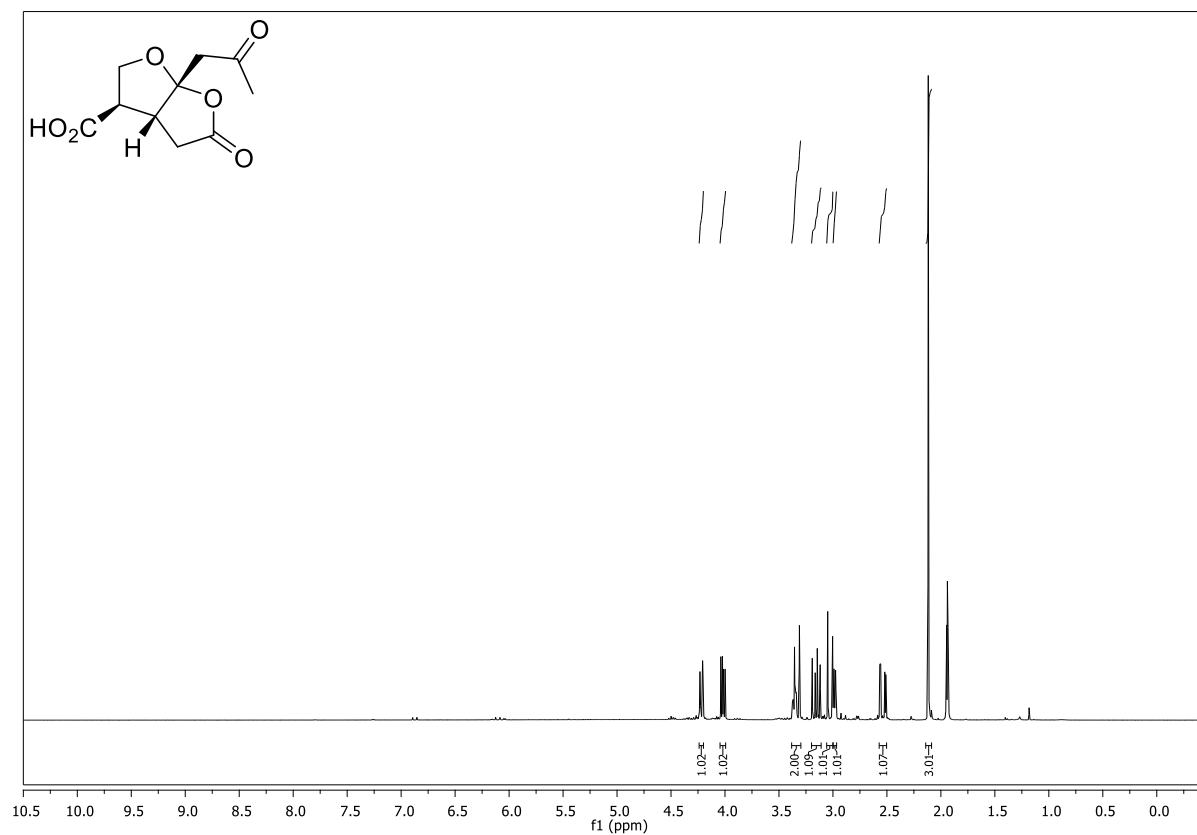
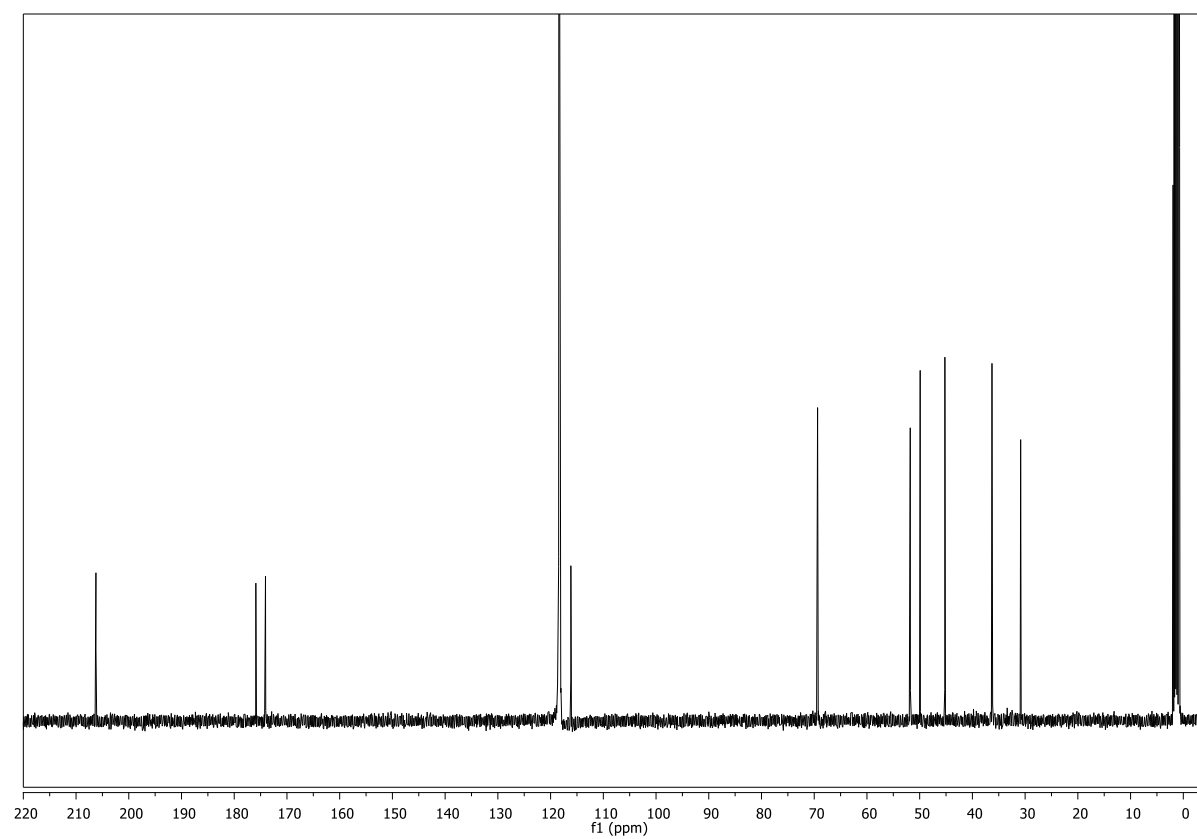
**(CDCl<sub>3</sub>, 101 MHz)**

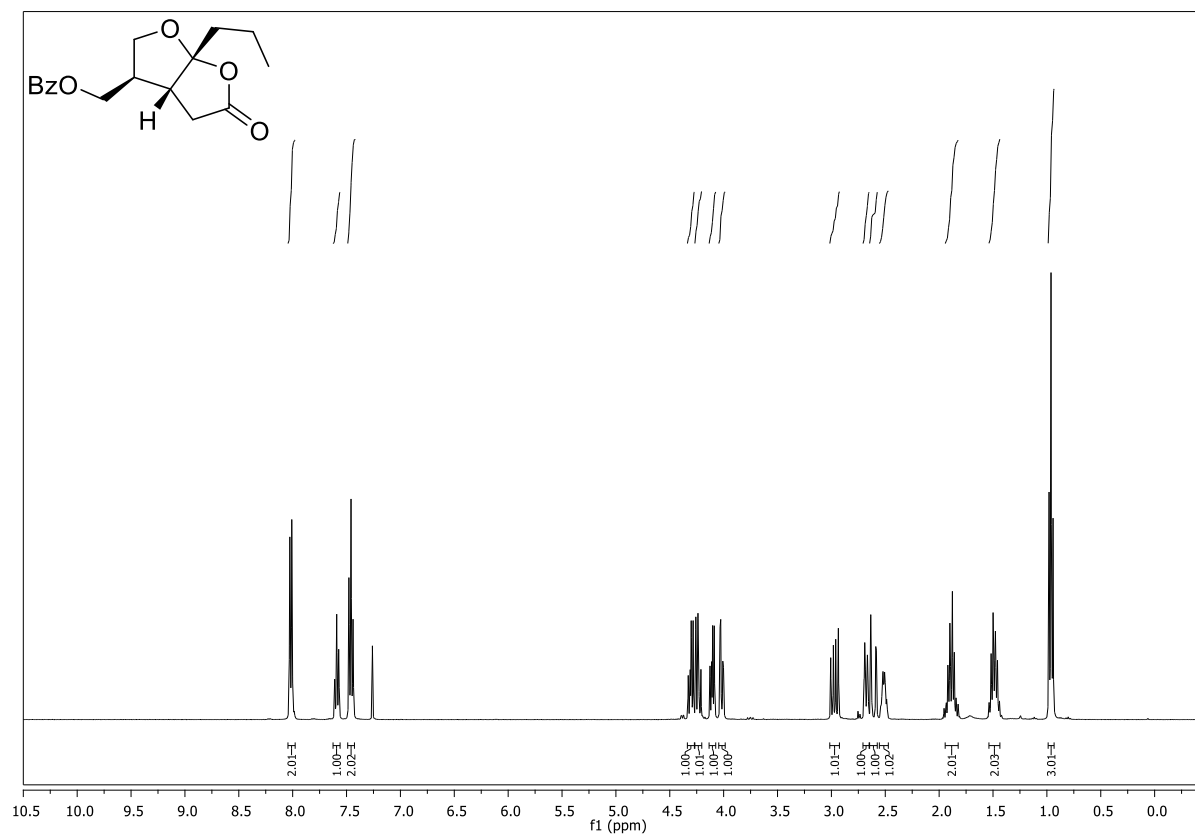
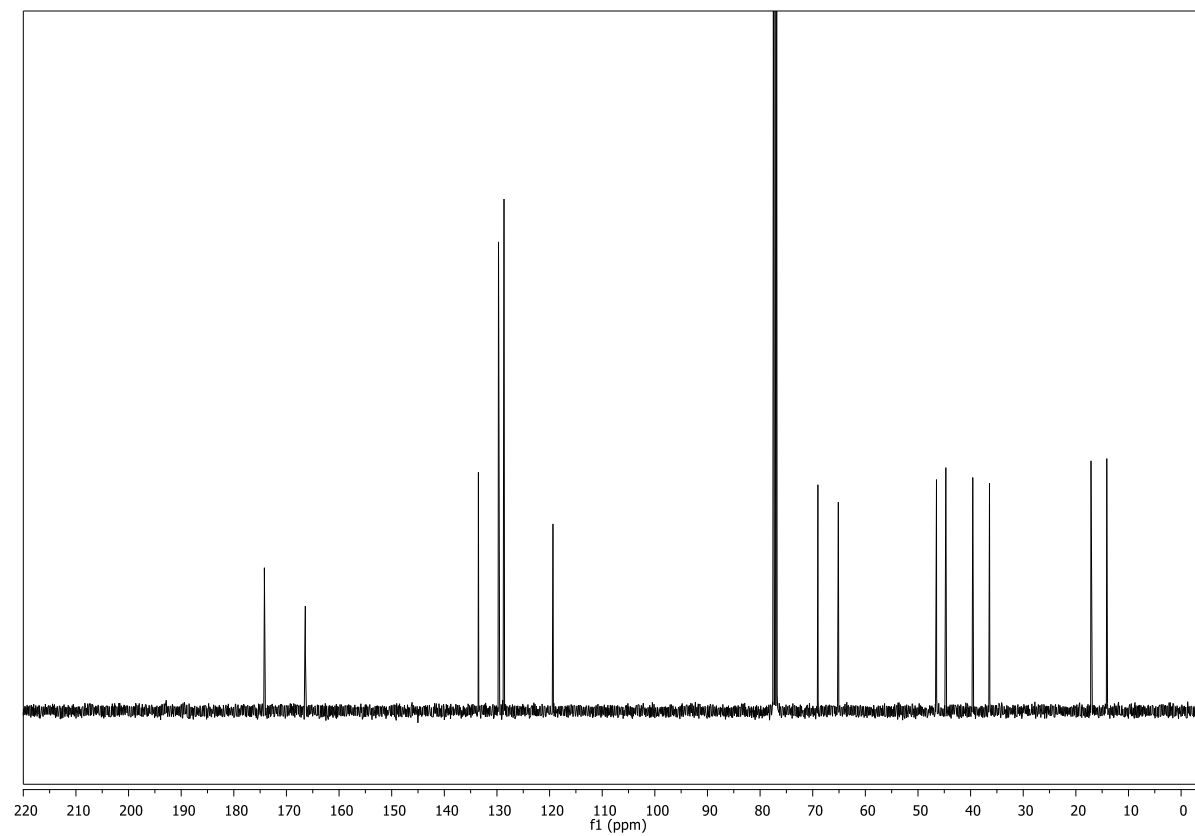


**(3*R*,3*aR*,6*aR*)-5-Oxohexahydrofuro[2,3-*b*]furan-3-carboxylic acid (178)****(Acetone, 400 MHz)****(Acetone, 101 MHz)**

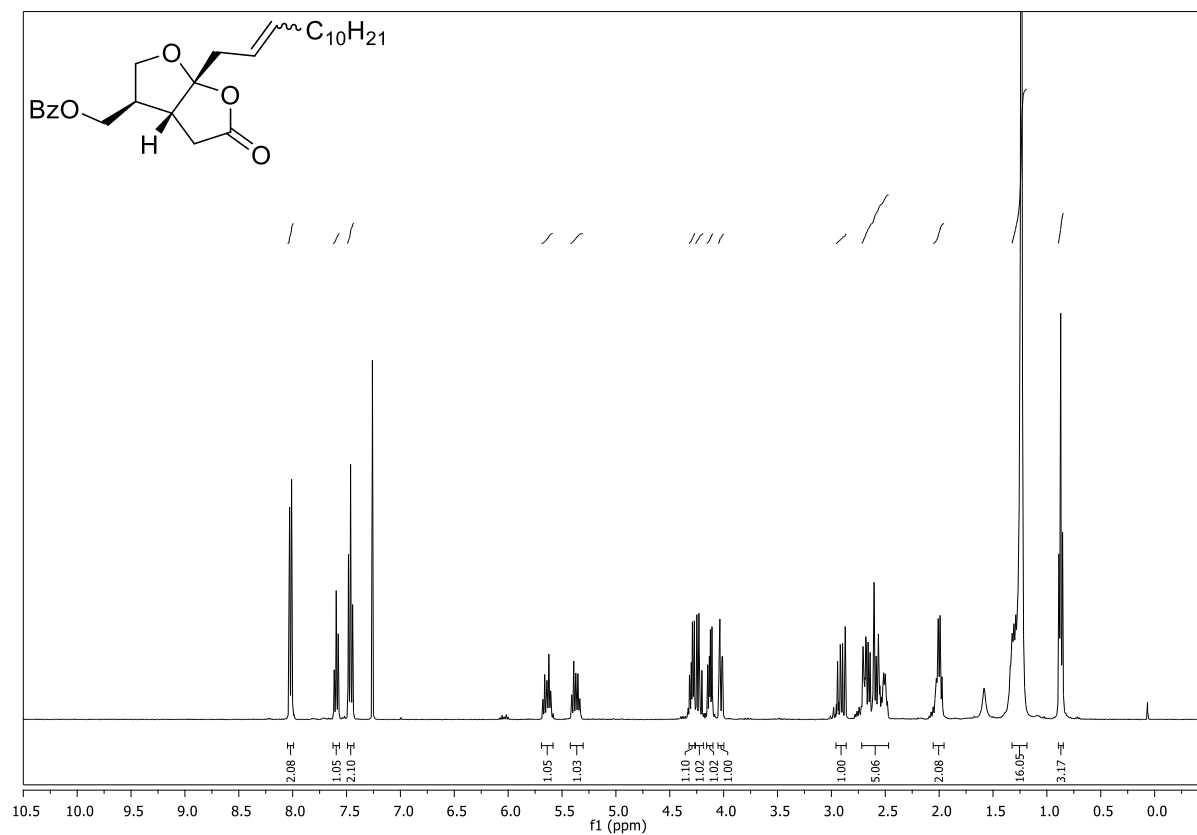
**(3*R*,4*R*)-4-(Carboxymethyl)-5-oxotetrahydrofuran-3-carboxylic acid (179)****(CD<sub>3</sub>CN, 400 MHz)****(CD<sub>3</sub>CN, 101 MHz)**

**(3*R*,3*aR*,6*aR*)-6*a*-Allyl-5-oxohexahydrofuro[2,3-*b*]furan-3-carboxylic acid (180)****(Acetone, 400 MHz)****(Acetone, 101 MHz)**

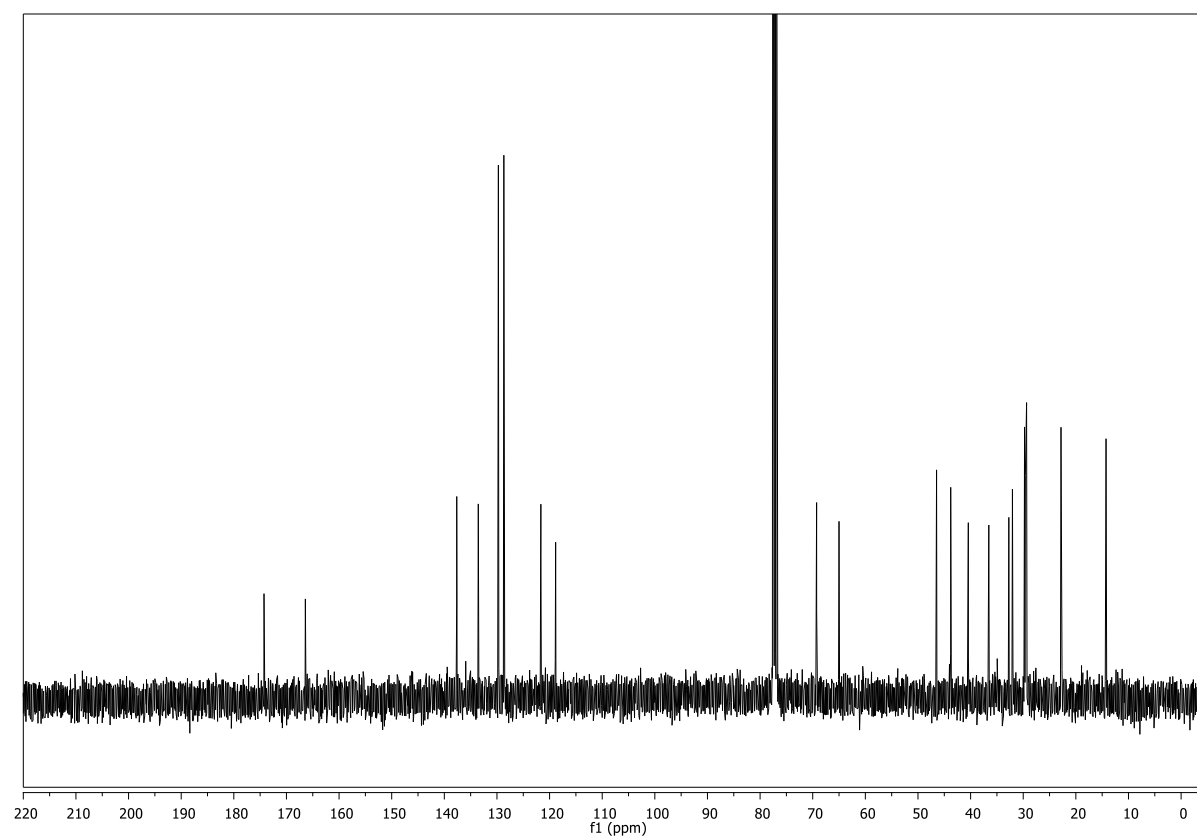
**(3*R*,3*aR*,6*aR*)-5-Oxo-6a-(2-oxopropyl)hexahydrofuro[2,3-*b*]furan-3-carboxylic acid (181)****(CD<sub>3</sub>CN, 400 MHz)****(CD<sub>3</sub>CN, 101 MHz)**

**((3*R*,3*aR*,6*aR*)-5-Oxo-6*a*-propylhexahydrofuro[2,3-*b*]furan-3-yl)methyl benzoate (182)****(CDCl<sub>3</sub>, 400 MHz)****(CDCl<sub>3</sub>, 101 MHz)**

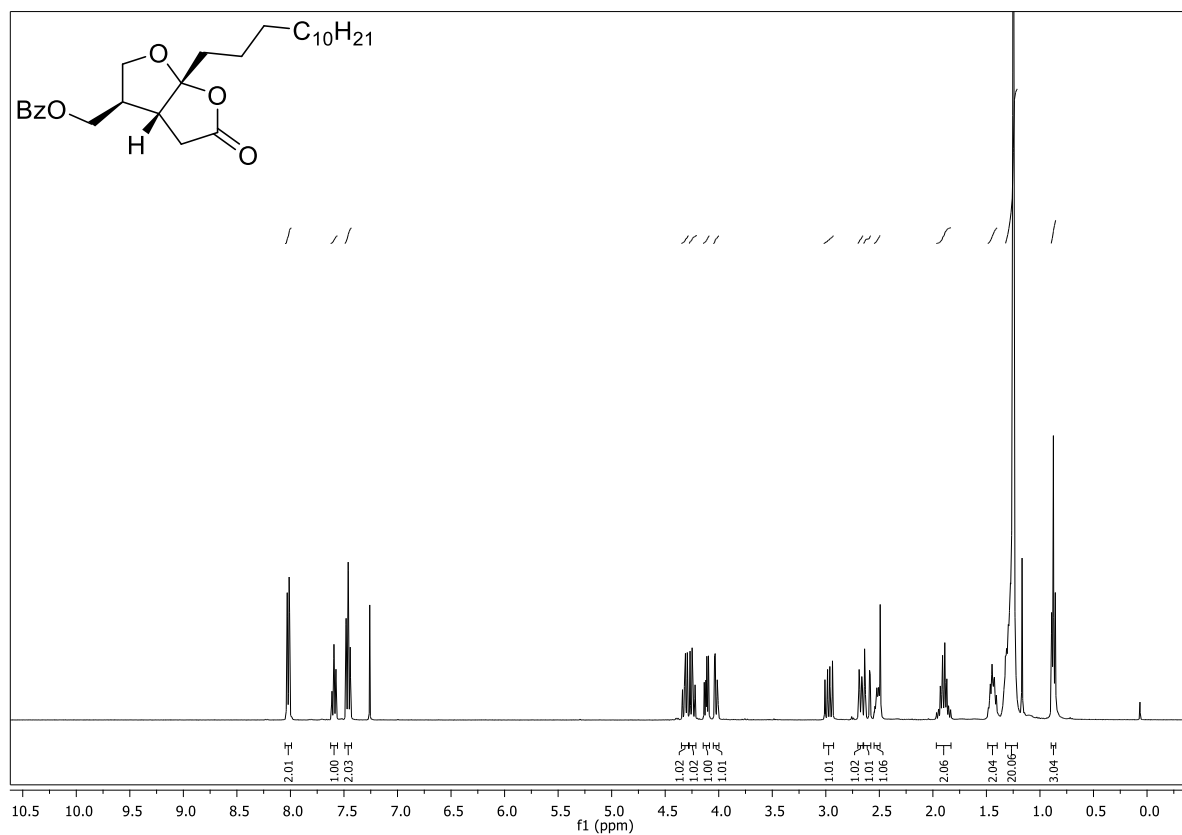
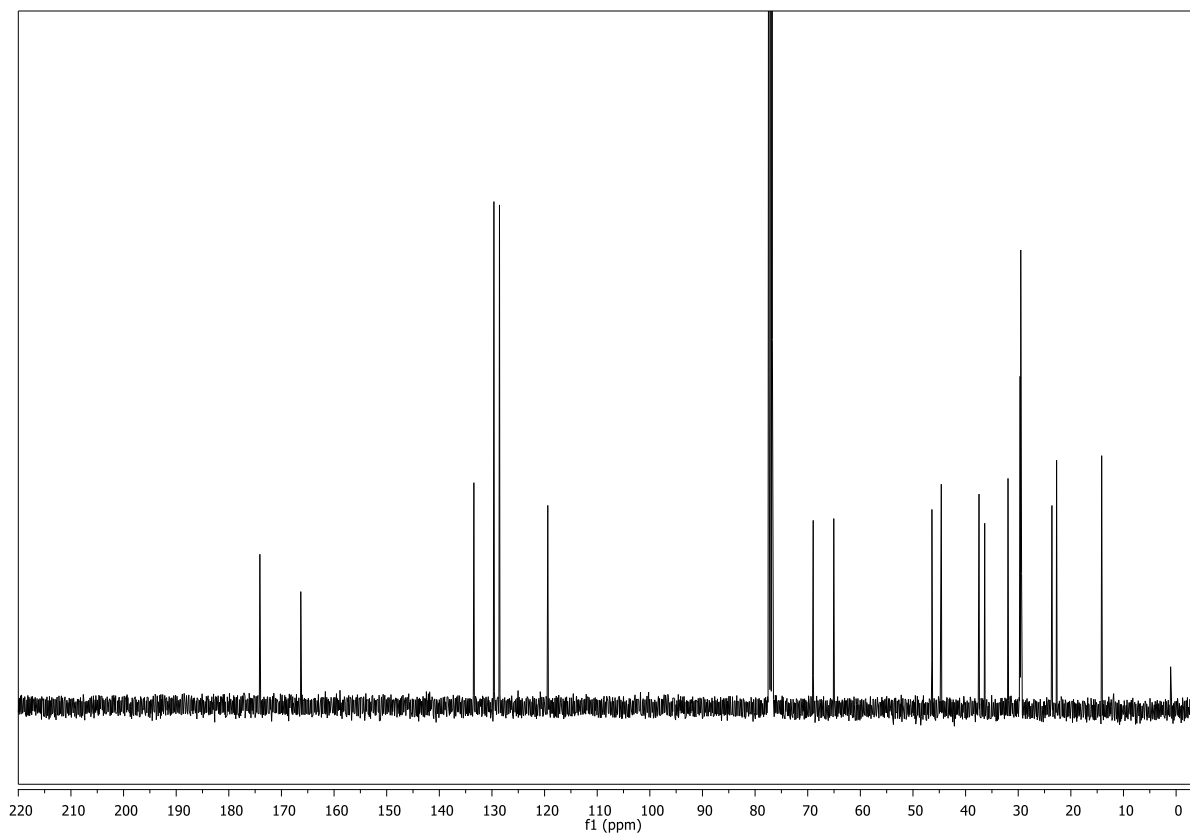
**((3*R*,3*aR*,6*aR*)-5-Oxo-6a-(tridec-2-en-1-yl)hexahydrofuro[2,3-*b*]furan-3-yl)methyl benzoate  
(183) (CDCl<sub>3</sub>, 400 MHz)**



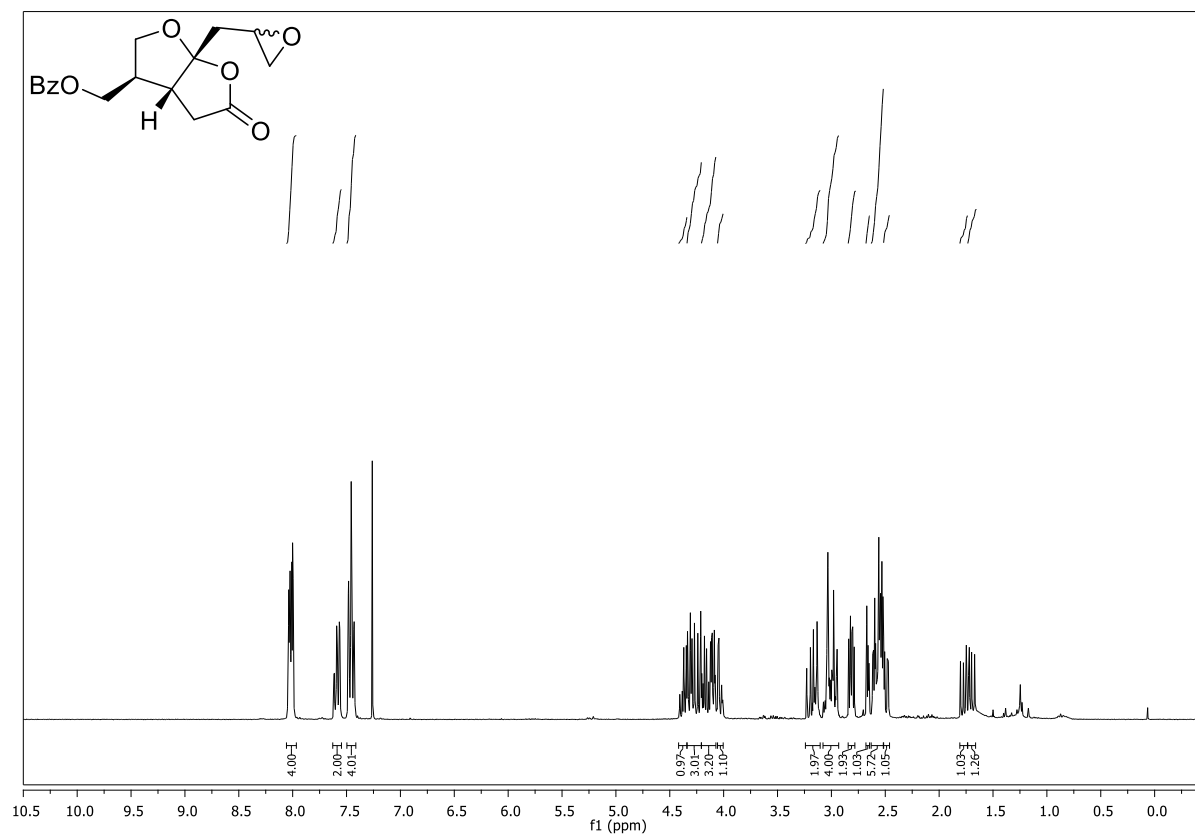
**(CDCl<sub>3</sub>, 101 MHz)**



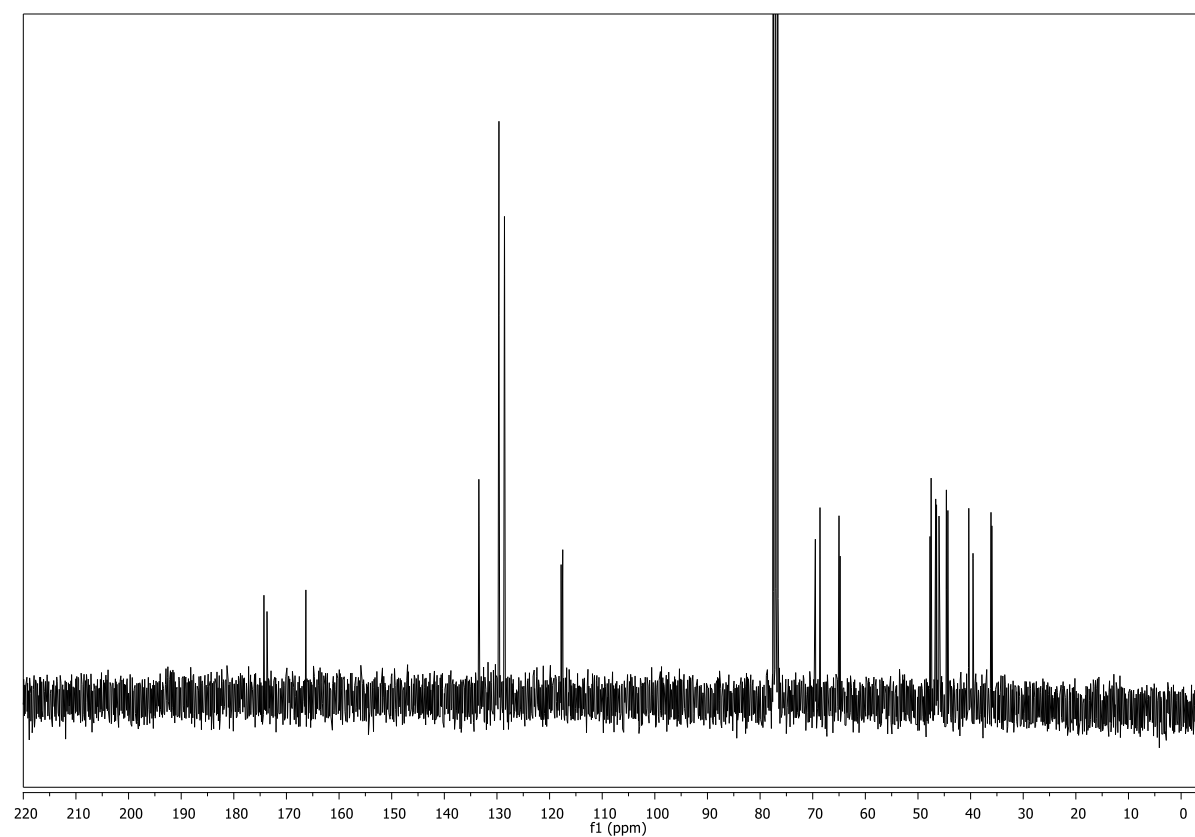


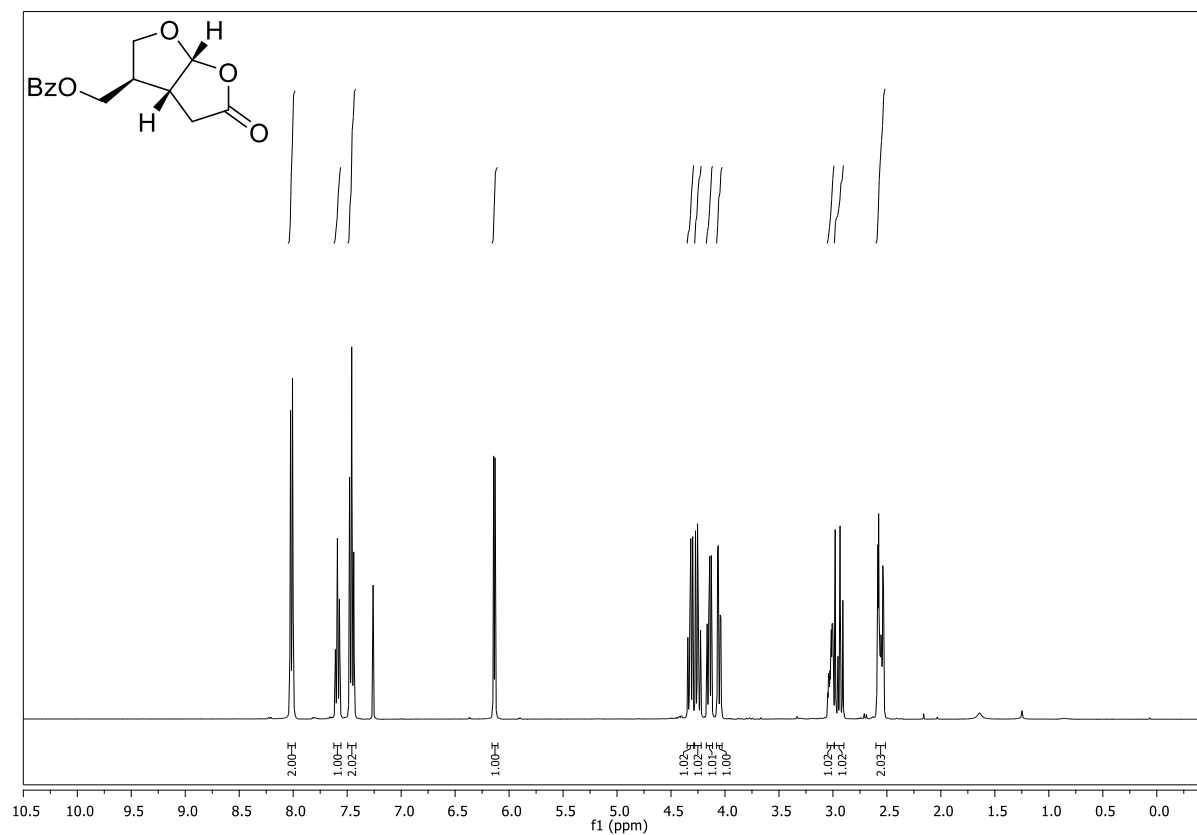
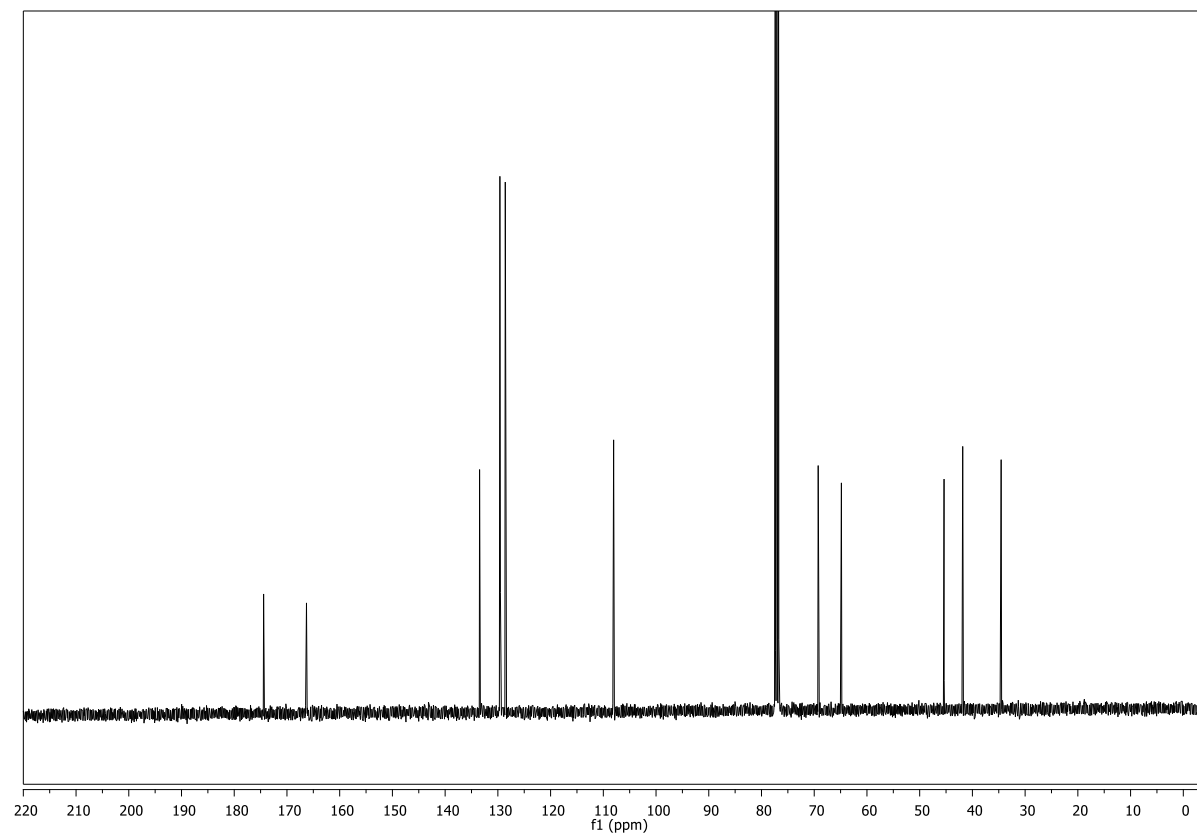
**((3*R*,3*aR*,6*aR*)-5-Oxo-6*a*-tridecylhexahydrofuro[2,3-*b*]furan-3-yl)methyl benzoate (184)****(CDCl<sub>3</sub>, 400 MHz)****(CDCl<sub>3</sub>, 101 MHz)**

**((3*R*,3*aR*,6*aR*)-6a-(Oxiran-2-ylmethyl)-5-oxohexahydrofuro[2,3-*b*]furan-3-yl)methyl benzoate (185) (CDCl<sub>3</sub>, 300 MHz)**

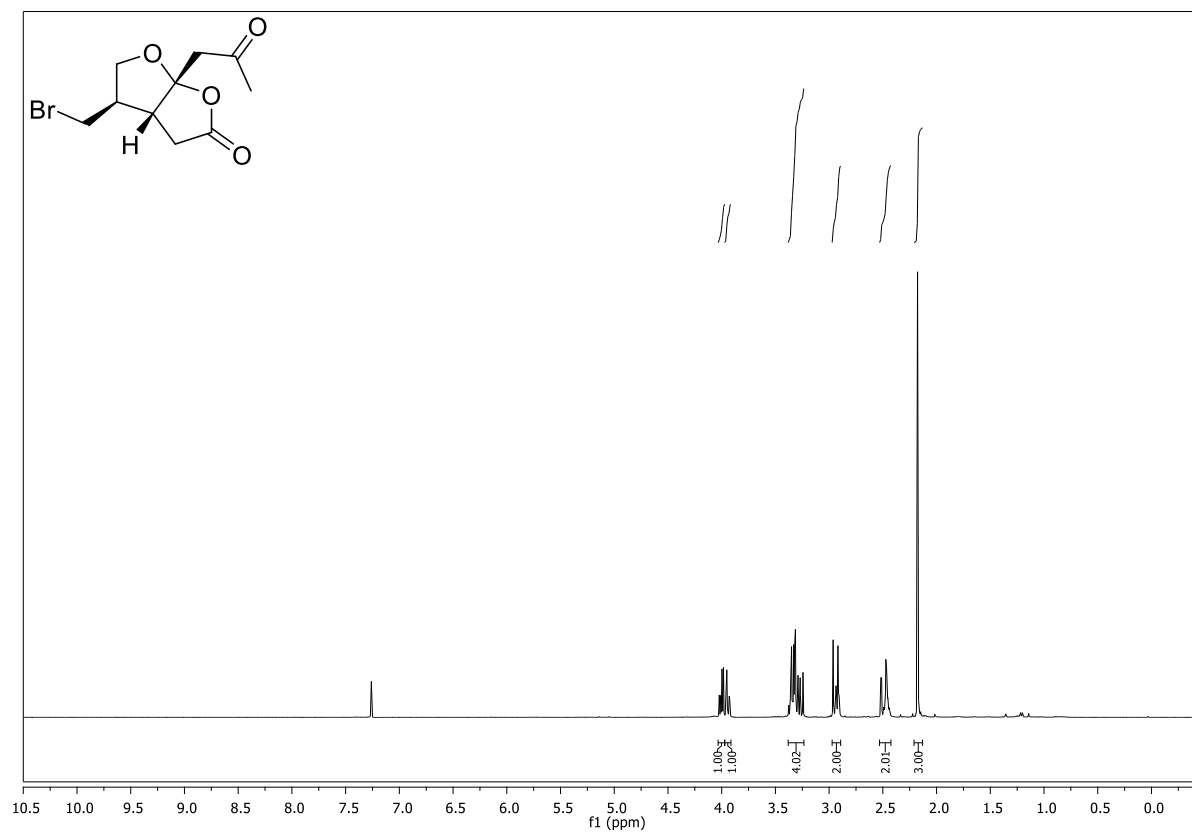


**(CDCl<sub>3</sub>, 75 MHz)**

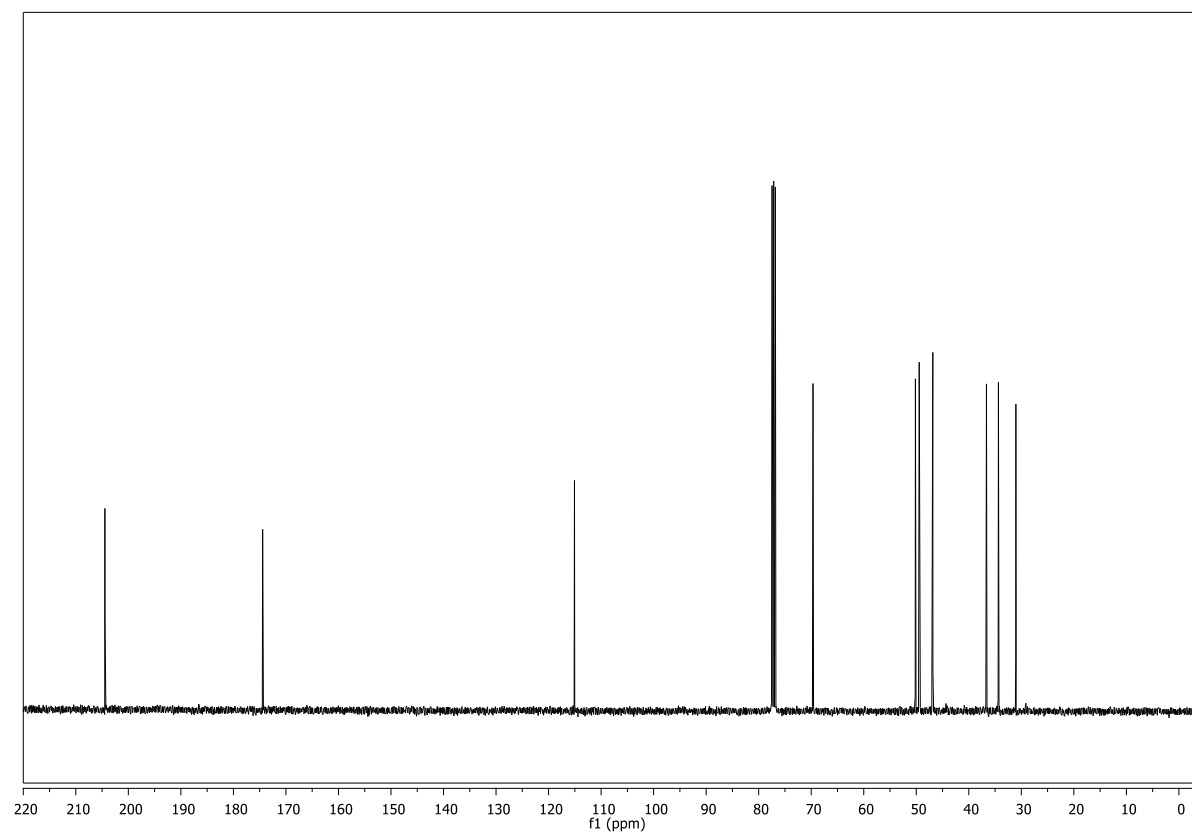


**((3*R*,3*aR*,6*aR*)-5-Oxohexahydrofuro[2,3-*b*]furan-3-yl)methyl benzoate (186)****(CDCl<sub>3</sub>, 400 MHz)****(CDCl<sub>3</sub>, 101 MHz)**

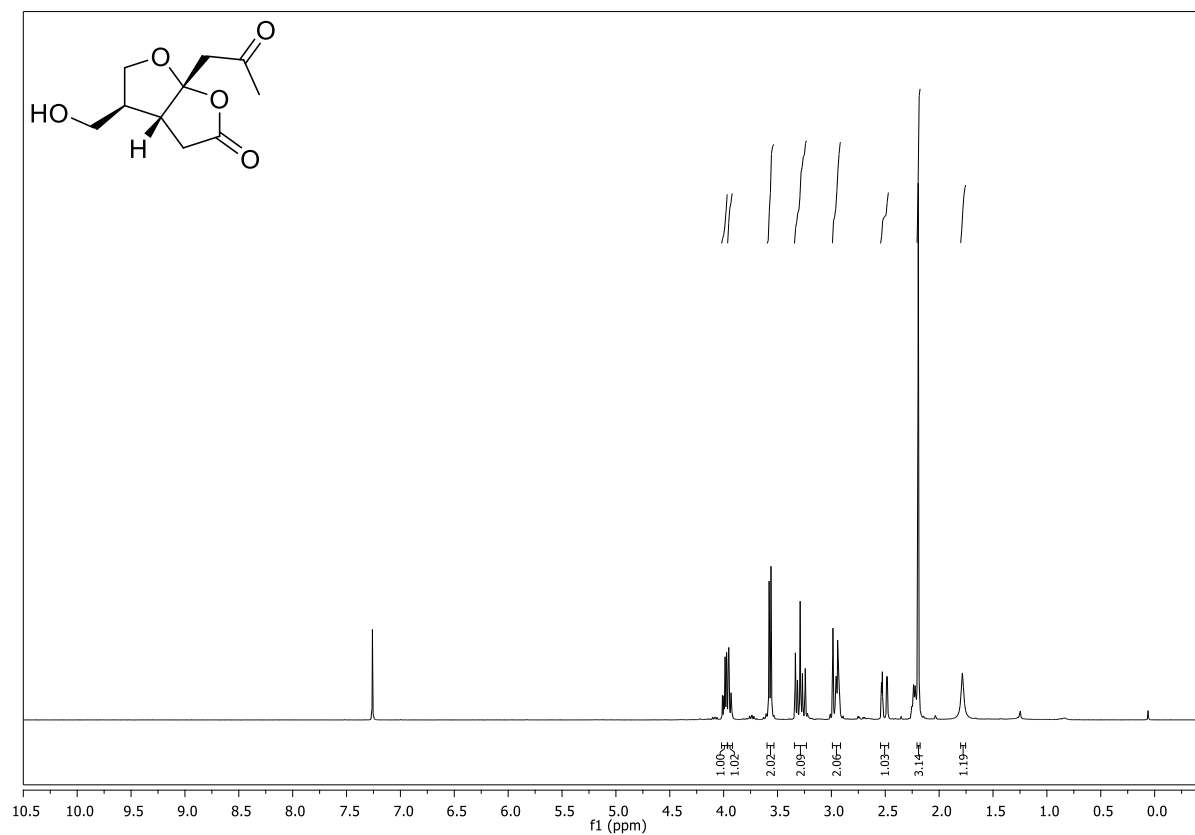
**(3aR,4R,6aR)-4-(Bromomethyl)-6a-(2-oxopropyl)tetrahydrofuro[2,3-b]furan-2(3H)-one**  
**(187) (CDCl<sub>3</sub>, 400 MHz)**



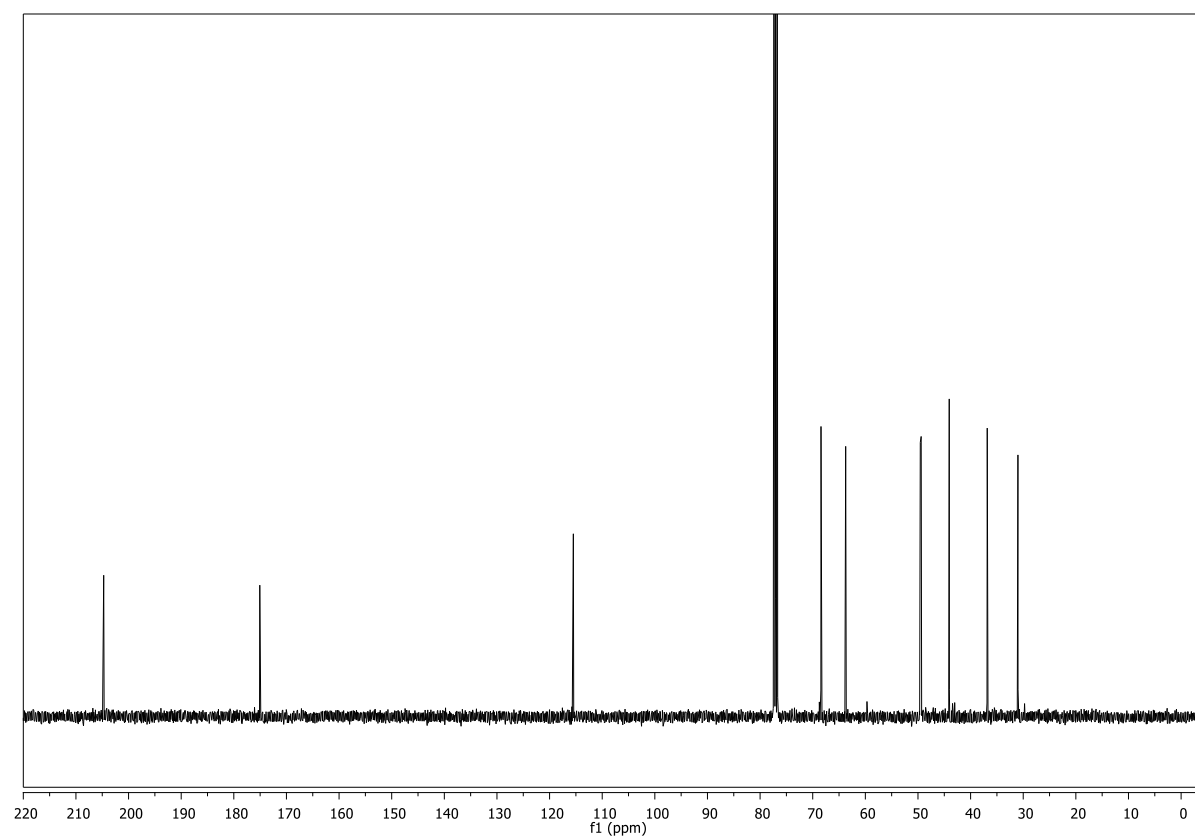
**(CDCl<sub>3</sub>, 101 MHz)**



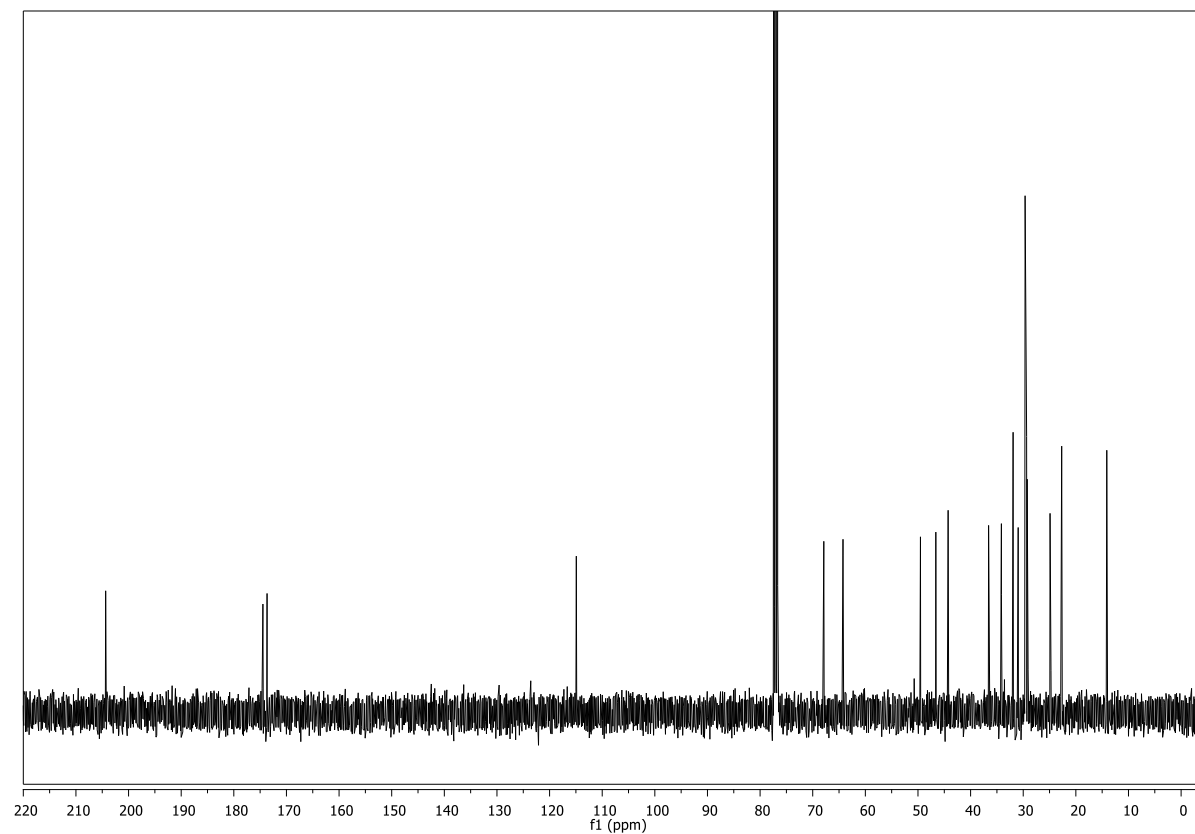
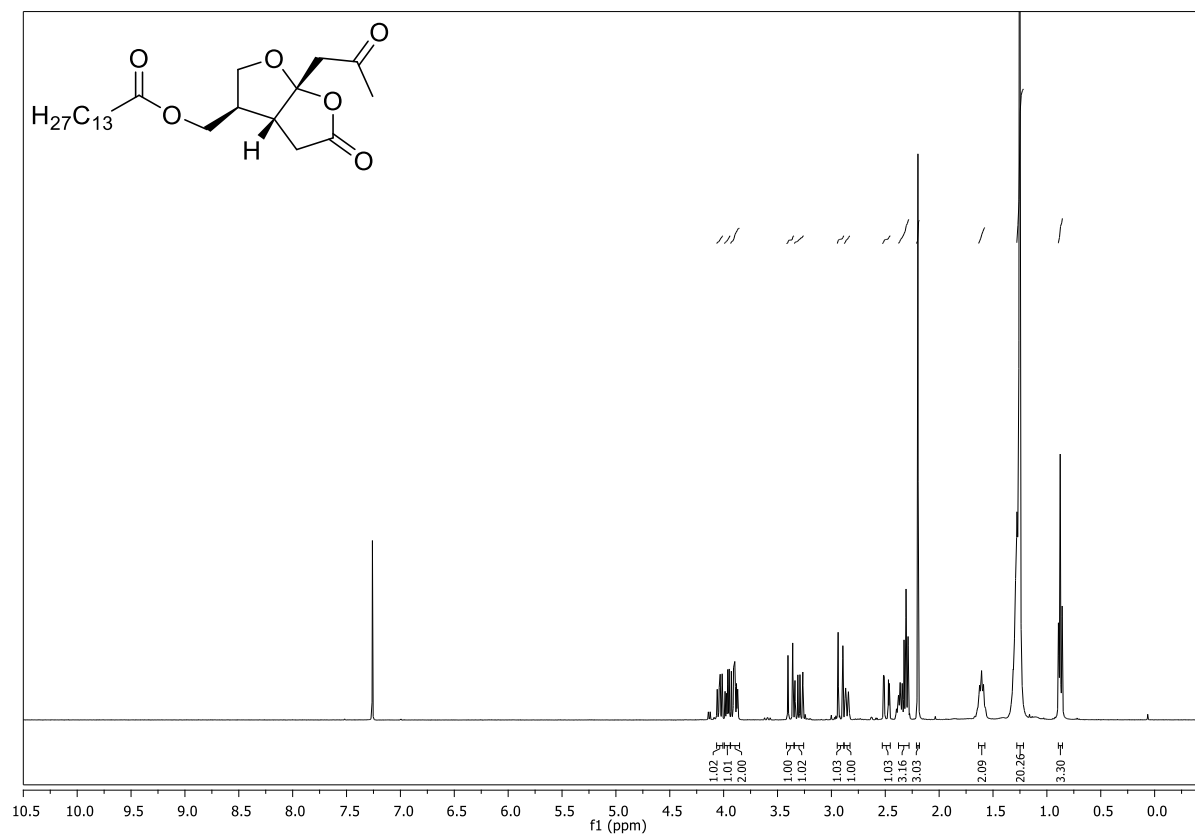
**(3*aR*,4*S*,6*aR*)-4-(Hydroxymethyl)-6*a*-(2-oxopropyl)tetrahydrofuro[2,3-*b*]furan-2(3*H*)-one**  
**(188) (CDCl<sub>3</sub>, 400 MHz)**



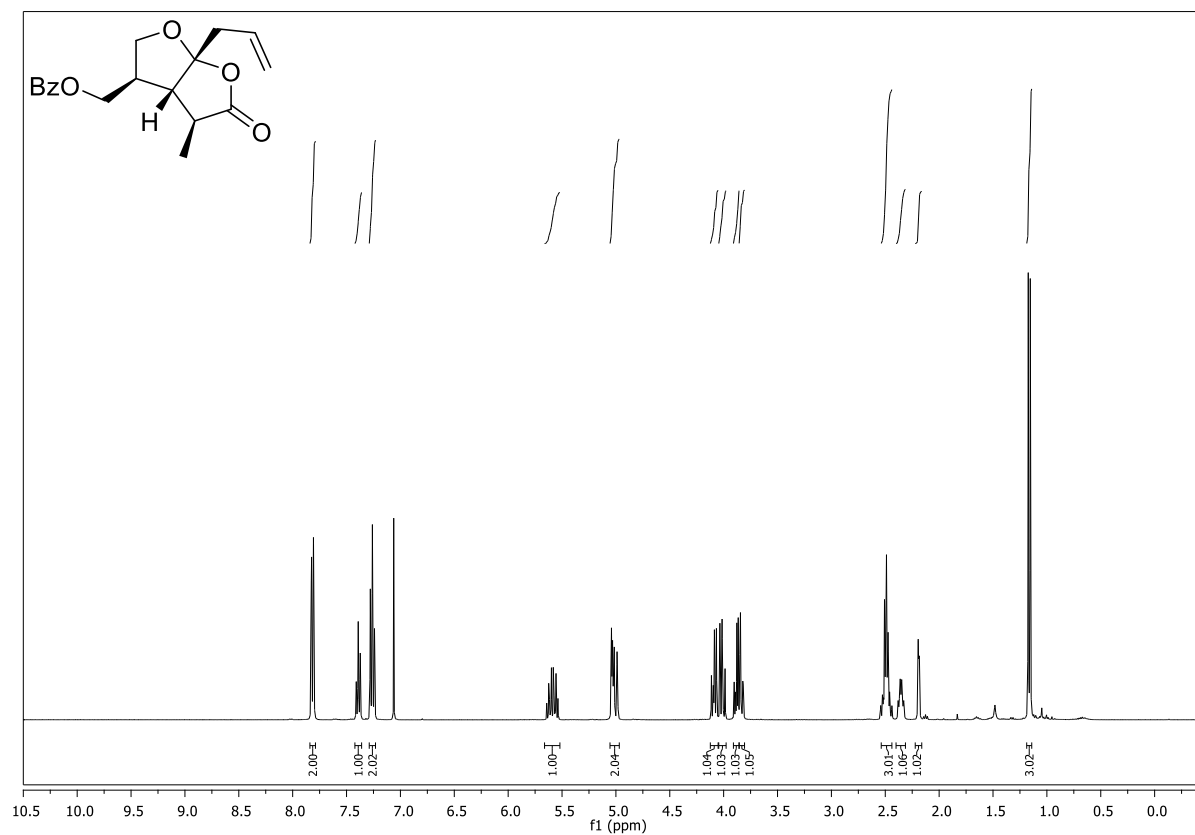
**(CDCl<sub>3</sub>, 101 MHz)**



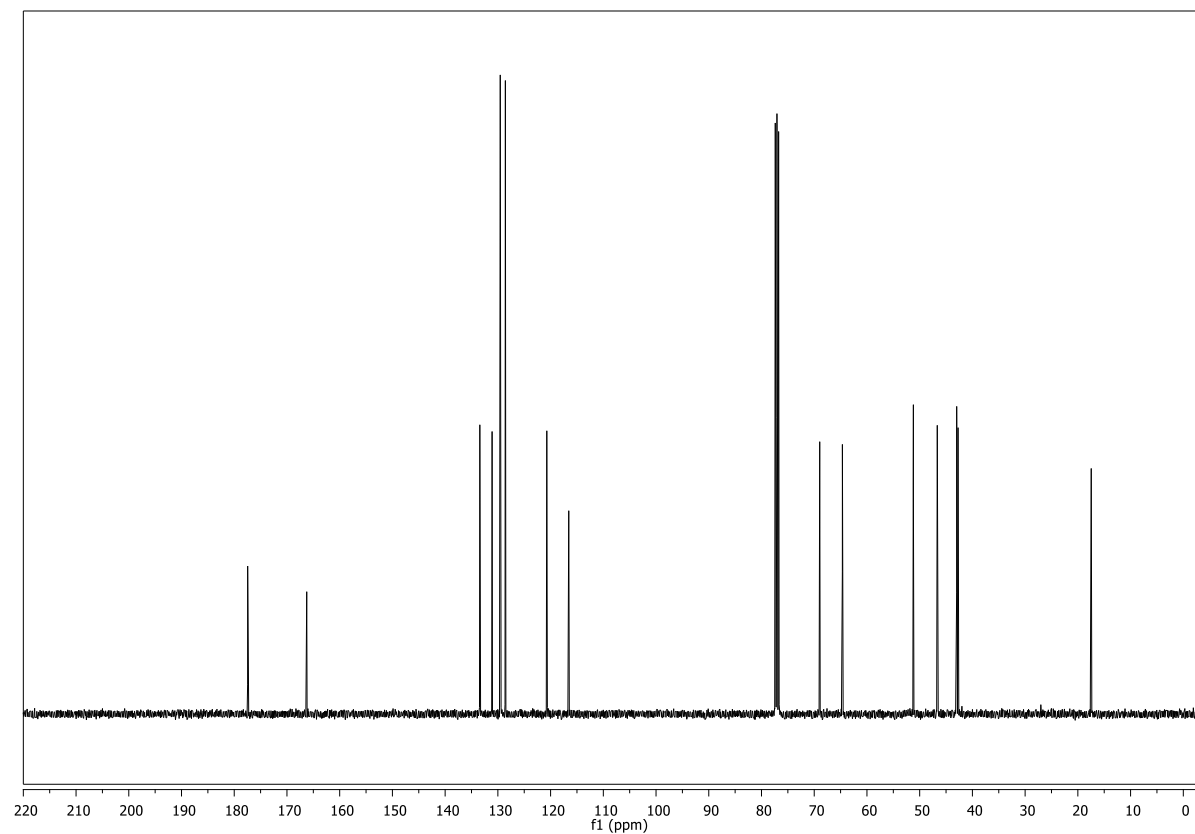
**((3*R*,3*aR*,6*aR*)-5-Oxo-6*a*-(2-oxopropyl)hexahydrofuro[2,3-*b*]furan-3-yl)methyl tetradecanoate (189) (CDCl<sub>3</sub>, 400 MHz)**



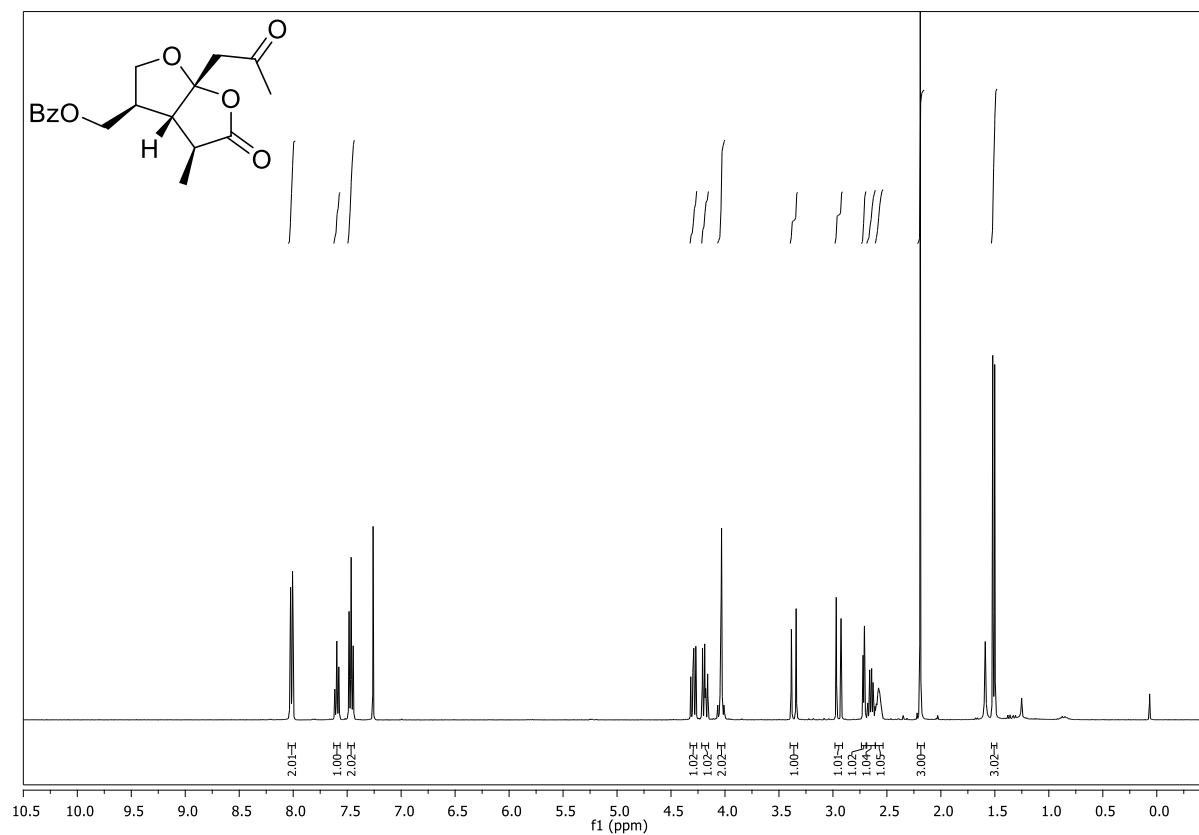
**((3*R*,3*aS*,4*S*,6*aR*)-6*a*-Allyl-4-methyl-5-oxohexahydrofuro[2,3-*b*]furan-3-yl)methyl benzoate  
(191) (CDCl<sub>3</sub>, 400 MHz)**



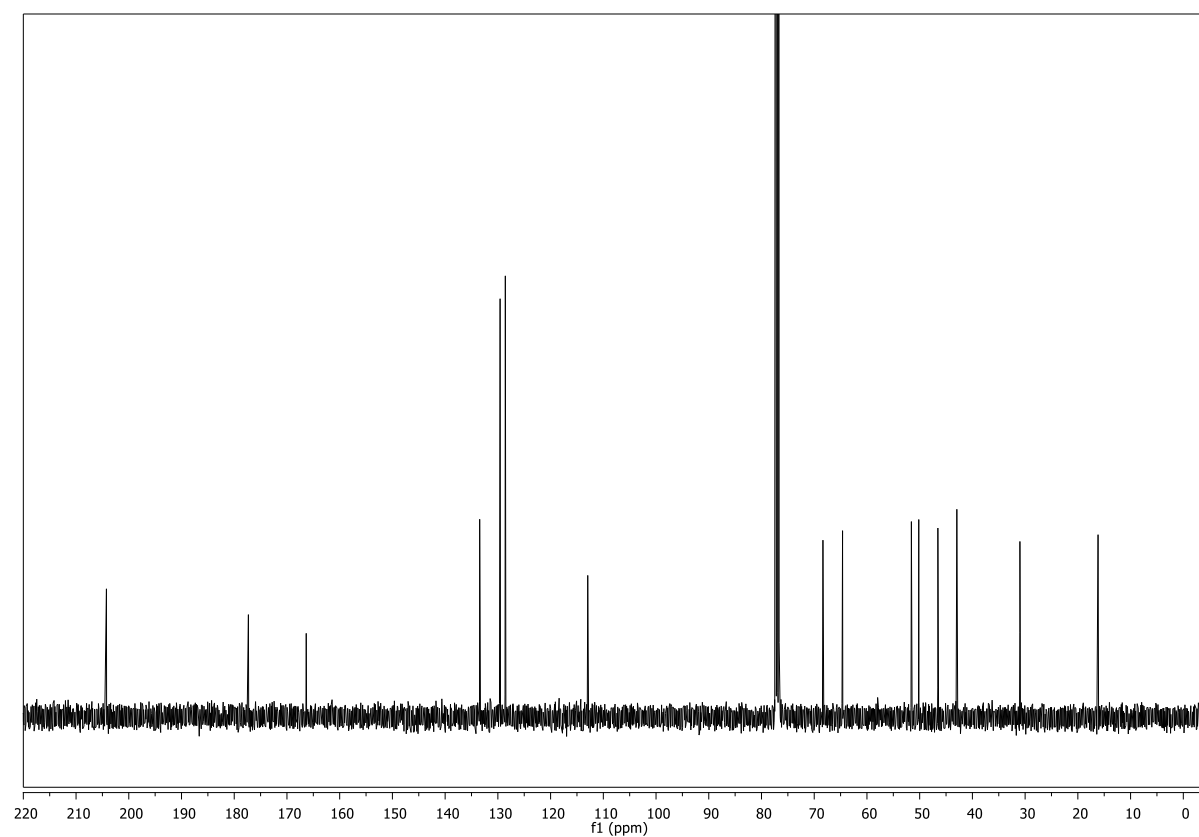
**(CDCl<sub>3</sub>, 101 MHz)**



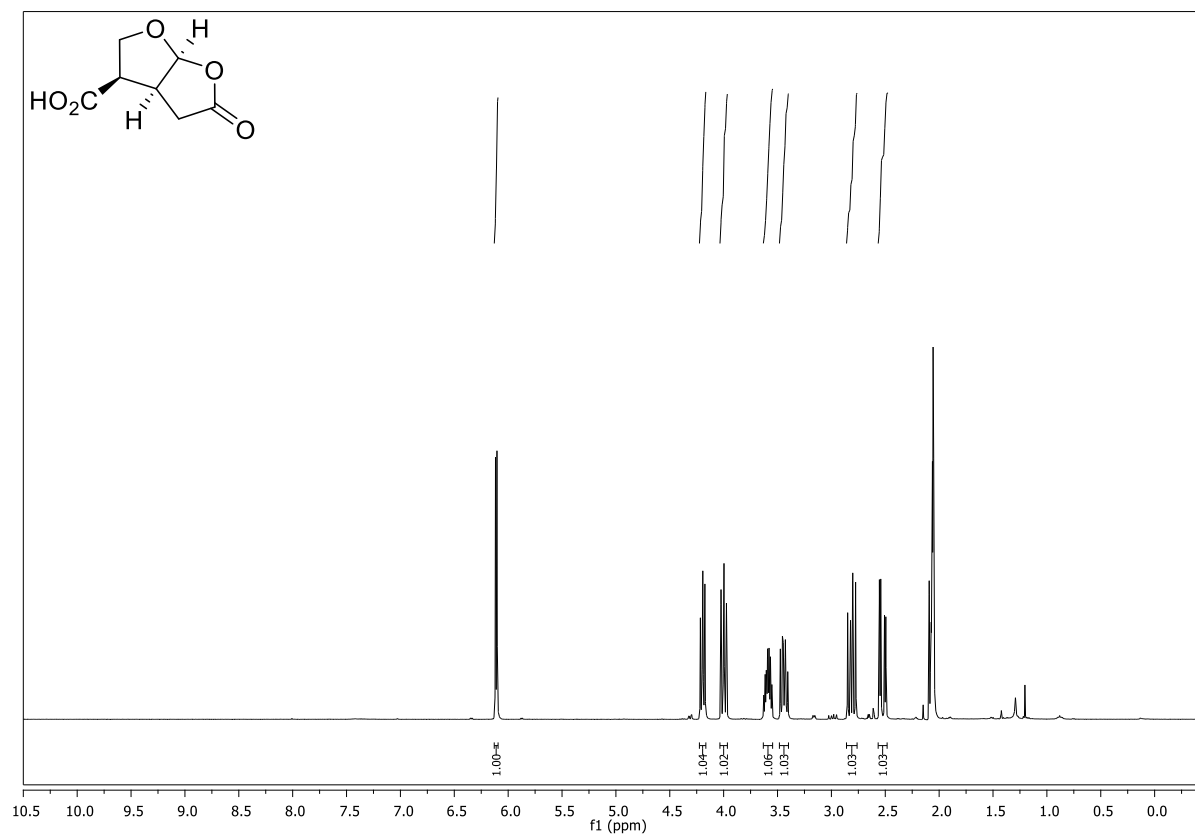
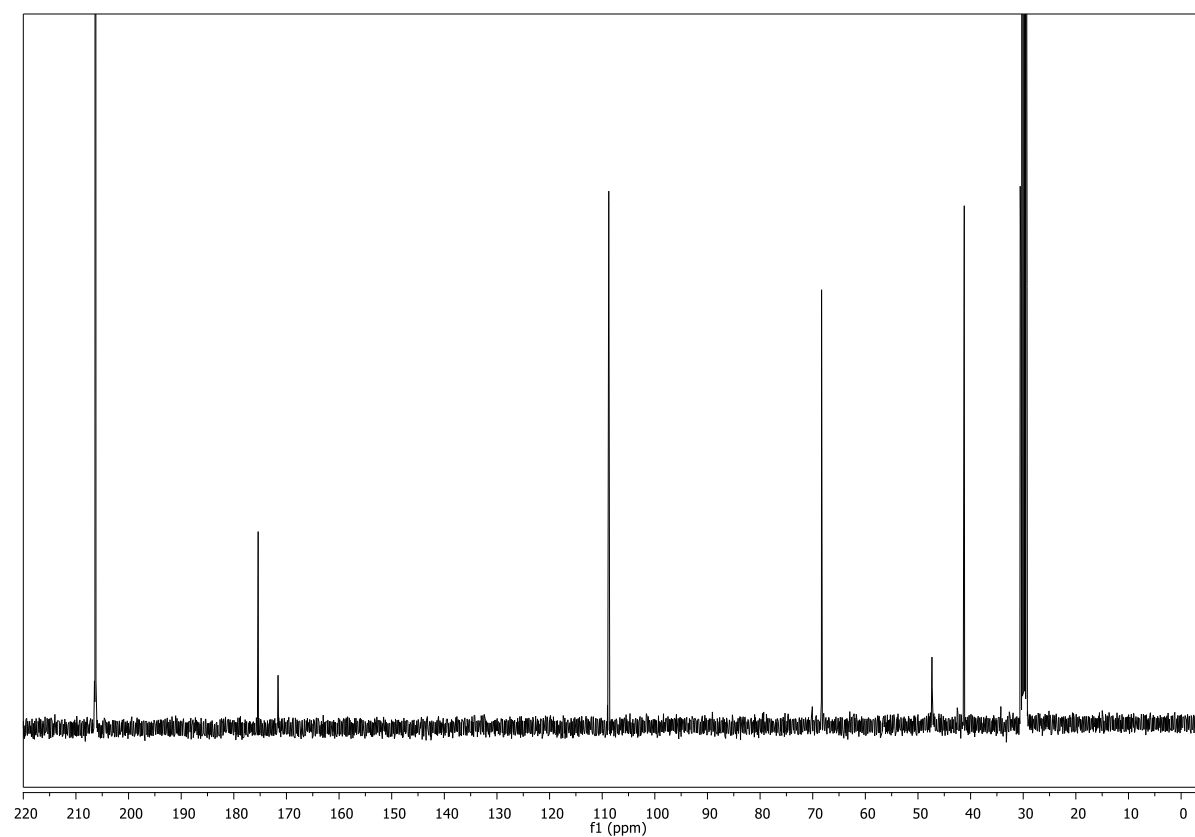
**((3*R*,3*aS*,4*S*,6*aR*)-4-Methyl-5-oxo-6a-(2-oxopropyl)hexahydrofuro[2,3-*b*]furan-3-yl)methyl benzoate (192) (CDCl<sub>3</sub>, 400 MHz)**

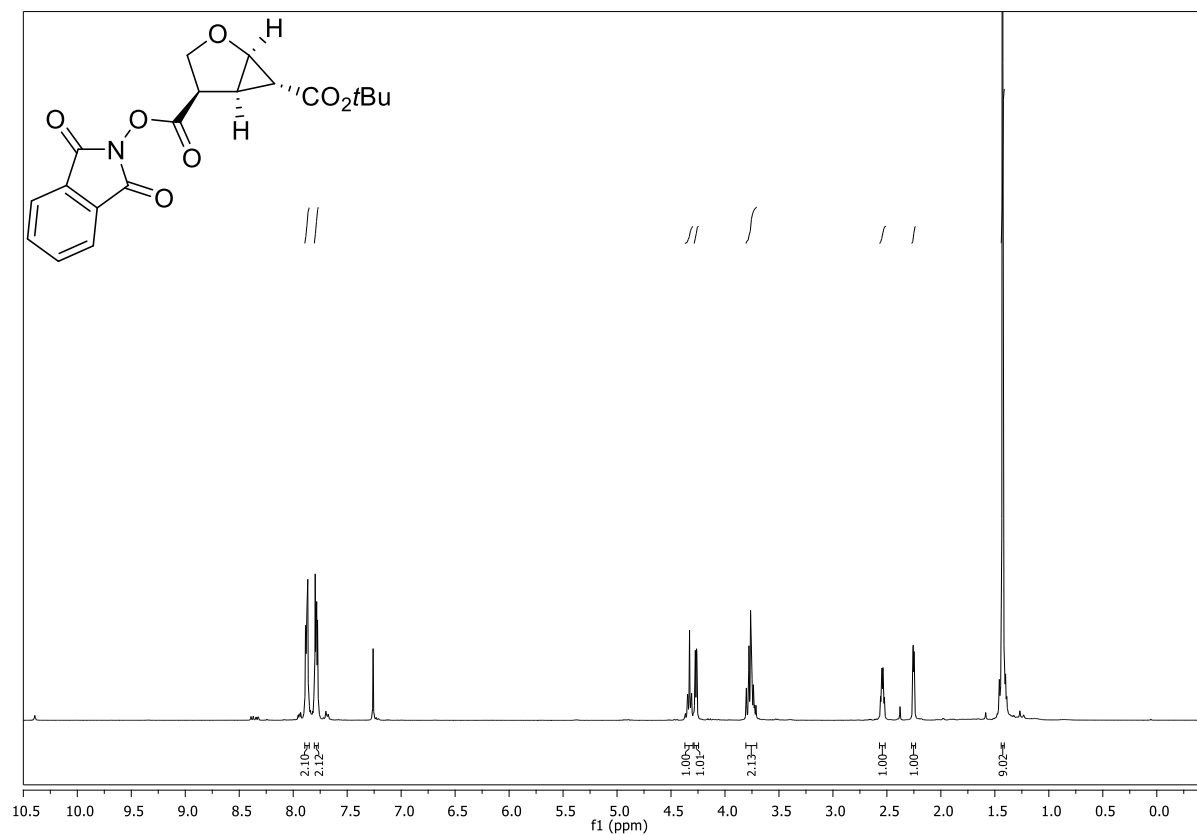
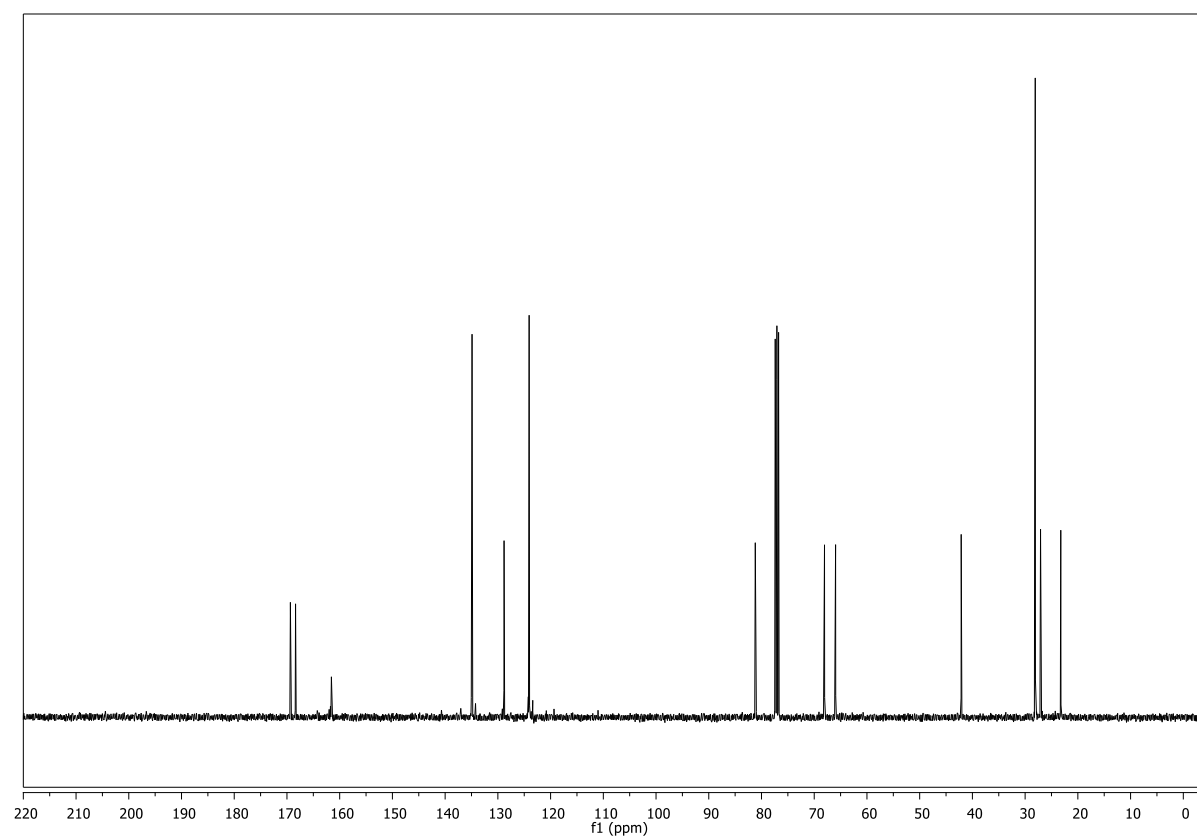


**(CDCl<sub>3</sub>, 101 MHz)**

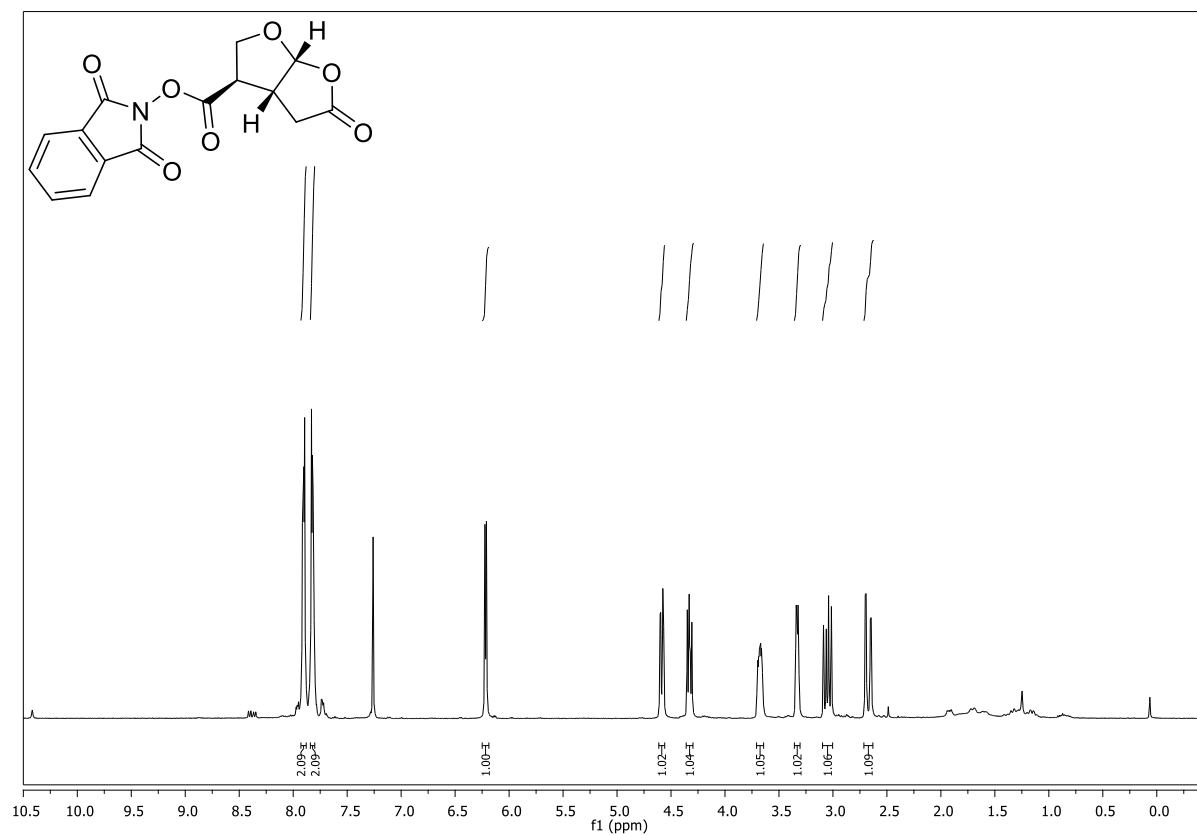




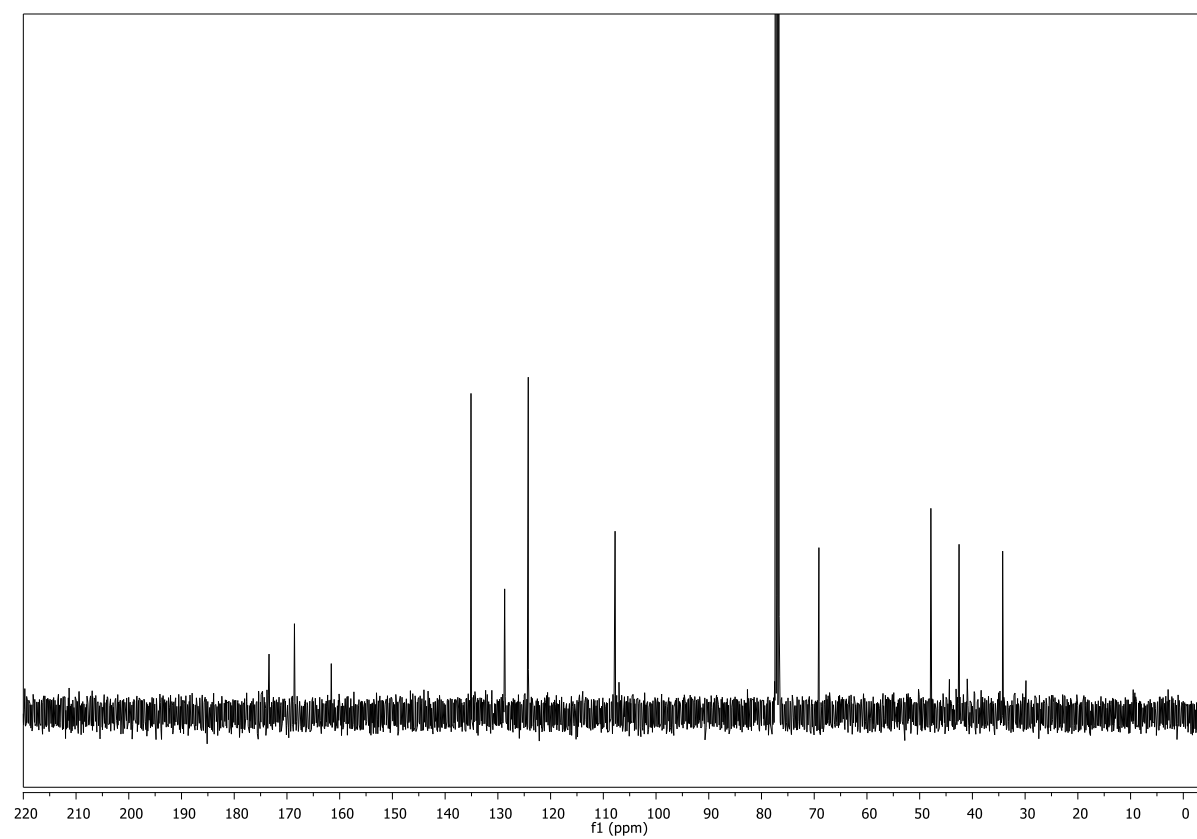
**(3*R*,3*aS*,6*aS*)-5-Oxohexahydrofuro[2,3-*b*]furan-3-carboxylic acid (238)****(Acetone, 400 MHz)****(Acetone, 101 MHz)**

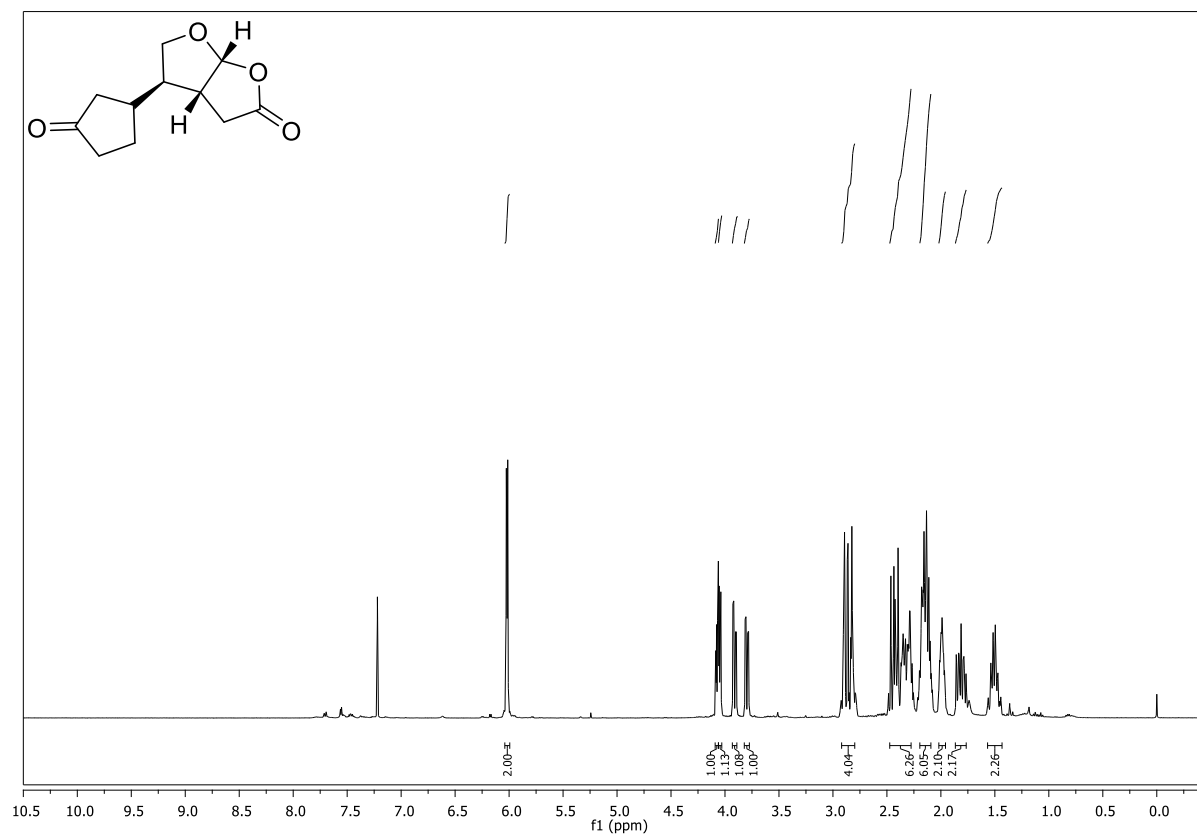
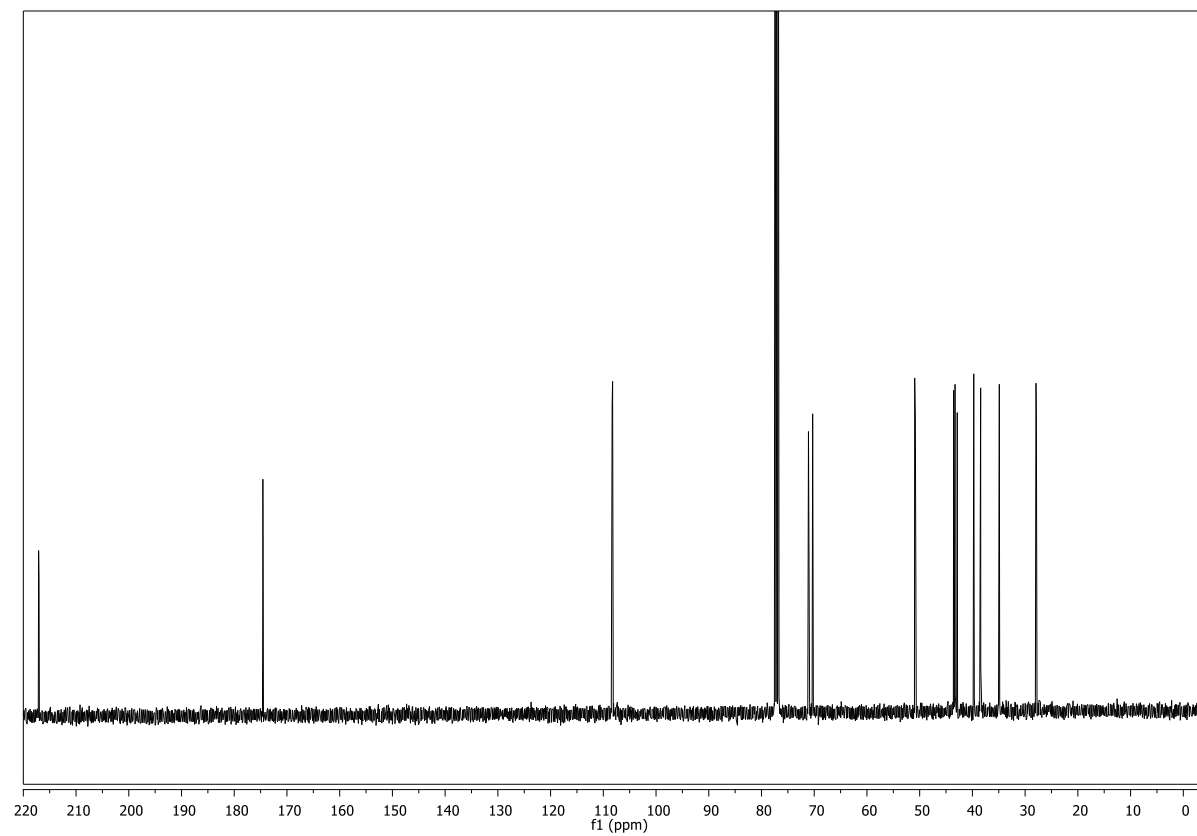
**6-(tert-Butyl) 4-(1,3-dioxoisindolin-2-yl) (1R,4R,5R,6R)-2-oxabicyclo[3.1.0]hexane-4,6-dicarboxylate (239) (CDCl<sub>3</sub>, 400 MHz)****(CDCl<sub>3</sub>, 101 MHz)**

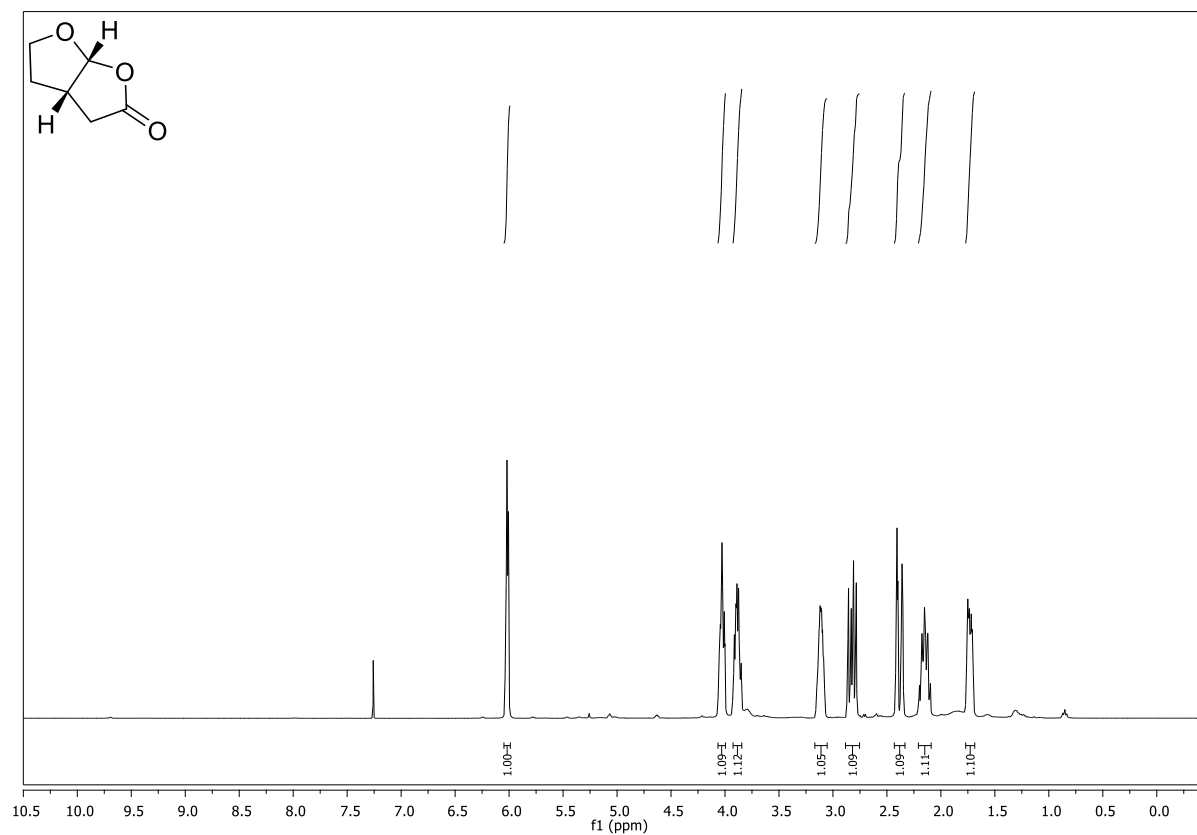
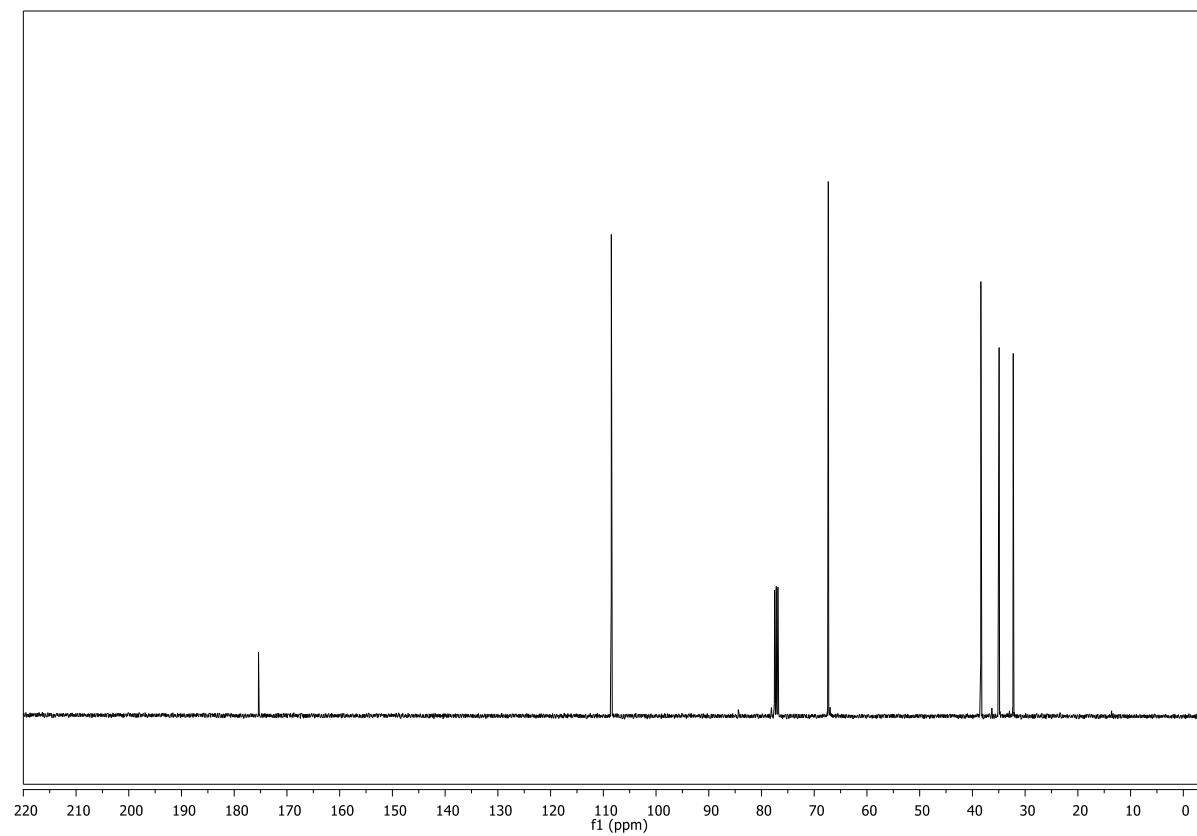
**1,3-Dioxoisindolin-2-yl (3*R*,3*aR*,6*aR*)-5-oxohexahydrofuro[2,3-*b*]furan-3-carboxylate (240)**  
(CDCl<sub>3</sub>, 400 MHz)

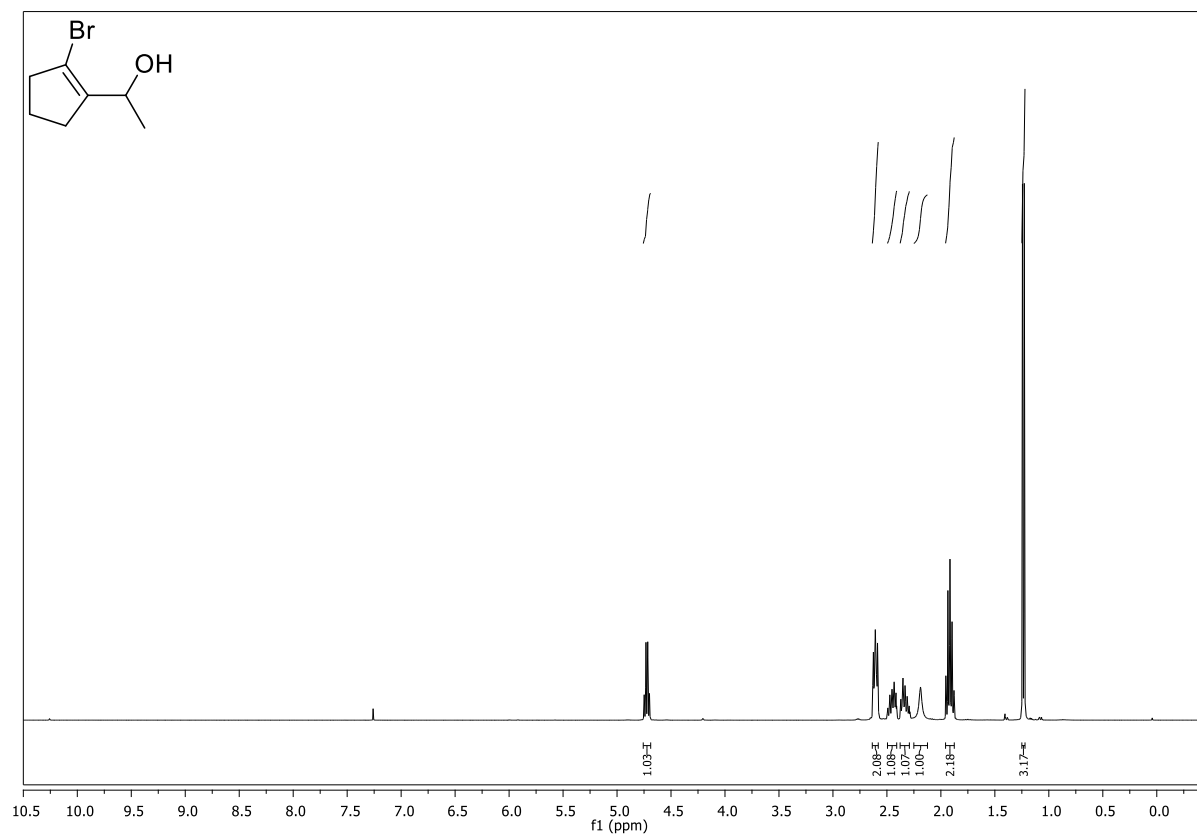
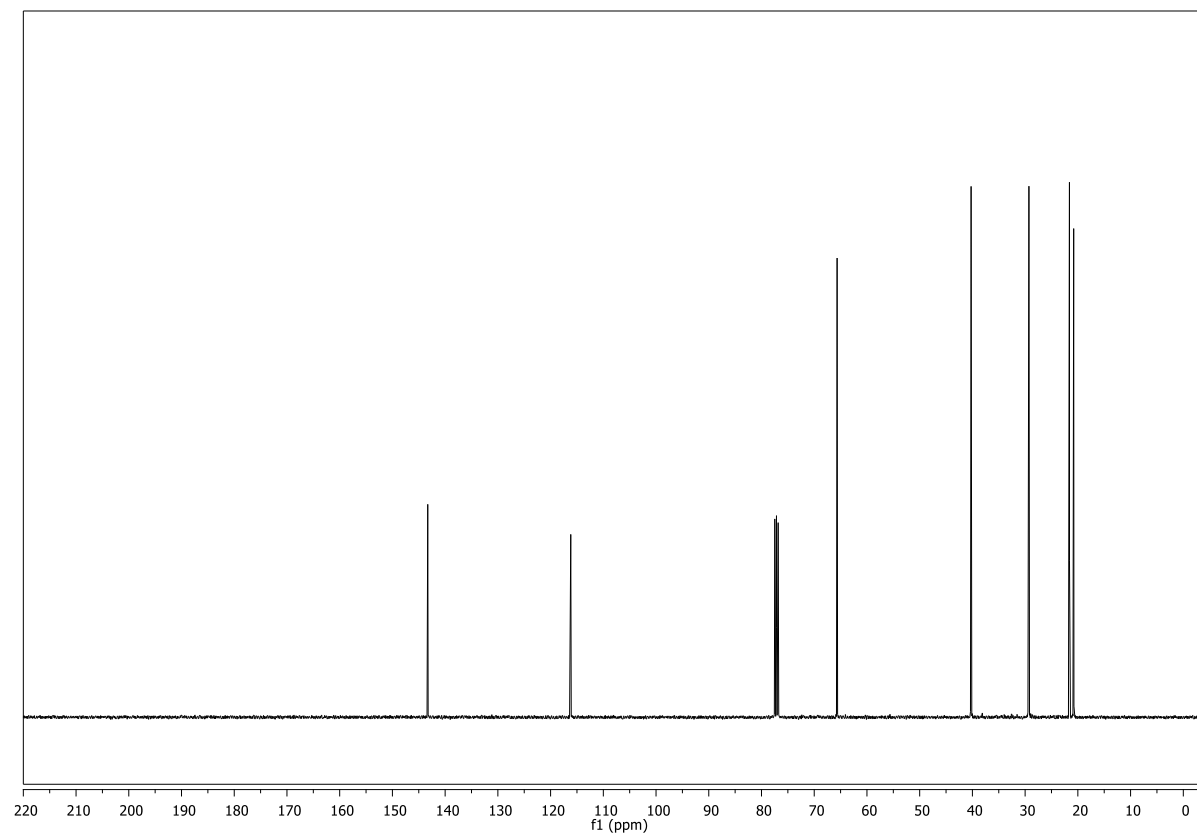


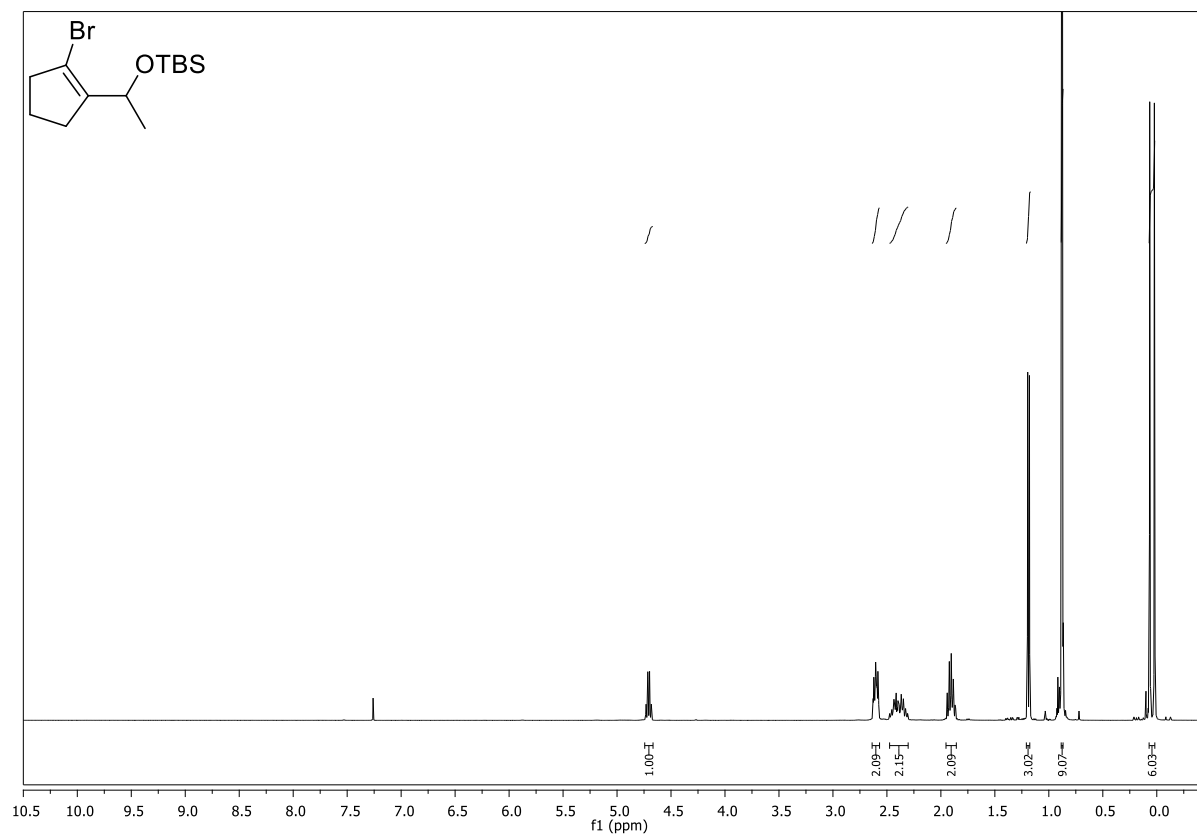
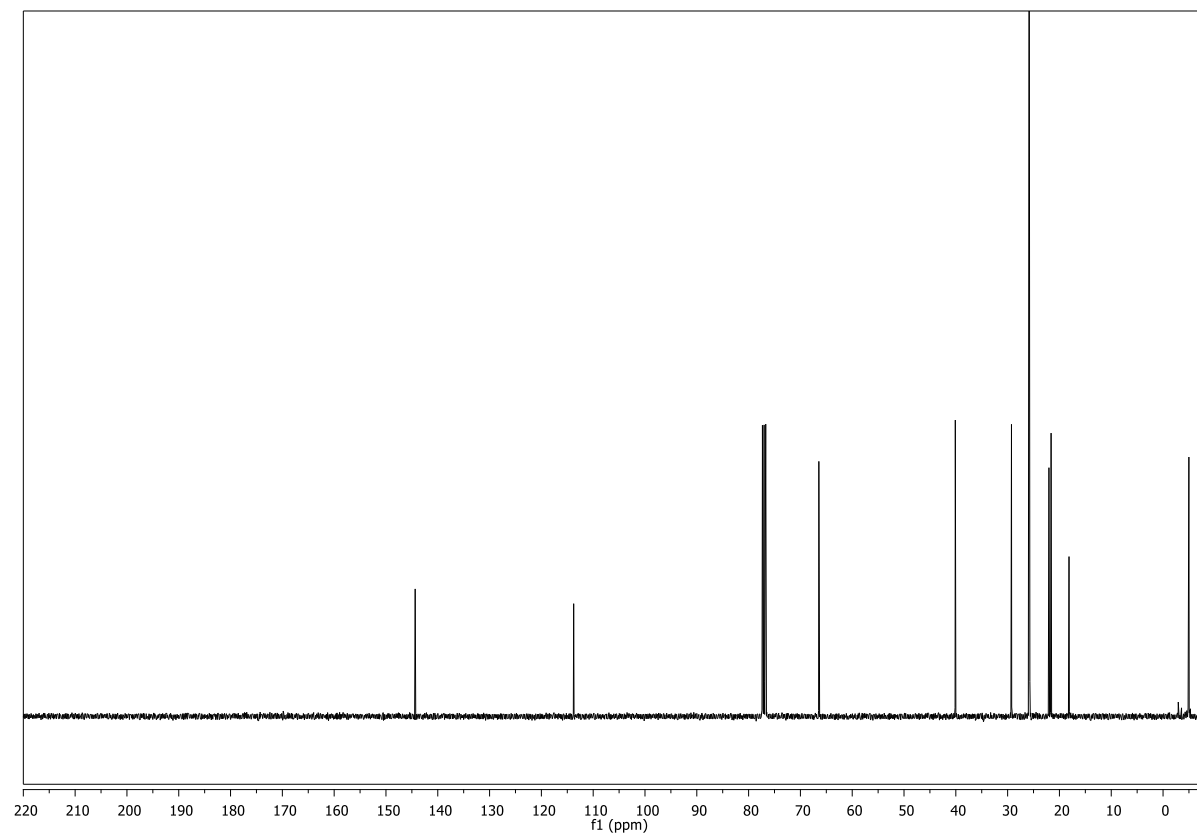
(CDCl<sub>3</sub>, 101 MHz)

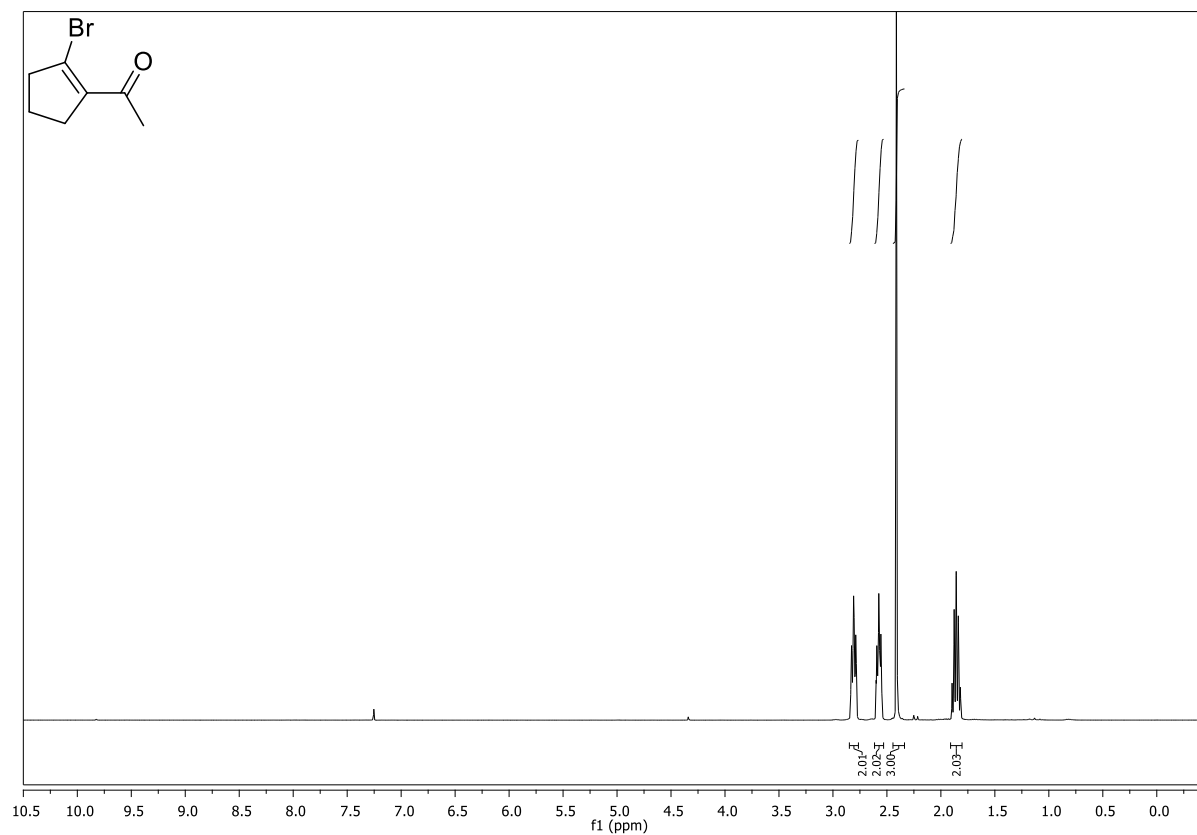
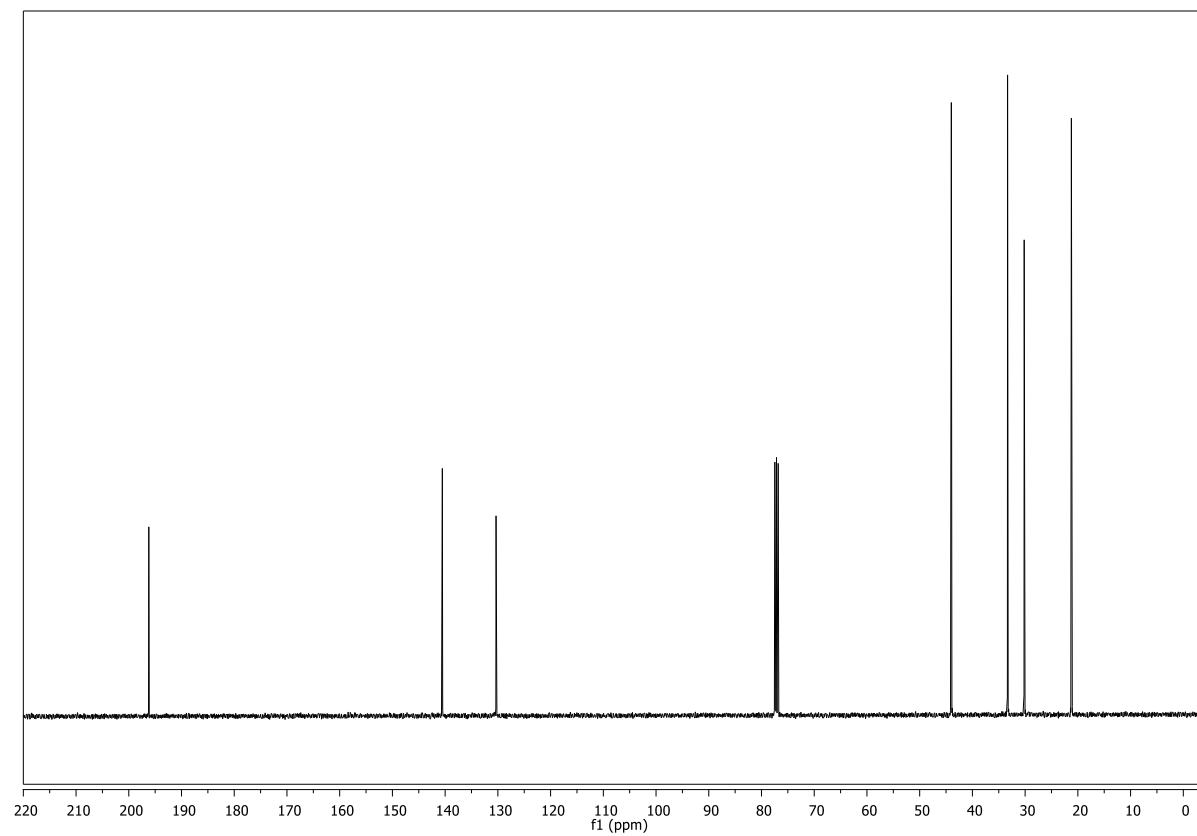


**(3aR,4R,6aR)-4-((R)-3-oxocyclopentyl)tetrahydrofuro[2,3-b]furan-2(3H)-one (242)****(CDCl<sub>3</sub>, 400 MHz)****(CDCl<sub>3</sub>, 101 MHz)**

**(3*aS*,6*aR*)-tetrahydrofuro[2,3-*b*]furan-2(3*H*)-one (243)****(CDCl<sub>3</sub>, 400 MHz)****(CDCl<sub>3</sub>, 101 MHz)**

**1-(2-Bromocyclopent-1-en-1-yl)ethan-1-ol (256)****(CDCl<sub>3</sub>, 400 MHz)****(CDCl<sub>3</sub>, 101 MHz)**

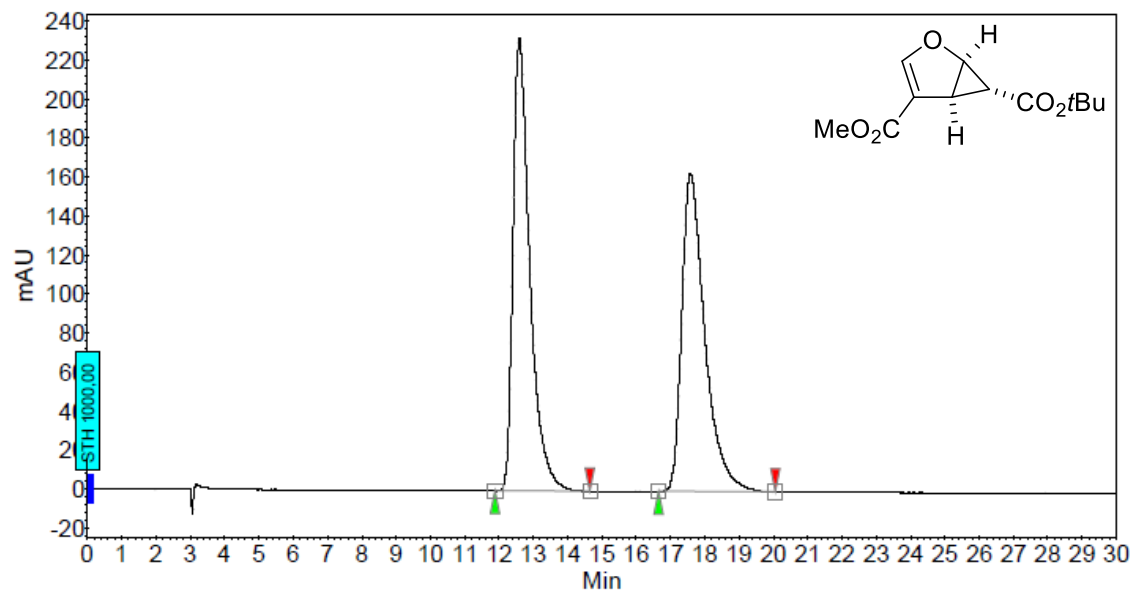
**(1-(2-Bromocyclopent-1-en-1-yl)ethoxy)(tert-butyl)dimethylsilane (257)****(CDCl<sub>3</sub>, 400 MHz)****(CDCl<sub>3</sub>, 101 MHz)**

**1-(2-Bromocyclopent-1-en-1-yl)ethan-1-one (260)****(CDCl<sub>3</sub>, 400 MHz)****(CDCl<sub>3</sub>, 101 MHz)**



## 2. HPLC Chromatograms

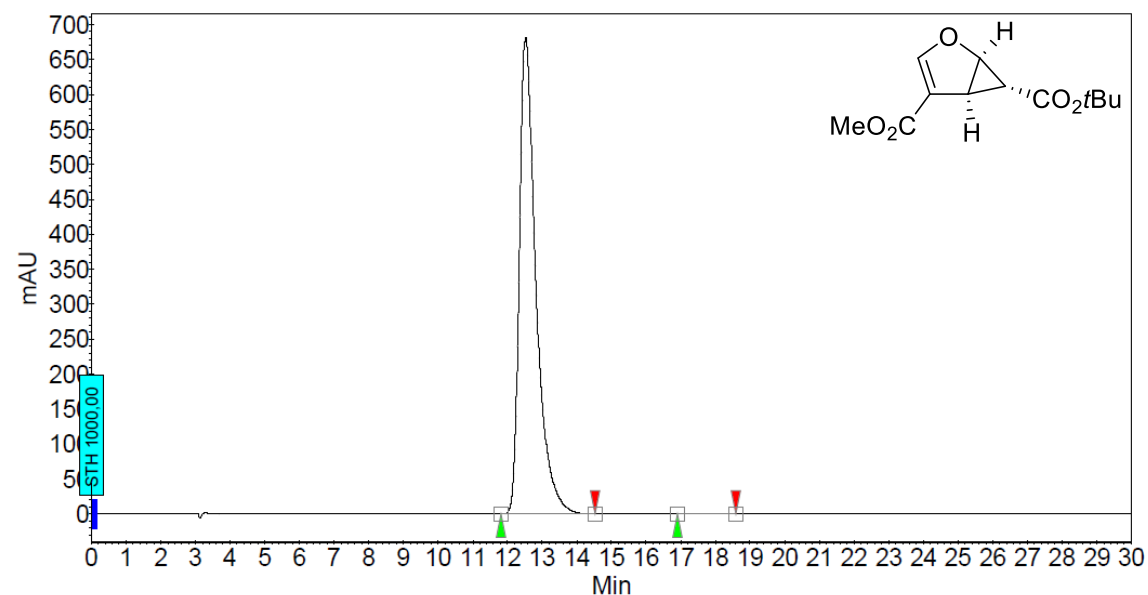
### 6-(*tert*-butyl) 4-methyl-2-oxabicyclo[3.1.0]hex-3-ene-4,6-dicarboxylate (racemic 142)



#### Peak Results :

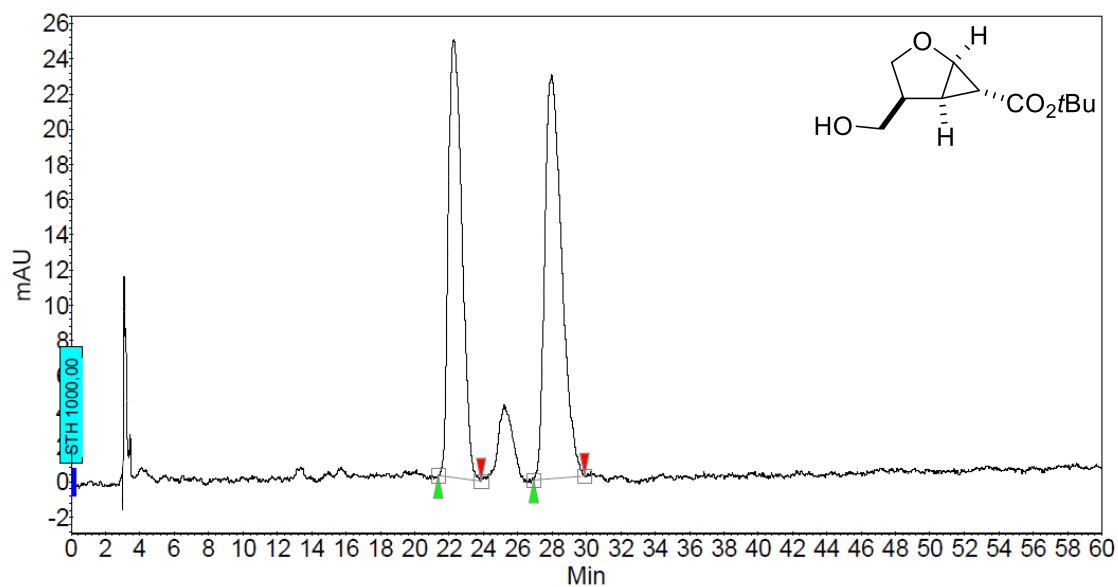
Index	Name	Time [Min]	Quantity [% Area]	Height [mAU]	Area [mAU.Min]	Area % [%]
1	UNKNOWN	12.59	50.95	232.2	132.2	50.947
2	UNKNOWN	17.59	49.05	163.1	127.3	49.053
Total			100.00	395.3	259.4	100.000

### 6-(*tert*-butyl) 4-methyl (1*R*,5*S*,6*R*)-2-oxabicyclo[3.1.0]hex-3-ene-4,6-dicarboxylate (142)

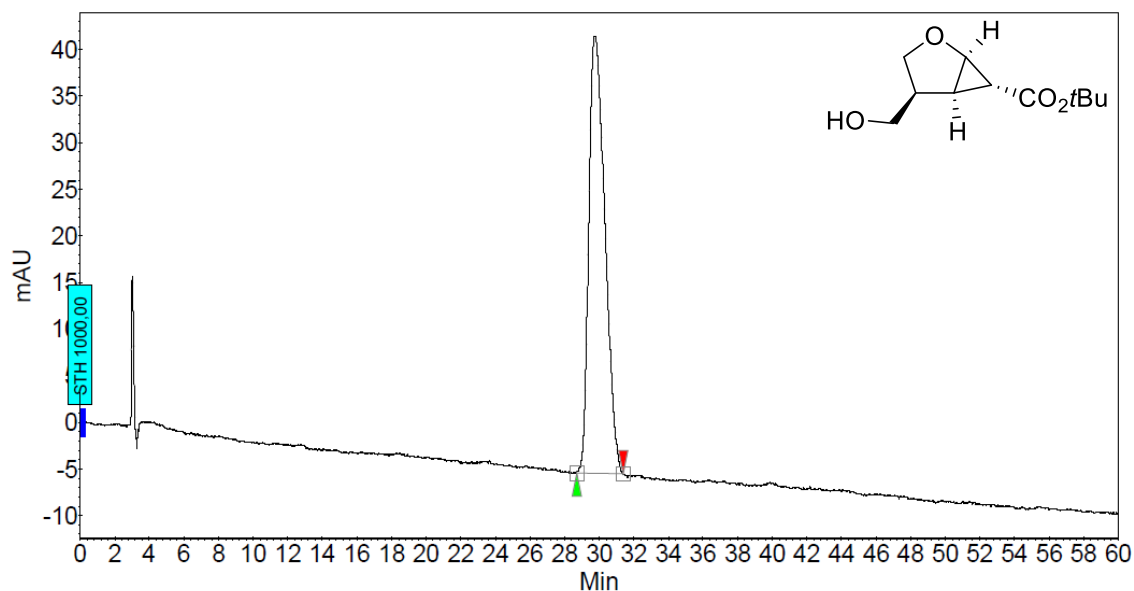


#### Peak Results :

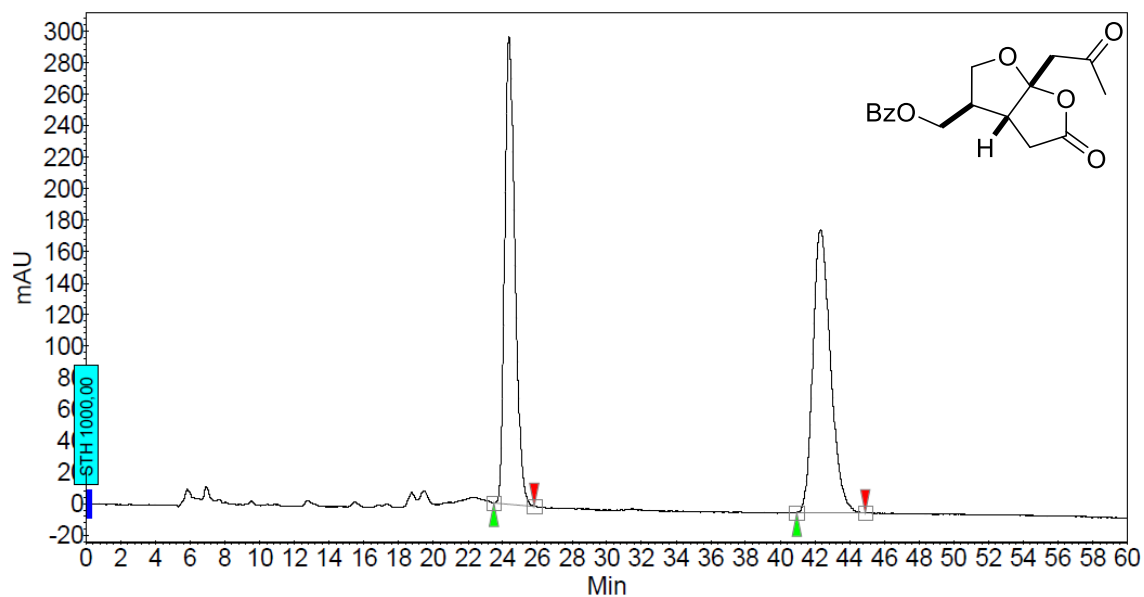
Index	Name	Time [Min]	Quantity [% Area]	Height [mAU]	Area [mAU.Min]	Area % [%]
1	UNKNOWN	12.52	99.87	681.8	378.0	99.868
2	UNKNOWN	17.54	0.13	0.7	0.5	0.132
Total			100.00	682.6	378.5	100.000

**tert-butyl-4-(hydroxymethyl)-2-oxabicyclo[3.1.0]hexane-6-carboxylate (racemic 157)**

**Peak Results :**

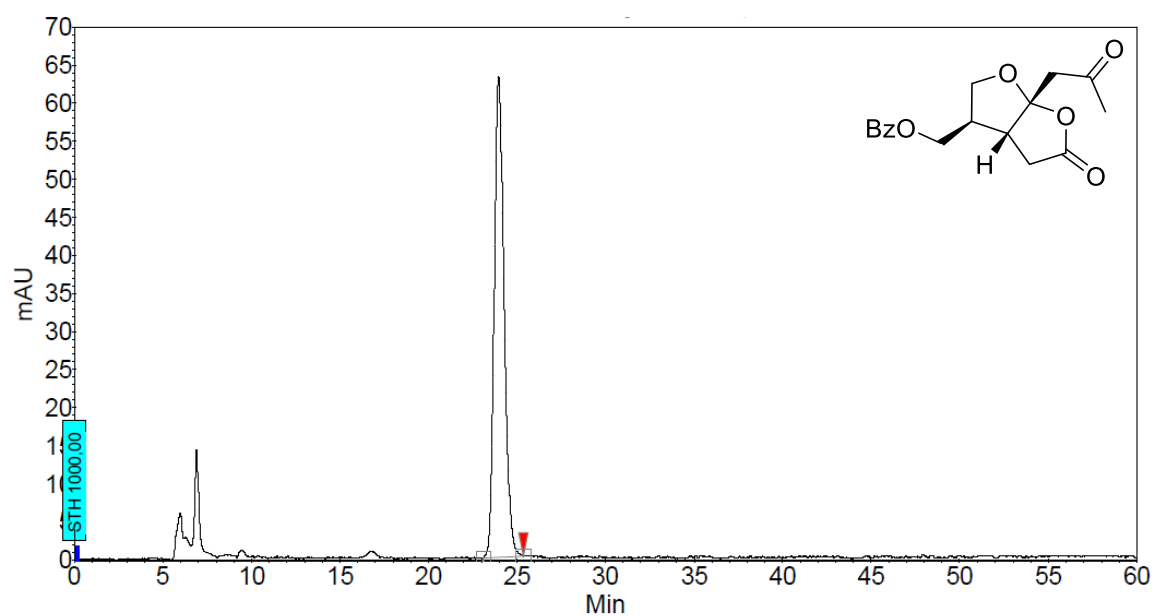
Index	Name	Time [Min]	Quantity [% Area]	Height [mAU]	Area [mAU.Min]	Area % [%]
2	UNKNOWN	22.28	46.65	24.9	22.9	46.647
1	UNKNOWN	27.95	53.35	22.9	26.2	53.353
Total			100.00	47.8	49.2	100.000

**tert-butyl (1R,4S,5R,6R)-4-(hydroxymethyl)-2-oxabicyclo[3.1.0]hexane-6-carboxylate (157)**

**Peak Results :**

Index	Name	Time [Min]	Quantity [% Area]	Height [mAU]	Area [mAU.Min]	Area % [%]
1	UNKNOWN	29.75	100.00	46.8	50.7	100.000
Total			100.00	46.8	50.7	100.000

**(5-oxo-6a-(2-oxopropyl)hexahydrofuro[2,3-b]furan-3-yl)methyl benzoate (racemic 49)****Peak Results :**

Index	Name	Time [Min]	Quantity [% Area]	Height [mAU]	Area [mAU.Min]	Area % [%]
1	UNKNOWN	24.37	49.04	296.9	204.1	49.043
2	UNKNOWN	42.32	50.96	179.7	212.1	50.957
Total			100.00	476.5	416.2	100.000

**((3R,3aR,6aR)-5-oxo-6a-(2-oxopropyl)hexahydrofuro[2,3-b]furan-3-yl)methyl benzoate (49)****Peak Results :**

Index	Name	Time [Min]	Quantity [% Area]	Height [mAU]	Area [mAU.Min]	Area % [%]
1	UNKNOWN	23.96	100.00	63.2	40.9	100.000
Total			100.00	63.2	40.9	100.000

### 3. X-ray crystallographic data

#### 6-(tert-Butyl) 4-methyl (1*R*,5*S*,6*R*)-2-oxabicyclo[3.1.0]hex-3-ene-4,6-dicarboxylate (**142**)

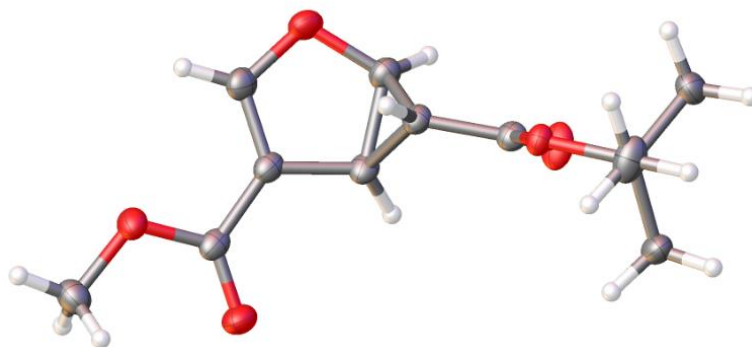
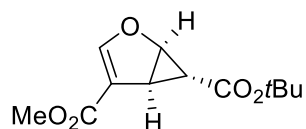


**Table 1.** Crystal data and structure refinement for **142**.

#### Crystal Data

Empirical formula	3(C <sub>12</sub> H <sub>16</sub> O <sub>5</sub> )
Formula weight	240.25
Crystal size	0.153 × 0.117 × 0.094 mm <sup>3</sup>
Crystal description	plate
Crystal colour	colourless
Crystal system	orthorhombic
Space group	P2 <sub>1</sub> 2 <sub>1</sub> 2 <sub>1</sub>
Unit cell Dimensions	a = 5.54420(6) Å; α = 90° b = 23.9671(3) Å; β = 90° c = 28.0722(4) Å; γ = 90°
Volume	3730.19(8) Å <sup>3</sup>
Z, Calculated density	4, 1.283 mg/mm <sup>3</sup>
Absorption coefficient	0.280 mm <sup>-1</sup>
F(000)	1536.0

#### Data Collection

Measurement Device Type	SuperNova, Single Source at offset, AtlasS2
Measurement Method	ω scans
Temperature	123.0 K
Radiation	CuKα (λ = 1.54184 Å)
2θ range for data collection	7.298 to 126.458°
Index ranges	-6 ≤ h ≤ 6, -25 ≤ k ≤ 27, -31 ≤ l ≤ 31
Reflections collected	25549

Independent reflections	5957 [ $R_{\text{int}} = 0.0336$ , $R_{\text{sigma}} = 0.0235$ ]
Reflections $I > 2\sigma(I)$	5683
Absorption correction	Multi-scan
Max. and min. transmissions	1.000 and 0.635

**Refinement**

Refinement methods	Full matrix least squares on $F^2$
Data/restraints/parameters	5957/0/472
Goodness-of-fit on $F^2$	1.020
Final R indexes [ $I \geq 2\sigma(I)$ ]	$R_1 = 0.0271$ , $wR_2 = 0.0709$
Final R indexes [all data]	$R_1 = 0.0290$ , $wR_2 = 0.0726$
Largest diff. peak/hole / $e \text{ \AA}^{-3}$	0.16/-0.15
Flack parameter	-0.07(5)

**Table 2.** Fractional Atomic Coordinates ( $\times 10^4$ ) and Equivalent Isotropic Displacement Parameters ( $\text{\AA}^2 \times 10^3$ ) for **142**.  $U_{eq}$  is defined as 1/3 of the trace of the orthogonalized  $U_{ij}$ .

Atom	x	y	z	$U_{eq}$
O9	-8131(2)	-3985.1(5)	-1620.2(4)	21.9(3)
O2	-8774(2)	-2769.2(5)	-4099.6(5)	29.2(3)
O4	-2975(2)	-4946.4(5)	-3259.0(5)	22.2(3)
O8	-10800(3)	-2228.7(5)	-1212.8(5)	30.8(3)
O7	-13966(2)	-1773.2(5)	-2479.0(4)	24.4(3)
O3	-5467(3)	-3156.3(6)	-2829.5(5)	33.1(3)
O1	-5613(3)	-3155.3(6)	-4477.0(5)	33.8(3)
C15	-10993(3)	-2190.5(7)	-2019.1(6)	20.4(4)
C2	-6638(3)	-3034.9(7)	-4109.8(7)	22.9(4)
C3	-5729(3)	-3154.5(7)	-3634.8(7)	23.6(4)
O6	-10702(2)	-2114.0(6)	-2855.7(5)	31.2(3)
O5	71(2)	-4316.0(5)	-3206.8(6)	34.3(3)
C9	-1402(3)	-5444.1(7)	-3279.6(7)	21.6(4)
C4	-6739(4)	-3003.2(8)	-3223.9(7)	28.3(4)
O10	-5138(2)	-3336.9(5)	-1637.3(5)	31.7(3)
C14	-11817(3)	-2033.2(7)	-2491.8(6)	20.2(4)
C23	-8333(4)	-4950.8(8)	-1537.7(8)	32.2(5)

Appendix

---

C8	-2048(3)	-4429.7(8)	-3234.1(7)	23.1(4)
C7	-4008(3)	-4011.4(7)	-3244.3(6)	23.2(4)
C5	-3500(3)	-3474.6(7)	-3528.5(7)	22.7(4)
C20	-7251(3)	-3466.4(7)	-1639.1(7)	21.6(4)
C21	-6529(3)	-4480.4(7)	-1599.2(7)	21.9(4)
C24	-4854(3)	-4446.5(8)	-1173.5(7)	27.8(4)
C13	-14835(4)	-1565.8(8)	-2930.2(7)	29.8(4)
C10	132(4)	-5423.4(9)	-3727.9(8)	32.3(5)
C16	-12052(4)	-2063.9(8)	-1606.6(7)	25.5(4)
C6	-3450(4)	-3470.9(8)	-2996.3(7)	27.4(4)
C1	-9767(4)	-2613.3(9)	-4555.3(7)	33.1(5)
C12	94(4)	-5493.3(8)	-2830.2(7)	31.2(5)
C17	-8759(3)	-2511.1(7)	-1917.4(6)	20.9(4)
C11	-3231(4)	-5912.1(8)	-3310.9(7)	29.2(4)
C18	-8753(4)	-2528.4(7)	-1382.2(6)	25.2(4)
C19	-9257(3)	-3058.7(7)	-1651.5(6)	21.9(4)
C22	-5171(4)	-4529.7(9)	-2066.5(7)	34.3(5)
O12	-1342(2)	-6251.3(5)	-715.0(5)	29.3(3)
O11	-4681(3)	-5963.0(6)	-1094.1(5)	34.1(3)
O14	-7409(2)	-4076.7(5)	26.7(4)	21.6(3)
O13	-4610(3)	-5808.0(5)	547.7(5)	29.6(3)
C34	-10759(4)	-3665.5(9)	-429.4(7)	30.5(4)
C32	-8249(3)	-4596.3(7)	89.6(7)	22.6(4)
C26	-3564(3)	-6026.8(7)	-726.8(7)	23.5(4)
C28	-3349(4)	-5981.8(8)	159.4(7)	26.7(4)
O15	-10353(2)	-4721.4(6)	136.0(6)	35.6(4)
C29	-6698(3)	-5563.3(7)	-158.0(7)	23.1(4)
C31	-6249(3)	-4999.6(7)	92.2(6)	21.5(4)
C33	-9070(3)	-3592.4(7)	-9.8(7)	22.6(4)
C27	-4435(3)	-5872.8(7)	-256.6(7)	23.2(4)
C25	-381(4)	-6430.3(9)	-1167.8(7)	32.0(4)
C30	-6697(3)	-5525.6(7)	373.0(7)	25.4(4)
C35	-10409(4)	-3513.3(8)	454.7(7)	30.9(4)
C36	-7321(4)	-3116.1(8)	-94.4(9)	37.7(5)

---

**Table 3.** Anisotropic Displacement Parameters ( $\text{\AA}^2 \times 10^3$ ) for **142**. The Anisotropic displacement factor exponent takes the form:  $-2\pi^2[h^2a^{*2}U_{11}+2hka^*b^*U_{12}+\dots]$ .

Atom	$U_{11}$	$U_{22}$	$U_{33}$	$U_{23}$	$U_{13}$	$U_{12}$
O9	17.9(6)	18.7(6)	29.0(7)	2.4(5)	-1.9(5)	1.5(5)
O2	26.7(7)	30.4(7)	30.4(7)	4.4(6)	4.2(6)	8.1(6)
O4	18.3(6)	17.1(6)	31.2(7)	1.0(5)	0.6(5)	1.1(5)
O8	38.0(8)	33.5(7)	20.8(7)	-0.8(6)	0.8(6)	11.2(6)
O7	21.9(6)	28.1(7)	23.3(7)	2.7(5)	0.3(5)	6.7(5)
O3	41.8(8)	31.5(7)	26.1(7)	-2.5(6)	4.9(6)	10.9(6)
O1	35.2(7)	38.9(8)	27.4(8)	-0.5(6)	8.4(6)	10.6(6)
C15	20.7(9)	17.0(8)	23.5(9)	1.0(7)	1.7(7)	0.3(7)
C2	22.0(9)	16.9(8)	29.8(10)	1.2(7)	6.9(8)	1.3(7)
C3	23.5(9)	17.5(9)	30(1)	1.6(7)	6.5(8)	2.7(7)
O6	31.6(7)	38.6(8)	23.5(7)	2.9(6)	6.3(6)	11.9(6)
O5	19.3(7)	24.9(7)	58.6(10)	1.5(6)	-2.8(6)	-2.3(5)
C9	20.9(8)	18.4(9)	25.4(10)	0.7(7)	1.1(8)	3.3(7)
C4	33.9(10)	22.1(9)	28.7(11)	2.6(8)	6.1(9)	7.5(8)
O10	18.5(6)	29.0(7)	47.4(9)	6.9(6)	-3.0(6)	-2.2(5)
C14	19.7(8)	17.1(8)	23.6(10)	0.5(7)	2.6(8)	1.3(7)
C23	29(1)	21.6(9)	45.9(13)	1.4(9)	-3.8(9)	-0.5(8)
C8	20.9(9)	20.4(9)	28.1(10)	2.1(8)	1.0(8)	-1.4(7)
C7	21.5(9)	20.1(9)	28(1)	2.2(8)	3.1(8)	0.9(7)
C5	22.6(9)	19.0(9)	26.5(10)	1.8(7)	5.9(8)	0.5(7)
C20	20.8(9)	21.2(9)	22.8(10)	3.9(7)	-0.4(7)	-0.7(7)
C21	20.3(8)	19.0(9)	26.6(10)	0.9(7)	-0.5(8)	4.0(7)
C24	26.8(9)	28.2(10)	28.3(11)	3.3(8)	-5.0(8)	4.3(8)
C13	29.7(10)	34.8(11)	24.8(10)	5.0(8)	-5.1(8)	7.8(9)
C10	33.9(10)	31(1)	32.1(11)	1.3(9)	9.2(9)	2.8(9)
C16	29.3(9)	22.4(9)	24.9(10)	1.0(8)	0.4(8)	5.0(7)
C6	29.1(10)	22.2(9)	31.0(11)	-2.1(8)	1.5(8)	3.5(8)
C1	32.4(10)	34.0(11)	32.8(11)	4.2(9)	-5.6(9)	3.4(9)
C12	34.6(11)	28.8(10)	30.3(11)	0.6(8)	-8.0(9)	4.8(9)
C17	19.1(8)	21.0(9)	22.6(9)	3.4(7)	0.2(7)	0.3(7)
C11	28.6(10)	19.4(9)	39.6(12)	-1.0(8)	0.3(9)	-1.6(8)
C18	27.8(9)	24.9(10)	22.9(10)	-0.8(8)	-0.8(8)	2.0(8)
C19	18.9(8)	21.5(9)	25.2(9)	4.1(8)	1.2(8)	0.3(7)
C22	36.9(11)	38.3(11)	27.7(11)	-4.9(9)	4.8(9)	4.0(9)

O12	25.3(7)	33.2(7)	29.4(7)	-7.1(6)	-5.8(6)	5.3(6)
O11	38.0(8)	37.3(8)	27.0(8)	-2.8(6)	-10.3(6)	8.2(7)
O14	19.1(6)	18.9(6)	26.8(7)	0.7(5)	-1.4(5)	1.8(5)
O13	37.9(8)	27.0(7)	23.8(7)	2.7(5)	-5.7(6)	4.7(6)
C34	29.1(10)	38.3(11)	24.1(10)	0.7(8)	-3.5(8)	9.0(9)
C32	21.3(9)	22.7(9)	23.9(10)	-1.4(8)	-2.7(7)	-2.3(7)
C26	25.0(9)	16.4(9)	29.2(10)	-1.2(7)	-7.1(8)	-1.1(7)
C28	31.7(10)	19.4(9)	29(1)	-0.7(8)	-2.6(8)	2.6(8)
O15	18.6(6)	28.5(7)	59.7(10)	-0.1(6)	0.6(6)	-3.2(6)
C29	21.9(9)	19.9(9)	27.6(10)	-3.7(7)	-6.3(8)	-1.6(7)
C31	19.7(8)	20.0(9)	24.8(10)	-1.1(7)	-3.8(7)	-0.4(7)
C33	22.3(8)	20.5(9)	24.9(10)	0.8(8)	-0.7(8)	4.9(7)
C27	24.9(9)	17.5(8)	27.1(10)	-0.6(7)	-6.1(8)	-0.4(7)
C25	32.4(11)	33.7(11)	30.0(11)	-6.3(9)	2.6(9)	0.6(9)
C30	27.1(9)	22.0(9)	27.2(10)	2.4(8)	-2.4(8)	0.3(8)
C35	36.2(11)	30(1)	26.4(11)	-3.8(8)	1.5(9)	7.4(9)
C36	30.9(10)	24.4(10)	57.7(15)	8.3(10)	-1(1)	1.2(9)

**Table 4.** Bond Lengths in Å for **142**.

Atom	Atom	Length/Å	Atom	Atom	Length/Å
O9	C20	1.336(2)	C7	C5	1.540(2)
O9	C21	1.484(2)	C7	C6	1.503(3)
O2	C2	1.345(2)	C5	C6	1.494(3)
O2	C1	1.442(2)	C20	C19	1.481(2)
O4	C9	1.479(2)	C21	C24	1.516(3)
O4	C8	1.343(2)	C21	C22	1.517(3)
O8	C16	1.364(2)	C17	C18	1.503(3)
O8	C18	1.425(2)	C17	C19	1.535(2)
O7	C14	1.345(2)	C18	C19	1.505(3)
O7	C13	1.443(2)	O12	C26	1.345(2)
O3	C4	1.363(2)	O12	C25	1.443(2)
O3	C6	1.428(2)	O11	C26	1.212(2)
O1	C2	1.212(2)	O14	C32	1.341(2)
C15	C14	1.453(3)	O14	C33	1.485(2)
C15	C16	1.333(3)	O13	C28	1.360(2)
C15	C17	1.486(2)	O13	C30	1.427(2)



C2	C3	1.454(3)	C34	C33	1.515(3)
C3	C4	1.333(3)	C32	O15	1.211(2)
C3	C5	1.485(2)	C32	C31	1.471(2)
O6	C14	1.210(2)	C26	C27	1.453(3)
O5	C8	1.209(2)	C28	C27	1.339(3)
C9	C10	1.520(3)	C29	C31	1.543(2)
C9	C12	1.515(3)	C29	C27	1.484(3)
C9	C11	1.515(3)	C29	C30	1.493(3)
O10	C20	1.212(2)	C31	C30	1.507(3)
C23	C21	1.517(3)	C33	C35	1.513(3)
C8	C7	1.479(2)	C33	C36	1.516(3)

**Table 5.** Bond Angles in ° for **142**.

Atom	Atom	Atom	Angle/°	Atom	Atom	Atom	Angle/°
C20	O9	C21	121.82(13)	C24	C21	C22	112.45(15)
C2	O2	C1	116.09(15)	C15	C16	O8	114.46(16)
C8	O4	C9	121.37(13)	O3	C6	C7	116.47(16)
C16	O8	C18	106.31(13)	O3	C6	C5	108.44(16)
C14	O7	C13	115.59(14)	C5	C6	C7	61.82(12)
C4	O3	C6	106.34(14)	C15	C17	C18	102.01(15)
C14	C15	C17	124.88(15)	C15	C17	C19	112.67(14)
C16	C15	C14	126.58(16)	C18	C17	C19	59.38(12)
C16	C15	C17	108.53(16)	O8	C18	C17	108.56(15)
O2	C2	C3	112.28(15)	O8	C18	C19	116.47(16)
O1	C2	O2	122.95(17)	C17	C18	C19	61.37(12)
O1	C2	C3	124.77(17)	C20	C19	C17	116.12(14)
C2	C3	C5	125.10(16)	C20	C19	C18	113.96(15)
C4	C3	C2	126.46(17)	C18	C19	C17	59.25(12)
C4	C3	C5	108.44(16)	C26	O12	C25	115.79(15)
O4	C9	C10	109.63(14)	C32	O14	C33	121.29(13)
O4	C9	C12	110.68(14)	C28	O13	C30	106.64(14)
O4	C9	C11	101.82(13)	O14	C32	C31	110.42(14)
C12	C9	C10	112.70(16)	O15	C32	O14	125.34(16)
C12	C9	C11	110.94(15)	O15	C32	C31	124.24(16)
C11	C9	C10	110.55(16)	O12	C26	C27	112.54(15)
C3	C4	O3	114.34(17)	O11	C26	O12	122.64(18)

O7	C14	C15	111.97(15)	O11	C26	C27	124.82(17)
O6	C14	O7	123.32(16)	C27	C28	O13	114.08(16)
O6	C14	C15	124.70(16)	C27	C29	C31	112.73(14)
O4	C8	C7	110.07(14)	C27	C29	C30	102.48(15)
O5	C8	O4	125.68(17)	C30	C29	C31	59.50(12)
O5	C8	C7	124.25(17)	C32	C31	C29	116.85(14)
C8	C7	C5	116.23(15)	C32	C31	C30	115.35(15)
C8	C7	C6	115.08(15)	C30	C31	C29	58.61(12)
C6	C7	C5	58.81(12)	O14	C33	C34	110.28(14)
C3	C5	C7	112.57(14)	O14	C33	C35	110.05(14)
C3	C5	C6	102.33(15)	O14	C33	C36	101.70(14)
C6	C5	C7	59.37(12)	C34	C33	C36	111.14(16)
O9	C20	C19	109.92(14)	C35	C33	C34	112.41(16)
O10	C20	O9	126.22(16)	C35	C33	C36	110.77(16)
O10	C20	C19	123.85(17)	C26	C27	C29	125.26(16)
O9	C21	C23	101.80(13)	C28	C27	C26	126.38(17)
O9	C21	C24	110.80(14)	C28	C27	C29	108.36(17)
O9	C21	C22	108.97(15)	O13	C30	C29	108.34(15)
C23	C21	C22	111.59(16)	O13	C30	C31	116.29(15)
C24	C21	C23	110.73(16)	C29	C30	C31	61.88(12)

**Table 6.** Torsion Angles in ° for **142**.

A	B	C	D	Angle/°	A	B	C	D	Angle/°
O9	C20	C19	C17	-149.92(15)	C16	O8	C18	C19	-63.58(19)
O9	C20	C19	C18	143.99(15)	C16	C15	C14	O7	-5.4(3)
O2	C2	C3	C4	-3.5(3)	C16	C15	C14	O6	173.28(19)
O2	C2	C3	C5	175.88(15)	C16	C15	C17	C18	-1.02(19)
O4	C8	C7	C5	-141.80(16)	C16	C15	C17	C19	60.59(19)
O4	C8	C7	C6	152.21(16)	C6	O3	C4	C3	-3.4(2)
O8	C18	C19	C20	-155.11(15)	C6	C7	C5	C3	-91.30(17)
O8	C18	C19	C17	97.66(17)	C1	O2	C2	O1	-2.2(2)
O1	C2	C3	C4	176.22(19)	C1	O2	C2	C3	177.55(15)
O1	C2	C3	C5	-4.4(3)	C17	C15	C14	O7	176.39(15)
C15	C17	C18	O8	-1.24(18)	C17	C15	C14	O6	-4.9(3)
C15	C17	C18	C19	109.39(14)	C17	C15	C16	O8	3.2(2)
C15	C17	C19	C20	165.59(15)	C17	C18	C19	C20	107.23(17)

Appendix

---

C15	C17	C19	C18	-90.85(17)	C18	O8	C16	C15	-3.9(2)
C2	C3	C4	O3	-178.17(16)	C18	C17	C19	C20	-103.56(18)
C2	C3	C5	C7	-118.08(19)	C19	C17	C18	O8	-110.63(16)
C2	C3	C5	C6	-179.79(17)	O12	C26	C27	C28	-6.5(3)
C3	C5	C6	O3	-1.66(18)	O12	C26	C27	C29	173.23(15)
C3	C5	C6	C7	109.09(15)	O11	C26	C27	C28	173.61(19)
O5	C8	C7	C5	38.2(3)	O11	C26	C27	C29	-6.6(3)
O5	C8	C7	C6	-27.7(3)	O14	C32	C31	C29	-141.18(16)
C9	O4	C8	O5	-3.1(3)	O14	C32	C31	C30	152.78(15)
C9	O4	C8	C7	176.91(14)	O13	C28	C27	C26	-177.61(16)
C4	O3	C6	C7	-64.0(2)	O13	C28	C27	C29	2.6(2)
C4	O3	C6	C5	3.0(2)	C32	O14	C33	C34	-60.1(2)
C4	C3	C5	C7	61.4(2)	C32	O14	C33	C35	64.5(2)
C4	C3	C5	C6	-0.31(19)	C32	O14	C33	C36	-178.06(16)
O10	C20	C19	C17	31.4(3)	C32	C31	C30	O13	-155.06(16)
O10	C20	C19	C18	-34.7(3)	C32	C31	C30	C29	107.24(17)
C14	C15	C16	O8	-175.31(16)	C28	O13	C30	C29	2.89(18)
C14	C15	C17	C18	177.47(16)	C28	O13	C30	C31	-64.16(19)
C14	C15	C17	C19	-120.92(18)	O15	C32	C31	C29	38.5(3)
C8	O4	C9	C10	-62.1(2)	O15	C32	C31	C30	-27.5(3)
C8	O4	C9	C12	62.8(2)	C29	C31	C30	O13	97.70(17)
C8	O4	C9	C11	-179.21(16)	C31	C29	C27	C26	-118.49(18)
C8	C7	C5	C3	163.98(16)	C31	C29	C27	C28	61.3(2)
C8	C7	C5	C6	-104.72(18)	C31	C29	C30	O13	-110.60(16)
C8	C7	C6	O3	-155.61(16)	C33	O14	C32	O15	-2.3(3)
C8	C7	C6	C5	106.69(17)	C33	O14	C32	C31	177.43(15)
C7	C5	C6	O3	-110.75(17)	C27	C29	C31	C32	163.88(16)
C5	C3	C4	O3	2.4(2)	C27	C29	C31	C30	-91.45(17)
C5	C7	C6	O3	97.71(18)	C27	C29	C30	O13	-1.40(18)
C20	O9	C21	C23	175.07(16)	C27	C29	C30	C31	109.20(15)
C20	O9	C21	C24	57.3(2)	C25	O12	C26	O11	-1.9(2)
C20	O9	C21	C22	-66.9(2)	C25	O12	C26	C27	178.23(15)
C21	O9	C20	O10	-0.7(3)	C30	O13	C28	C27	-3.5(2)
C21	O9	C20	C19	-179.34(14)	C30	C29	C31	C32	-104.67(18)
C13	O7	C14	C15	175.62(15)	C30	C29	C27	C26	179.60(16)
C13	O7	C14	O6	-3.1(2)	C30	C29	C27	C28	-0.60(19)
C16	O8	C18	C17	3.00(19)					

---

**Table 7.** Hydrogen Fractional Atomic Coordinates ( $\times 10^4$ ) and Equivalent Isotropic Displacement Parameters ( $\text{\AA}^2 \times 10^3$ ) for **142**.  $U_{eq}$  is defined as 1/3 of the trace of the orthogonalized  $U_{ij}$ .

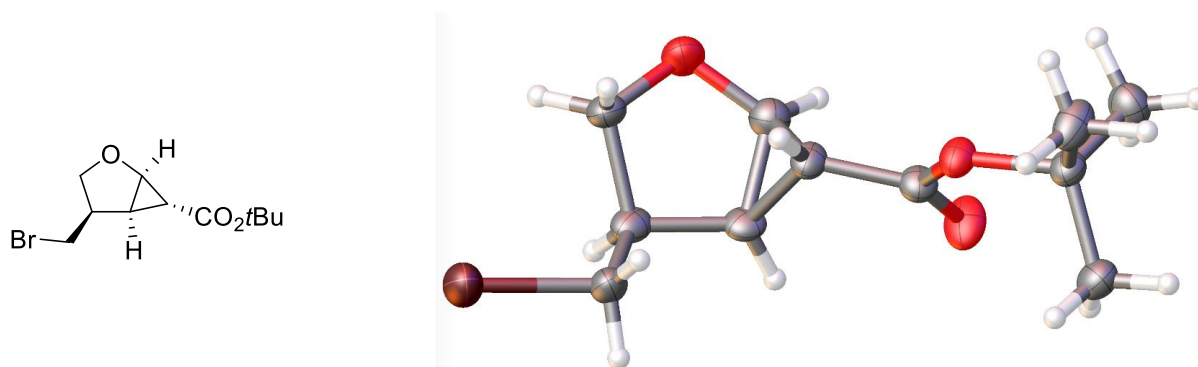
Atom	x	y	z	$U_{eq}$
H4	-8222	-2805	-3207	34
H23A	-9502	-4941	-1799	48
H23B	-9179	-4906	-1234	48
H23C	-7482	-5309	-1540	48
H7	-5708	-4150	-3233	28
H5	-1998	-3428	-3722	27
H24A	-5781	-4343	-890	42
H24B	-3611	-4164	-1233	42
H24C	-4087	-4810	-1123	42
H13A	-16523	-1451	-2897	45
H13B	-14714	-1861	-3171	45
H13C	-13858	-1245	-3029	45
H10A	1390	-5139	-3691	49
H10B	-888	-5329	-4001	49
H10C	883	-5788	-3780	49
H16	-13555	-1875	-1588	31
H6	-1864	-3429	-2830	33
H1A	-11450	-2498	-4515	50
H1B	-9692	-2933	-4773	50
H1C	-8833	-2303	-4688	50
H12A	-954	-5454	-2551	47
H12B	1322	-5199	-2826	47
H12C	883	-5859	-2822	47
H17	-7244	-2452	-2104	25
H11A	-4238	-5859	-3594	44
H11B	-4251	-5909	-3026	44
H11C	-2388	-6271	-3333	44
H18	-7185	-2490	-1210	30
H19	-10945	-3206	-1651	26
H22A	-4000	-4225	-2092	51
H22B	-6313	-4508	-2332	51
H22C	-4322	-4888	-2077	51
H34A	-11957	-3953	-354	46

Appendix

---

H34B	-9832	-3779	-710	46
H34C	-11582	-3312	-495	46
H28	-1832	-6164	181	32
H29	-8211	-5637	-341	28
H31	-4569	-4848	88	26
H25A	1317	-6534	-1129	48
H25B	-512	-6125	-1399	48
H25C	-1297	-6753	-1283	48
H30	-8257	-5568	548	31
H35A	-9254	-3508	719	46
H35B	-11548	-3822	500	46
H35C	-11293	-3159	446	46
H36A	-6411	-3185	-388	56
H36B	-6201	-3089	175	56
H36C	-8220	-2766	-125	56

---

**tert-Butyl (1*R*,4*R*,5*S*,6*R*)-4-(bromomethyl)-2-oxabicyclo[3.1.0]hexane-6-carboxylate (158)****Table 1.** Crystal data and structure refinement for **158**.**Crystal Data**

Empirical formula	C <sub>11</sub> H <sub>17</sub> BrO <sub>3</sub>
Formula weight	277.15
Crystal size	0.30 × 0.10 × 0.02 mm <sup>3</sup>
Crystal description	plate
Crystal colour	colourless
Crystal system	orthorhombic
Space group	P2 <sub>1</sub> 2 <sub>1</sub> 2 <sub>1</sub>
Unit cell Dimensions	a = 5.6797(4) Å; α = 90° b = 9.1270(4) Å; β = 90° c = 24.0021(13) Å; γ = 90°
Volume	1244.24(12) Å <sup>3</sup>
Z, Calculated density	4, 1.480 mg/mm <sup>3</sup>
Absorption coefficient	4.408 mm <sup>-1</sup>
F(000)	568.0

**Data Collection**

Measurement Device Type	SuperNova, Single Source at offset, Atlas
Measurement Method	ω scans
Temperature	123.0 K
Radiation	CuKα (λ = 1.54184 Å)
2θ range for data collection	7.366 to 148.370°
Index ranges	-6 ≤ h ≤ 6, -11 ≤ k ≤ 11, -29 ≤ l ≤ 29
Reflections collected	13224
Independent reflections	2481 [R <sub>int</sub> = 0.1020, R <sub>sigma</sub> = 0.0549]
Reflections I > 2σ(I)	2244
Absorption correction	Gaussian
Max. and min. transmissions	1.000 and 0.360

**Refinement**

Refinement methods	Full matrix least squares on F <sup>2</sup>
Data/restraints/parameters	2481/0/204
Goodness-of-fit on F <sup>2</sup>	1.068
Final R indexes [ $I \geq 2\sigma(I)$ ]	R <sub>1</sub> = 0.0345, wR <sub>2</sub> = 0.0800
Final R indexes [all data]	R <sub>1</sub> = 0.0409, wR <sub>2</sub> = 0.0841
Largest diff. peak/hole / e Å <sup>-3</sup>	0.361/-0.547
Flack parameter	-0.09(3)

**Table 2.** Fractional Atomic Coordinates ( $\times 10^4$ ) and Equivalent Isotropic Displacement Parameters ( $\text{\AA}^2 \times 10^3$ ) for **158**.  $U_{eq}$  is defined as 1/3 of the trace of the orthogonalized  $U_{ij}$ .

Atom	x	y	z	$U_{eq}$
Br1	5801.3(11)	5467.2(6)	6568.3(2)	46.68(19)
O3	5297(5)	5296(3)	3765.8(12)	27.9(6)
O1	14(6)	6255(4)	5169.4(15)	37.7(8)
O2	2800(7)	3399(3)	3888.1(15)	40.2(9)
C6	3277(8)	5180(4)	4600.9(18)	26.9(9)
C8	5982(9)	4906(4)	3186.3(18)	26.9(9)
C7	3730(8)	4513(5)	4051.2(17)	28.2(9)
C4	721(9)	5157(4)	4796.2(18)	31.9(9)
C2	2761(9)	4715(4)	5652.1(19)	30.6(10)
C3	1676(9)	6258(5)	5625(2)	32.1(10)
C5	5305(9)	4701(6)	5812.4(19)	35.3(11)
C9	7690(11)	6132(5)	3049(2)	38.9(12)
C10	7220(10)	3436(5)	3182(2)	34.6(11)
C1	2429(9)	4155(4)	5060(2)	29.0(10)
C11	3867(10)	4934(6)	2808(2)	37.7(11)

**Table 3.** Anisotropic Displacement Parameters ( $\times 10^4$ ) **158**. The anisotropic displacement factor exponent takes the form:  $-2\pi^2[h^2a^{*2} \times U_{11} + \dots + 2hka^* \times b^* \times U_{12}]$ .

Atom	$U_{11}$	$U_{22}$	$U_{33}$	$U_{23}$	$U_{13}$	$U_{12}$
Br1	58.5(4)	49.1(3)	32.4(2)	-6.1(2)	-6.8(3)	16.7(3)
O3	34.3(18)	22.0(12)	27.3(14)	-1.7(11)	6.0(12)	-5.3(12)
O1	35.2(19)	41.8(17)	36.0(18)	-1.3(14)	-0.5(13)	13.8(14)
O2	54(2)	29.9(15)	36.7(18)	-5.9(13)	4.2(16)	-20.1(15)
C6	35(3)	20.5(17)	26(2)	1.5(15)	5.1(17)	-2.7(16)
C8	32(2)	21.9(16)	26.4(19)	-1.0(13)	1.1(19)	-1.5(17)
C7	34(3)	21.8(16)	28(2)	2.7(16)	1.1(17)	-2.6(19)
C4	32(3)	31.1(19)	33(2)	1.1(15)	0(2)	0.6(19)

C2	38(3)	21.6(19)	32(2)	5.2(17)	8.0(19)	1.3(18)
C3	41(3)	24.5(19)	31(2)	0.5(16)	1.0(19)	8.7(19)
C5	43(3)	35(2)	28(2)	-2.6(19)	-1.6(19)	15(2)
C9	47(3)	32(2)	38(3)	-5.3(19)	17(3)	-10(2)
C10	40(3)	29(2)	35(3)	-5.1(18)	0(2)	4(2)
C1	35(3)	17.9(19)	34(2)	5.8(15)	3.0(19)	-2.4(16)
C11	37(3)	43(2)	33(3)	0.7(17)	-4(2)	0(2)

**Table 4.** Bond Lengths in Å for **158**.

Atom	Atom	Length/Å	Atom	Atom	Length/Å
Br1	C5	1.965(5)	C6	C1	1.524(6)
O3	C8	1.488(5)	C8	C9	1.517(6)
O3	C7	1.331(5)	C8	C10	1.515(6)
O1	C4	1.403(6)	C8	C11	1.506(7)
O1	C3	1.445(6)	C4	C1	1.476(7)
O2	C7	1.211(6)	C2	C3	1.539(6)
C6	C7	1.476(6)	C2	C5	1.496(7)
C6	C4	1.526(7)	C2	C1	1.521(7)

**Table 5.** Bond Angles in ° for **158**.

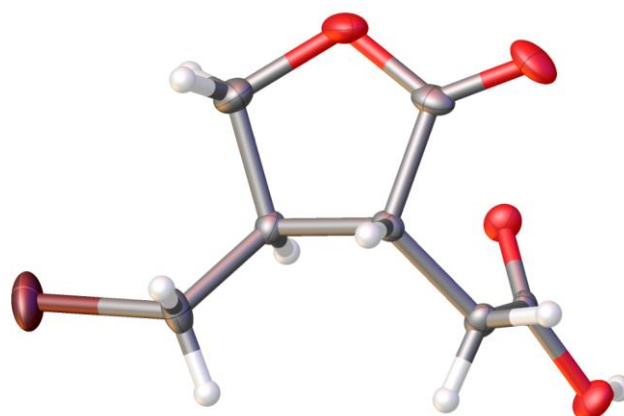
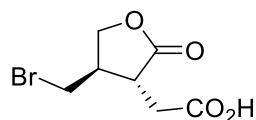
Atom	Atom	Atom	Angle/°
C7	O3	C8	121.9(3)
C4	O1	C3	107.3(3)
C7	C6	C4	115.8(4)
C7	C6	C1	116.7(3)
C1	C6	C4	57.9(3)
O3	C8	C9	101.2(3)
O3	C8	C10	109.9(3)
O3	C8	C11	110.5(4)
C10	C8	C9	110.8(4)
C11	C8	C9	111.5(4)
C11	C8	C10	112.4(4)
O3	C7	C6	110.8(4)
O2	C7	O3	125.2(4)
O2	C7	C6	124.0(4)
O1	C4	C6	117.3(4)
O1	C4	C1	110.9(4)
C1	C4	C6	61.0(3)
C5	C2	C3	113.9(4)
C5	C2	C1	110.9(4)



C1	C2	C3	102.6(4)
O1	C3	C2	107.0(4)
C2	C5	Br1	111.9(3)
C4	C1	C6	61.1(3)
C4	C1	C2	105.9(4)
C2	C1	C6	115.5(3)

**Table 6.** Hydrogen Fractional Atomic Coordinates ( $\times 10^4$ ) and Equivalent Isotropic Displacement Parameters ( $\text{\AA}^2 \times 10^3$ ) for **158**.  $U_{eq}$  is defined as 1/3 of the trace of the orthogonalized  $U_{ij}$ .

Atom	x	y	z	$U_{eq}$
H5A	6250(90)	5290(50)	5590(20)	24(12)
H3A	810(90)	6480(50)	5980(20)	22(11)
H5B	6020(100)	3750(60)	5860(20)	30(13)
H6	4210(100)	5960(60)	4700(20)	33(13)
H10A	6160(100)	2680(60)	3290(20)	30(13)
H10B	8460(110)	3420(60)	3440(30)	43(15)
H4	-560(100)	4850(60)	4540(20)	37(15)
H11A	4300(110)	4910(70)	2430(30)	52(17)
H9A	9020(120)	6160(70)	3330(30)	49(16)
H9B	8250(110)	5920(60)	2660(30)	44(17)
H2	1900(110)	4170(70)	5910(30)	46(17)
H1	2420(100)	3160(50)	4990(20)	26(12)
H9C	7080(100)	7040(60)	3090(20)	34(14)
H11B	3080(120)	5870(80)	2890(30)	53(19)
H3B	2750(90)	6970(50)	5560(20)	22(12)
H10C	7920(110)	3310(60)	2800(30)	40(15)
H11C	2830(110)	4110(70)	2880(30)	42(16)

**2-((3*R*,4*R*)-4-(Bromomethyl)-2-oxotetrahydrofuran-3-yl)acetic acid (167)****Table 1.** Crystal data and structure refinement for **167**.**Crystal Data**

Empirical formula	C <sub>7</sub> H <sub>9</sub> BrO <sub>4</sub>
Formula weight	237.05
Crystal size	0.23 × 0.20 × 0.16 mm <sup>3</sup>
Crystal description	irregular
Crystal colour	colourless
Crystal system	orthorhombic
Space group	P2 <sub>1</sub> 2 <sub>1</sub> 2 <sub>1</sub>
Unit cell Dimensions	a = 5.4766(10) Å; α = 90° b = 10.8666(3) Å; β = 90° c = 15.2378(3) Å; γ = 90°
Volume	906.83(3) Å <sup>3</sup>
Z, Calculated density	4, 1.736 mg/mm <sup>3</sup>
Absorption coefficient	6.021 mm <sup>-1</sup>
F(000)	472.0

**Data Collection**

Measurement Device Type	SuperNova, Single Source at offset, Atlas
Measurement Method	ω scans
Temperature	123.0 K
Radiation	CuKα (λ = 1.54184 Å)
2θ range for data collection	9.998 to 153.066°
Index ranges	-6 ≤ h ≤ 6, -13 ≤ k ≤ 13, -19 ≤ l ≤ 17
Reflections collected	11296
Independent reflections	1913 [R <sub>int</sub> = 0.0487, R <sub>sigma</sub> = 0.0234]
Reflections I > 2σ(I)	1869

Absorption correction	Gaussian
Max. and min. transmissions	1.000 and 0.680

**Refinement**

Refinement methods	Full matrix least squares on F <sup>2</sup>
Data/restraints/parameters	1913/0/110
Goodness-of-fit on F <sup>2</sup>	1.088
Final R indexes [ $I \geq 2\sigma(I)$ ]	R <sub>1</sub> = 0.0261, wR <sub>2</sub> = 0.0651
Final R indexes [all data]	R <sub>1</sub> = 0.0270, wR <sub>2</sub> = 0.0657
Largest diff. peak/hole / e Å <sup>-3</sup>	0.425/-0.638
Flack parameter	-0.055(15)

**Table 2.** Fractional Atomic Coordinates ( $\times 10^4$ ) and Equivalent Isotropic Displacement Parameters ( $\text{\AA}^2 \times 10^3$ ) for **167**.  $U_{eq}$  is defined as 1/3 of the trace of the orthogonalized  $U_{ij}$ .

Atom	x	y	z	$U_{eq}$
Br01	3464.4(8)	6411.3(3)	5914.7(2)	34.15(14)
O002	8034(4)	6812(2)	2024.4(15)	21.9(5)
O003	9562(4)	5631(2)	3096.2(14)	18.2(4)
O004	7676(5)	2984(2)	2902.4(18)	27.0(5)
O005	7563(5)	3322(2)	4344.1(16)	29.1(6)
C5	7863(5)	5950(3)	2638.3(18)	14.2(6)
C4	5332(5)	5418(3)	2696.7(18)	15.3(6)
C2	5004(5)	4584(3)	3489.4(18)	13.5(5)
C1	5306(6)	5183(3)	4395.3(18)	15.0(5)
C3	6866(5)	3560(3)	3517(2)	19.2(6)
C7	2940(6)	5737(3)	4736(2)	23.4(7)
C6	6231(7)	4112(3)	4948(2)	25.8(7)

**Table 3.** Anisotropic Displacement Parameters ( $\times 10^4$ ) **167**. The anisotropic displacement factor exponent takes the form:  $-2\pi^2[h^2a^{*2} \times U_{11} + \dots + 2hka^* \times b^* \times U_{12}]$ .

Atom	$U_{11}$	$U_{22}$	$U_{33}$	$U_{23}$	$U_{13}$	$U_{12}$
Br01	52.8(2)	29.4(2)	20.19(18)	-10.03(14)	12.50(16)	-6.54(18)
O002	21.7(11)	23.8(12)	20.2(10)	8.0(9)	3.0(9)	-2.9(9)
O003	14.1(10)	22.3(11)	18.3(10)	1.8(8)	-1.4(8)	-0.7(9)
O004	26.5(12)	16.5(11)	38.0(13)	-9.8(10)	6.4(10)	2.8(9)
O005	34.9(13)	22.2(12)	30.2(13)	9.1(9)	4.4(10)	12.5(10)
C5	18.8(15)	13.4(13)	10.5(12)	-3.0(10)	2.7(10)	-0.3(11)
C4	12.6(13)	19.4(14)	13.9(13)	1.7(11)	-1.2(10)	0.5(11)
C2	13.1(14)	10.8(12)	16.5(13)	-0.8(10)	1.5(10)	-0.2(11)
C1	17.6(14)	14.1(12)	13.2(12)	0.2(10)	1.2(10)	-0.8(11)

C3	18.4(14)	10.6(12)	28.6(15)	1.6(12)	2.1(11)	1.0(13)
C7	23.8(17)	27.0(17)	19.5(14)	-9.6(12)	4.7(12)	2.0(13)
C6	31.4(18)	24.9(16)	21.2(14)	8.6(13)	4.2(13)	7.4(16)

**Table 4.** Bond Lengths in Å for **167**.

Atom	Atom	Length/Å	Atom	Atom	Length/Å
Br01	C7	1.962(3)	C5	C4	1.505(4)
O002	C5	1.327(4)	C4	C2	1.521(4)
O003	C5	1.214(4)	C2	C1	1.535(4)
O004	C3	1.211(4)	C2	C3	1.510(4)
O005	C3	1.342(4)	C1	C7	1.519(4)
O005	C6	1.455(4)	C1	C6	1.523(4)

**Table 5.** Bond Angles in ° for **167**.

Atom	Atom	Atom	Angle/°
C3	O005	C6	109.8(2)
O002	C5	C4	112.2(2)
O003	C5	O002	123.6(3)
O003	C5	C4	124.2(3)
C5	C4	C2	112.6(2)
C4	C2	C1	116.7(2)
C3	C2	C4	112.4(2)
C3	C2	C1	102.4(2)
C7	C1	C2	112.5(3)
C7	C1	C6	113.4(3)
C6	C1	C2	102.1(2)
O004	C3	O005	121.5(3)
O004	C3	C2	127.4(3)
O005	C3	C2	111.1(3)
C1	C7	Br01	109.6(2)
O005	C6	C1	105.5(2)

**Table 6.** Hydrogen Fractional Atomic Coordinates ( $\times 10^4$ ) and Equivalent Isotropic Displacement Parameters ( $\text{Å}^2 \times 10^3$ ) for **167**.  $U_{eq}$  is defined as 1/3 of the trace of the orthogonalized  $U_{ij}$ .

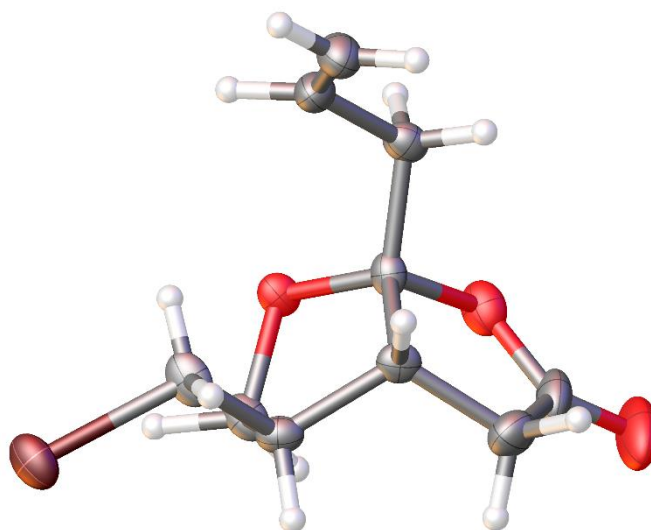
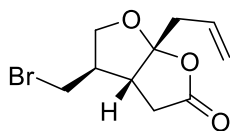
Atom	x	y	z	$U_{eq}$
H002	9451.42	7051.44	1992.11	33
H4A	4995.12	4951.82	2167.51	18
H4B	4157.66	6084.78	2728.9	18

Appendix

---

H2	3374.4	4214.55	3459.01	16
H1	6563.4	5823.01	4365.14	18
H7A	1682.25	5109.04	4755.55	28
H7B	2398.91	6384.63	4343.3	28
H6A	7296.61	4405.05	5411.84	31
H6B	4876.94	3670.23	5211.2	31

---

**(3a*R*,4*R*,6a*R*)-6a-Allyl-4-(bromomethyl)tetrahydrofuro[2,3-*b*]furan-2(3*H*)-one (169)****Table 1.** Crystal data and structure refinement for **169**.**Crystal Data**

Empirical formula	C <sub>10</sub> H <sub>13</sub> BrO <sub>3</sub>
Formula weight	261.11
Crystal size	0.12 × 0.09 × 0.06 mm <sup>3</sup>
Crystal description	plate
Crystal colour	colourless
Crystal system	orthorhombic
Space group	P2 <sub>1</sub> 2 <sub>1</sub> 2 <sub>1</sub>
Unit cell Dimensions	a = 6.0973(2) Å; α = 90° b = 8.1724(4) Å; β = 90° c = 21.2159(10) Å; γ = 90°
Volume	1057.18(8) Å <sup>3</sup>
Z, Calculated density	4, 1.641 mg/mm <sup>3</sup>
Absorption coefficient	5.153 mm <sup>-1</sup>
F(000)	528.0

**Data Collection**

Measurement Device Type	SuperNova, Single Source at offset, Atlas
Measurement Method	ω scans
Temperature	123.01(10) K
Radiation	CuKα (λ = 1.54184 Å)
2θ range for data collection	8.336 to 146.750°
Index ranges	-7 ≤ h ≤ 7, -10 ≤ k ≤ 9, -26 ≤ l ≤ 25

Reflections collected	6746
Independent reflections	2086 [R <sub>int</sub> = 0.0508, R <sub>sigma</sub> = 0.0380]
Reflections I > 2σ(I)	2009
Absorption correction	gaussian
Max. and min. transmissions	1.000 and 0.874

**Refinement**

Refinement methods	Full matrix least squares on F <sup>2</sup>
Data/restraints/parameters	2086/0/175
Goodness-of-fit on F <sup>2</sup>	1.066
Final R indexes [I ≥ 2σ(I)]	R <sub>1</sub> = 0.0334, wR <sub>2</sub> = 0.0905
Final R indexes [all data]	R <sub>1</sub> = 0.0348, wR <sub>2</sub> = 0.0921
Largest diff. peak/hole / e Å <sup>-3</sup>	0.591/-0.734
Flack parameter	-0.03(2)

**Table 2.** Fractional Atomic Coordinates (×10<sup>4</sup>) and Equivalent Isotropic Displacement Parameters (Å<sup>2</sup>×10<sup>3</sup>) for **169**.  $U_{eq}$  is defined as 1/3 of the trace of the orthogonalized  $U_{ij}$ .

Atom	x	y	z	$U_{eq}$
Br1	876.4(8)	4084.0(6)	2008.1(2)	32.40(19)
O1	6248(5)	4694(4)	3208.6(16)	21.0(6)
O2	7585(6)	3297(5)	4078.0(17)	30.7(8)
C1	1499(7)	4155(7)	2917(2)	27.7(10)
C3	3745(7)	3107(5)	3816(2)	21.3(9)
C8	5644(8)	5789(5)	4237(2)	24.5(9)
C5	5486(7)	3382(6)	2812(2)	23.7(9)
C4	5760(8)	4272(5)	3830(2)	20.4(8)
C2	3271(7)	2945(5)	3096(2)	23.1(9)
C6	4542(10)	1559(6)	4140(3)	34.6(12)
C7	6948(11)	1784(7)	4257(3)	34.4(13)
C9	3846(9)	6931(5)	4046(2)	28(1)
C10	2061(10)	7212(6)	4385(3)	31.1(11)
O3	8241(10)	837(7)	4480(2)	57.8(13)

**Table 3.** Anisotropic Displacement Parameters (×10<sup>4</sup>) for **169**. The anisotropic displacement factor exponent takes the form:  $-2\pi^2[h^2a^{*2} \times U_{11} + \dots + 2hka^* \times b^* \times U_{12}]$ .

Atom	$U_{11}$	$U_{22}$	$U_{33}$	$U_{23}$	$U_{13}$	$U_{12}$
Br1	19.4(3)	49.7(3)	28.1(3)	-5.0(2)	-5.01(19)	3.7(2)
O1	13.1(14)	27.5(14)	22.5(15)	-0.7(12)	2.7(12)	-2.9(11)

O2	20.4(16)	42.5(19)	29.2(18)	0.6(16)	-1.7(15)	6.6(15)
C1	9.9(19)	46(3)	27(2)	-2(2)	-1.0(16)	2.0(17)
C3	15(2)	23.7(19)	26(2)	-1.1(17)	3.0(17)	-3.7(15)
C8	23(2)	26.2(19)	25(2)	-2.9(18)	-0.5(18)	-4(2)
C5	12(2)	36(2)	23(2)	-4.4(18)	1.4(16)	2.5(16)
C4	14.3(18)	27.1(19)	20(2)	2.7(16)	-0.9(16)	1.4(19)
C2	18(2)	21.3(17)	30(3)	-5.0(18)	1.1(18)	-1.4(15)
C6	43(3)	25(2)	36(3)	4(2)	2(2)	-3(2)
C7	44(3)	36(3)	23(2)	6(2)	-2(2)	17(2)
C9	38(3)	22.4(19)	23(2)	0.1(17)	0(2)	1.2(19)
C10	37(3)	30(2)	27(3)	-2(2)	-2(2)	5(2)
O3	71(3)	65(3)	37(2)	10(2)	-9(2)	37(3)

**Table 166.** Bond Lengths in Å for **169**.

Atom	Atom	Length/Å	Atom	Atom	Length/Å
Br1	C1	1.965(5)	C3	C6	1.519(7)
O1	C5	1.439(6)	C8	C4	1.513(6)
O1	C4	1.395(5)	C8	C9	1.496(7)
O2	C4	1.466(5)	C5	C2	1.522(6)
O2	C7	1.351(7)	C6	C7	1.499(9)
C1	C2	1.514(6)	C7	O3	1.201(8)
C3	C4	1.555(6)	C9	C10	1.325(8)
C3	C2	1.560(7)			

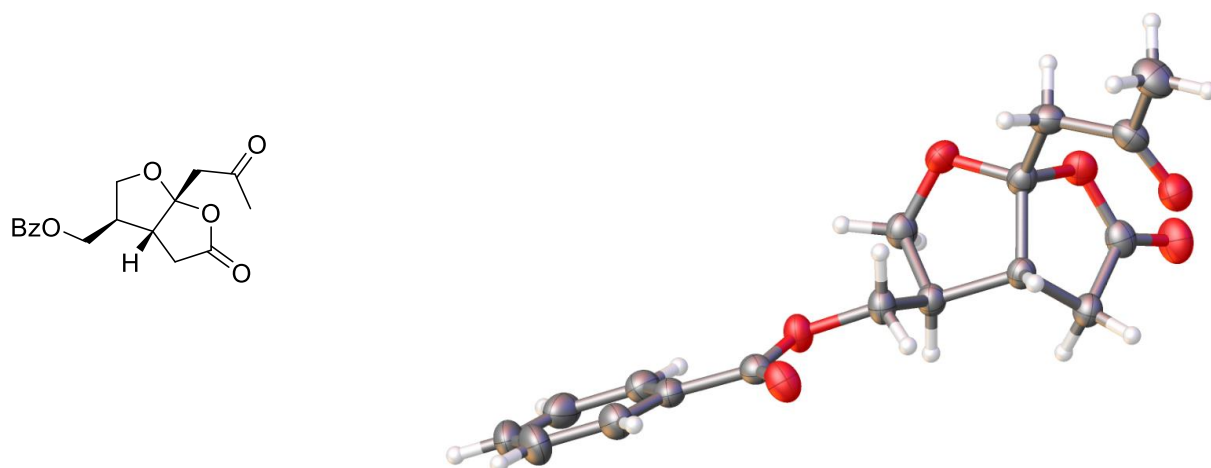
**Table 5.** Bond Angles in ° for **169**.

Atom	Atom	Atom	Angle/°	Atom	Atom	Atom	Angle/°
C4	O1	C5	107.4(4)	O2	C4	C3	105.9(3)
C7	O2	C4	112.4(4)	O2	C4	C8	106.0(4)
C2	C1	Br1	111.4(3)	C8	C4	C3	118.4(4)
C4	C3	C2	102.5(3)	C1	C2	C3	108.9(4)
C6	C3	C4	104.4(4)	C1	C2	C5	112.4(4)
C6	C3	C2	115.5(4)	C5	C2	C3	101.7(4)
C9	C8	C4	113.0(4)	C7	C6	C3	106.6(4)
O1	C5	C2	103.3(4)	O2	C7	C6	110.3(4)
O1	C4	O2	108.2(4)	O3	C7	O2	120.8(7)
O1	C4	C3	107.6(3)	O3	C7	C6	128.9(6)
O1	C4	C8	110.3(3)	C10	C9	C8	124.2(5)



**Table 6.** Hydrogen Fractional Atomic Coordinates ( $\times 10^4$ ) and Equivalent Isotropic Displacement Parameters ( $\text{\AA}^2 \times 10^3$ ) for **169**.  $U_{eq}$  is defined as 1/3 of the trace of the orthogonalized  $U_{ij}$ .

Atom	x	y	z	$U_{eq}$
H2	2844.41	1824.27	2986.73	28
H3	2320(110)	3560(70)	4040(30)	28(15)
H6A	4390(140)	630(90)	3870(30)	43(18)
H1A	1870(110)	5270(80)	2990(30)	35(16)
H5A	5510(110)	3830(70)	2340(30)	24(14)
H5B	6590(100)	2460(70)	2850(30)	22(14)
H1B	170(130)	3810(80)	3080(30)	40(18)
H8A	5440(110)	5430(70)	4660(30)	23(14)
H6B	3690(130)	1320(80)	4560(30)	40(19)
H8B	7130(160)	6440(100)	4190(40)	60(20)
H9	3870(150)	7490(90)	3630(40)	50(20)
H10A	930(130)	7940(80)	4250(30)	33(15)
H10B	1910(100)	6690(70)	4760(30)	22(14)

**((3*R*,3*aR*,6*aR*)-5-Oxo-6a-(2-oxopropyl)hexahydrofuro[2,3-*b*]furan-3-yl)methyl benzoate (49)****Table 1.** Crystal data and structure refinement for **49**.**Crystal Data**

Empirical formula	C <sub>17</sub> H <sub>18</sub> O <sub>6</sub>
Formula weight	318.31
Crystal size	0.23 × 0.07 × 0.04 mm <sup>3</sup>
Crystal description	needle
Crystal colour	colourless
Crystal system	monoclinic
Space group	P2 <sub>1</sub>
Unit cell Dimensions	a = 9.9840(2) Å; α = 90° b = 6.4871(10) Å; β = 98.909(2)° c = 12.1144(2) Å; γ = 90°
Volume	775.15(2) Å <sup>3</sup>
Z, Calculated density	2, 1.364 mg/mm <sup>3</sup>
Absorption coefficient	0.868 mm <sup>-1</sup>
F(000)	336.0

**Data Collection**

Measurement Device Type	SuperNova, Single Source at offset, Atlas
Measurement Method	ω scans
Temperature	122.99(12) K
Radiation	CuKα (λ = 1.54184 Å)
2θ range for data collection	7.386 to 150.158°
Index ranges	-12 ≤ h ≤ 12, -8 ≤ k ≤ 7, -15 ≤ l ≤ 15
Reflections collected	18748

Independent reflections	3079 [ $R_{\text{int}} = 0.0415$ , $R_{\text{sigma}} = 0.0232$ ]
Reflections $I > 2\sigma(I)$	2977
Absorption correction	gaussian
Max. and min. transmissions	1.000 and 0.825

**Refinement**

Refinement methods	Full matrix least squares on $F^2$
Data/restraints/parameters	3079/1/209
Goodness-of-fit on $F^2$	1.069
Final R indexes [ $I \geq 2\sigma(I)$ ]	$R_1 = 0.0333$ , $wR_2 = 0.0850$
Final R indexes [all data]	$R_1 = 0.0346$ , $wR_2 = 0.0862$
Largest diff. peak/hole / $e \text{ \AA}^{-3}$	0.309/-0.137
Flack parameter	0.09(9)

**Table 2.** Fractional Atomic Coordinates ( $\times 10^4$ ) and Equivalent Isotropic Displacement Parameters ( $\text{\AA}^2 \times 10^3$ ) for **49**.  $U_{eq}$  is defined as 1/3 of the trace of the orthogonalized  $U_{ij}$ .

Atom	x	y	z	$U_{eq}$
O4	5852.4(10)	8649.8(17)	7068.2(9)	33.9(2)
O2	7914.1(10)	3073.7(17)	4187.8(8)	33.2(2)
O3	5357.2(9)	6292.4(18)	5615.6(8)	34.0(2)
O1	8875.2(12)	10.1(17)	4669.1(9)	37.9(2)
O6	6782.3(11)	6119.6(19)	9060.9(8)	38.1(3)
O5	7156.4(13)	11225.8(18)	7821.9(9)	43.0(3)
C7	8477.3(12)	1284(2)	3970.7(11)	28.9(3)
C15	7063.0(15)	9519(2)	7428.1(11)	31.9(3)
C11	7522.4(12)	6126(2)	6763.7(10)	26.2(3)
C12	5981.3(13)	6510(2)	6724.2(11)	29.4(3)
C16	5794.7(15)	5131(3)	8669.8(12)	34.1(3)
C8	7757.6(14)	3403(2)	5349.3(10)	30.5(3)
C10	6365.7(14)	6644(2)	4901.4(11)	32.5(3)
C6	8561.1(13)	1027(3)	2756.4(12)	31.9(3)
C14	8198.3(13)	8100(2)	7246.0(11)	30.7(3)
C9	7655.4(14)	5697(2)	5530.1(11)	28.2(3)
C5	8243.0(15)	2614(3)	1990.0(12)	37.0(3)
C13	5222.3(14)	5183(3)	7440.1(13)	33.6(3)
C1	8975.9(16)	-876(3)	2408.2(13)	40.4(4)
C4	8361.5(17)	2290(3)	870.9(14)	46.2(4)
C17	5059.2(18)	3740(3)	9355.8(14)	46.5(4)
C3	8777.9(18)	398(4)	531.1(14)	51.2(5)
C2	9083.4(18)	-1193(4)	1289.2(15)	51.6(5)

**Table 3.** Anisotropic Displacement Parameters ( $\times 10^4$ ) for **49**. The anisotropic displacement factor exponent takes the form:  $-2\sigma^2[h^2a^{*2} \times U_{11} + \dots + 2hka^* \times b^* \times U_{12}]$ .

Atom	$U_{11}$	$U_{22}$	$U_{33}$	$U_{23}$	$U_{13}$	$U_{12}$
O4	33.2(5)	31.9(6)	36.0(5)	8.0(4)	3.4(4)	-0.5(4)
O2	40.3(5)	34.3(6)	24.5(4)	5.4(4)	3.7(4)	-2.2(4)
O3	28.1(4)	41.5(6)	30.5(5)	1.9(4)	-1.8(4)	-0.1(4)
O1	50.3(6)	31.1(6)	34.3(5)	4.4(5)	13.0(4)	2.8(4)
O6	41.6(5)	43.2(7)	30.4(5)	-0.5(5)	8.1(4)	-0.2(5)
O5	59.5(7)	28.0(6)	41.8(6)	2.9(5)	9.2(5)	-5.4(5)
C7	27.0(6)	29.7(7)	30.5(6)	-2.9(5)	6.1(5)	-1.8(5)
C15	40.9(7)	29.1(8)	26.1(6)	3.9(6)	6.5(5)	2.2(5)
C11	27.4(6)	26.5(7)	24.1(6)	1.8(5)	1.9(4)	-0.5(5)
C12	28.7(6)	29.7(8)	28.5(6)	3.5(5)	0.4(5)	-2.3(5)
C16	33.1(6)	34.4(8)	36.6(7)	5.4(6)	11.4(5)	1.6(6)
C8	37.8(7)	30.3(8)	22.9(6)	2.0(5)	3.3(5)	-2.4(5)
C10	35.5(7)	33.8(8)	27.0(6)	3.4(6)	1.2(5)	0.9(5)
C6	25.4(6)	41.5(8)	29.2(6)	-4.8(6)	5.3(5)	-4.7(6)
C14	32.2(6)	30.9(7)	28.6(6)	-2.1(6)	3.6(5)	-4.5(5)
C9	30.0(6)	29.9(8)	24.3(6)	0.7(5)	3.3(5)	-1.4(5)
C5	31.0(6)	47.5(10)	32.4(7)	-2.0(6)	4.1(5)	0.3(6)
C13	26.5(6)	36.9(8)	38.1(7)	-0.0(5)	6.8(5)	-0.1(6)
C1	37.9(7)	45.0(10)	38.6(7)	0.2(7)	7.6(6)	-8.8(7)
C4	35.7(8)	70.6(13)	31.9(7)	-5.8(7)	3.4(6)	4.2(7)
C17	51.4(9)	45.8(10)	46.0(9)	-2.1(8)	19.7(7)	5.7(7)
C3	43.3(8)	81.6(15)	29.7(7)	-7.0(8)	8.9(6)	-13.9(8)
C2	49.7(9)	63.7(13)	43.6(9)	0.3(9)	13.5(7)	-21.1(9)

**Table 4.** Bond Lengths in Å for **49**.

Atom	Atom	Length/Å	Atom	Atom	Length/Å
O4	C15	1.3436(18)	C11	C9	1.5458(18)
O4	C12	1.4607(19)	C12	C13	1.507(2)
O2	C7	1.3341(19)	C16	C13	1.511(2)
O2	C8	1.4553(15)	C16	C17	1.494(2)
O3	C12	1.3974(16)	C8	C9	1.510(2)
O3	C10	1.4437(17)	C10	C9	1.5203(19)
O1	C7	1.2050(19)	C6	C5	1.390(2)
O6	C16	1.210(2)	C6	C1	1.389(2)
O5	C15	1.204(2)	C5	C4	1.395(2)
C7	C6	1.4955(18)	C1	C2	1.392(2)
C15	C14	1.502(2)	C4	C3	1.379(3)
C11	C12	1.5520(17)	C3	C2	1.384(3)
C11	C14	1.522(2)			

**Table 5.** Bond Angles in ° for **49**.

Atom	Atom	Atom	Angle/°	Atom	Atom	Atom	Angle/°
C12	O4	C15	112.12(10)	C13	C16	O6	122.35(14)
C8	O2	C7	115.46(11)	C17	C16	O6	122.90(14)
C10	O3	C12	108.15(10)	C17	C16	C13	114.74(14)
O1	C7	O2	124.16(13)	C9	C8	O2	107.74(11)
C6	C7	O2	112.34(12)	C9	C10	O3	104.54(11)
C6	C7	O1	123.49(14)	C5	C6	C7	122.21(14)
O5	C15	O4	121.68(14)	C1	C6	C7	117.54(14)
C14	C15	O4	110.90(12)	C1	C6	C5	120.25(14)
C14	C15	O5	127.42(14)	C11	C14	C15	105.79(11)
C14	C11	C12	104.78(11)	C8	C9	C11	109.59(11)
C9	C11	C12	103.43(10)	C10	C9	C11	102.64(11)
C9	C11	C14	115.03(11)	C10	C9	C8	113.35(12)
O3	C12	O4	108.92(11)	C4	C5	C6	119.52(17)
C11	C12	O4	105.94(11)	C16	C13	C12	115.66(12)
C11	C12	O3	107.80(11)	C2	C1	C6	119.92(18)
C13	C12	O4	107.72(11)	C3	C4	C5	119.94(17)
C13	C12	O3	107.84(11)	C2	C3	C4	120.76(15)
C13	C12	C11	118.36(12)	C3	C2	C1	119.61(19)

**Table 6.** Hydrogen Fractional Atomic Coordinates ( $\times 10^4$ ) and Equivalent Isotropic Displacement Parameters ( $\text{\AA}^2 \times 10^3$ ) for **49**.  $U_{eq}$  is defined as 1/3 of the trace of the orthogonalized  $U_{ij}$ .

Atom	x	y	z	$U_{eq}$
H11	7825.4(12)	4938(2)	7236.8(10)	31.5(3)
H8a	6945.5(14)	2719(2)	5509.5(10)	36.6(4)
H8b	8531.3(14)	2844(2)	5841.2(10)	36.6(4)
H10a	6108.9(14)	5979(2)	4182.6(11)	39.0(4)
H10b	6484.6(14)	8107(2)	4782.9(11)	39.0(4)
H14a	8736.4(13)	8709(2)	6728.9(11)	36.8(3)
H14b	8784.3(13)	7823(2)	7946.5(11)	36.8(3)
H9	8454.0(14)	6401(2)	5332.4(11)	33.8(3)
H5	7953.3(15)	3883(3)	2221.5(12)	44.4(4)
H13a	4293.6(14)	5669(3)	7360.4(13)	40.4(4)
H13b	5199.8(14)	3784(3)	7154.6(13)	40.4(4)
H1	9181.6(16)	-1938(3)	2922.2(13)	48.4(4)
H4	8159.8(17)	3349(3)	354.5(14)	55.5(5)
H17a	5452(10)	3856(18)	10128(2)	69.7(6)
H17b	4121(4)	4130(15)	9267(10)	69.7(6)
H17c	5132(13)	2342(4)	9113(8)	69.7(6)
H3	8854.4(18)	189(4)	-216.1(14)	61.4(6)
H2	9358.9(18)	-2466(4)	1052.2(15)	62.0(6)

**(4*S*,5*R*)-4-Methyl-3-((3*R*,3*aR*,6*aR*)-5-oxohexahydrofuro[2,3-*b*]furan-3-carbonyl)-5-phenyl-oxazolidin-2-one (176)**

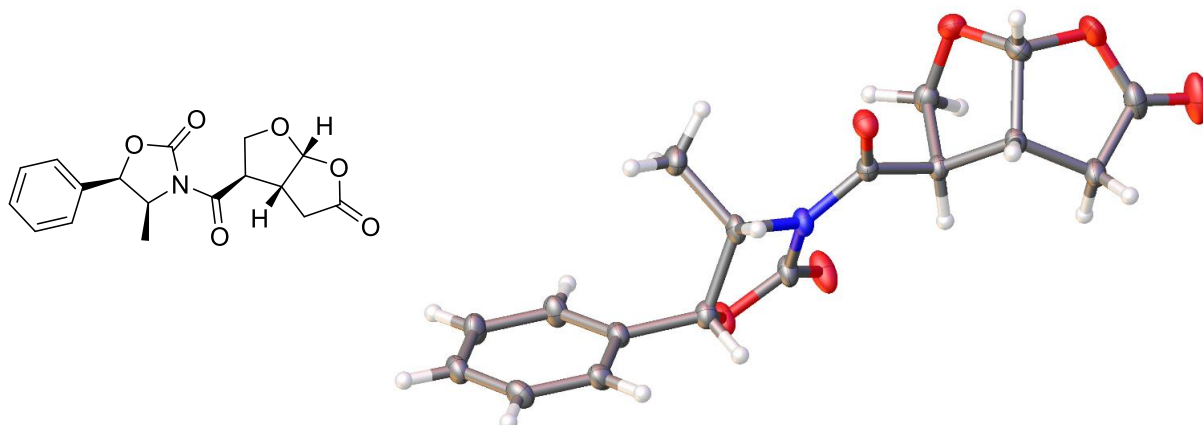


**Table 1.** Crystal data and structure refinement for **176**.

**Crystal Data**

Empirical formula	C <sub>17</sub> H <sub>17</sub> NO <sub>6</sub>
Formula weight	331.31
Crystal size	0.32 × 0.24 × 0.15 mm <sup>3</sup>
Crystal description	prism
Crystal colour	colourless
Crystal system	monoclinic
Space group	P2 <sub>1</sub>
Unit cell Dimensions	a = 8.1085(3) Å; α = 90° b = 10.0941(4) Å; β = 110.347(4)° c = 10.2184(4) Å; γ = 90°
Volume	784.17(6) Å <sup>3</sup>
Z, Calculated density	2, 1.403 mg/mm <sup>3</sup>
Absorption coefficient	0.902 mm <sup>-1</sup>
F(000)	348.0

**Data Collection**

Measurement Device Type	SuperNova, Single Source at offset, Atlas
Measurement Method	ω scans
Temperature	123.01(10) K
Radiation	CuKα (λ = 1.54184 Å)
2θ range for data collection	9.230 to 147.056°
Index ranges	-10 ≤ h ≤ 9, -12 ≤ k ≤ 10, -12 ≤ l ≤ 12
Reflections collected	8169

Independent reflections	2879 [ $R_{\text{int}} = 0.0219$ , $R_{\text{sigma}} = 0.0191$ ]
Reflections $I > 2\sigma(I)$	2828
Absorption correction	gaussian
Max. and min. transmissions	1.000 and 0.618

**Refinement**

Refinement methods	Full matrix least squares on $F^2$
Data/restraints/parameters	2879/1/218
Goodness-of-fit on $F^2$	1.069
Final R indexes [ $I \geq 2\sigma(I)$ ]	$R_1 = 0.0278$ , $wR_2 = 0.0696$
Final R indexes [all data]	$R_1 = 0.0285$ , $wR_2 = 0.0701$
Largest diff. peak/hole / $e \text{ \AA}^{-3}$	0.147/-0.206
Flack parameter	0.04(7)

**Table 2.** Fractional Atomic Coordinates ( $\times 10^4$ ) and Equivalent Isotropic Displacement Parameters ( $\text{\AA}^2 \times 10^3$ ) for **176**.  $U_{eq}$  is defined as 1/3 of the trace of the orthogonalized  $U_{ij}$ .

Atom	x	y	z	$U_{eq}$
O1	6160.8(16)	6416.3(15)	6654.4(13)	24.5(3)
O3	1582.5(16)	4283.4(14)	7099.8(12)	22.5(3)
O4	-321.6(18)	2917.9(14)	4238.5(14)	27.9(3)
O2	4105.5(16)	6003.1(18)	4568.1(13)	32.9(4)
N1	3737.1(18)	5380.1(16)	6648.4(14)	18.7(3)
O5	-3171(2)	3642.8(17)	3101.7(17)	40.3(4)
O6	-4664(2)	5051(2)	1429.1(15)	45.6(5)
C10	4593(2)	5945(2)	5821.9(18)	22.4(4)
C6	8042(2)	6375.1(19)	9118.5(17)	19.0(3)
C11	2035(2)	4869.4(18)	6243.5(17)	17.9(3)
C12	802(2)	5072.1(18)	4750.0(16)	17.0(3)
C13	-1114(2)	5093.7(19)	4721.4(17)	18.2(3)
C8	4944(2)	5290.9(19)	8114.8(17)	19.4(4)
C2	10103(2)	7015(2)	11366.4(18)	22.7(4)
C7	6185(2)	6438(2)	8097.0(17)	20.0(3)
C1	8426(2)	7077.2(19)	10359.5(19)	21.3(4)
C17	814(2)	3834(2)	3882.5(18)	23.2(4)
C3	11397(2)	6255(2)	11137.3(18)	22.3(4)
C5	9351(2)	5632(2)	8881.7(18)	23.3(4)
C4	11029(2)	5571(2)	9889.5(19)	23.6(4)
C15	-3544(2)	4876(2)	2545(2)	29.4(4)
C14	-2396(2)	5884(2)	3521.7(19)	22.8(4)
C9	5775(2)	3932(2)	8430.1(19)	25.4(4)

C16	-1699(2)	3645(2)	4403(2)	26.6(4)
-----	----------	---------	---------	---------

**Table 3.** Anisotropic Displacement Parameters ( $\times 10^4$ ) for **176**. The anisotropic displacement factor exponent takes the form:  $-2\pi^2[h^2a^{*2} \times U_{11} + \dots + 2hka^* \times b^* \times U_{12}]$ .

Atom	$U_{11}$	$U_{22}$	$U_{33}$	$U_{23}$	$U_{13}$	$U_{12}$
O1	14.8(6)	37.5(8)	18.5(6)	6.1(5)	2.3(4)	-3.7(5)
O3	18.5(6)	28.9(8)	19.0(6)	3.7(5)	5.2(5)	-1.9(5)
O4	26.4(7)	19.3(7)	33.5(7)	-0.7(6)	4.8(5)	-0.4(5)
O2	19.2(6)	60.4(11)	17.5(6)	6.0(6)	4.5(5)	-5.5(6)
N1	13.9(7)	25.5(9)	14.8(6)	1.9(5)	2.5(5)	0.2(5)
O5	21.9(7)	32.0(9)	50.4(9)	-10.0(7)	-8.2(6)	-6.0(6)
O6	24.9(7)	74.2(13)	26.8(7)	-8.8(8)	-4.8(6)	11.0(8)
C10	13.2(8)	31.3(11)	21.0(8)	3.7(7)	3.8(6)	0.9(7)
C6	14.7(8)	21.5(9)	18.9(8)	1.3(7)	3.5(6)	-1.7(7)
C11	14.6(8)	19.8(9)	18.1(7)	-0.1(6)	4.4(6)	0.8(6)
C12	13.7(7)	19.8(9)	15.8(7)	1.3(7)	2.9(6)	0.5(7)
C13	13.7(7)	21.7(9)	18.4(7)	0.8(7)	4.7(6)	-0.6(7)
C8	13.3(7)	27.3(10)	15.2(7)	1.7(6)	1.8(6)	0.9(7)
C2	21.4(9)	26.6(10)	18.8(8)	-4.7(7)	5.1(7)	-5.4(7)
C7	15.6(8)	24.5(9)	18.5(8)	2.2(7)	4.1(6)	1.2(7)
C1	17.0(8)	21.7(10)	25.7(8)	-2.1(7)	8.1(7)	-1.8(7)
C17	21.8(9)	24.5(10)	20.9(8)	-3.5(7)	4.5(7)	1.9(7)
C3	15.8(8)	27.3(10)	20.0(8)	1.4(7)	1.5(6)	-2.9(7)
C5	18.3(8)	30.3(11)	19.2(8)	-5.2(7)	3.9(7)	0.4(7)
C4	15.8(8)	28.4(11)	25.7(9)	-2.3(7)	6.0(7)	2.8(7)
C15	16.1(8)	41.9(13)	26.6(9)	-4.5(8)	2.8(7)	2.2(8)
C14	14.4(8)	26.6(10)	25.5(8)	5.9(7)	4.3(6)	0.6(7)
C9	18.5(8)	27.4(11)	26.0(9)	4.8(7)	2.2(7)	1.6(7)
C16	20.2(9)	24.2(11)	31.9(10)	1.6(8)	4.5(7)	-4.6(7)

**Table 4.** Bond Lengths in Å for **176**.

Atom	Atom	Length/Å	Atom	Atom	Length/Å
O1	C10	1.347(2)	C6	C5	1.388(3)
O1	C7	1.468(2)	C11	C12	1.520(2)
O3	C11	1.214(2)	C12	C13	1.544(2)
O4	C17	1.438(2)	C12	C17	1.534(3)
O4	C16	1.395(3)	C13	C14	1.528(2)
O2	C10	1.204(2)	C13	C16	1.536(3)
N1	C10	1.389(2)	C8	C7	1.538(3)



N1	C11	1.394(2)	C8	C9	1.513(3)
N1	C8	1.480(2)	C2	C1	1.393(3)
O5	C15	1.358(3)	C2	C3	1.384(3)
O5	C16	1.445(2)	C3	C4	1.388(3)
O6	C15	1.198(2)	C5	C4	1.393(2)
C6	C7	1.506(2)	C15	C14	1.501(3)
C6	C1	1.390(3)			

**Table 5.** Bond Angles in ° for **176**.

Atom	Atom	Atom	Angle/°	Atom	Atom	Atom	Angle/°
C10	O1	C7	108.63(13)	C16	C13	C12	103.02(15)
C16	O4	C17	107.56(15)	N1	C8	C7	98.45(13)
C10	N1	C11	128.59(14)	N1	C8	C9	111.07(15)
C10	N1	C8	110.28(14)	C9	C8	C7	116.11(15)
C11	N1	C8	121.03(14)	C3	C2	C1	120.20(17)
C15	O5	C16	112.09(15)	O1	C7	C6	110.87(13)
O1	C10	N1	108.81(14)	O1	C7	C8	102.74(14)
O2	C10	O1	122.94(16)	C6	C7	C8	117.43(15)
O2	C10	N1	128.22(17)	C6	C1	C2	120.16(17)
C1	C6	C7	117.61(16)	O4	C17	C12	104.15(14)
C5	C6	C7	122.88(16)	C2	C3	C4	119.85(16)
C5	C6	C1	119.49(16)	C6	C5	C4	120.28(17)
O3	C11	N1	118.84(15)	C3	C4	C5	120.00(17)
O3	C11	C12	122.09(15)	O5	C15	C14	110.28(16)
N1	C11	C12	119.06(14)	O6	C15	O5	121.2(2)
C11	C12	C13	109.10(13)	O6	C15	C14	128.5(2)
C11	C12	C17	109.67(14)	C15	C14	C13	105.76(16)
C17	C12	C13	102.06(14)	O4	C16	O5	109.16(17)
C14	C13	C12	114.98(14)	O4	C16	C13	108.99(15)
C14	C13	C16	104.64(14)	O5	C16	C13	106.98(15)

**Table 6.** Hydrogen Fractional Atomic Coordinates ( $\times 10^4$ ) and Equivalent Isotropic Displacement Parameters ( $\text{\AA}^2 \times 10^3$ ) for **176**.  $U_{eq}$  is defined as 1/3 of the trace of the orthogonalized  $U_{ij}$ .

Atom	x	y	z	$U_{eq}$
H12	1093.57	5874.25	4335.29	20
H13	-1170.34	5374.26	5622.9	22
H8	4311.58	5494.11	8751.92	23
H2	10354.38	7486.02	12195.36	27

Appendix

---

H7	5651.56	7269.44	8246.6	24
H1	7560.17	7589.51	10517.53	26
H17A	365.67	4034.85	2892.47	28
H17B	1994.03	3477.63	4127.01	28
H3	12510.41	6202.85	11817.66	27
H5	9106.88	5172.22	8046.7	28
H4	11902.23	5072.51	9726.31	28
H14A	-3097.08	6474.59	3865.21	27
H14B	-1764.95	6405.89	3052.08	27
H9A	4875.79	3279.59	8321.49	38
H9B	6591.81	3912.65	9371.63	38
H9C	6384.64	3742.42	7797.36	38
H16	-2043.75	3272.28	5155.01	32

---

**(4*S*,5*R*)-4-Methyl-3-((3*R*,3*aS*,6*aS*)-5-oxohexahydrofuro[2,3-*b*]furan-3-carbonyl)-5-phenyl-oxazolidin-2-one (177)**

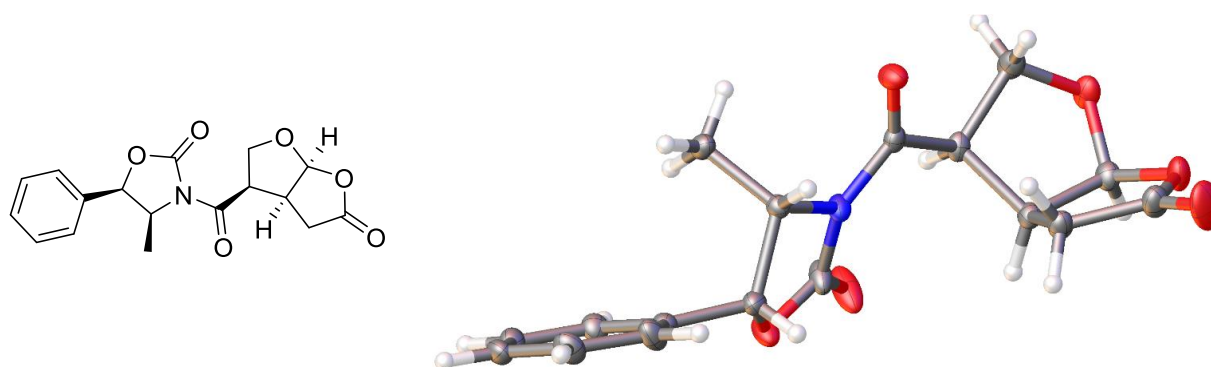


**Table 1.** Crystal data and structure refinement for **177**.

**Crystal Data**

Empirical formula	C <sub>17</sub> H <sub>17</sub> NO <sub>6</sub>
Formula weight	331.31
Crystal size	0.32 × 0.24 × 0.15 mm <sup>3</sup>
Crystal description	prism
Crystal colour	colourless
Crystal system	monoclinic
Space group	P2 <sub>1</sub>
Unit cell Dimensions	a = 6.6963(2) Å; α = 90° b = 11.2066(3) Å; β = 106.983(3)° c = 10.5591(3) Å; γ = 90°
Volume	757.83(4) Å <sup>3</sup>
Z, Calculated density	2, 1.452 mg/mm <sup>3</sup>
Absorption coefficient	0.933 mm <sup>-1</sup>
F(000)	348.0

**Data Collection**

Measurement Device Type	SuperNova, Single Source at offset, Atlas
Measurement Method	ω scans
Temperature	123.01(10) K
Radiation	CuKα (λ = 1.54184 Å)
2θ range for data collection	8.756 to 152.602°
Index ranges	-8 ≤ h ≤ 7, -14 ≤ k ≤ 14, -13 ≤ l ≤ 13
Reflections collected	9087
Independent reflections	3096 [R <sub>int</sub> = 0.0298, R <sub>sigma</sub> = 0.0290]

Reflections $I > 2\sigma(I)$	3008
Absorption correction	gaussian
Max. and min. transmissions	1.000 and 0.856

**Refinement**

Refinement methods	Full matrix least squares on $F^2$
Data/restraints/parameters	3096/1/218
Goodness-of-fit on $F^2$	1.040
Final R indexes [ $I \geq 2\sigma(I)$ ]	$R_1 = 0.0284$ , $wR_2 = 0.0700$
Final R indexes [all data]	$R_1 = 0.0301$ , $wR_2 = 0.0722$
Largest diff. peak/hole / $e \text{ \AA}^{-3}$	0.165/-0.166
Flack parameter	-0.04(8)

**Table 2.** Fractional Atomic Coordinates ( $\times 10^4$ ) and Equivalent Isotropic Displacement Parameters ( $\text{\AA}^2 \times 10^3$ ) for **177**.  $U_{eq}$  is defined as 1/3 of the trace of the orthogonalized  $U_{ij}$ .

Atom	x	y	z	$U_{eq}$
O3	9351(2)	3714.3(14)	3704.7(13)	22.5(3)
O4	11770(3)	2748.1(13)	7601.4(13)	23.6(3)
O5	13234(2)	4599.3(14)	8298.9(14)	25.0(3)
O1	3487(2)	5464.7(16)	3905.5(13)	28.0(4)
O2	4806(3)	4245(2)	5631.4(15)	41.2(5)
N1	6507(2)	4572.9(15)	4023.1(14)	17.2(3)
O6	14346(3)	6250.5(17)	7549(2)	45.4(5)
C4	5810(3)	5059.2(17)	2662.6(17)	15.8(4)
C11	8312(3)	3894.5(17)	4457.2(17)	16.6(4)
C13	9680(3)	4488.7(18)	6904.0(17)	17.9(4)
C8	-766(3)	6645.4(19)	-686(2)	22.3(4)
C12	8981(3)	3472.8(16)	5881.5(17)	17.1(4)
C2	2415(3)	6231.1(18)	1643.8(19)	18.9(4)
C14	11380(3)	3872.8(19)	8033.3(18)	19.9(4)
C1	586(3)	5560.2(19)	1354.3(19)	21.2(4)
C15	10836(3)	5521.9(17)	6486.0(19)	20.6(4)
C3	4218(3)	5983.6(18)	2849(2)	19.9(4)
C10	4936(3)	4710(2)	4636.6(19)	26.0(5)
C5	4895(3)	4091.4(18)	1665.5(18)	21.0(4)
C6	2645(3)	7114.0(19)	774(2)	25.5(4)
C16	12987(4)	5540(2)	7463(2)	26.2(4)
C17	10921(4)	2687.1(19)	6187.8(19)	23.9(4)
C9	-1003(3)	5770(2)	194(2)	22.4(4)
C7	1054(4)	7310.8(19)	-398(2)	26.8(4)

**Table 3.** Anisotropic Displacement Parameters ( $\times 10^4$ ) for **177**. The anisotropic displacement factor exponent takes the form:  $-2\sigma^2[h^2a^{*2} \times U_{11} + \dots + 2hka^* \times b^* \times U_{12}]$ .

Atom	$U_{11}$	$U_{22}$	$U_{33}$	$U_{23}$	$U_{13}$	$U_{12}$
O3	23.9(7)	27.3(7)	16.7(6)	0.4(5)	6.4(5)	7.0(6)
O4	27.9(8)	18.4(7)	19.3(7)	4.8(5)	-1.0(6)	0.9(6)
O5	21.3(7)	23.9(7)	23.3(6)	0.3(6)	-4.0(5)	-1.7(6)
O1	17.2(7)	50.4(10)	17.0(6)	-0.9(7)	6.0(5)	7.3(7)
O2	19.9(7)	85.0(15)	20.4(7)	13.1(8)	8.2(6)	4.4(9)
N1	14.0(7)	25.0(8)	13.2(7)	0.4(6)	4.8(6)	-1.3(7)
O6	30.4(10)	31.0(9)	62.9(12)	1.9(9)	-4.6(9)	-15.9(8)
C4	14.7(9)	17.8(8)	14.6(7)	0.8(7)	3.7(7)	1.9(7)
C11	16.7(9)	15.4(8)	15.8(8)	-0.9(7)	1.8(7)	-3.0(7)
C13	16.9(9)	22.5(10)	13.8(8)	-0.4(7)	3.6(7)	0.8(8)
C8	19.0(10)	22.8(9)	22.0(9)	-1.6(7)	1.2(8)	7.3(8)
C12	17.6(9)	17.7(9)	14.9(8)	2.1(7)	3.0(7)	-4.2(7)
C2	15.5(9)	19.2(9)	20.9(9)	-3.7(7)	3.7(8)	3.7(7)
C14	19.2(9)	23.9(10)	15.7(8)	1.5(7)	3.5(7)	-0.3(8)
C1	17.5(9)	25.3(10)	21.7(9)	-0.5(8)	7.2(7)	-0.8(8)
C15	21.5(10)	15.1(9)	22.0(9)	-0.8(7)	1.3(8)	-0.9(8)
C3	15.2(9)	22.3(10)	21.3(9)	-5.2(7)	3.8(8)	0.7(7)
C10	15.1(9)	46.4(13)	15.4(8)	-1.3(9)	2.9(7)	-0.5(9)
C5	22.4(10)	20.1(9)	17.4(8)	-2.2(7)	0.7(7)	4.9(8)
C6	16.5(9)	19.1(9)	37.6(11)	1.0(9)	2.8(8)	-0.3(8)
C16	24.5(11)	19.0(10)	29.8(10)	-2.7(8)	-0.2(8)	-1.7(8)
C17	30.0(12)	17.8(9)	19.4(9)	0.8(8)	-0.1(8)	4.8(8)
C9	16.7(9)	25.8(10)	24.0(9)	-3.9(8)	4.7(8)	-1.1(8)
C7	24.8(11)	19.7(10)	33.6(11)	6.5(8)	5.2(9)	3.8(8)

**Table 4.** Bond Lengths in Å for **177**.

Atom	Atom	Length/Å	Atom	Atom	Length/Å
O3	C11	1.216(2)	C11	C12	1.514(2)
O4	C14	1.391(3)	C13	C12	1.545(3)
O4	C17	1.435(2)	C13	C14	1.549(3)
O5	C14	1.442(3)	C13	C15	1.528(3)
O5	C16	1.354(3)	C8	C9	1.392(3)
O1	C3	1.464(2)	C8	C7	1.385(3)
O1	C10	1.348(3)	C12	C17	1.524(3)
O2	C10	1.198(3)	C2	C1	1.393(3)
N1	C4	1.479(2)	C2	C3	1.502(3)
N1	C11	1.388(3)	C2	C6	1.389(3)
N1	C10	1.396(2)	C1	C9	1.388(3)

O6	C16	1.192(3)	C15	C16	1.507(3)
C4	C3	1.540(3)	C6	C7	1.394(3)
C4	C5	1.511(3)			

**Table 5.** Bond Angles in ° for **177**.

Atom	Atom	Atom	Angle/°	Atom	Atom	Atom	Angle/°
C14	O4	C17	109.20(15)	C6	C2	C1	119.97(18)
C16	O5	C14	112.25(16)	C6	C2	C3	118.34(19)
C10	O1	C3	109.92(16)	O4	C14	O5	110.00(16)
C11	N1	C4	121.34(15)	O4	C14	C13	108.51(15)
C11	N1	C10	127.50(16)	O5	C14	C13	107.18(16)
C10	N1	C4	110.09(15)	C9	C1	C2	120.03(19)
N1	C4	C3	99.08(14)	C16	C15	C13	106.03(16)
N1	C4	C5	111.16(16)	O1	C3	C4	103.20(16)
C5	C4	C3	114.62(16)	O1	C3	C2	110.73(17)
O3	C11	N1	118.97(16)	C2	C3	C4	115.57(16)
O3	C11	C12	122.53(18)	O1	C10	N1	108.51(17)
N1	C11	C12	118.39(16)	O2	C10	O1	123.4(2)
C12	C13	C14	102.37(16)	O2	C10	N1	128.1(2)
C15	C13	C12	115.62(15)	C2	C6	C7	119.7(2)
C15	C13	C14	103.87(16)	O5	C16	C15	110.23(18)
C7	C8	C9	119.81(19)	O6	C16	O5	121.7(2)
C11	C12	C13	113.93(15)	O6	C16	C15	128.1(2)
C11	C12	C17	112.18(16)	O4	C17	C12	104.31(16)
C17	C12	C13	102.23(15)	C1	C9	C8	120.1(2)
C1	C2	C3	121.60(19)	C8	C7	C6	120.4(2)

**Table 6.** Hydrogen Fractional Atomic Coordinates ( $\times 10^4$ ) and Equivalent Isotropic Displacement Parameters ( $\text{\AA}^2 \times 10^3$ ) for **177**.  $U_{eq}$  is defined as 1/3 of the trace of the orthogonalized  $U_{ij}$ .

Atom	x	y	z	$U_{eq}$
H4	6969.99	5457	2443.33	19
H13	8519.65	4774.93	7212.31	21
H8	-1827.3	6782.87	-1466.23	27
H12	7834.83	3028.11	6063.65	21
H14	10914.53	3805.28	8828.4	24
H1	428.96	4971.51	1938.73	25
H15A	10921.64	5398	5594.17	25
H15B	10119.47	6269.88	6511.29	25

Appendix

---

H3	4946.05	6733.79	3163.54	24
H5A	5906.38	3468.79	1737.16	32
H5B	4524.82	4421.46	788.58	32
H5C	3671.03	3769.12	1837.39	32
H6	3854.84	7572.02	971.99	31
H17A	10557.5	1872.7	5900.91	29
H17B	11911.58	2988.66	5754.33	29
H9	-2226.7	5324.75	4.67	27
H7	1215.88	7892.08	-988.63	32

---

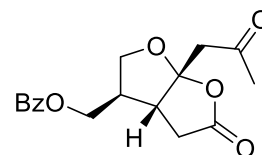
#### **4. Light transmission aggregometry**

Sample with antagonist: upper graph

Sample without antagonist: lower graph

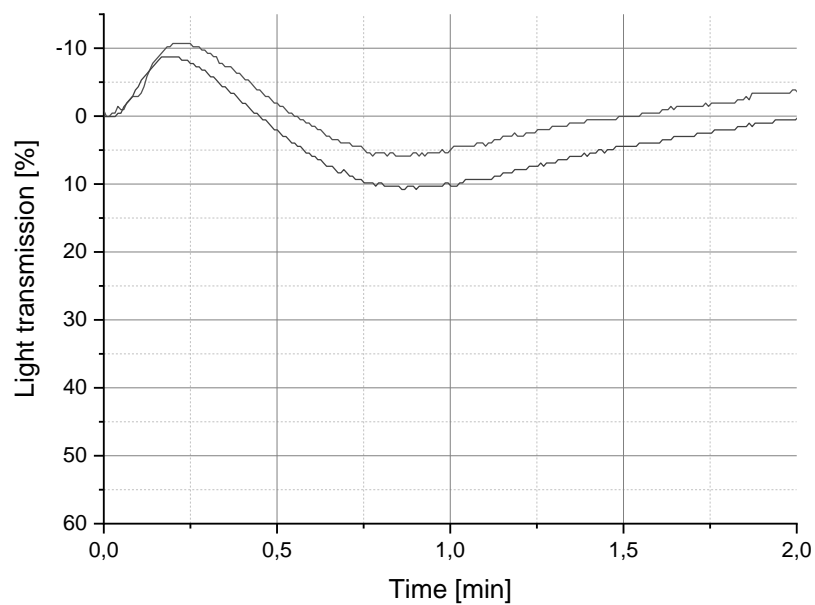
Concentrations are stated at each spectrum.



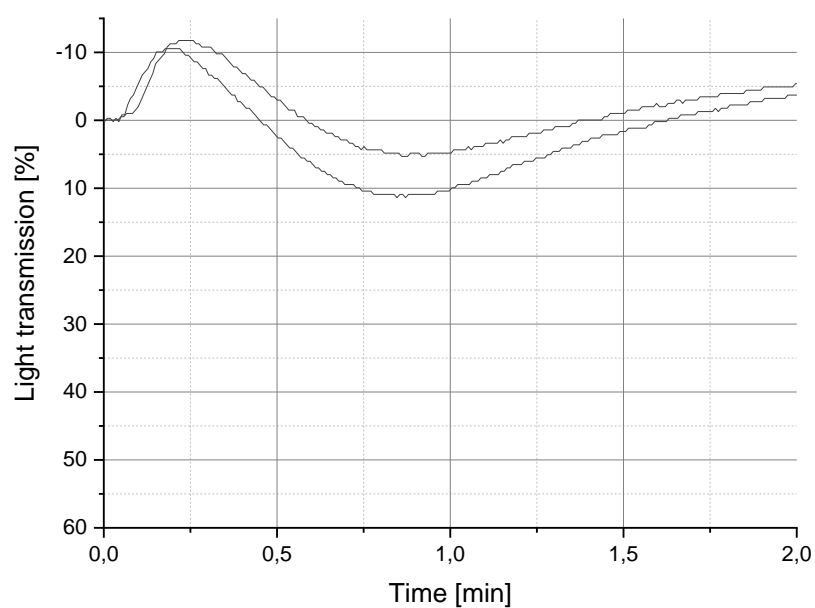


**((3R,3aR,6aR)-5-Oxo-6a-(2-oxopropyl)hexahydrofuro[2,3-b]furan-3-yl)methyl benzoate (49)**

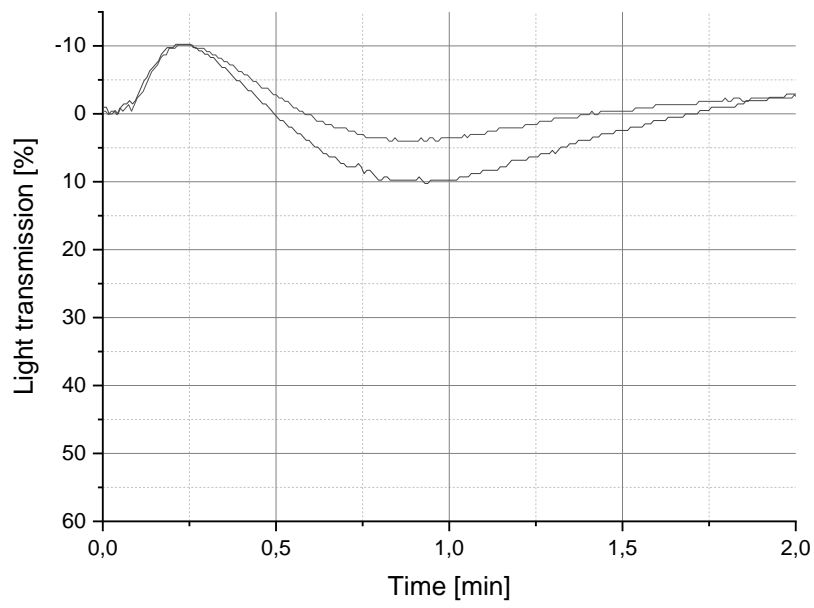
10 µg/mL



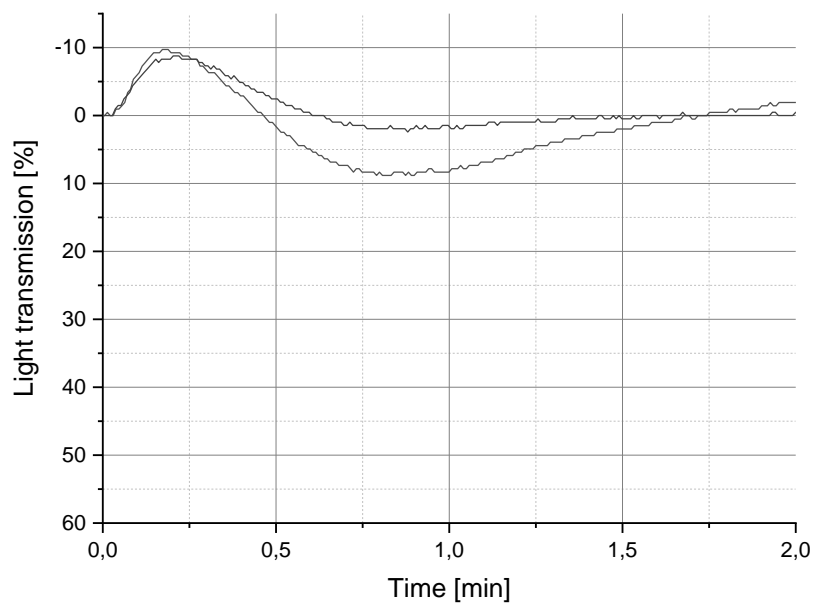
25 µg/mL



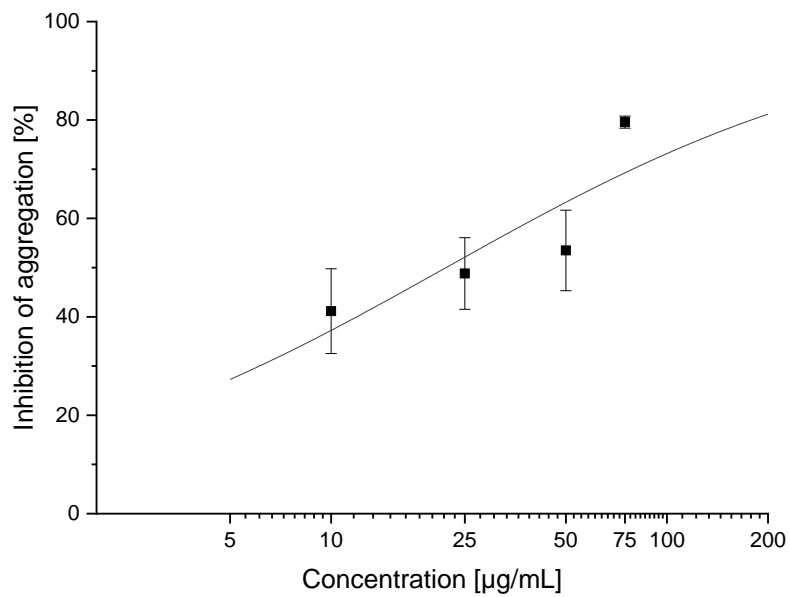
50 µg/mL



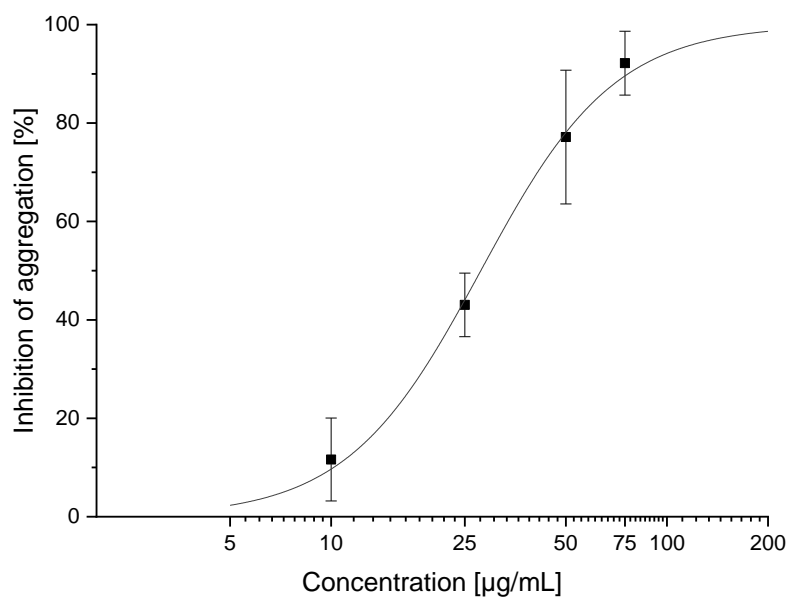
75 µg/mL

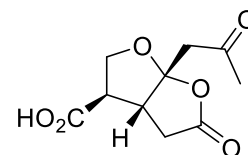


Maximum aggregation:



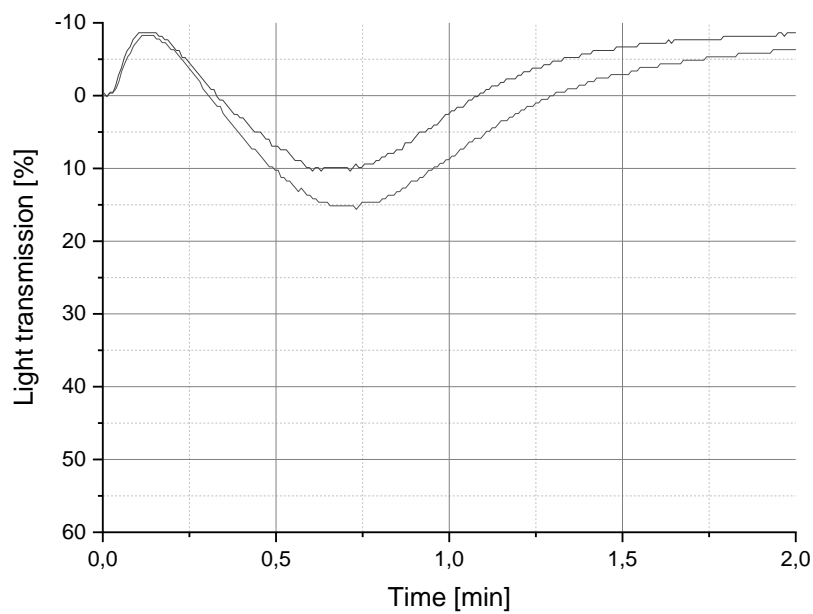
Slope:



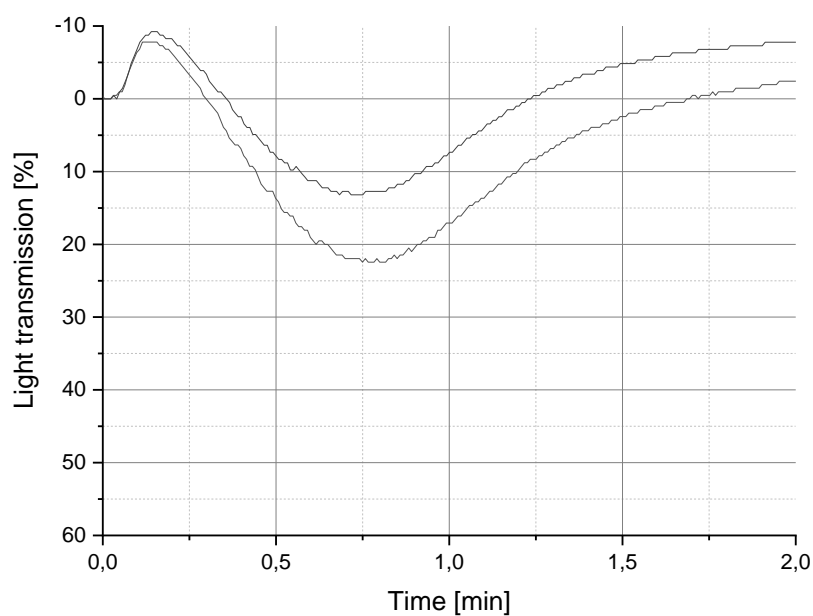


**(3R,3aR,6aR)-5-Oxo-6a-(2-oxopropyl)hexahydrofuro[2,3-*b*]furan-3-carboxylic acid (181)**

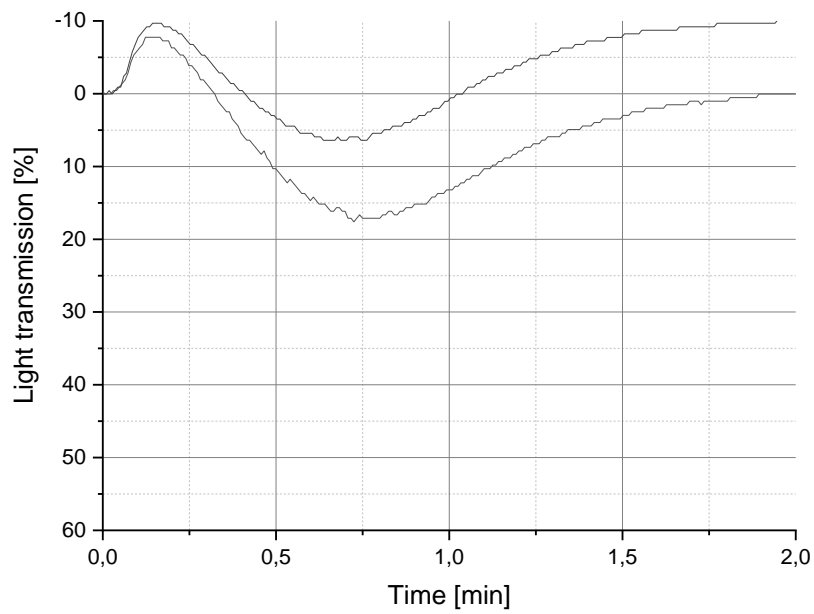
50 µg/mL



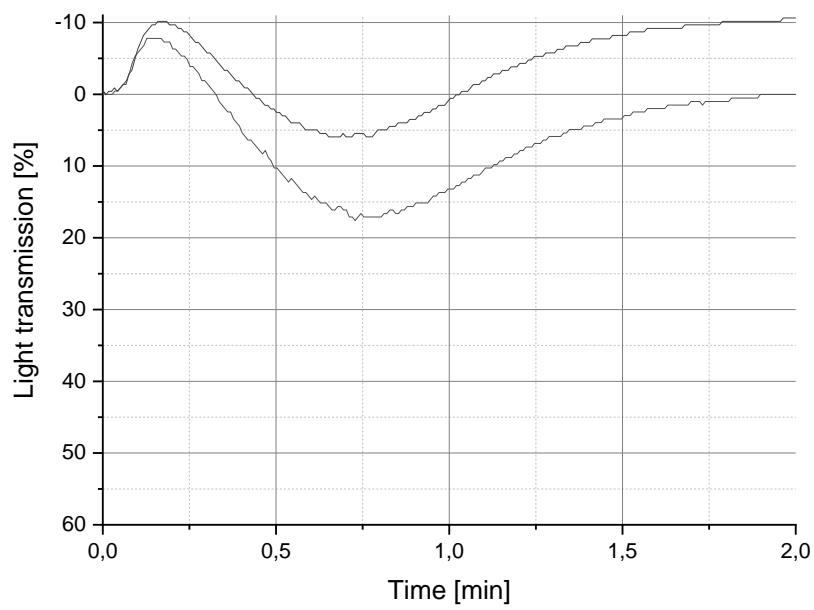
100 µg/mL



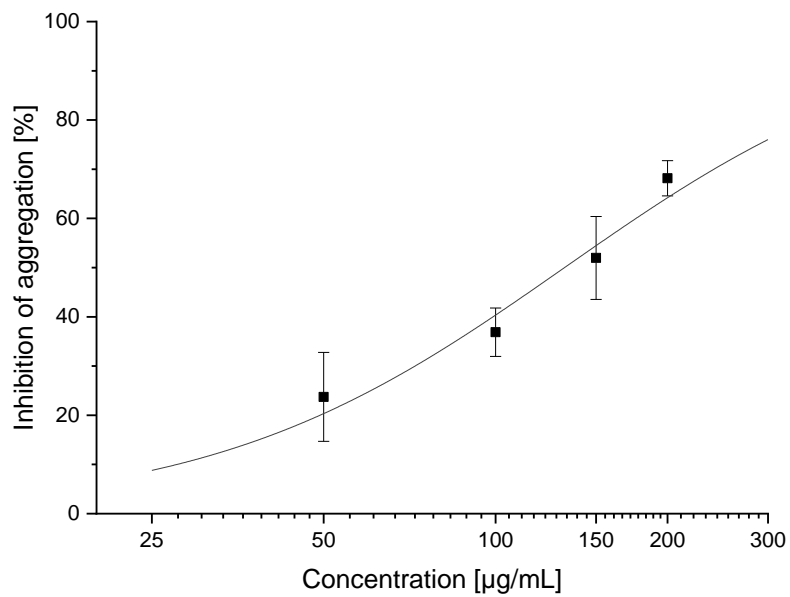
150 µg/mL



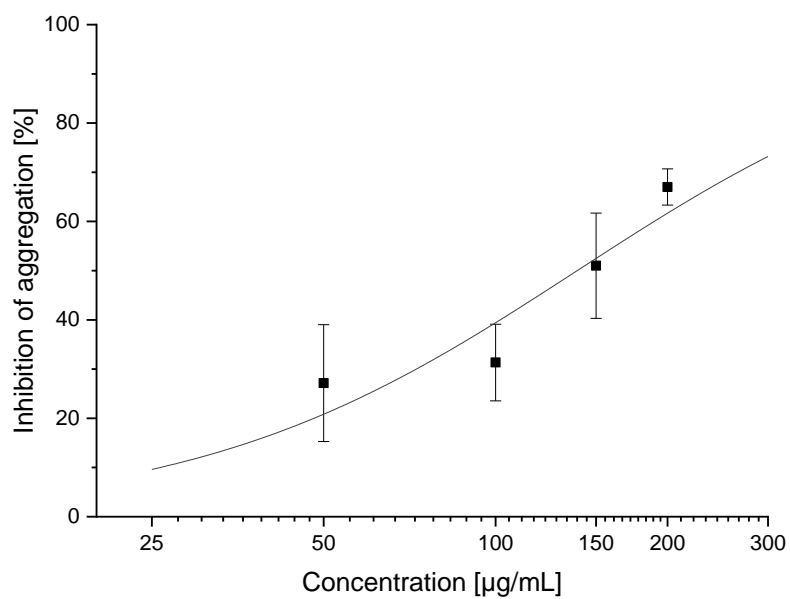
200 µg/mL

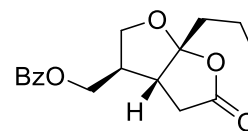


Maximum aggregation:

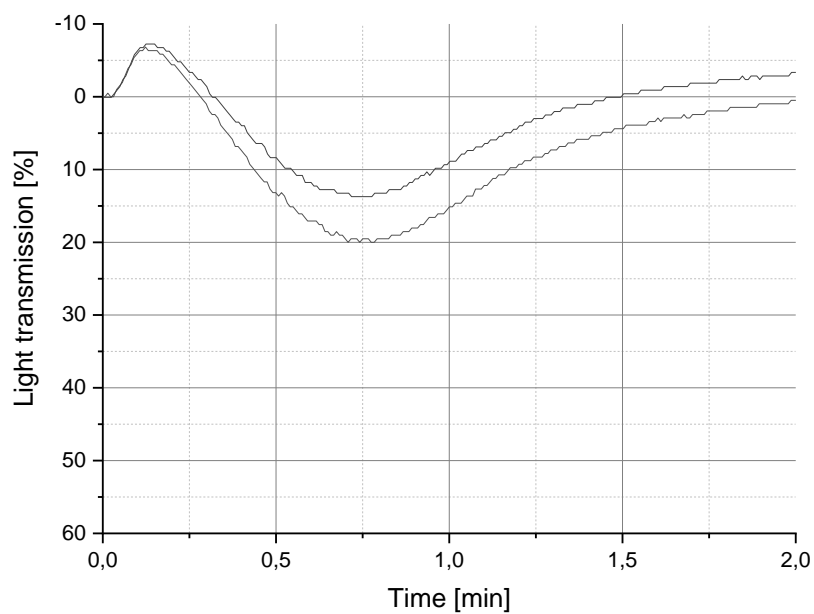


Slope:

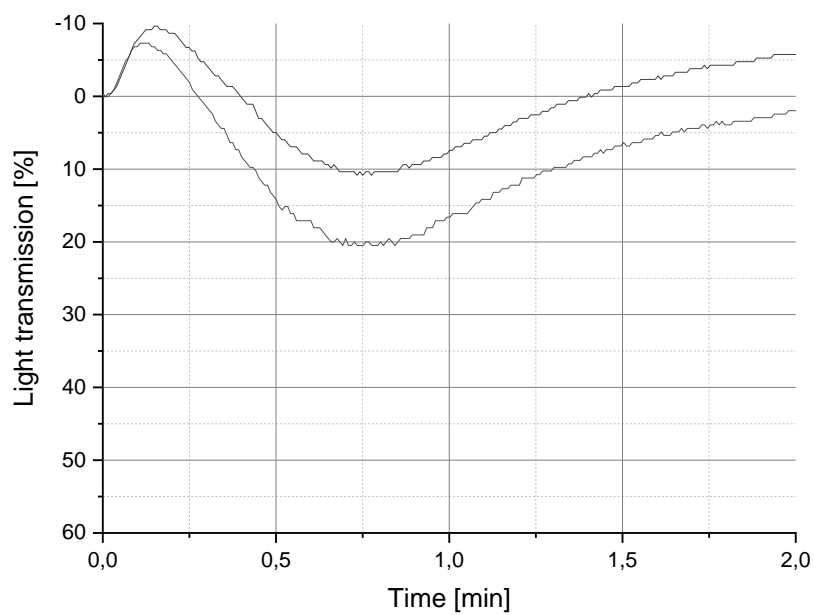


**((3R,3aR,6aR)-5-Oxo-6a-propylhexahydrofuro[2,3-b]furan-3-yl)methyl benzoate (182)**

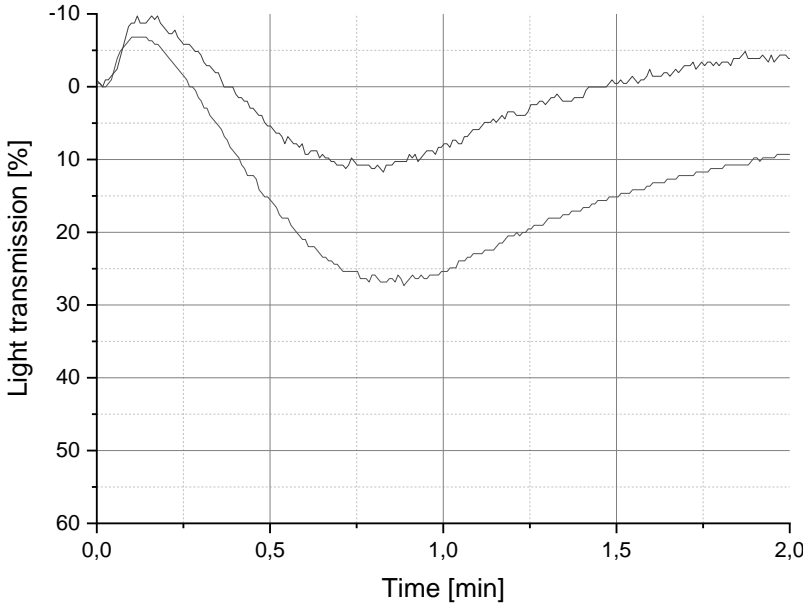
50 µg/mL



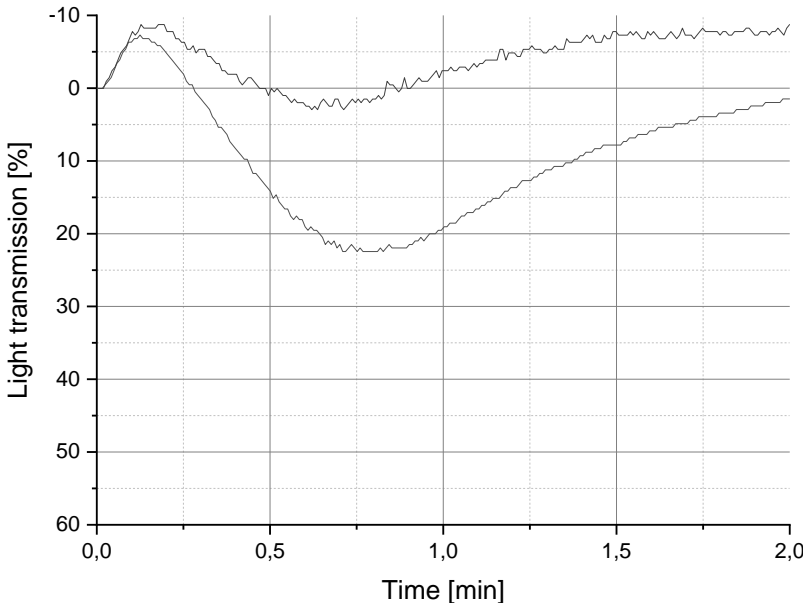
100 µg/mL



150 µg/mL

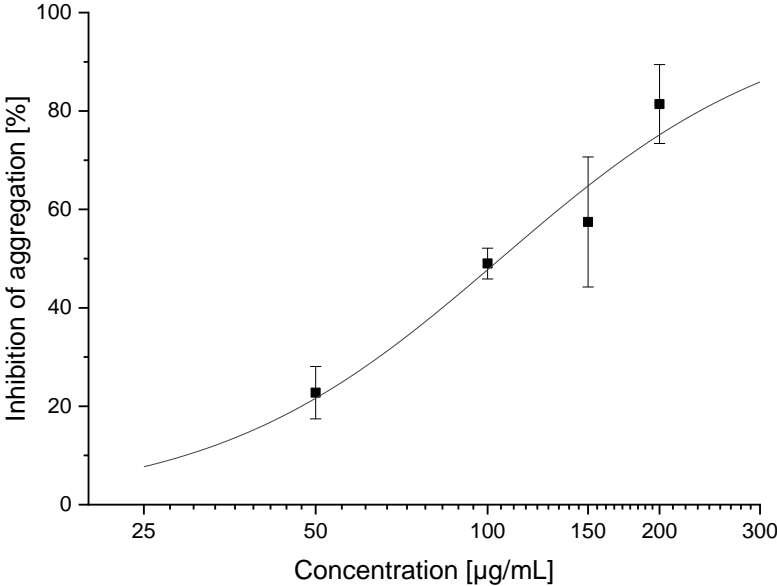


200 µg/mL

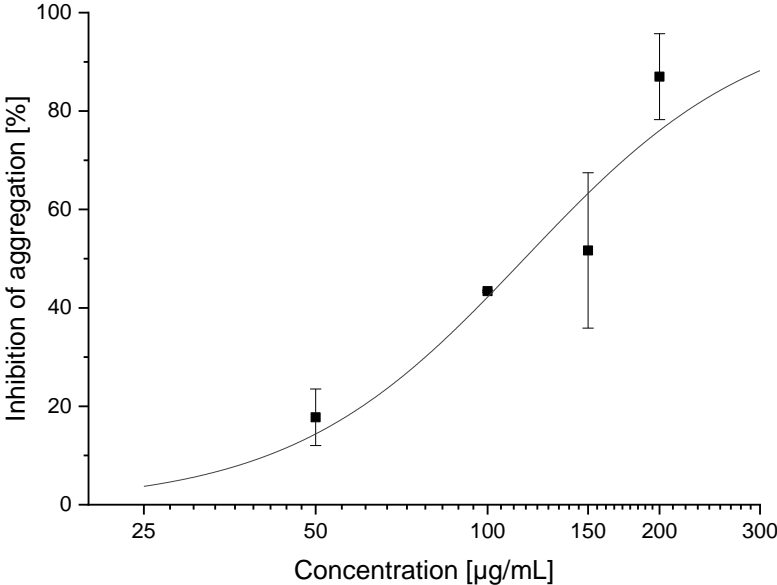


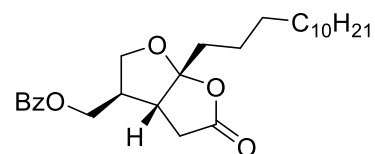


Maximum aggregation:

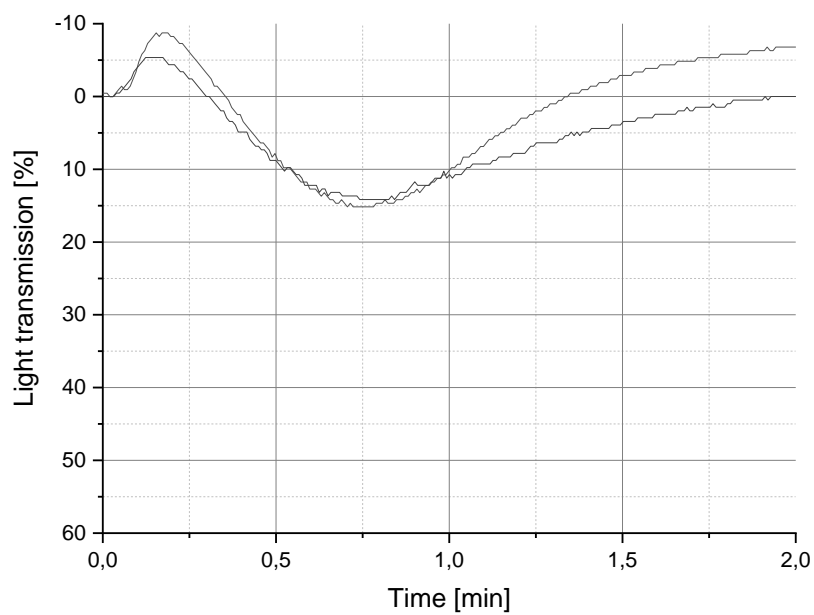


Slope:

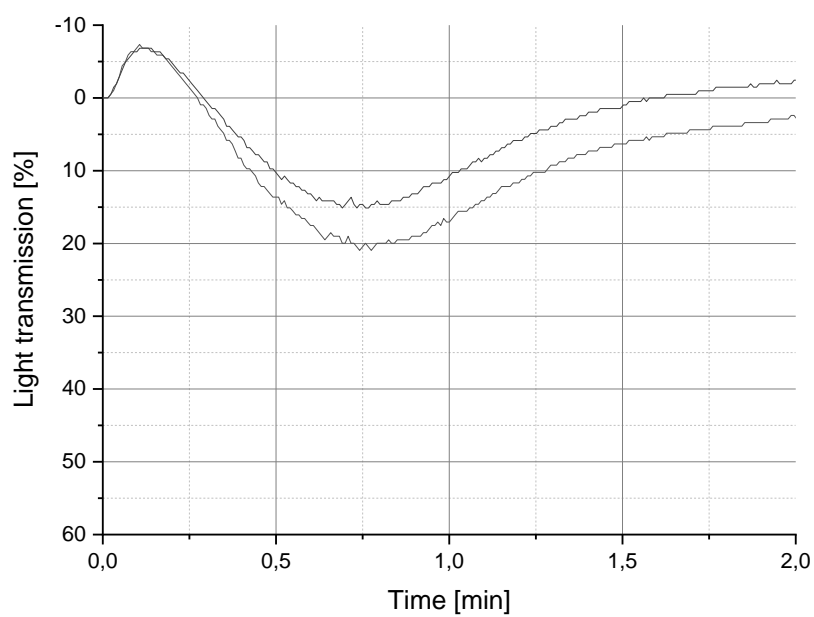


**((3R,3aR,6aR)-5-Oxo-6a-tridecylhexahydrofuro[2,3-b]furan-3-yl)methyl benzoate (184)**

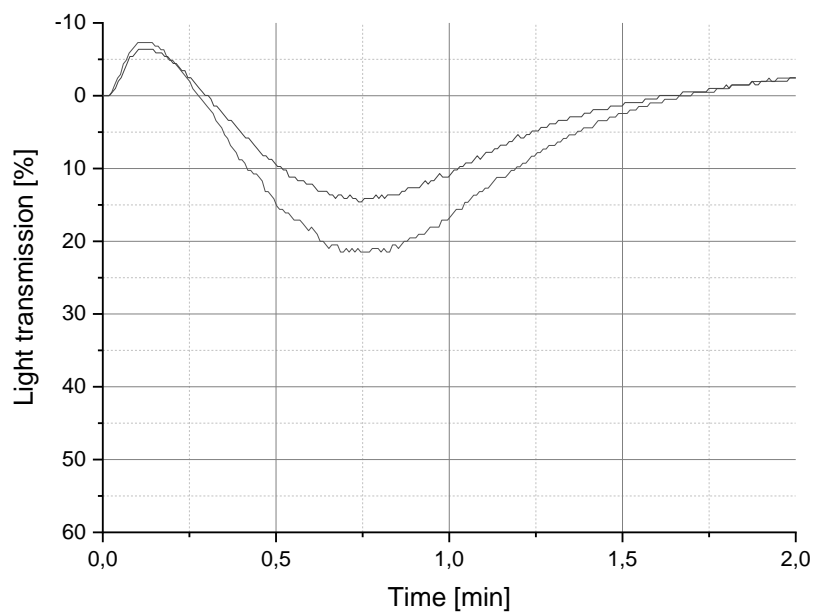
50 µg/mL



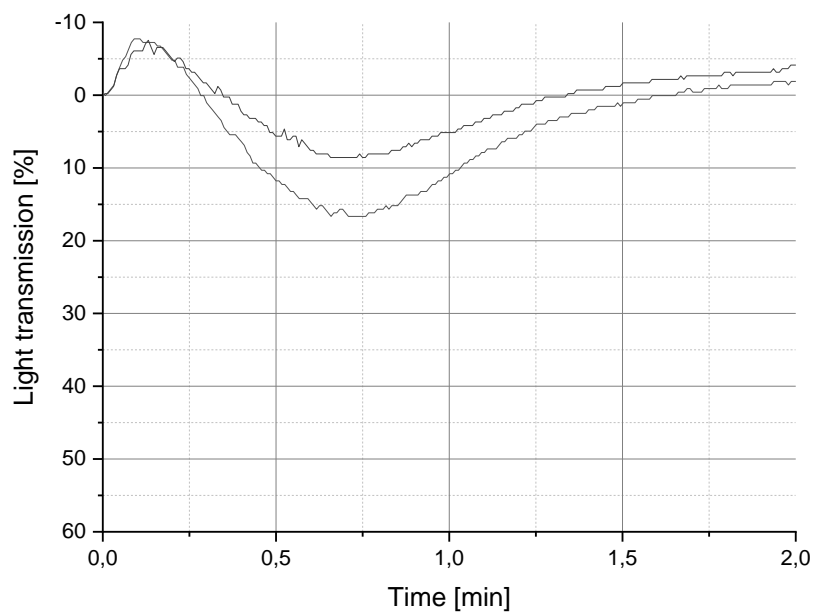
100 µg/mL



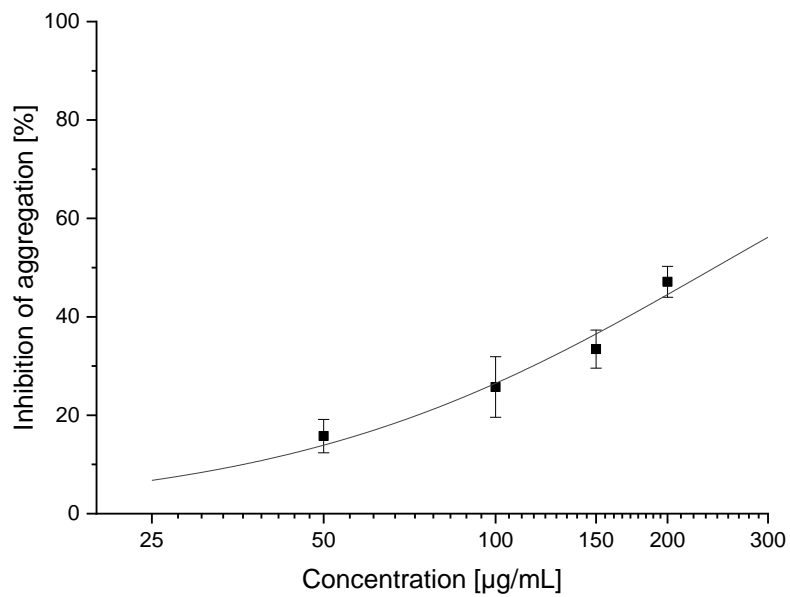
150 µg/mL



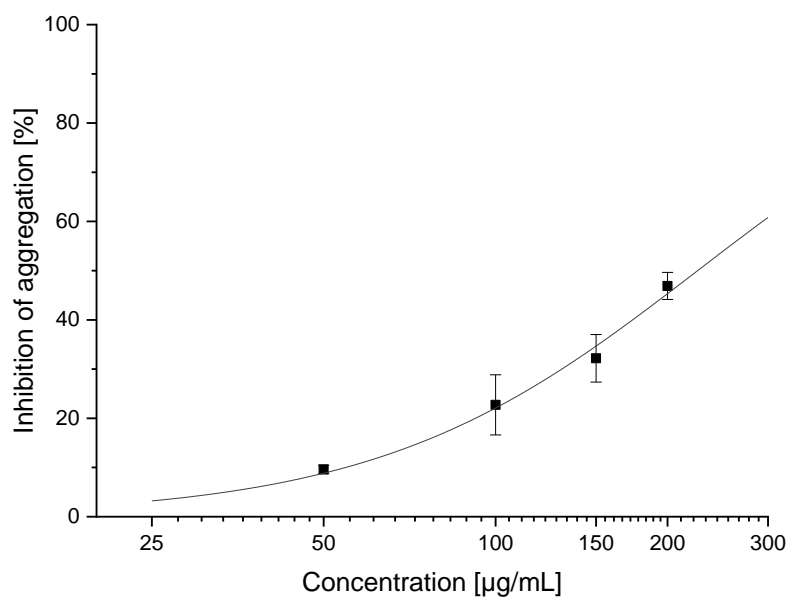
200 µg/mL

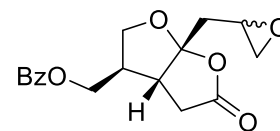


Maximum aggregation:



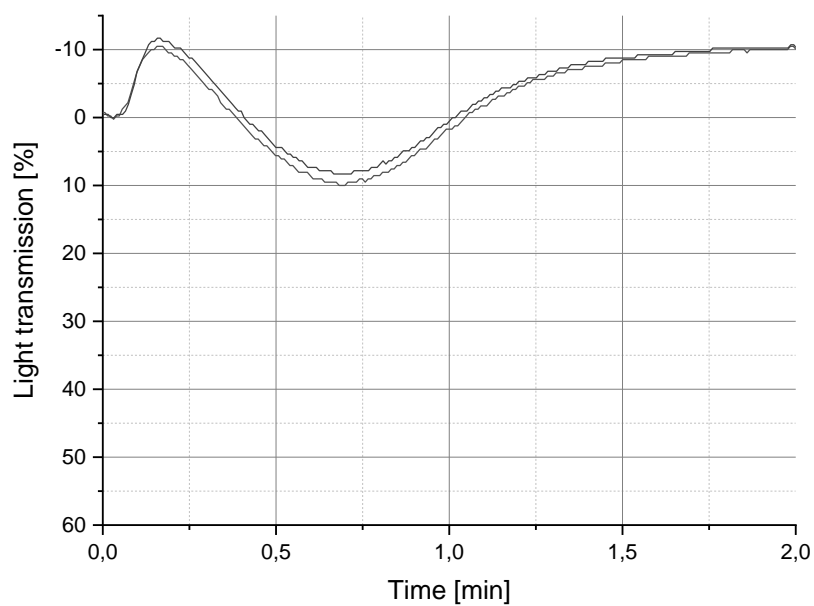
Slope:



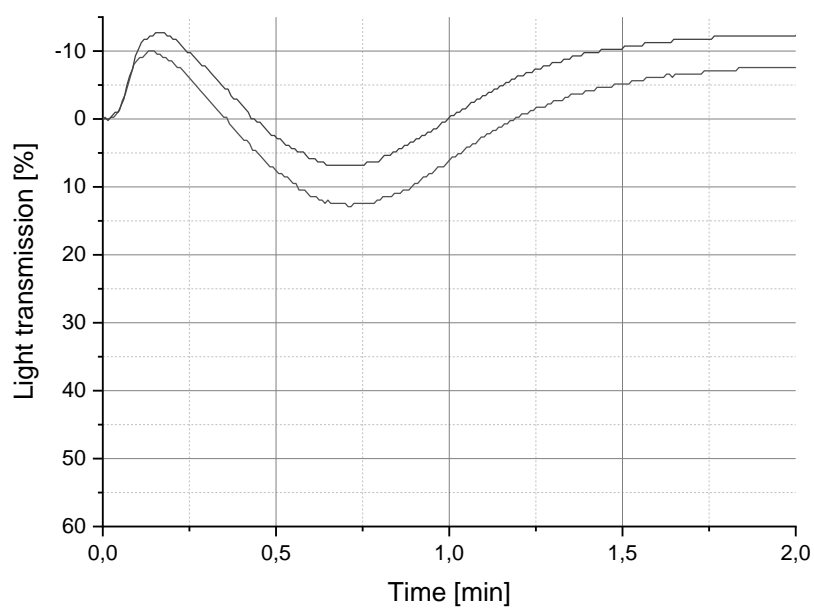


**((3*R*,3*aR*,6*aR*)-6*a*-(Oxiran-2-ylmethyl)-5-oxohexahydrofuro[2,3-*b*]furan-3-yl)methyl benzoate (185)**

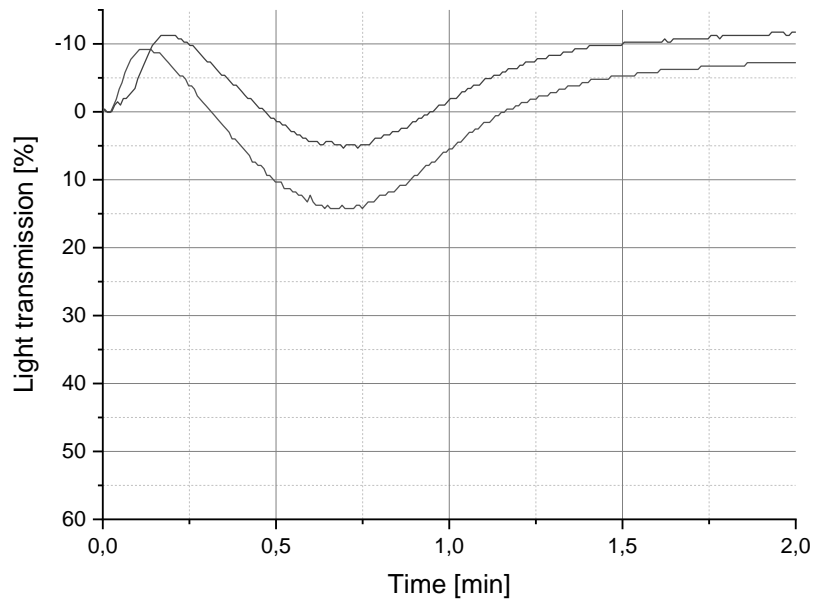
12.5 µg/mL



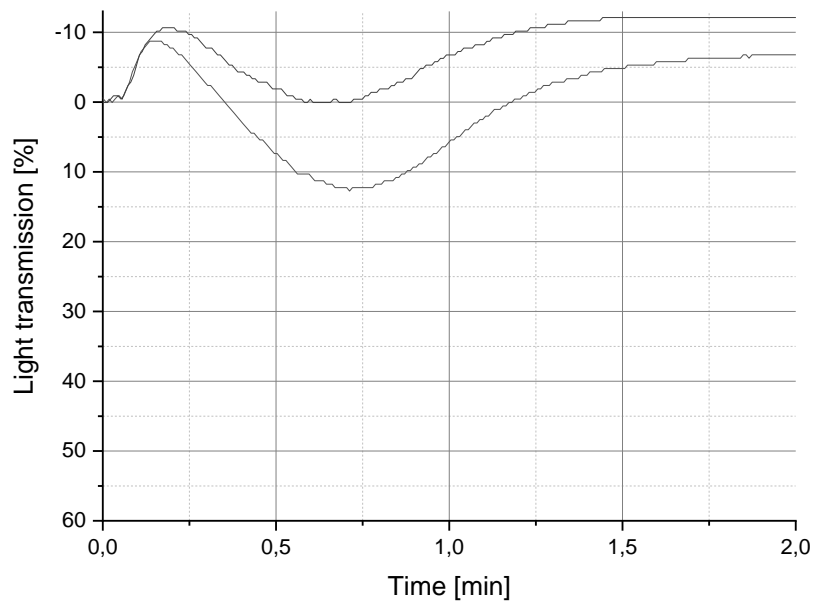
25 µg/mL



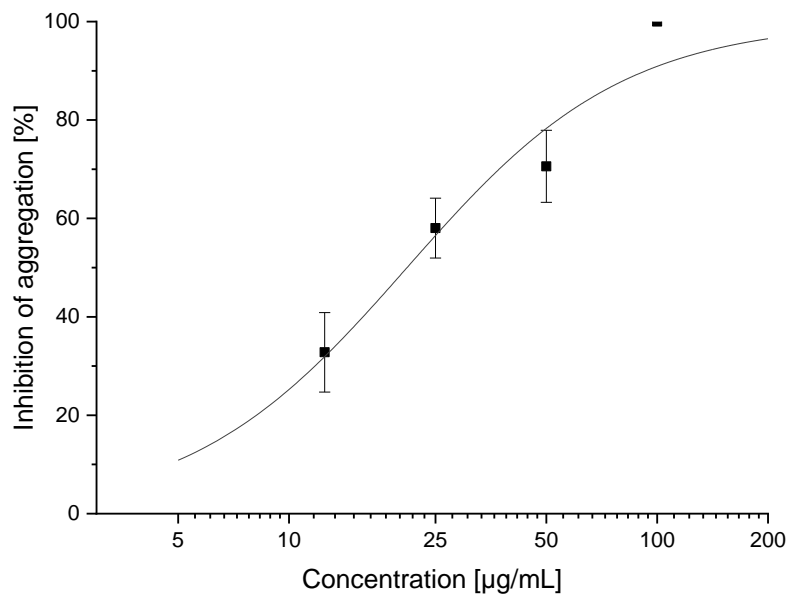
50 µg/mL



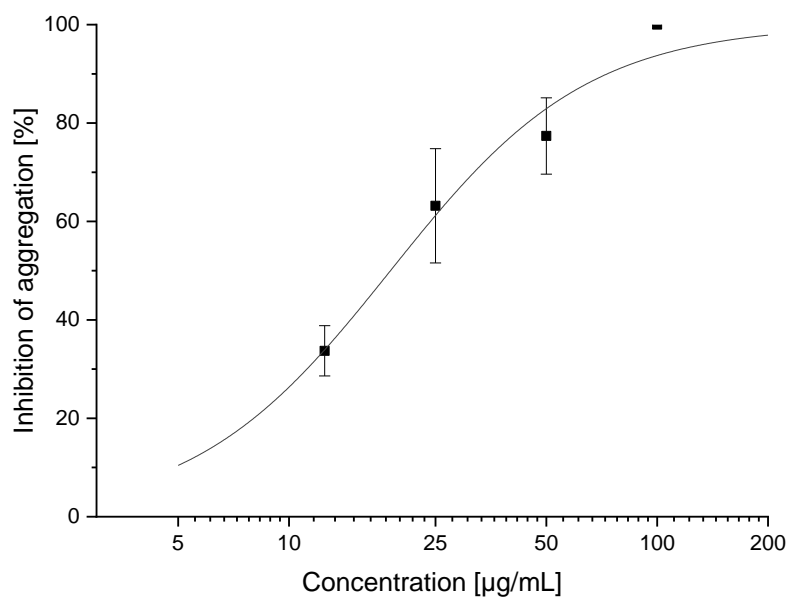
100 µg/mL

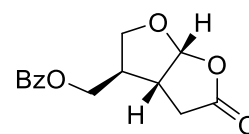


Maximum aggregation:

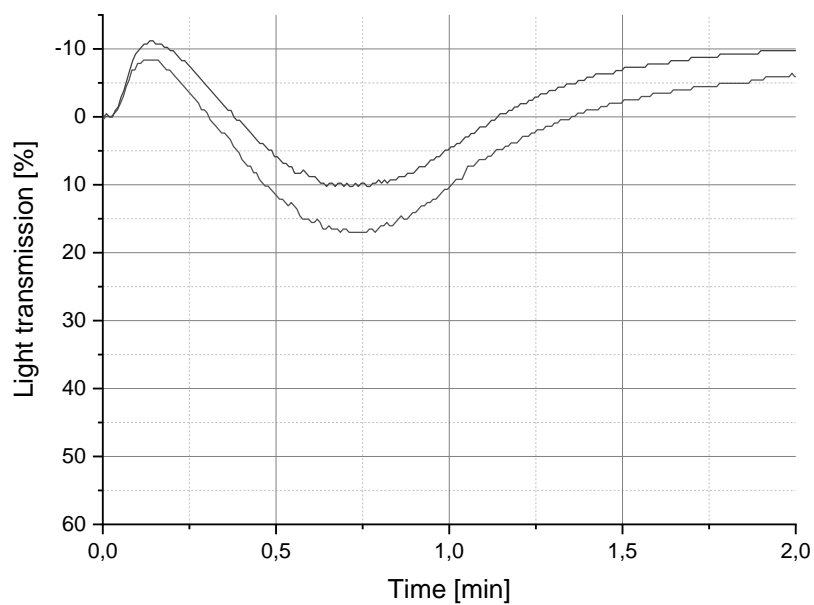


Slope:

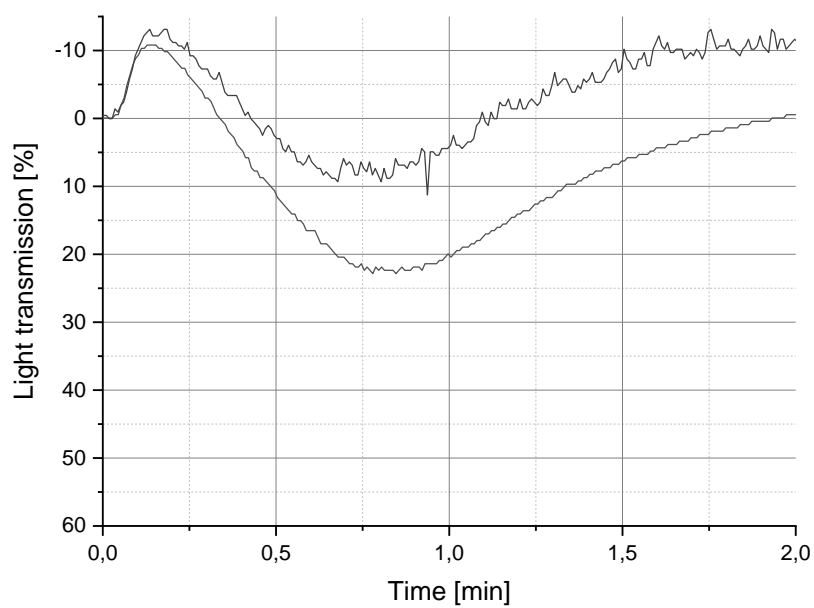


**((3R,3aR,6aR)-5-Oxohexahydrofuro[2,3-*b*]furan-3-yl)methyl benzoate (186)**

50 µg/mL

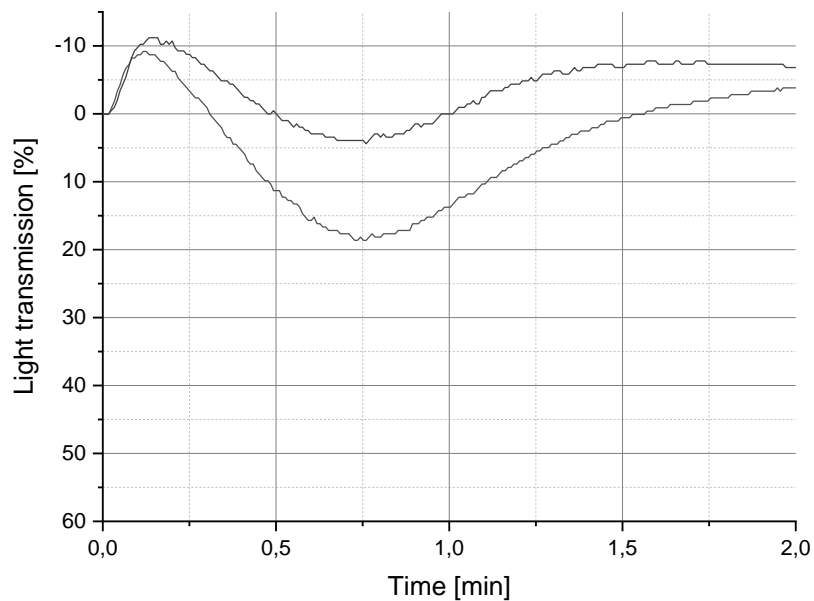


100 µg/mL

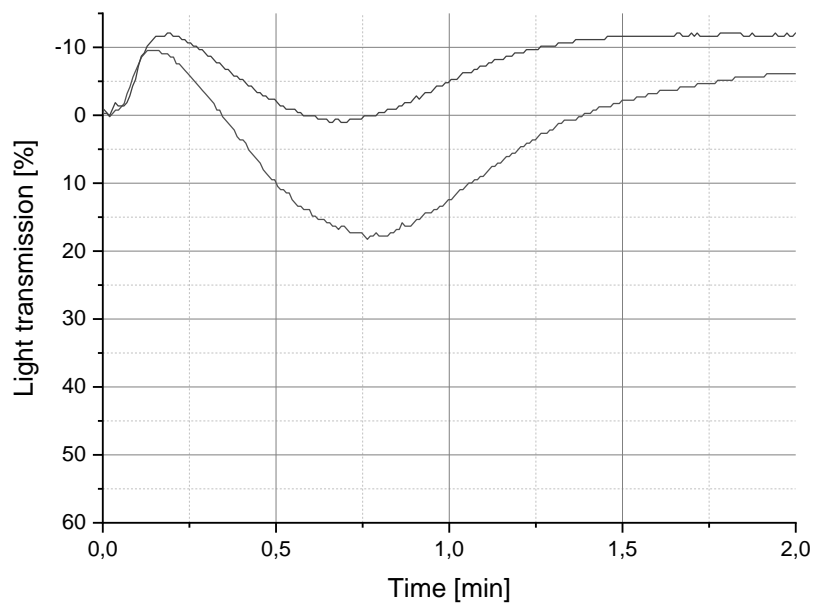




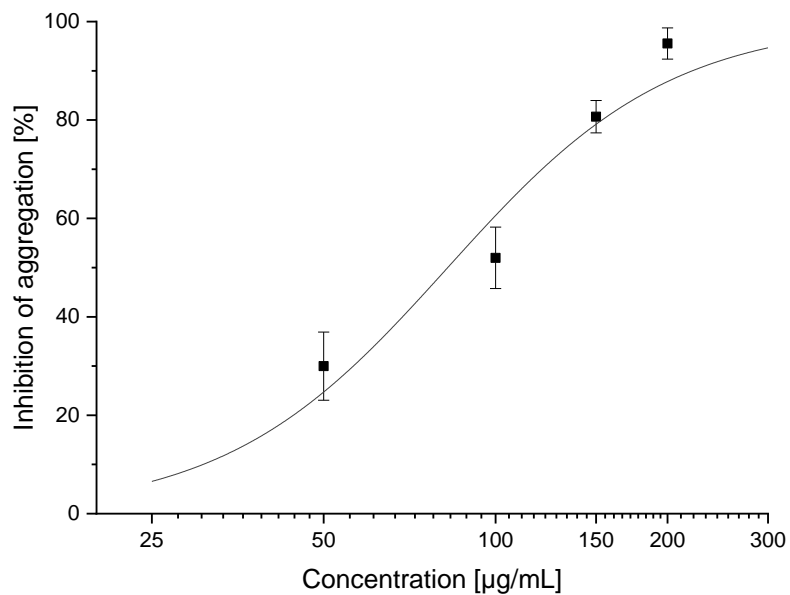
150 µg/mL



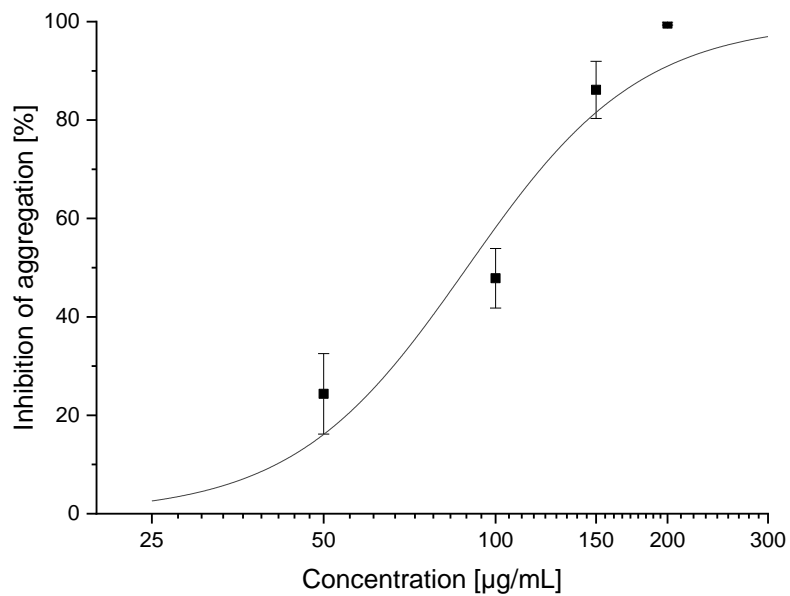
200 µg/mL

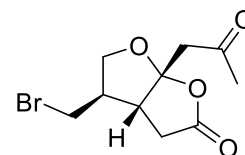


Maximum aggregation:



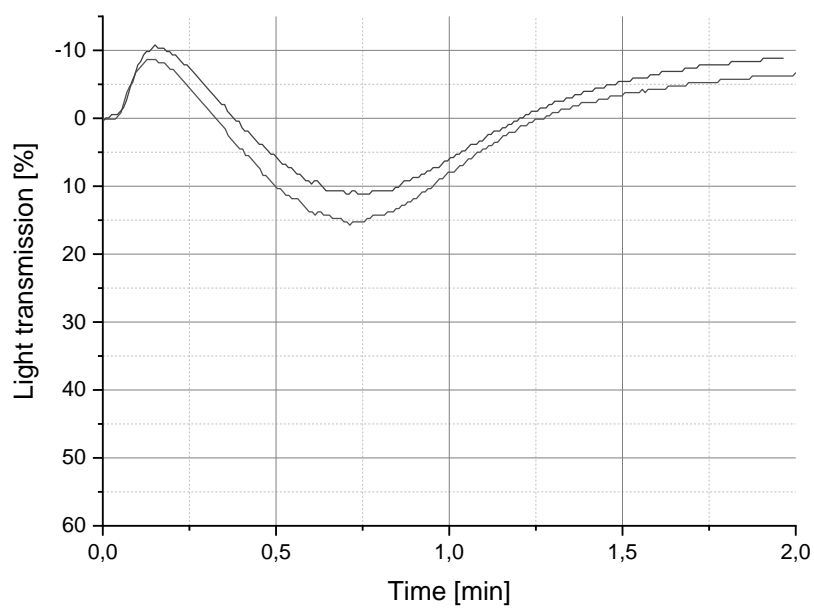
Slope:



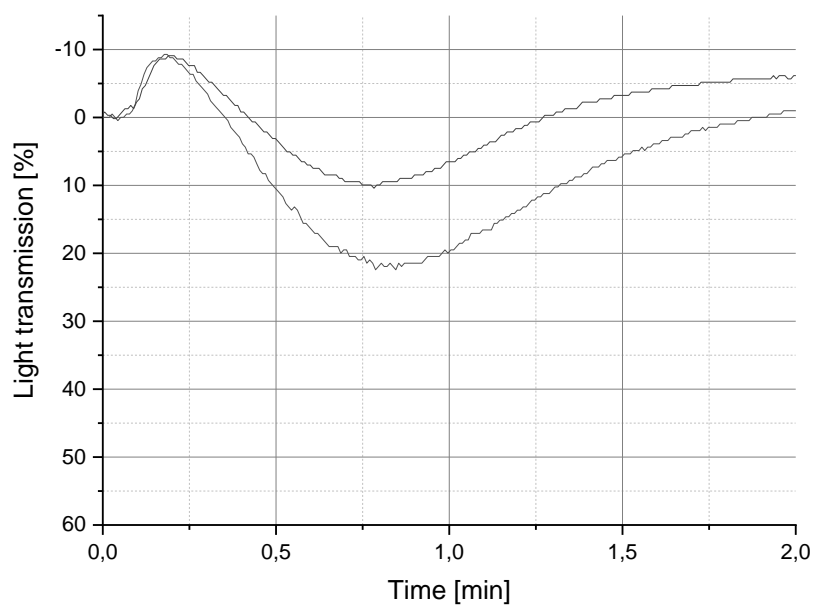


**(3aR,4R,6aR)-4-(Bromomethyl)-6a-(2-oxopropyl)tetrahydrofuro[2,3-b]furan-2(3H)-one  
(187)**

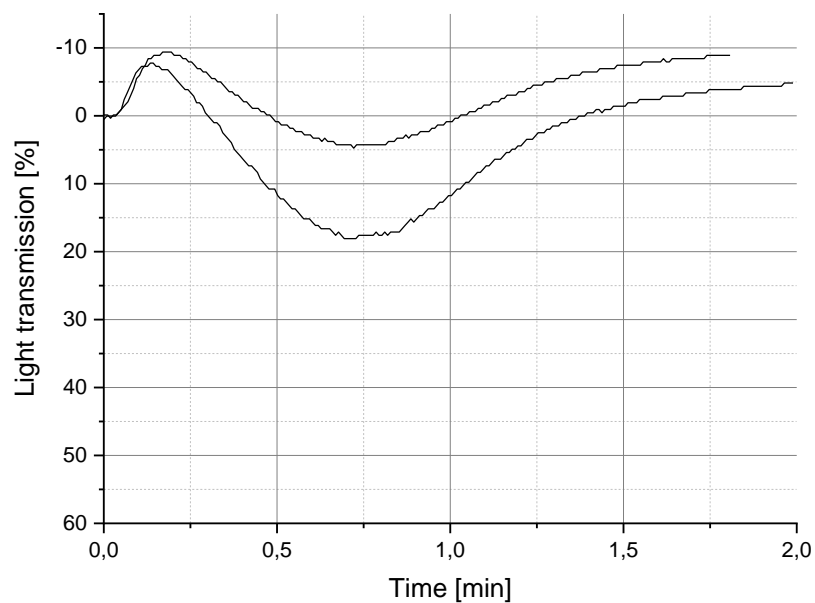
10 µg/mL



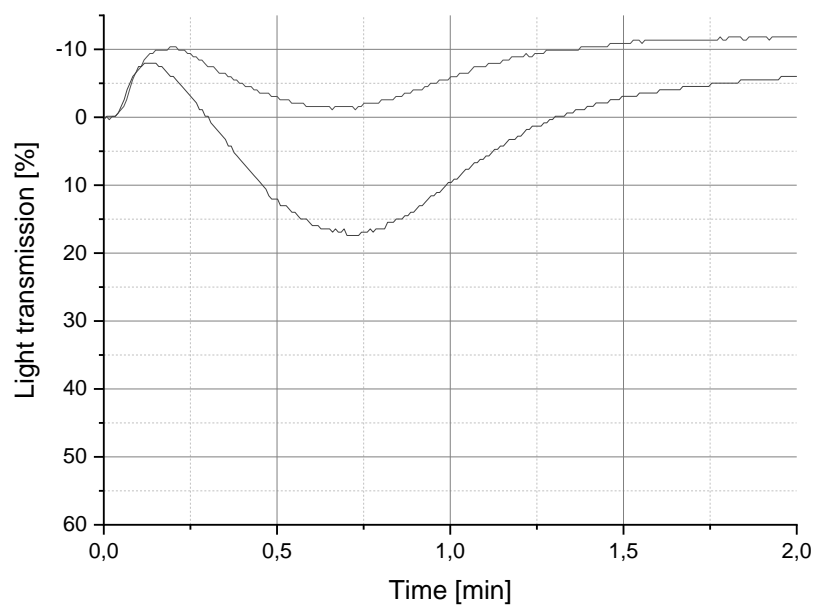
50 µg/mL



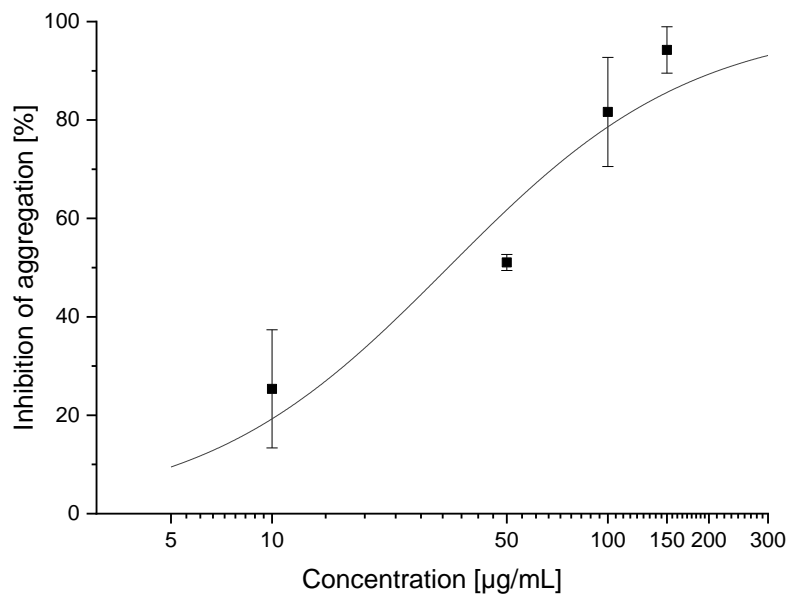
100 µg/mL



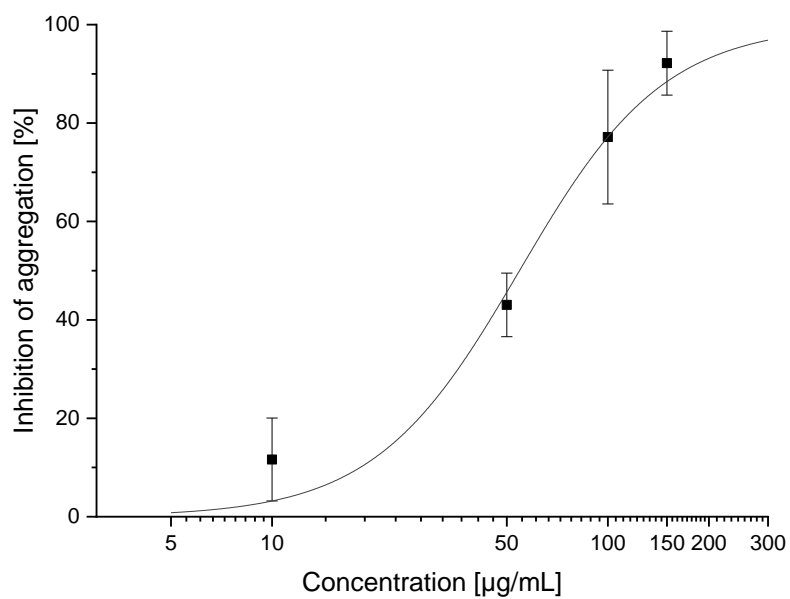
150 µg/mL

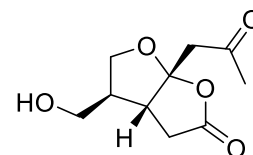


Maximum aggregation:



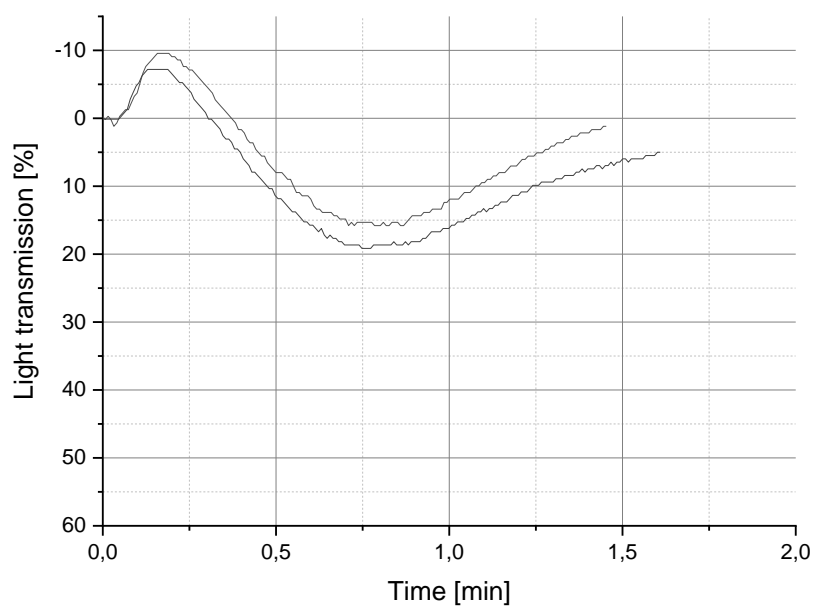
Slope:



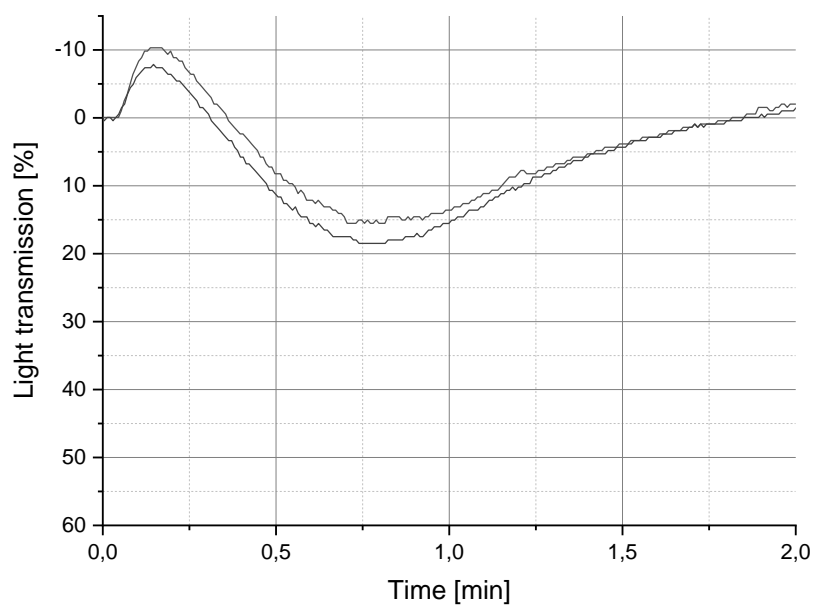


**(3aR,4S,6aR)-4-(Hydroxymethyl)-6a-(2-oxopropyl)tetrahydrofuro[2,3-b]furan-2(3H)-one  
(188)**

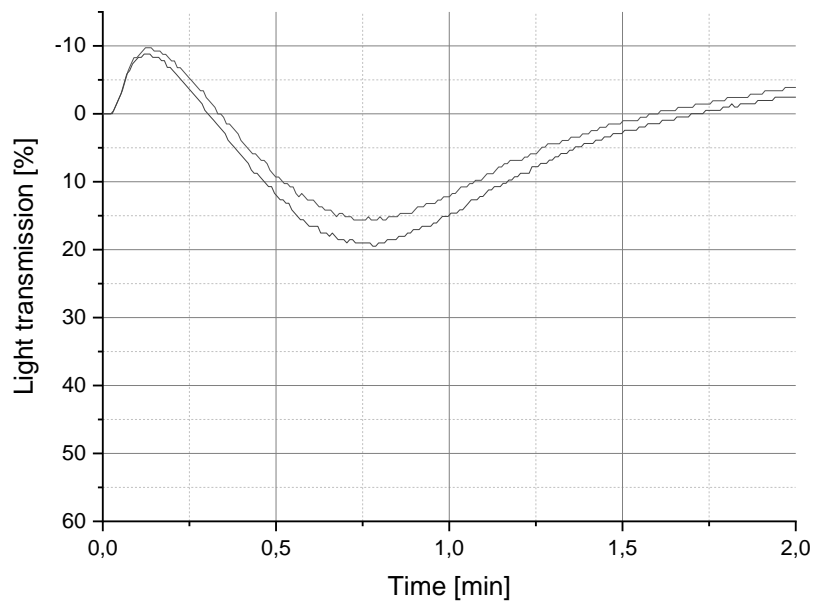
50 µg/mL



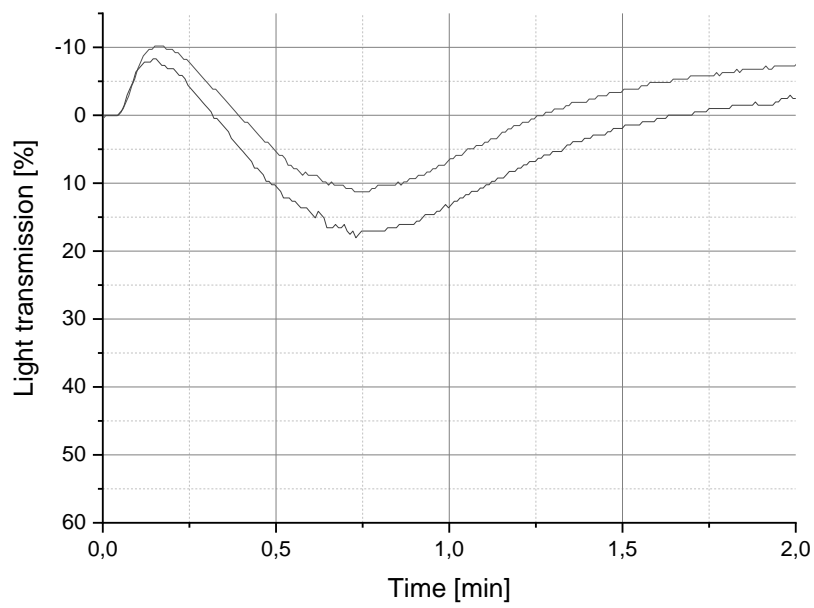
100 µg/mL



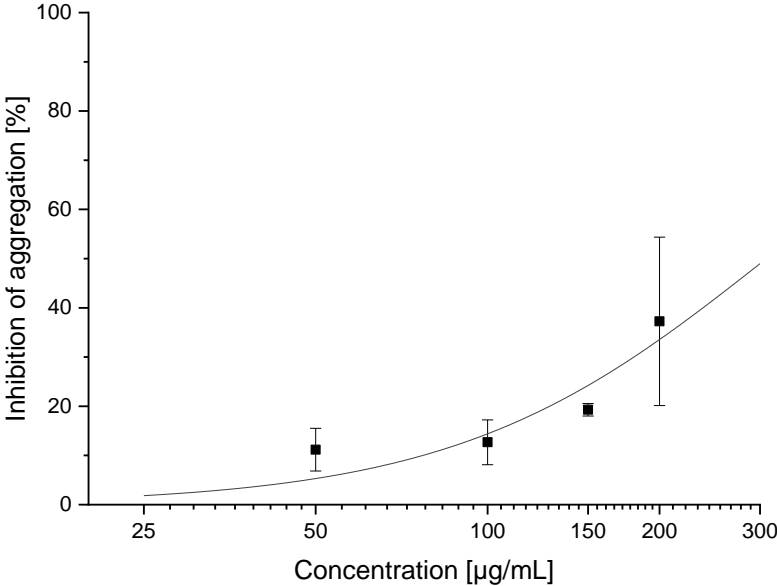
150 µg/mL



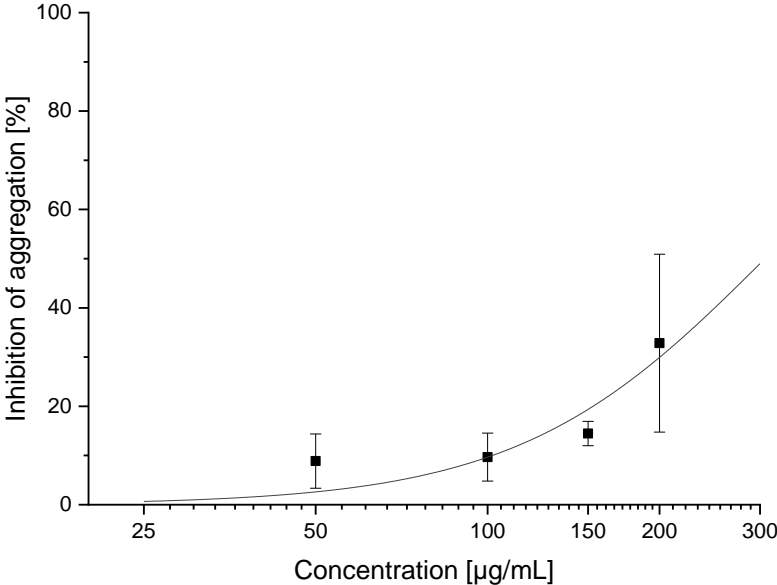
200 µg/mL



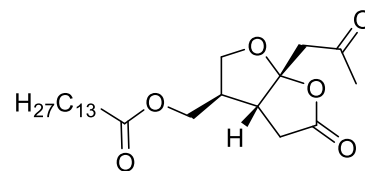
Maximum aggregation:



Slope:

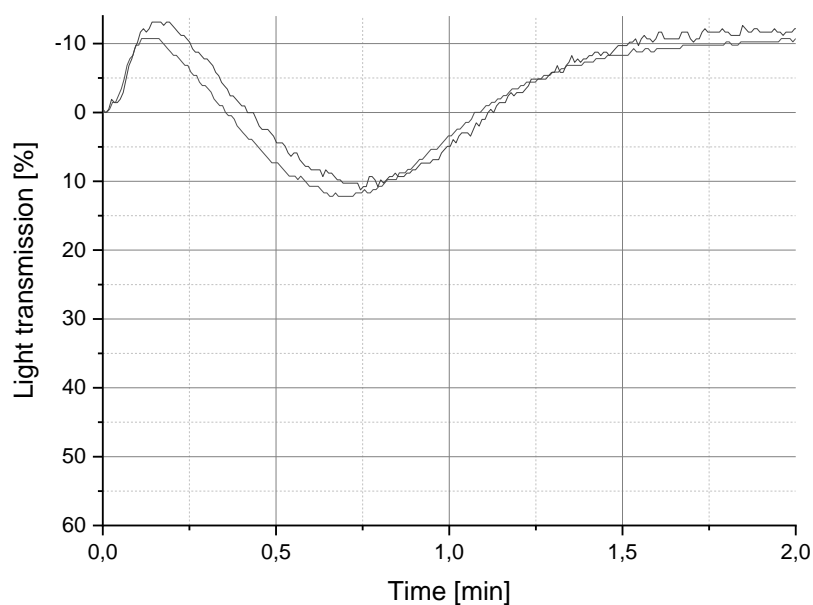




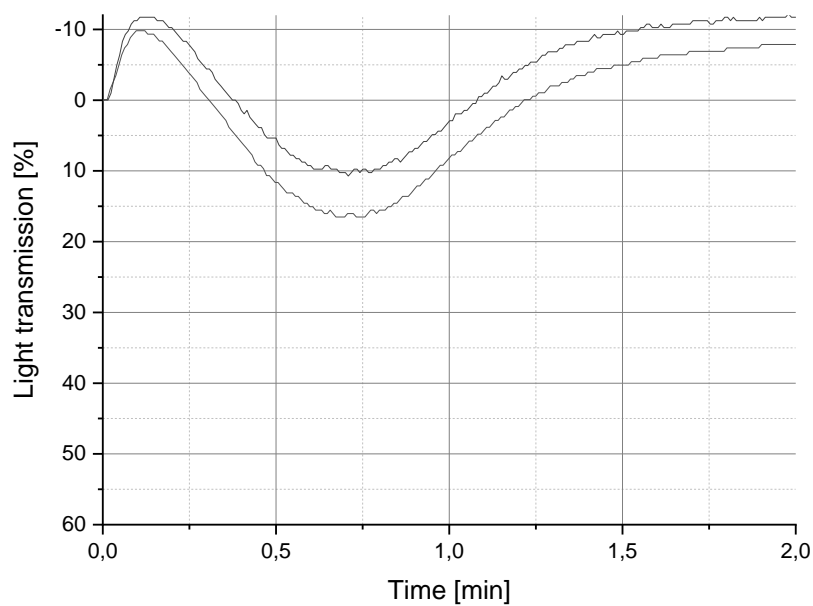


**((3*R*,3*aR*,6*aR*)-5-Oxo-6*a*-(2-oxopropyl)hexahydrofuro[2,3-*b*]furan-3-yl)methyl  
tetradecanoate (189)**

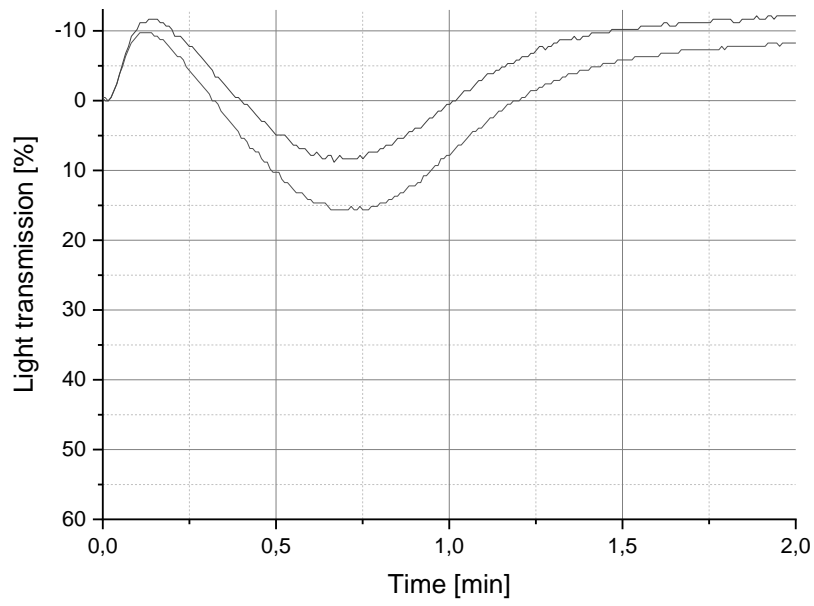
50 µg/mL



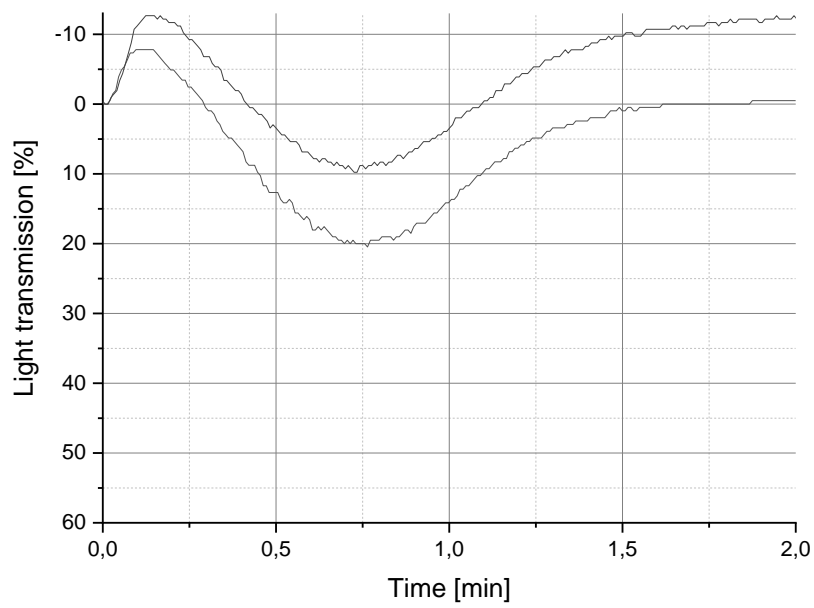
100 µg/mL



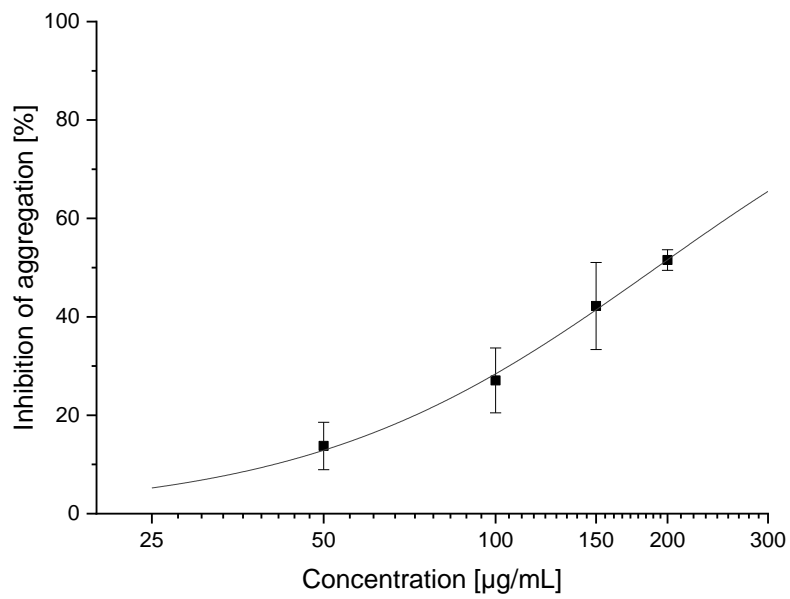
150 µg/mL



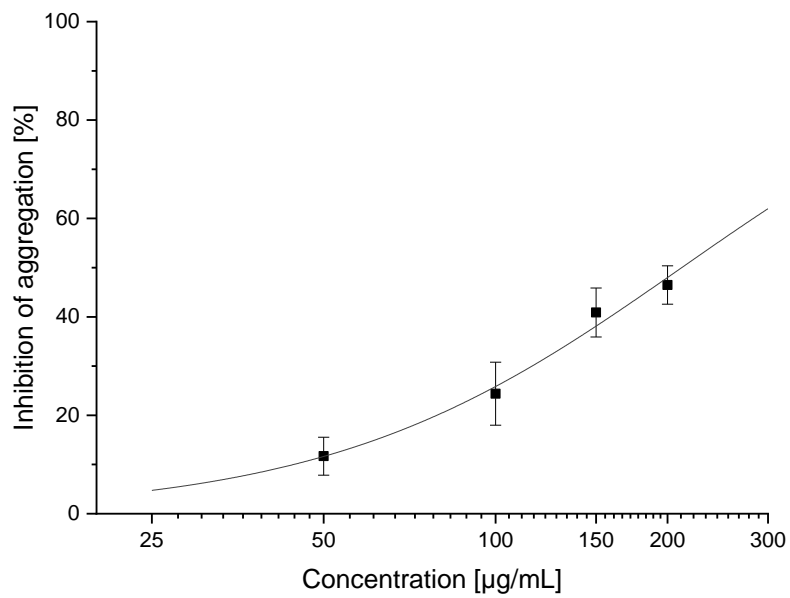
200 µg/mL

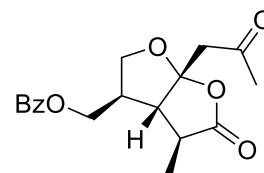


Maximum aggregation:



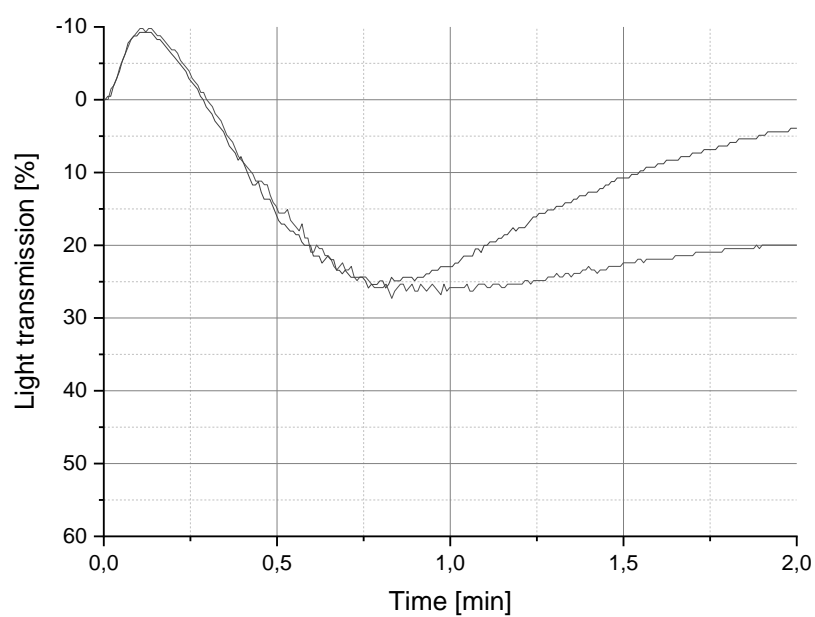
Slope:



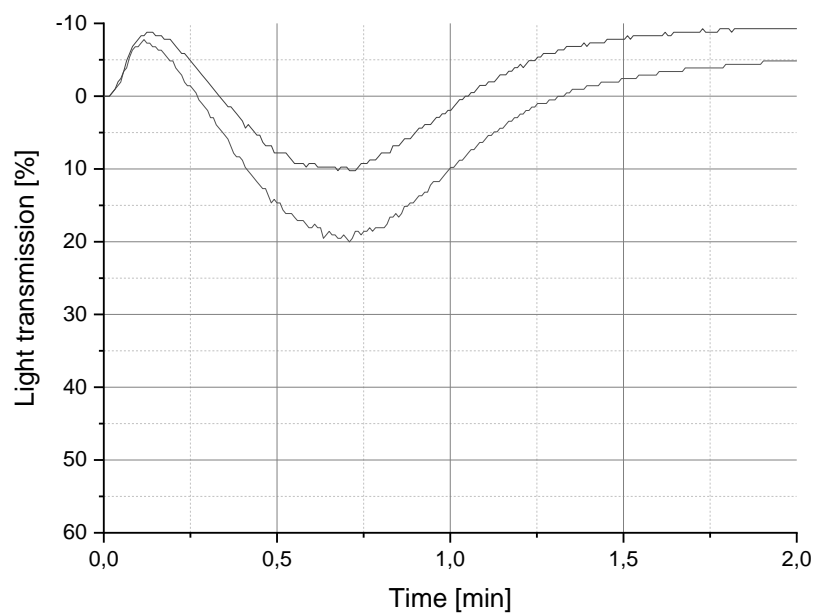


**((3*R*,3*aS*,4*S*,6*aR*)-4-Methyl-5-oxo-6*a*-(2-oxopropyl)hexahydrofuro[2,3-*b*]furan-3-yl)methyl benzoate (192)**

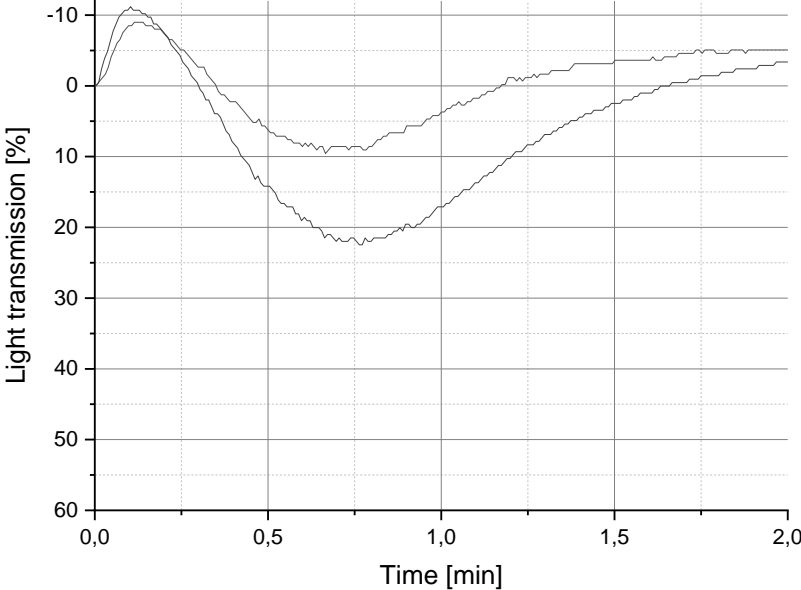
3  $\mu\text{g/mL}$



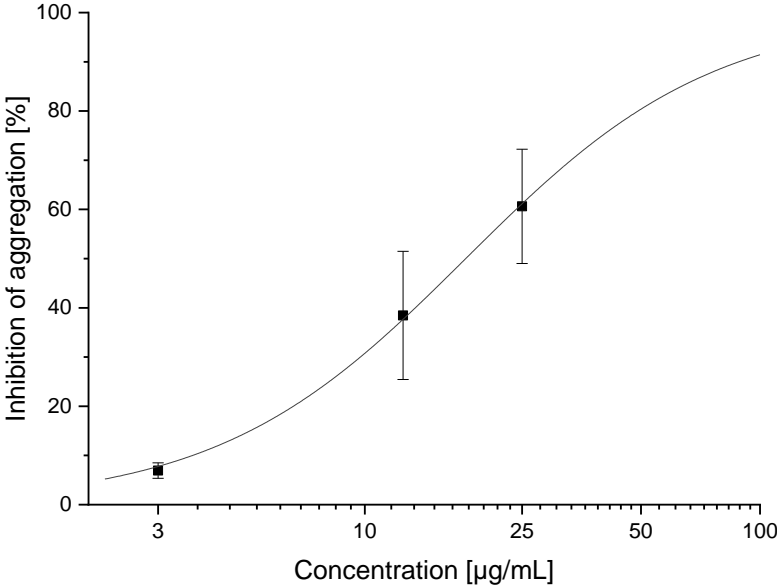
12,5  $\mu\text{g/mL}$



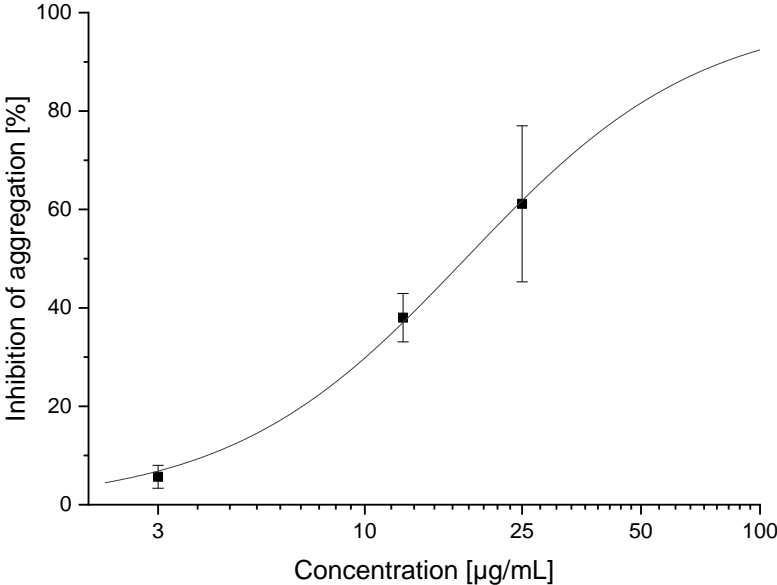
25 µg/mL



Maximum aggregation:



Slope:



## 5. Curriculum Vitae

### Personal data

---

Name	Matthias Gnahn
Date and place of birth	January 30, 1990 in Amberg
Nationality	German
Email	Matthias.Gnahn@chemie.uni-regensburg.de

### Education

---

11/2014 – current	PhD thesis in the research group of <i>Prof. Dr. Oliver Reiser</i> (University of Regensburg, Germany)
09/2014	Master of Science in chemistry
01/2014 – 09/2014	Master thesis in the research group of <i>Prof. Dr. Oliver Reiser</i> (University of Regensburg, Germany)
10/2012 – 09/2014	Advanced studies in chemistry (University of Regensburg, Germany)
09/2012	Bachelor of Science in chemistry
07/2012 – 09/2012	Bachelor thesis in the research group of <i>Prof. Dr. Oliver Reiser</i> (University of Regensburg, Germany)
10/2009 – 09/2012	Studies in chemistry (University of Regensburg, Germany)
09/2000 – 06/2009	Allgemeine Hochschulreife (A-levels), Herzog-Christian-August-Gymnasium, Sulzbach-Rosenberg, Germany

### Publications

---

1. Gnahn, M.; Schlossmann, J.; Reiser, O.; *Manuscript in preparation*  
“Synthesis, derivatization and biological evaluation of (+)-paeonilide”

## Conferences

---

**GDCh Wissenschaftsforum 2017** – Berlin (Germany), September 10–14, 2017.

*“Synthesis of (+)-Paeonilide derivatives”* (Poster).

**26<sup>th</sup> ISHC Congress 2017** – Regensburg (Germany), September 03–08, 2017.

*“The furo[2,3-b]furan motif as core structure of natural products”* (Poster).

**6<sup>th</sup> EuCheMS Chemistry Congress** – Seville (Spain), September 11–15, 2016.

*“Studies towards the enantioselective synthesis of (+)-Paeonilide derivatives”* (Poster).

**GDCh Wissenschaftsforum 2015** – Dresden (Germany), August 30 – September 02, 2015.

*“Synthesis and derivatization of (+)-Paeonilide”* (Poster).

## Professional References

---

Prof. Dr. Oliver Reiser

Institut für Organische Chemie

Universität Regensburg

Universitätsstr. 31

93053 Regensburg, Germany

Phone: 0049 941 943 4631

Email: [Oliver.Reiser@chemie.uni-regensburg.de](mailto:Oliver.Reiser@chemie.uni-regensburg.de)



## **G. Acknowledgement – Danksagung**

Bedanken möchte ich mich zunächst sehr herzlich bei meinem Doktorvater Prof. Dr. Oliver Reiser für die freundliche Aufnahme in seinen Arbeitskreis, die Überlassung des interessanten und abwechslungsreichen Themas, die Unterstützung und die hilfreichen Diskussionen während der gesamten Arbeit.

Mein aufrichtiger Dank gebührt Prof. Dr. Jens Schlossmann und seinen Mitarbeitern für die Ermöglichung der biologischen Messungen der (+)-Paeonilid Derivate.

Den Mitarbeitern der zentralen Analytik möchte ich für die zahlreichen Messungen, fachlichen Diskussionen und die bereitwillige Unterstützung bei der Auswertung danken. Vielen Dank auch an Regina Hoheisel für die CV-Messungen.

Für die geduldige Hilfe bei allen chemischen und technischen Problemen sowie für die Herstellung von Startmaterialien möchte ich mich ganz besonders bei Dr. Peter Kreitmeier bedanken.

Ein herzliches Dankeschön an die Mitarbeiterinnen des Sekretariats der Arbeitsgruppe, Antje Weigert und Michaela Schüle, für das Regeln aller bürokratischen Anliegen sowie die Unterstützung in allen organisatorischen und sonstigen Fragen.

Für die technische sowie synthetische Hilfestellung bedanke ich mich bei Roxane Harteis, Brigitte Eichenseer, Helena Konkell und Klaus Döring. Besonders möchte ich mich bei Roxane Harteis für die vielen tollen Gespräche und die schöne Zeit, sowohl an der Universität als auch außerhalb, bedanken, die den Uni-Alltag erleichtert haben.

Meinen Laborkollegen Dr. Verena Lehner, Dr. Martin „Jimmy“ Hofmann, Carina Sonnleitner, Robert Eckl und Urszula Klimczak möchte ich für die schöne Zeit und Zusammenarbeit im „PowerLabor“ danken. Des Weiteren möchte ich mich bei meinem „Laborvorgänger“

Dr. Andreas Bergmann für die Unterstützung bei chemischen Fragen und vor allem die unterhaltsamen Besuche am Arbeitskreis bedanken.

Mein ganz besonderer Dank gilt Dr. Verena Lehner und Dr. Martin „Jimmy“ Hofmann, die mir nicht nur den Einstieg ins Laborleben erleichtert haben, sondern mir auch später immer mit Rat und Tat zur Seite standen. Die vielen Unternehmungen inner- und außerhalb der Universität sowie die tollen Gespräche und Erlebnisse mit euch haben die letzten Jahre zu einer unvergesslichen Zeit gemacht.

Ein riesengroßes Dankeschön geht an Benjamin Kastl und Sabine Kerres. Auch wenn wir uns erst später im Studium richtig kennengelernt haben, seid ihr zu meinen besten Freunden geworden. Mit euch konnte man über alles reden und ihr habt die Laborzeit und das Zusammenschreiben zu einer schönen Zeit gemacht. Die tollen und erlebnisreichen Unternehmungen mit euch werden mir für immer in Erinnerung bleiben.

Meinen besonderen Dank möchte ich auch aussprechen an Michael Leitner, Lisa Stadler, Dr. Thomas Ertl, Saerom Park, Thomas „Easy“ Föll, Peter Ehrnsberger und Carina Sonnleitner für die schöne Zeit am Arbeitskreis und vor allem die tollen Abende, die wir miteinander verbracht haben.

Für das sorgfältige Korrekturlesen dieser Arbeit gebührt Martin „Jimmy“ Hofmann, Thomas „Easy“ Föll, Michael Leitner, Carina Sonnleitner und Robert Eckl mein herzlicher Dank.

Ich danke allen ehemaligen Kollegen am Arbeitskreis, insbesondere Dr. Ludwig Pils, Dr. Daniel Dobler, Dr. Corina Neumeister, Dr. Paul Kohls, Dr. Daniel Rackl, Dr. Andreas Okun, Dr. Christian Faderl, Dr. Matthias Knorn, Dr. Viktor Kais, Dr. Roland Linhardt, Dr. Francesca Besostri, Dr. Soraia Fernandes, Dr. Thomas Rawner sowie allen aktuellen Mitarbeitern des AK Reiser.

Mein Dank gilt auch meinen Studienkollegen und Freunden aus anderen Arbeitskreisen, insbesondere Dr. Andreas Seegerer, Felix Riedlberger, Marco Peteranderl, Dr. Marleen Häring, Dr. Sabine Möhle, Bernadette Pils, Julian Rieder, Romy Freund und Elisabeth Grünstein.

Meinen Bacheloranten und Forschungspraktikanten Roman Kučera, Maximilian Sehr, Tomislav Krolo, Sebastian Fischer, Johannes Gramüller, Johannes Moser, Diana Braun, Katrin Schwank, Lena Cook und Peter Bellotti danke ich für ihre Unterstützung bei der Laborarbeit und die zahlreichen Säulen.

Neben meinen Freunden und Kollegen innerhalb der Universität möchte ich mich auch bei allen meinen Freunden, sowohl in Regensburg, als auch in Leinhof, für ihre Hilfe und die vielen gemeinsamen Unternehmungen, die für die nötige Ablenkung gesorgt haben, bedanken.

Liebe Lisa, danke für deinen Rückhalt, dein Vertrauen und deine Geduld, die das Fertigstellen dieser Arbeit möglich gemacht haben. Ich danke dir auch, dass du immer für mich da bist und bin unendlich glücklich, dass du Teil meines Lebens bist.

Zum Schluss möchte ich meiner Familie danken: Vor allem meinen Eltern, Georg und Monika, die mich immer unterstützt haben und ohne die dieses Studium nicht möglich gewesen wäre, und meiner ganzen Familie für die Unterstützung im Laufe der Jahre.

Sollte ich noch jemanden vergessen haben, so bitte ich dies zu verzeihen und spreche auch hier meinen aufrichtigen Dank aus.

## **H. Declaration**

Herewith I declare that this present thesis is a presentation of my original work prepared single-handed. Wherever contributions from others are involved, all of them are marked clearly, with reference to the literature, license and acknowledgement of collaborative research.

Regensburg, October 19, 2018

---

Matthias Gnahn